SEPTEMBER 8-10, 2021
BUDVA, MONTENEGRO
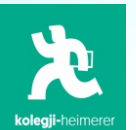
ICONST EST'21
ENGINEERING SCIENCE

4th INTERNATIONAL CONFERENCE ON ENGINEERING SCIENCE AND TECHNOLOGY

www.iconst.org

Proceedings & Abstracts Book

ICONST EST 2021

International Conferences on Science and Technology

Engineering Science and Technology

September 8-10 in Budva, MONTENEGRO

ABSTRACTS
&
PROCEEDINGS BOOK

ICONST EST 2021

International Conferences on Science and Technology

Engineering Science and Technology

September 8-10 in Budva, MONTENEGRO

Editors

Dr. Mustafa Karaboyacı
Dr. Kubilay Taşdelen
Dr. Abdullah Beram
Dr. Hamza Kandemir
Dr. Ergin Kala
MSc. Serkan Özdemir

Technical Editors

MSc. Tunahan Çınar
MSc. Şerafettin Atmaca
MSc. Doğan Akdemir
Ma. Fıratcan Çınar

Cover design & Layout
MSc. Kubilay Yatman

Copyright © 2021

Published by

ICONST EST 2021

International Conferences on Science and Technology

Engineering Science and Technology

September 8-10 in Budva, MONTENEGRO

Scientific Honorary Committee

Prof. Dr. Rade RATKOVIC, Fakultet za biznis i turizam Budva University, MONTENEGRO
Prof. Dr. İlker Hüseyin ÇARIKÇI, Suleyman Demirel University, TURKEY
Prof. Dr. İbrahim DİLER, Isparta University of Applied Sciences, TURKEY
Prof. Dr. Vujadin VEŠOVIĆ, Faculty of Transport Communications and Logistics, MONTENEGRO
Prof. Dr. Bujar DEMJAHA, Rector of AAB College, KOSOVO
Prof. Dr. Samedin KRRABAJ, University of Prizren, KOSOVO
Prof. Dr. Edmond HAJRİZİ, University for Business and Technology, KOSOVO
Prof. Dr. Fadıl HOCA, International Vision University, MACEDONIA
Prof. Dr. Naime BRAJSHORİ, Kolegji Heimerer, KOSOVO
Prof. Dr. Harun PARLAR, Parlar Research & Technology-PRT, GERMANY
Prof. Dr. Ahmad UMAR, Science of Advanced Materials, KINGDOM OF SAUDI ARABIA
Prof. Dr. Kürşad ÖZKAN, Isparta University of Applied Sciences, TURKEY
Prof. Dr. Mehmet KILIÇ, Suleyman Demirel University, TURKEY

Organizing Committee

Dr. Mustafa Karaboyacı, Suleyman Demirel University, TURKEY
Dr. Hamza Kandemir, Isparta University of Applied Sciences, TURKEY
Dr. Kubilay Taşdelen, Isparta University of Applied Sciences, TURKEY
Dr. Abdullah Beram, Isparta University of Applied Sciences, TURKEY
MSc. Serkan Özdemir, Isparta University of Applied Sciences, TURKEY
Dr. Ergin Kala, University of Prizren, KOSOVO

Technical Committee

MSc. Kubilay Yatman, Isparta University of Applied Sciences, TURKEY
MSc. Doğan Akdemir, Balıkesir University, TURKEY
MSc. Şerafettin Atmaca, Suleyman Demirel University, TURKEY
MSc. Fatih Yiğit, Isparta University of Applied Sciences, TURKEY
MSc. Tunahan Çınar, Isparta University of Applied Sciences, TURKEY
Ma. Fıratcan Çınar, Isparta University of Applied Sciences, TURKEY

ICONST EST 2021

International Conferences on Science and Technology

Engineering Science and Technology

September 8-10 in Budva, MONTENEGRO

Scientific Committee

Dr. Alev Akpınar Borazan, Bilecik Seyh Edebali University, Turkey
Dr. Amer Kanan, Al-Quds University, Palestine
Dr. Andrea G. Capodaglio, University of Pavia, Italy
Dr. Aybeyan Selim, International Vision University, North Macedonia
Dr. Apostolos Kiritsakis, Alexander Tech. Educational Ins. of Thessaloniki, Greece
Dr. Ayodeji Olalekan Salau, Obafemi Awolowo University, Nigeria
Dr. Bülent Derviş, International Vision University, North Macedonia
Dr. Cristian Fosalau, Technical University of Iasi, Romania
Dr. Driton Vela, University of Business and Technology, Kosovo
Dr. Eda Mehmeti, University of Business and Technology, Kosovo
Dr. Elvida Pallaska, University of Business and Technology, Kosovo
Dr. Ermek A. Aubakirov, Al – Farabi Kazakh National University, Kazakhstan
Dr. Fecir Duran, Gazi University, Turkey
Dr. Gauss M. Cordeiro, Federal University of Pernambuco, Brazil
Dr. Gholamhossein Hamedani, Marquette University, USA
Dr. Gülcan Özkan, Süleyman Demirel University, Turkey
Dr. Hamid Doost Mohammadian,FHM University of Applied Sciences, Germany
Dr. Ines Bula, University of Business and Technology, Kosovo
Dr. Izabela Zimoch, Silesian Universum of Technology, Poland
Dr. Joanna Boguniewicz-Zabłocka, Opole University of Technology, Poland
Dr. Kari Heliövaara, University of Helsinki, Finland
Dr. Kłosok-Bazan Iwona, Opole University of Technology, Poland
Dr. Kubilay Akçaözoğlu, Niğde Ömer Halisdemir University, Turkey
Dr. Leyla Tavacıoğlu, Istanbul Technical University, Turkey
Dr. Lulzim Beqiri, University for Business and Technology, Kosovo
Dr. Mathew Ademola Jayeola, Obafemi Awolowo University, Nigeria
Dr. Mehmet Kılıç, Suleyman Demirel University, Turkey
Dr. Mehmet Kitiş, Suleyman Demirel University, Turkey
Dr. Merita Barani, University for Business and Technology, Kosovo
Dr. Meruyert Kaygusuz, Pamukkale University, Turkey
Dr. Mirosław Kwiatkowski, AGH- University of Science And Technology, Poland
Dr. Mohd Aswadi Bin Alias, Unıversıty Kuala Lumpur- Bmı, Malaysia
Dr. Muhamet Ahmeti, University of Business and Technology, Kosovo
Dr. Naushad Ali Mamode Khan, University of Mauritius, Mauritius
Dr. Nicholas Baldacchino, Malta College of Arts, Science & Technology, Malta
Dr. Nuray Benli Yıldız, Duzce University, Turkey
Dr. Rahmon Ariyo Badru, Obafemi Awolowo University, Nigeria
Dr. Ramazan Şenol, Suleyman Demirel University, Turkey
Dr. Salina Muhamad, Universiti Selangor, Malasıa
Dr. Sami Makolli, University of Business and Technology, Kosovo
Dr. Serhat Oğuzhan Kıvrak, Hitit University, Turkey
Dr. Shpend Dragusha, University of Business and Technology, Kosovo
Dr. Şule Sultan Uğur, Suleyman Demirel University, Turkey
Dr. Valmir Hoxha, University of Business and Technology, Kosovo
Dr. Vehebi Sofiu, University of Business and Technology, Kosovo
Dr. Vincenzo Naddeo, University of Salerno, Italy
Dr. Zhandos T. Mukayev, Shakarim State University of Semey, Kazakhstan

ICONST 2021

International Conferences on Science and Technology
Engineering Science and Technology
Life Science and Technology
Natural Science and Technology
September 8-10, 2021 in Budva, MONTENEGRO

Dear Readers;

The fourth of ICONST organizations was held in Budva/Montenegro between 8-10 September 2021 with the theme of '*science for sustainable technology*' again. In recent years, weather changes due to climate change have reached a perceptible level for everyone and have become a major concern. For this reason, scientific studies that transform technological progress into a sustainable one is seen as the only solution for humanity's salvation. Here we ask ourselves "which branch of science is responsible for sustainability?". Sustainability science is an interdisciplinary field of study that covers all basic sciences with social, economic, ecological dimensions. If we consider technology as the practical application of scientific knowledge, the task of scientists under these conditions is to design products that consume less energy, require less raw materials, and last longer.

ICONST organizations organize congresses on sustainability issues of three main fields of study at the same time in order to present different perspectives to scientists. This year, 157 papers from 28 different countries presented by scientists in **ICONST Organizations**.

85 papers from 17 countries presented in our **International Conference on Engineering Science and Technology** organized under ICONST organizations. Turkey leads the way with 49% of the participants, followed by Kosovo and Moldova with 8.2%, North Macedonia 4.7%, Algeria, Azerbaijan, Hungary, Italy, Montenegro and Poland 3.5%, Croatia, Czech Republic, Kingdom of Saudi Arabia, Japan, Kyrgyzstan, Portugal and Russia with 1.2%.

57 papers from 13 countries presented in our **International Conference on Life Science and Technology** organized under ICONST organizations. Turkey leads the way with 49% of the participants, followed by Poland with 12.7% and Kosovo 11%, United Kingdom 5.4%, Kazakhstan, USA, Tunisia and Croatia 3.6%, Serbia, Israel, Czech Republic and Montenegro with 1.8%.

Finally, 15 papers from 8 countries presented in our **International Conference on Natural Science and Technology** organized under ICONST organizations. Turkey leads the way with 47% of the participants, followed by Kosovo with 11% and Serbia, Egypt, Bosnia and Herzegovina, Italy, Poland, North Macedonia and Romania with 6%.

As ICONST organizations, we will continue to organize organizations with the value you deserve in order to exchange ideas against the greatest threat facing humanity, to inspire each other and to contribute to science. See you at future events.

ICONST Organizing Committee

ICONST EST 2021

International Conferences on Science and Technology

Engineering Science and Technology

September 8-10 in Budva, MONTENEGRO

Contents

Advanced Functional Nanomaterials: From Growth to Applications

Ahmad Umar[1,2]*

Abstract: Nanoscale materials, which are at the foundation of Nanoscience and Nanotechnology, have sparked a lot of interest and anticipation in recent years because they possess high surface area and exhibited better chemical and physical characteristics that are different from both the bulk phase and individual molecules. Nanoscale materials or nanomaterials research has grown at a rapid pace, and it is now one of the most popular research topics among scientists and engineers due to their diverse structures, intriguing properties, and high-tech applications in electronics, catalysis, chemical engineering, pharmaceutics, biology, magnetic recording, and other fields. Due to their broad structural, physical, and chemical characteristics and functions, metal oxide semiconductor nanostructures stand out as one of the most prevalent, most diversified, and most likely richest classes of materials among semiconductor nanostructures. Metal oxide nanostructures' unique and tunable characteristics, such as optical, optoelectronic, magnetic, electrical, mechanical, thermal, catalytic, and photo-electrochemical, among others, making them ideal candidates for a variety of high-level technological applications.

In this lecture, I will demonstrate the growth, properties and applications of functional nanomaterials, especially the pure and doped metal oxide nanomaterials. Various metal oxide nanomaterials such as zinc oxide (ZnO), copper oxide (CuO), iron oxide (Fe2O3), cerium oxide (CeO2), etc and their composites will be explored from their synthesis to the potential applications. This lecture will cover a variety of applications based on metal oxide nanostructures, including chemical and biosensors, photocatalysis, dye-sensitized solar cells, and so on.

[1]Department of Chemistry, Faculty of Science and Arts, Najran University, Najran-11001, Kingdom of Saudi Arabia
[2]Promising Centre for Sensors and Electronic Devices (PCSED), Najran University, Najran-11001, Kingdom of Saudi Arabia
* Corresponding author: ahmadumar786@gmail.com

Efficiency of Singularity and PCA Mapping of Mineralization-Related Geochemical Anomalies: A Comparative Study Using BLEG and <180µm Stream Sediment Geochemical Data in Eskişehir-Sivrihisar Region

Fatma Nuran Sönmez[1], Hüseyin Yılmaz[1]*

Abstract: Fine-grained stream sediments are the most common sampling media in regional geochemical exploration programs, with analysis of Au, Ag and other elements extracted by bulk cyanide leach (BLEG methods) used in the early stages of stream sediment-based exploration followed up with aqua regia extractions at follow-up stages. The Eskisehir-Sivrihisar region in Western Turkey includes several orogenic type mineral deposits including Au-bearing quartz vein systems. The purpose of this study is to delineate geochemical anomalies of ore and related elements and track their dispersion, which may lead to discovery of unknown ore deposits. Using a geochemical database generated through company's exploration campaigns (Eurogold, Normandy Mining Ltd., Australia), this research also compares the capability of conventional statistical methods (such as Q-Q, Mean + 2STD, 3SD and 4SD) and principal component analysis (PCA), with concentration area (C-A) and number-size/concentration (N-S/C) fractal methods and singularity index method to differentiate anomalous and background Au distributions or define areas with geochemical signals related to mineralization (given singularity index mapping/S.M does not define threshold values). Known Au mineralization in the region of interest is strongly reflected in stream sediment BLEG Au patterns, which have robust singularity indices with C-A and N-S multifractal modeling and PCA. A hundred % of the Au deposits were detected using either BLEG Au and Ag singularity index mapping with C-A fractal analysis whereas those of factor analysis revealed 85% efficiency. Several strong Au-Ag anomalies defined by the singularity index and factor analysis in this study needs further follow up for the discovery of new deposits. Conventional approaches to anomaly detection in the BLEG and <180µm stream sediment data failed to detect a significant proportion of the deposits, including some major deposits in the vicinity of Sivrihisar

Keywords: Singularity mapping; C-A; N-S; PCA; multi-fractal models, Eskişehir.

[1] Dokuz Eylül University, Faculty of Engineering, Department of Geology, İzmir, Turkey
* Corresponding author: huseyin.yilmaz@deu.edu.tr

The approach of the critical size bone defects by decellularized vascularized bone allografts. Preliminary report of the *in-vivo* experiment.

[1]Pavlovschi Elena, [1,2]Stoian Alina, [2]Verega Grigore, [1]Nacu Viorel

Abstract: Tissue transplantation is a successful approach to rebuild the osteoarticular defects. Critical bone defects remain a dilemma for reconstructive surgery. Decellularization of organs, including bone, gives an acellular biological graft, which keeps their extracellular three-dimensional structure. Theoretically, maintaining the osteoplastic properties of the vascularized autograft, combining them with the orthotopic characteristics of an allogenic bone, the vascularized bone allograft would be a successful alternative for the reconstructive surgery of the skeletal system. To extract the cellular component from the vascularized bone allograft by the combined method, according to the algorithm, without injuring the extracellular structure and matrix, for obtaining a graft to be able for next inclusion in the host blood circulation, without immunosuppression by decellularization.

The bone segment was taken from the domestic rabbit- New Zealand White Rabbit. The femur was taken with the internal iliac artery, located between the upper part of the great trochanter and the distal 1/3 of the femoral shaft, respecting the vascular continuity. The graft was processed, gradually, with a series of solutions, during mechanical agitation.

The optimal segment for vascularized allografting (the rabbit model) was determined the upper third of the femur with the up to the level of the internal iliac artery. The decellularization process was applied according to the established protocol. Used decellularizing agents were physical, chemical, and biological. They assured the efficient removal of cellular content from the tissue, without damaging the three-dimensional structure of the extracellular matrix. The greatest part - the cells, were removed first, and then the protein and lipid residues. In the last step, the smallest compartments DNA and RNA, were eliminated. The grafts were examined radiologically, histological and morphologically.

The combined process of decellularizing of vascularized bone tissue can generate bone grafts devoid of immunological agents. The vascularized allogeneic bone without immunosuppression would be a perfect alternative in the treatment of the massive bone defects.

Keywords: vascularized bone allograft, combined decellularization, surgical revascularization

[1]Laboratory of Tissue Engineering and Cellular Culture, the University of Medicine and Pharmacy "Nicolae Testemițanu", Chișinău, Republic of Moldova.
[2]Department of Orthopaedics and Traumatology, the University of Medicine and Pharmacy "Nicolae Testemițanu", Chișinău, Republic of Moldova
[*]Corresponding author: pavlovschi.elena@gmail.com, tel. +373 79 050 049

Submarine Active and Potentially Active Faults, Gas Seeps and Diapirs in the Kusadasi Gulf and Surroundings, Aegean Sea

Savas Gurcay[1*]

Abstract: Gulf of Kuşadası and surroundings is an important area in terms of active faults both under the sea and on land. Karaburun Fault, Tuzla (Orhanlı) Fault, Seferihisar Fault, Gümüldür Fault and Küçük Menderes Fault are the most important faults in the study area and surroundings. Each of them can be traced until the shore line of the study area. Compare to the previous marine seismic data collected around the study area the high resolution Chirp marine seismic data, which were benefited from on this study, both have much higher resolution and comprises larger area than the others. In the light of the data, the features and distributions of the seafloor deformation made by submarine active faults, potentially active faults, gas seeps and diapirs in Kuşadası Gulf and surroundings were investigated. For this purposes, the high resolution Chirp marine seismic data which collected previously were processed to obtain two dimensional seismic profiles. The results were illustrated on a map in detail after interpretation of these profiles depending on their structural properties.

Keywords: Chirp-Seismic, Submarine Active Faults, Aegean Sea

[1]Canakkale Onsekiz Mart University, Marine Technology Vocational School, Canakkale, Turkey
* Corresponding author: savasgurcay@comu.edu.tr

Determination of Geological-Geochemical Properties of Magnesite Formations Observed in Kızıldağ Ophiolites

Yusuf Topak[1*]

Abstract: In this study, the geochemical characteristics of the economically valuable magnesite (MgCO3) in an area of approximately 200 km2 in the region between the Samandağ Central district of Hatay province and Iskenderun in southeast Turkey were evaluated by geological-geochemical analyzes. In this study, magnesite mineralizations developed along the cracks of ultramafic rocks of Kızıldağ ophiolite were sampled to determine their formation and origins. The study area is geologically composed of Arabian Platform, melange, Kızıldağ ophiolite and cover sediments. The sedimentary units of the Arabian platform include Lower Cambrian to Lower Carboniferous and Triassic to Cretaceous sediments and outcrops in the Amanos Mountains. The Arabian platform starts with fine-coarse-grained clastic units at the bottom and passes upwards to limestone-bearing units. The Mesozoic units of the platform start with large clastic units and pass the Cenomanian-Turanian aged platform carbonates and unconformably overlie the Paleozoic units. The melange unit presents small outcrops under the Kızıldağ ophiolite within the tectonic window observed around Kömürçukuru, which is called the Amanos olistostrome. The matrix of the unit consists of sheared serpentinites and is observed on the eastern and western slopes of the Amanos Mountains. The blocks within the matrix are diverse and include harzburgite, dunite, gabbro and pillow lavas, as well as limestone and sandstones. The Kızıldağ ophiolite melange unit is tectonically located around the town of Kömürçukuru with a low-angle fault. The ophiolite begins with serpentinized tectonites containing large limestone blocks that were combined with peridodites during thrust on the continent at the bottom. The Kızıldağ ophiolite represents one side of the spreading ridge and the other side of this spreading ridge is represented by the Troodos ophiolite. For geochemical analysis, 10 samples, all of which are magnesite, were taken from the field from 3 different locations and XRD analyzes were performed. As a result of the analyzes made, the whole rock geochemistry analyzes show that magnesite is in a more pure structure with other elements compared to dolomites and it accepts less main, trace and soil elements into its structure. As a result of isotope analysis, the low δ-18OV-PD (%) value shows that the origin of the water, which is effective in the formation of magnesite, is meteoric waters. As a result, the magnesite found in the study area was formed as a result of the alteration caused by the circulation of meteoric water in the ultramafics. For this reason, it has been determined that magnesite is not located along the fracture and crack zones.

Keywords: Hatay-Çevlik, Magnesite, Carbon and oxygen isotopes, Geochemistry

[1] AdıyamanUniversity, Mining and Mineral Extraction Department, Adıyaman, Turkey
* Corresponding author: ytopak@adiyaman.edu.tr

Denim Clothing Design with Ecological Footprint

Sukriye Yuksel[1*]

Abstract: Natural resources in the world are being consumed rapidly. Consumption preference of the environmental friendly people are turning to invest sustainable products in fashion, which aim is less harm/no harm to nature. Because, textile industry takes the major scale of using natural resources. Accordingly, to resent fashion researches, since 70's, especially denim become top desired material for the global fashion industry and use of denim varieties in textile developed for decades. However, the process of a denim, from cotton to a garment means waste of 1kg cotton and about 10800lt* water. For this reason, Denim companies, conscious about how to design denim products with less damage to nature and they formulated the process with this program called Eim Score (Environmental Impact Measuring).In this design project, denim clothing design's Eim score technically measured as a green project. The process and the testing of denim wash water consumption formulated to lower the impact and the dying steps of denim material explained. Fit and scale of the denim garment design process explained thru presentation, not only considered sustainable and "green label" for future fashion trends, but also made of "redone look" which is highly adding value to the products, presented for global fashion followers, for merchandise buyers and for nature conscious consumers. The design creation and the collection production with details of technical drawings, aim to involve as an important inspiration part in textile Industry for future Eco system.*(https://www.vatekcevre.com/blog/bir-urunun-uretimi-asamasinda-ne-kadar-su-kullaniliyor -biliyor-muyuz)

Keywords: EIM score, Denim clothing, Ecological garment designs, Sustainable Denim textile

Istanbul Technical University, Textile Engineering Faculty, Textile Technologies and Design Department, Istanbul, Turkey/
Yıltem Konfeksiyon, Yıkama ve Boya, Istanbul; Turkey
* Corresponding author: yuksels@itu.edu.tr

Extraction of heavy elements using liquid-liquid extraction

F. GHEBGHOUB[1*] , D. BARKAT[2*]

Abstract: The extraction of Co(II) and Cu(II) with bis(2-ethylhexyl)phosphoric acid is investigated at 25°C with the following parameters: pH, concentration of the extractant, and the nature of diluent. The effect of the diluent using polar and nonpolar solvents in the extraction of nickel(II) is discussed. The extracted copper(II) species were $CoiL_2$ in 1-octanol and methyl isobutyl ketone and CuL_2 $2HL$ in toluene, carbon tetrachloride, and cyclohexane. The extracted cobalt(II) species were CoL_2 in 1-octanol and methyl isobutyl ketone and CoL_2 $2HL$ in toluene, carbon tetrachloride, and cyclohexane.

Keywords: liquid–liquid extraction; cobalt(II);copper(II) ;di(2-ethylhexyl)phosphoric acid; diluent effect

[1] University of Biskra, Biskra, Algeria.
* Corresponding author: ghebghoub_fatima@yahoo.com

Encryption Technique With Catalan Numbers

Aybeyan Selim[1*]

Abstract: The permanent development of information technologies enables us to exchange and process a large amount of data. Due to the expansion of computer networks and the development of attack techniques, every computer connected is potentially endangered and primarily treated data. Protecting data from unwanted attacks with cryptological methods that allow unauthorized access and offer data modification is necessary. The paper provides an overview of cryptographic techniques that ensure data security to exchange or store. The method in this research explains data protection with Catalan numbers and computational geometry. Computational geometry is a discipline from computer sciences that deals with solutions to geometrical problems with computers and today have various areas of applications. Our encryption scenario contains four phases. In the first phase, we triangulate the 3D object with the Delaunay triangulation algorithm. Selection of polygon in the triangulated object we done in the second phase. The third phase contains the creation of Catalan keys with a triangulation problem. In the fourth phase, we encrypt the information with our technique. After presenting our developed procedure, we made cryptoanalysis for generated cryptographic keys gave proposals for practical application of the scenario developed in this research.

Keywords: Encrytion, Decryption, Catalan numbers, Cryptographic keys and Polygon triangulation.

---

[1] International Vision University, Faculty of Engineering and Architecture, Department of Computer Science, Gostivar, North Macedonia
* Corresponding author: aybeyan@vizyon.edu.mk

Between History And Technology: The Small Villas Of The Late Nineteenth Century In The Syracuse Countryside. The Recovery Of Villa Ortisi

Fernanda Cantone[1*], Francesca Castagneto[2*]

Abstract: The building heritage claims the unity of a culture that, to manifest itself completely, uses different linguistic structures, all referable to a single expressive code. It is also an expression of "conflict between oblivion and memory, between protection and abuse, between Viollet-le-Duc and Ruskin, between present and future, between tourism and museum ...". Today the interventions on the building heritage approve an overlap of traces and documents that make it a protected asset but above all usable.

The research theme is the built heritage of the late nineteenth century and, in particular, the small villas, "villini" in italian language, built by wealthy families to spend some periods of the summer season. In particular, the architectural model is a cottage, an imposing building, located in a peripheral area of Syracuse, Sicily, Italy close to others, which is in a state of neglect.

The research objective is to preserve these unique testimonies of a very interesting and particular past and to reuse these villini for a contemporary use.

The sustainable arrangement of a space, composed of several levels of liveability, plays a central role in the reuse project carried out as part of this research. In this sense, the re-use project does not only entail recovery but absolute 'fitting' to the environment, intention and invasion. The aim is to obtain close correspondence between the environmental and technological systems so that they fit together, developing a set of values that are contiguous with that of the past.

The intention of such research is to recover the lost identity of materials, geometric forms, volumes and empty spaces and foster the emergence of social, civil and symbolic values in which we recognize the architectural model of "villini" in Syracuse, Sicily, Italy. A project that aims to reconcile conservation and change, defining the possibilities of transforming the building property, enhancing its identity. The pre-existence becomes, in this sense, the starting point and the main reference system, in a contemporary vision of intervention. These aspects governed the design process with regards to the environment, the sites and the identity of the architectural model.

Keywords: adherence, integration, compatibility, respect.

---

[1] University of Catania, SDS Architecture, Department DICAR, Siracuse, Italy
* Corresponding author: fernanda.cantone@unict.it
[2] University of Catania, SDS Architecture, Department DICAR, Siracuse, Italy
* Corresponding author: francesca.castagneto@unict.it

General usage and features of data visualization software

Fehmi Skender*[1], Aybean Selim, Ilker Ali

Abstract: With the development of technology, the importance of easy presentation and perception of data has increased. People give a lot of importance to visuals. In addition to attracting attention within the content, the contents also make it easier to remember. Today, with the use of multiple devices and the widespread use of the internet compared to the past, visuals in the modern digital world have begun to attract the attention of users more than text. The visualization and processing of data has reached the crux.

In the research, besides visualizing the data, it is explained how important it is when firstly science researches and then analysis in other fields. Production data, which has different geographies around the world, has been accumulated and processed. There are different big data visualization software available today. Although they have different interfaces and algorithms, most of them have common functions.

Keywords: big data, data visualization, data visualization tools.

[1] International Vision University, Faculty of Informatics, Gostivar , North Macedonia
* Corresponding author: fehmi.skender@vizyon.edu.mk

The chance of architectural heritage of our recent history

Péter Fejérdy[1*]

Abstract: Nowadays it becomes important requirement the ecological point of wiev of the buildings. Even it becomes more clear that it means not only energetical renewal, but it is important to take into account the ecological circle of a building. The buildings of the recent history is in a special situation. Not enough time has passed, that the value, which is clear for professionals can be accepted by the society. Becouse of this, the buildings of this period is in danger. Throught restauration the can easily loose their caracter by changeing their shutters, or by covering them with heat insulation without thinking about the caracter of the former facade. Many time they demolish this buildings just becouse in the post-communist region the assessment of this period is negative. We have to change the relation with this buildings, becouse they are the part of our memory.

Keywords: recent past, monuments, renewal, heritage

[1] Budapest University of Technology and Economics, Faculty of Architecture, Dept. of Public Building Design, Budapest, Hungary,
* Corresponding author: fejerdy.peter@epk.bme.hu

Identification And Measures to Eliminate Delays in The Construction Sector In Kosovo

Muhamet AHMETI[1*]

Abstract: In the construction sector in Kosovo, whether in the public or private sector, there are delays and non-compliance with the dynamic plans approved in the implementation of contracted projects. Delays in the implementation of various projects directly affect the Kosovo economy in general. Delays in implementation of the construction of various projects also mean the slowdown of development in all other interrelated areas. Therefore, the main objective of this paper is to analyze the different types of delays based on the results of questionnaires and identify the reasons for causing these delays that are currently affecting the implementation of various construction projects in Kosovo. Delays in the construction industry are one of the acute and common problems in the construction sector. Moreover, in writing this paper we have analyzed 132 questionnaires that were realized by various construction companies which operate in different municipalities of Kosovo and carry out various construction works.

Based on the data from these assessments, there are proposed measures aiming to reduce or eliminate these delays in general, based on various methods that affect the reduction and mitigation of delays. Hence, there are different types of delays identified. It is important to identify whether the delay is critical or not as identifying critical delays helps to take appropriate action on time. Delays may be unjustifiable (caused by the contractor or other factors) for which the client or consultant must have the means of organizing and managing the project to effectively manage compensatory delays or delays (caused by the employer) of which are owed to the employer.

Delays can come from both parties and can be harmful at the same time and directly affect the deadline for completion of works. The reasons for delays are mainly due to an unreasonable project goal, project defects, inadequate organization and planning, and lack of risk management systems and measures. The contractor further contributes to the delay due to a lack of resources (financial, manpower, mechanization, etc.) and labor productivity.

On ambitious assessments of the company's capacity, inaccurate assessment of the task and work to be performed, lack of clarity of task, lack of experience for various construction works, delays of the main project/approval of changes, and interference in the decision-making process by the employer are factors that directly affect the delay in the implementation of projects in general.

Keywords: Delays, construction, factors, critical, employer.

[1] UBT – Higher Education Institution – Prishtinë Kosovë
* Corresponding author: muhamet.ahmeti@unt-uni.net

The Impact of Digital Technology on Advanced Business Processes

Ylber Limani[1*] , Edmond Hajrizi [1]

Abstract: Business processes are undergoing complex challenges related to the fasttechnological changes. The proper functionality of processes necessitates increased flexibility, higher reliability and augmented working speed of production systems and processes. The integration of information technology is accomplished by the development and use of cyberphysical systems, which actually are the enablers of the industrial alteration named "Industry 4.0". The debates about the digital transformation and competitive challenging advantages directed the industries to the creation of a new business vision named "Industry 4.0". Since the concept of Industry 4.0 and its impact on business processes is creating various challenges, this research addresses and examines the consequences and potentials of Industry 4.0 on advanced business transformation processes. The scope of this research is limited to the study of functional integration of Cyber-Physical Systems, Artificial Intelligence (AI) and Data Science (data security) providing the potential for the functioning of new technologies with focus on developing countries. The research utilizes qualitative and quantitative approaches to data collection and analysis based on literature and on the case studies. The contribution of this research is focused on the identification and analyses of needs, problems, and benefits related to the implementation of digital technology on business automated processes in developing countries.

Keywords: Digital technology, AI, Data Science, Industry 4.0.

[1] University for Business and Technology, 10000, Prishtina, Kosovo.
* Corresponding author: ylber.limani@ubt-uni.net

The Geology And Paleogegraphıc Evolutıon of Saraykoy(Denizli)

Mahmut Ziya GÖRÜCÜ [1*]

Abstract: Basement rocks of the Tırkaz-Sarayköy area consist of the Palaeocene-Early Eocene Zeybekölen Tepe Formation and tectonically overlying Late Triassic-Early Jurassic Gereme Formation and Mid Jurassic-Late Cretaceous Çataltepe Limestone all of which belong to the Menderes Massif (Okay, 1989). All this formations are unconformably overlain by the Kolonkaya Formation which belong to Denizli group of the Neocene age (Late Miocene). Kolonkaya Formation is overlain by Asartepe formation of Pleistocene age. After all these formation, are covered with travertene, some terrestrial sediments, slope debris and allivual sediments. We have collected some diatomite samples from differents levels of Sazak, Sakızcılar and mostly Kolonkaya formations for describing the species by comparing the electron microscope view to diatome catalogue. During this study we described *Cymbella brehmii* Hustedt, *Eunotia sudetica* Müller, *Navicula* cf. *Phyllepta* Kützing, *Cyclotella meneghiana* Kützing, *Stephanodiscus subtranssylvanicus* Gasse, *Cyclotella plitvicensis* Hustedt, *Fragilaria* sp., *Cyclotella meneghiana* Kützing, *Raphoneis amphiceros* Ehrenberg and put in the spreading map.

According this work and research we realize that especially Neogene sediments includes the diatoms. These diatoms are usually found in Sazak, Sakızcılar and Kolonkaya formations which are of Late Miocene age. At the same time wherever we find diatomites are together with marl deposits. Strata alternation shows that all over the colomn we had drilled 13 point, marl and diatomite levels are together. Therefore it is certain that marl and diatomite deposited the place which includes silica enough and the basin was shallow or marinal mesopelagic zone. According to these core data, we try to describe paleogeographic conditions and climate by looking both the vertical and horizontal spreading of diatoms. On the other hand there are many gypsium levels as well and we use and comment these data too for describing the paleogeographic conditions of the region.

Keywords: Diatomite, Upper Miocene, Paleogeographic, Denizli, Tırkaz, Jips.

[1] Istanbul University-Cerrahpasa, Engineering Faculty, Department of Geology Hadımkoy-Istanbul-Turkey
* Corresponding author: gorucu@iuc.edu.tr

Lessons learnt from Chernobyl and Fukushima accidents applicable for the protection against CBRN attacks

Jozef Sabol[1*]

Abstract: Both accidents involving nuclear power plants at Chernobyl in Ukraine and Fukushima in Japan have caused releases of tremendous amount of radioactive materials into the environment which resulted in huge contamination and resulted in overexposure of some workers as well as the general public especially in the vicinity of these nuclear facilities. This year, it is the 10th anniversary of the nuclear accident at Fukushima which occurred almost exactly 25 years after the Chernobyl nuclear accident in 1986. Analysis of each of these accidents and their consequences provided valuable late and early lessons that could prove helpful to minimize the impact of any emergency situation with massive radioactivity discharges which may contribute to the exposure of people affected. These events have been extensively publicized and led to the creation of a negative attitude towards the application of radiation and nuclear technologies for peaceful purposes. It is well known that some of this information has been exaggerated and formed undesirable perception especially among lay population. It is obvious that this was partially produced because of the lack and negligence in radiation risk communication with the public. Now, after so many years, the situation has considerably improved namely in terms of the upgraded nuclear safety and security, quantification and monitoring of radiation exposure in the case of accidents, and enhanced risk assessment and its mitigation. Most of these incentives come as lessons learned from the accidents at Chernobyl and Fukushima. The paper will discuss two major issues: a) the factual assessment of the impact of nuclear accidents on the human exposure and the environment, and b) the current state of the preparedness and response to a similar accident based on our present knowledge and lessons learned from the past misfortunes.

Keywords: Chernobyl, nuclear, Ukraine.

[1] Police Academy of the Czech Republic
* Corresponding author: sabol@polac.cz

Effect of Rare Earth Metals on Electrode Potential in Anodic Oxidation as A Novel Electrode for Different Kind of Contaminants

Dilara ÖZTÜRK[1*], Abdurrahman AKYOL[2*]

Abstract: Nowadays, novel metal electrodes have become a very interesting subject for both electrooxidation (EO) studies and catalyst production. Many different types of alloys and coatings are tried to increase the catalytic activity of the electrodes to be produced. Rare earth elements have started to gain an important place among the studies. The fact that rare earth elements are so abundant in nature and they are not processed, they are named as rare earth elements, which has made it an interesting research area. It was thought that rare earth elements could increase the catalytic activity and the fast transfer. It is well known that rare earth oxides are powerful oxidants and widely used as catalysts for oxidation reaction. So, various rare earth oxides were used to modify coating to increase the electrochemical performance of electrode.

In this study, we intend to improve the electro-catalytic activity and stability of Ti/TuO2-IrO2 electrode by modification of Lantane and Cerium. The electro-catalytic activity and stability of the La and Ce modified Ti/TuO2-IrO2 electrode were compared with those of undoped Ti/TuO2-IrO2, Ce-La doped Ti/TuO2-IrO2, and BDD electrodes, it has been tried both in the removal of paracetamol, which is a model pharmaceutical compound, and in the use of anodic oxidation in the removal of textile wastewater. Commercial electrodes in PST removal, Ti $/IrO_2/RuO_2$ electrodes exhibit the same performance with BDD electrode, providing 40% TOC and 100% PST removal at pH 5 and the current density of 350 A/m² for 90 minutes. In textile wastewater treatment trials, it was achieved faster and higher removal efficiency than BDD electrode, which is the most efficient commercial electrode known at the point of color removal, and 98% removal was achieved for both electrodes at the same conditions at 15 minutes. The results show promise for the new electrode compositions to be used in EO systems.

Keywords: Rare earth elements, anode materials, anodic oxidation, textile wastewater, paracetamol.

[1] Gebze Technical University, Engineering Faculty, Environmental Engineering, Kocaeli, Turkey
* Corresponding author: akyol@gtu.edu.tr

Biomimetic Approaches to Develop Safe-By-Design Antimicrobial Textiles

Isabel C. Gouveia[1]*, Frederico Nogueira, Cláudia Mouro, Ana P. Gomes

Abstract: Antimicrobial textile materials may significantly reduce the risk of infections and because they are able to absorb substances from the skin and release therapeutic compounds to the skin, they can also find applications as complementary therapy of skin-diseases as part of standard management. Although functional textiles may be a promising area in skin disease/injury management, as part of standard management, few offer complementary treatment even though they are well known to reduce scratching and aiding emollient absorption, reducing infection, and alleviating pruritus. The reason for this may rely on the low quality of supporting evidence and negative effect that antimicrobial agents may exert on skin microbiome, as for example additional irritation of the vulnerable skin, and by causing resistant bacteria.

Several antimicrobial agents have been tested in textiles: quaternary ammonium compounds, silver, polyhexamethylene-biguanides and triclosan have been used, with success. They have powerful bactericidal activity but the majority have a reduce spectrum of microbial inhibition and may cause skin irritation, ecotoxicity and bacteria resistance. Furthermore, the rising flow of strains resistant to last-resort antibiotics rekindles interest in alternative strategies. In this regard, new functional textiles incorporating highly specific antimicrobial agents towards pathogenic bacteria, are required. Recent research has been conducted on naturally occurring antimicrobials as novel alternatives to antibiotics. Conscious of this need our team firstly reported new approaches using L-cysteine and antimicrobial peptides (AMP). Briefly, we were able to develop different immobilization processes towards 6 Log Reduction against bacteria such as S. aureus and K. pneumoniae. Therefore, here we present several innovative antimicrobial textiles incorporating AMP and L-Cysteine which may open new avenues for the medical textiles market and biomaterials in general. Team references will be discussed as an overview and for comparison purposes in terms of potential therapeutic applications.

[1] FibEnTech Research Center, Faculty of Engineering University of Beira Interior, Covilhã – Portugal.
* Corresponding author: igouveia@ubi.pt

An Estimation of the Hydrologic Water Budget Components of the Seyfe Lake Basin By Using Hydrologic Characteristics and Hydrometeorological Data

Cansu Yurteri[1*], Türker Kurttaş[2*]

Abstract: A water budget calculated for a defined system, consists of the account of all water flowing into and out of an area of interest, along with the change of water storage in the area. The water budget, also known as the water balance, is computed over a specific time period for a particular system or region and is based on the conservation of the mass equation. Water budgets can help to provide a clearer understanding of past circumstances, as well as provide an indication of how future changes in hydrology, population, supply, demand, land use, and climate factors may influence the water resources in the basins. Water budget calculations are an essential tool for devising sustainable solutions regarding surface water and groundwater resources, water supply planning, and monitoring and designing water systems. Human activities such as groundwater withdrawals and irrigation alter natural flow patterns, which must be accounted for in the water budget calculation. In this research, the Seyfe Lake Basin was selected as a study area. Seyfe Lake is a closed basin and the lake area and its surroundings are a protected Ramsar Site. Lake area is located 15 km northeast of the Mucur district, Kırşehir province of Central Anatolia. Lake basin has a 1447 km^2 catchment area, in which 10.192 inhabitants reside. This paper aims to estimate the water budget components in the Seyfe Lake basin and the influence of budget components over a 50 year (1970-2020) period. The estimate of groundwater budget components is one of the most difficult issues in basin-scale management. The main issue with calculating the water budget components is a lack of routinely collected data. In this study, precipitation, evapotranspiration, surface outflow data were calculated by using annual data for the lake catchment area and the changes in storage reserves were calculated for the study area. Seyfe Lake Basin is recharged by precipitation and groundwater inflow. Discharge of the lake area via evaporation, drainage channels and withdrawal of water for irrigation and drinking purposes. The difference between lake recharge and discharge components for the period 1970-2020 was calculated to be 15.7 x10^6 m^3/year. Based on groundwater budget calculations, the sum of annual groundwater recharge of 554.49x10^6 m^3/year comes from precipitation (552x10^6 m^3/year), water flow returning from irrigation (1.59x10^6 m^3/year) and the recharge from marble lithologies into the basin (0.90x10^6 m^3/year). The total annual groundwater discharge was calculated as 570.6 x10^6 m^3/year. Discharge components include evapotranspiration loss (474.23x10^6 m^3/year), surface runoff taken up by drainage canals (63.1x10^6 m^3/year), domestic water usage (0.73x10^6 m^3/year), irrigation water usage (13.28x10^6 m^3/year), evaporation (16.26 x10^6 m^3/year) from the swamp-wetland surface and discharge of groundwater from the marble units out of the basin (3.17 x10^6 m^3/year). According to the budget results, evaporation and human activities are effective processes in the lake basin. Furthermore, the difference between recharge and discharge quantity causes a decrease in the flow rates of the springs throughout the basin. This corresponds to a decrease in groundwater levels in the wells thus, leading to an overall decrease in the lake level throughout the entire the basin.

Keywords: Water balance, human activities, precipitation, irrigation water usage, Seyfe Lake Basin, Central Anatolia

[1] Hacettepe University, Engineering Faculty, Hydrogeological Engineering Department, Ankara, Turkey
* Corresponding author: cyurteri@hacettepe.edu.tr

Comparative Analysis of Dimension Reduction and Classification using Cardiotocography Data

Mahmut TOKMAK[1*], Ecir Uğur KÜÇÜKSİLLE[2]

Abstract: Dimension reduction is the transformation of data from a high-dimensional space to a low-dimensional space in a way that does not lose its meaning. Processing a high-dimensional data requires more processing overhead. Therefore, dimension reduction is frequently used in fields such as signal processing, speech recognition, pattern recognition and bioinformatics where a large number of observations and variables are examined. Cardiotocography (CTG) is a tool used for recording of the fetal heart rate (FHR) and uterine contractions (UC) during the intrauterine life. As a technique for diagnosing fetal well-being, CTG is often used to help obstetricians obtain detailed physiological information of the fetus and pregnant woman.

In this work three of the prominent dimensionality reduction techniques, Principal Component Analysis (PCA), Auto-Encoder (AE) and Stacked Auto-Encoder (SAE) are investigated on popular Machine Learning (ML) algorithms, Support Vector Machine (SVM), Random Forest Classifier, Naive Bayes Classifier and using publicly available Cardiotocography (CTG) dataset from University of California and Irvine Machine Learning Repository. The obtained results are presented comparatively.

Keywords: Cardiotocography, Machine Learning, Dimension Reduction, Classification

[1] Isparta University of Applied Sciences, Gelendost Vocational School, Gelendost, Isparta, Turkey
[2] Süleyman Demirel University, Engineering Faculty, Department of Computer Engineering, Isparta, Turkey
* Corresponding author: mahmuttokmak@isparta.edu.tr

Main Sources of Microplastic Pollution in Aquatic Environments

Kamila Sobkowiak[*]

Abstract: Micro plastics can be intentionally added to products (primary microplastics) or randomly formed (secondary micro plastics) - they arise as a result of the degradation of larger plastic products such as plastic bags, bottles, fishing nets or due to the mechanical wear of materials. The last aspect states nearly two-thirds (63.1%) of global microplastics emissions to the seas and oceans occuring in the wake of washing of synthetic fabrics (34.8%) or abrasion of car tires while driving (28.3%). It is suspected that microplastics accumulating in living organisms may play a large role in the development of neoplastic diseases and hormonal disorders and therefore can be toxic in the long run. Cosmetics represent only a small fraction of all sources of plastic microbeads found in the aquatic environment, however, consciously eliminating products containing these elements from our daily life might have enormous influence on both fauna and flora of aquatic environments. Accordingly, the introduction of a restriction on the use of microplastics in cosmetic products will not solve the environmental problem, on the other hand, these are pollutants added to products on purpose, so it is worth limiting their emissions, especially if the scale of these emissions is contingent on us.

Keywords: Microplastics, aquatic, environment, effects.

[1] Lodz University of Technology, Chemistry Faculty, Polymer and Dye Technology Department, Lodz, Poland
* Corresponding author: camilla.river.50@gmail.com

Product Debugging Facility Design Using Image Processing For Defense Industry Gunpowder Production

Fatih ILGIN[1]*, Mustafa İlker ERDURSUN[2]*

Abstract: Nowadays, mechatronic systems are using extensively at industry due to technological developments and Industry 4.0. Defense Industry is one of the essential area which uses different axis robotic arms. In this study, it was aimed to separate the gunpowder used in the firing of artillery shells in the defense industry with the help of robot arms using image processing techniques to extract the faulty products formed after manufacturing. The grain shapes of cannonball gunpowder are cylindrical single or multi-bore. In multi-hole gunpowder, the number of holes is usually seven. A knife that slices gunpowder can sometimes close existing holes by plastering them. It is important that the holes in the middle of the Gunpowder are open, as the closing of these holes affects the combustion surface of the gunpowder, the combustion pressure, and therefore the rate of bullet output.

Our system consists of two conveyor belts and 3-axis robot arms working in opposite direction. After manufacturing, the products coming out of the first conveyor belt are checked and packaged, and from the other conveyor belt running in the opposite direction, the faulty products go to production for re-processing. Gunpowder images coming through the moving tape were taken with the help of the existing camera, and these images were detected by applying the image processing technique with the Python program. The process of taking the faulty object over the tape and transferring it to the opposite direction tape was carried out with the help of a robot arm.

Thanks to this system, which is controlled in real time, the detection of products suitable for packaging or not has been carried out. The system created in this study is a prototype and will save time and labor if it is adapted to real systems. In addition, because the substance produced is dangerous, work accidents that may be caused by individual errors will be prevented. This system can also be used in different industrial production plants using new algorithms.

Keywords: Defense technologies, Mechatronics, İmage processing, Robotic arm, Gunpowder

[1] Machinery Chemistry Industry, Gunpowder Factory, Maintenance and Repair Directorate, Kırıkkale/ TÜRKİYE
[2] Hitit Universty, Osmancık Ömer Derindere Vocational School, Computer Programing (Lecturer)

* Corresponding author: milkererdursunhitit.edu.tr

Concentrated Kefir Production by Ultrafiltration

Firuze Ergin[1*], Gülfide Tair[1], Ezgi Tekşan, [1] Gözde Nuran Balcı[1], Ahmet Küçükçetin[1]

Abstract: Milk-based powders (skim milk powder, sodium caseinate, whey concentrate/isolate) or several filtration techniques (traditional cloth bag, centrifugation, reverse osmosis) can be used in manufacture of concentrated dairy products due to improve the texture, chemical and nutritional properties of products. Besides, membrane technology is one of the methods used to concentrate milk components. In ultrafiltration technique, a membrane with pores of certain sizes that allows the passage of water and small molecules is used. When skim milk is ultrafiltrated, concentration of casein and whey proteins that are larger than membrane pores collected in the retentate. Lactose and minerals in soluble phase of milk are removed with permeate. In previous studies, the ultrafiltration technique was used for Greek-style yoghurt, dahi and labne productions. In recent years, consumption of kefir has increased due to their nutritive value and positive health properties. Kefir is acidic, slightly alcoholic and a viscous fermented dairy beverage that has a health benefits including anti-obesity, anti-oxidative, cholesterol-lowering, anti-allergenic, anti-inflammatory, anti-tumour, and anti-microbial properties. The aim of this work was to manufacture of concentrated kefir by using ultrafiltration technique. In this study, concentrated kefir was produced with two different ultrafiltration techniques: ultrafiltration of milk prior to the fermentation process (UFM) and ultrafiltration of kefir (UFK). Kefir was filled into cloth bag to produce traditional concentrated kefir (TCK). The concentrated kefir samples were stored at 4°C for 30 days and the physicochemical, microbiological, and sensory properties of the kefir samples were determined on days 1, 15 and 30 of the storage.

Keywords: kefir, rheology, storage, ultrafiltration,

[1] Akdeniz University, Faculty of Engineering, Department of Food Engineering, Antalya, TURKEY
* Corresponding author: fergin@akdeniz.edu.tr

Behavior of sugar consumption and lifestyle in the Republic of Moldova

Aurica Chirsanova [1*], Tatiana Capcanari[2*], Rodica Sturza[3*], Olga Deseatnicova[4*]

Abstract: The population of the Republic of Moldova faces the double burden of the consequences related to nutritional behavior. On the one hand, malnutrition and nutritional deficiencies, characteristic of developing countries, on the other hand - overweight and obesity, characteristic of developed countries. 6% of children up to 5 years have growth retardation, caused by insufficient energy, and one-fifth of children suffer from anemia. About a third of women of childbearing age and more than 40% of pregnant women have anemia. Half of the adult population is overweight or obese.

The main objectives of the study were focused on the decisive aspects of food consumption behavior in relation to lifestyle trends, culture and traditions, common values and economic and social changes and the identification of knowledge about the risk of eating foods and beverages high in sugar. The data collection was carried out between January and April 2021 by applying a questionnaire structured in three types of questions: related to the socio-demographic profile; style and food preferences and consumption of high-sugar products. In the study were taken into account 1989 responses of adults. It was found that the citizens of the Republic of Moldova consume an amount of sugar four times higher than the daily limit recommended by the WHO. This leads to an increase in the number of cases of weight gain, obesity, diabetes, fatty liver disease, hypertension, etc., which, in the context of the COVID-19 pandemic, considerably increases the risk of severe complications.

It is worth mentioning that adult citizens of the Republic of Moldova consume large amounts of foods rich in sugar, but predominantly low in nutritional value, instead of a balanced diet based on fresh vegetables and fruits, meat, fish, etc. At the same time, the adult citizens in this study have an excessive consumption of table salt, refined carbohydrates, unhealthy fats and others. A close relationship has been established between the culinary traditions applied by consumers, the unfavorable economic environment and food consumption habits in the Republic of Moldova. The eating behavior research of the respondents allows us to conclude that it is in line with international trends based on fast and cheap food with a high sugar content.

Keywords: sugar consumption, questionnaire, nutritional behaviour, Republic of Moldova

[1] Technical University of Moldova, Faculty of Food Technology, Food and Nutrition Department, Chisinau, Republic of Moldova[1]
[2]Technical University of Moldova, Faculty of Food Technology, Department of Oenology and Chemistry, Chisinau, Republic of Moldova

* Corresponding author: aurica.chirsanova@toap.utm.md

A Research on Urban Furniture Design: Example of Isparta

Abdullah Beram[1*]

Abstract: Urban construction and renewing efforts become more important in last years. Most of the municipalities are aware of the importance of renovation works. This situation is included in many studies. Urban furniture is an indispensable phenomenon for municipalities to satisfy the public. Local administrators aim to provide urban functions in common areas and to give the city a contemporary and aesthetic look.

The furniture in use in the city center of Isparta was evaluated. A face-to-face interview was conducted with 128 people from different age groups. Questions were asked about the function, aesthetics, form, material, color, texture and ergonomics of Isparta urban furniture. As a result, the original and creative designs of urban furniture satisfy the 16-25 and 26-35 age groups. It has been revealed that the group between the ages of 46-55 cares about materials and ergonomics. Design, color and aesthetic importance are more prominent in young and middle age groups.

Keywords: Urban furniture, design, local, ergonomic, satisfy.

[1] Isparta University of Applied Sciences, Faculty of Forestry, Isparta, Turkey
* Corresponding author: beramabdullah@gmail.com

Impact of Pandemic (Covid 19) on air quality in Prishtina

Besa Veseli[1*], Shkumbin Shala [2*], Vehebi Sofiu[3*]

Abstract: Kosovo is a small country with an area of about 10.887 km², pollution at country level is very big, but the main pollution problems are in urban areas which are highly polluted as the main cause of this pollution are: industries, power plants KEK, Road Transport, District Heating Companies (in Prishtina, Gjakova and Mitrovica), Urban and Industrial Waste Disposal (with different local impact), Wood and lignite for home heating. (World, 2011). Regarding the regions Prishtina region is the area with the highest air quality pollution caused by KEK power plants located nearby, other smaller industries, transport, heating, and other individual heating facilities. (Botrore, 2011). Since air pollutants know no bounds, Of greater concern are; volatile organic compounds (VOC), CO_2, NO_x, CO, sulfur compounds SO_2, PM10, PM2,5 etc. (MESP, 2015). During this paper we will present air quality in the Prishtina region, where air quality analyzes were obtained from KHMI for the Pandemic Period (COVID-19) by measuring these parameters, SO_2, CO, NO_2, O_3, PM 10 and PM 2.5 all of these measuring (µg / m3), and always referring to the Directive (2008/50 / EC) and the Law on Air Protection from Pollution (No. 03 / L-160).

Keywords: Air, Pollution, CO, NOX, SO2, O3, PM10, PM2.5, MESP, IHMK, WHO.

[1] Institution of Higher Education, UBT-College, Energy Efficiency Engineering
* Corresponding author: besa.veseli@ubt-uni.net

The light metals minerals of Montenegro

Biljana Zlaticanin[1*], Sandra Kovacevic[2*]

Abstract: In the area of Montenegro, which belongs to the southeastern Dinarides, there are red karst bauxites and white karst bauxites. According to conditions and way of origin, bauxite deposits are divided into three genetic groups: weathering deposits, sedimentary deposits and metamorphosed deposits. Significant results were achieved regarding knowledge on characteristics of the bauxite formations. Their economic significance was successfully defined long time ago. This study based on the up-to-date technical achievements which undertaken for the processing of bauxites.

Keywords: red karst bauxites, white bauxites

[1] University of Montenegro, Faculty of Metallurgy and Technology, Cetinjski put bb, 81000 Podgorica, Montenegro
[2] Central School of Chemical Technology Spasoje Raspopović, 81000 Podgorica, Montenegro
* Corresponding author: biljana@ucg.ac.me

The influence of the process parameters on the microstructure of Al-Cu-Mg-Ti alloys

Biljana Zlaticanin[1*], Sandra Kovacevic[2]

Abstract: Results presented in this paper contribute to investigation of the influence of process parameters on the microstructure of samples during solidification of Al-Cu-Mg-Ti alloys. In this aim the 30 samples was solidified by different growth rate. The growth rate has been very important factor in the crystallization process. Obtained results give us possibility to create the desired microstructure by growth parameters. The similar microstructure was observed for the very close values of growth rate.

Keywords: Al-Cu-Mg-Ti alloys, growth rate

[1] University of Montenegro, Faculty of Metallurgy and Technology, Cetinjski put bb, 81000 Podgorica, Montenegro
[2] Central School of Chemical Technology Spasoje Raspopović, 81000 Podgorica, Montenegro
* Corresponding author: biljana@ucg.ac.me

Multivariate methods for seasonal characterization of air pollution

Virgjina Lipoveci[1], Mirjana Čurlin[2*]

Abstract: A multivariate analysis of air quality monitoring data in the Kosovo region was performed. The aim of this work is seasonal classification based on air quality monitoring datasets in 2017. Different chemometric methods were used to process the dataset, such as basic statistical methods, Pearson correlation coefficients, principal component analysis (PCA) and cluster analysis (CA). The results obtained show and explain the seasonal distribution of SO_2 and NO_2 as air quality indicators. This study makes it possible to obtain new information from the monitoring datasets, which is necessary for the establishment of guidelines in the framework of the health protection of the population in this region.

Keywords: multivariate analysis, correlation, air pollution, quality indicators

[1]National Centre of Labour Medicine in Gjakova, Kosovo
[2*]University of Zagreb, Faculty of Food Technology and Biotechnology, Department of Process Engineering, Section for Fundamental of Engineering Pierottijeva 6, 10000 Zagreb
*Corresponding author: mcurlin@pbf.hr

The Assessment of Trihalomethanes (THMs) Concentrations in Drinking Water from Selected Distribution Systems in Opole Province

Iwona Klosok-Bazan[1*], Joanna Boguniewicz[2*], Agnieszka Drozdek[3*]

Abstract: Decreasing water abstraction, low flow velocities and variable water transport directions have become the cause of mineral and organic sediment deposition in water supply networks. This element in the presence of chlorine increases the likelihood of THMs formation, the main representative of which is chloroform. These compounds have carcinogenic and mutagenic effects on humans and animals, so their presence in water should be strictly controlled. Biofilm development contributes to an increase in color intensity, turbidity and organic matter content in tap water. The result is a significant increase in the risk of microorganisms and coliforms in the water. It is therefore necessary to maintain an adequate amount of disinfectant in the water, such as chlorine, which at a rate as low as 0.2g Cl_2/m^3 ensures that the microbiological risk of the water is reduced. Using high doses of Cl_2 for water treatment increases the risk of trihalomethanes in the water. The selection of an appropriate water disinfection method is important in this case.

Analyses of THMs levels in water from the water supply network in selected distribution systems in Brzeg, Glubczyce, Opole, Nysa and Krapkowice were performed. None of the five selected distribution systems exceeded the total THMs concentration in the analyzed period, however, it can be noticed that in a few measurement points the concentration of this compound reaches 19 μg/l, while in the remaining measurement points it does not exceed 8 μg/l. This may indicate good technical conditions of water supply networks as well as efficient operation of disinfection methods.

Additionally, the analysis of the data obtained from these five distribution systems, show that 67% of them have a slight excess of chloroform concentration, while in 7% of cases the excess is almost three times higher than the recommendations. The reasons for this may be sought in the quality of the intake water at the given measurement points for which the exceedance occurred. The temperature of the water was considerably elevated due to the time of the year, pH within 7 and the content of total organic carbon could have led to such effects. In order to maintain the sanitary safety of the drinking water, it is therefore necessary to control not only microbiological contamination but also the results of disinfection i.e. disinfection by-products.

Keywords: drinking water, disinfection by-products, trihalomethanes, distribution system,

[1] Opole University of Technology, Faculty of Mechanical Engineering, Department of Thermal Engineering and Industrial Facilities, Mikolajczyka 5, Opole 45-271, Poland
* Corresponding author: i.klosok-bazan@po.edu.pl

Application of the Rutherford Backscattering Method in powder nanotechnology

A.A. Tatarinova[1] [*], A.S. Doroshkevich, M. Kulik,
M.A. Balasoiu, V. Almasan, D. Lazar

Abstract: Rutherford Backscattering Spectrometry (RBS) is an ion scattering technique used for compositional thin film that are less than 1μm thick analysis. During an RBS analysis, high-energy He^{2+} ions with energies in the region from several hundred kiloelectron-volts to 2 - 3 MeV are directed onto the sample and the energy distribution and yield of the backscattered He^{2+} ions at a given angle is measured. Since the backscattering cross section for each element is known it is possible to obtain a quantitative compositional depth profile from the RBS spectrum obtained. The capabilities of this method can be significantly expanded. In particular, the method can be used in powder nanotechnology to study elemental composition in microscopically small objects. The application of methods based on Rutherford Backscattering Spectrometry is extremely interesting for adsorption energy devices, in particular, these methods can be used with maximum efficiency for various chemoelectronic converters. A unique opportunity is to study the elemental surface of adsorbates on the surface phase separation in functional nanostructured layers. For this reason, the preparation of planar-distributed chemoelectronic converters and the study of the elemental composition of adsorbates using the Rutherford Backscattering Spectrometry technique was the purpose for the investigation. The tasks of this study included: development and optimization of the technology for producing planar chemoelectronic converters a functional layer in the form of rounded drops containing monodisperse nanosized (7.5 μm) particles of a solid solution of the ZrO_2 system - 3 mol% Y_2O_3 (YSZ) in the PVA polymer matrix, study of the theoretical characteristics of the obtained chemoelectronic converters [1], study of the elemental composition of the obtained chemoelectronic converters using Rutherford Backscattering Spectrometry. The atomic and chemical composition of these layers has been studied using nuclear and atomic methods. The thickness of the oxide layers was found to be approximately the same for all implanted samples. These values were determined on the basis of Rutherford Backscattering Spectrometry and nuclear reactions (RBS/NR).

Keywords: RBS, Powder Nanotechnology, chemoelectronic converters.

[1] Joint Institute for Nuclear Research, Dubna, Russia
[2] University, Faculty, Department, City, Country
[*] Corresponding author: w99_9@yahoo.com

Process of Drying Peaches by Forced Convection

Natalia Tislinscaia[1]*, Vitali Visanu, Mihail Balan, Mihail Melenciuc

Abstract: For the Republic of Moldova peaches represent a strategic economic product, especially on the fresh fruit market, but due to the fact that peaches are perishable product huge quantities remain unused. The solution would be dehydration, which involves both economic and health benefits. As raw material or dry on average peaches with firmness 1.05 kgf/cm2, dry matter 11.5%, humidity 88.5%); by forced convection at temperatures 50-90°C; with different speeds of the working agent: 0.5-2.5 m/s, and at different thicknesses of the product layer: 2-10mm.

The study of peaches convective drying kinetics revealed that the increase both thermal agent temperature, speed and decreasing the thickness of the rolls, leads to an intensification of the process. Therefore, for the convective drying of peaches, the temperature of 60°C with the speed of the heating agent 2.0 m$\cdot$s^{-1} and the thickness of the rolls ± 3 10^{-3}m are recommended for getting an optimal drying process.

Keywords: Moldova, material, health.

[1] Technical University of Moldova, Moldova
* Corresponding author: vitali.visanu@pmai.utm.md

Innovation strategies of functional plant yogurt production for personalized nutrition

Tatiana Capcanari[1*], Aurica Chirsanova[1], Rodica Siminiuc[1]

Abstract: Speaking of personalized nutrition, we are talking about the exclusion of specific foods or chemical elements from the diet of a certain person for various reasons. It can be both a state of health and personal taste preferences, principles of life. For a long time, the issues of the individuality of our organisms from the point of view of biochemical functioning worried people. The reaction of different people to the same ingredient can be completely opposite. A person's energy, health and resilience largely depends on his nutrition. With prolonged malnutrition, this quickly leads to cardinal health problems.

The frequency of iron deficiency anemia in the Republic of Moldova is high, being detected in certain population groups, such as women of childbearing age (especially pregnant women), young children and adolescents. The risk groups also include the elderly, vegetarians, people with a poor socio-economic level, as well as people suffering from certain chronic conditions. Hypocalcemia is a decrease in the level of calcium in the blood, which can be caused by a problem with the parathyroid glands, as well as by bad nutrition. As hypocalcemia progresses, muscle cramps are common, as well as confusion, depression, memory problems, tingling in the lips, fingers and toes, but also tension and muscle pain. So that the elaboration of the assortment of functional fermented products for the Republic of Moldova is extremely relevant.

A technology for plant yogurt producing was developed using fermentation technology. The range of natural, fortified and enriched yoghurts were developed. Rice, oat and coconut milk was used as the main raw material. Flax, sesame and chia seeds, which are rich in vitamins, minerals, dietary fibers were used to produce a range of enriched yoghurts. To obtain fortified yoghurts, the minerals as iron and calcium were used, which prevent the development of anemia and hypocalcemia. The problem solved by the invention consists in expanding the base of fermented vegetarian products for personalized nutrition for people with anemia, hypocalcemia, lactose intolerant people, people with avitaminosis, gastrointestinal disorders by improving the chemical composition and increasing the biological value of yogurts by fortifying with vitamins, minerals, dietary fiber, natural antioxidants with a high activity, by reducing the amount of stabilizer and the duration of fermentation.

Experimental assortment of plant yoghurts was assessed by physicochemical and organoleptic methods. All developed samples meet the standards of technical documentation for this type of food product. The organoleptic characteristics were highly appreciated. Developed products are an opportunity for many people to return to a normal healthy diet.

Keywords: personalized nutrition, functional food products, hypocalcemia, iron deficiency anemia, natural antioxidants, dietary fiber, yogurt production.

[1] Technical University of Moldova, Faculty of Food Technology, Food and Nutrition Department, Chisinau, Republic of Moldova
* Corresponding author: tatiana.capcanari@toap.utm.md

Evaluatıon Des Bıomaterıaux A Base Des Resıdus Agrıcoles [Coques De Noıx] Actıvee Par L'acıde De Cıtron, Naoh Et H₃po₄. Applıcatıon Au Traıtement Des Eaux

Amel Aidi [1*], Assia Slimani[2*],Ammar Fadel[3*]

Abstract: Les eaux de surface contiennent des matières organiques(substances humiques). Elles sont responsables de la coloration de l'eau, possèdent des propriétés d'échangeurs d'ions et des propriétés de complexassions. Elles peuvent être un véhicule pour la plupart des substances toxiques (métaux lourds…), participent également à la corrosion du système de distribution et au colmatage des résines et des membranes. Pour cela l'adsorption est l'une des techniques les plus adoptées pour cette élimination de polluants, à cause de sa grande capacité d'épurer les eaux contaminées. Dans ce contexte l'objectif principal de ce travail est de préparer trois biomatériaux avec une fortes capacités d'adsorption de la matière organique SH: il s'agit des matériaux à base d'un résidu de l'agricole il subit un traitement thermique jusqu'a 600°C, puis une activation chimique par trois activant (hydroxyde de sodium NaOH, l'acide phosphorique H_3PO_4et l' acide de citron) . La caractérisation des matériaux a été déterminée par la technique de spectroscopie infrarouge IR-TF ainsi que par diffraction des rayons X (DRX).Par la suit mettre en évidence leurs capacités dans les procédés d'adsorption pour l'élimination des substances organiques (SH) dans les traitements des eaux. Les valeurs optimales pour les paramètres réactionnelles ont été déterminé pour chaque activant notamment, la température, la vitesse d'agitation, le temps de contact, et la masse du matériau et la comparaison entre eux par la suite. L'étude de l'isotherme montre que les modelés de Langmuir et Freundlich décrit bien le processus d'adsorption de la substance humique avec des coefficients de corrélation linéaires arrive à 97%. Le modèle de pseudo-second-ordre est le modèle établi dans ces études. On peut conclure aussi que les coques de noix forment un résidu naturel non coûteux représentant un avantage majeur pour le traitement les eaux de surfaces.

Keywords: H_3PO, substances humiques, NaOH

[1] Département de Chimie Industrielle / Université Mohamed Khider, Biskra, Algérie
* Corresponding author: a.aidi@univ-biskra.dz

Physico-chemical properties of rapeseed honey from the Republic of Moldova

Chirsanova Aurica[1*], Tatiana Capcanari[2*], Alina Boistean[3*]

Abstract: Bee honey is an empirical and image product of the Republic of Moldova. At the same time, rapeseed honey is becoming more and more appreciated and sought after by local consumers. In the last 5 years, the surface of agricultural lands sown with rapeseed is constantly growing (from 36 thousand hectares in 2019 to 45 thousand hectares in 2021), which also ensured the increase of the volume of rapeseed honey proposed for consumption. In the context of a major focus on the authenticity of bee honey worldwide, this study is relevant.

Melisopalinological analysis of rapeseed honey samples showed that the dominant pollen is Brassica spp. in proportion of 57.4% -68.3%. Therefore, the presence of over 45% of the pollen grains of Brassica spp allows us to say that the honey samples are part of the monofloral category. The moisture content ranged from 17.02% to 18.6%, and the pH from 4.19 to 4.28. Free acidity analysis is useful for assessing the freshness of honey. With the alteration of honey, the value of free acidity increases as a result of the fermentation of sugars into organic acids. A low acidity of 16.02-16.9 milliequivalents acid / kg was recorded in the analyzed samples. Another physico-chemical parameter that indicates the degree of freshness of honey is the content of hydroxymethylfurfural (HMF) which varied in the range from 11.21 mg / kg to 38.12 mg / kg which is below the maximum limit of 40 mg / kg allowed by European standards. The electrical conductivity gives us information about the botanical origin of honey. The analysis of this parameter is very often used, being considered a good criterion to be able to identify the botanical origin and implicitly the purity of honey. Thus, in the rapeseed honey samples, the electrical conductivity was in the range of 160.1 µS / cm to 182.9 µS / cm, which denotes a low electrical conductivity. The functional properties of honey are related to the amount of natural antioxidants in bee pollen and floral nectar. The antioxidant effects of bee honey are attributed to polyphenols, flavonoids and others. Thus in the analyzed samples the total content of polyphenols was between 23.71 mg GAE / 100 g and 25.09 mg GAE / 100 g and flavonoids of 19.05 mg QE / 100 g and 21.15 mg QE / 100 g honey . The DPPH method was used as a means to determine the antioxidant activity of honey samples. DPPH radical inhibition activity in rapeseed honey ranged from 53.12% to 56.78%. Thus, the researches showed that rapeseed honey from the Republic of Moldova meets the requirements of the admissible norms and is recommended for consumption.

Keywords: rapeseed honey, physical and chemical indicators, HMF, polyphenols, flavonoids

---

[1] Technical University of Moldova, Faculty of Food Technology, Food and Nutrition Department, Chisinau, Republic of Moldova
* Corresponding author: aurica.chirsanova@toap.utm.md

Study Of The Ohrid Traditional Ottoman Houses Local Architecture In Sustainability Context

Levent Menga[1*]

Abstract: Ohrid is the most important city in North Macedonia in terms of tourism. One of the most important reasons why it is the most important city in terms of tourism is Ohrid lake, from which the town takes its name. Ohrid lake is the largest of the three natural lakes in North Macedonia. Within the scope of this study, we examine the historical settlement area around the Ohrid castle. This area, one of the first residential areas in the region, has historical buildings and monasteries built with stone streets around the castle. In this paper, we show a residential area as an example of a sustainable local settlement and analyze the sustainability of the local architecture. The analysis we do is about the socio-economic, socio-cultural, and environmental analysis criteria. In analyzing the socio-economic context, supporting autonomy, promoting local events, optimizing construction work, extending the building life, and protecting resources are examined. In the environmental context, respect for nature, suitable location selection, reducing pollution and waste material, contributing to health quality, and reducing natural hazards items are analyzed. Cultural protection, transferring building cultures, developing creativity, recognizing moral values, and promoting social cohesion are considered in the socio-cultural context. As a result of these examinations, we have rated each criterion as "good," "bad," "average," and "ineffective, we converted the results in the table, and we have got conclusions for the sustainability of this area.

Keywords: Sustainability, local architecture, environment, old town and cultural protection.

[1] International Vision University, Faculty of Engineering and Architecture, Department of Computer Science, Gostivar, North Macedonia
* Corresponding author: levent.menga@vizyon.edu.mk

Cluster Analysis of Mobile Devices

Samedin Krrabaj[1]*

Abstract: Today, with the rapid development of technology, mobile devices have become one of the most important elements of our lives. With the hardware and software developments, mobile devices have become more than just a means of communication and have become used in many parts of our daily lives with software applications developed in many areas such as health, finance, social, photography, games, education and business life. Technology companies make various strategic plans in the production and marketing of mobile devices that have become a part of daily life. Mobile device manufacturers aim to produce mobile devices that will appeal to every budget by making various pricing according to various hardware features. Thus, they provide targeted mobile device sales in the market share and increase their profit share. In this study, 8 attributes were determined by using hardware (processor speed, battery, ram, storage space, camera, weight, NFC, fingerprint) data of mobile devices. Together with the attributes obtained, the price information of 163 mobile devices was discussed in four categories as 0-249 €, 250-499 €, 500-749 €, 750-1000 €. Cluster analysis was performed according to attribute and price categories. In the study, Expectation Maximization, one of the clustering analysis algorithms, was used and a success rate of 88 percent was achieved.

Keywords: Artificial Intelligence, Data Mining, Clustering.

[1] University of Prizren, Faculty of Computer Science, Prizren, Kosovo.
* Corresponding author: samedinkrrabaj@gmail.com

Proposal and Analysis of the Geothermal Energy Based Plant; Thermodynamic Assessment

Oğuzhan AKBAY[1*], Fatih YILMAZ[2*]

Abstract: Due to global warming and environmental problems, the importance of renewable energy sources continues to increase day by day, so it can be specified that research on renewable energy power generation plants has increased in recent years. In this proposed study, thermodynamic investigation of the geothermal energy supported plant is conducted according to the n-butane fluid. In this regard, the energy and exergy efficiency of the flash-binary geothermal power plant is examined, and also, the impacts of some limitations such as geothermal fluid temperature, geothermal outlet pressure, and environmental temperature on system performance are examined. According to the thermodynamic results, the energy and exergy efficiency of the proposed total plant is found to be 15.97% and 44.63%, respectively.

Keywords: Energy, exergy, geothermal, sustainability, renewable energy

1. Introduction

By rising the population and industrial development lead to rising in the need for energy and the use of fossil fuels has increased in parallel. The consumed fossil fuels have caused global warming problems due to the effect of various greenhouse gases (Ratlamwala et al., 2012). It is known that renewable energy sources are more preferable than fossil fuels because they are clean, environmentally friendly, reliable and sustainable (Takan and Kandemir, 2020). There is increasing interest in geothermal energy source derived from hot liquid or hot dry rock systems produced by the Earth's core (Altun and Kilic, 2020).

Geothermal fluid is used in low and medium temperature ranges in organic Rankine cycles (ORC). ORC systems are capable of generating electricity at sources of 150 °C and lower temperatures (Yilmaz, 2018). In power generation cycles with a low temperature source, organic fluid is preferred, which has a high saturation pressure at atmospheric pressure at condensation temperature and is in the state of hot steam at the turbine output. There are several studies in the literature on the performance analysis of power plants driven by geothermal.

Erdemir, (2020) has developed an underground pumped hydro-energy storage system (UPHES) with geothermal sources integrated with ORC and regional heating. As a result of thermodynamic analysis, 60 MWh of electricity was stored by UPHES. The heating needs of 100 homes of 2.8 MW were met and 1.7 MW of energy was produced by the orc system. Siddiqui et al., (2019) developed a new renewable energy source model. The system comprised

[1] Isparta University of Applied Science, Graduate Education Institute, Isparta, Turkey
[2] Isparta University of Applied Science, Faculty of Technology, Mechatronics Engineering, Isparta, Turkey
* Corresponding author: fatiyilmaz7@gmail.com

of a flash steam plant and Cu-Cl process. As a result of the study, the energetic and exergetic performance of the trigeneration model were computed as 19.6% and 19.1% respectively. Yilmaz and Koyuncu, (2020) modeled and optimized the dual geothermal power plant in Afyon province using artificial neural network-based genetic algorithm method. After that, they found the repayment period of the electricity produced at the plant to be 2.87 years and the exergy cost to be 0.0176 $/kWh. Yuksel and Ozturk, (2020) performed a thermodynamic evaluation of a multigeneration system with geothermal resources. As a result of their studies, they concluded that multi-generation plants are more efficient than single and co-generation systems because. Gnaifaid and Ozcan, (2020) studied the thermodynamic and economic analysis of power plant for the generation of natural freshwater, power, cooling and heating using geothermal energy. Furthermore, they calculated that the total energy and exergy efficiency of the plant could be as high as 61% and 37.8%, respectively, and the cost of the plant ranged from $160-330/hour.

In the above studies, it is seen that different geothermal power plants in our country are examined, thermodynamic performance analyzes are made and cycle proposals with different refrigerants are presented. The thermodynamic performance examination of the geothermal energy supported power generation plant is made according to the n-butane fluid. According to the n-butane refrigerant of the flash-binary power generation model, the energetic and exergetic effectiveness are investigated and compared with different refrigerants. In addition, in this study, the influence of some limitations such as geothermal fluid temperature, geothermal outlet pressure and ambient temperature on the plant performance is examined.

2. Modeled plant description

This suggested model contains of a flash unit, a direct steam turbine and an ORC system. The geothermal water pass in the plant at 200 °C temperature and 1600 kPa pressure and it is assumed that it emerges from the geothermal well as a liquid vapor mixture. The flow chart of the system is given in Figure 1.
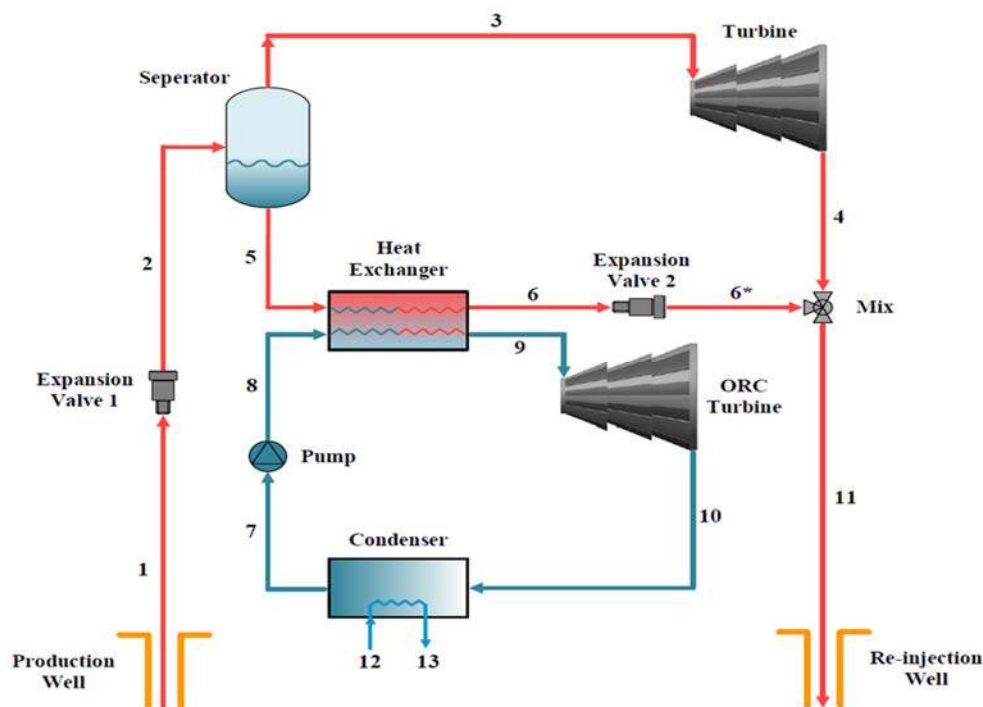
Figure 1. The layout of the working point of modeled plant

Briefly, the geothermal fluid entering the separator at state 2, goes to the steam turbine as saturated steam at point 3. Afterward, the geothermal fluid in the saturated liquid phase at state 5 transfers its heat to the subsystem ORC system in the heat exchanger (HEX) and the thermal energy required for the ORC is provided. Finally, at state 11, it returns back to the re-injection well.

2.1. Thermodynamic analysis

In this proposed study, thermodynamic performance analysis was examined parametrically with respect to the n-butane fluid. Thermodynamic analyses are performed in this studied system according to four basic balance equations (Cengel and Boles, 2015; Dincer and Rosen, 2013). In Table 1, general thermodynamic balance equations are mentioned. According to thermodynamic laws, balance equations for the proposed model are presented in Table 1.

Table 1. Thermodynamic balance equations

	Balance equations
Mass	$\sum \dot{m}_i = \sum \dot{m}_{out}$
Energy	$\dot{Q} - \dot{W} = \sum \dot{H}_{out} - \sum \dot{H}_{in}$
Entropy	$\sum \dot{m}_{in} S_{in} + \sum \left(\dfrac{\dot{Q}}{T}\right)_{in} + \dot{S}_{gen} = \sum \dot{m}_{out} S_{out} + \sum \left(\dfrac{\dot{Q}}{T}\right)_{out}$
Exergy	$\sum \dot{m}_{in} ex_{in} + \sum Ex_{in}^{W} + \sum Ex_{in}^{\dot{Q}} = \sum \dot{m}_{out} ex_{out} + \sum Ex_{out}^{\dot{W}} + \sum Ex_{out}^{\dot{Q}} + \sum \dot{Ex}_{dest}$

In addition, the four equilibrium equations of the whole system, namely mass, energy, entropy and exergy, are presented in Table 2.

Table 2. General thermodynamic analysis of system subcomponents

System subcomponents	Balance equations			
	Mass	**Energy**	**Entropy**	**Exergy**
Seperator	$\dot{m}_2 = \dot{m}_3 = \dot{m}_5$	$\dot{m}_2 h_2 = \dot{m}_3 h_3 + \dot{m}_5 h_5$	$\dot{m}_2 s_2 + \dot{S}_{gen,Sep} = \dot{m}_3 s_3 + \dot{m}_5 s_5$	$\dot{m}_2 ex_2 = \dot{m}_3 ex_3 + \dot{m}_5 ex_5 + \dot{Ex}_{dest,Sep}$
Turbine	$\dot{m}_3 = \dot{m}_4$	$\dot{m}_3 h_3 = \dot{m}_4 h_4 + \dot{W}_T$	$\dot{m}_3 s_3 + \dot{S}_{gen,T} = \dot{m}_4 s_4$	$\dot{m}_3 ex_3 = \dot{m}_4 ex_4 + \dot{W}_T + \dot{Ex}_{dest,T}$
ORC turbine	$\dot{m}_9 = \dot{m}_{10}$	$\dot{m}_9 h_9 = \dot{m}_{10} h_{10} + \dot{W}_{ORC\_T}$	$\dot{m}_9 s_9 + \dot{S}_{gen,ORC\_T} = \dot{m}_{10} s_{10}$	$\dot{m}_9 ex_9 = \dot{m}_{10} ex_{10} + \dot{W}_{ORC\_T} + \dot{Ex}_{dest,ORC\_T}$
Condenser	$\dot{m}_{10} = \dot{m}_7$; $\dot{m}_{12} = \dot{m}_{13}$	$\dot{m}_{10} h_{10} + \dot{m}_{12} h_{12} = \dot{m}_7 h_7 + \dot{m}_{13} h_{13}$	$\dot{m}_{10} s_{10} + \dot{m}_{12} s_{12} + \dot{S}_{gen,Con} = \dot{m}_7 s_7 + \dot{m}_{13} s_{13}$	$\dot{m}_8 ex_8 + \dot{m}_{11} ex_{11} = \dot{m}_9 ex_9 + \dot{m}_{12} ex_{12} + \dot{Ex}_{dest,Con}$
Pump	$\dot{m}_7 = \dot{m}_8$	$\dot{m}_7 h_7 + \dot{W}_P = \dot{m}_8 h_8$	$\dot{m}_7 s_7 + \dot{S}_{gen,P} = \dot{m}_8 s_8$	$\dot{m}_7 ex_7 + \dot{W}_P = \dot{m}_8 ex_8 \dot{Ex}_{dest,P}$
Heat exchanger	$\dot{m}_5 = \dot{m}_6$; $\dot{m}_8 = \dot{m}_9$	$\dot{m}_5 h_5 + \dot{m}_8 h_8 = \dot{m}_6 h_6 + \dot{m}_9 h_9$	$\dot{m}_5 s_5 + \dot{m}_8 s_8 + \dot{S}_{gen,Hex} = \dot{m}_6 s_6 + \dot{m}_9 s_9$	$\dot{m}_5 ex_5 + \dot{m}_8 ex_8 = \dot{m}_6 ex_6 + \dot{m}_9 ex_9 + \dot{Ex}_{dest,Hex}$

Taking into account the balance equations in Tables 1 and 2, the overall energy and exergy efficiency of the entire system was found using the following equations.

$$\eta_{overall} = \frac{\dot{W}_{net,overall}}{\dot{Q}_{in}} = \frac{\dot{W}_{overall}}{\dot{m}_1 h_1 - \dot{m}_{11} h_{11}} \qquad (2.1)$$

$$\psi_{overall} = \frac{\dot{W}_{net,overall}}{\dot{m}_1 ex_1 - \dot{m}_{11} ex_{11}}$$

<div align="right">(2.2)</div>

3. Results and Discussion

In this suggested work, power generation from the flash-binary power plant supported by geothermal energy was examined from a thermodynamic point of view. In the ORC subsystem, n-butane fluid was used as the working fluid and thermodynamic examination was also performed. In the study, all calculations were modeled using the EES package program. The results obtained are tabulated in Table 3.

Table 3. Analysis results of the proposed plant and the ORC system

	ORC	Overall system
Energy efficiency	10.24	15.97
Exergy efficiency	42.09	44.63
Net power generation	565.4	3038
Total exergy destruction rate	-	3663

A net power of 3038 kW is produced from the cycle with a reservoir temperature of 70 °C. The energetic and exergetic performance of the planned model are computed as 15.97% and 44.63%, respectively. After that, the influence of the flash pressure change on the performance of the ORC is observed and specified in Figure 2. As a result of increasing the flash pressure from 300 kPa to 800 kPa, the energy and exergy performance of the ORC decrease by 0.15% and 0.95%, respectively.
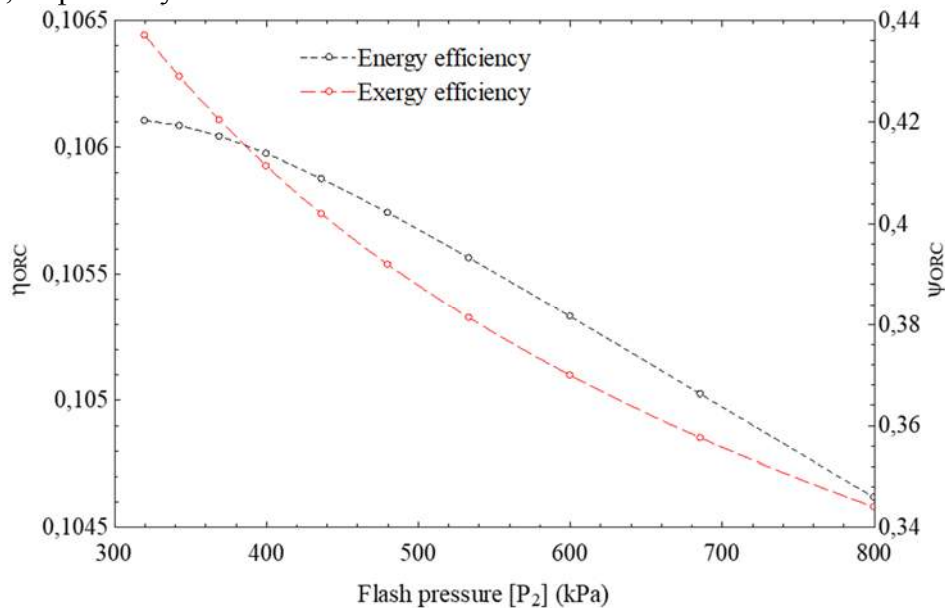
Figure 2. Impact of flash pressure change on the performance of the ORC

In Figure 3, the influence of flash pressure change on the performance of the whole model was examined and as a result of increasing the flash pressure from 300 kPa to 800 kPa, the energy efficiency of the whole plant increased from 0.15% to 0.21%, and the exergy efficiency from 0.4% to 0.59%. The reason for this increase is that with the increase of flash pressure, the fluid going to the steam turbine goes at higher pressure and temperature, so the performance of the proposed plant also increases.
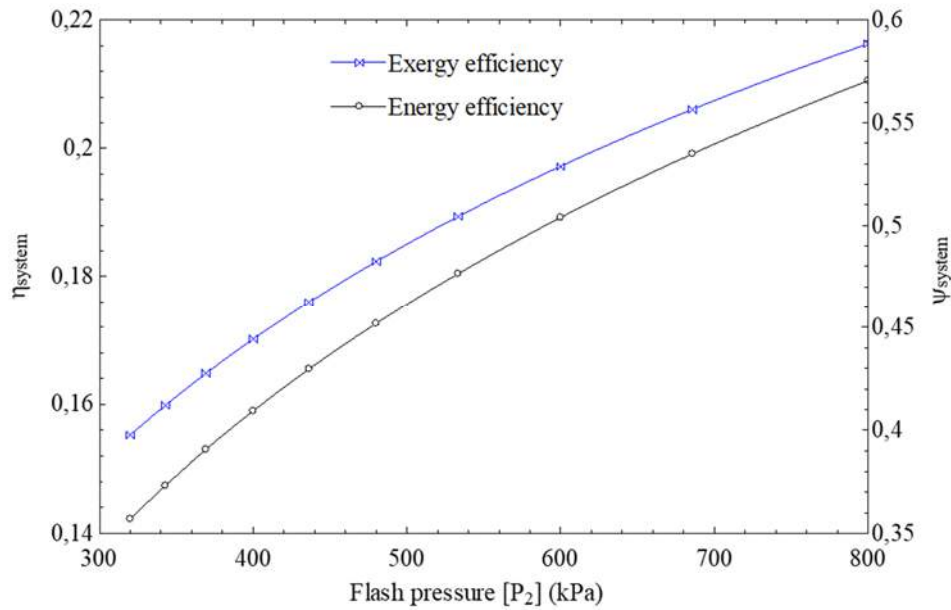
Figure 3. Effect of flash pressure variation on the performance of the entire plant

The effect of flash pressure change on turbine inlet temperature and net power production of the whole plant has been investigated and given in Figure 4. When the flash pressure increases from 300 kPa to 800 kPa, the produced power rate increases and the turbine inlet temperature also increases by about 33 °C. The cause for this rise can be expressed as the higher temperature and enthalpy of the fluid going to the steam turbine at high flash pressures. In Figure 5, the influence of turbine isentropic efficiency change on the net power generation of the suggested plant is examined and given in Figure 5. As a result of increasing the turbine isentropic efficiency by 20%, the turbine and ORC system power generation rate also increments.
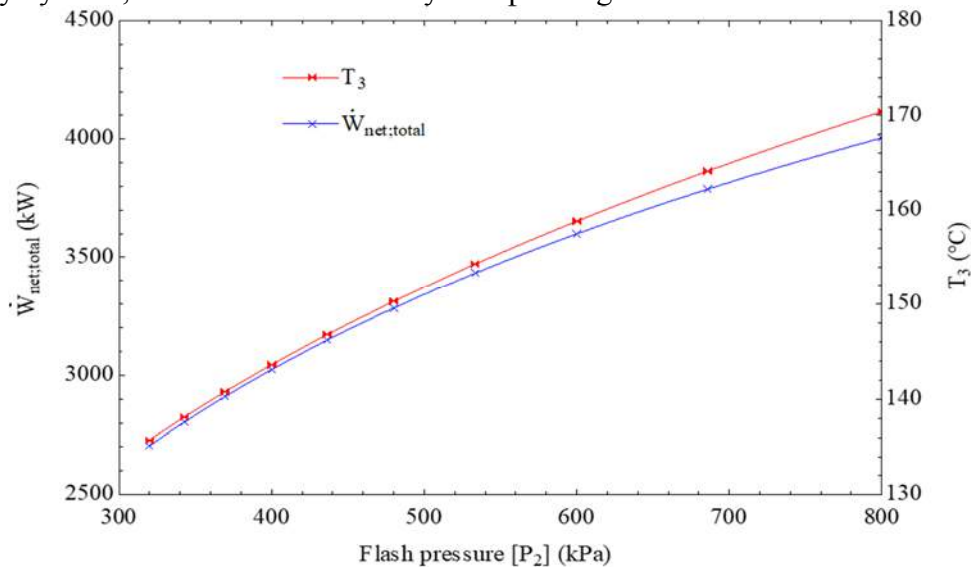
Figure 4. Effect of flash pressure change on turbine inlet temperature and power generation
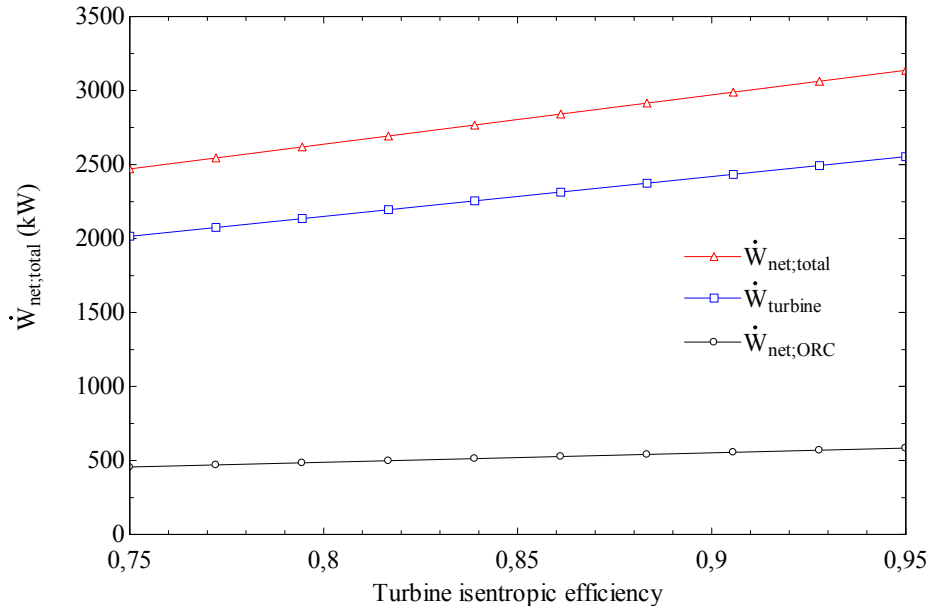
Figure 5. Net power generation according to turbine isentropic efficiency change

Changes in the performance of the modeled plant and ORC versus various turbine isentropic efficiency are presented in Figure 6. As a result of 20% rise in turbine isentropic efficiency, the energy efficiency of the suggested plant increases from approximately 12.8% to 15.97%, and the exergy efficiency increases from 37.2% to 44.63%. Under the same situations, the energetic efficiency of the ORC increased from about 8% to 10.24%, and the exergy performance increased from 34% to 42.09%.
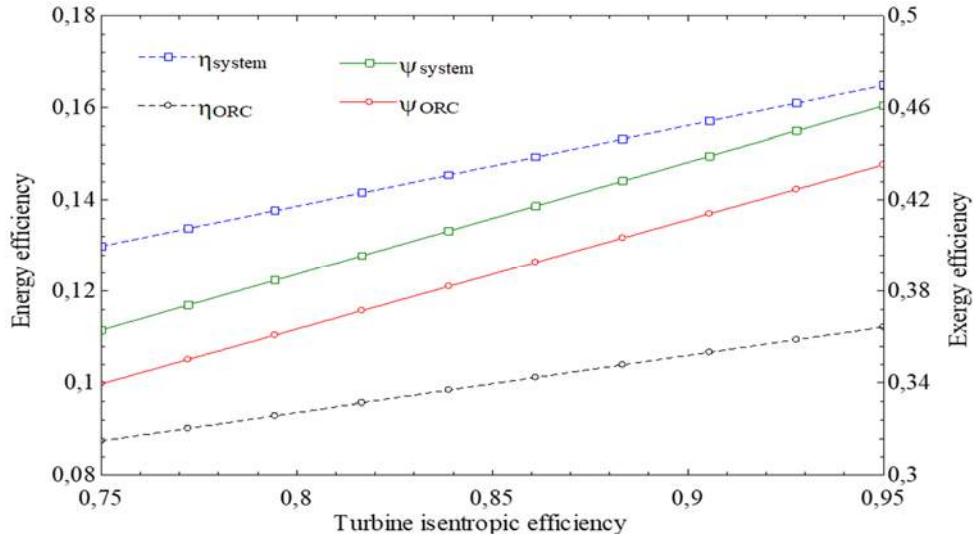
Figure 6. ORC and overall system performance change according to turbine isentropic efficiency change

In Figure 7, the change in net power generation according to the ORC turbine input pressure is examined. Once the ORC turbine input pressure is increased from 1500 kPa to 2500 kPa, it is realized that the power generation rate obtained from both ORC and the overall system tends to increase. The cause for this tendency is that with the rise of turbine input pressure, the fluid entering the turbine reaches higher enthalpy values.
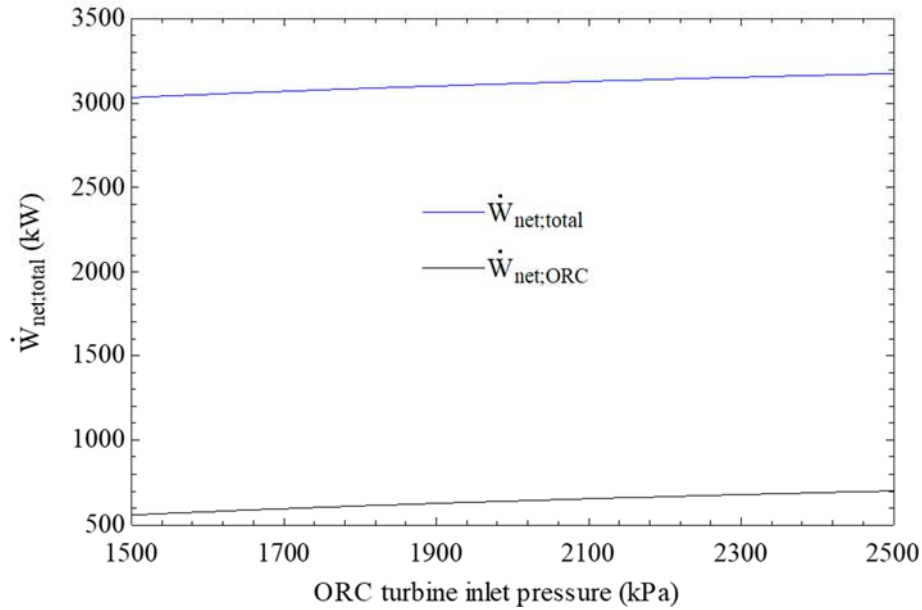
Figure 7. Power generation rate with various ORC turbine inlet pressure

The influence of ORC turbine input pressure on the ORC and whole system performances was investigated and given in Figure 8. By increasing the ORC turbine pressure by 1000 kPa, the energetic and exergetic performances of the ORC enhance by approximately 2.75% and 10%, respectively.
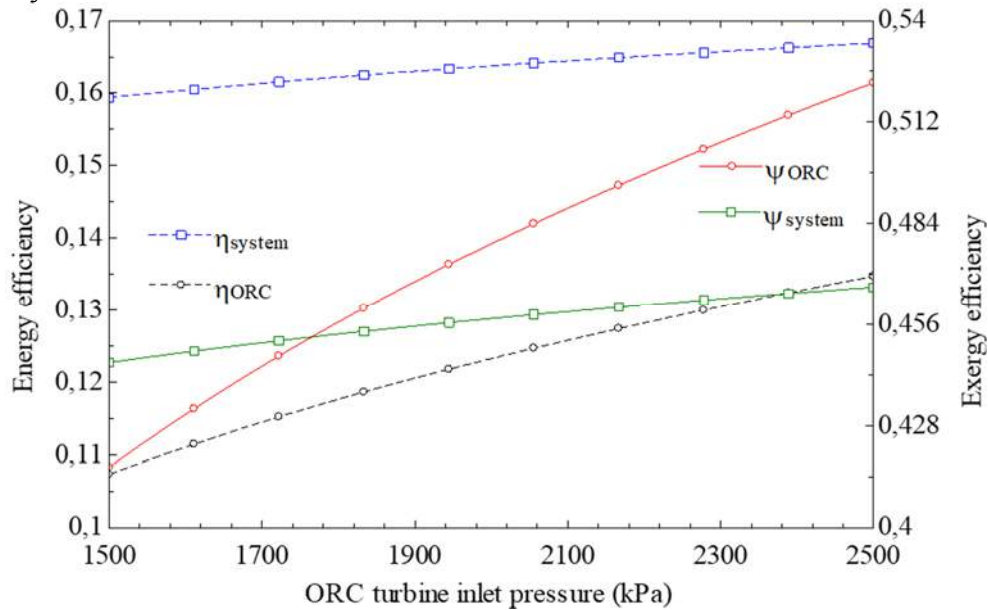
Figure 8. System and ORC performance variation at different ORC turbine inlet pressures

In Figure 9, the effects on the overall system due to the PPT of HEX change are examined. When the PPT of HEX is increased by about 25 °C, a linear reduction is occurring in the energetic and exergetic performance of the total model. The reason for this decrease is that as the temperature of the coolant entering the ORC turbine decreases with the increase of the PPT of HEX, the enthalpy of the working fluid decreases, so the power generation drops in and as a result its performance decreases.
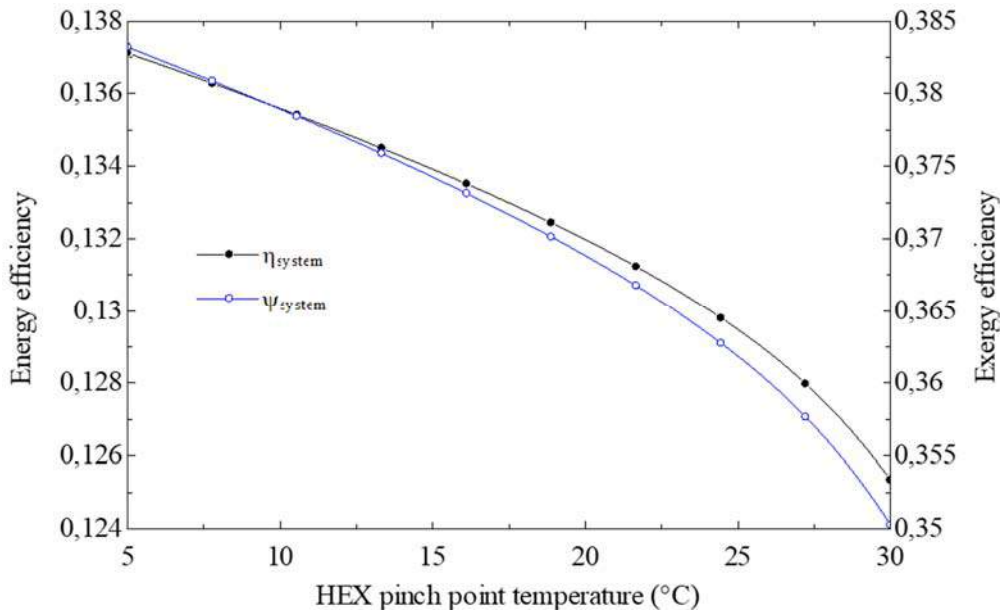
Figure 9. Effect of PPT of HEX change on overall system performance

In Figure 10, the energetic and exergetic performance of two different fluids used as cycle fluids in the proposed system are given for the entire system. As can be seen in Figure 10, in the case of using n-butane as the work fluid, the energetic and exergetic performance of the plant was calculated as 15.97% and 44.63%, respectively. If isopentane is used in the work fluid, the energy and exergy performance of the suggested model was found to be 14.40% and 40.26%, respectively. Once these two fluids are compared under the same conditions, the performance of n-butane fluid is higher than isopentane.
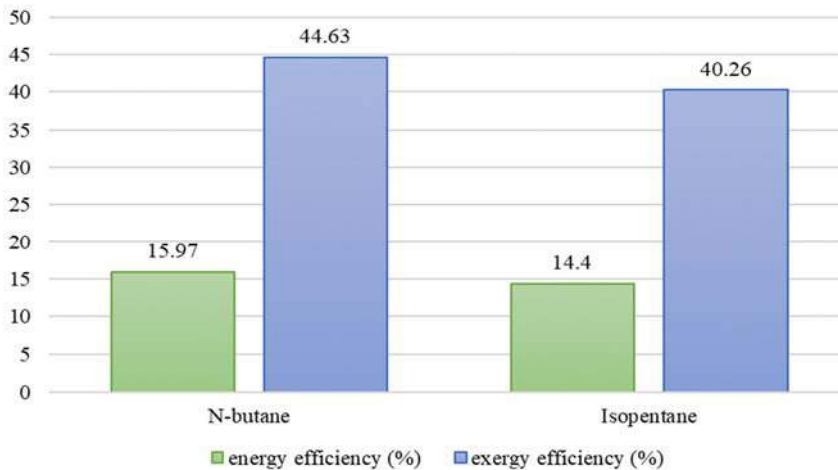
Figure 10. Performance comparison of the whole plant for two working fluids

4. Conclusion

Geothermal energy, which is one of the renewable energy sources, has widespread use today... In this planned work, thermodynamic performance analyses of geothermal energy assisted power generation system were examined according to n-butane fluid. Under the same circumstances; the influence of some parameters such as flash pressure, turbine isentropic efficiency, ORC turbine inlet pressure and TPP of HEX on the modeled system were examined

and presented in graphs. By applying the first and second laws of thermodynamics, performance analyses of this system were performed and some important results obtained are as follows:

1. The power generated from the entire plant was calculated as 3038 kW for the n-butane fluid.
2. Energetic and exergetic efficiencies of the modeled ORC for the n-butane fluid were calculated as 10.24% and 42.09%, respectively.
3. Energy and exergy performance of the total power plant are found as 15.97% and 44.63% for n-butane fluid, respectively.

References

Altun, A. F., & Kilic, M. (2020). Thermodynamic performance evaluation of a geothermal ORC power plant. Renewable Energy, 148, 261-274.

Cengel, Y. A., & Boles, M. A. (2015). Thermodynamics: An Engineering Approach 8th Editon. The McGraw-Hill Companies, Inc., New York.

Dincer, I., & Rosen, M. (2013). Exergy: energy, environment, and sustainable development.

Erdemir, D. (2020). Development and assessment of geothermal-based underground pumped hydroenergy storage system integrated with organic Rankine cycle and district heating. International Journal of Energy Research, 44(13), 10894-10907.

Erdogan, A., & Kucuka, S. (2019). Bir jeotermal enerji santralinin termodinamik analizi ve hava ve su soğutmalı çevrim performanslarının değerlendirilmesi. Ulusal Tesisat Mühendisliği Kongresi, 17-20 Nisan 2019, İzmir.

Gnaifaid, H., & Ozcan, H. (2021). Development and multiobjective optimization of an integrated flash-binary geothermal power plant with reverse osmosis desalination and absorption refrigeration for multi-generation. Geothermics, 89, 101949.

Ratlamwala, T. A. H., Dincer, I., & Gadalla, M. A. (2012). Thermodynamic analysis of a novel integrated geothermal based power generation-quadruple effect absorption cooling-hydrogen liquefaction system. International Journal of hydrogen energy, 37(7), 5840-5849.

Siddiqui, O., Ishaq, H., & Dincer, I. (2019). A novel solar and geothermal-based trigeneration system for electricity generation, hydrogen production and cooling. Energy Conversion and Management, 198, 111812.

Takan, M. A., & Kandemir, S. Y. Türkiye'deki Jeotermal Enerjinin Birincil Enerji Arzı Yönünden Değerlendirilmesi. Avrupa Bilim ve Teknoloji Dergisi, 381-385.

Yilmaz, F. (2018). Jeotermal enerji destekli güç ve temiz su üretim sisteminin incelenmesi ve termodinamik analizi. Akademik Platform Mühendislik ve Fen Bilimleri Dergisi, 6(2), 86-93.

Yilmaz, C., & Koyuncu, I. (2021). Thermoeconomic modeling and artificial neural network optimization of Afyon geothermal power plant. Renewable Energy, 163, 1166-1181.

Yuksel, Y. E., & Ozturk, M. (2020). Jeotermal enerji destekli çok fonksiyonlu enerji üretim sisteminin termodinamik analizi. Pamukkale Üniversitesi Mühendislik Bilimleri Dergisi, 26(1), 113-121.

Comparative Performance Investigation of a Transcritical CO₂ Power Plant Using with Waste Heat

Fatih YILMAZ[1*]

Abstract: The energy generation sector is one of the most important players in the emergence of environmental challenges today. Therefore, the effective use of energy resources such as energy management with using the waste heat is important for humanity at this point. The proposed study deals with thermodynamic performance analysis of the transcritical CO_2-based Rankine cycle with waste heat as an energy source. This system mainly comprised of a Rankine cycle (RC) with CO_2 refrigerant at the transcritical situation. system A detailed performance analysis are made to investigate the RC and overall system. To examined the effects of some important parameters on the system performance and exergy destruction rate, parametric analysis is also conducted. In addition, the efficiency comparison for co-generation is discussed by making some modifications in this Rankine cycle. Thermodynamic analysis results show that energetic and exergetic efficiency of the overall system are 55.66% and 36.06%, respectively.

Keywords: Energy, exergy, Rankine cycle, waste heat

1. Introduction

Today, as a result of the excessive use of fossil fuels, it is a known fact that greenhouse gases both to the environment and to the atmosphere cause great harm not only to the atmosphere but also to human health (Karapekmez and Dincer, 2021). However, despite these known damages of fossil fuels, the fact that they are still in the first place in energy generation (Gunderson et al., 2020; Zhang et al, 2020) and then continue to increase in environmental problems day by day. One of the most important ways to prevent this increase and to fight as humanity is the use of renewable energy sources and use of energy efficiency methods. In this context, energy production with waste heat comes to the fore, and in recent years, there are many academic researches in this field, both in real studies and in the literature.

Liao et al. (2020) planned an organic Rankine cycle (ORC) using waste heat in terms of advanced exergy analysis method. They also conducted an energy and exergy analysis to examine the impact of some constraints on the system performance. They computed that optimum compression rate for simple supercritical CO_2 ORC as 1.8. Kizilkan (2020) suggested a performance evaluation of a cement plant driven by waste heat. Also, this author conducted a detailed comparative analysis for supercritical fluids. He stated that the highest energy efficiency was obtained in the closed CO_2 Brayton cycle with 27.9%. Feng et al. (2020) modeled a parametric and thermo-economic analysis of ORC that is the usage of the waste heat.

[1] Isparta University of Applied Science, Faculty of Technology, Mechatronics Engineering, Isparta, Turkey
* Corresponding author: fatiyilmaz7@gmail.com

In their proposed study, parametric analyzes of supercritical and subcritical cycles are performed according to R1234ze fluid Butcher and Reddy (2007) examined an excess heat recovery power plant using the exergy analysis method. Also, they investigated that some important parameters such as the effect of heat recovery steam generation (HRSG) temperature on the system performance. They stated that increasing the HRSG pinch point temperature (TPP) decreased the exergetic efficiency of the proposed system.

In short, it is a fact that there are many studies on waste heat management and power production. However, in this study, the CO_2-based transcritical (t-CO_2) cycle is preferred for power generation. In this proposed study, a detailed analysis of energetic and exergetic performance analyzes for the performance evaluation of the waste heat-assisted tCO_2-RC system is discussed.

2. Explanation of Proposed System

In this work, a waste heat supported RC system, with t-CO_2 working fluid, is proposed as shown in Fig. 1. In short, the thermal energy for the RC plant is met by waste heat. first of all, the waste heat centers in the heat recovery steam generator (HRSG), at state 7, and then the heat transfer occurs in this component. Then, the CO_2 fluid enters the turbine of the Rankine cycle from state 3 in the superheated vapor phase, where power production takes place. The high temperature CO_2 at the turbine outlet transmits its heat to the water in the heat recovery system. The water entering the HEX 1 under environmental conditions is heated here and hot water is produced and cogeneration is made with this proposed system, as revealed in Fig.1. The working fluid entering the pump in the saturated liquid phase at the gas cooler outlet and then it is pressurized and enters the HRSG component again. As a result, the RC system employs for heating and power generation application from waste heat.
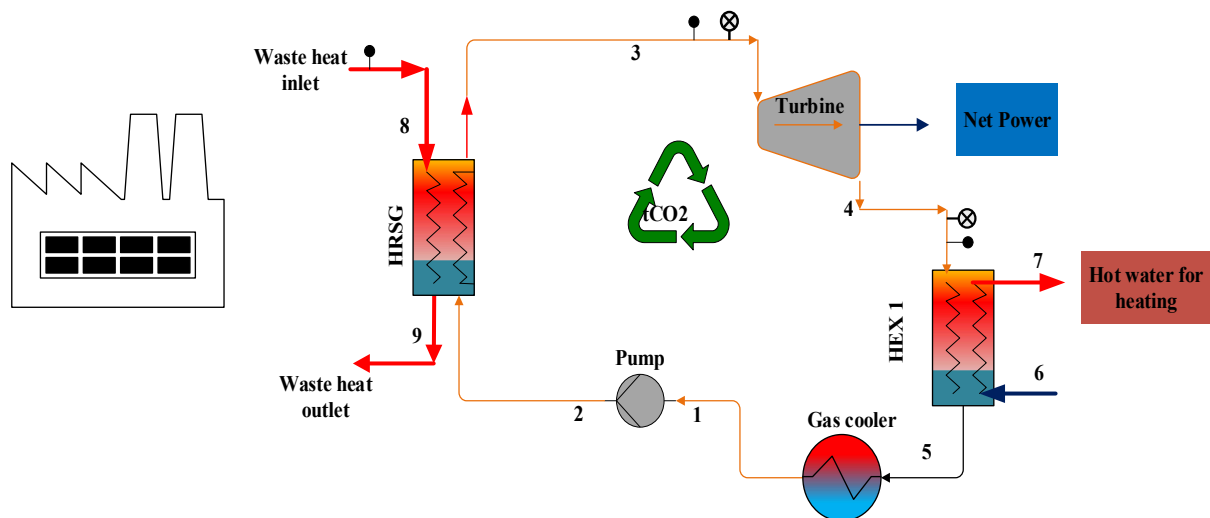
Fig.1 Design Layout of the proposed model system

2.1. Thermodynamic Modeling

In this suggested study, as above mentioned in Fig.1, a detailed thermodynamic performance evaluation is conducted to examine of the plant effectiveness in terms of the energy and exergy efficiency perspectives. Before moving on to the thermodynamic analysis in a system in its most general form, some of the assumptions made are given below;

- The modeled plant is expected to operate under steady-state flow circumstances
- The kinetic and potential energy disregarded
- Waste heat is considered as air in the analysis
- The employing fluid at the turbine inlet is modeled according to the saturated vapor phase.
- Pumps and turbines considered adiabatic
- The efficiency of the heat exchangers is accepted as 80%.
- Reference temperature and pressure values are accepted as 25 °C and 101.325 kPa.

With the aforementioned assumption, the general thermodynamic balance equivalences, for the modeling of the thermodynamic evaluation, should be described as (Cengel and Boles, 2007; Dincer and Rosen, 2012; Kotas, 2013);

Mass Balance: $\sum \dot{m}_i = \sum \dot{m}_e$ (1)

Energy Balance: $\sum \dot{m}_i h_i + \sum \dot{Q}_i + \sum \dot{W}_i = \sum \dot{m}_e h_e + \sum \dot{Q}_e + \sum \dot{W}_e$ (2)

Entropy Balance: $\sum \dot{m}_i s_i + \sum \left(\frac{\dot{Q}}{T}\right)_i + \dot{S}_{gen} = \sum \dot{m}_e s_e + \sum \left(\frac{\dot{Q}}{T}\right)_e$ (3)

Exergy Balance: $\sum \dot{m}_i ex_i + \sum \dot{Ex}_i^{\dot{Q}} + \sum \dot{Ex}_i^W = \sum \dot{m}_e ex_e + \sum \dot{Ex}_e^{\dot{Q}} + \sum \dot{Ex}_e^W + \dot{Ex}_{Des}$ (4)

In equation (3), $\sum \dot{Ex}_i^{\dot{Q}} \; and \; \sum \dot{Ex}_i^W$ terms describe the heat and work exergy transfer rates, and also, should be written as below;

$$\dot{Ex}^{\dot{Q}} = (1 - \frac{T_0}{T_c})\dot{Q}$$ (5)

$$\dot{Ex}^W = \dot{W}$$ (6)

After these assumptions and general equations, the specific exergy term, ie physical exergy, can be defined as follows;

$$ex = h - h_0 - T_0(s - s_0)$$ (7)

As a result, the power generation and inlet of the thermal energy for the modeled system can be depicted as;

$$\dot{Q}_{HRSG} = \dot{Q}_{in} = \dot{m}_8(h_8 - h_9) = \dot{m}_3(h_3 - h_2)$$ (8)

$$\dot{W}_T = \dot{m}_3(h_3 - h_4)$$ (9)

$$\dot{W}_P = \dot{m}_2(h_2 - h_1)$$ (10)

After calculating the produced and consumed power rate, the net power generation rate can be formulated as below;

$$\dot{W}_{net} = \dot{W}_T - \dot{W}_P$$ (11)

At the end of the formulation, the overall system's energy and exergy efficiency as;

$$\eta_{system} = \frac{\dot{W}_{net} + \dot{Q}_{DHW}}{\dot{Q}_{in}}$$ (12)

$$\psi_{system} = \frac{\dot{W}_{net} + \dot{Ex}_{DHW}^{\dot{Q}}}{\dot{Q}_{in}}$$ (13)

3. Results

The suggested proposed study addresses the thermodynamic analysis of the waste heat-supported tCO2-RC for cogeneration purposes. For this purpose, power generation and system

performance are investigated in terms of energetic and exergetic efficiencies by using waste heat at 200 ºC in an RC system with CO_2 fluid for advanced energy management. In the light of the assumptions presented in Table 1, thermodynamic analysis is applied to the proposed system with the EES program and the results are shown in Table 2.

Table 1. Proposes system assumptions

	unit	Value
Waste heat inlet temperature	ºC	200
Waste heat inlet pressure	kPa	101.325
Pump compression rate	-	1.5
Pinch Point Temperature of HRSG	ºC	15
Pump inlet pressure	kPa	5800
Pump isentropic efficiency	%	85
Turbine isentropic efficiency	%	92
HEX effectiveness	%	80
Reference temperature	ºC	25
Reference pressure	kPa	101.325

The total net power generation capacity of the proposed system is 92.43 kW, by using the waste heat. According to the results presented in Table 2, the system produces 463.4 kW of heating load, and also the energetic and exergetic efficiency of the RC plant is 9.08% and 31.08%, respectively. As a result, the modeled power plant has an energy performance of 55.66% and an exergy performance of 36.06%.

Table 2. Thermodynamic analysis results

	Unit	Value
Net power generation rate	kW	92.43
Heat production rate	kW	463.4
Energy efficiency for RC	%	9.08
Exergy efficiency for RC	%	31.08
Energy efficiency for whole system	%	55.66
Exergy efficiency for whole system	%	36.06
Total exergy destruction rate	kW	279.6

In this study, since the basis of the study is waste heat, this temperature change is an important parameter. Fig. 2 examines the impact of waste heat temperature change on the performance of the RC plant. With the rise in the waste heat temperature, the energy efficiency of the proposed RC plant increases from 8.9% to 9.25%, since the temperature of the fluid entering the system at point 3 increases. However, at the same time, the exergy performance of the RC system decreases as the exergy entering the system with heat increases.

Another figure, Fig. 3, discusses the effect on overall system performance in the same waste heat temperature range. As can be seen in this figure, the rise in the waste heat temperature increases the energy efficiency as it increases the useful outputs in the whole system. However, it reduces the exergy efficiency. Therefore, waste heat temperature management is important in system designs.
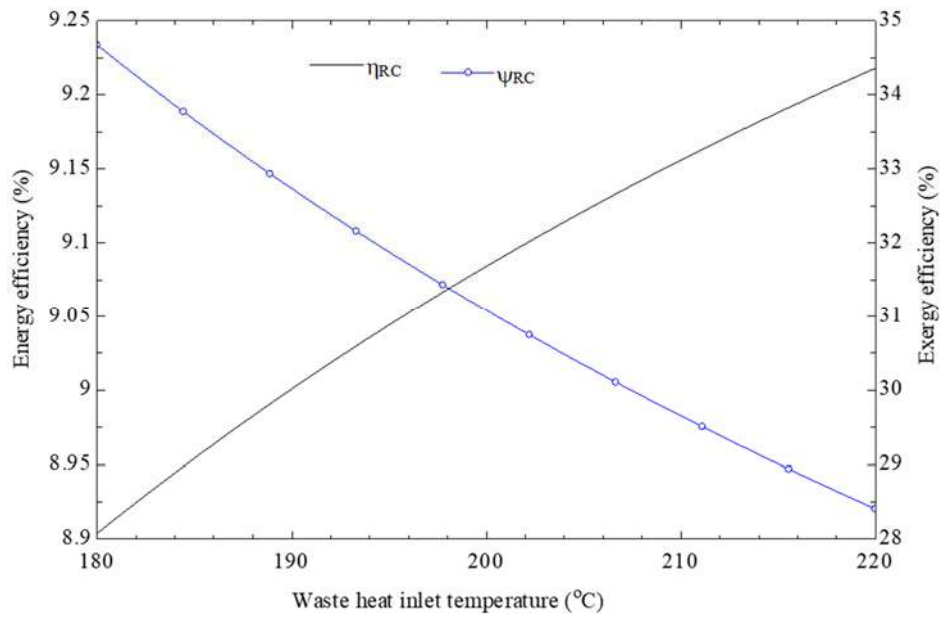
Fig.2. Impact of the waste heat inlet temperature on the RC plant performance
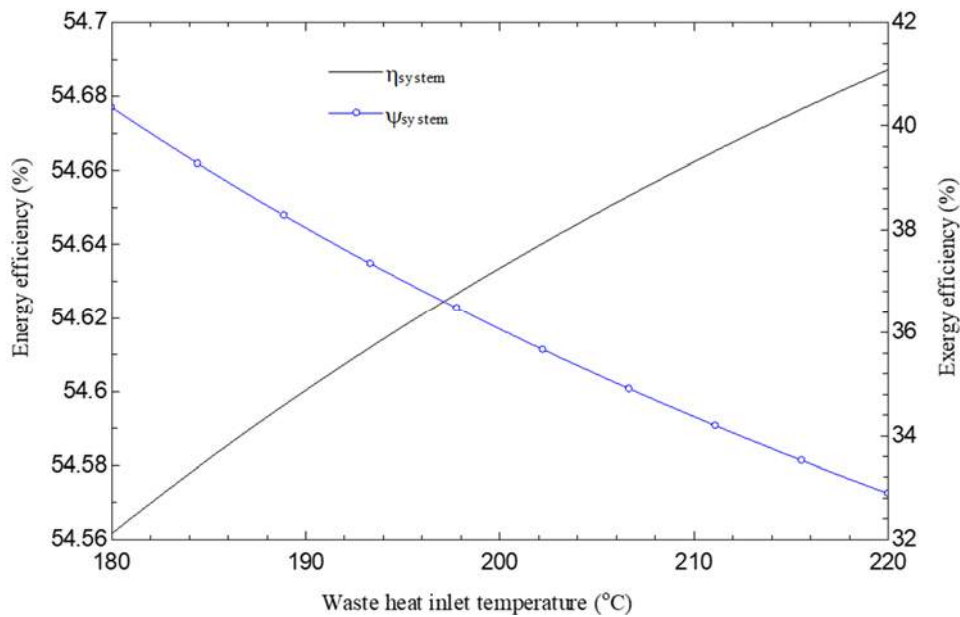
Fig.3. Impact of the waste heat inlet temperature on the overall plant performance

The last figure on waste heat temperature, Fig.4, evaluates the net power generation and the irreversibility of the entire plant. With the increase in waste heat temperature, both the power produced and the irreversibility increase. While the rise in electricity production is a positive situation, the rise in the irreversibility is an undesirable situation. Therefore, waste heat temperature management in power generation systems can be expressed as a very important parameter.
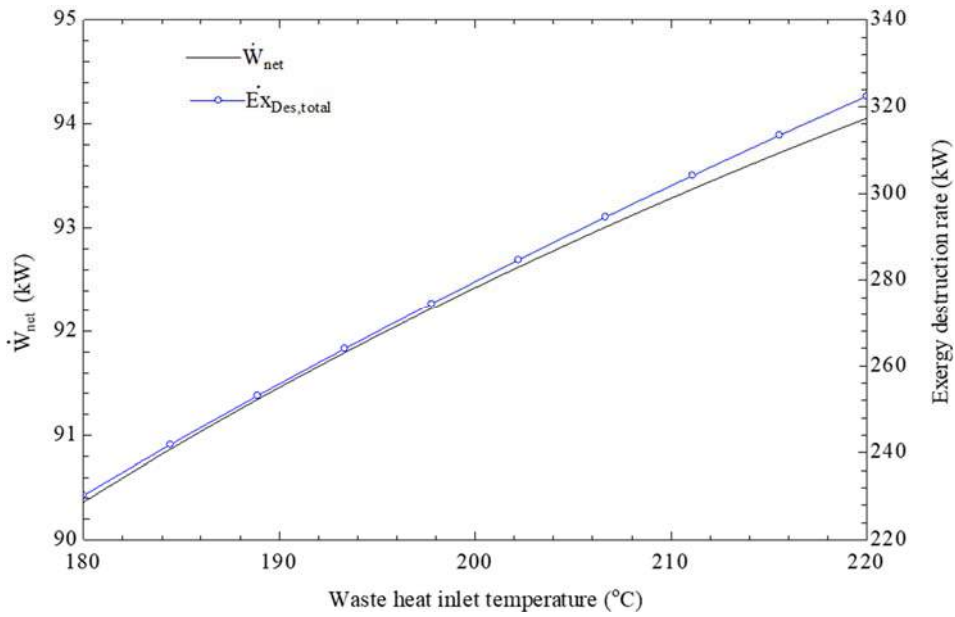
Fig.4. Influence of the waste heat inlet temperature on the net power and irreversibility

Fig. 5 and 6 examine the impact of pump compression ratio on net power production, irreversibility, RC performance and, overall system performance, respectively. In short, it is clearly realized in Fig. 5 that while the power generation from the system increases with the increase of pump compression ratio, the exergy destruction of the whole system decreases. Depending on this situation, the energetic and exergetic efficiency of the plant and RC, as in Fig. 6, is also increased.
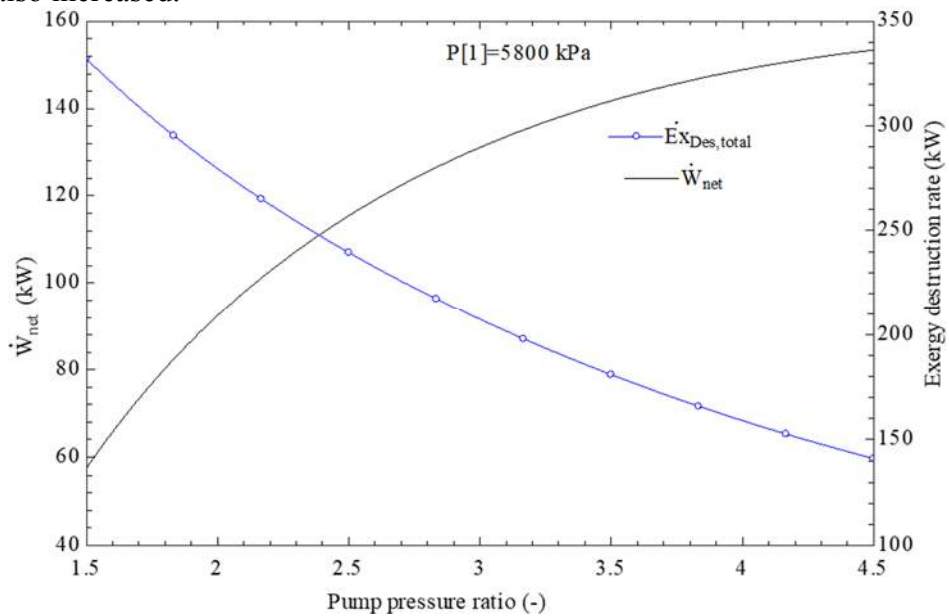
Fig.5. Net power and total irreversibility vs pump pressure ratio
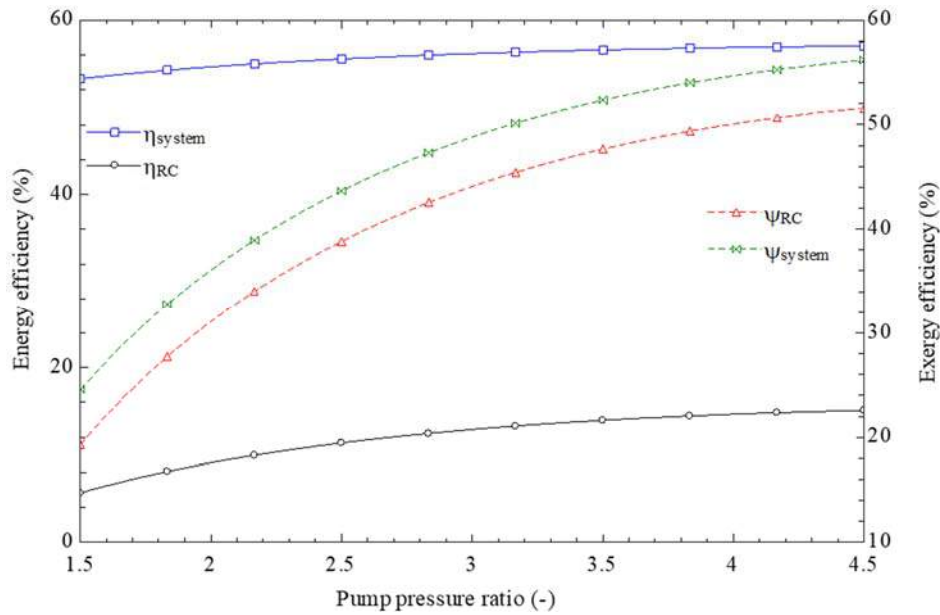
Fig.6. Performance of the whole and RC plant vs pump pressure ratio

In this proposed study, the last figure, Fig. 7, presents the change in overall system performance and power rate with increasing pinch point temperature of the HRSG. As the HRSG temperature rises from 5 °C to 35 °C, the net power output drops by approximately 2.5 kW. Depending on this situation, both energy efficiency and exergy performance are in a downward trend.
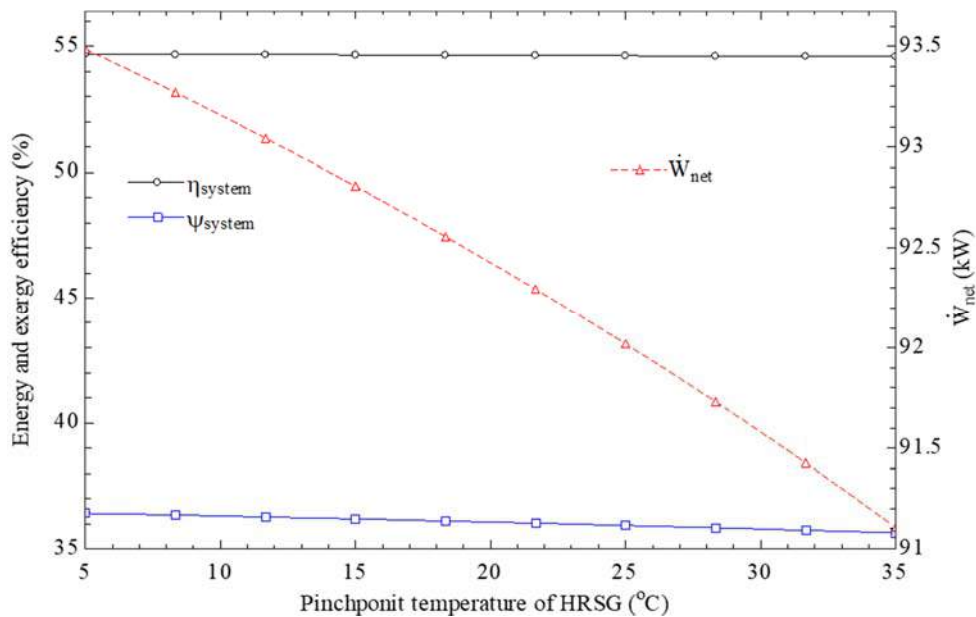
Fig.7. Effect of the PPT of HRSG on net power rate and system's performance

4. Discussion and Conclusions

The intent of this suggested plant is to study the thermodynamic performance examination of the waste heat supported transcritical CO_2-RC for power and heating production applications. In this context, a parametric study is made to examine the effects of changes in some parameters such as waste heat inlet temperature, compression ratio and pinch point temperature of HRSG on system performance. To summarize, some important results obtained as stated by the results of the analysis can be declared as follows;

i. The power and heat generation capacity of the whole system was determined as 92.43 kW and 463.4 kW. In addition, the total exergy destruction was calculated as 279.6 kW.
ii. While the entire system has an energy efficiency of 55.66%, it has an exergy efficiency of 36.06%.
iii. The highest exergy destruction was seen in the HRSG subcomponent.

As a result, it is very important to increase system efficiencies with cogeneration, trigeneration or waste heat management and to design environmentally friendly systems by applying energy management.

References

Butcher, C. J., & Reddy, B. V. (2007). Second law analysis of a waste heat recovery based power generation system. *International Journal of Heat and Mass Transfer*, *50*(11-12), 2355-2363.

Cengel, Y. A., & Boles, M. A. (2007). *Thermodynamics: An Engineering Approach 6th Editon (SI Units)*. The McGraw-Hill Companies, Inc., New York.

Dincer, I., & Rosen, M. A. (2012). *Exergy: energy, environment and sustainable development*. Newnes.

Feng, Y. Q., Zhang, W., Niaz, H., He, Z. X., Wang, S., Wang, X., & Liu, Y. Z. (2020). Parametric analysis and thermo-economical optimization of a Supercritical-Subcritical organic Rankine cycle for waste heat utilization. *Energy Conversion and Management*, *212*, 112773.

Gunderson, R., Stuart, D., & Petersen, B. (2020). The fossil fuel industry's framing of carbon capture and storage: Faith in innovation, value instrumentalization, and status quo maintenance. *Journal of Cleaner Production*, *252*, 119767.

Karapekmez, A., & Dinçer, İ. (2021). Development of a multigenerational energy system for clean hydrogen generation. *Journal of Cleaner Production*, *299*, 126909.

Kizilkan, O. (2020). Performance assessment of steam Rankine cycle and sCO2 Brayton cycle for waste heat recovery in a cement plant: A comparative study for supercritical fluids. *International Journal of Energy Research*, *44*(15), 12329-12343.

Kotas, T. J. (2013). *The exergy method of thermal plant analysis*. Elsevier.

Liao, G., Jiaqiang, E., Zhang, F., Chen, J., & Leng, E. (2020). Advanced exergy analysis for Organic Rankine Cycle-based layout to recover waste heat of flue gas. *Applied Energy*, *266*, 114891.

Zhang, W., Yan, Q., Yuan, J., He, G., Teng, T. L., Zhang, M., & Zeng, Y. (2020). A realistic pathway for coal-fired power in China from 2020 to 2030. *Journal of Cleaner Production*, *275*, 122859.

The Effects of Coronavirus in the Construction Industry: A Case of Turkey

Pınar Usta[1*], Başak Zengin[2] and Kübra Arslan[3]

Abstract: The coronavirus (COVID 19) pandemic, which has affected the whole world, has changed the balance of life. Unconfirmed the epidemics in history, it has become a more effective global problem. While searching for solutions to problems on the health side, new problems have emerged in different sectors within the scope of the measures taken. The construction area, which is one of the sectors that affect global economic development, the fluctuation in the construction sector, was greatly affected by this process.

The quantitative measurement techniques to investigate the impact of the pandemic on descriptive analysis of the construction sector in Turkey by applying the survey fieldwork was conducted. In the study, it was felt that the construction industry was affected by global economic difficulties. Even though precautions were taken in terms of health, there was unemployment anxiety as well as the health problems of the employees and their environment. In addition, another major problem was in the procurement of the material. Due to the findings, economic contractions were observed in the construction sector. According to the study, it was revealed that more measures should be taken for the further progress of the pandemic or for a similar situation.

Keywords: COVID 19, Epidemic, Construction Sector and Descriptive Study

1. Introduction

Epidemic diseases have affected the health of living creatures and deteriorated their quality of life. The recent COVID-19 epidemic has caused strong damage to community levels. While certain systems and locations are not equally affected, it is noteworthy that the coronavirus outbreak is global, rapid and significantly widespread disrupting current practices. For the post-epidemic period, it has been called "the beginning of a new era". Following the rapid infection of 3 million patients worldwide by the pandemic, the health organization announced the increase of measures (COVID-19 STRATEGY UPDATE 2020). Many cities/countries have implemented quarantine measures and have made decisions to close many borders and roads while workplaces, schools and universities were closed.

The anxiety, fear, and depression caused by the epidemic caused psychological, sociological and economic problems by disturbing both individuals and sectors, and therefore businesses.

[1] [1] Isparta University of Applied Sciences Technology Faculty, Civil Engineering Department, Isparta- Turkey
ORCID Code: 0000-0001-9809-3855
* [2] Kahramanmaraş Istiklal University, Elbistan Vocational High School Kahramanmaraş, Turkey.
ORCID Code: 0000-0003-3719-9423
[3] Istinye University, Faculty of Fine Arts, Design and Architecture, Interior Architecture and Environmental Design, Istanbul Turkey ORCID Code: 0000-0002-2803-7185.
* zenginbasak@gmail.com

Due to these effects, problems related to the epidemic progressed faster (Barua); (Wang et al. 2020). While the pandemic is a serious problem in countries, the rapid increase in deaths and the threat of the virus is seen as an enemy that must be fought collectively, the importance of the measures that the world will work together to eliminate this problem has emerged.

While investigating the effects of COVID 19, it was seen that there were major crises. In addition to the crises experienced in terms of health, there were wide-ranging crises. When the effect of the epidemic on the economy was investigated, a meta-transition was encountered. It has been specified as a meta-transition due to the fact that the pandemic infects more than one regime at the same time. According to this transition theory, multiple system elements must be taken into account, including technology and innovation, markets, business, government, behaviors and norms, regulatory and governance frameworks, and pathways of change. This multi-parameter way of working is integrated into the analysis. Such systematic changes are examined under two valid conditions; government (management and regulation) and economics (business, markets and finance). States have faced major problems in applying these multiple parameters. It is a process where states are not ready. Sectors that progress due to globalization have experienced the most difficult constraints.

International air travel, shipping and trade suffered the most. Small businesses and self-employed people have gone through more troublesome processes (Wells et al. 2020). When the COVID-19 pandemic first manifested itself, production and general economic activities in China, and later on all over the world, led to shrinkage in demand together with production. These negativities were felt in most countries. Vasiev et al. (2020) conducted input-output analyses in 42 sectors in 31 provinces in order to investigate how and how much the Chinese economy was affected by the epidemic during the pandemic. In this context, they developed various scenarios for changes in production and consumption depending on 22 different parameters in economic, environmental and social fields. According to the analysis, it has shown that there are 23 sustainable factors for China's regional development and the pandemic has a strong impact on hazardous waste, carbon dioxide emissions and energy resource efficiency. When countries are examined from different angles, they estimated that the revenue would decrease by 8.5% in the positive scenario during the pandemic process of the Galician economy, and 12.7% in the case of the negative scenario, if the pandemic lasts more than a quarter (Ellison, 2020). During the Covid-19 pandemic, the economy in Iran contracted, and according to preliminary data, a 30% decrease in oil exports was found (Duddu 2020).

Fornaro and Wolf (2020) examined the effects of supply and demand shocks on economic growth within the scope of the macroeconomic effects of the COVID-19 pandemic (Fornaro and Wolf 2020). The Covid-19 crisis has dragged many sectors to collapse in many countries around the world, a rapid acceleration in high inflation and unemployment rates of economies, and if this process continues for a few more periods, there will be profits in production (Chakraborty and Maity 2020) (Fig 1).

Figure.1 After-Before Covid crisis process affects different sectors

When discussed the Indian economy, he examined the impact of the Covid-19 pandemic on sectors such as agriculture, industry, tourism, finance and economy in the period of March-June 2020 (Jaya 2020). According to these findings, financial and real estate services in India 17.3%, mining and quarrying 14.7%, basic consumption/energy (electricity, gas and water supply) 13.9%, construction/building sector 13.3%, general production 6.3%, trade, tourism While the travel sector emphasizes a decrease of 9% and safety by 0.4%, it has been determined that the agriculture, forestry, fishing and nutrition sectors have increased by 1.3% compared to the past. In the research findings of it was observed that industrial production decreased during the COVID-19 pandemic in India, unemployment reached the highest level in the last 45 years, and private sector investments have recently started to decline rapidly (Dev and Sengupta 2020).

The subsistence of individual beings relies on critical items during the outbreak and that can be content by appropriately exploit the critical resource, like crude materials, employees, and active logistics systems as explain in the internal coterie of Figure 2.
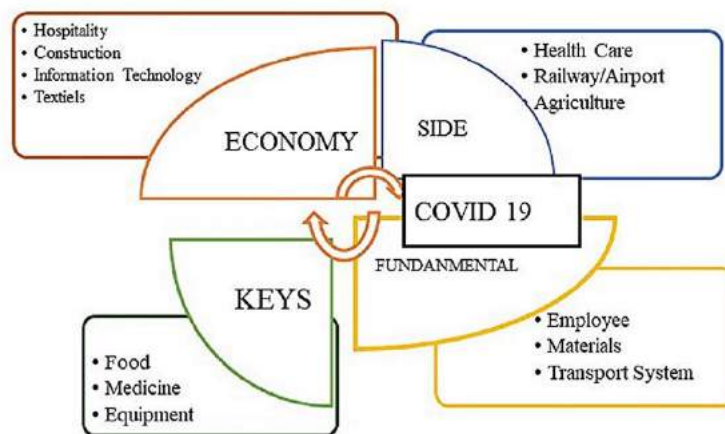
Fig.2 Covid crisis process affects different sectors

The recent example of the coronavirus COVID-19 outbreak clearly shows the necessity of this new perspective. This research introduces a new angle in SC resilience research when resistance to extraordinary disruptions needs to be considered at the scale of viability. The integrity ISN is elaborated with viability. The system illustrates the viability formation through dynamic game-theoretic modelling of a biological system that resembles the ISN. That compares some future research areas (Ivanov and Dolgui 2020; Mishra et al. 2021, Singh et al., 2021).

While examining the Egyptian economy under the influence of the pandemic process, if the pandemic continues, the income revenue in the Egyptian economy will decrease by 0.7-0.8% every month and the consumption of the people will decrease by 10%, if the crisis continues for 3 or 6 months, the revenue will be approximately% at the end of 2020. They mentioned the possibility of a decrease of 2.1- 4.8%. (Diao et al. 2020). Investigating the impact of the pandemic process across different areas. has compared 63 sectors such as agriculture, transportation, mining and construction in Myanmar. According to the findings, they predicted that with the contraction of the economy by 41% during the pandemic process, the demand and the decline in exports to the agriculture and food sector would play an important role in this. In their study (Cajner et al. 2020) found that approximately 13 million wage earners lost their jobs in two weeks in employment due to the pandemic in the USA, and this rate was twice as much during the period followed, compared to the 2008 Global Financial Crisis.

Examining the reflections of COVID-19 on a sectoral basis, emphasized that the tourism sector has an important share in the economy of Namibia and that the impact of the pandemic is pessimistic in the manufacturing, construction, mining and quarrying sectors, as well as in the tourism sector, and the agriculture, forestry and fishing sector and technology are optimistic (Evelina et al. 2020) After the date of start detecting the first case in the world countries in parallel with the effect seen since March 11, which detected the first case of 2020 in Turkey, the economic side of health, social, was observed to be felt largely sociological and psychological effects. Covidien-19 of Turkey's economy also impact the pandemic is obvious that affected so many other countries. Considering this process, sectoral employment has become more fragile (Koyuncu and Meçik, 2020).

Although there were negative effects on the sectors after the pandemic, it ensured that precautions were taken for the problems that may occur from now on. Larger investments and budgets began to be allocated for management systems, especially in the education and health sectors. Vaccination studies were carried out, which affected the treatment process on a large scale. Equipment used in hospitals was developed. A new era has begun in the education system that concerns all fields. The distance education system, which is generally preferred in adult education, has turned into a system used by everyone. Compulsory education and working environments were created with the remote system. In that period, the tendency towards the virtual shopping system increased. With the increasing trend in e-commerce, developments in this direction have been observed. The tendency towards agriculture has increased with renewable energy resources. With the transition of life online, the need for cyber precautions has increased even more. The most significant improvement in this process has been observed in energy resources. Considering the carbon dioxide measurements, it was determined that the rates in the emission measurements decreased (Karakaş 2021; Karakaya, and Uzmanı 2021; Doğan and Doğan 2020).

1.1   New coronavirus disease (COVID-19)

It is a virus that was first identified on January 13, 2020, as a result of research conducted in a group of patients who developed respiratory symptoms (fever, cough, shortness of breath) in the Wuhan Province of China at the end of December. When we analyze COVID-19, the "Co" of "Corona", the "vi" of "virus", the "d" of the word "disease" in English, and the number "19" for the first time in 2019 The World Health Organization (WHO) declared the coronavirus-borne Covid-19 disease, which threatens the whole world, as a "pandemic", which means a global epidemic (Cucinotta and Vanelli 2020). With the impact of Covid-19 on the global

community, it was declared a pandemic (epidemic) by the World Health Organization (WHO) on March 11 (Valtonen et al. 2019).

Coronaviruses (COV) are a large family of viruses that cause a variety of illnesses, from the common cold to more serious diseases such as Middle East Respiratory Syndrome (MERS) and severe acute respiratory syndrome (SARS) (UNCTAD 2020). The new type of coronavirus, coded as COVID-19, usually causes diseases in the respiratory and gastrointestinal system in humans. According to clinical results in adults; common cold, bronchitis, pneumonia, severe acute respiratory distress syndrome (ARDS) and multiple organ failure resulting in death (Reyad 2020; Aslan and Özdemir 2020). According to the WHO report, public health and social measures must be implemented with the participation of all members of the society in order to slow down or stop the spread of Covid19, and a global struggle must be carried out (World Health Organization, 2020). When we examine from history to the present, the Plague Epidemic, also known as "Black Death" in the 1300s, "Bleeding Fever" in the 1500s, "Cholera" in the 1900s, "SARS" in the early 2000s, and later in 2009 and 2014. Outbreaks such as "Swine Flu and Ebola" have threatened public health and the economy in large areas around the world. As in all pandemics in world history, the Covid-19 pandemic manifests itself not only in health but also in many areas such as economy, finance, education, transportation, industry, public services and tourism (WHO, 2020).

The global epidemic spread from China and the Far East countries to other Asian, European, American and African countries and spread rapidly. Despite the coronavirus (Covid-19) epidemic, while countries are struggling with different approaches, they have also revealed that they are generally caught unprepared (Dyer (2020); Manderson and Levine (2020)). So much so that while the health system and infrastructure in many countries were questioned, the insufficiency of the health personnel, the lack of medical equipment and supplies created complete confusion.

1.2   The effect of covid-19 on the construction industry

The construction sector is one of the sectors affected by the coronavirus epidemic in the world and in our country. Like many other industries, it negatively affected the construction industry. The slowdown in building products in the sector, the decrease in the working capacity, the disruption of the allowances, the insufficient supply of the material needs and the adverse effects of the rising exchange rates caused great negativities. Looking at the sectoral study in Turkey has emerged worldwide contraction. Studies have shown that the construction sector is affected by this epidemic in crises, except for tourism, trade, aviation and social areas. Especially during the pandemic in China, it has been observed in the findings of the studies on the tunnel construction sites that are far from the settlements that there are great difficulties in the availability of workers and the sustainability of the work (Guo et al. 2020). As the stretch of COVID-19 has sustained after December 2019, stay at residence demand about the globe have modified how mostly from physical to practical interface, similar as going to institution and doing our jobs; though, some activities are in substance impracticable to accomplish virtually, such as construction exercise.

Therefore, the construction sector has been highly impaired by the current pandemic. The construction sector lay out a key constituent of countries' economies—it is approximately 13% of global GDP—as such, adopted the availability to perform construction activities with a least spread of COVID-19 might support with the financial feedback to the outbreak. Particular this context, this analysis aims to comprehend the capability impact of COVID-19 on construction

employee using an agent-based modelling approach. Activities are classified as being of low-medium-high hazard for workers, and the stretch of COVID-19 is simulated in the midst of construction workers in a project. This research establishes that the workforce from a construction project might be reduced by 30% to 90% due to the spread of COVID-19. Understanding how COVID-19 may spread among construction workers may assist construction project managers in creating adequate conditions for workers to perform their job, minimizing the chances of getting polluted with COVID-19. That way investigations given contribute to quantifying the benefits of using multiple working shifts to ease the spread of COVID - 19 in between construction laborer. (Araya 2021a; Araya 2021b)

Singapore's construction sector applies more than 450,000 laborers. In the course of the summit of the COVID-19 pandemic in Singapore from April to June 2020, migrant workers were disproportionately impaired, including plenty operation in the construction industry. Divided adaptation and structure worksites emerged as connection for COVID-19 transmittal. Official government resources including COVID-19 epidemiological data, 43 advisories and 19 circulars by Singapore's Ministries of Health and Manpower were examined over an 8-month period from March to October 2020. From a peak COVID-19 incidence of 1,424.6/100,000 employee in May 2020, the prevalence declined to 3.7/100,000 workers by October 2020. Multilevel safe management measures were performed to enable the phased resumption of construction worksites from July 2020. Using the Swiss cheese risk management model, the authors described the several governmental, industry, supervised and worker-specific intrusion to prevent, detect and contain COVID-19 for safe resumption of work for the structure industry (Zhang et al. 2021)

COVID-19 prevention policies have also been found to hinder the arrival of materials to be used in construction (García-Alberti et al. 2021) Events similar to these have been experienced in our country. For the construction sector, which covers hundreds of businesses lines and contributes to the economy and employment, in order to revive the construction sector in our country, packages such as reducing the down payment to 10% in the housing, discounts in credit rates in banks and facilitation in loan usage have been prepared. The search for bigger incentives has begun. For a while, there has been trading activity in the sector. Adhering to this research study data to analyze the situation in the construction sector in Turkey is made. It caused some problems in terms of working conditions in the sector, work follow-up, allowances. With the effect of this process on people, a study has been carried out on what kind of problems are experienced in construction. Based on the data obtained as a result of the studies, the main reasons for COVID 19 to affect the construction industry are;

- Import and export issues.
- Changing oil prices.
- Social distance effect.
- Curfew situation.
- Impact on newly graduated and experienced engineers.
- The subject of taking adequate precautions.
- New policies developed.
- New conditions in the working environment.
- Measures.

This approach concise discuss that the COVID-19 pandemic exposes the break in the current world-wide socio-technical command and offers the chance of multiple various option outlook. The policy brief explores the pandemic through the lens of the multi-level perspective on socio-

technical transitions. The pandemic is devised as a meta-transition event at the scenery level of unprecedented scale, pace, and pervasiveness such that it permeates all socio-technical regimes simultaneously. The prospects for the future are then defined on a array that compares the toughness of civil society and that financial structures. The result is four dissimilar eventualities for are linked to contemporary conversation on socio-economic futures: trade as usual; managed transition; chaotic transition; and succeeded degrowth. A socio-technical transitions perspective for assessing future sustainability following the COVID-19 pandemic. The eventuality is presented as a starting point for policy discussion and the participation of societal actors to define social and economic option for the future, and the involvement that the various forward would have for ecological responsibility. It is all over that the COVID 19 pandemic can act as a catalytic event in which the authenticity and efficacy of existing economic and political structures will be questioned and reformed, and hence is an opportunity to redefine the ecological responsibility our action cause.

2.   Material and Method

In this section, the research design, population and sample, measurement tool, validity and reliability study and analysis of the data are explained.

2.1   Material and researched background

The aim of this research is to investigate how the construction industry is affected by COVID-19 pandemic. By determining these effects, it is aimed to share the existing problems with the public, civil engineers, techniques and company managers. As a result of this, awareness will be provided on the creation of emergency action plans against other possible future epidemics. It is thought that this research will fill an important gap since there are a limited number of studies conducted abroad and domestically on how the epidemic has affected the construction sector.

The research population, located in the Republic of Turkey civil engineer, civil engineering technicians and includes the final year students. The study universe of the research consists of civil engineers, technicians and civil engineering senior students working in the districts of the European side of Istanbul. The major different people live in these districts in terms of socio-economic and socio-cultural aspects. Based on this, civil engineers, technicians and civil engineering senior students working in these districts have the variety and number to reflect this structure (Figure 3).
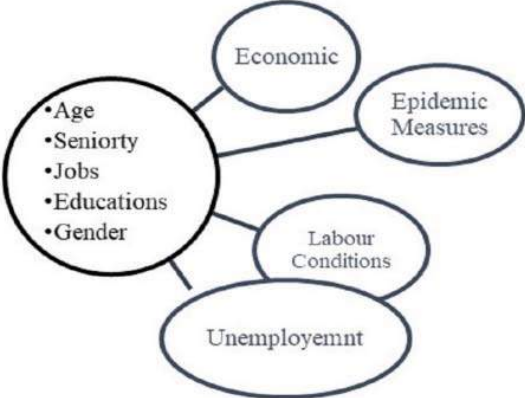
Figure. 3. Survey researched group

In line with the calculations made, the contact information of 170 of the civil engineers, technicians and civil engineering senior students who were determined from the research area was reached and 156 people who were able to get responses from 156 people who answered the scale as well-marked questionnaires formed the study group of this study. The general characteristics of the research groups are given in Table 1.

Table 1. Total research group

		n	**%**
Gender	Male	136	87.2
	Female	20	12.8
Age	20-27	59	37.8
	28-35	35	22.4
	36-43	30	19.2
	44 and-	32	20.5
Seniority	0-4 years	95	60.9
	5-10 years	42	26.9
	11-15 years	12	7.7
	16-20 years	3	1.9
	21 years and-	4	2.6
Jobs	Engineering	78	50
	Technician	63	40.4
	Intern	15	9.6
Education	Undergraduate	22	14.1
	License	91	58.3
	Postgraduate	43	27.6
Total		156	100

When Table 1. is examined, the distribution of the participants by gender; 87.2% male (n = 136), 12.8% female (n = 20), distribution by age groups; 37.8% were aged 20-27 (n = 59), 22.4% were aged 28-35 (n = 35), 19.2% were aged 36-43 (n = 30) and 20.5% of those aged 44 and over (n = 32), their distribution by seniority; 60.9% 0-4 years (n = 95), 26.9% 5-10 years (n = 42), 7.7% 11-15 years (n = 12), 1% 9 of them 16-20 years, 2.6% of them 21 years and above (n = 4), their distribution by profession; 50% of them are engineers (n = 78), 40.4% are technicians (n = 63), 9.6% are trainees (n = 15), their distribution by education level; 14.1% were associate degree (n = 22), 58.3% were undergraduate (n = 91) and 27.6% were graduate (n = 43).

2.2. Collection of data

In this study, the data were collected with the "Effect of Coronavirus on the Construction Industry" scale. According to the validity and reliability results of the Cronbach's Alpha values of the managerial strength scale were calculated as .88. The Cronbach Alpha value of the technology literacy scale, whose validity and reliability calculations were made by was calculated as 0.86. According to Cronbach Alpha values being 0.60 and above indicate that the scale is highly reliable and valid, and .80 and above indicates that the scale is highly reliable and valid. Table 2 gives the evaluation according to the questions according to the subtitles of the research.

Table 2. Evaluation according to the subtitles of the research and the questions

Dimensions	Item	Factor	Variances	Cronbach's Alpha	Average	S. Deviation
Epidemic Measures	Q1	0.755	60.25	0.95	4.21	0.59
	Q 2	0.719				
	Q 3	0.71				
	Q 4	0.701				
	Q 5	0.699				
Economics	Q6	0.732	9.686	0.86	4.26	0.51
	Q 7	0.727				
	Q 8	0.721				
	Q9	0.823				
	Q 10	0.541				
	Q11	0.558				
	Q12	0.668				
Labour conditions	Q13	0.591	10.18	0.83	4.16	0.63
	Q14	0.726				
	Q15	0.679				
	Q16	0.657				
	Q17	0.763				
	Q 18	0.673				
	Q 19	0.627				
State assistance	Q20	0.664	4.83	0.81	4.27	0.54
	Q 21	.837				
	Q 22	.871				
	Q 23	.833				
	Q 24	.859				
	Q 25	.817				
	Q 26	.865				
Unemployment	Q 27	0.531	11.21	0.83	3.96	0.66
	Q 28	0.823				
	Q 29	0.793				
	Q 30	0.558				
KMO=0.897	xsquare= 14021.932					

As can be seen in Table 2. in the scale factor analysis assessment of the impact of the pandemic on the construction industry, attention was paid to the factor load values being higher than 0.50 and the variance explained to be greater than 50%. In the phase of determining the factors, a total of six factors were determined by paying attention that the eigenvalues of the factors were greater than 1. These factors are; Pandemic measures are Economy, Working conditions, State aid and Unemployment factors. The variance value for items 1, 2, 3, 4 and 5 of the scale, which constitutes the pandemic precautions factor, was found to be 60.25 and the "Cronbach Alpha" value to be 0.95. The variance value for the 6, 7, 8, 9, 10, 11 and 12 items of the scale, which constitutes the economy factor, was found to be 9.686 and the "Cronbach Alpha" value to be 0.86. The variance value for the 13, 14, 15, 16, 17, 18 and 19 items of the scale, which constitutes the working conditions factor, was 4.83 and the "Cronbach Alpha" value was 0.81. The variance value for the 20, 21, 22, 23, 24, 25 and 26th items of the scale,

which constitutes the state aid factor, was found to be 11.21 and the "Cronbach Alpha" value as 0.83. The variance value for items 27, 28, 29 and 30 of the scale, which constitutes the unemployment factor, was found to be 4.7 and the "Cronbach Alpha" value to be 0.8

2.3 Data Analysis

After the data was obtained, the data were expressed in the form of distributions of frequencies and percentages, and comparisons were made between them by creating various graphics and tables. In the analysis of the data, the findings obtained in the study were evaluated using the arithmetic mean, standard deviation (s), percentage (%) among the descriptive statistical methods. SPSS (Statistical Package for Social Sciences) 20.0 For Windows software was used in the analyses.

In the study, firstly, normality distribution coefficients were examined to determine whether the data points obtained from the "Technology Literacy Scale", "Managerial Strength Scale" showed normal distribution or not. Normal distribution of data is required to perform parametric tests. In this study, Kolmogorov-Smirnov Test was used to test the normality of data distribution. Kolmogorov-Smirnov Test is used when the group size is greater than 50 A p <0.05 value obtained from the Kolmogorov-Smirnov Test indicates that the data are not normally distributed; A p> 0.05 has been interpreted as the data distributed normally For the comparison of scale items and variance in paired groups (gender), parametric t-test and ANOVA test for multiple groups (age, seniority, occupation, educational status) were used.

3. Recent Finding

Findings Regarding the Relationship Between the Impact of the Pandemic on the Construction Sector and Demographic Variables. In Table 3, the analysis of the study was made by gender

Table 3. Analysis of the research by gender

	Gender	n	Average	SS	t	p
Epidemic Measures	Male	20	3.08	.97	2.20	.071
	Female	136	3.50	.76		
Economics	Male	20	2,07	.57	6.96	.369
	Female	136	3.02	.57		
Laboure conditions	Male	20	2.85	.98	3.51	.114
	Female	136	3.52	.76		
State assistance	Male	20	2.76	.90	3.03	.061
	Female	136	3.23	.59		
Unemployment	Male	20	1.71	.67	7.07	.109
	Female	136	2.99	.76		

When Table 3 is examined, the effect of the pandemic on the construction sector does not differ significantly in terms of gender in the dimension of pandemic measures (p = 0.071, t = 2.20) The average of the female participants is at the I agree level ($\bar{x}$ = 3.08) and the average of the male participants is partially at the level of agree ($\bar{x}$ = 3.50). Gender does not cause a significant difference again in the economy sub-height (p = .369, t = 6.96). The average of the female participants is at the level of disagree ($\bar{x}$ = 2.07), and the average of the male participants is at the level of undecided ($\bar{x}$ = 3.02). Working conditions sub-dimension did not differ significantly in terms of gender (p = .114, t = 3.51). The average of the female participants is at the undecided level ($\bar{x}$ = 2.85), and the average of the male participants is at the level of agree ($\bar{x}$ = 3.52). The state support sub-dimension does not differ significantly in terms of gender (p = .061, t = 3.03). The average of the female participants is at the undecided level ($\bar{x}$ = 2.76), the average of the male participants is at the level of agree ($\bar{x}$ = 3.23). The unemployment sub-dimension does not differ significantly in terms of gender (p = .109, t = 7.07). The average of the female participants is at the level of disagree ($\bar{x}$ = 1.71), and the average of the male participants is at the level of undecided ($\bar{x}$ = 2.99). In table 4 the analysis of the study was researched by groups.

Table 4. Analysis of the research by different education group

	Sources of Variation	Sum of Squares	Sd	Quadratic Mean	f	Significance Level
Epidemic Measures	Between groups Within groups Total	3.570 96.810 100.380	2 153 155	1.78 .633	2.82	.063
Economics	Between groups	9.589	2	4.795	12.751	.000
	Within groups	57.533	153	.376		
	Total	67.122	155			
Laboure conditions	Between groups	6,475	2	3.238	4.981	.008
	Within groups	99.450	153	.650		
	Total	105.926	155			
State assistance	Between groups	1.842	2	.921	2.165	.118
	Within groups	65.101	153	.425		
	Total	66.943	155			
Unemployment	Between groups	24.640	2	12.320	20.525	.000
	Within groups	91.835	153	.600		
	Total	116.476	155			

As a result of the responses of the participants to the scale of the impact of the pandemic on the construction sector in Table 4, there is no significant difference between the pandemic measures sub-dimension and the educational status (F = 2.82, p <.05). It shows a significant difference between the economics sub-dimension and educational status (F = 12.75, p <.05). Tukey test was applied to understand from which educational status this difference arises. According to the results of the Tukey test, the averages of the participants with a postgraduate degree are higher than the participants with an associate degree. There is a significant difference in terms of working conditions sub-dimension and educational status (F = 4.98, p <.05). Tukey test was applied to understand from which educational status this difference arises. According to the results of the Tukey test, the averages of undergraduate graduate participation are lower than the average of the graduate graduates. There is no significant difference between the sub-dimension of state support and educational status (F = 2.16, p <.05). It shows a significant difference in terms of unemployment sub-dimension and educational status (F = 4.98, p <.05). Tukey test was applied to understand from which educational status this difference arises. According to the results of the Tukey test, the averages of the participants with a postgraduate degree are higher than the graduates of the undergraduate and graduate departments. In table 5 the analysis professional of the study was researched by groups.

Table 5. Analysis of the research by different groups

	Sources of Variation	Sum of Squares	Sd	Quadratic Mean	f		Significance Level
Epidemic Measures	Between groups Within groups Total	3.327 97.053 100.380	2 153 155	1.663 .634	2.62		.076
Economics	Between groups	97,053	153	6,870	19,690		.000
	Within groups	100.380	155	.349			
	Total	13.740	2				
Laboure conditions	Between groups	53.383	153	5.454	8.783		.000
	Within groups	67.122	155	.621			
	Total	10.909	2				
State assistance	Between groups	95.017	153	1,770	4.272		.016
	Within groups	105.926	155	.414			
	Total	3.41	2				
Unemployment	Between groups	63.403	153	18.469	35.529		.000
	Within groups	66.943	155	.520			
	Total	36.939	2				

As a result of the responses of the participants to the scale of the impact of the pandemic on the construction sector in Table 5, the sub-dimension of pandemic measures does not show a significant difference in terms of occupation variable (F = 2.62, p <.05). Economics sub-dimension shows a significant difference in terms of the profession (F = 18.69, p <.05). Tukey test was applied to understand which profession caused this difference. According to the results of the Tukey test, the average of the participants working as technicians is lower than the other participants. Working conditions sub-dimension shows a significant difference in terms of the profession (F = 8.78, p <.05). Tukey test was applied to understand which profession caused this difference. According to the results of the Tukey test, the average of the participants working as technicians is lower than the other participants. The state support sub-dimension shows a significant difference in terms of the profession (F = 4.27, p <.05). Tukey test was applied to understand which profession caused this difference. According to the results of the Tukey test, the average of the participants who are working as interns is lower than the other participants. The unemployment sub-dimension shows a significant difference in terms of occupation (F = 35.52, p <.05). Tukey test was applied to understand which profession caused this difference. Tukey test was applied. According to the results of the Tukey test, the average of the participants working a technician is lower than the other participants. In table 6 the analysis professional of the study was researched by groups.

Table 6. Analysis of professional the research by different groups

	Sources of Variation	Sum of Squares	Sd	Quadratic Mean	f	Significance Level
Epidemic Measures	Between groups Within groups Total	3.327 91.114 100.380	4 151 155	2,316 .603	3.83	.075
Economic	Between groups	15.608	4	3.902	11.438	.090
	Within groups	51.514	151	.341		
	Total	67.122	155			
Laboure conditions	Between groups	11.753	4	2.938	4,711	.001
	Within groups	94.172	151	.624		
	Total	105.926	155			
State assistance	Between groups	6.978	4	1.745	4.393	.072
	Within groups	59.965	151	.397		
	Total	66.943	155			
Unemployment	Between groups	37.937	4	9.484	18.234	.000
	Within groups	78.539	151	.520		
	Total	116.476	155			

As a result of the responses of the participants to the scale of the impact of the pandemic on the construction sector in Table 6, the sub-dimension of pandemic measures does not show a significant difference in terms of seniority variable (F = 3.83, p <.05). The economy sub-dimension does not show a significant difference in terms of seniority (F = 11.43, p <.05). Working conditions sub-dimension shows a significant difference in terms of seniority (F = 4.71, p <.05). Tukey test was applied to understand from which seniority interval this difference arises. According to the results of the Tukey test, the averages of the participants in the 0-4 years seniority range are lower than the average of the participants in the 11-15 years seniority range. The state support sub-dimension does not show a significant difference in terms of seniority (F = 4.39, p <.05). The unemployment sub-dimension shows a significant difference in terms of seniority (F = 18.23, p <.05). Tukey test was applied to understand from which seniority interval this difference arises. Tukey test was applied. According to the results of the Tukey test, the average of the participants in the 0-4 years seniority interval is lower than the participants in the other seniority interval. In table 7 the analysis seniority of the study was researched by groups.

Table 7. Analysis of seniority the research by different groups

	Sources of Variation	Sum of Squares	Sd	Quadratic Mean	f	Significance Level
Epidemic Measures	Between groups	5.724	3	1.908	3.064	.030
	Within groups	94.657	152	.623		
	Total	100.380	155			
Economics	Between groups	31.260	3	10. 420	44.166	.000
	Within groups	35.862	152	.236		
	Total	67.122	155			
Laboure conditions	Between groups	17.723	3	5.908	10. 180	.000
	Within groups	88.203	152	.580		
	Total	105.926	155			
State assistance	Between groups	5.162	3	1.721	4.233	.007
	Within groups	61.781	152	.406		
	Total	66.943	155			
Unemployment	Between groups	90.157	3	30.052	173.568	.000
	Within groups	26.318	152	.173		
	Total	116.476	155			

As a result of the responses of the participants to the scale of the impact of the pandemic on the construction sector in Table 7, the sub-dimension of pandemic measures shows a significant difference in terms of the age variable (F = 3.06, p <.05). According to the results of the Tukey test conducted regarding the source of this difference; The averages of the participants aged 44 and over are higher than those between the ages of 20-27. The economy sub-dimension shows a significant difference in terms of age (F = 44.16, p <.05). Tukey test was applied to understand from which age range this difference arises. According to the results of the Tukey test, the average of the participants between the ages of 20-27 is lower than the other age groups. Working conditions sub-dimension shows a significant difference in terms of age (F = 10.18, p <.05). Tukey test was applied to understand from which age range this difference arises. According to the results of the Tukey test, the averages of the participants between the ages of 20-27 are lower than the averages of the participants between the ages of 36-43 and 44 and over. State support sub-dimension shows a significant difference in terms of age (F = 4.23, p <.05). Tukey test was applied to understand from which age range this difference arises.

According to the results of the Tukey test, the averages of the participants aged 44 and over are higher than the participants between the ages of 20-27. The unemployment sub-dimension shows a significant difference in terms of age (F = 173.56, p <.05). Tukey test was applied to understand from which age range this difference arises. Due to the results of the Tukey test, the averages of the participants between the ages of 20-27 are lower than the averages of the other participants.

4. Conclusion
By Turkey in the sector of shocks should be reconstructed employment considering the sensitivity and education policy in the country, the inclusion in the role of providing financing in these areas of employment policies and public sector are expected to increase the effectiveness of doubt macroeconomic policy. This pandemic of the Covidien-19 works in Turkey, especially during the short-term effects of changes in the industry and construction sector will then be a source for measures to be taken.

Analyzing the effects of the pandemic in the short, medium and long term with new research at both macroeconomic and sectoral level will be of great importance in terms of understanding the impact mechanisms of this process that affects all segments of the economy.

When examined in general, according to the findings, the areas that continue with the application are experiencing difficulties in this sense. Materials could not be procured. The workers could not work at full capacity. Necessary occupational health measures could not be taken. It was stated that unemployment is increasing and a new job area has not been created. With the increasing anxiety of people, different problems have arisen. Due to this natural abrupt process, tenders have been extended and it has been revealed that some companies have difficulties. People with shifted priorities have tried to pay more attention to nutrition and health.

In this context, the priority of the implementation of sector-specific policies in the economy, and the emphasis on digital transformation in the medium and long-term, especially in the industry, manufacturing, retail trade and service sectors, can alleviate the sectoral effects in possible epidemics, and strengthening and encouraging remote work opportunities in these sectors will reduce the fragility in the sectors and it is thought that employment losses in these sectors will be prevented.

In the light of the research, the decrease in the share of the working group from the national income during the pandemic, the decrease in wages, the increase in unemployment and the contraction of capital reflected economic problems. In this context, it is emphasized that institutional opportunities such as transfers in the short term and basic income system and family insurance should be strengthened in the long term in order not to worsen the income inequality conditions of those who do not have access to financial markets. By improving standards in construction project and cost management and applying new technologies, construction can play an important part in economic recovery from the coronavirus. The sessions in the Working Week examine problems and potential solutions in construction investment and delivery and link new technologies to these potential solutions in a pragmatic way. Longer term, these improvements will allow construction to contribute meaningful to the attainment of sustainable development goals and which will remain a problem long after the pandemic has abated.

Refences

Araya, F., (2021a). Modeling Working Shifts in Construction Projects Using an Agent-Based Approach to Minimize the Spread of COVID-19. Journal of Building Engineering 41 doi: 10.1016/j.jobe.2021.102413.

Araya, F., (2021b). Modeling the Spread of COVID-19 on Construction Workers: An Agent-Based Approach. Safety Science 133 (September 2020). doi: 10.1016/j.ssci.2020.105022.

Aslan, M., T., Aslan, I., O., Özdemir. O., (2020). COVID-19 (Yeni Tip Koronavirüs) Günlerinde Dahi Anne Sütü Yine Çok Önemli!" Journal of Biotechnology and STtrangeic Health Research 1 (April). Journal of Biotechnology and Strategic Health Research: 111–115. doi:10.34084/bshr.721702.

Barua, S.,. 2020. Archive Understanding Coronanomics: The Economic Implications of the Coronavirus (COVID-19) Pandemic Understanding Coronanomics: The Economic Implications of the Coronavirus (COVID-19) Pandemic.

COVID-19 STRATEGY UPDATE. 2020. https://www.who.int/docs/default-source/coronaviruse/covid-strategy-update-14april2020.pdf.

Domenico, C., Vanelli. M., (2020). WHO Declares COVID-19 a Pandemic. Acta Biomedica.. 91. Mattioli 1885. doi:10.23750/abm.v91i1.9397.

Dev, S. M., Sengupta, R., (2020). Covid-19: Impact on the Indian Economy. Indian Journal of Labour Economics 63 (October). Springer: 105–111. doi:10.1007/s41027-020-00264-z.

Diao, X., Nilar A., Wuit Y. L., Zone P, P., Thurlow J. (2020). Assessing the Impacts of COVID-19 on Myanmar's Economy: A Social Accounting Matrix (SAM) Multiplier Approach. doi:10.2499/p15738coll2.133745.

Doğan, Y., Doğan S., (2020). Koronavirüs Pandemisi ve Türkiye'de Bitkisel Üretime Etkisi. Artuklu Kaime International Journal of Economics and Administrative Researches Y.2020. Vol. 3. https://dergipark.org.tr/en/pub/artuklu/729961.

Duddu P., (2020). Iran Coronavirus (Covid-19): Updates on the Outbreak, Measures & Impact. https://www.pharmaceutical-technology.com/features/iran-coronavirus-covid-19-death-toll-cases-ncov-measures-impact/.

Dyer, O., (2020). Trump Claims Public Health Warnings on Covid-19 Are a Conspiracy against Him. BMJ (Clinical Research Ed.) 368 (March). NLM (Medline): m941. doi:10.1136/bmj.m941.

Ellison, G. (2020). Implications of Heterogeneous SIR Models for Analyses of COVID-19. Cambridge, MA. doi:10.3386/w27373.

Evelina, J, Nuugulu S, Julius L H. (2020). Estimating the Economic Impact of COVID-19: A Case Study of Namibia, April.

Fornaro, L, Martin Wolf. (2020). Covid-19 Coronavirus and Macroeconomic Policy." Economics Working Papers. Department of Economics and Business, Universitat Pompeu Fabra. https://ideas.repec.org/p/upf/upfgen/1713.html.

García-Alberti, M, Fernando S, Isabel C, Juan C. (2021). Challenges and Experiences of Online Evaluation in Courses of Civil Engineering during the Lockdown Learning Due to the COVID-19 Pandemic. Education Sciences 11 (2). MDPI AG: 59. doi:10.3390/educsci11020059.

Ghebreyesus, T. A. 2020BC. "WHO Director-General's Opening Remarks at the Media Briefing on COVID-19 - 25 March 2020." Ghebreyesus, T. A.

Guo, Yan Rong, Qing Dong Cao, Zhong Si Hong, Yuan Yang Tan, Shou Deng Chen, Hong Jun Jin, Kai Sen Tan, De Yun Wang, and Yan Yan. 2020. "The Origin, Transmission and Clinical Therapies on Coronavirus Disease 2019 (COVID-19) Outbreak- A n Update on the Status." Military Medical Research. BioMed Central Ltd. doi:10.1186/s40779-020-00240-0.

Hamins-Puertolas, A., Kurz C. (2020). Tracking Labor Market Developments during the COVID-19 Pandemic: A Preliminary Assessment. Finance and Economics Discussion Series 2020 (030). Board of Governors of the Federal Reserve System. doi:10.17016/feds.2020.030.

Indranil C., Maity. P., (2020). COVID-19 Outbreak: Migration, Effects on Society, Global Environment and Prevention. Science of the Total Environment 728 (August). Elsevier B.V.: 138882. doi:10.1016/j.scitotenv.2020.138882.

Ivanov, Dmitry, and Alexandre Dolgui. 2020. "Viability of Intertwined Supply Networks: Extending the Supply Chain Resilience Angles towards Survivability. A Position Paper Motivated by COVID-19 Outbreak." International Journal of Production Research 58 (10). Taylor & Francis: 2904–2915. doi:10.1080/00207543.2020.1750727.

Jaya S, S. 2020. "COVID-19: An Overview of Economic Waves on Indian Economy." Shanlax International Journal of Economics 8 (3). Shanlax International Journals: 114–119. doi:10.34293/economics.v8i3.3201.

Karakaş M. 2021. "Covid-19 Salgınının Çok Boyutlu Sosyolojisi ve Yeni Normal Meselesi." İstanbul Üniversitesi Sosyoloji Dergisi 40 (1): 541–573. Accessed May 3.

doi:10.26650/SJ.2020.40.1.0048.

Karakaya, E, İklim Değişikliği, and Enerji Uzmanı. 2021. COVID-19 Krizinin Ekonomi, Enerji ve Emisyonlara Etkileri: Mevcut Durum ve Olası Post-Corona Senaryoları. Accessed May 3. https://www.iklimhaber.org/covid-19-krizinin-ekonomi-enerji-ve-emisyonlara-etkileri-mevcut-durum-.

Koyuncu, T., Meçik O. (2020). COVİD-19 Pandemics of Sectoral and Cross-Sectoral Effects on Economic Growth in Turkey . Ankara. http://www.is-be.org/Content_Files/Content/ISBE2020 Proceeding.pdf.

,
Manderson, L, Susan L., (2020). COVID-19, Risk, Fear, and Fall-Out." Medical Anthropology: Cross Cultural Studies in Health and Illness. Taylor and Francis Inc. doi:10.1080/01459740.2020.1746301.

Rahimi, R., (2014). The Effect of Using Different Rock Failure Criteria in Wellbore Stability Analysis. http://scholarsmine.mst.edu/masters_theses.

Reyad, O., (2020). Novel Coronavirus COVID-19 Strike on Arab Countries and Territories: A Situation Report I. ArXiv. arXiv.

UNCTAD. 2020. "How COVID-19 Is Changing the World : A Statistical Perspective." Committee for the Coordination of Statistical, 1--90. https://unstats.un.org/unsd/ccsa/%0Ahttps://unstats.un.org/unsd/ccsa/documents/covid19-report-ccsa.pdf.

Valtonen, M, Matti W, Tytti V, Erkki E, Antti J. H, Katja M., Wilma G., Olli J. H., Olli R. (2019). Common Cold in Team Finland during 2018 Winter Olympic Games (PyeongChang): Epidemiology, Diagnosis Including Molecular Point-of-Care Testing (POCT) and Treatment. British Journal of Sports Medicine 53 (17). BMJ Publishing Group: 1093–1098. doi:10.1136/bjsports-2018-100487.

Vasiev, M., Kexin B., Artem D., Vladimir B., (2020). How COVID-19 Pandemics Influences Chinese Economic Sustainability. Foresight and STI Governance (Foresight-Russia till No. 3/2015) 14 (2). National Research University Higher School of Economics: 7–22. https://ideas.repec.org/a/hig/fsight/v14y2020i2p7-22.html.

Wang, C., Riyu P., Xiaoyang W., Yilin T., Linkang X., Cyrus S, Roger C. (2020). Immediate Psychological Responses and Associated Factors during the Initial Stage of the 2019 Coronavirus Disease (COVID-19) Epidemic among the General Population in China. International Journal of Environmental Research and Public Health 17 (5). MDPI AG: 1729. doi:10.3390/ijerph17051729.

Wells, P., Wessam A., Stephen P., Anthony B., (2020). A Socio-Technical Transitions Perspective for Assessing Future Sustainability Following the COVID-19 Pandemic. Sustainability: Science, Practice, and Policy 16 (1). Taylor & Francis: 29–36. doi:10.1080/15487733.2020.1763002.

Zhang, Xiaofeng, Huanyun Yu, Fangbai Li, Liping Fang, Chuanping Liu, Weilin Huang, Yanhong Du, Yemian Peng, and Qian Xu. 2021. "Covid 19 and Retuen to Work for the

Construction Sector: Lessons from Singapore." Science of the Total Environment. Occupational Safety and Health Research Institute, 136204. doi:10.1016/j.shaw.2021.04.001.

Sustainable thinking, educational opportunities in interior architecture projects

Munteanu Angela[1*]

Abstract: The current ecological situation in the world has become a catastrophic problem, and sustainability can provide many opportunities to protect and save the world. The primary concern of mankind must be the rational use of natural resources in protecting the environment and for the benefit of future generations, one of the major challenges of our time. Therefore, an approached thinking of the existentialism of humanity to solve the objectives, can be intervened through institutional educational projects in various fields, including interior architecture, offering solutions for recycling and reuse of different materials, and technologies for transformation into objects of furniture, lighting fixtures, wall finishes, floors, etc.Thus, the method of sustainability is an example to follow, which offers many opportunities to protect and save the environment. The architecture of residential and non-residential interior space is the field of application through sustainable and effective design methods of recycling, reuse, reorganization, in a comfortable space. Thus, we get more spacious, brighter, healthier interiors through materials that regain a new utility. Sustainable theoretical and practical research models reflect results in the design of engineering products, sustainable design, which ensures an impact on future generations of specialists - architects, engineers, and interior designers, with a sustainable vision of the environment and the future of humanity.

Keywords: : interior architecture, sustainability, design, recycled materials

1. Today's reality

For centuries, the Earth has changed beyond recognition. The air has become poisoned by emissions. Even ecologically clean areas and regions are no longer the same as they were a few centuries ago. Impurities will be present almost everywhere. Today we are facing multiple ecological problems: environmental pollution, floods, and fires that devastate everything around us, global warming which leads to a global disaster. Thus, the destruction of nature as a result of climate change is the most pressing problem facing humanity. The problem affecting today's world, demonstrated by scientific research, is that humans are responsible for global climate change. Through a prompt approach and thinking of rational use of natural resources, stopping harmful emissions, reducing energy consumption, recycling, and reuse, etc., we can save the future of generations [1; 6].

2 Consciously approached thinking

[1] Technical University of Moldova, Faculty of Urbanism and Architecture, Department of Architecture, Chisinau, Moldova

* Corresponding author: angela.munteanu@arh.utm.md

Therefore change starts with us! Why throw away and pollute nature if it is possible to reduce the impact, reuse and recycle - the result of sustainability! Sustainability is the ability to exist and develop without depleting natural resources for the future. And sustainable development is the impetus that meets the needs of the present without compromising the ability of future generations to meet their own needs. Earth's resources are finite and should therefore be used conservatively and carefully to ensure that they are sufficient for future generations without diminishing the quality of life today. A sustainable society must be socially responsible, focusing on environmental protection and dynamic balance in human and natural systems. Sustainability offers many opportunities to protect and save the world. [2].

2.1 Education and sustainable approach

SUSTAINABLE education through existentialist thinking and approach, healthy for a sustainable and bright future starts in college. The principles of the existentialism of contemporaneity and the environment, are manifested in the sense that it puts the destiny of humanity in the hands of itself. Starting from the famous observation of the French philosopher, Rene Descartes - "I think, so I exist" is a current issue, focused on a lived experience of thought, senses, actions in becoming a responsible human being for the environment. [3].

Table 1. Eco-design principles

	Low impact materials: the use of non-toxic materials, durable or recycled products, which require little energy for processing;
	Energy efficiency: the use of manufacturing processes and the production of products that require less energy;
Eco design principles	***Quality and durability:*** products that last longer and work better will need to be replaced less often, reducing the impact of replacements;
	Design for recycling: „ Products, processes and systems should be designed for performance in a "life beyond" commercial ";
	Renewability: materials should come from nearby renewable sources (local or bioregional), sustainably managed, which can be composted when their usefulness has been exhausted;

Sustainable design also includes social considerations: occupational safety and health; utility; responsible social use; the origin of the materials; design according to human needs. Sustainable design is the philosophy of designing physical objects, the built environment, and services to respect the principles of social, economic, and ecological sustainability. Namely, through the interior architecture, we can intervene with the principles of sustainability, by designing spaces and using intelligent and economical lighting systems, with many windows to provide natural lighting during the day, and the use of materials and furniture by reuse.

Eco-innovation, creativity is any innovation that leads to significant progress and the goal of sustainable development. Ecodesign supports the need to incorporate environmental and sustainability criteria into the basic requirements of product design, such as cost, function, utility, aesthetics, reliability, safety, etc. (tab. 1) [4; 5].

Thus, together with the student-architects, year V from the Technical University of Moldova, Faculty of Urbanism and Architecture, Architecture department, within the course unit: Interior

space architecture, we both researched and approached the topic of ecodesign, through recycling and reuse, through creative thinking in the elaboration of objects for interior architecture. Event of the Institutional Project, highly publicized by the media (TV, press, radio, news portals on the Internet, etc.), presented in several Scientific-Practical Seminars (2019, first edition, 2021, second edition), which each this time gathers more and more public, interested in the issue of sustainability [8; 9].

Figure 1. Cionanu Jana, Iordan Ana-Lucia, st. gr. ARH-161, UTM, FUA, Architecture department. Living room table, made of recycled wood

Examples of sustainability are student works, transformable and functional furniture, lighting objects made from recycled materials: cardboard sheets and tubes, wood material (plywood, construction wood, old or degraded furniture), envelopes, old objects, metal, etc. . For example - the wood used for multiple purposes and shapes, forests, represent the lungs of the earth, affected today. The most important use in the world is fuel. Wood is also used as a building material in the architecture of wooden houses, bridge industry, railway sleepers, furniture, parquet, various interior design elements. But it is often the case of mass deforestation, and the impact is imminent on the environment: intensifying the processes of soil erosion; droughts are becoming more frequent; impoverishment of flora and fauna leading to global warming; intensification of landslides [5; 6; 7].

Figure 2. Malanici Maria, st. gr. ARH-162, UTM, FUA, Architecture department. Sustainable lighting fixture

To avoid harmful problems, it can present an approach by recycling and reusing garden crates and wooden pallets, to create a table for the living room, made of four elements with storage spaces that aesthetically complete the space in a harmony of chromatic contrast, work by the authors, students gr. ARH-161, Architecture department, UTM, FUA Cionanu Jana, Iordan

Ana-Lucia (fig. 1). A lamp that mimics the shape of the human body, made of solid wood, can be comfortable and can serve as a support for a book or phone, is the work of student gr. ARH-162, Malanici Maria (fig. 2). Thus, as the authors mention - art is contemplation, it is the pleasure of the mind that seeks in nature and describes the spirit with which Nature itself is animated ...

Figure 3. Iordan Ana-Lucia, st. gr. ARH-161, UTM, FUA, Architecture department. Project with sustainable furniture
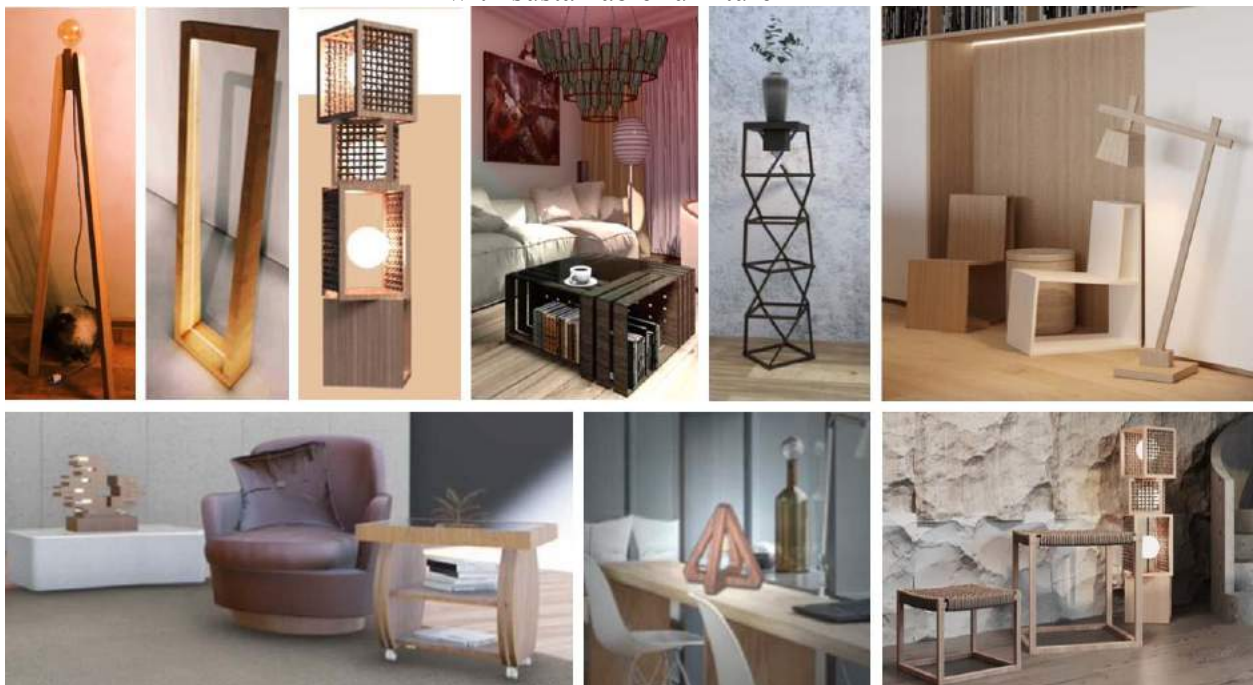
Figure 4. Furniture models, sustainable lighting objects, presented at the Scientific-Practical Seminar eco-design, developed by architecture students, DA, FUA, UTM

The final results of the project, models of utilitarian and functional objects, aesthetically defined by finishes, framed in residential and non-residential spaces developed within the

interdisciplinary project "Urban Metamorphosis of 31 AUGUST 1989, Chisinau" and kept in the EXPO hall of the FUA and the museum Department of Architecture (fig. 3, 4) [10].

Student satisfaction is culminated by the desire of the theme approached for the recycling and reuse of unnecessary objects and things, not to be thrown in nature. The educational message of the Project is addressed to the academic environment and society for recycling and reuse, each contributing through healthy thinking, behavior for a healthy environment of our planet Earth!

> *... What human needs is not only the persistent questioning of the final questions, but the sense of what is feasible, of what is possible, of what is right, here and now ...*
> /Hans-Georg Gadamer, Truth and method /

3. Conclusions

In conclusion, we mention that the architecture of the residential and non-residential interior space is the field through which we can manage and educate sustainability in the academic and social environment, through our own examples of recycling and reuse.

Following the elaboration of these projects, we notice that there are no non-recyclable materials. Various materials can be combined to obtain original and interesting objects for interior architecture. Such an approach can lead to both technological and economic progress. Through work and creation, we achieve pleasant goals, both in terms of aesthetics and quality

References

1. Aloone M., Bey, N., (2009). Improving the environment through product development - guide, Danish EPA, Copenhagen Denmark, ISBN 978-87-7052-950-1, 46 p.
2. Benyus J., (1997). Biomimicry: Innovation Inspired by Nature. New York, USA: William Morrow & Company. ISBN 978-0-688-16099-9.
3. Descartes R., (1701). Regulae ad directionem ingenii, Amsterdam.
4. Kant I., (2008). Observations on the feeling of beauty and sublime, translated by Rodica Croitoru, All Publishing House, Bucharest, ISBN 5-322-00020-8, 120 p.
5. Lindahl M., (2003). Designer's use of environmentally friendly and sustainable methods. Progress of the first international workshop on "Sustainable Consumption", Tokyo, Japan, Non-Traditional Technology Society (SNTT) and the Life Cycle Assessment Research Center (AIST).
6. Shedroff N., (2010). Design is the problem: the future of design must be sustainable. Design Journal: vol 13, nr. 1.
7. What is sustainability - https://www.twi-global.com/locations/romania/ce-facem/intrebari-frecvente-faq/ce-este-sustenabilitatea (visited 09.05.2021).
8. Sustainability - Wikipedia, the free encyclopedia, https://ro.wikipedia.org/wiki/Sustenabilitate (visited 25.06.2021).
9. World Recycling Day https://utm.md/blog/2021/03/22/fua-utm-a-marcat-ziua-reciclarii-mondiale-prin-seminarul-eco-design/.
10. The interdisciplinary project Metamorphosis str. 31 august, Chisinau https://utm.md/blog/2021/01/27/studentii-arhitecti-ai-fua-utm-isi-propun-un-proiect-de-metamorfoza-urbana/.

Reducing the Estimation Error of the Measure of Proximity Between Objects in Pattern Recognition

Rahim Mammadov[1*], Gurban Mammadov[2], Sevinj Aliyeva[3]

Abstract: When similar or close objects are recognized in a report, the reliability of recognition becomes very low when the price of the measure of proximity between objects is close to the price of the resulting error. There are several reasons for this: The presence of a modular sign in the existing formulas for the assessment of the measure of proximity between objects; The correlation coefficient between the measurements is not taken into account (it is assumed that there is no) but the correlation exists; gross errors that appearing during measurements are not taken into account. To reduce random errors, it is necessary to carry out repeated measurements, which reduces the processing speed. İn the report suggests an algorithm for solving this problem. In this algorithm, the reference parameters are subjected to a large number of measurements in the training mode. The parameter of the researched object is measured in such a number that does not affect the speed of the system. During recognition, each measured parameter is compared with all measured values of the reference parameter. Thus, the number of repeated measurements is artificially increased enough. Since the comparison process is performed on a computer by software, it does not affect the speed of the system. In this case, errors caused by statistical processing, the correlation coefficient, the use of the modular sign in formulas, and gross error are eliminated, resulting in increased accuracy. This algorithm was simulated on a computer and the positive results were obtained. The distance between objects is decided by analyzing the range of change of parameters, not on the basis of Manhattan or other formulas. During separate measurements, 3 options are proposed, replacing the values of the lower, middle and upper limits of the range over which the current distances fall. The processing of the results showed that the proposed algorithm can significantly increase the accuracy of estimating the measure of proximity between objects in all three options. In this case, the speed of the system will not be affected.

Keywords: pattern recognition, recognition reliability, measurement errors, random errors, interval analysis, correlation coefficient.

1. Introduction

The efficiency of flexible automated production (FAP) and mobile robots (MR) largely depends on the reliability of the pattern recognition (PR) of the technical vision system (TVS), which is one of the main components giving them flexibility and adaptability [1-7]. The reliability of pattern recognition is determined by the accuracy of the estimation of the measure of proximity between objects, the features of which are determined by measurement. The errors allowed when measuring the values of the features of images, summing up

[1]Azerbaijan State Oil and Industry University, "Instrumentation engineering" department, Baku, Azerbaijan,
[2] Azerbaijan State Scientific-Research Institute for Labor Protection and Occupational Safety, Baku, Azerbaijan
[3] Azerbaijan Technical University, Baku, Azerbaijan
 * Corresponding author: rahim1951@mail.ru

according to the most complex law, create an error in assessing the measure of proximity between objects, which in the computer vision system is commensurate with the actual value of the distance between the features of objects [8-10]. Therefore, these errors, reducing the values of the reliability of image recognition, are a serious obstacle to the use of technical vision systems for the widespread introduction of flexible automated production and mobile robots [11,12].

2. Analysis of the current situation

Many works have been devoted to minimizing systematic errors in estimating the proximity measure between objects, and recommendations have been given to reduse them [13-15].

However, theoretical and experimental studies of errors in estimating the measure of proximity between objects show that these methods cannot significantly increase the accuracy of estimating of the final assessment to the fact that random errors associated with hidden influences and commensurate with the actual value of the measure of proximity between objects are large enough and minimize these errors are necessary. They arise due to the fact that the nature and function of the impact of these destabilizing factors on the occurrence of errors in estimating the measure of proximity between objects are somewhat different from our knowledge. For example, the transfer characteristic of the converter, contrary to our knowledge, may differ slightly from the linear one, and even in different areas these nonlinearities are different in value and direction. The current technique is not able to detect the nonlinearity of these.

To do this, it is necessary to analyze the sources of the occurrence of random errors, and it is important to eliminate them. In the search for methods to reduce random errors in estimating the measure of proximity between objects, various destabilizing factors were analyzed as sources of creating systematic and random errors.

The action of these factors creates additive, multiplicative, and higher-order errors. The latter, along with the existing destabilizing factors, which are either not identified, or their effect is difficult to take into account, or these actions individually are so small that they are not taken into account separately. However, these errors add up to create random errors in value and polarity, which are impossible to predict. Experiments have shown that random errors in measuring the values of the features of the recognized σ_x and the reference image σ_y are distributed according to the normal law. On the basis of these errors and the ρ - correlation coefficient between them, it is possible to find random errors in estimating the measure of proximity between objects, since the latter are a composition of the laws of distribution of random errors in measuring the values of features of the recognizable and reference images and should also be distributed according to the normal law. Whereas in the computer vision system all features are measured by one measuring device and under the same conditions, then when assessing the measure of proximity between objects, the random errors in measuring the values of individual features by subtracting should have significantly reduced the total error in assessing the measure of proximity between objects [13-16].

However, the presence of the modulus sign in the formulas for assessing the measure of proximity between objects has a negative impact on the formation of random errors in estimating the measure of proximity between objects. In this case, since errors with a negative sign become positive, the distribution of errors in estimating the measure of proximity between objects becomes truncated and the estimated value shifts to the positive direction. This disadvantage appears when the recognized and reference images are so close that their measure of proximity between objects is commensurate with the error in estimating its value. Since there are a lot of such cases in the practice of using the technical vision system, the additional error that appears, commensurate with the value of the standard deviation of the estimate of the measure of proximity between objects, makes a significant negative contribution to pattern recognition [17,18].

Therefore, when evaluating the measure of proximity between objects, its value is shifted to the right side by an indefinite amount, which makes the result incorrect and there is an error associated with the use of the modulus sign in formulas for evaluating the measure of proximity between objects. The displacement continues until the real value of the measure of proximity between objects becomes equal to or greater than the minimum of the differences between the values of individual features of the recognized and reference objects. Such real distributions of random errors in estimating the measure of proximity between objects is completely in the positive plane of the Euclidean metric. Therefore, the use of different methods and techniques to reduce the influence of these destabilizing factors does not have a significant effect. Thus, the direct reduction of random errors in the estimation of the measure of proximity between objects is necessary.

The use of traditional methods of statistical processing of measurement results using multiple measurements of the values of the features of patterns increases the time of pattern recognition, which is undesirable.

Therefore, the development of algorithms that use a certain number of repeated measurements of feature values, which does not reduce the capabilities of the computer vision system in terms of pattern recognition time, significantly reducing the level of random errors in estimating the measure of proximity between objects is actual [17-19].

3. Problem statement

It is known that scientific research is carried out not only on the Earth, but also by sending mobile robots to uninhabitable space, underwater and other planets. In order for the sent robots to adapt to the environment and perform the given tasks, it is important to first recognize the images. The main issue of reliability of image recognition is to find a match between images taken from real objects and reference images. But in some cases, it is impossible to get a reference images and to pass certain trainings, since it is impossible for a person to go to the listed places. At that time, the recognition operation is done only on the basis of the real images of the input. The reliability of the image recognition depends on the correct calculation of the measure of proximity between objects. Certain formulas (for example, Manhattan, Euclidean, Camberra, etc.) are used to find measure of proximity between objects in known recognition and control systems. These formulas are highly

integrated and all of them use modul sign. Because these formulas are integral, the characteristics of the individual values are not taken into account. The object is given an overall price. The modular sign also cuts its characteristic and leans in a positive direction. Therefore, it is not possible to determine the exact value of measure of proximity between objects.

The reliability of pattern recognition depends on the correct calculation of the measure of the proximity between objects. The more accurately we calculate the measures of the proximity between objects, the more accurate the results will be In addition, the following shortcomings lead to incorrect results using these formulas:The presence of a modular sign in the existing formulas for the assessment of the measure of proximity between objects;

1.   The correlation coefficient between the measurements is not taken into account (it is assumed that there is no) but the correlation exists;
2.   To reduce random errors, it is necessary to carry out repeated measurements, which reduces the processing speed;
3.   Gross errors that appearing during measurements are not taken into account.
   For these reasons, the processing of algorithms that use a certain number of repeat measurements of feature values, which do not reduce the capabilities of the technical vision system in terms of the duration of recognition of pattern, significantly reduce the level of random errors in the evaluation of the measure of proximity between objects is actualistic.

4. Problem solving

Modern development of nanotechnology, information technology and computers allows a more intelligent approach to estimating the size of proximity between objects, abandoning formulas, it possible the development of new methodologies for analyzing errors in measuring the values of each parameter of known and comparable images. In the presented report, an algorithm is proposed that achieves the solution of this issue. The algorithm is implemented as follows:

The input and reference parameters $\{ x_i | i = \overline{1,n} \}$ and $\{ y_i | i = \overline{1,n} \}$ are entered into the computer. The program method finds in the calculation of the numerical average, the standard deviation, the correlation coefficient and the final error of the measures of the proximity between objects values of the input and reference parameters [3,5].

According to the Manhattan formula, the input and reference parameters are checked for compatibility with each other [2]:

$$Z = \sum_{i=1}^n |x_i - y_i| \qquad\qquad (1)$$

Because σ_x and σ_y obey the normal distribution, σ_z will obey in the normal distribution the law. Therefore, it is necessary to find out in what part of this distribution the difference between the input and reference parameters falls. The difference between the input and reference parameters is $a = x_i - y_j$. x and y are measured in n times, it is usually checked with each value of y for each value of x. That is:

$$x_1 - y_1, \quad x_1 - y_2, \quad \ldots \quad x_1 - y_n$$
$$x_2 - y_1, \quad x_2 - y_2, \quad \ldots \quad x_2 - y_n$$
$$\ldots \qquad \ldots \qquad \ldots \qquad \ldots$$
$$x_n - y_1, \quad x_n - y_2, \quad \ldots \quad x_n - y_n$$

(2)

The difference - a is checked in the range a -3*σ_z - +3*σ_z by every $0.5 \cdot \sigma_z$ step ([-3*σ_z, -2,5*σ_z], [-2,5*σ_z, -2*σ_z], [-2*σ_z, -1,5*σ_z], [-1,5*σ_z, -σ_z], [-σ_z, -0,5*σ_z], [-0,5*σ_z, 0], [0, 0,5*σ_z], [0,5*σ_z, σ_z], [σ_z,1,5*σ_z], [1,5*σ_z,2*σ_z], [2*σ_z,2,5*σ_z] və [2,5*σ_z,3*σ_z]).

If a does not fall in the interval, the program checks whether it falls in other intervals. In the case of an interval falls, then as the price of a, the smallest price of the interval is accepted and sent to the total input and the possible deviations are minimized. In the measurement technique, errors are accepted up to ± 3*σ. Greater than it, is thrown like a gross error. Therefore, a's greater than $-3 \cdot \sigma_z$ and $+3 \cdot sz_0$ are not taken into account. Then the a's in the interval $[-3 \cdot \sigma_z, 0]$ and $[0, 3 \cdot \sigma_z]$ are collected and the average value is found by dividing by the number of measurements. The final values found in the general order by the Manhattan formula and found by the operation of our algorithm are given. We take the number of pre-measurements as NK instead of n. NK varies from 1 to n. It is interesting to us how the algorithm performs itself in the number of different measurements. That is, the result should actually be "0". Because the X and Y arrays are deliberately taken from the same in advance. They differ from zero simply because they came by mistake and were collected by the module sign. According to mathematical statistics, the greater the number of repeated measurements, the smaller the random errors. However, the presence of a modular sign in the formula greatly weakens this rule. Thus, the effectiveness of repeated measurements is lost. Therefore, the use of interval analysis, taking a relatively small number of repeated measurements, both slows down the speed of the recognition system, and has the appropriate accuracy, which is reflected in this program. It is better to say that the values of *zm (Manhattan) and zk (suggested)* in the algorithm are closer to the corresponding values obtained at the maximum value of *n*.

The proposed algorithm for estimating the size of proximity between objects was mathematical modeling in software on the computer. By replacing the value of the current parameter-*a* with the minimum (Table 1 and Figure 1), average (Table 2 and Figure 2) and maximum (Table 3 and Figure 3) values of the given interval, the program calculates the *zk* (*suggested*) values. Then the errors of the calculated values of *zm (Manhattan)* and *zk (suggested)* are calculated by repeating measurements once again the *NK* times.

First of all, when analyzing Table 1 and Figure 1 obtained at the minimum price of the current parameter-*a*, it appears that as a result of the proposed algorithm by performing repeated measurements *NK*, the random measurement error is smaller and can be considered the best among the options.

When taking the average value of the current parameter-*a* in the given interval, the results are very good and the accuracy increases significantly when the *NK* performs repeated measurements.

The results obtained in computer modeling are good when the current parameter-*a* receives the maximum value in that interval and much higher compared to in classical use.

Thus, as can be seen from the tables and figures, the result of the proposed algorithm is much higher than the results obtained by the classical method, and when using the proposed algorithm, the accuracy of the technical vision system increases significantly and the processing speed remains at the required level.

Table 1. The results obtained when the number of repeated measurements of the reference and input parameters is the same

NK	MZNK	ZM	ZK(min)	ZK(max)	ZK (orta)
1	9	9	8,74	13,11	10,92
2	4,5	4,5	6,55	10,92	7,1
3	-0,33	6,33	4,85	6,74	5,07
4	-2	6,5	4,37	5,94	4,61
5	-1,2	5,6	4,19	6,04	4,5
6	-4,33	8	5,58	6,87	6,23
7	-2	8,57	4,91	6,06	5,26
8	-1,5	7,75	4,58	5,9	4,96
9	-0,66	7,55	4,8	5,88	5,2
10	-0,1	7,3	4,42	6,21	4,87
11	-0,09	6,81	4,88	6,14	5,42
12	-0,33	6,67	4,67	6,29	5,23
13	-1,07	6,92	4,66	6,02	5,25
14	-0,93	6,5	4,3	6,11	5,05
15	-1,73	6,93	4,99	6,03	5,77
16	-1,125	7	4,63	5,68	5,42
17	-0,411	7,23	4,17	5,34	4,81
18	0	7,22	4,52	5,43	5,27
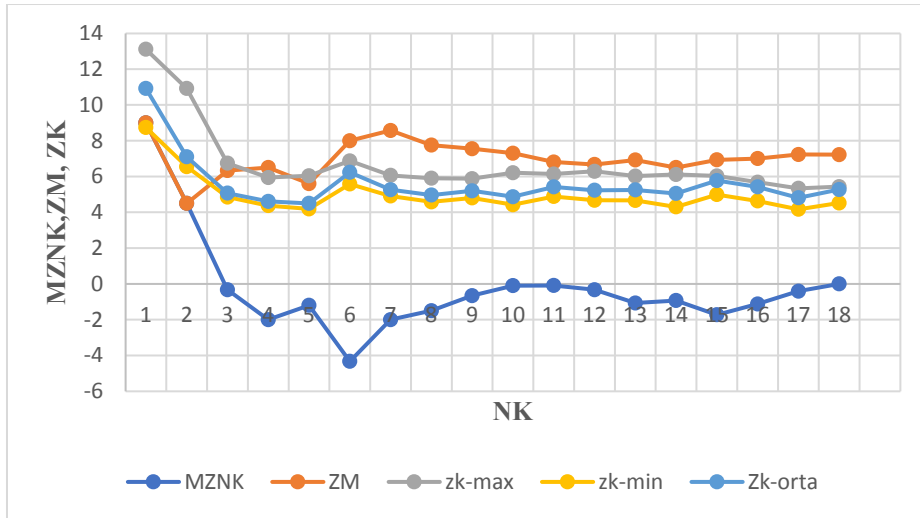
Figure 1. The results obtained when the number of repeated measurements of the reference and input parameters is the same

Table 2.Results obtained when the number of repeated measurements is different under time constraints

NK	zm (Manhattan)	zk_max	zk_orta	zk_min
1	9	8,01	5,820	3,640
2	4,5	7,28	5,340	3,400
3	6,33	7,77	5,780	3,800
4	6,5	7,65	5,640	3,640
5	5,6	7,57	5,560	3,540
6	8	7,36	5,480	3,600
7	8,57	7,25	5,390	3,530
8	7,75	7,19	5,290	3,400
9	7,55	7,12	5,240	3,370
10	7,3	7,09	5,220	3,350
11	6,81	7,19	5,320	3,440
12	6,66	7,2	5,310	3,420
13	6,92	7,32	5,410	3,510
14	6,5	7,32	5,400	3,480
15	6,93	7,41	5,480	3,560
16	7	7,36	5,440	3,530
17	7,23	7,34	5,430	3,520
18	7,22	7,31	5,400	3,490
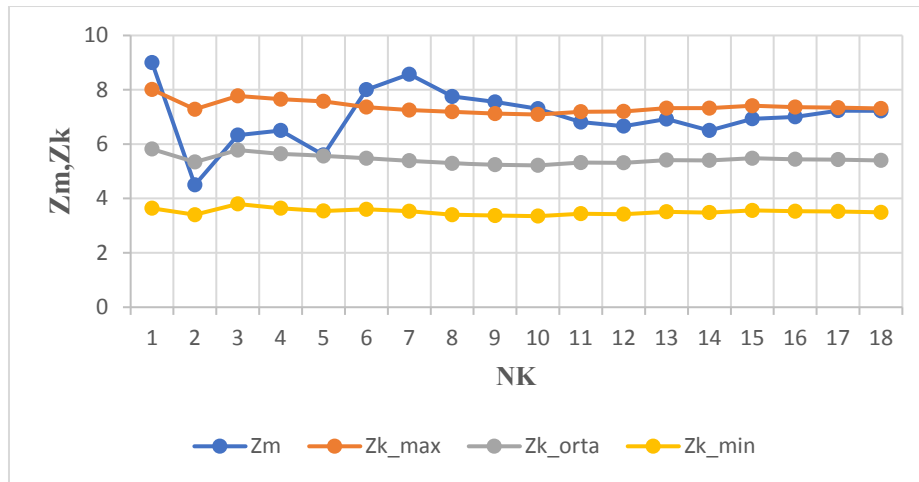
Figure 2. Results obtained when the number of repeated measurements is different under time constraints

5. Conclusion

It should be noted that since all these shortcomings have been eliminated, it is more expedient to use this methodology in recognition and control systems instead of the existing formulas. Thus, along with the elimination of shortcomings, there are a number of advantages. In this case, errors caused by statistical processing, the correlation coefficient, the use of the modular sign in formulas, and gross error are eliminated, resulting in increased accuracy. This algorithm was simulated on a computer and the results were obtained. The distance between objects is determined not by a formula, but by analyzing the range of changes in parameters. As can be seen from the mathematical analysis of the given graphs, the best option is to take the minimum of *a*, and the random error is reduced by 15-30%. The processing of the results showed that the proposed algorithm can significantly increase the accuracy of estimating the measure of proximity between objects. In this case, the speed of the system will not be affected.

References

1. Bastian Hartmann, Christoph Schauer and Norbert Link, "Worker Behavior Interpretation for Flexible Production," Engineering And Technology International Journal Of Industrial And Manufacturing Engineering, 2009, pp. 1224-1232.
2. Tushar Jain and Meenu, "Automation and Integration of Industries through Computer Vision Systems," International Journal of Information and Computation Technology, 2013, pp. 963-970.
3. Keith Jacksona, Konstantinos Efthymioua, John Borton, "Digital manufacturing and flexible assembly technologies for reconfigurable," Changeable, Agile, Reconfigurable & Virtual Production Conference, 2016, pp. 274-279.
4. F. Leighton, R. Osorio, G. Lefranc, "Modelling, Implementation and Application of a Flexible Manufacturing Cell," International Journal of Computers, Communications & Control, 2011, pp. 278-285.
5. Phansak Nerakae, Pichitra Uangpairoj, Kontorn Chamniprasart, "Using machine vision for flexible automatic assembly system," International Conference on Knowledge Based and Intelligent Information and Engineering Systems, 2016, pp. 428-435.

6. Petar Marić, "Computer Vision Systems For The Enhancement Of Industrial Robots Flexibility," Facta Universitatis, Ser. Mechanics, Automatic Control and Robotics, 2011, pp. 1-18.
7. Herakovic N., "Robot Vision in Industrial Assembly and Quality Control Processes," Robot Vision / Edited by Ales Ude, 2010, pp. 501-534.
8. Mammadov R.K., Mutallimova A.S., Aliyev T.Ch., "Ispol'zovaniye momentov inertsii izobrazheniya dlya invariantnogo k affinnym preobrazovaniyam raspoznavaniya," Vostochno-Yevropeyskiy zhurnal peredovykh tekhnologiy, 2012, pp. 4-7.
9. Caldwell D.G., "Robotics and automation in the food industry. Current and future technologies," Woodhead Publishing Limited, 2013, 523.
10. Siciliano B., Khatib. O., "Springer Handbook of Robotics," Springer-Verlag Berlin Heidelberg, 2008, 1628 p.
11. Vimal Sudhakar Bodke, Omkar S Vaidya, "Object Recognition in a Cluttered Scene using Point Feature Matching," International Journal for Research in Applied Science & Engineering Technology, 2017, pp. 286-290.
12. Toshiaki Ejima, Shuichi Enokida, Toshiyuki Kouno, "3D Object Recognition based on the Reference Point Ensemble," International Conference on Computer Vision Theory and Applications, 2014, pp. 261-269.
13. Mammadov R.K., Aliyev T.Ch., "Kontrol' polozheniya 3D-ob"yektov v gibkikh avtomatizirovannykh sistemakh. Povysheniye dostovernosti raspoznavaniya". LAP Lambert academic publishing, 2014, 90 p.
14. Мамедов.Р.К, Иманова.У.Г. Повышение достоверности принятия решений при распознавании образов, Электрон моделирование, Киев, 2014, т.36, №5, с.115-121.
15. Скачков В.В., Чепкий В.В.,и др. Минимизация доминирующей погрешности в задачах измерения информационных параметров «зашумленной» выборки сигнала, Information and Telecommunication Sciences, 2016, Volume 7, Number 2 Одесса, Украина , с.62-69.
16. Володин И.Н. Лекции по теории вероятностей и математической статистике. - Казань: (Издательство), 2006. - 271с.
17. Xiang Bai, Xingwei Yang, Longin Jan Latecki, "Detection and recognition of contour parts based on shape similarity," Pattern Recognition, 2008, pp. 2189-2199.
18. Konrad Schindler, David Suter, "Object Detection by Global Contour Shape," Pattern Recognition, 2008, pp. 3736-3748.
19. Mohammad Arafah, Qusay Abu Moghli, "Efficient Image Recognition Technique Using Invariant Moments and Principle Component Analysis," Journal of Data Analysis and Information Processing, 2017, pp. 1-10.

Hide Data In 24-Bit And 8-Bit Bmp and Tiff Files, Reading Confidential Data and Comparing with Image Quality Criteria According to Steganography Principles

Remzi Gürfidan[1][*], Ziya DİRLİK[2]

Abstract: Information hiding techniques are a subject area that all societies from the past to the present work on and care about. Steganography means " secret writing "in ancient Greek and is the name given to the science of concealing knowledge. Many different data hiding methods have been found and used in history and today. The biggest advantage of steganography over encryption is that a person who sees information cannot understand that what they see is important information. So, when people look at an object hidden inside them in the view of nature, they do not look for information in it. Moreover, an encrypted message attracts attention because of its mystery, even if it is difficult to solve. The carrier containing the confidential data is called stego. Although encryption methods are preferred in information protection methods, it has a significant advantage in that steganography can perform this function without attracting attention. In the study, different sizes of data are stored in Bmp and Tiff format image images. After that, the stego image and the original image were calculated by using different image quality.

Keywords: Steganography, Image Quality, Data Hiding, Confidential Data

1. Introduction

The confidentiality of information has been of great importance in the communications of persons in important positions of all kingdoms and states from the past to the present. For this reason, many different data hiding methods have been found and used from the earliest times to the present day. Steganography means " hidden writing "in ancient Greek and is the name given to the science of concealing knowledge. The biggest advantage of steganography over encryption is that a person who sees information cannot realize that what they see is important information, so when he looks at an object that is hidden in it, he does not look for information in it. However, an encrypted message attracts attention because of its mystery, even if it is difficult to solve (Narayana and Prasad, 2010, Seth and Ramanathan et al., 2010, Usha and Kumar et al., 2011). The carrier containing confidential data is called stego (Usha and Kumar et al., 2011,Koçak, 2015). Although encryption methods are preferred in information protection methods, steganography has a significant advantage due to its lack of attention (Gençoğlu, 2021).

If you need to explain exactly the purposes and methods of the science of steganography, it is useful to look at the most known examples from history to the present day. Covering the

[1] Isparta University of Applied Sciences, Yalvac TBMYO VHS, Isparta, Turkey
[*] Corresponding author: remzigurfidan@isparta.edu.tr

inscriptions engraved on wooden tablets in history with a candle can be considered the first example of steganography in history. After the hair of an agent who scraped the scalp and made a tattoo containing a secret message on the skin grew, the tattoo disappeared, and the agent took the desired message to the desired place without attracting attention. An example of the use of steganography is when a tortured prisoner opens and closes his eyes in accordance with Morse code. 2. during World War II, a Japanese agent sent American movements by hiding them among letters containing baby orders is one of the most beautiful striking examples of steganography in history. 2 again. during World War II, messages were transmitted those enemy forces, which seemed very ordinary in radio news, would bomb the city tomorrow. During World War I, Washington D.C. the German Embassy in Berlin sent two messages via telegrams to its headquarters in Berlin. If read instantly, the message does not give a meaningful idea of what the Germans are doing. Reading the first letter of each word in the first message or the second letter of each word in the second message gives confidential information about the entire message (https://e-bergi.com/y/veri-gizleme-bilimi/ Date: 17.07.2021, Johnson and Sushil, 1998).

Many different techniques have been used to store data. In a series of articles, methods such as storing information within certain rules, storing information through psychomotor movements in mutual communication, storing data in images, storing data in audio files were used. In this study, the method of storing data into visuals from communication methods performed using technological infrastructure was experimentally studied. In the details of the study, an attempt was made to store data in visual formats with bitmap and tiff extensions. The data stored in visual data is decoded and the data is compared to stego visual in terms of raw visual quality. This benchmarking was carried out using six different quality benchmarking criteria.

Zhang and Luo's study proposed a most significant bit (MSB) replacement-based high-capacity reversible data hiding method that could embed hidden messages into color images. In the study, our multiple MSB replacement-based technique performed better both in terms of data embedding rate and PSNR values of the restored images. Furthermore, it does not contain very complex calculations, and therefore it has performed very quickly in terms of computational complexity (Zhang and Luo, 2020). Kumar and colleagues conducted a study on Gray paintings similar to this study (Zhang and Luo, 2020). Here, there has been a highly imperceptible information hiding technique that uses the characteristics of MSBs of implicit image (CI) pixels. CI was initially grouped into two different segments. Later, segments, along with the MSBs of each pixel, were used to embed hidden bits into the LSBs of each pixel. The results of the study were compared with some high-quality existing techniques. From a comparison of various metrics, the proposed study has been shown to outperform other related studies (Kumar and Kumar et al., 2021).

2. Proposed Method

The first step is to choose the image in which the information will be stored, by the application user. 8-bit or 24-bit pixel format is determined by the application according to the quality of the selected picture. After this process, the size of the data that can be stored in the picture, the size of the header and the size of the picture in terms of bits, bytes are calculated. Afterwards, the message to be kept in the picture is entered by the user. The size of the entered message in bytes is displayed to the user. When the storage process is completed, the image with data embedded in it is presented to the user. The user can save this picture via the application to send it to someone else. The uploaded picture and the stored message regarding

the picture are shown in the left and middle part of Figure 1. The mentioned information hiding process is explained in detail in sections 2.1 and 2.2.

In the same application, it is in the section that reveals the message of the picture in which data is hidden. The data stored image is uploaded to the application by the user. The uploaded image is determined whether it belongs to 8-bit or 24-bit pixel format. With the initiation of the read process, the low bits of the picture are read, and the hidden message is revealed. Said reading process can be seen in the middle and right part of Figure 1. How the secret message on the picture is revealed is explained in detail in 2.3.
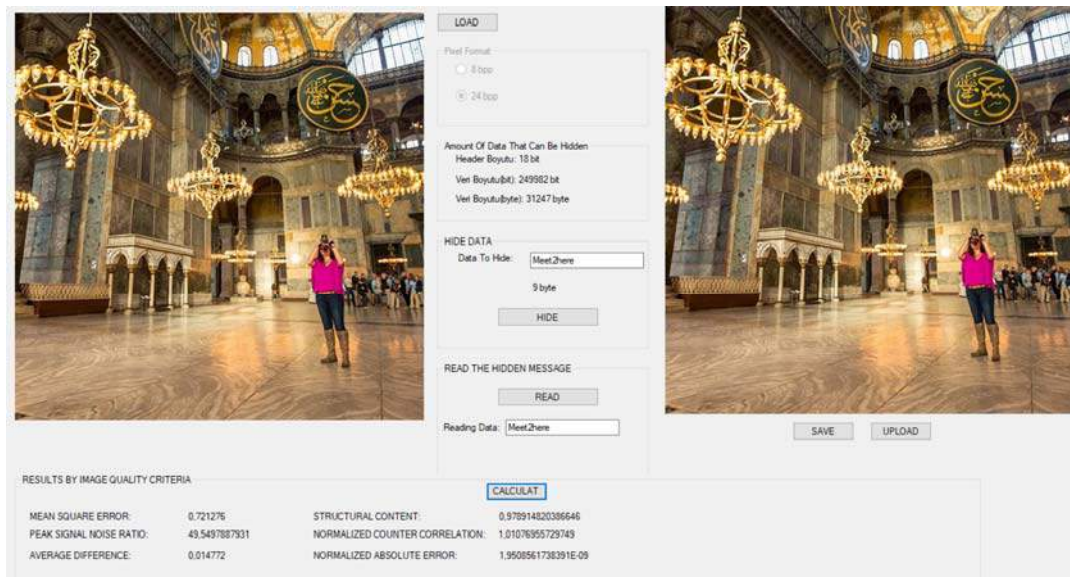
Figure 1. Fully functional screenshot of the application

Quality criteria based on different mathematical models were selected to calculate the quality criteria of the image in which the information is stored. The calculated values are shown at the bottom in Figure 1. How the values of the quality criteria are calculated is explained in detail in 2.4.

2.1. Image upload process

In the image loading process, three global variables named bit size, byteBoyut and baslikBoyut were used. bitBoyut variable hold a total of how many bits of data can be hidden in the image. byteBoyut variable hold a total of how many bytes of data can be hidden in an image. baslikBoyut variable hold stores the maximum number of bits of information that contains the number of bits to hide, depending on the size of the image.

A bmp or tiff image file is selected from the dialog box and loaded onto picureBox1. It is set to the selected state of radioButton1 or radiobutton2, depending on whether the loaded image is 24 bits or 8 bits. According to whether the uploaded image is 24 bits or 8 bits, the contents of the bit size, byteBoyut and baslikBoyut variables are calculated and these variables are shown in the corresponding label places on the form. bit size is the aspect multiplication of the image. byteBoyut consists of 8 sections of bitBoyut. baslikBoyut is to contain information about how many bits consists of the bitBoyut value.

2.2. Data hiding process

The data to be hidden entered by the user is compared to the maximum number of bytes stored in the byteBoyut variable, ensuring that the amount of data to be hidden does not exceed the image capacity. Data storage has been started according to whether the loaded image is 24 bits or 8 bits.

Algorithm 1: Data hiding algorithm.

Input: Message

Output: Picture with data hidden inside

1 Calculate char lenght x 8
2 **mesajBoyut ! = baslikBoyut ?** Adding "0" : ConvertStringArray
3 for (i=0; i<image.height;i++)
4   for (k=0; k<image.width; k++)
5   GetBlueValues();
6   WriteLSB ();
7 return new_image;

2.2.1 Data hiding process for 24 bits

The veriGizle24Bit method takes the data to be hidden as a parameter. First, the number of characters of the text stored in the message variable is multiplied by 8, which indicates how many bits this message consists of, and the number found is also translated into a binary base. This information is stored in the message size variable. Then, by adding 0 next to the message size value as needed, the message size variable contains as many bits as the number of bits in the baslikBoyut variable. Then the message is converted to a string of bits consisting of 1 and 0. This value is passed in the binaryMesaj variable. It is then delivered to each pixel of the image with two nested loops. Only the B value is taken from the RGB values of the Pixel. the bits in the message size variable are written to the lowest valence (LSB) bit of each pixel, which contains information about how many bits the message consists of, to the first bits as much as the number of bits held in the header size. In order for the bits that follow this, the bits contained in the binaryMesaj string are written from left to right to the lowest bit of the B value of each pixel, hiding the message.

2.2.2 Data hiding process for 8 bits

The veriGizle8Bit method takes the data to be hidden as a parameter. First, the number of characters of the text stored in the message variable is multiplied by 8, which indicates how many bits this message consists of, and the number found is also translated into a binary base. This information is stored in the message size variable. Then, by adding 0 next to the message size value as needed, the message size variable contains as many bits as the number of bits in the baslikBoyut variable. The message is then converted to a string of 1 and 0. This value is kept in the binaryMesaj variable. Then, with two nested loops, each pixel of the image is reached. the bits in the message size variable are written to the lowest valence (LSB) bit of each pixel, which contains information about how many bits the message consists of, to the first bits as much as the number of bits held in the header size. In order for the bits that follow this, the bits contained in the binaryMesaj string are written to the lowest bit of each pixel from left to right, hiding the message.

2.3. Data reading process

If the image expected to be solved is 24 bits, the veriOku24Bit method is executed, and the veriOku8Bit method is executed if it is 8 bits. Both methods accept the carrier image as a parameter value.

Algorithm 2: Data reading algorithm

Input: Image

Output: Hidden_mesage

```
1   for (i=0; i<image.height;i++)
2     for (k=0; k<image.width; k++)
3       CheckBlueValues();
4       Hidden_message += FirstBit(baslikBoyut)
5   for (i=0; i< Hidden_message_Lenght; i++)
6     for (k=0; k< Hidden_message_Lenght; k++)
7   Hidden_message += ReadLSB ();
8       for (j=0; j< Hidden_message_Lenght; j++)
9         Hidden_message += (Convert_Int(Hidden_message / 8)).ToChar()
10 return Hidden_message;
```

2.3.1 Data reading process for 24 bits

First, with two nested loops, successive pixels of the image are scanned from the beginning, and the B value of each pixel is checked. a string is added by taking the first bit of the B value of consecutive pixels, as well as the number of bits held in the baslikBoyut variable. This sequence of bits obtained from the first Pixels is converted to numbers, which allows you to find out how many bits of information are hidden in the image. Again, the image is scanned with two nested loops from the first Pixel, and the pixels that come after the pixels containing the header information are sequentially taken and added to the string variable, taking the lowest first bit of B values. In this loop structure, the bits of the hidden message are obtained in a string. Then this sequence of bits is divided into groups of 8. Each 8 i is first converted to a numeric value of byte type, then to a character of char type. A hidden string value is obtained by combining characters. The function completes the operation by returning the text it obtained.

2.3.2 Data reading process for 8 bits

First, with two nested loops, successive pixels of the image are scanned from the beginning and the value of each pixel is checked. a string is added by taking the first bit of the value of consecutive pixels, as well as the number of bits held in the baslikBoyut variable. This sequence of bits obtained from the first Pixels is converted to numbers, which allows you to find out how many bits of information are hidden in the image. Again, the image is scanned with two nested loops from the first Pixel, and the pixels that come after the pixels containing the header information are sequentially taken and added to the string variable, taking the lowest first bit. In this loop structure, the bits of the hidden message are obtained in a string. Then this sequence of bits is divided into groups of 8. Each 8 i is first converted to a numeric value from byte type and then to a character of char type. A hidden string value is obtained by combining characters. The text obtained by the function is returned.

2.4. Picture quality measurements and value calculations

Quality assessment algorithms are needed for optimization operations where quality is maximized at a certain cost, to perform comparative analysis between different alternatives, or to perform quality monitoring in real-time applications (Silpa and Mastani, 2012).

In the calculation operations, cover and carrier images are compared according to image quality criteria and values are calculated according to six different criteria.

2.4.1. Mean square error calculation

Image quality assessment is important in various image processing processes. Experimental results show that MSE and PSNR are simple, easy to implement, and have low computational complexity. In addition, these methods do not give good results. MSE and PSNR are acceptable for image similarity measurement only when images differ by increasing distortion of a particular type. However, they cannot capture image quality when used to measure types of distortion (Silpa and Mastani, 2012).

The mathematical model shown in Equation 1 was used to calculate the mean square error value.

$$MSE = \frac{1}{M*N}\sum_{i=1}^{M}\sum_{j=1}^{N}(Y_{i,j} - S_{i,j})^2 \qquad \text{Equation (1)}$$

2.4.2. Peak Signal Noise Ratio calculation

Peak Signal Noise Ratio (PSNR) is a metric that shows the ratio of a sign's maximum possible power to the power of noise on the sign. The signal represents the original data, while the noise represents the compression-induced error. When comparing compression encodings, PSNR can actually be considered as an approach to human quality perception. The mathematical model shown in Equation 2 was used to calculate the Peak Signal Noise Ratio value.

MSE = Mean Square Error

$$PSNR = 10\log_{10}\frac{R^2}{MSE} \qquad \text{Equation (2)}$$

2.4.3. Average difference calculation

The mathematical model shown in Equation 3 was used to calculate the average difference value.

$$AD = \sum_{j=1}^{M}\sum_{k=1}^{N}\frac{[F(j,k)-F\prime(j,k)]}{M*N} \qquad \text{Equation (3)}$$

2.4.4. Structural Content calculation

Structural difference is the type of metric that calculates the similarity between reference and test images. The mathematical model shown in Equation 4 was used to calculate the structural content value.

$$AC = \frac{\sum_{j=1}^{M}\sum_{k=1}^{N}[F(j,k)]^2}{\sum_{j=1}^{M}\sum_{k=1}^{N}[F\prime(j,k)]^2}$$

Equation (4)

2.4.5. Normalized Counter Correlation calculation

Normalized Counter Correlation between left and right images is calculated using the sum of the normalized cross correlation (NCC). The NCC algorithm is preferred because some metrics are affected by light change (Mohamed and Adulla et al, 2018, Dankers and Barnes et al., 2007, Zhang and Tay et al., 2011).

$$NK = \frac{\sum_{j=1}^{M}\sum_{k=1}^{N}F(j,k)F\prime(j,k)}{\sum_{j=1}^{M}\sum_{k=1}^{N}[F(j,k)]^2}$$

Equation (5)

2.4.6. Normalized Absolute Error

This technique measures exactly what is the difference between the processed image and the original image. It's the numerical variance between the restored and the original image. The result of this method falls into the interval of values between 0 and 1 (Gustafson and Yu, 2012). Moreover, the results that are near to zero means that the image have high similarity to the original one and the results near the value one indicates that the image have a very poor quality. The mathematical model shown in Equation 6 was used to calculate the normalized absolute error value.

$$NAE = \frac{\sum_{j=1}^{M}\sum_{k=1}^{N}|O\{F(j,k)\}-O\{F'(j,k)\}|}{\sum_{j=1}^{M}\sum_{k=1}^{N}|O\{F(j,k)\}|}$$

Equation (6)

3. Results

Quality metric values were measured by hiding the same information inside bmp and tiff image. The resulting values are shown in Table 1.

Table 1. Quality metric values of image file in different hiding data size

Image Format	Pixel Size	Hiding Data Size (Byte)	MSE	PSNR	AD	SC	NCC	NAE
BMP / TIFF	500x500	30	7,5277	38,7771	00872	0,9915	1,0096	8,3784
BMP / TIFF	500x500	15	4,7379	40,7879	0,0509	1,0022	0,9911	4,8921
BMP / TIFF	500x500	10	3,1824	42,5161	0,0352	0,9975	0,9973	3,3871
BMP / TIFF	500x500	5	1,8557	44,8585	0,0207	1,0074	0,9955	1,9896

MSE, NAE, and PSNR values changed significantly depending on the hidden data sizes. Although SC, NCC, and AD values vary depending on the hidden data size, the change amounts remain negligible.

4. Discussion and Conclusions

In this study, data hiding operation was performed on images in tiff and bmp formats. Depending on the size of the data hidden in the image, the measurement of the error metrics of these two formats was carried out. Obtained findings are shown in detail in the previous section. As a result of these findings, the error metric values calculated in both formats decrease depending on the decrease in the amount of hidden data. When the rate of change of error metrics is examined according to the size of the hidden data, it has been determined that the MSE metric changes more than the other metric values. In the next step of the study, it is planned to perform error metric measurements in data hiding operations in different image formats and different resolutions.

References

DANKERS, Andrew; BARNES, Nick; ZELINSKY, Alex. MAP ZDF segmentation and tracking using active stereo vision: Hand tracking case study. *Computer Vision and Image Understanding*, 2007, 108.1-2: 74-86.

Dolay, B. https://e-bergi.com/y/veri-gizleme-bilimi/ , Erişim Tarihi: 29.07.2021

GENÇOĞLU, M. T. (2021). Enhancing The Data Security by using Audio Steganography with Taylor Series Cryptosystem. *Turkish Journal of Science and Technology*, *16*(1), 47-64.

GUSTAFSON JR, William I.; YU, Shaocai. Generalized approach for using unbiased symmetric metrics with negative values: normalized mean bias factor and normalized mean absolute error factor. *Atmospheric Science Letters*, 2012, 13.4: 262-267.

Johnson, Neil F., and Sushil Jajodia. (1998) "Exploring steganography: Seeing the unseen." Computer 31.2 : 26-34.

Koçak, C. (2015). Kriptografi ve stenografi yöntemlerini birlikte kullanarak yüksek güvenlikli veri gizleme. *Erciyes Üniversitesi Fen Bilimleri Enstitüsü Fen Bilimleri Dergisi*, *31*(2), 115-123.

Kumar, K. S., Kumar, C. M., Kumar, B. S., & Cristin, R. (2021). Highly imperceptible data hiding technique using MSB in the grayscale image. *Materials Today: Proceedings*.

MOHAMED, Abdulla, et al. Depth Estimation Based on Pyramid Normalized Cross-correlation Algorithm for Vergence Control. *IEEE Access*, 2018, 6: 65199-65211.

ZHANG, Xuejie; TAY, Leng Phuan. A spatial variant approach for vergence control in complex scenes. *Image and Vision Computing*, 2011, 29.1: 64-77.

NARAYANA, Sujay; PRASAD, Gaurav. Two new approaches for secured image steganography using cryptographic techniques and type conversions. *Signal & Image Processing: An International Journal (SIPIJ) Vol*, 2010, 1.2: 60-73.

SETH, Dhawal; RAMANATHAN, L.; PANDEY, Abhishek. Security enhancement: Combining cryptography and steganography. *International Journal of Computer Applications*, 2010, 9.11: 3-6.

SILPA, K.; MASTANI, S. Aruna. Comparison of image quality metrics. *Int. J. Eng. Res. Technol*, 2012, 1.4: 1-5.

Usha, S., Kumar, G. S., & Boopathybagan, K. (2011, December). A secure triple level encryption method using cryptography and steganography. In *Proceedings of 2011 International Conference on Computer Science and Network Technology* (Vol. 2, pp. 1017-1020). IEEE.

ZHANG, Yike; LUO, Wenbin.2020. A Multi-MSB Replacement Based Approach for High Capacity Data Hiding in Color Images.

Detection of Hail Damage in Fruits Using Image Processing Techniques with Kinect Sensor

Enes AÇIKGÖZOĞLU[1*], Remzi GÜRFİDAN

Abstract: A study was carried out on the determination of damage caused by hail of fruits, which have an important share in agricultural production. Images of the lateral surface of six apples randomly taken from a random apple tree exposed to hail damage were obtained and the damage rates were tried to be determined by applying various image processing techniques on these images. In order to take the image, the damage detection table was designed and the images were processed in the Matlab environment. It is planned to develop methods to differentiate disease damage and hail damage in future studies.

Keywords: Image processing, fruit damage detection, hail damage

1. Introduction

All living things must be fed in order to survive. People started to meet their nutritional needs by hunting in ancient times, and over time they focused on agriculture and animal husbandry. Agriculture, which has developed with its economic dimension in addition to the field of basic needs, has become a source of livelihood for many people today. The agricultural sector has spread to many fields of study, such as agricultural machinery production, pesticide initiatives, air-conditioning environments, soilless farming techniques, disease detection and separation in harvested products by taking advantage of the developing technology. Although it is supported by technological infrastructures, the agricultural production sector, which is carried out in the open field, is exposed to the natural conditions of the environment and climate. Among the natural factors affecting agricultural production in the open field, precipitation, winds, frost events and extreme temperatures can be shown. When choosing the products they will buy, consumers look at whether there is damage to the external appearance of fruits or vegetables (Wang etc., 2013).

Producers strive to grow their produce as much as possible without contaminating diseases and meeting optimum irrigation needs. However, there is no measure that can be taken to prevent precipitation damage. For this reason, producers resort to insuring their production gardens in order to eliminate possible grievances they may encounter.

Insurance transactions can be carried out in the categories of garden area, amount of trees, productivity value, agricultural disease and precipitation damage. Insurance transactions are carried out manually by experts who are agricultural engineers by going to the producer's production garden. Persons who carry out this process are called experts. In order to determine the insurance cost, the experts take random product samples from different sides of

[1] Isparta University of Applied Sciences, Keçiborlu VHS, Isparta, Turkey
* Corresponding author: enesacikgozoglu@isparta.edu.tr

different trees from the products in the production garden. They evaluate and decide based on their experience for the purpose of the insurance, with the samples they receive.

In this study, a system was designed to determine the damage detection rate of a tree fruit affected by precipitation damage by image processing methods. The motivation of this study is to transfer the damage detection process, which will be carried out by the expert by hand and eye, to a technological autonomous system. Thanks to this proposed design, it is foreseen that the mistakes of carelessness, fatigue and bias that can be made by the expert will be minimized and a standard will be established among the experts in determining the damage detection rates. In order to test the proposed model, apple fruit, which is easily accessible in the region where the study was carried out, was preferred.

Processes such as quality classification of harvested fruits and vegetables and damage detection can be achieved faster and more reliable by utilizing technological opportunities. A model using image processing and artificial intelligence technologies is proposed for fast and accurate damage detection of litchi fruit. In the study, the damage areas are determined by the image processing infrastructure, and the support vector machine algorithm is operated for the classification process and the results are obtained (Xiong, Lin etc., 2018). In another study, studies were carried out on different packaging methods by classifying the fruits (Eissa and FR, 2009, Pathmanaban and Gnanavel etc., 2019). Lü and Tang proposed a system for detecting occult caries by hyperspectral imaging of kiwifruit. According to the experimental results of their study, the hidden bruises of kiwifruit could only be detected at a rate of 14.5% with hyperspectral imaging (Lü and Tang, 2011). Again using the hyperspectral imaging technique, Pan et al. tried to detect the detection of cold damage for peach fruit with artificial neural networks. In the proposed model, they achieved an accuracy rate of 70% to 90% according to different cold temperatures (Pan and Zhang etc., 2016). Along with hyperspectral systems, artificial vision systems and ultraviolet rays are used to reveal invisible defects in fruits and vegetables and to determine the quality of fruits and vegetables (Cubero etc., 2011). In a study on Jonagold apples, a few images taken from apple surfaces were processed to classify the fruits (Leemans and Destain, 2004). Pattnayak and Patra identified the damaged parts in fruits without human intervention using the salience detection technique on different fruits (Pattnayak and Patra, 2020). It can be said that his work is promising in this field.

In the second part of the study, the architecture of the proposed model is explained in Figure 1, the working principle of the system is shown with the flow diagram in Figure 2, and the electronic circuit drawing of the proposed system is shown in Figure 3. In the third part, image processing techniques and application images obtained for damage detection are given. According to the values obtained in the second part, the results of the study are mentioned.

2. Proposed Method

In the proposed model, there is a shaft attached to the rotation shaft of the stepper motor on which the apple fruit will be positioned on the damage detection table. Opposite the shaft is the camera that takes the image. The architecture of the proposed system is shown in Figure 1.

[1] Isparta University of Applied Sciences, Keçiborlu VHS, Isparta, Turkey
* Corresponding author: enesacikgozoglu@isparta.edu.tr
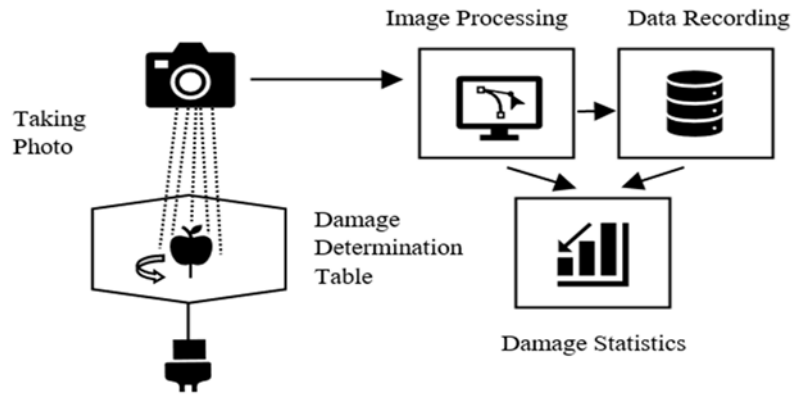
Figure 1. Architecture of Fruit Damage Detection System

After the fruit is placed on this spindle, by pressing the button, the codes in the Arduino Uno are started to be run beforehand and the motor calibrates itself according to the initial rotation position. Then it starts to rotate to scan the entire lateral surface of the fruit. After each 120 degree rotation, there is a 1 second wait for the image to be taken. The acquired images are combined side by side so that the entire lateral surface is flattened. Afterwards, feature extractions are performed using image processing techniques and fruit damage data is calculated. The flow diagram of the system is shown in Figure 2 in detail.
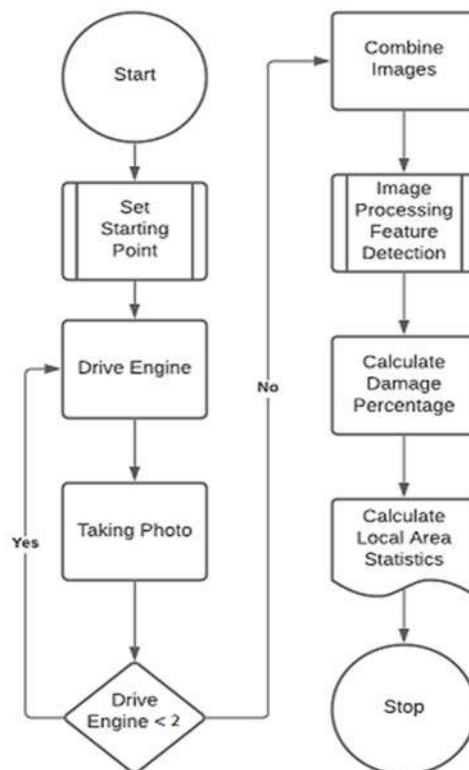
Figure 2. Flow Diagram of Fruit Damage Detection System

The electronic circuit diagram of the proposed system is shown in Figure 3 in detail.

[1] Isparta University of Applied Sciences, Keçiborlu VHS, Isparta, Turkey
* Corresponding author: enesacikgozoglu@isparta.edu.tr
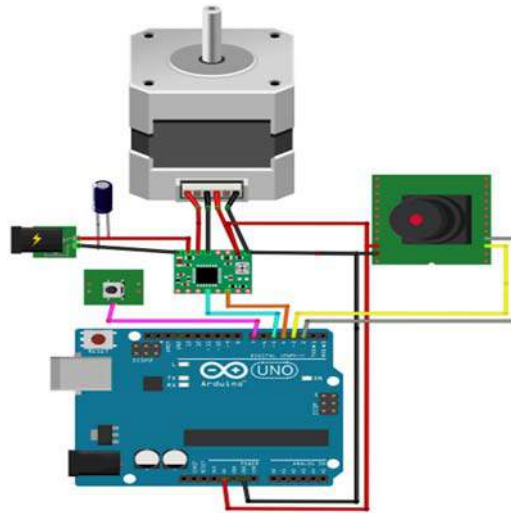
Figure 3. Circuit Diagram of Fruit Damage Detection System

Using image processing techniques, the damaged fruit image was first converted to gray scala form. Afterwards, the image obtained was converted to binary format and the damaged spots on the lateral area of the fruit were clarified. The counting process was completed by coloring the damaged spots.
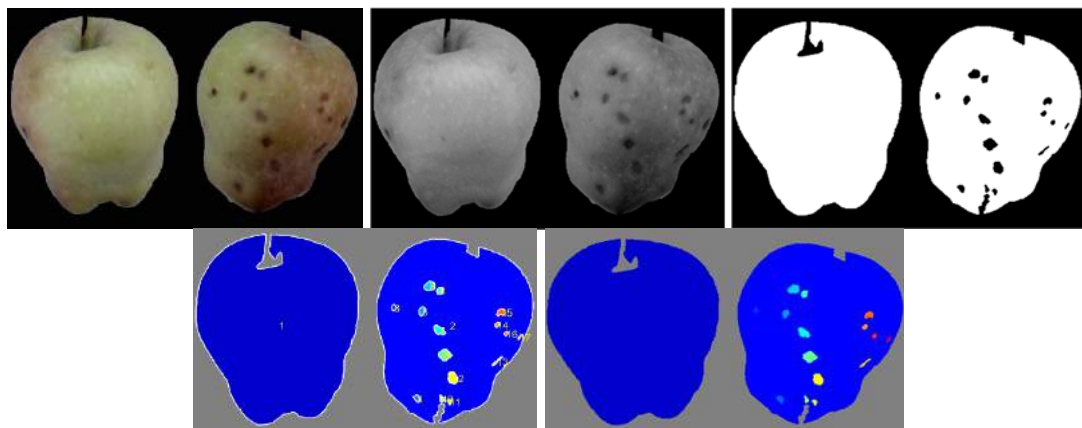
Figure 4. Image Processing Algorithms Results of Fruit Damage Detection System

3. **Discussion and Conclusions**

The results obtained by evaluating the sample selected for the detection of damaged fruit in the system proposed in the study are shown in Table 1. In Table 1, a scenario was prepared on the evaluation of fruit samples taken from a tree exposed to hail damage. In Table 1, starting from the first image of the damaged fruit, pictures of the image processing processes, the calculated total lateral area of the fruit, the detected damaged area, the number of damage points and the total damage percentage are given.

Table 1. Evaluation Data of the Proposed Model in the Sample Selected for the Sample Scenario

Image Sample	Total Area of Fruit	Detected Damaged Area	Number of Damaged Points	Damage Percentage of Fruit

[1] Isparta University of Applied Sciences, Keçiborlu VHS, Isparta, Turkey
* Corresponding author: enesacikgozoglu@isparta.edu.tr

	616547	9850	40	1,597607319
	437077	6509	19	1,489211283
	481148	2153	10	0,447471464
	347412	926	4	0,266542319
	249317	3868	15	1,55143853

[1] Isparta University of Applied Sciences, Keçiborlu VHS, Isparta, Turkey
* Corresponding author: enesacikgozoglu@isparta.edu.tr

	243827	3920	16	1,607697261
The Overall Total	2375328	27226	104	6,959968176

In this study, the proposed system is presented as a prototype. The necessary hardware and costs for the installation of the system are given in Table 2. The prototype cost of the proposed system was realized with a very affordable budget of 2165 TL.

Table 2. Hardware Components and Costs of the Proposed System

Hardware Component	Hardware Cost
Arduino Uno Development Board	54 TL
Step Motor	34 TL
Step Motor Driver Circuit	15 TL
Camera	40 TL
Button	1 TL
Capacitor	1 TL
Supply Circuit	20 TL
Computer	2000 TL
The Overall Total	2165 TL

The agricultural expert using the system proposed in this study will be able to quickly obtain the damage detection rates in numerical data from the sample taken from the tree he is interested in. We hope this benefit will provide a solution to personal measurement and evaluation random errors. In future studies, we plan to develop on the differentiation of hail damage and wounds and fruit diseases.

References

Cubero, S., Aleixos, N., Moltó, E., Gómez-Sanchis, J., & Blasco, J. (2011). Advances in machine vision applications for automatic inspection and quality evaluation of fruits and vegetables. Food and bioprocess technology, 4(4), 487-504.

Eissa, A., & F R, G. (2009). OPERATIONAL MODAL ANALYSIS AND DAMAGE DETECTION IN FRUIT QUALITY ASSESSMENT USING DIFFERENT METHODS OF PACKAGING. *ERJ. Engineering Research Journal*, *32*(1), 33-47.

Leemans, V., & Destain, M. F. (2004). A real-time grading method of apples based on features extracted from defects. Journal of Food Engineering, 61(1), 83-89.

Lü, Q., & Tang, M. (2012). Detection of hidden bruise on kiwi fruit using hyperspectral imaging and parallelepiped classification. *Procedia Environmental Sciences*, *12*, 1172-1179.

[1] Isparta University of Applied Sciences, Keçiborlu VHS, Isparta, Turkey
* Corresponding author: enesacikgozoglu@isparta.edu.tr

Pan, L., Zhang, Q., Zhang, W., Sun, Y., Hu, P., & Tu, K. (2016). Detection of cold injury in peaches by hyperspectral reflectance imaging and artificial neural network. *Food chemistry*, *192*, 134-141.

Pathmanaban, P., Gnanavel, B. K., & Anandan, S. S. (2019). Recent application of imaging techniques for fruit quality assessment. *Trends in Food Science & Technology*, *94*, 32-42.

Pattnayak, S. B., Patra, T. K. (2020). An Image Processing Approach to Detect Fruit Damage. International Research Journal of Engineering and Technology, 667-671.

Wang, L., Li, A., & Tian, X. (2013, November). Detection of fruit skin defects using machine vision system. In 2013 Sixth International Conference on Business Intelligence and Financial Engineering (pp. 44-48). IEEE.

Xiong, J., Lin, R., Bu, R., Liu, Z., Yang, Z., & Yu, L. (2018). A micro-damage detection method of litchi fruit using hyperspectral imaging technology. *Sensors*, *18*(3), 700.

[1] Isparta University of Applied Sciences, Keçiborlu VHS, Isparta, Turkey
* Corresponding author: enesacikgozoglu@isparta.edu.tr

# A Novel Multi-attribute Visual CAPTCHA Model Approach

Ziya DİRLİK[1*], Ayhan ARISOY

Abstract: One of the methods we encounter in the data entry screens of applications and used to distinguish between real users and artificial users is to use CAPTCHA. With the development of technology, the problem of correctly estimating CAPTCHAs has arisen for bot applications that imitate real users. In order to overcome this problem, CAPTCHAs have changed over time and, pictures, questions, shapes, etc. have been used instead of simple letters and numbers. In this study, a new CAPTCHA model created with color, shape and numerical value is presented.

Keywords: Captcha, bot detection, user confirm, secure verification

1. Introduction

One of the most important problems encountered in user-interactive platforms is the difficulty in distinguishing the real user from the artificial user. It is one of the main features that will increase the security of the system by correctly distinguishing the artificial users designed to use a created system and the real users, and maintaining the correct operation by the system. They have developed interactive solution methods to distinguish the real user and the artificial user correctly. The most well-known of these methods is captcha. Captcha can be defined as an automatic verification test developed to correctly distinguish between real users and artificial users. CAPTCHA (Completely Automated Public Turing test to tell Computers and Humans Apart), meaningless as a word, is a concept formed from the initials of the Fully Automated Public Turing Test to Separate Computers and Humans (Von Ahn, Luis, et al., 2003).

In the operation of the captcha technique, there is the continuation of the workflow according to the correctness of the answers to the simple questions directed to the software user. T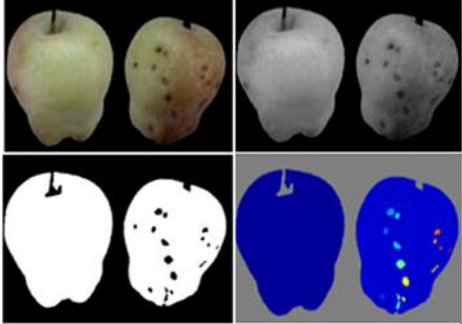he characteristics of the question asked should be capable of distinguishing between real users and artificial users. As the captcha formats were solved and answered successfully by artificial users over time, the captcha structure was differentiated and strengthened. Different techniques have been developed, such as printing text-based expressions presented to the system user by the user, asking the user for the results by calculating simple mathematical operations, and selecting objects shared over different visual expressions. However, for each new technique developed, artificial users have discovered different breaking methods for each of them over time (Athanasopoulos and Antonatos, 2006, Chow and Susilo, 2011, Desai and Patadia, 2009). When the process is considered, the determination of real users by traditional captcha methods seems to be an endless chase, which seems to never end, in which new

[1] Isparta University of Applied Sciences, Keçiborlu VHS, Isparta, Turkey
* Corresponding author: ziyadirlik@isparta.edu.tr

cracking solutions are developed in addition to the closed gaps. Some examples of captcha developed in different techniques are shown in figure 1.
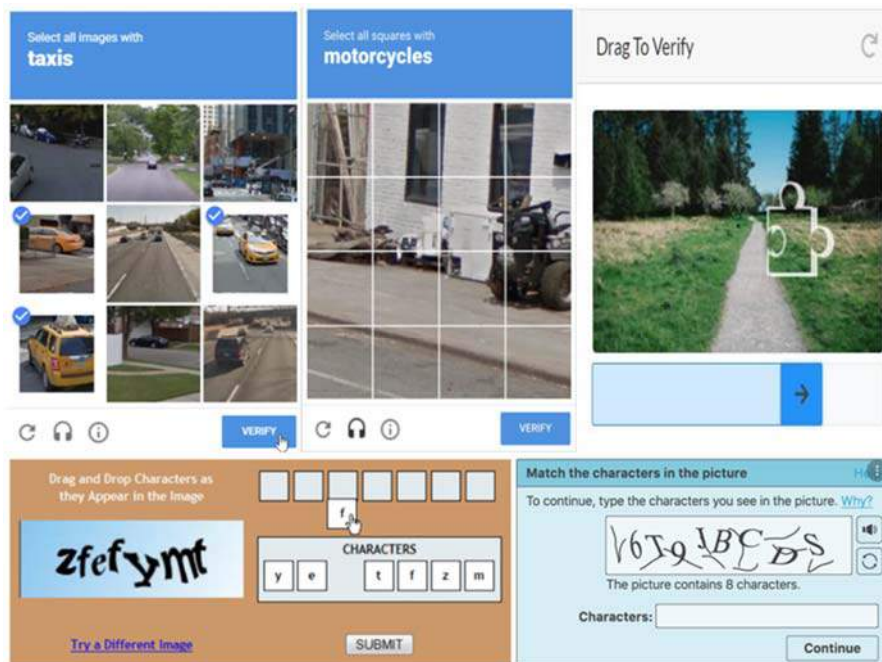
Figure 1. The most well-known captcha examples

The main purpose of the scientists in the captcha studies carried out is to develop techniques that real users can easily perceive and perform, while artificial users will fall into complexity and err. For this purpose, the studies aimed at demanding the result to be obtained by inserting two simple numbers into basic mathematical operations, asking the users to rewrite the textual expressions with letter and number complexity written on the image in different thicknesses and angles (Imsamai and Phimoltares 2010, Singh and Pal, 2014, Saalo, 2010), asking the user for results through logical gates (Choudhary and Kaur, 2015), asking the user to select images with common objects by mixing them with images that are similar to that image but do not contain a common object, next to more than one visual piece containing a common object (Fujita and Sano et al.,2016), by dividing an image into a different number of parts, asking the user to select the images containing the part of an object scattered on the parts (Gao, 2010), asking the user to write what he hears by listening to a simple sound (Gritzalis and Soupionis, 2 010), asking the user to select a genre from a set of small images that are very similar to each other on an image (Lin, 2011), cutting a small piece on an image from where it is located, positioning it at a random point in the image by providing drag-and-drop features to that piece, and asking the user to select a genre from it (Lin, 2011). It reveals different methods such as asking the part to be dragged and seated where it belongs (Ali and Karim, 2014, Chaudhari et al., 2011), asking the user to choose with face recognition (Goswami and Gaurav et al., 2012). Some field experts, on the other hand, argue that captcha is not a strong enough parser on its own and think that captcha and graphic cipher schemes should be used together (Bin and Zhu et al., 2014). However, the weak point of their work is that the model they developed is quite open to brute-force attacks.

In the second part of the study, the models of the suggested captcha method will be shown. In the third part, statistical data of real people using the proposed captcha test are shown

[1] Isparta University of Applied Sciences, Keçiborlu VHS, Isparta, Turkey
* Corresponding author: ziyadirlik@isparta.edu.tr

according to different criteria. In the last part of the study, the evaluation of the findings of the proposed model and the future study plans of the proposed model are given.

2. Prpposed Method

The captcha model proposed in this study contains all of the shape, color and numerical relationship criteria. The user trying to log in to the system should interpret all three criteria at the same time and choose the right option. Some captcha examples of the proposed model are shown in Figure 2.
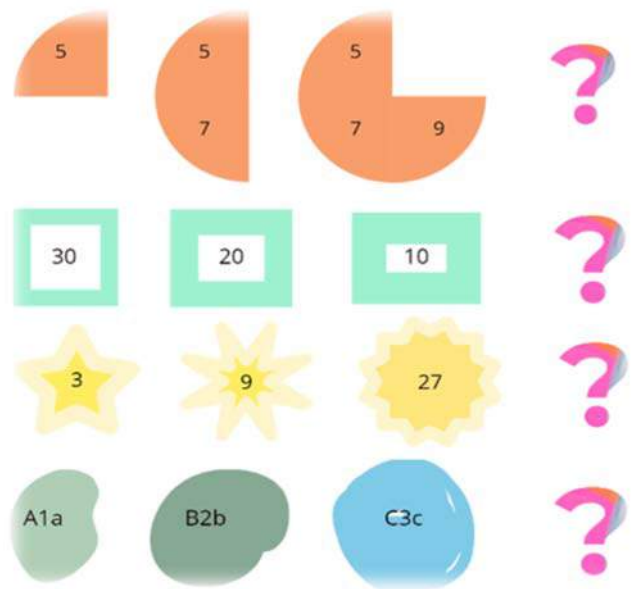
Figure 2. Some captcha examples of the proposed model

In the designed captcha examples, inductive and deductive methods are preferred in figure flow. Numerical and character expressions written on the figures also form a meaningful sequence in themselves.

3. Results

The test of the proposed captcha model was tested with the participation of 208 people. The classification of the number of participants according to age range and educational status is shown in Figure 3. It is seen that the number of participants between the ages of 20 and 30 is higher than the number of participants in the other age range.
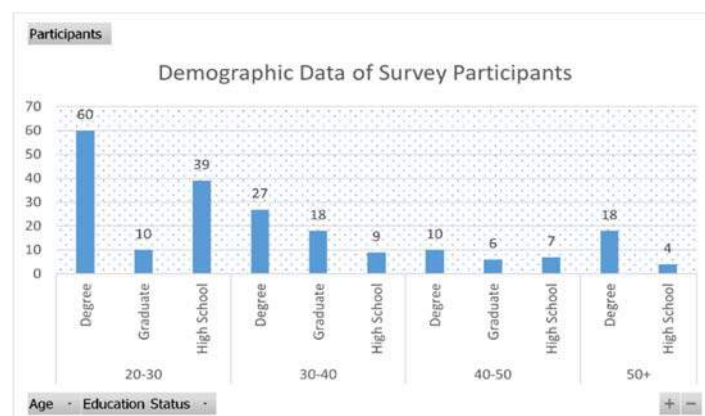
Figure 3. Demographic data of survey participants

[1] Isparta University of Applied Sciences, Keçiborlu VHS, Isparta, Turkey
* Corresponding author: ziyadirlik@isparta.edu.tr

The average time spent per question by the participants performing the captcha test is shown in Figure 4. Participants spent an average of 51 seconds for the second question and 18 seconds on average for the fourth question.
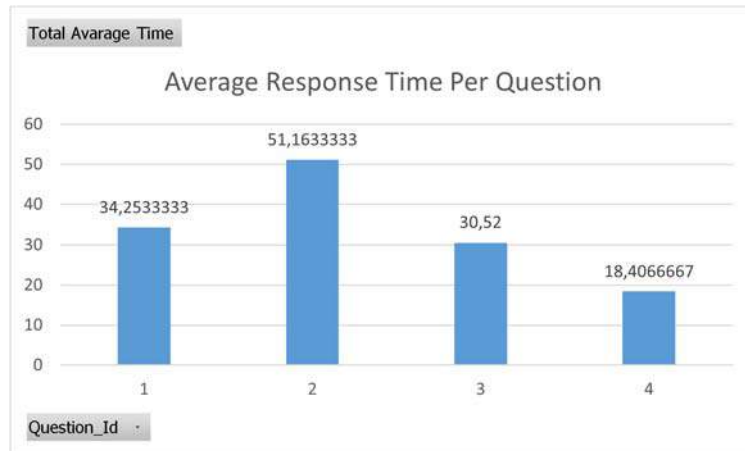
Figure 4. Average response time per questios

The total time spent by the participants on the 4 suggested captcha questions exceeds 5 hours. The average and total times spent per question are shown in Table 1.

Table 1. Average Response Time and Total Time Per Question

Question Id	Average Time (sec)	Total Time (hour)
1	00:00:34.2533333	01:21:38.4600000
2	00:00:51.1633333	01:53:24.5933333
3	00:00:30.5200000	01:05:06.5366667
4	00:00:18.4066667	00:40:48.2266667

The number of correct and incorrect answers given by all participants to the captcha questions and the average percentage of correct answers per question are shown in Figure 5. An accuracy rate of 86% was achieved in the fourth question.
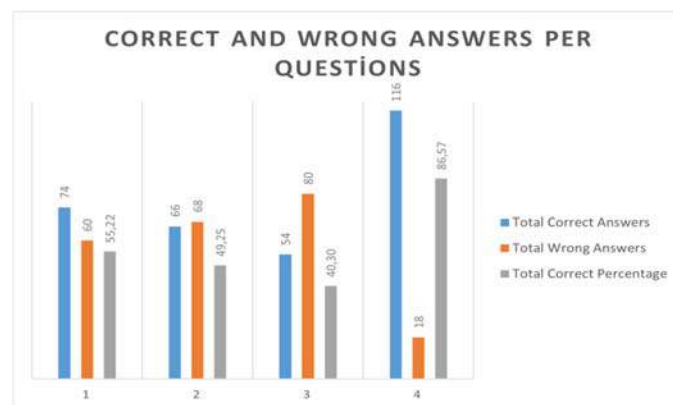
Figure 5. Correct and wrong answer per questions

4. Discussion and Conclusions

In the proposed capthca model, it was seen that the 2nd capthca question was more challenging than the other questions, and the 4th capthca question was answered faster and

[1] Isparta University of Applied Sciences, Keçiborlu VHS, Isparta, Turkey
* Corresponding author: ziyadirlik@isparta.edu.tr

with higher accuracy than the other capthca questions. The measurement values obtained in the capthca questions with these two extreme values of the proposed model are at an acceptable level when compared with the values accepted in the literature studies and practice. For this reason, the proposed models are considered to be suitable for daily use. In the next study, it is planned to replicate capthca examples and to test their security against cyber attacks that they may be exposed to during implementation and to strengthen their vulnerabilities.

References

Alı, Firkhan Ali Bin Hamid; Karım, Farhana Bt. Development Of Captcha System Based On Puzzle. In: 2014 International Conference On Computer, Communications, And Control Technology (I4ct). Ieee, 2014. P. 426-428.

Athanasopoulos, Elias; Antonatos, Spiros. Enhanced Captchas: Using Animation To Tell Humans And Computers Apart. In: Ifıp International Conference On Communications And Multimedia Security. Springer, Berlin, Heidelberg, 2006. P. 97-108.

Chaudharı, S. K., Et Al. 3d Drag-N-Drop Captcha Enhanced Security Through Captcha. In: Proceedings Of The İnternational Conference & Workshop On Emerging Trends İn Technology. 2011. P. 598-601.

Chow, Yang-Wai; Susılo, Willy. Anicap: An Animated 3d Captcha Scheme Based On Motion Parallax. In: International Conference On Cryptology And Network Security. Springer, Berlin, Heidelberg, 2011. P. 255-271.

Desaı, Arpan; Patadıa, Pragnesh. Drag And Drop: A Better Approach To Captcha. In: 2009 Annual Ieee India Conference. Ieee, 2009. P. 1-4.

Gao, Haichang, Et Al. A Novel İmage Based Captcha Using Jigsaw Puzzle. In: 2010 13th Ieee International Conference On Computational Science And Engineering. Ieee, 2010. P. 351-356.

Goswamı, Gaurav, Et Al. Face Recognition Captcha. In: 2012 Ieee Fifth International Conference On Biometrics: Theory, Applications And Systems (Btas). Ieee, 2012. P. 412-417.

Imsamaı, Montree; Phımoltares, Suphakant. 3d Captcha: A Next Generation Of The Captcha. In: 2010 International Conference On Information Science And Applications. Ieee, 2010. P. 1-8.

Kaur, Ramanpreet; Choudhary, Pooja. A Novel Captcha Design Approach Using Boolean Algebra. International Journal Of Computer Applications, 2015, 975: 8887.

Lın, Rosa, Et Al. A New Captcha İnterface Design For Mobile Devices. 2011.

Saalo, V. (2010). Novel Captcha Schemes.

[1] Isparta University of Applied Sciences, Keçiborlu VHS, Isparta, Turkey
* Corresponding author: ziyadirlik@isparta.edu.tr

Sano, Ayane; Fujıta, Masahiro; Nıshıgakı, Masakatsu. Directcha: A Proposal Of Spatiometric Mental Rotation Captcha. In: 2016 14th Annual Conference On Privacy, Security And Trust (Pst). Ieee, 2016. P. 585-592.

Sıngh, Ved Prakash; Pal, Preet. Survey Of Different Types Of Captcha. International Journal Of Computer Science And Information Technologies, 2014, 5.2: 2242-2245.

Soupıonıs, Yannis; Grıtzalıs, Dimitris. Audio Captcha: Existing Solutions Assessment And A New İmplementation For Voıp Telephony. Computers & Security, 2010, 29.5: 603-618.

Von Ahn, Luis, Et Al. Captcha: Telling Humans And Computers Apart Automatically. In: Proceedings Of Eurocrypt. 2003.

Zhu, Bin B., Et Al. Captcha As Graphical Passwords—A New Security Primitive Based On Hard Aı Problems. Ieee Transactions On İnformation Forensics And Security, 2014, 9.6: 891-904.

[1] Isparta University of Applied Sciences, Keçiborlu VHS, Isparta, Turkey
* Corresponding author: ziyadirlik@isparta.edu.tr

Assistant Referee Offside Signals Training Simulator System Design

Ayhan ARISOY*, **Enes AÇIKGÖZOĞLU²**

Abstract: The football industry has been growing in recent years and the number of stakeholders is increasing. Football has become more than a sport with the increase in the number of fans of league teams such as national teams and league teams of countries. Undoubtedly, the share of referees who manage football matches is very important in this sector. The skills and correct management of the referees in the match are followed by all fans and clubs. For this reason, referee training and training is an issue that should be carefully considered. In this study, a simulation system is proposed to assist the training and training of the linesmen in executing the offside decisions. In the last part of the study, the cost analysis of the proposed system was carried out and its attractiveness was revealed. We hope that the system will be adopted and put into practice in a short time.

1. Introduction

Football, the most well-known and most followed sport today, was founded in England in 1857. There are 403 professional football clubs in the world. This number increases considerably when football teams and amateur initiatives are included (Aydın, 2008). The worldwide football economy consists of clubs, players, facilities, broadcasters, and fan expenditure stakeholders. The economy in question has a budget of more than billion Euros. This large budget is distributed to professional clubs in proportion to their success in competitions on official platforms. This situation shows that it is of vital importance that the competitions are managed fairly and in accordance with the football game rules. The most critical football stakeholder to execute and fulfill these conditions is the referees. As in every sport, certain rules are determined and updated in the football branch. In the field, a total of 7 referees, including VAR (Video Assistant Referee) referees, are responsible for the fair and proper administration of football matches, with new applications. During the match, all spectators, technical team and football players follow the game flow with the physical signs of the referee and assistant referees specified in the football game rules. For this reason, referees must reflect the game rules on the field physically and mentally during the game (Kürkçü and Uluşar, 2014). Possible misleading or wrong physical sign negatively affects the course of the game.

---

¹ Isparta University of Applied Sciences, Senirkent VHS, Isparta, Turkey
* Corresponding author: ayhanarisoy@isparta.edu.tr

Assistant referees notify their decisions in the competition through the referee flag. For this reason, the use of flags by the assistant referees must be error-free and closed to interpretation. During the referee training process, the flag holding positions and angles of the assistant referees is the main issue that needs to be studied meticulously. Even today, this physical training and education process is carried out by the referee candidates watching each other, recording the images and watching them later, or in front of a mirror. In learning psychology, the immediate feedback given to the learner at the time of learning contributes positively to the effectiveness and quality of learning. For this reason, the need for a system that can give instant feedback to the learner in training and flag training of assistant referees is clearly seen. The motivation source of the study is the preparation of the necessary training and training environment for the referees to have the right effect of the football game rules on the field.

The adaptation of football, which appeals to large audiences, with technology started at the end of the 90s by increasing the communication quality of the referee and assistant referee. These systems enabled the referee and assistant referees to communicate independently of distance and ambient noise. The growing economic portfolio of the football industry has caused all stakeholders in the field to get closer to technology to optimize their roles. The goal line technology, which is one of the most well-known of these technologies, is a system that helps the referee by deciding whether the ball has crossed the goal line through electronic sensors (FIFA, 2012). This system has been developed by scientists and a system based on radio frequency recognition and faster decision making has been proposed (Ghosh and Sasmal et al., 2019). The contribution of the goal line technology to the continuation of the match with the right decisions has been accepted by all football segments. This satisfaction has created the opinion that a technological structure that will help the referee in all critical decisions, except the goal line technology, will be positive. The VAR model, which started to be constructed after 2010, was officially implemented for the first time in 2016 in a preparation competition (IFAB, 2016). As a result of the positive feedback received, it has been actively used in many national and international organizations today. The technological infrastructures developed for the scenarios during the competition are not limited to the competition, athlete, referee analysis, injury evaluations, athlete and referee training, athlete and referee training. Scientists develop various software to analyze the competition (Abdullah and Razali et al., 2016) or make use of artificial intelligence technologies (Kumar, 2013). Similarly, the running distances, game zones, defense and attack contributions, tactical compatibility, and physical strength of the football players and referees in the competition can also be followed [Gong and Cui et al., 2019, Kürkçü and Uluşar, 2014]. Thanks to the developed IoT (Internet of Things) based systems, the training environments and training programs of football players and referees can be prepared in an optimized way. In order to realize this system, using ZigBee technology, parameters such as the athlete's blood pressure, blood oxygen rate, body movements, sweating rate, body temperature, past health stories are instantly taken and transferred to cloud-based systems. Thus, the responsible personnel who manage the training or training can follow the instant physical conditions of all learners (Ikram and Alshehri et al, 2015). As a result of the researches, it has been determined that the technological structures developed are designed for the detection and monitoring of the physical conditions of the athletes. It is obvious that the systems developed for education are very limited and the sector's hunger in this regard. With the proposed model, it is aimed to

[1] Isparta University of Applied Sciences, Senirkent VHS, Isparta, Turkey
* Corresponding author: ayhanarisoy@isparta.edu.tr

contribute to the physical training of the assistant referee, who is an important figure in the football industry.

In the second part of the study, how the proposed model was developed and its working principles, the findings obtained in the third part, and the results of the study carried out in the fourth part are given.

2. Proposed Method

The Kinect V2 is a capable sensor for game consoles that can detect human movements, skeletal and joint structure. It is used by scientists in academic studies thanks to the library supports that we can define the skeletal structure and joints (Taşdelen and Gürfidan, 2015). The Kinect sensor has an infrared camera, RGB camera, infrared emitter and multiple microphones. The resolution of the infrared camera is 512x424 pixels (px), the resolution of the RGB camera is 1920x1080 px. The lens viewing angle capability of the RGB camera is 70x60 degrees. It has an image detection rate of 30 frames per second. The detection area ranges from 0.5 meters to 4.5 meters. The Kinect v2 sensor is shown in Figure 1.
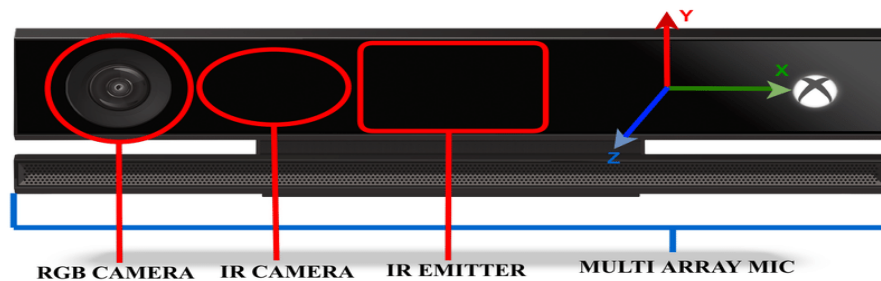
Figure 1. Kinect V2 Sensor

True and false flag positions taken from the proposed system are shown in Figure 2.

Figure 2. Assistant referee offside flag positions

[1] Isparta University of Applied Sciences, Senirkent VHS, Isparta, Turkey
* Corresponding author: ayhanarisoy@isparta.edu.tr

To determine the accuracy of the movements, the length from the wrist to the elbow and the length from the elbow to the shoulder are obtained from the absolute difference of the x-axes. Then the obtained value is converted to vector unit. The same process is done for the length from elbow to shoulder, and this value is also converted to vector. The angle between these structures, which are then converted into vectors, is calculated using the cosine theorem. As shown in Figure 3, angle calculation is performed when x, y, and z points are known. In order to apply the cosine theorem, the distance between the joints must first be converted to a vector. This conversion is calculated with Formula 1 and Formula 2.

$$\overrightarrow{PA} = x1 - x2, y1 - y2, z1 - z2 \qquad \text{(Formula 1)}$$

$$\overrightarrow{PB} = x3 - x2, y3 - y2, z3 - z2 \qquad \text{(Formula 2)}$$

The expressions $\overrightarrow{PA}$, $\overrightarrow{PB}$ express the vector norm between points. The expressions x1, x2, x3, y1, y2, y3, z1, z2, z3 express the vector coordinates of the joints. In order to calculate the angle between two vectors starting from the same point and extending in different directions, the lengths of the vectors must be calculated separately. Calculation of the lengths of the vectors is calculated as shown in Formula 3 and Formula 4.

$$|\overrightarrow{PA}| = \sqrt{(A_X . P_X)^2 + \left((A_y . P_y)^2\right) + (A_z . P_z)^2} \qquad \text{(Formula 3)}$$

$$|\overrightarrow{PB}| = \sqrt{(B_X . P_X)^2 + \left((B_y . P_y)^2\right) + (B_z . P_z)^2} \qquad \text{(Formula 4)}$$
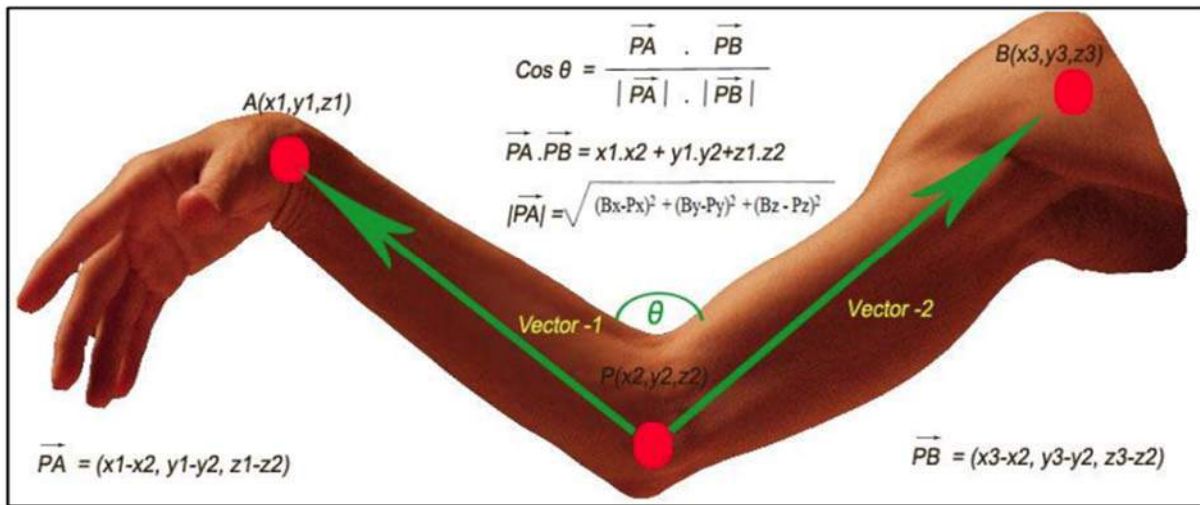
Figure 3. Converting joint distances to vector and calculating the angle between them
(Taşdelen and Gürfidan, 2015)

After the preprocessing required to calculate the angle between the two vectors is completed, the decision calculation that allows us to calculate the angle between the two vectors is shown in Formula 5.

$$Cos\theta = \frac{\overline{P_a}.\overline{P_b}}{|P_a|.|P_b|} \qquad \text{(Formula 5)}$$

[1] Isparta University of Applied Sciences, Senirkent VHS, Isparta, Turkey
* Corresponding author: ayhanarisoy@isparta.edu.tr

3. Discussion and Conclusions

In order to apply the model proposed in the study to real life, cost analyzes were carried out. All components required for efficient and correct use of the system are given in Table 1 with cost calculations.

Table 1. Components of the System and Cost Analysis

Hardware Equipment	Cost Accounting
Notebook / Desktop	3500 TL
Monitor	1500 TL
Operating System	600 TL
Kinect V2 Sensor	1100 TL
TOTAL COST	6700 TL

As can be seen in Table 1, this training and training system, which can be installed at a cost of 6700 TL, is a very appropriate amount considering the critical role of the referees. In addition, with the development of software suitable for the system, it has the potential to contribute not only to the offside training and training of the linesman, but also to many physical training and training.

References

Abdullah, Mohamad Razali, et al. Development of tablet application based notational analysis system and the establishment of its reliability in soccer. *Journal of Physical Education and Sport*, 2016, 16.3: 951.

Aydın, E. *Futbol Ekonomisi: 2 Ülke Kıyaslaması (İngiltere ve Türkiye)*. 2008. PhD Thesis. Yüksek Lisans Tezi, Marmara Üniversitesi Sosyal Bilimler Ens. İşletme Anabilim Dalı Uluslararası İşletmecilik Bilim Dalı.

FIFA (2012). "Testing Manual". *FIFA Quality Programme for Goal Line Technology*.

Ghosh, S., Sasmal, S., Bhui, S., Dutta, S., Mukherjee, S., Majumder, A., & Ganguly, B. (2019, March). Radio Frequency Identification based Goal Line Technology for Quick Decision Making in a Football Match. In *2019 Devices for Integrated Circuit (DevIC)* (pp. 441-445). IEEE.

Gong, Bingnan, et al. The validity and reliability of live football match statistics from champdas master match analysis system. *Frontiers in psychology*, 2019, 10: 1339.

Ikram, Mohammed Abdulaziz; ALSHEHRI, Mohammad Dahman; HUSSAIN, Farookh Khadeer. Architecture of an IoT-based system for football supervision (IoT Football). In: *2015 IEEE 2nd World Forum on Internet of Things (WF-IoT)*. IEEE, 2015. p. 69-74.

Kumar, G. (2013). Machine learning for soccer analytics. *University of Leuven*.

Kürkçü, Cengiz; Uluşar, Ümit Deniz. Position and motion analysis of referees during soccer games. In: *2014 22nd Signal Processing and Communications Applications Conference (SIU)*. IEEE, 2014. p. 124-127.

[1] Isparta University of Applied Sciences, Senirkent VHS, Isparta, Turkey
* Corresponding author: ayhanarisoy@isparta.edu.tr

Minutes of the 130th Annual General Meeting of the International Football Association Board". IFAB. pp. 13–17, 2016.

Taşedelen K., Gürfidan R. "*Control of robot arm by using kinect technology*". *Yüksek Lisans Tezi, Süleyman Demirel Üniversitesi Elektronik Bilgisayar Eğitimi Anabilimdalı, 2015.*

[1] Isparta University of Applied Sciences, Senirkent VHS, Isparta, Turkey
* Corresponding author: ayhanarisoy@isparta.edu.tr

Internet of Things Based Real-Time Fatigue Detection System for Drivers with Kinect Sensors

Enes AÇIKGÖZOĞLU[1*], Ziya DİRLİK[2], Ayhan ARISOY[3]

Abstract: A precaution and warning system has been proposed by making use of internet-based objects and image processing techniques in order to detect fatigue of vehicle drivers. In the study, the Kinect sensor, which can detect human joints, was preferred in order to detect the forward tilt of the head during diving and sleep. In addition, a simple camera that sees the driver's face was used to detect the state of closing the eyes without tilting the head in case of fatigue and sleep. Data obtained and processed in real time can make decisions for fatigue detection and play an accident-preventing role by warning the driver.

Keywords: Internet of things, fatigue detection, Kinect sensor, image processing

1. Introduction

As of 2020, there are approximately one billion two hundred and fifty million vehicles in the world. These vehicles are used for public transportation, logistics services, commercial activities and personal purposes. Transportation has become an essential need in every aspect of daily life. For this reason, traffic is a multidimensional phenomenon that is active, alive and growing every moment of the day. Traffic phenomenon has stakeholders such as traffic rules and violations, traffic accidents, road conditions, number of vehicles and pedestrians. Among these stakeholders, traffic accidents appear as the dimension that most concerns and affects human life. According to official figures, over 14 million accidents have occurred in our country in the last 10 years. In these accidents, a total of 64,634 people lost their lives and over 3 million 247 thousand people were injured (Tuik, 2021). This number is much larger worldwide. Although there are many reasons for traffic accidents, driver faults constitute 89.39% of the accident causes. When the causes of the accidents are examined, it is distributed as 2% hitting a stationary vehicle, 6% hitting a fixed object, 15% going off the road, and 6% mutual collision (Polis Academy, 2019). When these reasons are examined, it is clear that the vehicle user is careless and careless in accidents. Vehicle companies such as Nissan, Toyota, Volkswagen are updating and developing driver assistance software to prevent vehicle accidents (Sikander and Anwar, 2018).

In this study, a system is proposed in which the driver's density can be detected in real time while the vehicles are in motion. In the proposed system, images taken from the Kinect sensor and images obtained from the camera are processed in real time by using image processing techniques, triggering a warning system. Fatigue detection is a subject that has been studied before. Scientists have tried to develop different methods to prevent drivers from diving or sleeping at the wheel (Wang and Yang etc., 2006). Wang et al. proposed a real-time driving fatigue detection system based on a wireless EEG headset. They used power spectrum and

sample entropy to detect the mental fatigue of the driver (Wang and Dragomir etc., 2018). In another study, fatigue detection was performed with the help of OpenCV library by detecting the face of the vehicle driver in both light and night vision mode by means of a camera system installed inside the vehicle (Brandt and Stemmer etc., 2004). Rogado et al. proposed a detection system to detect early signs of fatigue, using data from biological and vehicle peripherals. With this detection system, it decides whether the driver of the vehicle is suitable for driving or not. In the study carried out, the driver's heart rate changes, the pressure on the steering wheel grip, the vehicle's interior and exterior temperature values are obtained and analyzed to determine fatigue indirectly (Rogado and Garciaetc.,2009). Kong et al. proposed a fatigue detection system based on artificial vision. They examined the face, eye and mouth regions of the driver with the images they took from the camera. The open-closed states of the eyes and the mouth opening conditions were examined and the fatigue status of the driver was determined (Kong and Zhou., 2015). Devi and Bajaj, on the other hand, suggested the detection of fatigue by monitoring and measuring eye opening (Devi and Bajaj., 2008, Eriksson and Papanikotopoulos, 1997).

Among the motivation sources of the study, accidents that can be prevented by using the system and injuries and deaths that can be prevented can be counted. In addition, a different method has been developed for fatigue detection based on the Kinect sensor, which is one of the elements of the Internet of Things, and the measurements of the angle that occurs in the neck angle of the driver. This method has not been used for fatigue detection before. In the second part of the study, the proposed model is explained in detail. In the third chapter, the findings obtained from the proposed model are discussed and the results are presented.

2. Proposed Method

In the proposed fatigue detection system, a two-legged fatigue verification method is preferred. First, the skeletal system of the vehicle driver was extracted by using the camera of the Kinect sensor and the infrared module. From the obtained image, the skeletal structure of the neck of the vehicle driver was converted into vectors and the angle between the neck movement was calculated. In normal use, the neck angle of the vehicle driver can vary between 169 and 174 degrees. In cases of fatigue and sleep, the neck bends forward, causing the angle between the skeletal system to decrease. In this way, a warning code is sent to the central control point in real time, considering that the vehicle driver is out of normal use. The measurement values suitable for the scenario of normal use and fatigue or sleep detection are shown in Figure 1.
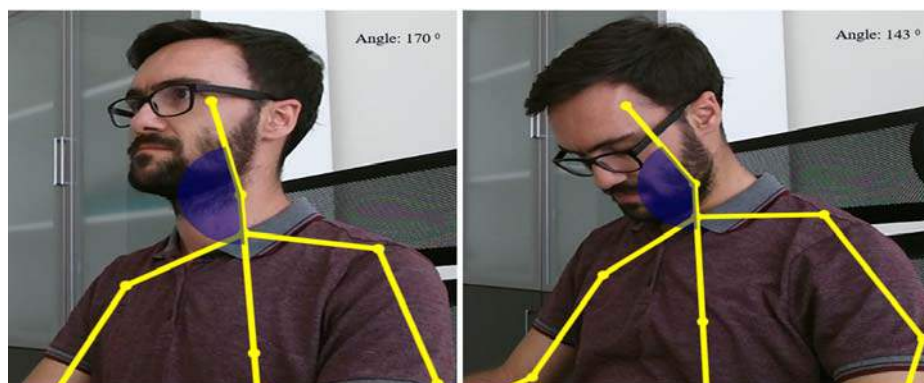
Figure 1: Fatigue detection by obtaining neck angle with Kinect sensor

For the accuracy of fatigue detection, the length from the chest to the neck and the length from the neck to the head are obtained from the absolute difference of the x-axes. Then the obtained values are converted to vector. Then, the angle between these structures, which are

[1] Isparta University of Applied Sciences, Keçiborlu VHS, Isparta, Turkey
* Corresponding author: enesacikgozoglu@isparta.edu.tr

converted into vectors, is calculated using the cosine theorem. As shown in Figure 2, angle calculation is performed when x, y and z points are known. In order to apply the cosine theorem, firstly the conversion to vector is calculated with Formula 1 and Formula 2. Calculation of the lengths of the vectors is calculated as shown in Formula 3 and Formula 4.
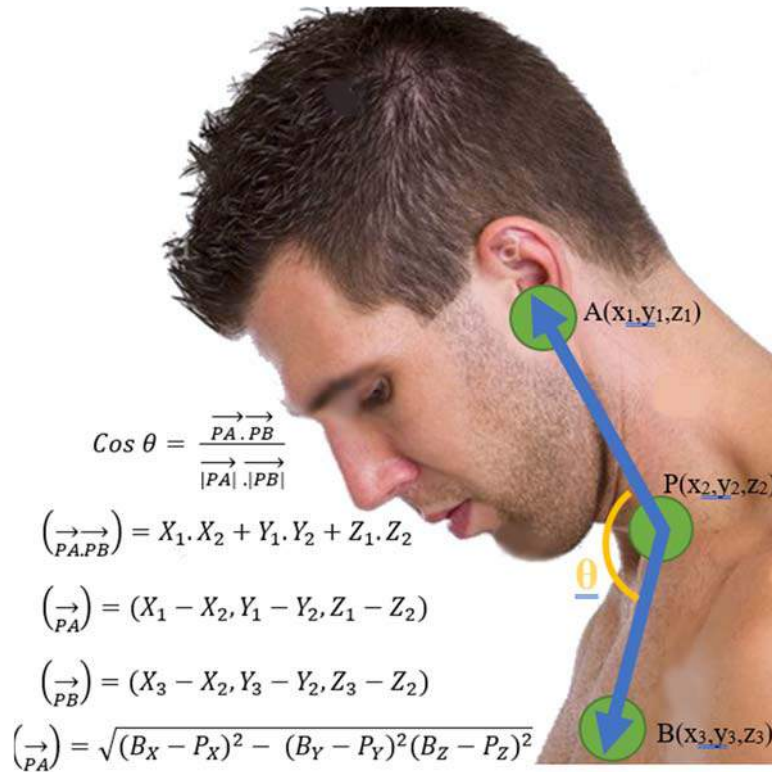
Figure 2: Converting distances to vectors and calculating the angle between

$$\left(\overrightarrow{PA}\right) = (X_1 - X_2, Y_1 - Y_2, Z_1 - Z_2) \qquad \text{(Formula 1)}$$

$$\left(\overrightarrow{PB}\right) = (X_3 - X_2, Y_3 - Y_2, Z_3 - Z_2) \qquad \text{(Formula 2)}$$

$$\left(\overrightarrow{PA.PB}\right) = X_1.X_2 + Y_1.Y_2 + Z_1.Z_2 \qquad \text{(Formula 3)}$$

$$\left(\overrightarrow{PA}\right) = \sqrt{(B_X - P_X)^2 - (B_Y - P_Y)^2 (B_Z - P_Z)^2} \qquad \text{(Formula 4)}$$

After the preprocessing required to calculate the angle between the two vectors is completed, the decision calculation that allows us to calculate the angle between the two vectors is shown in Formula 5.

$$Cos\,\theta = \frac{\overrightarrow{PA}.\overrightarrow{PB}}{|\overrightarrow{PA}|.|\overrightarrow{PB}|} \qquad \text{(Formula 5)}$$

The second fatigue verification step is a system positioned in front of the vehicle driver and constantly monitoring the driver's eyes. Here, the driver's eyes are detected by image processing techniques, and a warning code is sent to the central control point in case of closing or squinting. The EmguCV library of the OpenCV framework was used in the software designed to detect the eyes of the driver. The fact that the driver of the vehicle is wearing glasses does not cause any loss or error in detecting the eyes. The images obtained from the software prepared for the detection of eyes are shown in Figure 3.

[1] Isparta University of Applied Sciences, Keçiborlu VHS, Isparta, Turkey
* Corresponding author: enesacikgozoglu@isparta.edu.tr

Figure 3: Checking the aperture of the eyes with image processing techniques

In the general operation of the system, the neck angle of the vehicle driver and the open-closed states of his eyes are constantly measured. If the obtained measurements are within the required values, the image measurement process continues. As soon as abnormal values are detected, a warning code is sent to the central control point. As soon as warning codes are sent from both the camera and the Kinect sensor, the warning system is inserted into the environment and the vehicle driver is warned with both sound and light warnings. The general operating architecture of the fatigue detection system is shown in Figure 4.
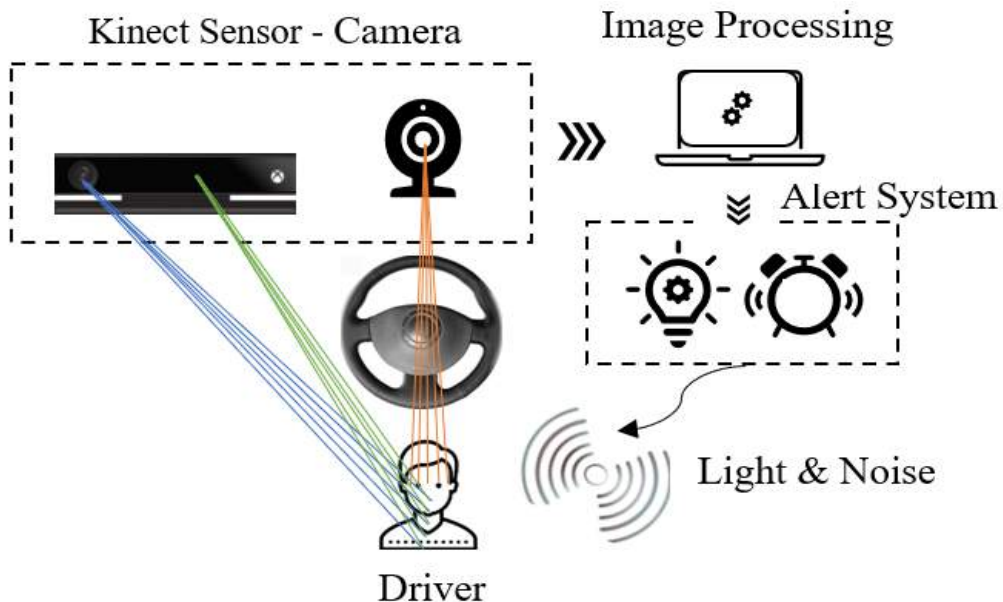
Figure 4: Architecture of the Proposed Fatigue Detection System

[1] Isparta University of Applied Sciences, Keçiborlu VHS, Isparta, Turkey
* Corresponding author: enesacikgozoglu@isparta.edu.tr

3. Discussion and Conclusions

In this study, a system is proposed in which the driver's density can be detected in real time while the vehicles are in motion. This system, which makes use of the values of pupil finding and neck angles for fatigue detection, gives successful results and is open to development. As with all developed and proposed systems, the system proposed in this study has limitations and difficulties. Within the limitations and difficulties of the system, it can be said that the driver of the vehicle pulls his head out of the camera angle for road control and similar purposes while driving. This situation can be said as the activation of the warning system, even if there is no fatigue, since it prevents the correct angle detection in the skeletal system and the perception of the eyes. In future studies, new techniques will be developed on the optimization of this problem.

Reference

Brandt, T., Stemmer, R., & Rakotonirainy, A. (2004, October). Affordable visual driver monitoring system for fatigue and monotony. In *2004 IEEE International Conference on Systems, Man and Cybernetics (IEEE Cat. No. 04CH37583)* (Vol. 7, pp. 6451-6456). IEEE.

Devi, M. S., & Bajaj, P. R. (2008, July). Driver fatigue detection based on eye tracking. In *2008 First International Conference on Emerging Trends in Engineering and Technology* (pp. 649-652). IEEE.

Eriksson, M., & Papanikotopoulos, N. P. (1997, November). Eye-tracking for detection of driver fatigue. In *Proceedings of Conference on Intelligent Transportation Systems* (pp. 314-319). IEEE.

Kong, W., Zhou, L., Wang, Y., Zhang, J., Liu, J., & Gao, S. (2015). A system of driving fatigue detection based on machine vision and its application on smart device. *Journal of Sensors*, *2015*.

Polis Akademisi, 2019. Trafik Kaza ve Denetim İstatistikleri. https://www.pa.edu.tr/Upload/editor/files/Trafik_ Kaza_ve_ Denetim_%C4%B 0statistikleri.pdf Erişim Tarihi: 05.08.2021

Rogado, E., Garcia, J. L., Barea, R., Bergasa, L. M., & López, E. (2009, February). Driver fatigue detection system. In *2008 IEEE International Conference on Robotics and Biomimetics* (pp. 1105-1110). IEEE.

Sikander, G., & Anwar, S. (2018). Driver fatigue detection systems: A review. *IEEE Transactions on Intelligent Transportation Systems*, *20*(6), 2339-2352.

Tuik. 2021. https://data.tuik.gov.tr/Bulten/Index?p=Road-Traffic-Accident-Statistics-2020-37436 . Erişim Tarihi : 05.08.2021

Wang, H., Dragomir, A., Abbasi, N. I., Li, J., Thakor, N. V., & Bezerianos, A. (2018). A novel real-time driving fatigue detection system based on wireless dry EEG. *Cognitive neurodynamics*, *12*(4), 365-376.

Wang, Q., Yang, J., Ren, M., & Zheng, Y. (2006, June). Driver fatigue detection: a survey. In *2006 6th world congress on intelligent control and automation* (Vol. 2, pp. 8587-8591). IEEE.

[1] Isparta University of Applied Sciences, Keçiborlu VHS, Isparta, Turkey
* Corresponding author: enesacikgozoglu@isparta.edu.tr

Performance analysis of advanced encryption standard algorithm using parallel computing for embedded systems

Muhammet Cihat MUMCU[1*], Güner TATAR[2]

Abstract: In today's technological world, data transfer is an important issue. It has even become one of the most discussed topics. With the advancement of technology, processing and storing vast quantities of data in computers and devices with limited resources in the middle of the Internet of things and transmitting them from one location to another through electronic communication channels has become a routine activity of everyday life. However, since the communication networks used for data processing are accessible to everyone's use or access, there is a risk that such data will be shared, lost, or accessed by unauthorized (third) parties. At this stage, some transformations must be performed for the messages to be rendered incomprehensible by third parties and transmitted via accessible electronic communication channels. This is accomplished by the use of encryption or cryptographic operations. The cryptographic algorithms used today may be insufficient in terms of security and efficiency, especially for limited resource devices used in Internet of Things environments. As a result, special lightweight cryptography algorithms built with the constraints of restricted devices are commonly used. The implementation and analysis of the symmetric AES algorithm in parallel computing using different methods on different platforms were performed in this research. AES algorithm has been computed in parallel using different software platforms in the Complex Instruction Set Computer (CISC) architecture, and better efficiency has been achieved by making parallel hardware design in the folded architecture.

Keywords: Internet of Things (IoT), Embedded Systems, Parallel Computing, Lightweight Cryptography.

1. Introduction

In today's world where technology is developing rapidly, the internet and computers have become indispensable elements of our lives. In parallel with this development, the security gaps that have emerged are also as important. It has become compulsory to use the most advanced encryption methods in applications requiring high security such as online sales (e-commerce), banking transactions and credit card transactions. Various encryption, keying and decoding algorithms are provided through the science of cryptography for reliable transmission and acquisition of data (Kahate 2013; Goldreich 2009).

Cryptography is a term that refers to a combination of math and security engineering. It provides us with the tools that are at the heart of most current security measures. It is the most

[1] Maltepe University, Faculty of Engineering and Natural Science, Department of Electrical and Electronics Engineering, Istanbul, Turkey
[2] Fatih Sultan Mehmet Vakıf University, Faculty of Engineering, Department of Electrical and Electronics Engineering, Istanbul, Turkey
* Corresponding author: cihatmumcu@maltepe.edu.tr

appropriate key enabling approach for safeguarding various systems, but it is regrettably difficult to implement correctly (Diffie and Hellman 1976). The cryptology communities and computer security have been drifting away over the last 20 years. The users of security systems do not always realize the cryptology's tools, and they do not always understand the real-world's problems.

In the face of hostile external attackers, cryptography is a method of transferring special information through communication routes. It includes many problems such as authentication, encryption and the key distribution to limited persons. The field of modern cryptography provides the users the ability to understand these problems depending on the theoretical foundation, evaluate the response protocols that can solve these problems, and build the needed protocols that achieve the confidence of security (Eisenbarth et al. 2007).

Today's cryptographic methods may be insufficient in terms of security and performance, particularly for devices with low resources utilized in Internet of Things environments. As a result, specific lightweight cryptography methods designed for limited devices are frequently employed. This work involved the implementation and analysis of the symmetric AES algorithm in parallel computing using various approaches on various platforms.The AES algorithm has been computed in parallel using different software platforms in the Complex Instruction Set Computer (CISC) architecture, and better efficiency has been achieved by making parallel hardware design in the folded architecture.

2. Material and Method

The cryptography techniques are generally divided into two groups:

2.1. Symmetric Algorithms

The same structure is used for encryption and decryption in symmetric key algorithms whose general structure is shown in Figure 1. This key is called a secret key. This secret key is known to both parties (sender and receiver).
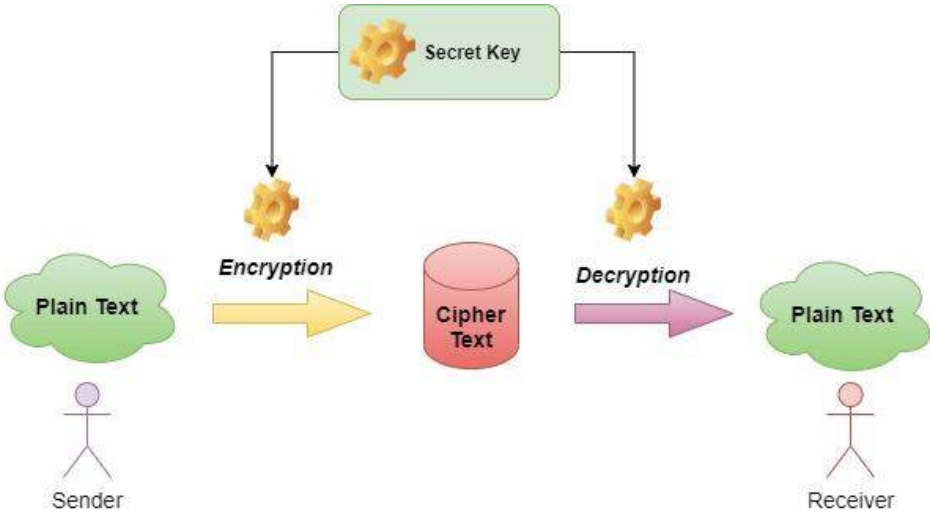
Figure 1. General Structure of Symmetric Key Algorithm

Symmetric algorithms work faster than asymmetric algorithms. Examples of symmetric algorithms include AES, DES, 3DES, Blowfish, IDEA, RC4 and TEA. Symmetric ciphers are still widely used, especially for data encryption, data decryption and integrity check of the messages. The symmetric cryptography algorithms can be rated into two types, block ciphers and stream ciphers (Chandra et al. 2014; Ebrahim et al. 2014).

2.2 Asymmetric Algorithms

Different keys termed public and private keys are used for encryption and decryption in this cryptography method, and the overall structure of systems with asymmetric keys is depicted in Figure 2. These two keys are used together. However, a person who has any of these keys cannot produce the other key, which is mathematically impossible.
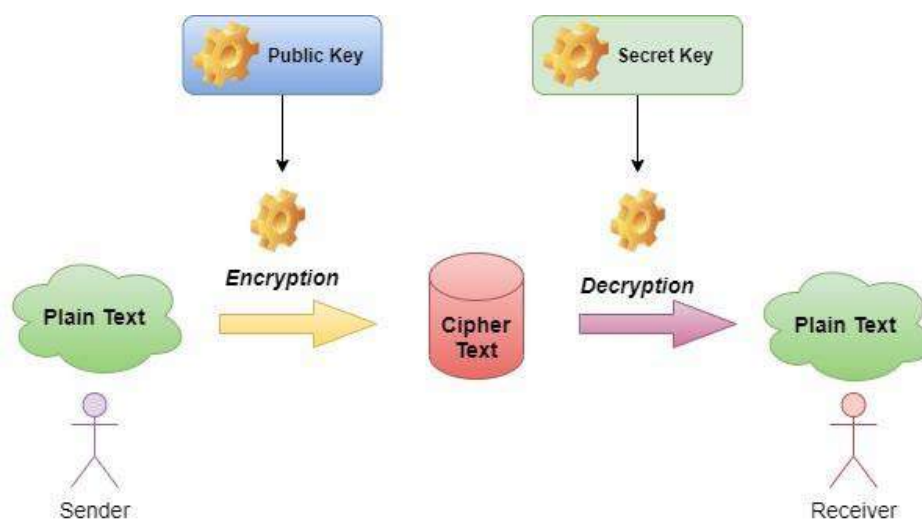
Figure 2. General Structure of Asymmetric Key Algorithm

Asymmetric algorithms are more secure and more difficult to break than symmetric algorithms. However, their performance is quite low compared to symmetric algorithms. In asymmetric algorithms, each person has a key pair. A person's private key is for his own use only and should not be in the hands of others. The only recipient can open the encrypted message with his private-key. Some examples of public-key cryptography algorithms are Elgamal, RSA, ECC, Diffie-Hellman and DSA (Maqsood et al. 2017; Garg and Yadav 2014).

2.3. Advanced Encryption Standard

AES is an encryption standard adopted by the United States. A standard block encoder, also known as Rijndael (Daemen and Rijmen 2001). The algorithm improved by two Belgian researchers Joan Daemen and Vincent Rijmen was determined as the new standard as a result of the competition organized by NIST (National Institute of Standards and Technology) in order to determine a new encryption standard with the weakening and credibility of the DES algorithm against the developing technology. After a long period of standardization and verification, it was published by NIST on 26 November 2001 as the AES FIPS 197 standard (Nechvatal et al. 2001; Schneier and Whiting 2000).

Advanced encryption standard (AES) is a block cipher algorithm that encrypts data in 128-bit chunks. There are three types, AES-128, AES192 and AES-256, according to the key length it

uses. In AES, 128-bit data blocks are considered 4 words, each consisting of 32-bits. When starting the encryption process with AES, a 128-bits data block consisting of 4 words is written into the state sequence and all the necessary operations during the algorithm are performed using this sequence. With the end of the last operation required for encryption, the last state of the sequence is written to the output sequence (Selent 2010).

The AES algorithm generally consists of two blocks, the first block is the round conversion and the second block is the key generation block. The algorithm has a repetitive structure, 128, 192 or 256-bit, depending on the length of the key sizes, is repeated 10, 12, or 14 times in turn. The number of repetitions is given in Table 1.

Table 1. AES Key-Block-Round Comparison

	Block Size (bit)	Key Length (bit)	Number of Rounds (Nr)
AES-128	128	128	10
AES-192	128	192	12
AES-256	128	256	14

The block to be encrypted at the beginning of the encryption is written to the status sequence according to Figure 3. Encryption process starts with the addition of the state sequence with the input key. Depending on the length of the key sizes, the round conversion is repeated 10, 12 or 14 times.
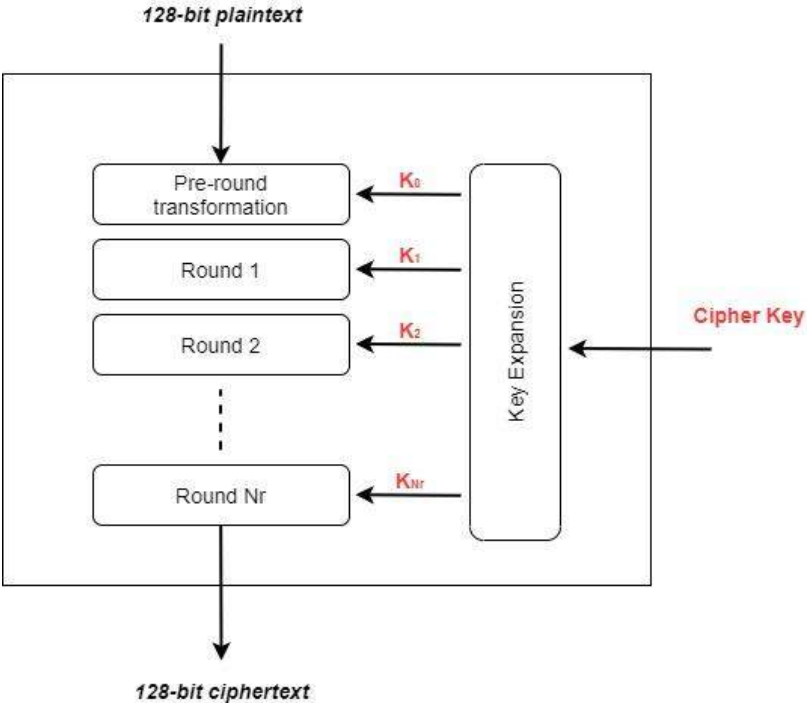
Figure 3. The Structure of AES Encryption

The block diagram of the detailed encryption and decryption process is given in Figure 4. During the tour conversion process, the Byte Change, Shifting Rows, Mixing Columns, and

Round Key collection sub-operations are applied on the status sequence. The 128-bit data obtained as the output of the round conversion process is collected by the key data generated as a result of the key generation process. Performing the last round operation and collecting with the key block results in the encrypted block. The operations performed in the last round differ from those performed in the previous rounds. Mixing Columns is not performed in the last round.
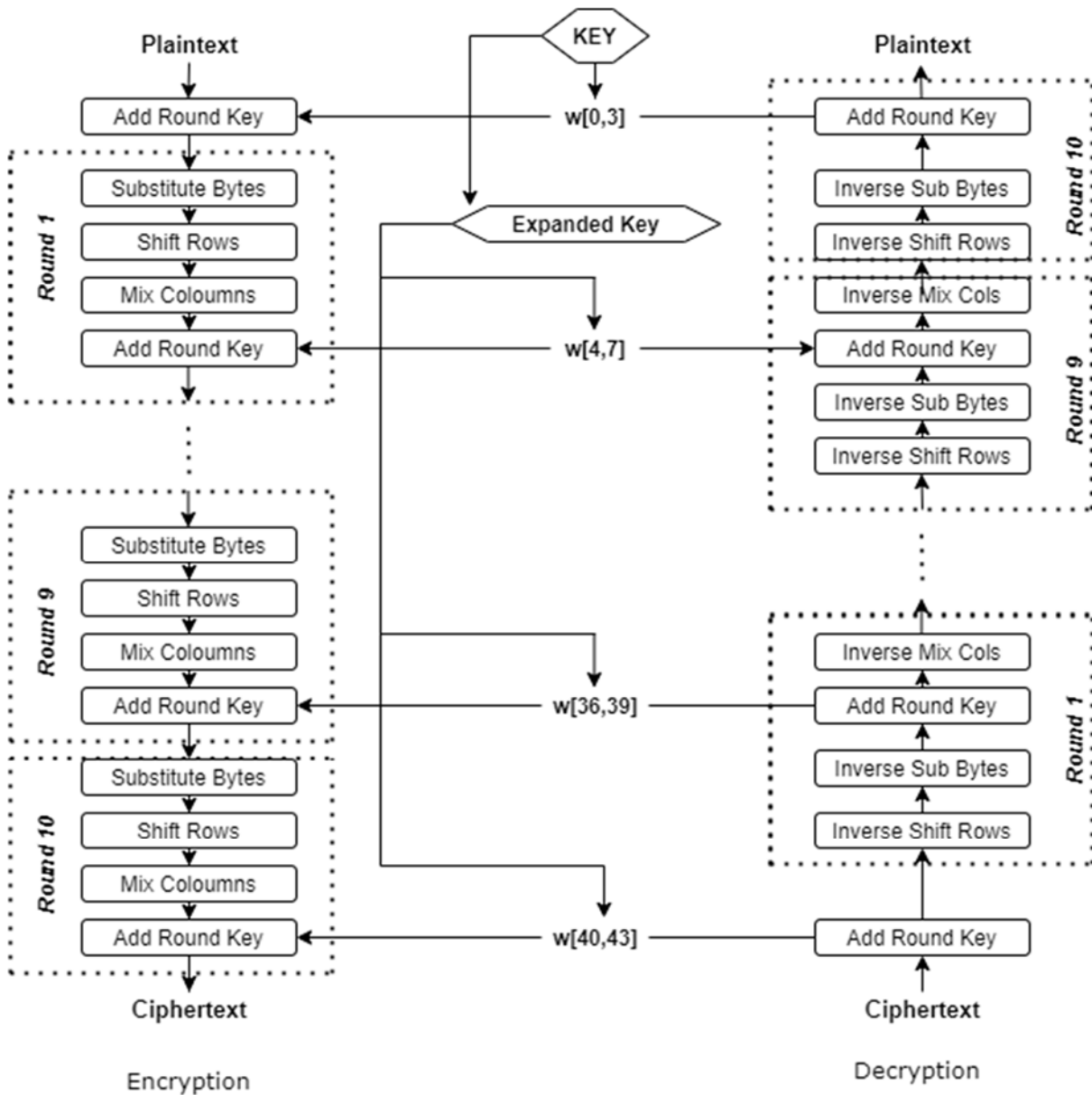
Figure 4. The Detailed Encryption and Decryption Rounds of AES-128

2.4. Instruction Set Architecture (ISA)

In computer science, an instruction set architecture (ISA), often known as computer architecture, is an abstract representation of a computer. Devices such as central processing units (CPUs) that implement an ISA are referred to as "implementations". I/O paradigm (such as memory consistency, addressing modes and virtual memory) and data type support are defined by an ISA for a family of ISA implementations (Goodcare and Sloss 2005).

An ISA specifies the behavior of machine code running on ISA implementations in a way that is independent of those implementations' characteristics, allowing binary compatibility across them. This allows multiple implementations of an ISA to run the same machine code while differing in performance, physical size, and monetary cost (among other things). This allows a lower-performance, lower-cost machine to be replaced with a higher-cost, higher-performance machine without replacing the software. It also enables the evolution of ISA implementation microarchitectures, allowing a newer, higher-performance ISA implementation to run software written for previous generations of implementations (Jamil 1995).

The architecture of processor instruction sets varies. Each architecture has its own length, structure, and complexity of commands. As a result of the alteration, there is a difference in design.

The first of the instruction set architectures, CISC (Complex Instruction Set Computing), is the first developing instruction set architecture. Commands in this architecture vary in length and complexity. Both memory and instruction number are saved since many instructions are merged into a single instruction. The intricacy of the instructions, on the other hand, adds to the complexity of the processor architecture. The instructions in the RISC instruction set architecture are all the same length and have a basic structure. This makes the processor design easier. In comparison to the CISC design, however, more instructions are required to execute an operation (Bhandarkar 1997).

2.4.1 Complex Instruction Set Computing (CISC)

When Intel's processor series based on the x86 architecture first appeared in the 1970s, some design architects who advocated for the support of high-level languages by utilizing these resources economically due to the expensive and limited RAMs collaborated to create the CISC architecture. This architecture is the result of a design philosophy that is simple to program and makes efficient use of memory. Despite the fact that it has poor performance and complicates the processor, it simplifies the software.

Variable-length commands are one of the two distinguishing features of CISC architecture, along with complex commands. Commands with variable and complex lengths save memory. Because complex instructions combine two or more instructions into a single instruction, they save both memory and the number of instructions that must be included in the program. A complex command necessitates a complex architecture. As the architecture becomes more complex, undesirable situations in processor performance arise. Low memory usage when installing and running programs, on the other hand, can eliminate this issue. A typical CISC instruction set contains 120-350 instructions in variable format. It has a good memory management system and more than a dozen addressing modes (Bhandarkar and Clark 1991).

The CISC architecture is based on the multi-stage processing model. The first tier is where the high-level language is written. The next level is machine language, which, as a result of compiling the high-level language, translates a series of commands into machine language. In the next step, the commands translated into machine language are decoded and converted into the simplest operable codes (microcode) that can control the hardware units of the microprocessor. At the lowest level, the necessary tasks are carried out through the hardware that receives the workable codes.

CISC processors are designed to complete the command before moving on to the next instruction. In practice, however, this is not the case because the commands are too complex

and are not processed in a single loop. They cause delays in the production line. As a result, most processors divide instruction execution into several distinct stages. When a stage is completed, the result is passed on to the next stage (Lee et al. 2002).

2.4.2 Reduced Instruction Set Computing (RISC)

RISC architecture was developed as an alternative to CISC architecture with the reaction of the market to eliminate the bad aspects of processors. Companies such as IBM, Apple, and Motorola have worked diligently to develop RISC. Adherents of the RISC philosophy believed that computer architecture needed to be completely overhauled and that almost all traditional computers had architectural flaws and were therefore obsolete (Wolfe and Chanin 1992). They believed that computers were becoming increasingly complex and that they needed to be set aside and restarted from scratch (Kane 1988).

Advances in semiconductor technology began to close the speed gap between main memory and processor chips in the mid-1970s. As memory speed rose and high-level languages supplanted assembly language, the CISC's primary benefits began to fade. Instead of only speeding up hardware, computer designers began to experiment with different methods to boost computer performance (Aletan 1992).

IBM is recognized as being the first to define the RISC architecture in the 1970s. In reality, the universities of Berkeley and Stanford expanded on this study in order to uncover core architectural models. Three essential concepts underpin RISC's philosophy. A requirement of performance parity is that all instructions be performed in a single cycle. It can only be realized if specific characteristics are present. Instruction code must have a set width equal to or smaller than the external bus to minimize decoding delays, operands must not be supported, and instructions must be vertical and simple. Only the "load" and "store" commands should be used to access the memory. This principle is a logical extension of the first. It takes many cycles to execute an instruction that directly manipulates memory for its own purpose. The command is retrieved, and memory is examined. The RISC processor loads data from memory into a register, reviews the register and then writes the contents of the register to the main memory. This sequence necessitates at least three commands. To maintain performance with register-based transaction processing, a large number of general-purpose loggers are required. All execution units must be run directly from the hardware, without the use of microcode. Using microcode necessitates a large number of cycles to load arrays and similar data. As a result, it is difficult to use in the execution of single-cycle execution units (Waterman 2016).

2.5. Parallel Programming Methods

In general terms, parallel programming is the principle of using multiple sources and processors to solve a problem. In this type of programming, the problem is divided into smaller steps and instructions are given to the processors to solve them simultaneously. Thus, compared to a work done using serial programming, a serious advantage is gained in the completion time of the work by using the parallel programming technique (Karunadasa and Ranasinghe 2009). Today, new types of computer systems have hardware that allows this type of programming. When parallel structures are used, it offers advantages over simultaneous programming in terms of accelerating all processes, achieving fast results and saving time. On the other hand, the use of parallel computing methods has high energy requirements as it uses a large number of processor cores, and besides, such programming methods are more difficult to learn than simultaneous programming. As it is known, there are five main methods in

parallel programming. One of them is the modern compilers, called compile aid, which are used to automatically parallelize the program written by the user. Examples are Intel AVX and Intel Parallel Studio XE. Another is the calling of parallelized libraries. Multi-core architectures can be exploited in this process, even NVIDIA GPUs, using libraries built on CUDA is a big step towards parallelization. Another one, even one of the important ones, is OpenMP (Graham et al. 2005; Gabriel et al. 2004). In basic terms, OpenMP is a multi-platform API as well as an application development interface that supports multi-platform shared memory multiprocessing in C, C++ and Fortran programming languages. OpenACC (open accelerator) is known as a programming standard for parallel computing. It makes parallel programming of standard heterogeneous CPU/GPU systems simpler. That is, it can initiate computational code on both CPU and GPU architectures. Our fourth parallel programming technique is known as low-level hardware targeting, and even includes hardware description languages used in FPGA programming such as VHDL and Verilog. The focus here is on CUDA programming, mostly CPU and GPU memory allocation, data transfer, and computing "kernels" mapped between thread blocks in the GPU (Farber 2011; Cheng et al. 2014). In GPUs, basically one-way multi-data paradigms called SIMD are implemented. CUDA is low level programming and it is clear that the problem is with knowing the basic structure of GPUs and how to map it to hardware. The last but not least important parallel programming method is MPI (message passing interface). MPI is the "standard" for distributed memory parallelism, that is, the parallel use of networked node clusters. Using efficient threading and intra-node communication methods, the MPI is a great fit for the symmetric multiprocessing (SMP) node. Performance-wise, it's just as good as direct threading methods like OpenMP. Today, it has become a standard for hybrid programming in which OpenMP and MPI are used together. MPIs are also used with hardware accelerators like GPUs. So multi-core architectures are suitable for MPI acceleration. An example of distributed shared memory is given in Figure 5. The relationship between Shared and Distributed memory can be understood here.
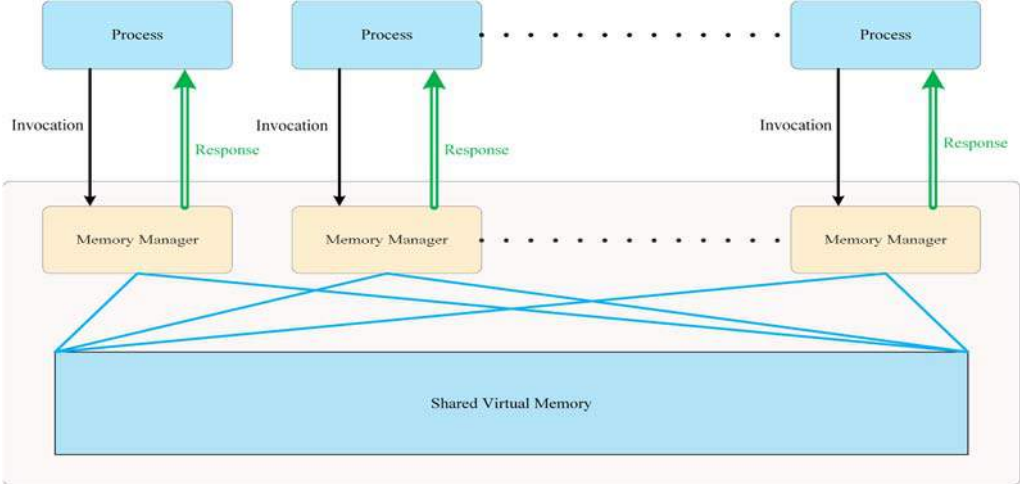
Figure 5. Distributed Shared Memory Architecture

3. Results

In this study, encryption and decryption performance analyses of the AES-128 algorithm on texts of different sizes were performed. During the comparison of the algorithm on serial, OpenMP and CUDA platforms, HP Workstation with Intel ® Core ™ i7-7700HQ @2.80 GHz (8CPUs) processor and NVIDIA Quadro M1200 graphics card was used in CISC structure.

The results of computing the AES-128 algorithm for both encryption and decryption in serial and parallel mode on plain texts are presented in Figure 6 and 7.
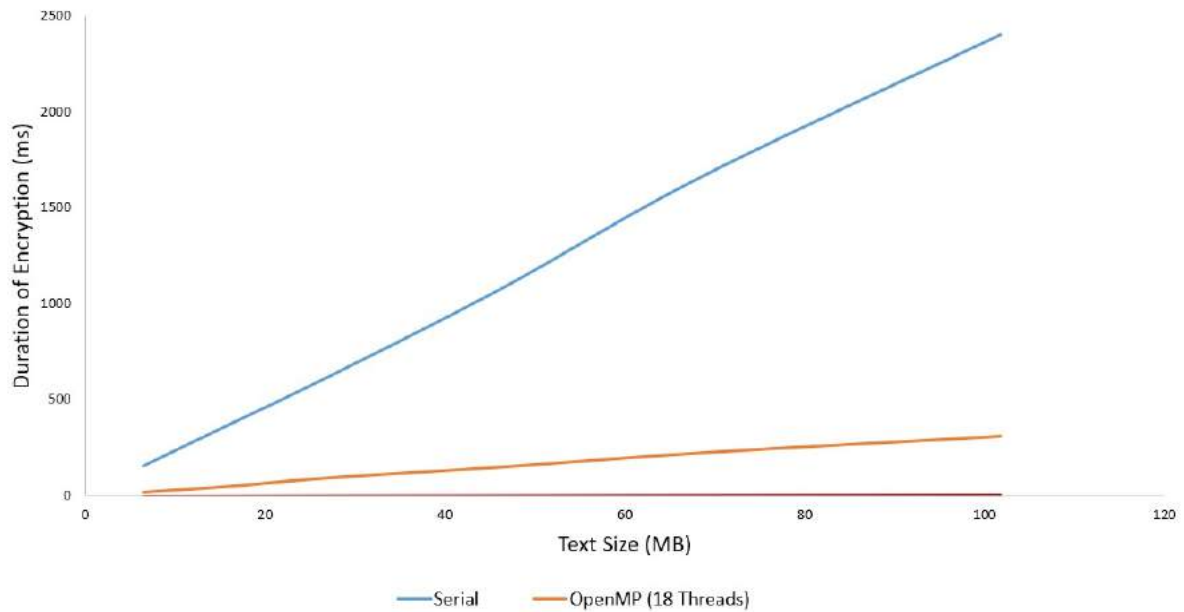
Figure 6. Comparison of Serial vs. Parallel Computing for Encryption
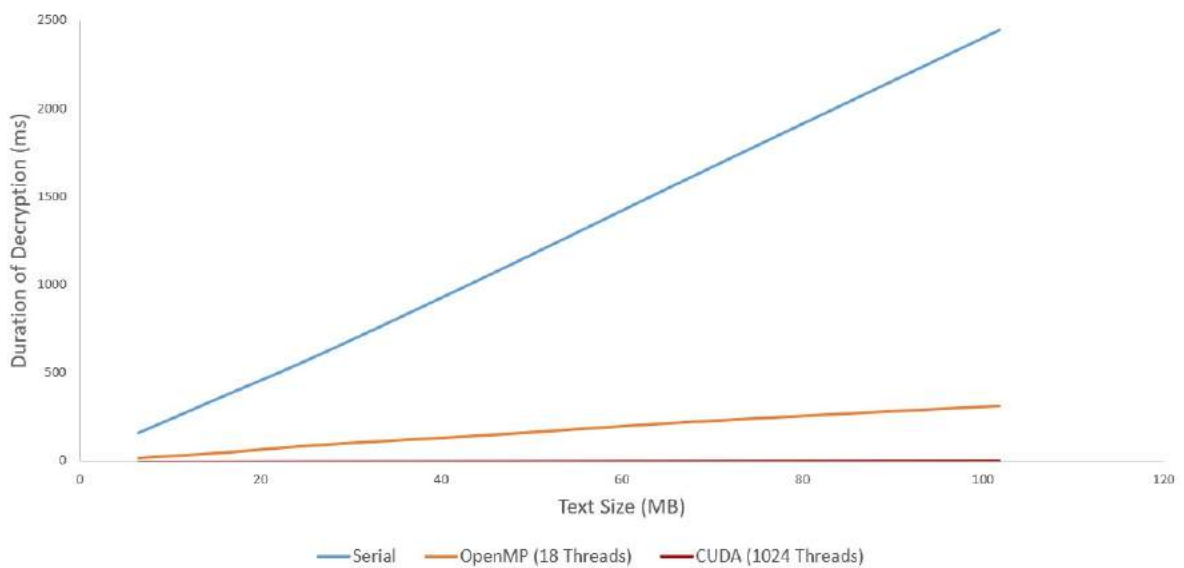
Figure 7. Comparison of Serial vs. Parallel Computing for Decryption

As can be seen in Figures 3 and 4, a significant performance improvement has been observed in the implementation of the AES algorithm using parallel computing methods. Especially CUDA showed a much better result compared to the OpenMP method. AES is a block cipher algorithm based on Substitution-Permutation design. Therefore, encryption and decryption times are expected to be similar. This similarity is observed in Figures 3 and 4 for all computing methods.

4. Discussion and Conclusions

In this work, encryption-decryption implementations of the AES-128 technique on texts of various sizes were created, and OpenMP and CUDA applications were created to boost performance. It has been discovered that the algorithm's parallel implementation yields considerable performance benefits when compared to executing in serial mode. It will make major contributions to research in the field of the internet of things and information security in the future with the application of comparable methodologies to different cryptology algorithms.

References

Aletan, S. O. (1992, April). An overview of RISC architecture. In *Proceedings of the 1992 ACM/SIGAPP Symposium on Applied computing: technological challenges of the 1990's* (pp. 11-20).

Bhandarkar, D., & Clark, D. W. (1991, April). Performance from architecture: comparing a RISC and a CISC with similar hardware organization. In *Proceedings of the fourth international conference on Architectural support for programming languages and operating systems* (pp. 310-319).

Bhandarkar, D. (1997). RISC versus CISC: a tale of two chips. *ACM SIGARCH Computer Architecture News*, *25*(1), 1-12.

Chandra, S., Bhattacharyya, S., Paira, S., & Alam, S. S. (2014, November). A study and analysis on symmetric cryptography. In *2014 International Conference on Science Engineering and Management Research (ICSEMR)* (pp. 1-8). IEEE.

Cheng, J., Grossman, M., & McKercher, T. (2014). *Professional CUDA c programming*. John Wiley & Sons.

Daemen, J., & Rijmen, V. (2001). Reijndael: The Advanced Encryption Standard. *Dr. Dobb's Journal: Software Tools for the Professional Programmer*, *26*(3), 137-139.

Diffie, W., & Hellman, M. (1976). New directions in cryptography. *IEEE transactions on Information Theory*, *22*(6), 644-654.

Ebrahim, M., Khan, S., & Khalid, U. B. (2014). Symmetric algorithm survey: a comparative analysis. *arXiv preprint arXiv:1405.0398*.

Eisenbarth, T., Kumar, S., Paar, C., Poschmann, A., & Uhsadel, L. (2007). A survey of lightweight-cryptography implementations. *IEEE Design & Test of Computers*, *24*(6), 522-533.

Farber, R. (2011). *CUDA application design and development*. Elsevier.

Gabriel, E., Fagg, G. E., Bosilca, G., Angskun, T., Dongarra, J. J., Squyres, J. M., ... & Woodall, T. S. (2004, September). Open MPI: Goals, concept, and design of a next generation MPI implementation. In *European Parallel Virtual Machine/Message Passing Interface Users' Group Meeting* (pp. 97-104). Springer, Berlin, Heidelberg.

Garg, N., & Yadav, P. (2014). Comparison of asymmetric algorithms in cryptography. *Journal of Computer Science and Mobile Computing (IJCSMC)*, *3*(4), 1190-1196.

Goldreich, O. (2009). *Foundations of cryptography: volume 2, basic applications*. Cambridge university press.

Goodacre, J., & Sloss, A. N. (2005). Parallelism and the ARM instruction set architecture. *Computer*, *38*(7), 42-50.

Graham, R. L., Woodall, T. S., & Squyres, J. M. (2005, September). Open MPI: A flexible high performance MPI. In *International Conference on Parallel Processing and Applied Mathematics* (pp. 228-239). Springer, Berlin, Heidelberg.

Jamil, T. (1995). Risc versus cisc. *Ieee Potentials*, *14*(3), 13-16.

Kahate, A. (2013). *Cryptography and network security*. Tata McGraw-Hill Education.

Kane, G. (1988). *mips RISC Architecture*. Prentice-Hall, Inc..

Karunadasa, N. P., & Ranasinghe, D. N. (2009, December). Accelerating high performance applications with CUDA and MPI. In *2009 International Conference on Industrial and Information Systems (ICIIS)* (pp. 331-336). IEEE.

Lee, J. H., Lee, W. C., & Cho, K. R. (2002, August). A novel asynchronous pipeline architecture for CISC type embedded controller, A8051. In *The 2002 45th Midwest Symposium on Circuits and Systems, 2002. MWSCAS-2002.* (Vol. 2, pp. II-II). IEEE.

Maqsood, F., Ahmed, M., Ali, M. M., & Shah, M. A. (2017). Cryptography: A comparative analysis for modern techniques. *International Journal of Advanced Computer Science and Applications*, *8*(6), 442-448.

Nechvatal, J., Barker, E., Bassham, L., Burr, W., Dworkin, M., Foti, J., & Roback, E. (2001). Report on the development of the Advanced Encryption Standard (AES). *Journal of Research of the National Institute of Standards and Technology*, *106*(3), 511.

Schneier, B., & Whiting, D. (2000, April). A Performance Comparison of the Five AES Finalists. In *AES Candidate Conference* (pp. 123-135).

Selent, D. (2010). Advanced encryption standard. *Rivier Academic Journal*, *6*(2), 1-14.

Waterman, A. S. (2016). *Design of the RISC-V instruction set architecture*. University of California, Berkeley.

Wolfe, A., & Chanin, A. (1992). Executing compressed programs on an embedded RISC architecture. *ACM Sigmicro Newsletter*, *23*(1-2), 81-91.

Changes in agrochemical indicators of soils under the rotational technique of pasture use in the conditions of the Kyrgyz Republic

Totubaeva N.E.[1*], Shalpykov K.T.

Abstract: Intensive use of pastures, without the use of rotational technique in the Kyrgyz Republic, over the past 30 years has led to the deterioration of their ecological condition, as a result more than 60% of the country's pastures are degraded. One of the indicators of pastures' state is the agrochemical indicators of pasture soils. Therefore, the purpose of our research was to study changes in agrochemical indicators of soils, with different types of pasture use. We created demonstration plots of 1 hectare each, with an interval of 1 year of withdrawal from common use. Our studies showed that the pasture plot that was fenced 1 year ago contained more particles the size of which were <0.001mm (18.04%), and the plot that was not fenced and subjected to overgrazing contained minimal particle content of size <0.001mm (15.64%). In contrast, the content of large particles of 1.0-0.25 mm, in the unfenced plot was elevated and was 9.45%, and in the fenced plot the content of particles of 1.0-0.25 mm was 2.49 and 2.71%. Ca^{2+} content in the unfenced plot was lower than in the fenced plots and was 0,008/0,40 %/mg.eq. As the increase of Ca^{2+} in soil is an important indicator of improvement of soil structure and general condition, we can assume that creation of rotational grazing is important to improve structure, pasture productivity, and possibility of good practice of successful sustainable grazing and improve life and health of local population vulnerable to climate change.
Keywords: sustainable pasture use, biodiversity, anthropogenic pressure, soil degradation, ecosystem, agrochemical indicators

Keywords: Kyrgyz, climate change., Cryptography

1. Introduction

Many works are devoted to methods of sustainable pasture management (Ehsan Elahi,2021; W. Crewett, 2012; Silva de Oliveria, 2017; Amorim H.C., 2020; Ragimov, A., 2020; Andreeva O.V. et al, 2021). The relevance is caused by the intensification of pasture degradation with the continuous growth of the world population and the possible problem with food security, especially in arid areas (Aerts R. , 2000; FAO, 2020; Xie et al., 2020; Elser J. J., 2010; Picasso, V. D.,2014). Many projects have been implemented to identify vulnerable communities and target areas to implement locally appropriate sustainable rangeland management options (FAO, 2020). However, most developments in sustainable pasture management focus on socio-economic management issues and decision-making theory rather than on natural processes and ecosystem responses to negative anthropogenic impacts (Andreeva O. V., 2021; Donald M., 2021; WOCAT Database, 2020). The most vulnerable link of unsustainable pasture management is soil, it is an indicator of the ecological

[1] Kyrgyz-Turkish Manas University, Bishkek, KYRGYZSTAN.
* Corresponding author: totubaevanurzat@gmail.com

state of the environment, the initial link in the productive chains of the ecosystem (Kovyazin V.F., 2008), ensuring its health is one of the most important tasks of our time. Soil health is the ability of soil to function as a single living system in nature and within the boundaries of land use, maintain plant and animal productivity, maintain or improve water and air quality, and contribute to plant and animal health (Reynolds, W. D., 2007; Duval, M. E., 2013). Anthropogenic decline in pasture soil health is a pressing environmental problem in the Kyrgyz Republic (Wibke Crewett, 2012; Dörre A., 2012). Pastures in the country occupy almost half of the country's land area, or about 80% of agricultural land (FAO, 2018). For more than half of the local population of the country, livestock farming is the main source of income (SIP "Kyrgyzgiprozem" under the Ministry of Agriculture and Food, 2018). Recently, the intensification of degradation of pastures has been observed, which in a moderately arid climate can lead to irreversible processes of aridization of vast areas not only of the Kyrgyz Republic, but also of all Central Asian countries, affecting the strategic resources of economic development, food security and environmental health (Nóbrega RLB, 2017). According to FAO (2000), pasture productivity in the Kyrgyz Republic has steadily declined since the 1960s, and by 1993 it was reported to be about 300 kg/ha dry substance due to increased grazing pressure and poor grazing management (FAO, 2018). One of the informative indicators of soil condition is its agrochemical characteristic, which can characterize the qualitative condition of soil (Alexander K.G., 1991; Pierret A., 1999; Dorana J, 2000; Hunke, P.,2015; Hunke P, 2015, Lavelle, Patrick, 2000; Mandal, A., 2020) and depends largely on its granulometric composition and degree of degradation (Donald R.G., 1987; Dolgopolova N., 2018). This indicator is often used for the ecological assessment of urban areas (Kovyazin V.F., 2008). However, its application to assess the condition of pastures is of particular interest. In this regard, the purpose of our research was to study changes in the agrochemical indicators of the country's pasture soil withdrawn from general use for different terms.

2. Materials and Methods

The studies were conducted in the spring and fall pastures of the Chu valley of the Kyrgyz Republic, located at an altitude of more than 1600 m a.s.l. Chui region is located in the northern part of the Kyrgyz Republic, and occupies Chui, Chon-Kemin, high-mountain Suusamyr valley, as well as slopes of Kyrgyz, Zaili, Kungey Ala-Too, Suusamyr-Too and Djumgal ranges.

Soil sampling was done in the Shamshy area of the Issyk-Ata District (map-scheme1).

Map-scheme1. points of experimental plots (Shamshy ur., Chui oblast, Kyrgyz Republic).
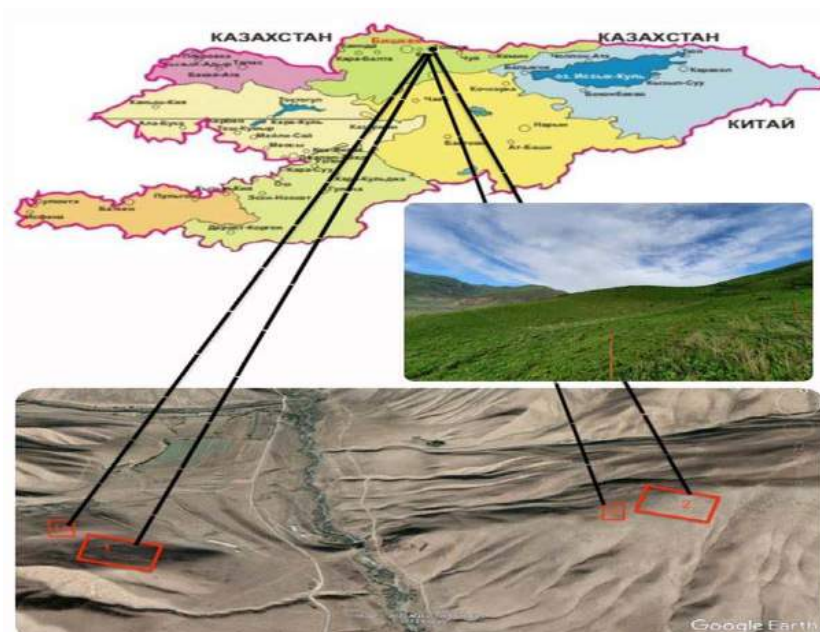
In order to study the agrochemical parameters of pasture soils, we selected soil samples shown in Table 1:

Table 1 **Soil sampling scheme**

#	Pilot site plans	Selection coordinates	Height above sea level
1	Demonstration plot withdrawn from pasture use in 2020, total area 1 ha	$42^o35^/29,1^{//}$N, $75^o24^/08,53^{//}$E 42.591411 75.402.371	1654
1a	Demonstration plot withdrawn from pasture use in 2019, total area 0.1 ha	42o35/29,1//N, 75o24/08,53//E 42.591411 75.402.371	1654
2	Demonstration plot withdrawn from pasture use in 2020, total area 1 ha	$42^o35^/17,64^{//}$N, $75^o27^/06,49^{//}$E 42.588233 75.451805	1948
3	Control, intensively used pasture type. A background soil sample was taken at a distance of 10 m from the fenced plots.	$42^o35^/17,64^{//}$N, $75^o27^/06,49^{//}$E 42.588233 75.451805	1948

Figure 1 shows the demonstration plots of the study areas (Figure 1)
a) Demonstration site #1
b) Demonstration site #2

Soil samples were taken according to GOST 17.43.01-83, at a depth of 0-20 cm, from a 1x1 m sample plot of 5 points that were combined into one total sample of 400-500 g.

Soil pH was measured with a universal ionometer EB-74.

Soil humus was determined by Tyurin's method modified by CINAO. Soil humidity was determined by gravimetric method by drying samples in a drying oven at a temperature of 105oC. Determination of total nitrogen was determined by Meshcheryakov method, determination of gross forms of phosphorus and potassium by Machigin method, mechanical method by sieve method, using sieves from 0.001 to 10.0 mm in size. Determination of the aqueous extract according to GOST 26423-85.

All data analyses were performed using Statistica 13.0 (USA). All figures created in the Excel program from the Microsoft Office program package.

Results and Discussion

According to the International Fund for Agricultural Development, Chui oblast in the Kyrgyz Republic is classified as a vulnerable region to climate change (Map 2).
Map-scheme 2: Levels of vulnerability to climate change in the Kyrgyz Republic (Source: IFAD, Livestock and Market Development Program II (LMDP II). Project Completion Report. WG 6. Impact of Climate Change on Pastures and Livestock Systems - Summary Report, 2017)
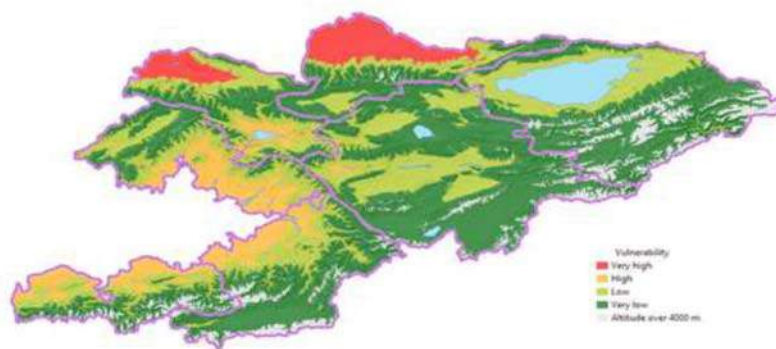
The situation is aggravated by unsustainable pasture use. The study of agrochemical properties of pastures under different pasture use showed that rotational technique significantly affects their composition.

The mechanical composition of soils is characterized by aggregates of different shapes and sizes, among which sandy particles (1-0.05 mm), dust (0.05-0.001 mm), silt (0.001-0.0001 mm), colloids (<0.0001 mm) stand out (Esenzhanova G.K., 2019). The soils we studied had the mechanical composition given in Table 2.

As shown in Table 2, the demonstration plots of pastures that were fenced 1 year ago (1a) contained more particles of size <0.001mm (18.04%), and the plot that was not fenced in and used in full contained minimal particles of size <0.001mm (15.64%) (Fig.2). In contrast, the content of coarse particles of 1.0-0.25mm size, in the unfenced plot was higher and was 9.45%, while in fenced plot 1 and 1a the content of particles of 1.0-0.25mm size was 2.49 and 2.71%, which was 6.74 times lower than in the unfenced plot (Fig.3).

Table 2 Mechanical and microaggregate composition of soils under different types of pasture use, in %

Sampling number	Fractional composition, % (particle size)						Sum of particles <0.01
	1.0-0.25	0.25-0.05	0.05-0.01	0.01-0.005	0.005-0.001	<0.001	
1	2,71	22,81	35,36	9,80	12,64	16,68	39,12
1a	2,49	24,35	35,16	8,64	11,32	18,04	38,00
2	8,24	27,36	30,40	5,52	11,24	17,04	33,80
3	9,45	24,27	34,60	5,52	10,52	15,64	31,68
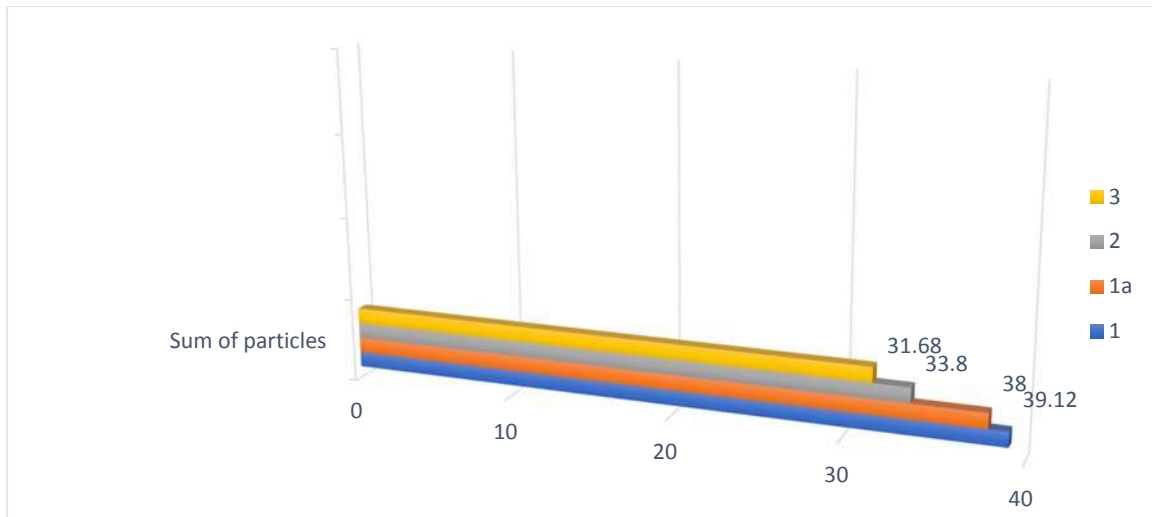
Fig.2 Change in the sum of particles <0.01 at different types of pasture use
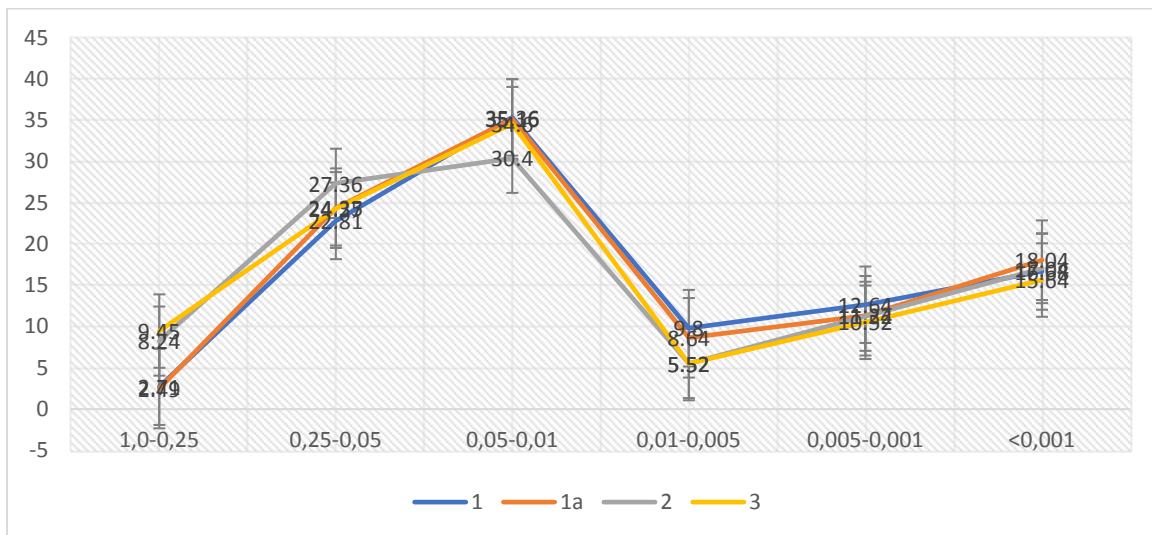
Fig.3. Changes in the texture of soils under different types of pasture use

Thus, in order to preserve and improve the productivity of mountain pastures, the use of rotational grazing is a necessary and important measure, with the resilience of mountain ecosystems to various types of risks. Further, according to the research program, we studied the chemical composition of the studied soils.

Indicators of soil chemical composition showed ambiguous indicators, according to which it is not possible to reveal any dynamics in changes of chemical composition with changes in the type of post-land use (Table 3), however, some changes can still be traced (Fig.4). The chemical composition of soils showed that the plot fenced for more than 1 year had the highest soil pH of 7.80, while the pH of the rest of the plots was 7.45 (Fig. 5). The CO_2 content in the unfenced plot was 0.4%, while the other plots had a value of 0.44%. However, the humus content in the unfenced plot was higher than in the other variants of the studied soils and was 8.85%, and in plot 1a (fenced more than 1 year ago) the humus content was 6.55%, which was the lowest of all soils studied.

Table 3 Chemical composition of soils, with different types of pasture use

№	pH	CO_2, %	Humus, %	Total nitrogen, %	The mobile form of phosphorus (P_2O_5) mg/kg	Exchangeable potassium (K_2O) mg/kg	Exchange capacity mg-eq./100 g soil	Absorbed Na, mg-eq
#1	7,45	0,44	7,17	0,245	18,2	600,0	29,0	0,25
#1a	7,80	0,44	6,55	0,215	21,0	240,0	28,0	0,20
#2	7,45	0,44	7,64	0,290	22,5	275,0	27,2	0,25
#3	7,45	0,40	8,85	0,323	24,0	240,0	28,6	0,25
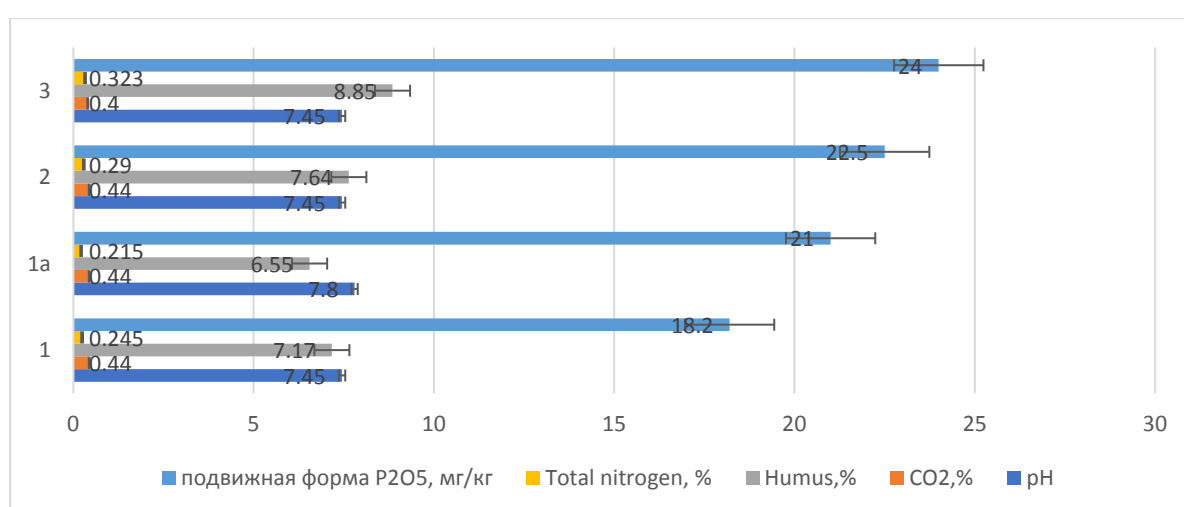
Fig.4 Changes in the chemical composition of the studied soils

However, as shown in Table 4, the Ca2+ content in the unfenced plot was lower than in the fenced plots and was 0.008/0.40 %/mg.eq., while its content in the plot fenced more than 1 year ago was highest at 0.012/0.24 %/mg.eq. (Fig.6). As Ca2+ increase is an important indicator of improved soil structure and general condition, it can be assumed that the establishment of rotational grazing is important to improve pasture structure, which entails the conservation of unique mountain plants and the entire biodiversity of the studied ecosystems.
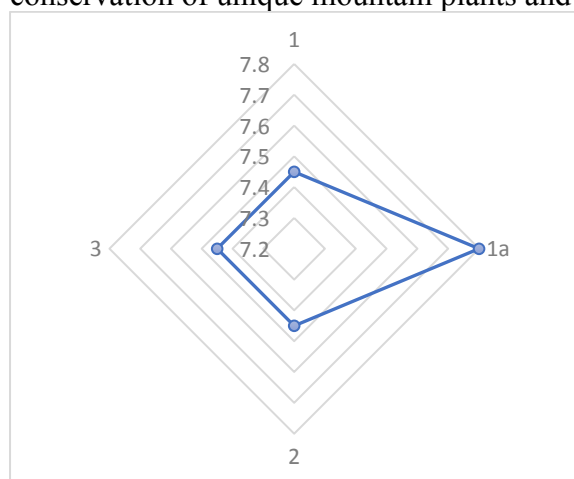
Fig.5 Changes in the pH of the studied soils

Table 4 **Indicators of aqueous extract of soils**

#	Dense sludge, %	alkalinity	Cl-	SO4^{2-}	Ca^{2+}	Mg^{2+}	Na
		Total by HCO3					
$\frac{\%}{\text{мг.экв}}$							
1	0,057	0,026	0,001	0,012	0,006	0,001	0,007
		0,43	0,03	0,24	0,80	0,08	0,32
1a	0,077	0,038	0,001	0,016	0,012	0,001	0,007
		0,62	0,03	0,32	0,60	0,08	0,29
2	0,081	0,046	0,001	0,012	0,010	0,001	0,010
		0,75	0,03	0,24	0,50	0,08	0,44
3	0,067	0,022	0,001	0,024	0,008	0,001	0,009
		0,36	0,03	0,48	0,40	0,08	0,39
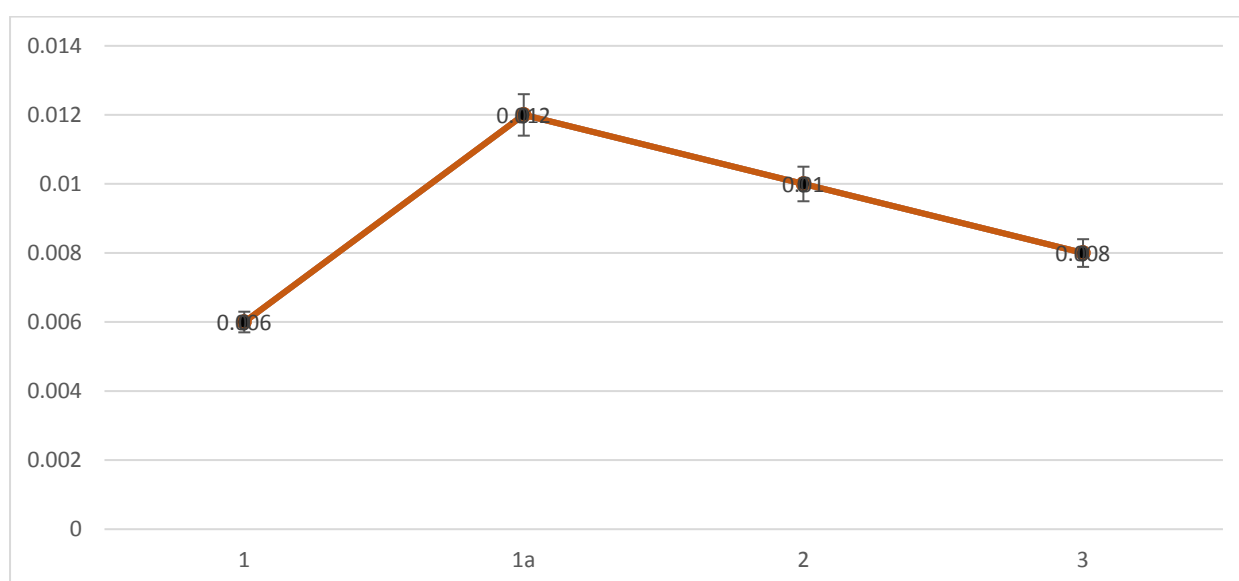
Fig.6 Ca2+ content in the studied soils

Thus, changes in the mechanical and microaggregate composition of soils of different types of pasture use have shown that the use of rotational pasture use and the creation of micro plots with a one year withdrawal from common use is an effective way to improve the microaggregate condition of soils, which further by chain reaction will lead to the restoration and improvement of ecological functions of pastures and create all necessary conditions for improving the productivity of the latter.

Acknowledgements

References

1. Andreeva O.V., Lobkovsky V.A., Kust G.S., Sonne I.S. Current status of the concept and development of a typology of sustainable land use models/Aridic ecosystems, 2021, Vol. 27, No. 1 (86), pp. 3-14
2. Dolgopolova N. V., Pigorev I. Y., Grudinkina V. V. Methodology of crop rotation design, agrochemical characteristics of soils and optimal structure of sown areas in adaptive-landscape farming (by example of Central Chernozem region) // Vestnik of Kursk State Agricultural Academy, 2018, no. 6.
3. State Research Institute "Kyrgyzgiprozem" under the Ministry of Agriculture of the Russian Federation. 2018г. Land resources of the Kyrgyz Republic. [Electronic resource http://data.movegreen.kg/indicator/6].
4. IFAD, Livestock and Market Development Programme II (LMDP II). Project Completion Report. WG 6. Climate Change Impacts on Pasture and Livestock Systems - Synthesis Report, 2017.
5. Esenzhanova G.K., Totubaeva N.E., Tokpaeva J.K., Talaibekova G.T., Kozhobaev K.A. Changes of some indicators of soils and grounds of Balykchy city polluted with oil products after remediation / Problems of Regional Ecology, 2019
6. Kovyazin V.F. Dynamics of agrochemical properties of soils of St.Petersburg / Fertility, 2008, № 3, p.34-37
7. FAO Carbon Sequestration through Climate Investment in Forests and Grasslands in the Kyrgyz Republic (SUPKILPCR), 2018, p.155Amorim, H. C., Ashworth, A. J., Moore Jr, P. A., Wienhold, B. J., Savin, M. C., Owens, P. R. & Xu, S. Soil quality indices following long-term conservation pasture management practices. Agriculture, Ecosystems & Environment, 2020, 301, 107060.
8. Alexander K.G. & Miller M.H. The effect of soil aggregate size on early growth and shoot-root ratio of maize (Zea mays L.). Plant and Soil, 1991, 138, 189–194.
9. Aerts R. and Chapin F. S. The mineral nutrition of wild plants revisited: a re-evaluation of processes and patterns. Adv. Ecol. Res., 2000, 30: 1–67.
10. Crewett Wibke "Improving the Sustainability of Pasture Use in Kyrgyzstan," Mountain Research and Development, 32(3), 267-274, (1 August 2012)
11. Dörre Andrei and Borchardt Peter "Changing Systems, Changing Effects—Pasture Utilization in the Post-Soviet Transition," Mountain Research and Development 32(3), 313-323, (1 August 2012). https://doi.org/10.1659/MRD-JOURNAL-D-11-00132.1
12. Donald R.G., Kay B.D. & Miller M.H. The effect of soil aggregate size on early shoot and root growth of maize (Zea mays L.). Plant and Soil, 1987, 103, 251–259.
13. Donald M. Ecological Intensification: A Step Towards Biodiversity Conservation and Management of Terrestrial Landscape. Ecological Intensification of Natural Resources for Sustainable Agriculture, 2021, p. 77-102.
14. Duval, M. E., Galantini, J. A., Iglesias, J. O., Canelo, S., Martinez, J. M., & Wall, L. Analysis of organic fractions as indicators of soil quality under natural and cultivated systems. *Soil and Tillage Research*, 2013, *131*, 11-19.
15. Dorana John W.Zeissb, Michael R.Soil health and sustainability: managing the biotic component of soil quality/ Applied Soil Ecology, Volume 15, Issue 1, August 2000, p. 3-11
16. Ehsan Elahia, Hongxia Zhanga, Xing Lironga, Zainab Khalid, Haiyun Xu Understanding cognitive and socio-psychological factors determining farmers' intentions to use improved grassland: Implications of land use policy for sustainable pasture production/ Land Use Policy, 2021, Vol.102, 105250
17. Elser J. J. et al. Biological stoichiometry of plant production: metabolism, scaling and ecological response to global change. New Phytol., 2010, 186: 593–608.
18. FAO. [Электронный ресурс http://www.fao.org/land-water/land/sustainable-land-management/slm-decisionmaking/ru (дата обращения 05.08.2020)].
19. Hunke, P., Roller, R., Zeilhofer, P., Schröder, B., & Mueller, E. N. Soil changes under different land-uses in the Cerrado of Mato Grosso, Brazil. *Geoderma Regional*, 2015, *4*, 31-43.
20. Hunke P, Mueller EN, Schröder B, Zeilhofer P. The Brazilian Cerrado: assessment of water and soil degradation in catchments under intensive agricultural use. Ecohydrology. 2015;8: 1154–1180.

21. Lavelle, Patrick Ecological challenges for soil science, Soil Science: January 2000, Volume 165, Issue 1, p 73-86
22. Mandal, A., Sarkar, B., Mandal, S., Vithanage, M., Patra, A. K., & Manna, M. C. Impact of agrochemicals on soil health. In *Agrochemicals Detection, Treatment and Remediation*, 2020, pp. 161-187.
23. Nóbrega RLB, Guzha AC, Torres GN, Kovacs K, Lamparter G, Amorim RSS. Effects of conversion of native cerrado vegetation to pasture on soil hydro-physical properties, evapotranspiration and streamflow on the Amazonian agricultural frontier. PLoS ONE, 2017, 12(6): e0179414. https://doi.org/10.1371/journal.pone.0179414
24. Pierret A., Moran C.J. & Pankhurst C.E. Differentiation of soil properties related to the spatial association of wheat roots and soil macropores. Plant and Soil, 1999, 211, 51–58.DOI: 10.1023/a:1004490800536
25. Picasso, V. D., Modernel, P. D., Becoña, G., Salvo, L., Gutiérrez, L., & Astigarraga, L. Sustainability of meat production beyond carbon footprint: a synthesis of case studies from grazing systems in Uruguay. *Meat science*, 2014, *98*(3), 346-354.
26. Ragimov, A., Mazirov, M., Nikolaev, V., Shitikova, A., & Malakhova, S. Impact Of Different Type Of Cattle Grazing On The Processes Of Agrochemical Degradation and Digression Of Soil Cover. In *E3S Web of Conferences*, 2020, Vol. 220
27. Reynolds, W. D., Drury, C. F., Yang, X. M., Fox, C. A., Tan, C. S., & Zhang, T. Q. Land management effects on the near-surface physical quality of a clay loam soil. *Soil and Tillage Research*, 2007, *96*(1-2), 316-330.
28. Silva de Oliveira, R., Barioni, L. G., Hall, J. J., Moretti, A. C., Veloso, R. F., Alexander, P., ... & Moran, D. Sustainable intensification of Brazilian livestock production through optimized pasture restoration. Agricultural systems, 2017, 153, 201-211.
29. Xie H., Zhang Y., Wu Z., Lv T. A bibliometric analysis on land degradation: Current status, development, and future direction // Land., 2020, No. 9. 37 p.
30. WOCAT Database Global Database on Sustainable Land Management, 2020 [Электронный ресурс https://www.wocat.net/en/global-slm-database].

The "sustainable" landscape: learning from the building tradition of the Hyblean countryside to prepare for the future

Gianfranco Gianfriddo[1*], Luigi Pellegrino[1], Matteo Pennisi[1]

Abstract: Artifacts built in the past in a different economic and social context often contain principles that are valid for building the present and foreshadowing the future. The necessary condition for such human artifacts to be still relevant is their ability to go beyond the historical reality that generated them. Observation of the few stones still standing thus becomes the means by which to draw out those "timeless" ideas and construction principles that are the foundation of architecture.

In Sicily, a particular geographical area contains a remarkable density of artefacts with these characteristics: the Hyblean plateau. Here, over time, man has succeeded in building an extraordinary landscape through a clear structuring of territory that leads from the city house, through the streets, to the country house. The buildings in the Hyblean countryside represent a lesson in sustainable living "ante litteram", capable of guiding us today through the increasingly necessary search for new approaches to building in terms of man's impact on the environment. Through comparisons and reflections, the text will make it clear that these "new" approaches have in fact already been placed at the foundation of the construction of the Hyblean landscape and that therefore the sustainability we seek has already been achieved in the past by these small but significant country houses.

The construction of the Hyblean countryside thus becomes a virtuous example of world-building from which to draw valuable lessons to be updated with today's means, capable of guiding us in imagining human life in the future, an increasingly urgent issue that can no longer be postponed given the times we live in.

Keywords: Countryside, Sustainability, Tradition, Landscape, Architecture, Project

1. Introduction: the farmer's knowledge

«Pay attention to the forms with which the farmer builds. For they are heritage handed down by the wisdom of the fathers. But try to discover the reasons that led to that shape [...] Don't think about the roof, but about the rain and the snow. This is how the farmer thinks, and consequently builds»[1].

This idea underlies the research conducted on the country houses of the Hyblaean plateau. A study centred on how the combination of several minimal living units, based on reasons of

---

[1] Loos, 1921.

[1] S.D.S. di Architettura di Siracusa, Università degli Studi di Catania, Catania, Italia.
* Corresponding author: luigi.pellegrino@unict.it

necessity and sustainability, has shaped the construction of the landscape. It must be said that research has never seen in all this heritage of houses a certain "minor architecture", testimonies as the expression of a less "elevated" knowledge than that of the most well-known architectures, although in any case pertaining to the so-called "spontaneous architecture"[2]. This work, on the contrary, aims to detect in these buildings the traces and reasons for Architecture, understood in its highest sense.

The study has been articulated through the analysis of artefacts that have not been studied so far from this point of view, both in the intrinsic relations between the parts and in those that they establish with the territorial palimpsest, in order to understand how these houses have managed to transform a territory into a landscape.

The tools of the research were drawing and history, for Siza the only two tools available to the architect to continue learning[3]. In essence, in relation to the research, drawing was necessary to translate historical knowledge into constructive experience. Drawing served to draw out from these artefacts the "timeless" lessons they contain. The orthogonal representation allowed the settlement reasons underlying an entire man-made landscape to appear. The fact that it was not possible to materially start from any existing documentation in this sense, if on the one hand obliged a greater effort, on the other hand forced a decisive intellectual effort in the quality of the research aimed at the "invention" of these drawings. These drawings are reasoned at several territorial scales and not according to a principle of approaching the studied artefact from the vast context, but following the idea that each scale communicates its own specific relations and reasons different from the others. On the largest scale, the relationship between the house and the neighbouring town and the territorial structure that holds them together emerges; on the intermediate scale, the relationship with the soil and the site of the "*cugno*" or the "*cava*"; on the more "architectural" scale, the spatial and dimensional relationship between the spaces of the house and their articulation is revealed.

The truly extraordinary thing was to be faced with constructions, each of which wisely solves all the questions of environmental sustainability that we are so convinced of today. These houses seem to come out of the ground and base their balance on that of the surrounding environment. Sustainability in this territorial context is not an aspect that was considered in the construction but a real settlement principle capable of shaping the whole Hyblean countryside. It is strange to think that centuries ago, with the few means available, they understood how to settle in the landscape without the risk of "impact", precisely because the building seems to fit into the metabolism of nature and form an integral part of it. This extraordinary context therefore represents a treasure trove of ideas for our future, from which we can take as many lessons as possible in an attempt to make sustainability truly a principle rather than a mere technical aspect.

2. The Hyblean minimum house

The Hyblean minimal house is a building, mostly single- or two-storey, made of limestone on sack masonry with cantonments of rough-hewn or sometimes squared stone and a wooden roof. An elementary structure whose essence is a state of necessity and limited economic possibilities. The house itself, in the sense of a covered volume, only covers a limited part of the plot, in most cases ranging from two to five "*tumuli*" (about 2,200 to 5,500 square

---

[2] (Rudofsky, 1979)
[3] "L'apprendimento – l'acquisizione della capacità di apprendere continuamente – continua a concentrarsi, a mio intendere, nel disegno – nell'imparare a vedere, a capire, a esprimere – e nella storia – nel senso di conquista della coscienza del presente in divenire." (Siza, 2008)

metres). Therefore, the uncovered areas used for the various tree crops were very important, the choice of which depended strictly on the characteristics of the soil and the most advantageous species to be cultivated. A valley with a strong presence of springs, for example, would have been more suitable for the cultivation of vegetables; an arid plateau for legumes; the slopes were perfect for grazing. In this extraordinary place, every human action is almost, we might say, the "artificial continuation" of a natural accident.

The social class that initiated this structuring of the landscape through the small rural house was that of sharecroppers and farm labourers. The economic conditions for this fragile section of the population were anything but flourishing due to the poorly paid work on the large estates, so much so that most of these people barely managed to procure enough to survive. It was therefore indispensable for them to *extend* their city house into the countryside, in order to acquire the land to be able to set up the small building to serve the crops necessary to guarantee the family a dignified survival. This is in fact the socio-economic function behind these buildings: to respond to a need arising from an imbalance in the distribution of wealth in society. Having said this, it is easy to see that the purpose of the small rural house is still that of a productive building, i.e. dedicated to the agricultural activity of the plot on which it stands. In this sense, this type of building constructs the Hyblean countryside in the true sense of the word, if by countryside we mean that part of the territory devoted to agricultural production. As we have seen, the house is only a small part of the area in which it stands. Other elements in fact, although without a real roof, contribute to the construction of the lot.

2.1. The elements of the house

Access to the lot is via the roads that connect the city to the countryside, the backbone of settlement throughout the area. A dense network of secondary roads branches off from these routes, giving shape with exceptional clarity to a "spontaneous" layout, in the sense that it is not the result of the application of a pre-established plan, but only of the condition of necessity due to the accidents of the soil and the shape of the plateau, an approach that has guided the choices of the people who have settled here. There are two ways of accessing the plot: if the building is far from the main road by means of a dirt track that cuts through the property; if, on the other hand, one of the sides of the building borders on the main or secondary road, then access is direct without a further route.

If the roads are the backbone, the dry-stone walls are the rest of the framework. In an overall view, dry-stone walls constitute a complex network that structures the territory geometrically, dividing it into smaller and smaller areas according to work requirements. Dry-stone walls are not only the most obvious anthropic sign in the landscape, but also those which, at a closer look, clearly reveal man's interaction with the land and his ability to make it a place to live in. The specific feature that a piece of the world must have in order to be "domestic", and therefore habitable, is size, and dry-stone walls tame the territory, on the one hand regulating the relationships between individuals in the subdivision of property, and on the other guaranteeing human feeling a sense of protection from the outside world, necessary to perceive living "inside" something.

Among the elements of the house there is the "Mediterranean garden", a space built up from a few elements which nevertheless manage to define an identifiable spatial idea, thanks to the clarity with which these objects are related. «[…] the Mediterranean Garden made up of small plots of land, with its small walls over which runs the tangle of suburban lanes, nestled between the whitewashed boundary walls surmounted by the glossy green foliage of the trees

[…]»[4]. What Sereni's words are worth highlighting is his ability to render the idea of a place where the interaction between man and nature is almost total in an artefact. The truth is that the Mediterranean garden, while not being a formally intended volume, is in any case a construction in its own right, part in turn of the general construction of the plot and the entire agrarian landscape of Hyblaean. This ability to pass from the garden to the whole landscape shows that what makes a construction "human" is its response to "internal" and at the same time "external" rules, fitting correctly into another, larger construction, without ever losing its recognizability and autonomy with respect to the whole it is composed of.

The "*baglio*" is the front part of the house and functionally its access. This space is characterized by dry stone walls which, according to the layout of the perimeter walls, run parallel to the elevations of the house. The "*baglio*" extends the inside of the house to the outside, delimiting an area and providing valuable shade on the hottest days, thanks to the work of a few necessary trees placed along the dry-stone walls.

The position of each of the elements listed in the plot, and therefore also of the house itself, is a consequence of the geology of the soils within the perimeter. The plateau is composed of a large limestone plateau which, in the places where the rock is not outcropping, guarantees the possibility of cultivation. In the innermost areas, in fact, there is a sufficient layer of ground above the stony layer to allow for some cultivation. In other places, however, the planking emerges, thus making cultivation impossible due to the lack of soil. In most cases both conditions are easy to find within a plot. In these cases, the farmer wisely sets up his house on the rock, relegating all the precious space with the soil to cultivation. The farmer's "choice" may seem to us, and rightly so, more a necessity than an arbitrary decision, so much so that in a certain sense we doubt whether it can really be called a "choice". In truth, the farmer chose the position of his house, and the fact that today, once the work has been completed, it seems to have come out of the earth, only testifies that the reasons that guided the farmer were those appropriate to the place and the right ones to shape it according to his needs and living conditions.

In analysing the elements, it becomes clear that the logic behind the construction of the small rural house is far removed from that which would see the house as "full" and the rest of the plot as "empty". Whoever built this landscape started from totally different assumptions. In these buildings there is an inseparable knot between house and lot, so much so that we could say that they are *the same thing*, since the idea behind them is the same. The house, the roofed unit, is as much a part of the living organism as the rest of the lot; it is only the place of functions that necessarily, for various reasons, require the presence of a roof. The house belongs to the same world as the garden, the wall and all the other elements that make up this *unicum*.

The small rural house has nothing more than what is strictly necessary to make a house "habitable", not only with respect to a rational organization of the rooms but precisely with respect to an idea of "measurability", a space in which a man can feel good as a human being living in the world. The rural house is in this sense "domestic", and the use of the most highly worked stone in the canton's buildings is enough to clarify the matter and add another fundamental aspect. The fact that in the cantonments it was often decided to sketch out a geometry, making a considerable effort, is not a marginal thing. Without the cut stone in the corner of a building it would be as if the corner *did not know* it was a corner, but at the same

---

[4] (Sereni, 1987)

time it is true that staggered stone blocks in the corner make the structure stronger and more solid. This correspondence between the static wellbeing of the building and the perception of solidity by those who live in it is the basis of the construction of the Hyblaean countryside.

3. The sustainability as principle of the minimum house

In the minimal house it is impossible to clearly identify the function of each element that builds it; take, for example, a tree whose role might be: to reduce the radiation on the perimeter walls, to create a comfortable shady space in which to stand, to produce fruit necessary for subsistence, to improve the perceptive wellbeing of the inhabitants. All these reasons coexist together and this is one of the greatest lessons of the Hyblean countryside: not to compartmentalize the world. This applies as much to the tree as to any other element that makes up the house.

A principle of sustainability pervades the meaning of these constructions. It is precisely an approach that unites both the individual technical-constructive choices and the general settlement idea underlying the relationship between man and the environment. Reducing radiation on the building volume goes hand in hand with the creation of a space of shade for the wellbeing of the inhabitants of the house; it would seem obvious that they go together, but in reality, it is not so evident that an apparently exclusive aim of the technological sphere (protection from the sun's rays) is mingled with one relating to the wellbeing of the inhabitants (a shaded outdoor space). This approach to the overall dimension of the Hyblaean plateau results in a human artefact that we could define as a "sustainable landscape" shaped by the perfect union of several choices made in individual lots, all of which are necessary, each of which is a wise response to the needs of man and the environment, which are never seen as two opposing realities but which conform to each other.

The systematic analysis of the object of the research through the tool of drawing, carried out with scientific precision, has made it possible to "make these artefacts speak", drawing from them all the questions and lessons that they still conceal beneath the surface. Drawing the small houses has made it possible to clarify, and to clarify, the characters that make this structure a landscape construction. By bringing together different scales of representation, from the broadest to the most detailed, the small houses showed all their capacity to construct both the specific area of relevance and the entire territorial palimpsest in general. These drawings are the most evident tools for understanding the relationships between the parts within the artefact and at the same time between the single artefact and the palimpsest: they are drawings for "doing". The idea was to produce drawings that could clearly show how these houses manage to build a landscape through a principle of necessity and sustainability. As a matter of fact, no regulation or prescription can ever ensure that new buildings are *really* sustainable, at most only the respect of certain parameters but separated from any constructive idea. On the contrary, we believe that drawings created with the aim of being useful to the work by explaining a possible way of sustainable building that has shaped a landscape in the past are the most effective tools for tracing the paths to be taken to reconnect, if possible, with that tradition and try to start doing it again today.

4. Discussion and Conclusions: from the minimum house to the future

Today, although the concept of sustainability is enormously widespread and on everyone's lips, surprisingly it seems to have lost the "active" role it had in the past when it was not actually the subject of discussion. As if in a real paradox, just when sustainability was not an

issue to be discussed it took on the far more incisive role of a building principle. While sustainability was not explicitly talked about, it was seen as a *principle* underlying the construction of the world. It is clear that there is a kind of inverse proportion: on the one hand sustainability is the subject of heated debate, but on the other hand it has lost its importance, being relegated to the fulfilment of specific requirements. Precisely today, at a time when ethically everyone seems to be sensitive to the subject, sustainability has gone from being a mere answer to specific technical questions, from a construction principle capable of holding together the small house with the whole landscape (which it was).

There is an increasing tendency to understand sustainability as a matter of law or environment. In this way, planners see only restrictions on their work and consequently their approach is limited to meeting requirements without sustainability being understood as a construction principle.

Making a building sustainable is commonly perceived as an obligation (mostly only bureaucratic-formal) and not as a fundamental necessity of living. If we look at the past, at country houses, it is clear that the well-being of the farmer who lived on his land was inextricably linked to the well-being of the land with which he had a relationship in which both parties interacted and benefited. Country houses are still able to clearly manifest the idea with which the farmer stood in relation to the surrounding environment, a way of standing in no way in opposition but collaborative, so that every element of the house is affected by this basic point of view. On the contrary, today we understand the surrounding environment as something that in any case will be attacked by our building action and therefore to be protected through the mitigation of our intervention. It would be far better for both man and the environment to learn from the farmer and try to establish a firm foothold in the land, to establish a relationship with it in which man's actions do not damage the environment but rather improve it, for example by maintaining it. Man's work in the countryside is in fact fundamental from this point of view too, in keeping a rural area in excellent condition, which in turn guaranteed the necessary fruits for the people who lived there. It is a symbiotic relationship in which human action takes the form of a corrugation of the soil, a modification that gives shape to the accidents of the orography.

The disconnect between our well-being and that of the environment is creating an ever-increasing hiatus that produces effects contrary to what we all hope for. Seeing the environment as something to be protected from our action rather than as an active element in shaping construction only aggravates our interaction with it.

It is clear that we cannot see the minimum house as a formal reference for sustainable building today. To give an example, we should not proceed thinking of re-proposing today all the elements of the minimal house as they are. It would not make much sense today to bring the cistern of the country house back into daily use as it was. Instead, we must seize, quoting Grassi, that "technical-practical power that the place holds"[5] and not so much the visible results of the application of that "power". The configuration and final appearance of the cistern in rural houses is in fact the result of numerous factors linked to the time when the house was built, the quality of the workforce and above all the resources and knowledge available at that time. Today we must use our technical knowledge but guided by the method and the idea that the "ancients" show us through what remains of their artefacts. Because while it is true that we can add newer techniques, knowledge and resources to those

---

[5] (Grassi, 1996)

techniques, it is also true that the theoretical scope and idea of that settlement are insurmountable, so much so that the only thing left for us, and that is no small thing, is to try to understand it in order to restore sustainability to its rightful place in today's world, not as an obligation to be formally respected but as an idea of minimal living
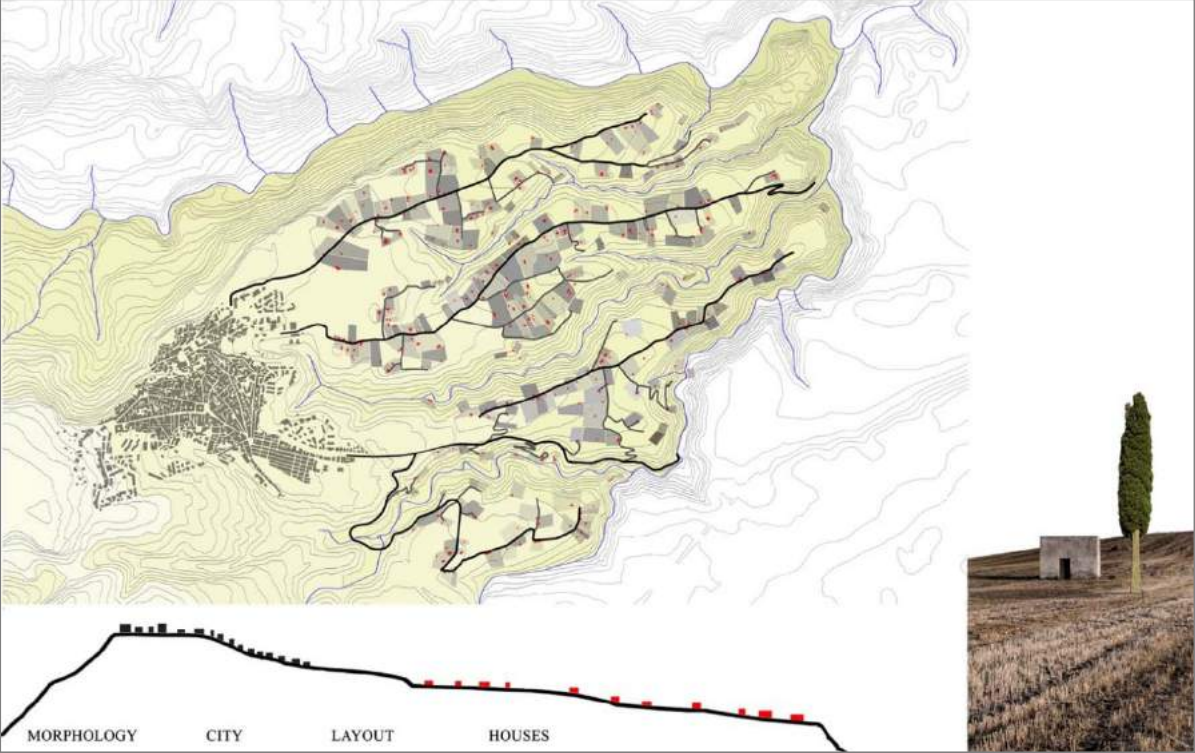
Figure 1. Relationship between the city and the minimal house

Figure 2. Minimum house near Buscemi
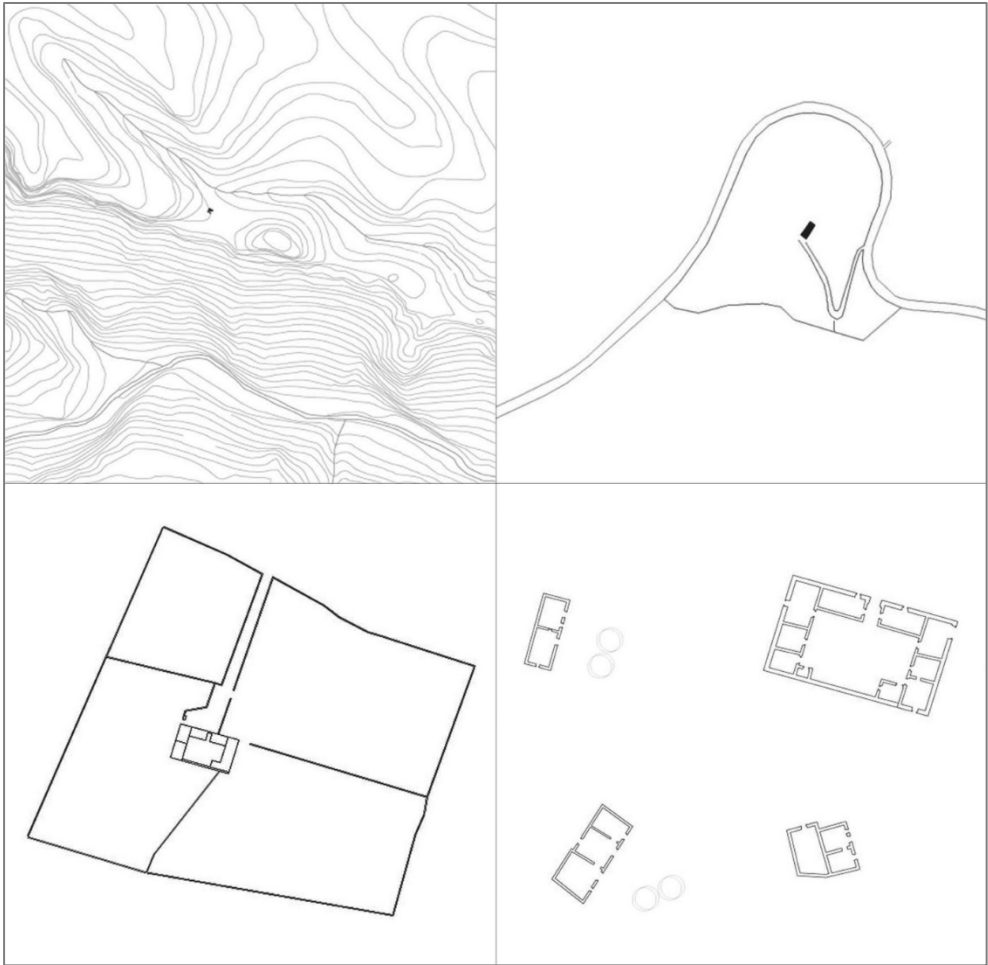
Figure 3. Settlement relations with the palimpsest and between the parts
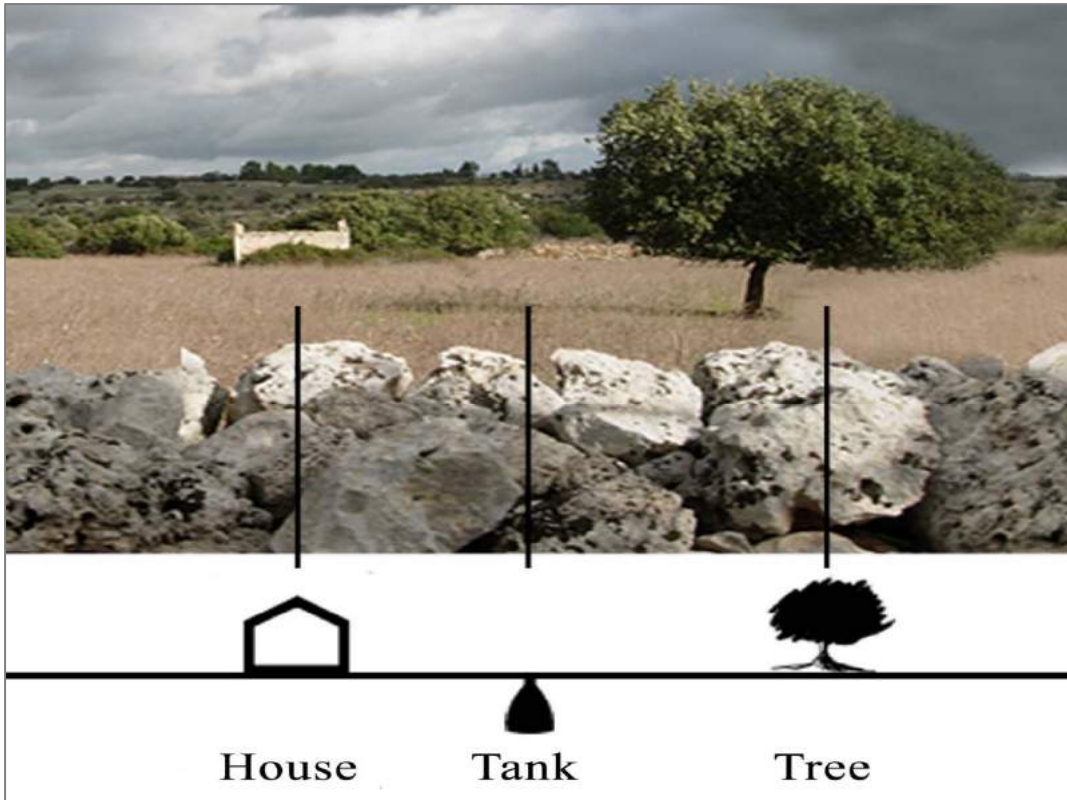
Figure 4. Synthesis of minimal living
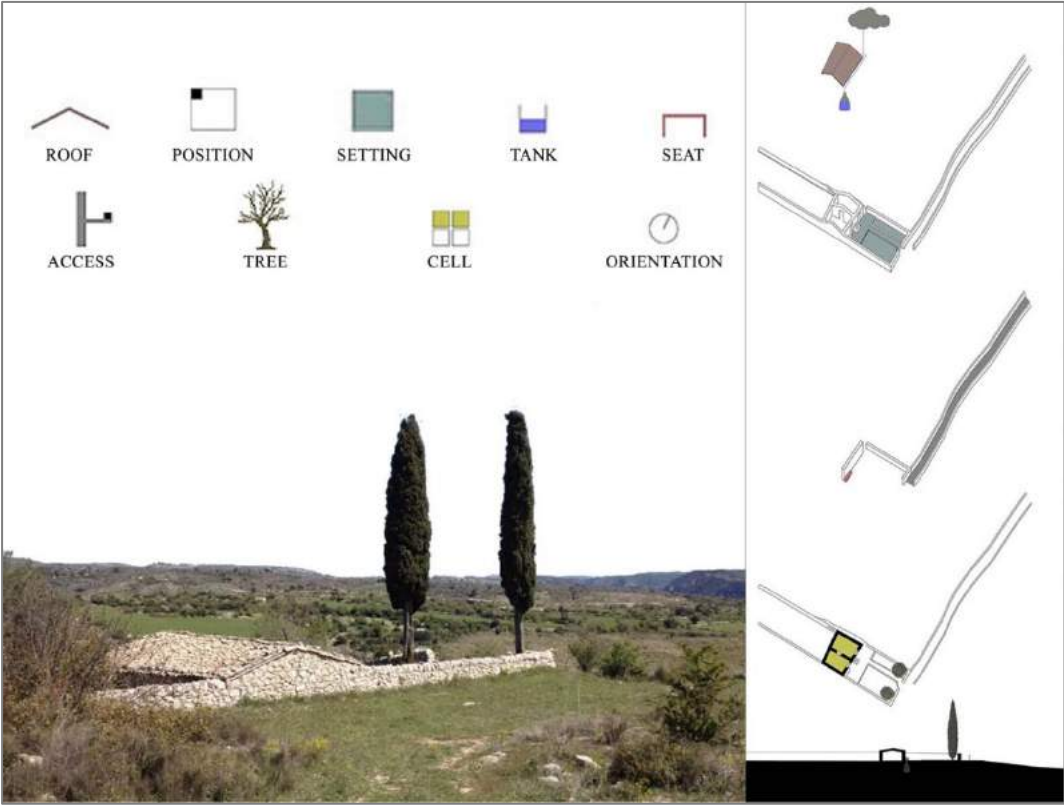
Figure 5. Abacus of the construction elements of the minimum house

References

Grassi, G., (1996). I progetti, le opere e gli scritti. Electa, Milano.

Loos, A., (1972, ed. or. 1921). Parole nel vuoto. Adelphi Editore, Milano, 271-272

Rudofsky, B., (1979). Le meraviglie dell'architettura spontanea: note per una storia naturale dell'architettura con speciale riferimento a quelle specie che vengono tradizionalmente neglette o del tutto ignorate. Editori Laterza, Bari.

Sereni, E., (1987). Storia del paesaggio agrario italiano. Editori Laterza, Roma-Bari, 268-268

Siza, A., (2008). Sulla pedagogia. Casabella, 770, 3-3

Evaluation of Parameters Affecting Frequency Response Analysis Measurements in Power Transformers /

Güç Transformatörlerinde Frekans Tepki Analizi Ölçümlerini Etkileyen Parametrelerin Değerlendirilmesi

Selim Köroğlu[1*], Akif Demirçalı[2*], Mustafa Yıldız[3*]

Abstract: Power transformers are one of the most expensive and important equipment in high voltage energy transmission systems. It is very important that these devices operate smoothly in order to maintain the power transmission safely. For this reason, power transformers are closely monitored until they complete their operational life, including the manufacturing phase. They are subjected to a series of routine controls and tests in the operation in order to monitor their general condition, to detect and prevent possible malfunctions early. Frequency response analysis (FRA) test, which has been implemented in recent years, is an effective and sensitive method used in the diagnosis of winding failures and structural defects in the core, especially in determining the structural shifts that occur in transformers. In this study, the basic principles of the FRA method used in the diagnosis of power transformer faults are given and test connection configurations are explained. In addition, the effects of the parameters such as tap changer, temperature, connection group, DC voltage, measurement direction etc. on the FRA results are discussed.

Keywords: Power Transformers, Fault analysis, Frequency Response Analysis

Özet: Güç transformatörleri, yüksek gerilimli enerji iletim sistemlerinde kritik görev alan en pahalı ve en önemli ekipmanlardan birisidir. Güç aktarımının güvenli bir şekilde sürdürebilmesi için bu aygıtların sorunsuz çalıştırılması oldukça önemlidir. Bu nedenle, güç transformatörleri imalat aşaması dahil işletme ömürlerini tamamlayana kadar yakın takip edilirler. Genel durumlarının izlenmesi, olası arızaların erken teşhisi ve önüne geçilmesi için işletmede bir dizi rutin kontrol ve testlere tabi tutulurlar. Son yıllarda uygulamaya başlanan frekans tepkisi analizi (FRA) testi; transformatörlerde meydana gelen sargı arızaları ve nüvedeki yapısal bozuklukların teşhisinde, özellikle de transformatörlerde meydana gelen yapısal kaymaların belirlenmesinde kullanılan etkin ve hassas bir yöntemdir. Bu çalışmada, güç transformatörleri arızalarının teşhisinde kullanılan FRA yönteminin temel prensipleri verilmiş, test bağlantı konfigürasyonları açıklanmıştır. Ayrıca, kademe değiştirici, sıcaklık, bağlantı grubu, DC gerilim, ölçüm yönü vb., parametrelerin FRA sonuçlarına etkileri tartışılmıştır.

Anahtar Kelimeler: Güç Transformatörleri, Hata analizi, Frekans Tepkisi Analizi

[1] Pamukkale Üniversitesi, Mühendislik Fakültesi, Elektrik Elektronik Mühendisliği, Denizli, Türkiye
[2] TEİAŞ 21. Bölge Müdürlüğü, Denizli, Türkiye
* Sorumlu yazar: skoroglu@pau.edu.tr

1. Giriş

Güç transformatörleri, elektrik enerji iletim sisteminin en pahalı ekipmanlılarından biri olup işletmede oldukça kritik bir görevi yerine getirmektedirler. Transformatörlerde yaşanacak bir arıza iletim siteminde sorunlara yol açacaktır. Bu açıdan transformatörlerin sağlıklı ve sorunsuz bir şekilde çalıştırılması, güç sistemi yönetimi açısından önemlidir. Bunlarda yaşanacak herhangi bir arıza nedeniyle meydana gelecek enerji kesintisi tüketiciler olumsuz yönde etkiler ve ciddi mali kayıplara neden olur. Bu nedenle, güç transformatörlerin en az sorunla çalıştırılması elektrik enerji sistemin sürekliliği açısından gereklidir (Bohatyrewicz et al., 2019; CIGRE Working Group A2.37, 2015). Bunların yanında, bir hata sonucu transformatörde meydana gelecek patlamalar, can ve mal gibi önemli kayıplara ve çevresel risklere de neden olur. Elektrik güç sistemlerinin sürdürülebilir bir şekilde işletilmesi, güç transformatörlerinin güvenilirliği ve kullanılabilirliği ile yakından ilgilidir (Mirzai et al., 2006). Güç transformatörlerinde yeni başlayan arızaların erken teşhis edilmesi ile arıza durumuna hızlı bir şekilde müdahale ederek arızanın ilerlemesi durdurulabilir, ekonomik kayıplar azaltılır ve onarım süresi kısaltılabilir.

Transformatörler imal edilirken mekanik ve elektriksel zorlanmalara dayanacak şekilde tasarlanmasına rağmen nakliye aşamasındaki dikkatsizlikler, depremler, doğal yaşlanma, izolasyon bozulması, kısa devre arızaları gibi durumlar sargı ve çekirdek deformasyonuna neden olabilir. Transformatörlerin işletmede sorunsuz bir şekilde çalışmasının sağlanması onun teknik durumuyla yakından ilgilidir. Transformatörlerin korunmasına yönelik birçok önlem alınmakla birlikte test ve bakımlarının düzenli yapılması gerekir. Bu amaçla işletmedeki durumlarının değerlendirilmesi, olası arıza durumlarına karşı erken önlem alınması, arıza durumunun acil bir şekilde belirlenmesi maksadıyla birçok koruma, mekanik ve elektrik testlerin yanında kimyasal analizlere tabi tutulurlar. Transformatörlere uygulan testlerle ilgili detaylı çalışmalar literatürde sunulmuştur. Korumaya yönelik önlemler içerisinde diferansiyel koruma örnek verilebilir (Faiz & Heydarabadi, 2015; Gajić, 2008). Arıza teşhisine yönelik uygulan elektriksel testler; AC-DC izolasyon, sarım oranı, DC direnç, yağ üzerinde yapılan güç faktörü (%PF), delinme dayanımı vb. şeklinde sıralanabilir (Koroglu, 2016; Mendes et al., 2004). Bunlarının yanında izlemeye yönelik test ve analizler arasında; kısmi deşarj ölçümü, frekans yanıt analizi (FRA), yağda çözünmüş gaz analizi (DGA), dielektrik tepki ölçümü, yağdaki nem, dinamik termal modelleme gösterilebilir (International Electrotechnical Commission, 2015; Tenbohlen et al., 2016).

Son yıllarda, güç transformatörleri arızaların tanılanmasında FRA, yeni nesil test yöntemleri arasındaki yerini almaktadır. FRA yöntemi özellikle transformatörlerde mekanik deformasyonun gözlenmesinde etkin bir yöntem olarak kullanılmaktadır (IEEE, 2013; Suwarno & Donald, 2010). Ancak, FRA ölçüm sonuçlarının karşılaştırma esasına dayanan bir yöntem olması nedeniyle hatanın türü ve ciddiyeti hakkında kesin bir bilgi elde etmek hala zordur. Referans verilerin karşılaştırılması ile birlikte aynı zamanda uzman bilgisine de ihtiyaç duyulmaktadır (Al-Ameri et al., 2021). Birçok araştırmacı, FRA sonuçlarının değerlendirilmesinde insan müdahalesini en aza indirmek veya kaldırmak maksatlı çalışmalar da yapmaktadır (Khalili Senobari et al., 2018). FRA sonuçlarının yorumlanmasının iyileştirilmesi için güç transformatörleri üzerinde farklı tipte mekanik arızaların test edilmesi gerekmektedir. Yapılan bir çalışmada, güç transformatörü üç boyutlu sonlu elemanlar yöntemi ile modellenmiştir. Bu modelde transformatör sargılarında oluşturulan çeşitli radyal deformasyonların, eksenel yer değiştirmelerin ve aynı zamanda radyal-eksenel deformasyonların FRA imzaları elde edilmiştir. Bu sonuçlar istatistiksel göstergeler

kullanılarak temel FRA izi ile karşılaştırılarak arıza değerlendirmesi yapılmıştır (Mahvi et al., 2020).

Tüm bunlara ilaveten FRA, transformatörün frekans cevabının karşılaştırması esasına dayalı bir yöntem olduğundan, her bir deney koşulunun birbirine yakın olmasına dikkat edilmelidir. Ölçme işlemini etkileyecek parametrelerin titizlikle dikkate alınması yine sağlıklı bir değerlendirme için önemli olacaktır. Bu çalışmada, FRA temel ölçme prosedürleri irdelenmiş ve FRA sonuçlarını etkileyen faktörlerin (kademe değiştirici, sıcaklık, bağlantı grubu, DC gerilim, ölçüm yönü ve diğer faktörler) sonuçlar üzerindeki etkileri tartışılmıştır.

2. Frekans Tepkisi Analizi

FRA, güç transformatörünün sargı ve demir çekirdekteki arızaların tespit edilmesinde hassas bir yöntem olup mekanik deformasyonların tespiti için etkili ve ekonomik bir teşhis tekniğidir. Aynı zamanda transformatörün aktif parçalarının geometrisi hakkında güvenilir bilgi sağlayabilir (Ni et al., 2020). Genel manada bir transformatör gövde, nüve ve sargılardan oluşmaktadır. Transformatör doğası gereği sargılarının direnci, endüktansı, sargı-gövde arasındaki kapasite değeri vb. gibi elektriksel parametrelerle ifade edilir. Bu yapı ve etkileşimler dikkate alındığında kompleks bir RLC devresi şeklinde düşünülebilir.
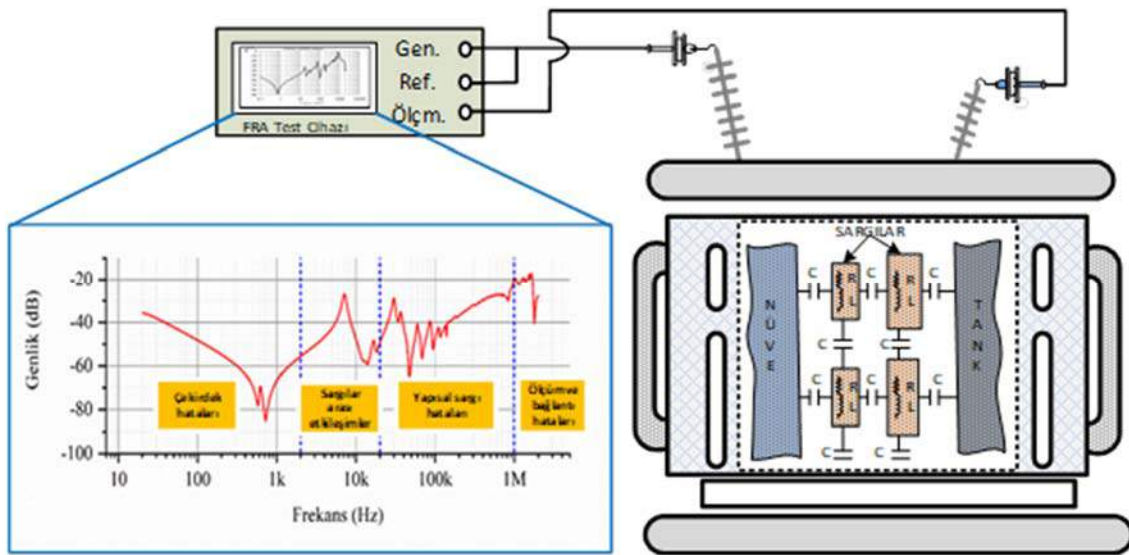
Şekil 1. Bir güç transformatörünü için temel FRA prensip şeması

FRA prensip şeması Şekil 1'de gösterildiği gibi geniş bir bant aralığında transformatörün frekans cevabının gözlenmesine dayanmaktadır. Frekans tepkisi, transformatörün bir terminaline uygulanan belli frekanslardaki alçak gerilim sinyalinin diğer bir terminalden genlik ve faz açısı olarak ölçülmesidir. Çıkıştaki sinyal küçük olacağından dolayı genellikle dB olarak ölçülür. Ölçüm ulaşılabilir olan bütün terminaller için yapılır. Her frekanstaki transfer fonksiyonu, transformatörün RLC ağının etkin empedansının bir ölçüsüdür (Alsuhaibani et al., 2016). Transfer fonksiyonu ölçülen V_2 çıkış geriliminin, referans V_1 giriş gerilimine oranı olup, sistemin genlik cevabı denklem 1'den, işaretin faz açısı cevabı ise denklem 2'den hesaplanır.

$$A_{,Genlik}\,[dB] = 20\log_{10}\left(\frac{V_2\,(jw)}{V_1\,(jw)}\right) \qquad (1)$$

$$\varphi_{,Faz}[°] = tan^{-1}\left(\frac{V_2\,(jw)}{V_1\,(jw)}\right) \qquad\qquad (2)$$

FRA ölçümü bir nevi transformatörler için tanımlanmış parmak izi olarak da değerlendirilir. Herhangi bir fiziksel ve elektriksel hata sonucu, transformatör RLC devresinin empedansında meydana gelecek değişimlere bağlı devrenin transfer fonksiyonunun da değeri değiştirecektir. Bu yöntemle, hataya bağlı empedans değişiklikleri etkin bir şekilde izlenebilir hale gelmektedir. Böylelikle transformatördeki hatalar, ölçülen FRA sonuçlarının, önceki test sonuçları ile karşılaştırılması neticesinde tespit edilebilir (Kraetge et al., 2009).

3. FRA Test Konfigürasyonu

FRA yöntemi transformatör empedansının frekans cevabının faz ve genlik olarak incelenmesini esas alır. Ölçme işlemi bu amaç için geliştirilmiş test cihazlarından yararlanılarak gerçekleştirilir. FRA test cihazlarında, bağlantı için genellikle referans ucu, sinyalin gönderildiği canlı uç ve ölçüm ucu şeklinde üç adet çıkış bulunur. Referans ucu toprağa bağlanırken, ölçümü yapılan transformatör ile aynı topraklama noktasına irtibatlı olmasına dikkat edilir. Ölçme işlemi her fazda ve istenilen kademelerde tamamlanır. Daha önce yapılmış sonuçlarla karşılaştırılarak, önceki değerlerle uygunluğu kontrol edilir. FRA ölçüm sonuçlarının karşılaştırılması zaman tabanlı, tip tabanlı ve fazlar arası karşılaştırma olmak üzere üç farklı biçimde yapılabilmektedir (Kraetge et al., 2009; Picher, 2008). Bunlardan zaman tabanlı karşılaştırma aynı transformatörde yapılan ölçümlerin daha önce kaydedilen FRA ölçümleriyle karşılaştırmasını ifade eder. Tip tabanlı karşılaştırma, bir transformatörün FRA sonuçlarının ikiz aynı tip başka bir transformatörün sonuçları ile karşılaştırılması anlamına gelir. Fazlar arası karşılaştırma ise her bir faza ait sonuçların birbiriyle kıyaslanmasından ibarettir. Karşılaştırılan sonuçlar arasında herhangi bir sapma yoksa transformatörün sağlıklı, tersi bir durum gözlenirse transformatörde anormal bir durumun varlığı değerlendirilir.

FRA ölçme yöntemleri standartlarda açıkça tanımlanmış olup temel olarak dört ölçümden ibarettir (IEEE, 2013; International Electrotechnical Commission, 2012). Bunlar sargı sonu-sargı sonu açık devre testi, sargı sonu-sargı sonu kısa devre testi, sargılar arası kapasitif test ve sargılar arası endüktif test şeklindedir.

3.1. Sargı sonu – sargı sonu açık devre testi

Sargı sonu-sargı sonu açık devre testindeki ölçümlerde, sinyal faz veya nötr terminalden uygulanabilmektedir. Sinyal bir fazın sargı ucundan uygulanır ve diğer terminalin sargı ucuna iletilen sinyal ölçülür. Bu test basit ve her faza uygulanabildiğinden, yaygın bir şekilde tercih edilmektedir. Şekil 2'de, YNyn0 bağlantı gruplu transformatör için sargı sonu-sargı sonu açık devre örnek ölçüm şeması verilmiştir. Bu ölçüm, her üç faza da uygulanır.
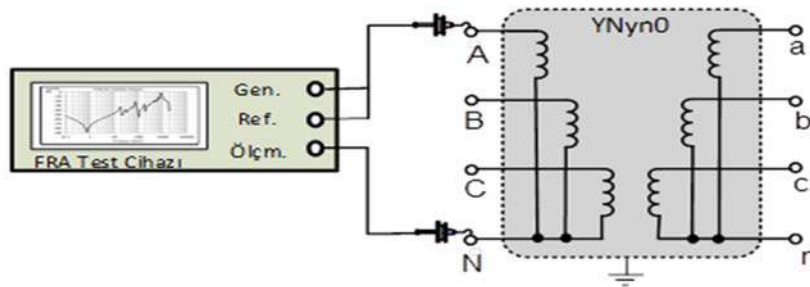
Şekil 2. Sargı sonu-sargı sonu açık devre testi şeması

3.2. Sargı sonu – sargı sonu kısa devre testi

Bu ölçüm sargı sonu-sargı sonu açık devre ölçümüyle benzer olup, tek farklı nokta, transformatörün sekonder faz sargılarının kısa devre edilmesi şeklindedir. Üç fazlı bir transformatörde, bu test için, her faz sargısı sırasıyla kısa devre edilebileceği gibi, üç fazın sargıları da kısa devre edilebilir. Şekil 3'te sargı sonu-sargı sonu kısa devre testine ait örnek ölçüm şeması verilmiştir.
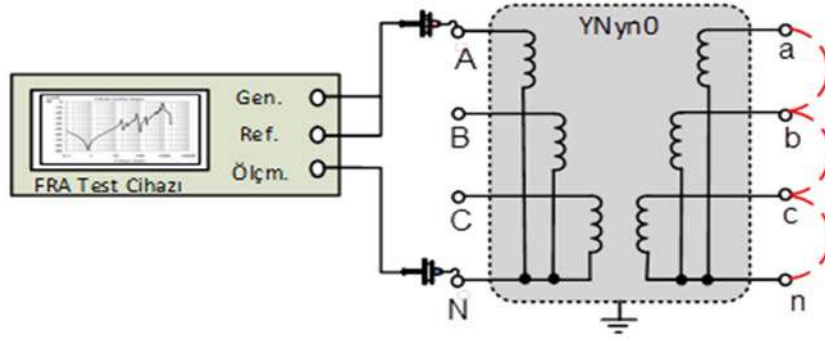
Şekil 3. Sargı sonu-sargı sonu kısa devre testi şeması

3.3. Sargılar arası kapasitif test

Bu ölçümde sinyal, primer sargının bir ucundan uygulanarak sekonder sargının aynı fazından sinyal çıkışı ölçülür. Bu işlem, oto transformatörlerin seri ve ortak sargılarında uygulanamaz. Bu ölçüm daha ziyade, transformatörlerde alçak frekans bölgesindeki değişimlerin gözlenmesi, yani nüve problemlerin tespiti amaçlı uygulanır. Şekil 4'te, ölçüm işlemi için gerekli bağlantı şeması verilmiştir.
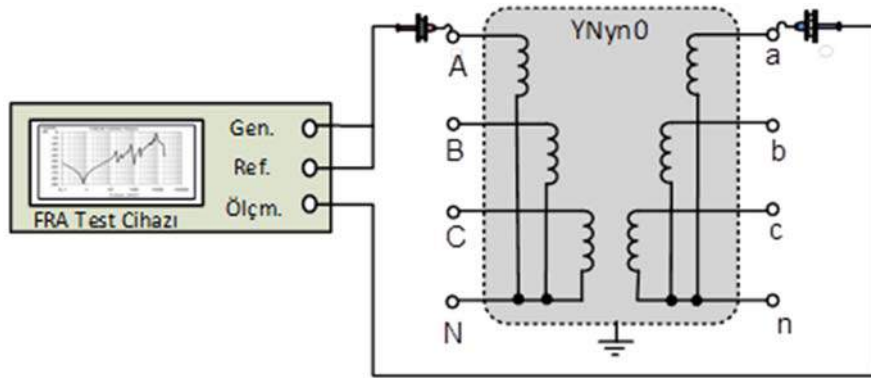
Şekil 4. Sargılar arası kapasitif test bağlantı şeması

3.4. Sargılar arası endüktif test

Bu ölçümde sinyal, primer sargının bir terminaline uygulanırken, çıkış sinyali sekonder sargının diğer ucundan ölçülür. Bu ölçüm tekniği ile kapasitif ölçüm arasındaki fark, bu ölçüm tekniğinde transformatör primer ve sekonder sargılarının birer uçlarının topraklanmasıdır. Bu ölçümün alçak frekans oranı, transformatörün sarım oranını verir. Şekil 5'te, sargılar arası endüktif ölçüm işleminin bağlantı şeması verilmiştir.
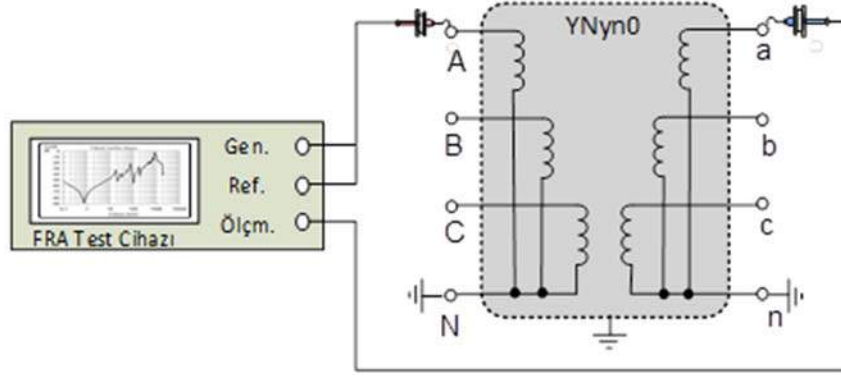
Şekil 5. Sargılar arası endüktif test bağlantı şeması

4. FRA Ölçümlerin Etkileyen Faktörler

Birkaç Hz'den birkaç MHz'e kadar olan FRA ölçümü, transformatör sargılarının durum değerlendirmesi için yaygın olarak kullanılmakta olup çeşitli mekanik ve elektrik arıza durumlarının tespit edilmesinde etkin bir yöntemdir. Test esansında elde edilen FRA sonucu, önceki bir ölçümle veya üç fazlı bir transformatörün fazları arasında frekans yanıtlarının görsel olarak karşılaştırılır (Picher et al., 2017). Güç transformatörü sargı yapısındaki yüksek frekanslı elektriksel etkileşimlerin karmaşıklığı, ölçüm esasındaki diğer ekipman ve çevresel faktörlerin varlığı FRA yorumlamasında bazı zorluklar getirmektedir. Dolayısıyla, doğru bir yorumlama için deneyimli uzman bilgisi yanında ölçme işlemine ait şartların da iyi bilinmesi gerekir. Karşılaştırma esasına dayanan bu yöntemde, sağlıklı bir değerlendirme yapılabilmesi için, test şartlarının benzer olması gerekmektedir. Bunların yanında FRA test işlemlerinde dikkate alınması gereken ve ölçüm sonuçlarını etkileyen önemli parametreler; kademe değiştirici etkisi, sıcaklık, bağlantı grubu, DC gerilim, ölçüm yönü vb. şeklinde sıralanabilir.

4.1. Kademe değiştirici etkisi

Transformatörlerde yapılan FRA ölçümünde, kademe pozisyonu önemli olmaktadır. Standartlarda önerilen, kademe değiştiricinin tüm sargıları içerisine alacak seviyede bulunmasıdır. Her kademe için ayrı ölçüm yapılabilir, ancak bu durum çok fazla ölçme gerektireceğinden pratik değildir (IEEE, 2013; International Electrotechnical Commission, 2012; Yousof et al., 2015). Bu nedenle, yapılan ölçümlerde kademe değiştiricinin pozisyon değeri mutlaka belirtilmelidir. Bununla birlikte, yük altında kademe değiştiricinin en düşük kademeden en yüksek kademeye doğru gitmesi ile tam tersi yönde gitmesi arasında yapılan ölçümlerde de farklılıklar olabileceği dikkate alınmalıdır.

4.2. Sıcaklık etkisi

FRA ölçümü, bir anlamda transformatör empedansının frekansa verdiği cevap olarak değerlendirilebilir. Dolayısıyla, sıcaklık ile direnç arasındaki ilişki ve sargı sıcaklığına bağlı olarak, direnç değerinde bir miktar değişim söz konusu olmaktadır. Direnç değeri değiştiğinden, ölçüm sonuçlarının genlik değerlerinde de bir miktar değişimler görülebilir. Değişim, yüksek frekanslı bölgede ve yüksek sıcaklık farklarında daha fazla gözlenmektedir (International Electrotechnical Commission, 2012; Reykherdt & Davydov, 2011). Bu sebeple, ölçme anındaki sıcaklık değerlerinin tespit edilip kaydedilmesi, yerinde olacaktır.

4.3. Bağlantı grubu ve tersiyer sargı etkisi

Bazı güç transformatörlerinde, primer ve sekonder sargıların haricinde, üçüncü sargı olarak tersiyer sargılar mevcuttur. Tersiyer sargı, yıldız bağlı transformatörlerde kullanılan yardımcı bir sargıdır. Yıldız bağlı transformatörlerde sargı sonları yıldız noktasına bağlı iken, üçgen sargılı transformatörlerde sargılar ardı sıra bağlıdır. Üçgen bağlantı uçlarının açık ve kapalı olması, özellikle orta frekansta rezonansa sebep olmakta, bu da ölçüm sonuçlarını etkilemektedir. Yıldız bağlı transformatörlerde, harici olarak yıldız noktası değiştirilebiliyor ise, yıldız noktasının bağlı veya açık olması da, yine ölçüm sonuçlarını değiştirecektir (Reykherdt & Davydov, 2011).

4.4. DC gerilim etkisi

Sahada yapılan test işlemlerinde, ilk olarak FRA ölçümü yapılması istenir. Bunun nedeni, ölçüm sonucu elde edilecek frekans cevabının diğer test cihazlarından kaynaklanan DC gerilimden etkilenmesini önlemektir. Nüvede meydana gelen artık mıknatısiyet, ölçüm sonuçlarını etkiler (International Electrotechnical Commission, 2012). Yapılan bir çalışmada, DC gerilimin FRA ölçüm sonuçları üzerindeki etkisi gözlenmiştir. İlgili çalışmada, DC gerilim uygulanmadan ve uygulandıktan sonra frekans cevabının 0-1 kHz bölgesinde, genlik bakımından önemli kaymalar görülmüştür (Abeywickrama et al., 2008). Bu nedenle, transformatör nüvesinden kaynaklı artık mıknatısiyet etkisinin en aza indirilmesi gerekir. Bunun sağlamak için, FRA ölçmeleri sargı direnç ölçümlerinden önce yapılmalı veya ölçme işleminden önce nüvedeki artık mıknatısiyet demagnetize edilmelidir.

4.5. Buşing ve ölçüm yönü etkisi

Bu ölçme yönteminde ölçüm cihazının bağlantı terminalleri, transformatör buşinglerine irtibatlandırılır. Sistem karakteristiğinin etkilenmemesi için, önceki ölçümde irtibatlanan buşing kullanılmalıdır. Farklı tip buşing kullanıldığı taktirde, buşing izolasyon malzemelerinin karakteristiğine bağlı olarak, ölçüm sonuçları da farklılık gösterebilir. Ayrıca, ölçüm yönü de, test sonuçlarını etkileyen diğer önemli bir faktör olarak karşımıza çıkmaktadır. Örneğin; A fazı sargısından Nötr (N) noktasına doğru yapılan ölçümle, N noktasından A fazına doğru yapılan ölçüm arasında farklılıklar meydana gelebilir. FRA analizinde bu etki, daha çok, yüksek frekans bölgesinde görülmektedir (International Electrotechnical Commission, 2012).

4.6. Diğer etkiler

Ayrıca, FRA ölçüm işlemini etkileyebilecek diğer faktörler ise; ölçüm cihazının standartlar dahilinde olmaması, bağlantı hataları, testi yapan operatörün ilgili testi standartlara uygun bir şekilde gerçekleştirmemesi şeklinde sıralanabilir. Bütün bu faktörler, test sonuçlarının güvenilirliği ve testlerin tekrar edilebilirliği açısından önemli birer unsurdur.

5. Sonuçlar

FRA, transformatörlerde meydana gelen sargı arızaları ve nüvedeki yapısal bozuklukların teşhisinde, özellikle de transformatörlerde meydana gelen sargı ve nüvedeki yapısal kaymaların belirlenmesinde kullanılan etkin bir yöntemdir. Bu çalışmada yöntemin temel prensipleri, ölçme yöntemleri, ölçmeyi etkileyen önemli faktörler açıklanarak tartışılmıştır.

FRA testlerinin yapılmasında, ölçüm sonuçlarının yorumlanması ve değerlendirilmesinde dikkat edilmesi gereken önemli etkenler aşağıdaki gibi not edilmiştir.

- Bir önceki FRA sonuçlarıyla karşılaştırmayla değerlendirme yapılacaksa test şartlarının ve ölçme yönteminin aynı olmasına dikkat edilmelidir.
- Ölçme işleminden önce transformatörde artık mıknatısiyetin olmadığından emin olunmalı veya demagnetize işlemi yapılmalıdır.
- Ölçme bağlantı uçlarının seçilmesinde ölçüm yönünün tüm test işlemleri için aynı seçilmesi önemlidir.
- Transformatördeki yaşlanma etkileri ve izolasyon yağının durumundaki değişimler de hesaba katılmalıdır.

Tüm bu durumlar dikkate alındığında FRA sonuçların yorumlanmasında uzmanlık bilgisine ihtiyaç duyulmaktadır. FRA yöntemi transformatör arızalarının teşhisinde hassas ve başarılı sonuçlar vermekte olup test şartlarının önceki şartlarla uygun olmasına dikkat edilmelidir. Aynı zamanda test esnasında deney şartları, ölçme yöntemi ve transformatöre ait karakteristik değerler (sıcaklık, nem, izalasyon yağının durumu vb.) titizlikle not edilmelidir.

Kaynaklar

Abeywickrama, N., Serdyuk, Y. V., & Gubanski, S. M. (2008). Effect of core magnetization on frequency response analysis (FRA) of power transformers. *IEEE Transactions on Power Delivery*, *23*(3). https://doi.org/10.1109/TPWRD.2007.909032

Al-Ameri, S. M., Kamarudin, M. S., Yousof, M. F. M., Salem, A. A., Siada, A. A., & Mosaad, M. I. (2021). Interpretation of frequency response analysis for fault detection in power transformers. *Applied Sciences (Switzerland)*, *11*(7). https://doi.org/10.3390/app11072923

Alsuhaibani, S., Khan, Y., Beroual, A., & Malik, N. H. (2016). A review of frequency response analysis methods for power transformer diagnostics. *Energies*, *9*(11). https://doi.org/10.3390/en9110879

Bohatyrewicz, P., Płowucha, J., & Subocz, J. (2019). Condition assessment of power transformers based on health index value. *Applied Sciences (Switzerland)*, *9*(22). https://doi.org/10.3390/app9224877

CIGRE Working Group A2.37. (2015). Transformer Reliability Survey. In *Cigre* (Issue December). Cigre.

Faiz, J., & Heydarabadi, R. (2015). Diagnosing power transformers faults. *Russian Electrical Engineering 2014 85:12*, *85*(12), 785–793. https://doi.org/10.3103/S1068371214120207

Gajić, Z. (2008). *Differential protection methodology for arbitrary three-phase power transformers* [Lund University]. https://doi.org/10.1049/cp:20080009

IEEE. (2013). C57.149-2012 - IEEE Guide for the Application and Interpretation of Frequency Response Analysis for Oil-Immersed Transformers. *IEEE*.

International Electrotechnical Commission. (2012). *IEC 60076-18 Ed. 1.0 b:2012 Power*

Transformers - Part 18: Measurement Of Frequency Response.

International Electrotechnical Commission. (2015). *IEC 60599:2015 Mineral oil-filled electrical equipment in service - Guidance on the interpretation of dissolved and free gases analysis.*

Khalili Senobari, R., Sadeh, J., & Borsi, H. (2018). Frequency response analysis (FRA) of transformers as a tool for fault detection and location: A review. *Electric Power Systems Research*, *155*, 172–183. https://doi.org/10.1016/j.epsr.2017.10.014

Koroglu, S. (2016). A Case Study on Fault Detection in Power Transformers Using Dissolved Gas Analysis and Electrical Test Methods. *Journal of Electrical Systems*, *12*(3), 442–459.

Kraetge, A., Krüger, M., Valásquez, J. L., Viljoen, H., & Dierks, A. (2009). Aspects of the Practical Application of Sweep Frequency Response Analysis (SFRA) on Power Transformers. *CIGRÉ 2009 6th Southern Africa Regional Conference.*

Mahvi, M., Behjat, V., & Mohseni, H. (2020). Analysis and interpretation of power auto-transformer winding axial displacement and radial deformation using frequency response analysis. *Engineering Failure Analysis*, *113*. https://doi.org/10.1016/j.engfailanal.2020.104549

Mendes, J. C., Marcondes, R. A., & Nakamura, J. (2004). On-site Tests on HV Power Transformers. *Cigre 2004*. http://www.cigre.org

Mirzai, M., Gholami, A., & Aminifar, F. (2006). Failures Analysis and Reliability Calculation for Power Transformers. *Journal of Electrical Systems*, *2*(1).

Ni, J., Zhao, Z., Tan, S., Chen, Y., Yao, C., & Tang, C. (2020). The actual measurement and analysis of transformer winding deformation fault degrees by FRA using mathematical indicators. *Electric Power Systems Research*, *184*. https://doi.org/10.1016/j.epsr.2020.106324

Picher, P. (2008). Mechanical Condition Assessment of Transformer Windings Using Frequency Response Analysis (Fra). *Evaluation, April*.

Picher, P., Tenbohlen, S., Lachman, M., Scardazzi, A., & Patel, P. (2017). Current state of transformer FRA interpretation: On behalf of CIGRE WG A2.53. *Procedia Engineering*, *202*. https://doi.org/10.1016/j.proeng.2017.09.689

Reykherdt, A. A., & Davydov, V. (2011). Case studies of factors influencing frequency response analysis measurements and power transformer diagnostics. *IEEE Electrical Insulation Magazine*, *27*(1). https://doi.org/10.1109/MEI.2011.5699444

Suwarno, & Donald, F. (2010). Frequency Response Analysis (FRA) for diagnosis of power transformers. *ECTI-CON 2010 - The 2010 ECTI International Conference on Electrical Engineering/Electronics, Computer, Telecommunications and Information Technology.*

Tenbohlen, S., Coenen, S., Djamali, M., Müller, A., Samimi, M. H., & Siegel, M. (2016).

Diagnostic measurements for power transformers. In *Energies* (Vol. 9, Issue 5). https://doi.org/10.3390/en9050347

Yousof, M. F. M., Ekanayake, C., & Saha, T. K. (2015). An investigation on the influence of tap changer on Frequency Response Analysis. *Proceedings of the IEEE International Conference on Properties and Applications of Dielectric Materials*, *2015-October*. https://doi.org/10.1109/ICPADM.2015.7295434

Simultaneous Hybrid Use of Drinking Water Pump Energy from Grid and Solar Energy

Aydın GULLU[1*]

Abstract: The importance of renewable energy sources has increased with the aim of efficient use of limited energy resources. Energy sources such as wind and sun are used in energy production. However, energy production in these energy sources varies depending on environmental conditions. In cases where there is a need for energy, energy may not be provided from the sun or wind due to environmental conditions. Energy can be stored by mechanical arrangement of the system. However, this may not always be enough. In this case, renewable energy sources and grid hybrids are used. In this study, a deep water well pump will be operated with electrical energy produced from solar panels. The water will be collected in a tank and given to the drinking water network. When the water level in the tank decreases, the pump will be activated automatically. The most efficient way of this work depends on the use of the solar panels at the maximum level. The energy from the solar panels is connected to the DC bus input of an AC motor drive. At the same time, the mains voltage is connected to the drive via a disconnector. The system was applied for Edirne İpsala Aliçopehlivan village. In this application, solar panels and electrical panels are placed on the existing infrastructure. In system tests, the pump must be operated in the range of 45-50Hz in order to extract water. For this reason, the use of maximum power tracking point has been used very limitedly. The grid is used when the energy of the solar panels is not sufficient. A separator is used for this transition. In cases where the sun is not enough, both the grid and the solar panels are connected at the same time to operate the system. In the developed setup, 25300 W solar panel, 22kW AC motor driver and 18.5kW pump were used.

Keywords: Hybrid Energy, Solar Energy, Solar Pump Control

1. Introduction

The use of clean energy sources is desired by many people. However, they are not sufficient in terms of continuity and installed power(Akinsipe, Moya, & Kaparaju, 2021). Solar panels generate electricity based on daylight. Wind turbines, on the other hand, are dependent on the wind. Since the control of resources in clean energy is not in the hands of human beings, electricity production cannot be provided at the desired power and at the desired time (Ozan & GÜLLÜ, 2016). It is used in the most efficient way with very good planning and statistical calculations. The aim of this study is to use solar panels for the energy of an electric pump working for water needs. Although the power provided by these solar panels can operate the pump, this operation will not be possible for 24 hours. Solar energy depends on sunlight. However, the water requirement is independent of daylight. For this reason, it is aimed to meet the energy of the pump, which will meet the water need, as a hybrid (Upasani & Patil, 2018). The hybrid worker model and the installed system are explained in chapter 3.

[1] Trakya University, Ipsala Vocational School, Electronics and Automations Dept., Edirne, Turkey
* Corresponding author: aydingullu@trakya.edu.tr

2. Materials and Methods

The material and method used to create the system are mentioned in this section. First, information about solar panels will be given. Then, the inverters used in the conversion of the energy produced in the solar panels will be mentioned.

2.1. Solar Panels

Solar panels convert the energy they receive from the sun into electricity. Solar cells are used for this conversion. Solar panels are produced by connecting more than one solar cell with each other in series or parallel. The structure of the cells determines the structure of the solar panel. They can be monocrystalline(Munzer, Holdermann, Schlosser, & Sterk, 1999) or polycrystalline according to cell types. monocrystalline or polycrystalline panel is shown in figure 1(Hörömpöli & Rácz, 2018). The energy produced as direct current is produced at a certain voltage and current. If the generated energy is to be used in DC, it is used by reducing it to the appropriate voltage level. If AC is to be used as a source of power, direct current must be converted to alternating current. This conversion is done with the help of inverters. Inverters are described in chapter 2.1.
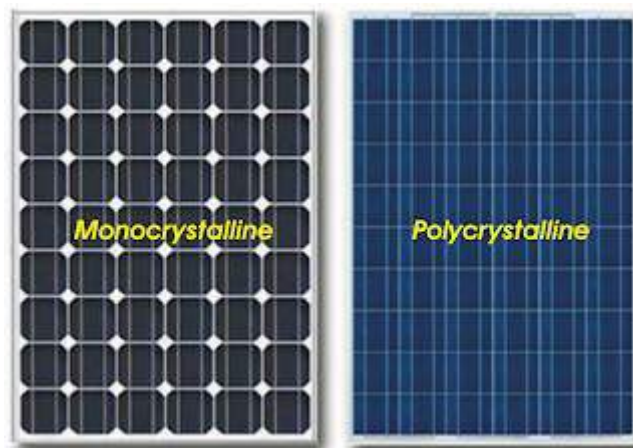
Figure 1. Types of Solar Panels

2.1. Inverters

In this study, energy will be used in the water pump working with alternating current. Since it works with alternating current, it is necessary to convert the direct current produced in solar panels. An inverter will be used for this conversion process. DC-AC inverters are produced and sold commercially(Dogga & Pathak, 2019). These inverters convert to AC voltage at grid frequency. The conversion power is constant for the device being produced. These devices are selected in accordance with the panel power(Güllü, Kuşçu, & Yılmazlar, 2020). There are varieties such as AC full-wave sine, or modified sine. There is an off-grid type that is independent of the grid, as well as on-grid inverters that work connected to the grid. The off-grid inverter connection diagram is shown in figure 2. On-grid inverters adjust the energy they produce in accordance with the grid frequency angle. In this way, the energy produced is in the same direction as the grid, and when desired, energy can be transferred to the grid with the help of these inverters(Chand, Prasad, Mamun, Sharma, & Chand, 2019). The on-grid inverter connection diagram is shown in figure2.
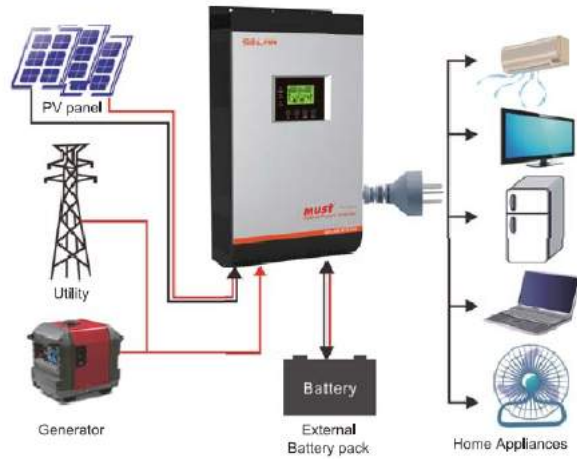
Figure 2. Off-grid inverters
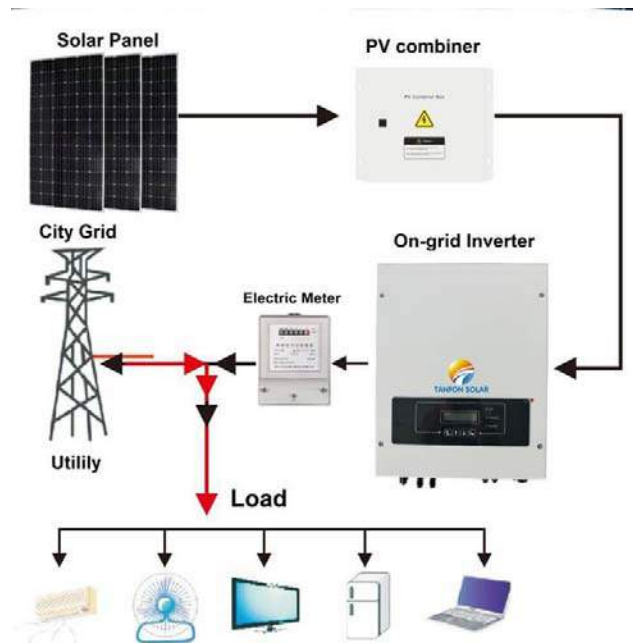
Figure 3. On-grid inverters

In this study, a motor control will be made. For this reason, a direct ac motor frequency inverter is used instead of a dc-ac inverter. The operation of AC motor drives is as follows. The supply is usually inputted as AC. This supply is then converted to DC. Then the dc voltage is converted back to ac at the desired frequency and transferred to the motor. DC-converted voltage terminals are available for use from most ac frequency inverters operating on this principle. It can also be used without AC input by applying external DC voltage to these terminals. However, since the output potential (phase-to-phase for Turkey) is AC380V, this voltage should be close as DC. When a 3-phase sine voltage is rectified with a blind rectifier, it is calculated as in equation 1.

$$V_{DC} = V_m \, 3\sqrt{3} \cos a \, /\pi \qquad \text{(I)}$$

$$V_m = \sqrt{2}xV_{rms} \tag{II}$$

Peak voltage is 311V for a voltage of 220V rms between phase and neutral.   In the formula I, if a=0 for maximum efficiency, the DC voltage will be 514V for 380 V.

This calculated voltage is the DC link voltage of the motor driver. If a voltage above this busbar voltage is applied externally to the DC bus, current will flow from here. The system structure is described in chapter 3.

The 22-kW delta c2000 series inverter used in this project. Figure 4 shows the inverter and its connection diagram. 3 phase input and motor connections are shown in the connection diagram. The energy from the solar panels will be connected to the DC bus (DC+ DC- terminals). Since it is the direction of the direct current, the connections must be paid attention to.
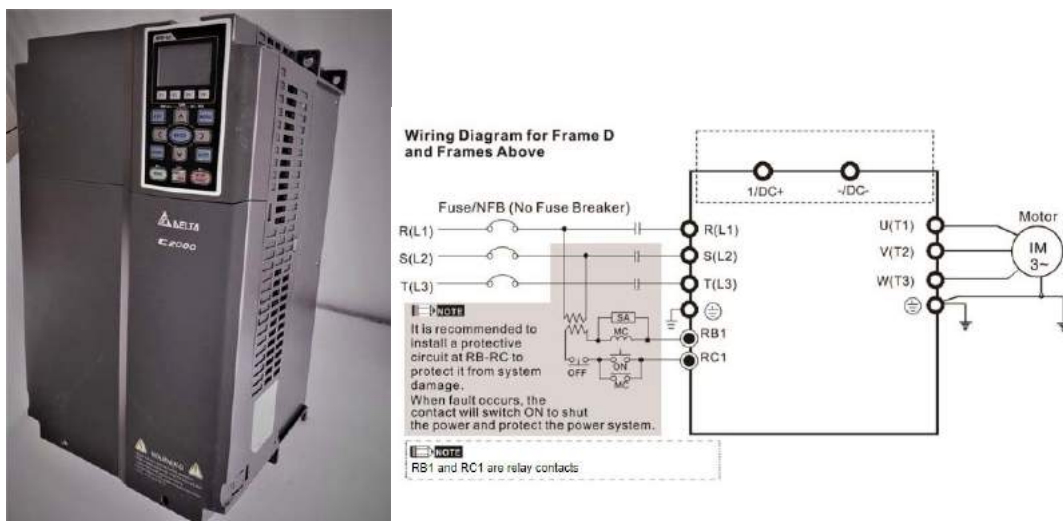
Figure 4. Delta C2000 Invertor

3. Structure of the System

The system is designed to supply the energy of the drinking water pump of the village of Ipsala Aliçopehlivan. The current drinking water pump is 18.5kW. The water needs of the village are met by transferring the water from the well to a high tank. The pump is designed to fill the tank. Since the water usage is high in the summer months, the pump must run 24 hours a day. In the summer, the tank is never fully filled. 110 solar panels are placed in the area next to this pumping station. The solar panel array is given in figure 6. Solar panels are planned in the form of 5 arms of 22 pieces. PLM-230P-60 model 230W polycrystalline solar panels are positioned on each arm. Solar panels are given in figure 5. The solar panels produce 30.15V DC voltage and the current capacity is 7.63A. With the calculation made from the formula 1, the dc bus voltage in the network becomes 514V. In some cases, voltage fluctuations may increase the mains phase-to-phase voltage above 380V. An increase is also observed in the DC bus voltage at the noses. In order for the panel currents to be used simultaneously with the grid, the panel potential is expected to be higher than the DC potential of the grid. Otherwise, there may be no current flow. For this, 22 branches were created by looking at the land layout on which this system will be installed and the number of 110 panels. Since each panel voltage is 30.15V, the branch voltage is 663.3V. For this voltage, 22 pieces of each arm are connected in series and 5 branches are connected in parallel. Separate + and − cables were drawn from

the arms. It is protected with a diode so that it is not exposed to reverse current for each arm. When there is no sun, reverse voltage is prevented from flowing through the panels. The electrical panel made for the system is shown in the figure 7.

Figure 5. Solar Panel

The current will flow unidirectionally from the panels to the DC bus development of the drive. With this method, both the network and the panels are integrated into the system at the same time. The system was operated with a hybrid energy source. In addition, a contactor is connected to the system. When the sun is sufficient, the mains current will be completely cut off and disconnection from the mains will take place. However, in the tests carried out, it was not possible to meet all of the pump energy from the sun. It has been observed that the efficiency of the panels is around 70%. The panels were used for a long time and were re-arrayed for this project.

Figure 6. Solar Panel Array

In order to use the sun efficiently in solar systems, the output is reduced in a controlled manner according to the efficiency of the sun. This is achieved by reducing the frequency from AC motor drives. With the method called maximum power point tracking, it is aimed to use the maximum power of the solar panels(Espinosa, 2017; Pathare et al., 2017). In this method, the power to be drawn from the panels is always at the maximum level and the output power is adjusted accordingly. However, in this system, water is drawn from the well. When the pump frequency drops below 45Hz, no water comes out. In this case, the frequency of the pump must be set at a very limited level. In places where water demand is high, maximum

operation of the pump is often desired. In this study, the MPPT method was used and the minimum level of the pump was controlled via the human-machine interface(figure 8). However, due to the preference of maximum 50Hz and low panel efficiency most of the time, it causes the system to work with network support.
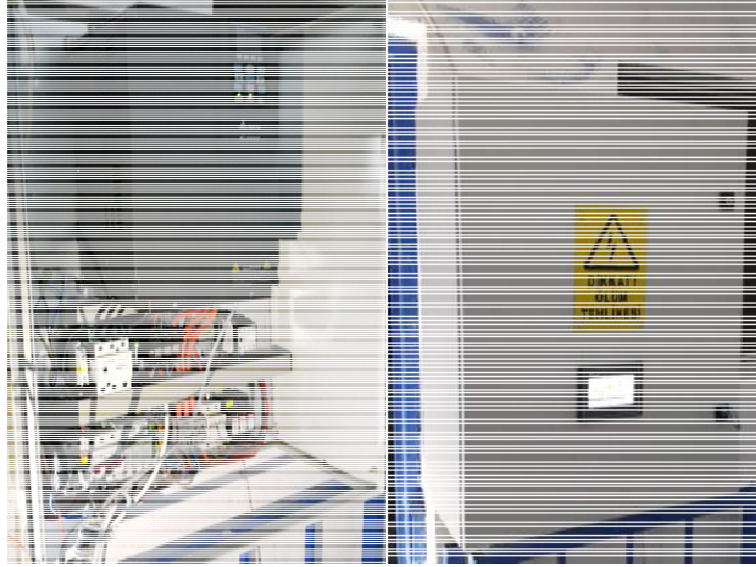
Figure 7. Electrical Panel

While the motor current is around 40A when the daylight is most efficient, it has not been observed that this current is drawn from the solar panels of the 10A network. However, in the tests and measurements, it was observed that the pump did not work only from the solar panels as the installed power. If the motor frequency is reduced to 38HZ, the motor can operate from the solar panels. However, in this case, the water does not come out. Hybrid operation is most suitable in terms of the performance of the system. If the number of panels is increased, the system can be switched and only panels can be operated.
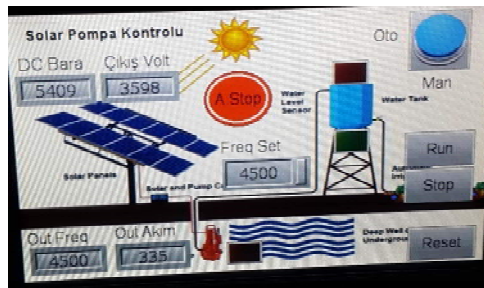
Figure 8. Human Machine Interface

4. Discussion and Conclusions

In this study, a 18.5kW pump was operated together with 110 solar panels of 25300W and the grid. In operation, current flows from the solar panels to the DC bus. According to the solar efficiency, some of the current is taken from the panels and some from the grid. In this way, the panels are integrated into my system around the clock. If sufficient energy is provided from the solar panels, it is ensured that the system is disconnected from the grid. In the measurements made during the day, it has been observed that 40A motor current is drawn from the mains, 10A is drawn from the mains and the rest from the panels. This has been

observed as the most efficient case. This situation is reversed when the efficiency of solar panels decreases. The solar panels are insulated with a diode so that no current flows. This allowed the current to flow in one direction. 22 panels are planned in each of the 5 branches, thus leaving the potential of the panels above the grid. Even if the panel voltage drops, protection is provided with a diode. It is planned to monitor the status of the system by monitoring the daylight data for a long time with a separate project. This study has been tested so that the solar panels are sufficient but the solar panels can be used actively when the grid is available. In this way, as there is daylight, there will always be a current flow from the solar panels according to the daylight level, which will make a serious contribution to the costs. In addition, the system will run continuously.

References

Akinsipe, O. C., Moya, D., & Kaparaju, P. (2021). Design and economic analysis of off-grid solar PV system in Jos-Nigeria. *Journal of Cleaner Production, 287*, 125055.

Chand, A. A., Prasad, K. A., Mamun, K. A., Sharma, K. R., & Chand, K. K. (2019). Adoption of grid-tie solar system at residential scale. *Clean Technologies, 1*(1), 224-231.

Dogga, R., & Pathak, M. (2019). Recent trends in solar PV inverter topologies. *Solar Energy, 183*, 57-73.

Espinosa, C. L. (2017). *Asynchronous non-inverter buck-boost DC to DC converter for battery charging in a solar MPPT system.* Paper presented at the 2017 IEEE URUCON.

Güllü, A., Kuşçu, H., & Yılmazlar, E. (2020). Efficiency Analysis in Solar Panel Energy Systems: AC-DC Conversion Cost and DC-DC Energy Use.

Hörömpöli, B., & Rácz, E. (2018). *Statistical analysis of power measurements made on mono-and polycrystalline solar cells.* Paper presented at the 2018 IEEE 16th World Symposium on Applied Machine Intelligence and Informatics (SAMI).

Munzer, K. A., Holdermann, K. T., Schlosser, R. E., & Sterk, S. (1999). Thin monocrystalline silicon solar cells. *IEEE transactions on electron devices, 46*(10), 2055-2061.

Ozan, A., & GÜLLÜ, A. (2016). *Solar Pump Project Feasibility Study For The Village Kumdere.* Paper presented at the UNITECH 16, Gabrova Bulgaria.

Pathare, M., Shetty, V., Datta, D., Valunjkar, R., Sawant, A., & Pai, S. (2017). *Designing and implementation of maximum power point tracking (MPPT) solar charge controller.* Paper presented at the 2017 International Conference on Nascent Technologies in Engineering (ICNTE).

Upasani, M., & Patil, S. (2018). *Grid connected solar photovoltaic system with battery storage for energy management.* Paper presented at the 2018 2nd International Conference on Inventive Systems and Control (ICISC).

Effects of different stitch combinations on the seam bursting characteristics of PET/Co workwear

Sukran Kara[1*]

Abstract: Workwears are produced to protect the wearer against occupational or environmental hazards. One of the shared properties of several workwear types is resisting external forces during occupation. As for workwear fabrics, the seams of the workwear should be strong enough to resist uniaxial or multiaxial forces to maintain the properties in the cut and sewn parts of the garment. Although the uniaxial seam strengths of classical fabrics for various end-products were determined in several studies, multiaxial strength of workwear fabrics have not been studied in details, yet. Therefore, in this study, effects of different stitch types and their combinations on the workwear bursting characteristics were evaluated in order to determine their resistance against multiaxial forces. According to results, usage of stitch combinations obviously contributed to the seam bursting strength. The stitch rows responded to the bursting forces together therefore the bursting failures occurred in 1-step.

Keywords: Seam bursting, bursting height, workwear, stitch combinations.

1. Introduction

Workwears should resist external forces during occupation and provide protection to the wearer. Therefore, workwears are produced with thick and heavy fabrics made of specialty fibres or traditional synthetic/natural fibers. Raw materials of the workwear fabrics are selected carefully in order to balance the performance and the cost of the end-products (Paul, 2019; Midha et al, 2010; Haifa, 2013). As for workwear fabrics, seams of the workwear should be strong enough to resist the forces in order maintain the unsewn fabric properties at the sewn areas.

In ready wear industry, six standard classes of stitches are used. They are chain stitch, hand stitch, lock stitch, overlock stitch, multi-yarn chain stitch and cover stitch (Gurarda, 2019; ASTM D6193, 2016). These stitch types can provide advantages such as security, strength, flexibility, low cost, ease to unstitch etc, for different application areas. So that, the effects of different stitch types on the seam quality of workwears should be investigated in details.

In the literature, seam strength of fabrics for different application areas were studied in details (Unal and Baykal, 2018; Choudhary and Goel, 2013; Vijay Kirubakar Raj and Renuka Devi, 2017; Frydrych and Greszta, 2016; Sular et al, 2015; Farhana et al, 2015; Namiranian et al, 2014; Bharani et al, 2012; Gurarda, 2008; Yesilpinar and Bahar, 2007; Tarafder et al, 2007; Gribaa et al, 2006; Mukhopadhyay et al, 2004; Chowdhary and Poynor, 2006). In most of these studies, lock stitch was utilized as it is a universal stitch type and lock stitch machine is

[1] Dokuz Eylul University, Engineering Faculty, Textile Engineering Department, Izmir, Turkey
* Corresponding author: sukran.kara@deu.edu.tr

the most available sewing machine. Nevertheless, in recent years, effects of other stitch types on the seam strength and other seam properties were evaluated (Kara, 2020; Islam et al, 2020; Ates et al, 2019; Akter and Khan, 2015). On the other hand, there is a very limited number of research studies on the bursting strength of sewn fabrics (Yusof, 2013; Kovalova et al, 2019; Rajput et al, 2018; Yesilpinar, 1997).

As seen from literature search, seam properties of workwear is very important as it ensures the continuity of the fabric properties in the joint areas. Although the uniaxial seam strengths of different fabrics were determined in several studies, multiaxial strength (bursting strength) of workwear fabrics have not been studied in details, yet. Therefore, the main goal of this study was to evaluate the effects of stitch types and stitch combinations on the multiaxial bursting strength of sewn workwear fabrics. This study differs from the literature as it determines the bursting strength of seams and as it compares 7 types of different stitch types/combinations for workwear.

2. Materials and Methods

As materials, a 280 g/m^2 PET/Co (65/35) blend fabric and 60 tex polyester core-spun sewing thread was utilized as they were suitable to be used for many workwear areas (Haifa, 2013; Midha et al., 2010; Verdu et al, 2009). The fabric was 0.46 mm thick and its weave was 2/2 warp rib. Warp and weft densities of fabric were 55.1 and 19.1 threads/cm, respectively. On the other hand, sewing yarn was a 2 ply yarn and its breaking strength was 34.5 N.

7 types of seams were produced by using basic stitch types (lock stitch, 2-yarn chain stitch and 3-yarn overlock stitch) and their combinations as 2-rows of stitches. The sample codes, stitch schematics and important stitch dimensions such as seam allowance and distances between stitch rows are given in Figure 1. Seam densities for all types of stitches were 3 stitches/cm. Seam allowances were folded in the back side of fabric and ironed before conditioning the test samples. For all samples, seams were formed both in warp direction and weft direction. All the samples were conditioned under standard atmosphere conditions (20±2ºC, 65±4 % relative humidity) for 24h before the tests.
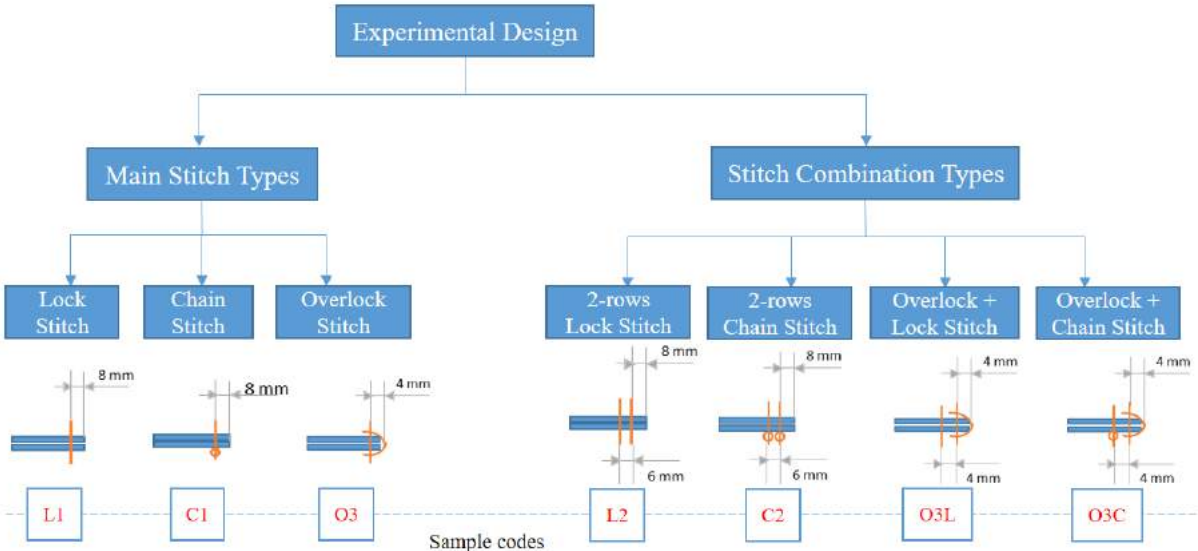
Figure1. Sample codes and seam and stitch information

Bursting strength and bursting height of non-sewn reference samples and sewn samples were determined according to ASTM D6797-15 standard, utilizing Instron 4411 Tensile Tester with a ball-burst attachment. Sample size was kept as 14 cm x 14 cm and the test speed was 300 mm/min. Normally, bursting strength test examines the strength of samples in all directions so that the test is not repeated for warp and weft directions. However, in this study, the bursting test samples were prepared to have seams in warp and weft directions, as shown in Figure 2.
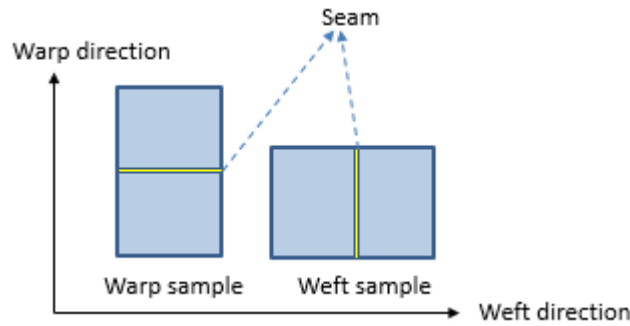
Figure 2. Seam placements and sample definition (Kara and Yesilpinar, 2021)

Also, seam bursting efficiencies of samples were calculated as given in Equation 1.

$$\text{Seam bursting efficiency (\%)} = \text{BE (\%)} = \frac{\text{Seam bursting strength}}{\text{Fabric bursting strength}} * 100 \qquad \text{Eq. (1)}$$

3. Results

Bursting strength results of samples are given in Figure 3. In addition, seam bursting efficiencies of samples are given in Table 1.

According to results, for the 3 main stitch types (L1, C1 and O3), bursting strength in warp and weft directions were lower than that of non-sewn reference samples (Figure 3). O3 exhibited the lowest bursting strength among these 3 stitch types. On the other hand, bursting strength of samples sewn with stitch combinations (L2, C2, O3L and O3C) exhibited higher bursting strengths when compared to non-sewn reference, especially for the warp samples. A similar result was obtained by Yesilpinar (1997), when she compared the bursting strength of 1 row lock stitched samples with 2 row lock stitched counterparts.

Second row of stitches in the combinations supported the seam line against bursting, importantly. Chain stitch containing samples (C1, C2, O3C) exhibited higher bursting strength when compared to lock stitch containing counterparts (L1, L2, O3L), but the differences were low. In the literature, the bursting strength of lock stitched samples were found slightly higher than chain stitched samples, but this study was made on knitted fabrics and bursting test procedure was different (Rajput et al, 2018).
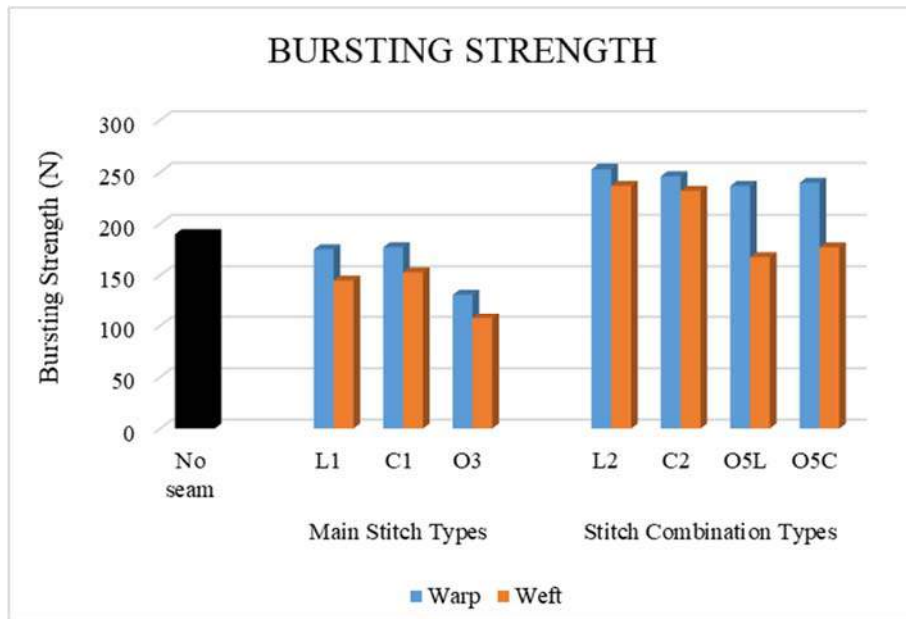
Figure 3. Bursting strength of samples

For stitch combinations, seam efficiencies against bursting were higher than 100% (Table 1). For all sample types, bursting efficiency of warp samples were higher than weft samples. During bursting tests, generally stitches were broken for 1 row stitch types (L1, C1, O3) whereas fabric tear near the seamline accompanied the stitch breakages or only the fabric tear near the seamline was observed in the bursting failure of combination stitches (L2, C2, O3L, O3C).

Table 1. Seam bursting efficiency

| Sample code | Seam Bursting Efficiency | |
	Warp (%)	Weft (%)
No seam	/	/
L1	92.25	76.25
C1	93.31	80.46
O3	68.95	56.64
L2	133.19	124.70
C2	129.69	122.15
O3L	124.71	88.23
O3C	126.33	93.23

Bursting height of samples are given in Figure 4. Only L2 and C2 samples exhibited slightly higher bursting heights for weft samples when compared to non-sewn reference. Also, bursting height of combination stitch samples were slightly higher when compared to main stitch samples (L1, C1, O3). The bursting heights for warp and weft samples were similar for all sample types.
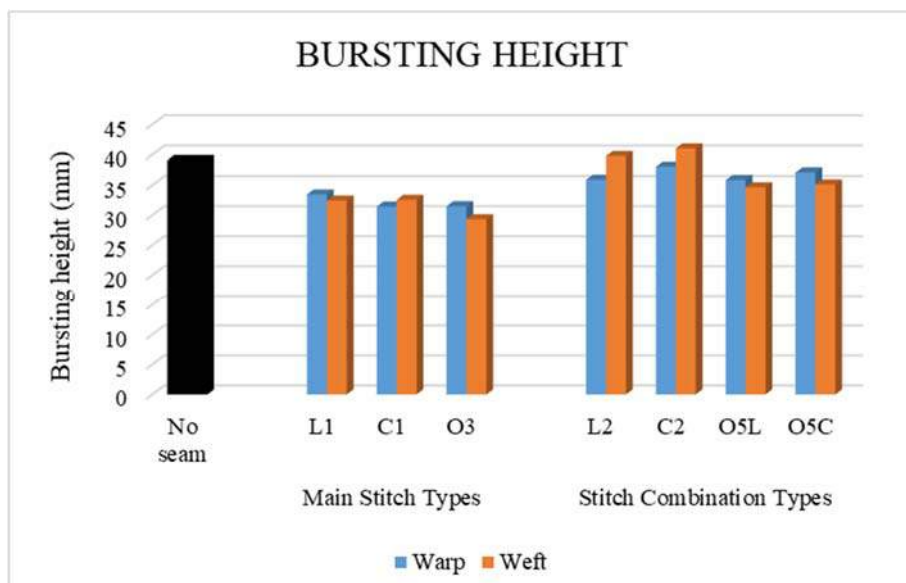
Figure 4. Bursting height of samples

4. Discussion and Conclusions

In this study, bursting properties of a workwear fabric sewn with 7 different stitches/stitch combinations were evaluated. Stitch combinations were formed by using lock stitch, chain stitch and overlock stitch together, as 2 rows stitches.

Normally, the main function of the second stitch row is to form a safety stitch rather than increasing the overall performance of textile items. In spite of this fact, in this study, usage of stitch combinations obviously contributed to the seam bursting strengths. Combined stitch rows responded to the bursting forces together and their bursting strengths were higher than non-sewn reference fabrics, especially in warp direction. This provided seam bursting efficiencies higher than 100 %. During the bursting tests, fabric tear near the seamline accompanied the stitch breakages or only the fabric tear near the seamline was observed for combination stitches. This phenomenon made it harder to repair the bursting failures for workwear. This situation was not valid for samples sewn with single row basic stitches. Bursting height of all sewn samples were similar to non-sewn reference samples.

In the further studies, seam strength of the selected samples will be determined to observe the behavior of stitch combinations during uniaxial seam strength tests. In addition, lock stitch or chain stitch can be selected and, the seam strength and seam bursting properties of workwear with lapped seams can be studied in the further studies.

References

Akter, M., Khan, M. R., (2015). The effect of stitch types and sewing thread types on seam strength for cotton apparel. International Journal of Scientific and Engineering Research, 6(7), 198-205.

ASTM D6193 – 16. Standard practice for stitches and seams.

ASTM D6797 – 15. Standard test method for bursting strength of fabrics constant-rate-of-

extension (CRE) ball burst test.

Ates, M., Gurarda, A., Ceven, E. K., (2019). Investigation of seam performance of chain stitch and lockstitch used in denim trousers. Tekstil ve Muhendis, 26(115), 263-270.

Bharani M., Shiyamaladevi P. S. S., Mahendra Gowda R. V., (2012). Characterization of seam strength and seam slippage on cotton fabric with woven structures and finish. Research Journal of Engineering Sciences, 1(2), 41-50.

Choudhary, A. K., Goel, A., (2013). Effect of some fabric and sewing conditions on apparel seam characteristics. Journal of Textiles, 2013, 1-7.

Chowdhary U, Poynor D., (2006). Impact of stitch density on seam strength, seam elongation, and seam efficiency. International Journal of Consumer Studies, 30(6), 561-568.

Farhana, K., Syduzzaman, M., Yeasmin, D., (2015). Effect of sewing thread linear density on apparel seam strength: A research on lapped and superimposed seam. Journal of Advancements and Engineering and Technology, 3(3), 1-7.

Frydrych, I., Greszta, A., (2016). Analysis of lockstitch seam strength and its efficiency. International Journal of Clothing Science and Technology, 28(4), 480-491.

Gribaa, S., Amar, S. B., Dogui, A., (2006). Influence of sewing parameters upon the tensile behavior of textile assembly. International Journal of Clothing Science and Technology, 18(4), 235-246.

Gurarda, A., (2008). Investigation of the seam performance of PET/nylon-elastane woven fabrics. Textile Research Journal, 78(1), 21-27.

Gurarda, A., (2019). Seam performance of garments. In: Textile Manufacturing Processes. ISBN: 178985105X, 9781789851052.

Haifa, I. H., (2013). Seam properties of workwear. Pakistan Textile Journal, 62(1), 42-46.

Islam, M. R., Asif, A. A. H., Razzaque, A., Al Mamun, A., Maniruzzaman, M., (2020). Analysis of seam strength and efficiency for 100% cotton plain woven fabric. International Journal of Textile Science, 9(1), 21-24.

Kara, S., (2020). Comparison of sewn fabric bending rigidities obtained by heart loop method: Effects of different stitching types and seam directions. Industria Textila 71(2), 105-111.

Kara, S., Yesilpinar, S. (2021). Comparative study on the properties of taped seams with different constructions. Fibres & Textiles in Eastern Europe, 29, 2(146), 54-60.

Kovalova, N, Kulhavy, P., Vosahlo, J., Havelka, A., (2019). Experimental and numerical study of sewing seams of automobile seat covers under unidirectional and multiaxial loading. Tekstil ve Konfeksiyon, 29(4), 322-335.

Midha, V. K., Kothari, V. K., Chattopadhyay, R., Mukhopadhyay, A., (2010). Effect of

workwear fabric characteristics on the changes in tensile properties of sewing threads after sewing. Journal of Engineered Fibers and Fabrics, 5(1), 31-38.

Mukhopadhyay, A., Sikka, M., Karmakar, A.K., (2004). Impact of laundering on the seam tensile properties of suiting fabric. International Journal of Clothing Science and Technology, 16(4), 394-403.

Namiranian, R., Shaikhzadeh Najar, S., Etrati, S. M., Manich, A. M., (2014). Seam slippage and seam strength behavior of elastic woven fabrics under static loading. Indian Journal of Fibre and Textile Research, 39(3), 221-229.

Paul, R. (Ed.)., (2019). High performance technical textiles. John Wiley & Sons.

Rajput, B., Kakde, M., Gulhane, S., Mohite, S., Raichurkar, P. P., (2018). Effect of sewing parameters on seam strength and seam efficiency. Trends in Textile Engineering and Fashion Technology, 4(1), 4-5.

Sular, V., Mesegul, C., Kefsiz, H., Seki, Y., (2015). A comparative study on seam performance of cotton and polyester woven fabrics. The Journal of the Textile Institute, 106(1), 19-30.

Tarafder, N., Karmakar, R., Mondal, M., (2007). The effect of stitch density on seam performance of garments stitched from plain and twill fabrics. Man-Made Textiles in India, 50(8), 298-302.

Unal, B. Z., Baykal, P. D., (2018). Determining the effects of different sewing threads and different washing types on fabric tensile and sewing strength properties. Tekstil ve Konfeksiyon, 28(1), 34-42.

Verdu, P., Rego, J. M., Nieto, J., Blanes, M., (2009). Comfort analysis of woven cotton/polyester fabrics modified with a new elastic fiber, part 1 preliminary analysis of comfort and mechanical properties. Textile Research Journal, 79(1), 14-23.

Vijay Kirubakar Raj, D., Renuka Devi, M., (2017). Performance analysis of the mechanical behaviour of seams with various sewing parameters for cotton canopy fabrics. Fibres and Textiles in Eastern Europe, 25, 4(124), 129-134.

Yesilpinar, S., (1997). Kullanim sirasinda giysilerde oluşan dikis patlamalari üzerine bir arastirma. Tekstil ve Mühendis, 11(56), 30-41.

Yeşilpınar, S., Bahar, S., (2007). The effect of sewing and washing processes on the seam strength of denim trousers. AATCC review, 7(10), 27-31.

Yusof, N. A., (2013). Effect of seam type on selected seam tensile behaviour under multi-axial forces (Doctoral dissertation, University of Otago).

Geomorphometric Analysis of the Sub-watersheds in the Eastern Black Sea region, Turkey

Senem TEKİN[1*], Tolga ÇAN[2]

Abstract: Topographic and drainage network features are important parameters in watershed management planning due to the physical characteristics of the watershed in terms of controlling the sustainability of water resources. In this study, physical characteristics and geomorphometric features were evaluated in the sub-waterheds of the Eastern Black Sea that is one of the 25 main watersheds of Turkey. GIS based geomorphometric analyses are important in terms of erosional processes and interpretation of the watershed condition. Geomorphometric evaluations were evaluated by considering linear (Bicking rate, Length Ratio, Texture ratio), areal (Drainage density, basin shape, Stream frequency) and surface morphometry (Hypsometric integral/curve) parameters.

Keywords: Watershed, drainage network, Eastern Black Sea, geomorphometric analysis.

1. Introduction

Watersheds morphometrics and the development of stream profiles are configured over long time periods, constructing the boundary condition that controls by river flow system. These controls constrain the range of river behaviour and associated morphological attributes within a watershed. By its nature, among others regional geologic and climatic factors mainly regulate the topography, sediment transport and the discharge regime (Fryirs and Brierley 2013). Topographic and drainage network features of watersheds are important parameters in watershed management planning due to the physical characteristics of the basin in terms of controlling the sustainability of water resources. With the surface morphometric features, erosion cycles of the basins can be determined, and numerical interpretations can be made. Therefore, geomorphometric studies using digital basin analyzes are important in terms of erosional processes in the basin and interpretation of the basin situation. Geomorphometric evaluations are evaluated by considering linear (Bidding ratio, Length Ratio, Texture ratio), areal (Drainage density, basin shape, Stream frequency) and surface morphometry (Hypsometric integral/curve) parameters. In this study, linear, areal and surface geomorphometric evaluations were made in 38 sub watersheds with an aerial size greater than 100 km^2 in the Eastern Black Sea main drainage basin of 22,867.06 km^2, which is one of the 25 main watersheds in Turkey (Figure 1).

[1] Adiyaman University, Mining and Mineral Extraction Department, School of Technical Sciences, Adıyaman, Turkey.
[2] Çukurova University, Department of Geology Engineering, Adana, Turkey
* Corresponding author: senemtekin@adiyaman.edu.tr
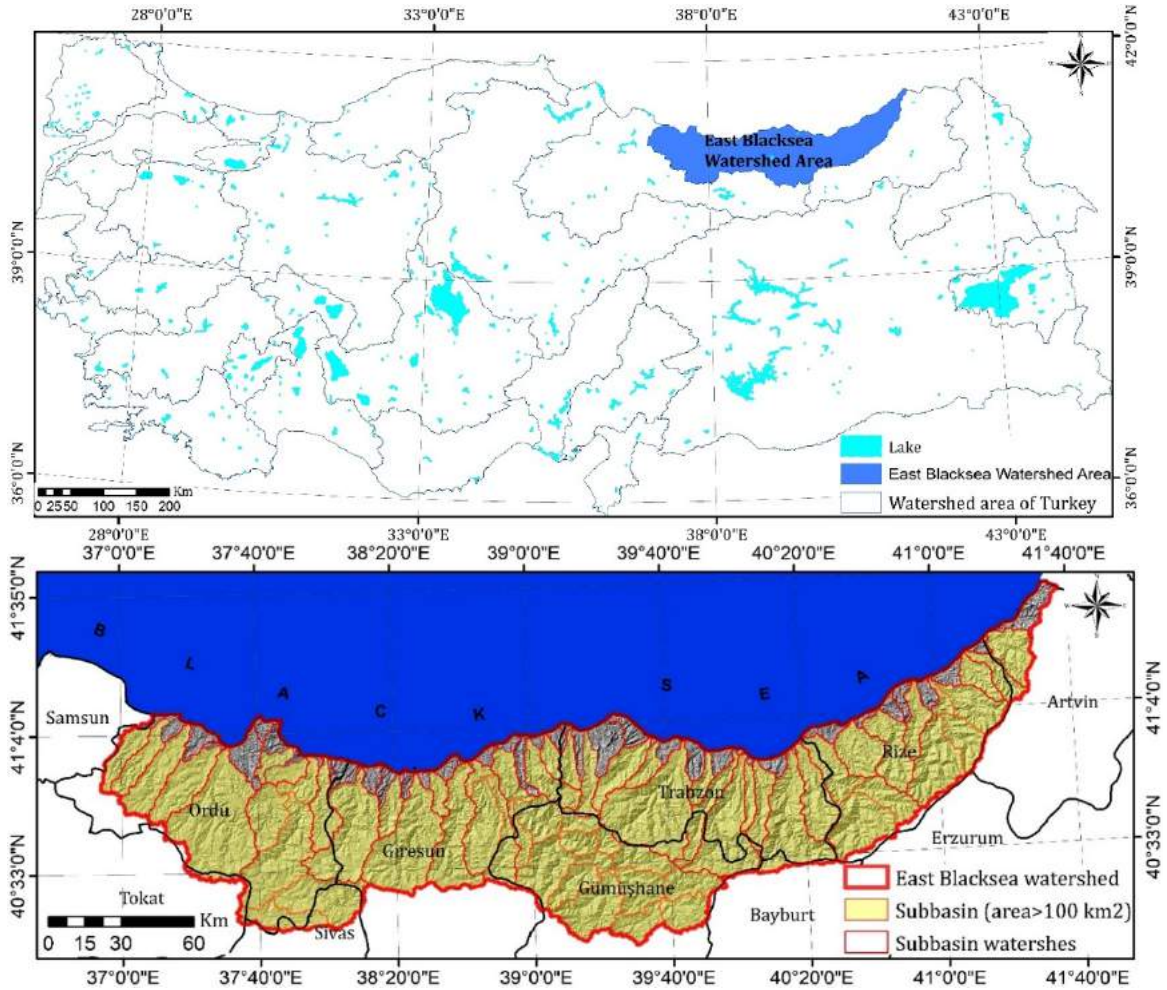
Figure 1.. Yer bulduru haritası.

2. Eastern Black Sea Basin of General Features

The Eastern Black Sea is one of the 25 main watershed of Turkey. The Black Sea region consists of 3 regions: East, Central and West. The Eastern Black Sea basin constitutes a region with a lower population compared to the Central and Western Black Seas in terms of both its climatic characteristics and mountainous settlements.

Digital elevation model (DEM) is the most basic parameter of geomorphometry studies. In this study, ASTER GDEM data, which is available free of charge and has a resolution of 28 meters, was used. According to this data, it varies between 0 - 3866 m in the Eastern Black Sea basin and increases relatively as one goes from the coast to the inner parts of the basin (Figure 2). Areas with an altitude below 1000 m in the basin have 40.44%, while the upper parts of the basin greater than 2000 m correspond to 20%. slope map was prepared by using DEM of the Eastern Black Sea basin (Figure 3). According to this map, slopes below 20° correspond to 44%, while areas with slopes greater than 40° correspond to 6% of the basin.
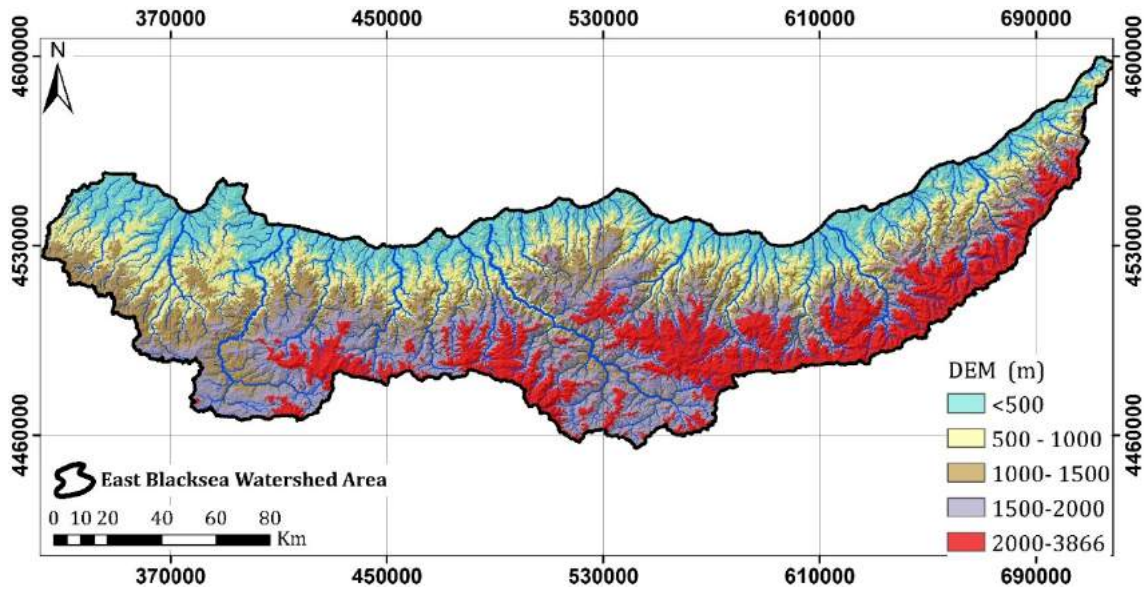
Figure 2. Digital elevation model of the Eastern Black Sea basin.
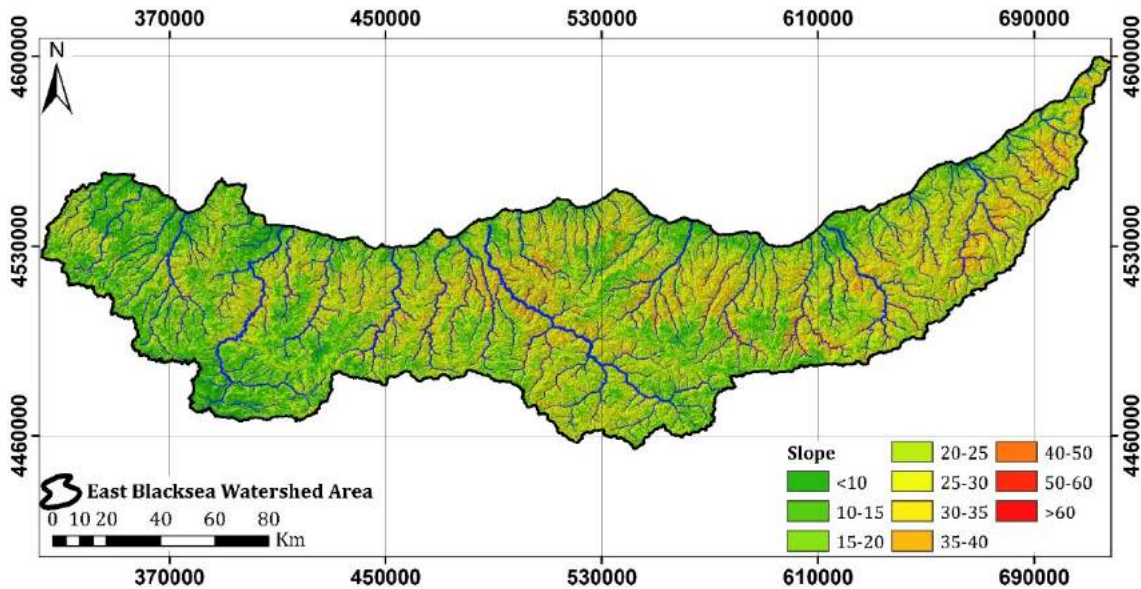
Figure 3. Slope map of the Eastern Black Sea basin.

The landform map was prepared according to Jenness (2006) by using the topographic position index (Figure 3). Accordingly, the basin consists of Valleys with 5.61% small drainage systems, 0.64% Lower Slopes, 17.25% Gentle Slopes, 16.08% Steep Slopes, 41.60% Upper Slopes and 18.81% very low slopes. ridges classes (Figure 4).

According to the 1/100000 scale CORINE Land Cover Classification, which consists of three different levels determined by the European Environment Agency; The Eastern Black Sea basin consists of 9 different classes (Figure 5). Among these classes, agricultural lands are generally located in areas below 1000 m and corresponds 34% of the basin. The forests cover that are seen throughout the basin and have the largest areal size with 37%, are generally located in the middle and upper parts of the basin.
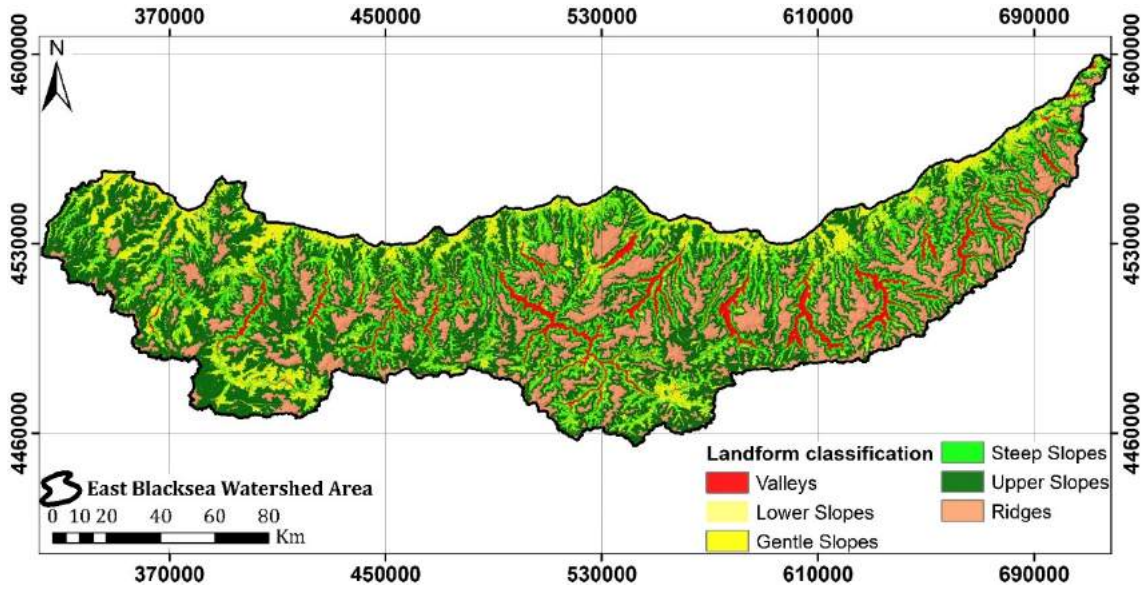
Figure 4.Landform classification of the Eastern Black Sea basin.
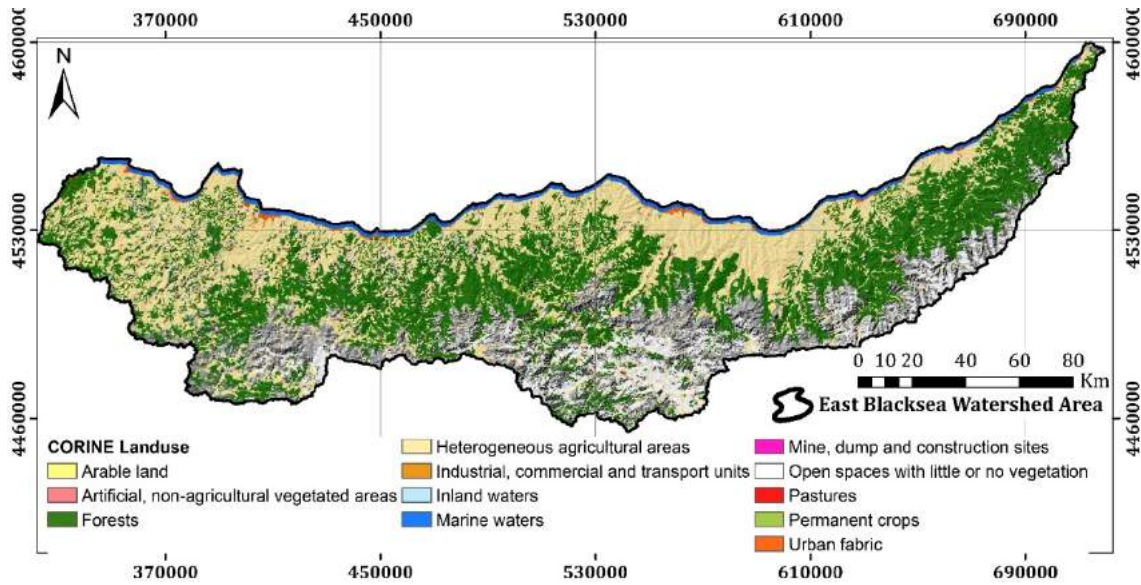
Şekil 5. CORINE of the Eastern Black Sea basin.

According to the KOPPEN classification, which is the most commonly used climate classification globally, there are 10 different climate types in Turkey. Climate data prepared by Worldclim (http://www.worldclim.org/version1) for a series of global climate layers with a spatial resolution of approximately 1 km^2 were evaluated for the Eastern Black Sea basin. According to the annual precipitation data of 1960-1990, the lowest precipitation in the basin was recorded as 463 mm and the highest precipitation as 2230 mm (Figure 6a). According to the predictions for the future using today's data, it is thought that there will be an increase in the annual precipitation amount of approximately 200 mm in the Eastern Black Sea basin in 2070 (Figure 6b).
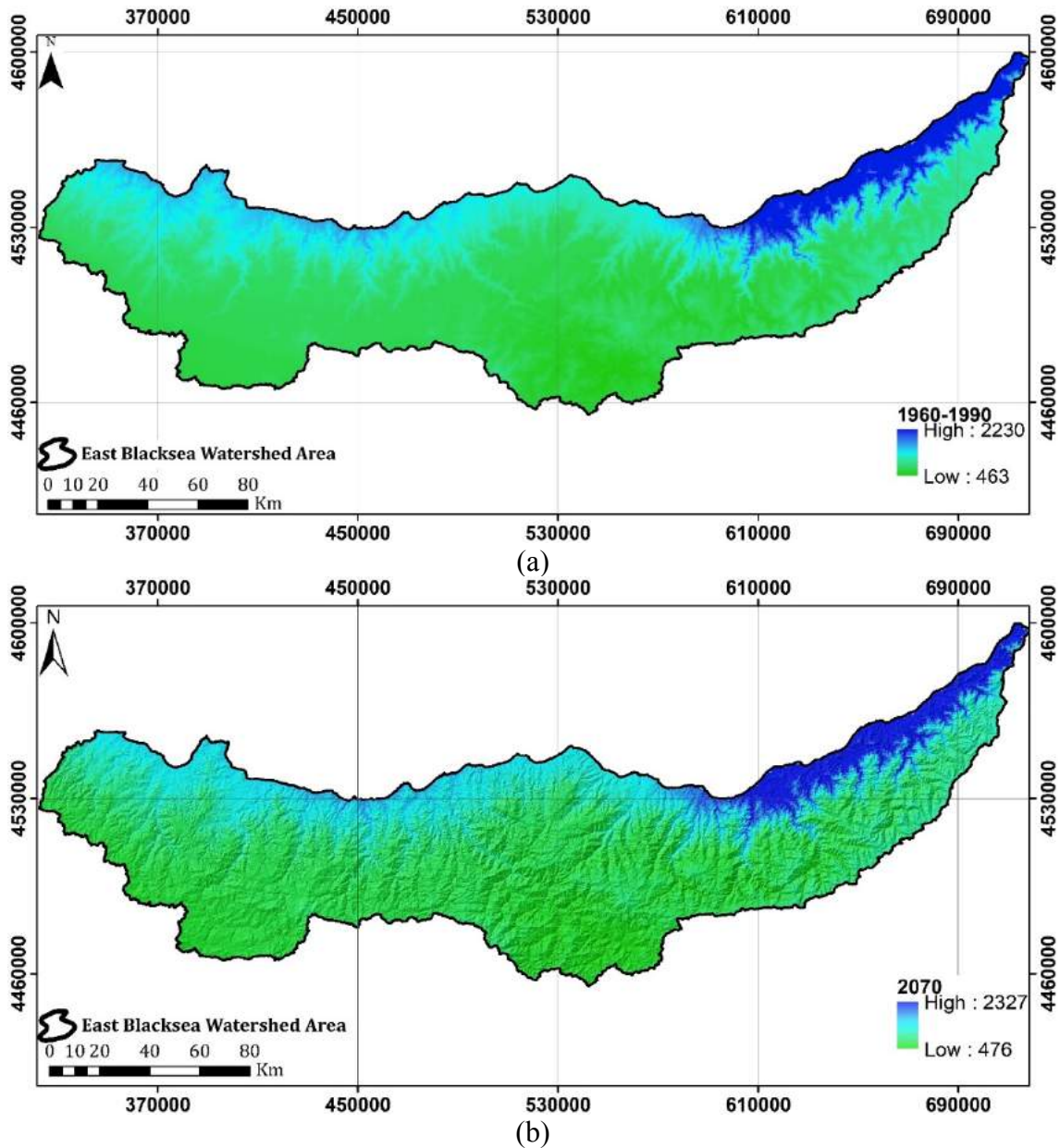
Figure 6. Annual precipitation values (a) for the years 1960-1990, annual precipitation data for the year 2070 (b) using current data (http://www.worldclim.org/version1).

3. Methodology

Depending on the formal features and numerical values of the rivers in the basins, the morphometric features of the river networks are evaluated numerically and the relationship between streams of different sizes, called the "drainage composition", can be expressed mathematically (Horton, 1945, Strahler, 1952). Geomorphometry is defined by Pike (2002), as "the science of digital land surface analysis". With geomorphometry, the characteristic features and morphological processes of water catchments are examined (Horton, 1932; Strahler, 1952; Chorley, 1957; Patton, 1976; Keller and Pinter, 1996; Pike, 2009).

When examined in general, geomorphometric analyzes are the whole of evaluations about the stage of erosion activities of streams. It is evaluated under three main headings as linear, areal and surfacial (Table 1). Linear morphometric analyzes include detailed examination of rivers in stream catchments. These analyzes mainly include the Bifurcation Ratio (Rb) (Schumm,

1956), Length Ratio (RL) (Schumm, 1956), and Texture Ratio (T) (Horton, 1945) parameters. While linear morphometric analyzes are evaluated only on the drainage network of the basin, areal morphometric properties are obtained with the values of both the drainage network and the entire basin surface (Ritter et al., 1995). They are important parameters in terms of collection of precipitation falling into the basin and accumulation of surface runoff. Surface morphometric evaluations consist of Drainage Density (Dd), Stream Frequency (Fs) (Horton, 1945), Basin Shape (RF) (Horton, 1945), parameters. Linear and areal morphometric features, total number of tributaries (Nu), total number of tributaries of the upper sequence (N(u+1)), basin diameter (P), basin area (A), total length (Lu) of the number of rivers, The next index number is calculated by calculating in-basin values such as length (Lu+1), Total number of indexes (N) (Table 1). The evaluations of the surface morphometry were determined by the hypsometric curve and hypsometric integral parameters. The hypsometric curve is obtained by comparing the ratio of the area above a contour line of height h passing through a basin to the area of the entire drainage basin (a/A, x) and the value of the contour line with the ratio of the highest elevation of the basin (h/H, y). The hypsometric integral (HI) is an important parameter in determining the watershed characteristics (Ritter et al., 2002). Basins are defined as old (monadnock: basin where erosional processes are balanced; $HI \leq 0.3$) according to Hı values, indicating that the catchment basin is completely balanced. Situations where HI value is between $0.3 \leq HI \leq 0.6$ defines mature stage, and $HI \geq 0.6$ defines basins as young or unequilibrium, that is, highly susceptible to erosion (Strahler 1952; Sarangi et al., 2001). The hypsometric analyzes were performed using the hypsometry extension in the ArcGIS environment.

Table 1. Lineer, areal and relief aspects calculated for morphometric analysis

İndisler	Eşitlik	Kaynak
Bifurcation Rate	Rb=Nu/N(u+1)	Schumm (1956)
Length Ratio	Rl=Lu/Lu+1	Horton (1945)
Texture Ratio	T = Nu1*(1/P)	Horton (1932)
Drainage Density	Dd = Lu/A	Horton (1932)
Stream frequency	Fs = Nu/A	Horton (1932)
Basin shape	Ff = A/Lb²	Horton (1932)

4. Eastern Black Sea Basin Geomorphometry

All basin classes, including stream drainage branches and micro dimensions of the Eastern Black Sea basin, were performed using DEM using the Hydrology extension in ArcGIS environment. Flow direction and cumulative flow values were prepared in raster format, drainage networks and basin boundaries were prepared in vector formats. By determining the starting points of the basin, the rivers in the Eastern Black Sea basin and all the basin boundaries formed by these rivers were created using the ArcGIS model configuration technique. For the calculation of geomorphometric analysis, the branches in the drainage network were ranked hierarchically according to their positions using the Strahler method. A drainage network model up to the 5th degree was obtained with the Strahler method in the 22,867.06 km² basin with a total of 1682 river segments. The Eastern Black Sea basin has 83 sub-basins. The areal size of these basins varies between 30.45 - 1241.04 km². In this study, linear, areal and surface geomorphometric evaluations were made in 38 basins (Figure 7) with an area of more than 100 km² in the Eastern Black Sea basin.
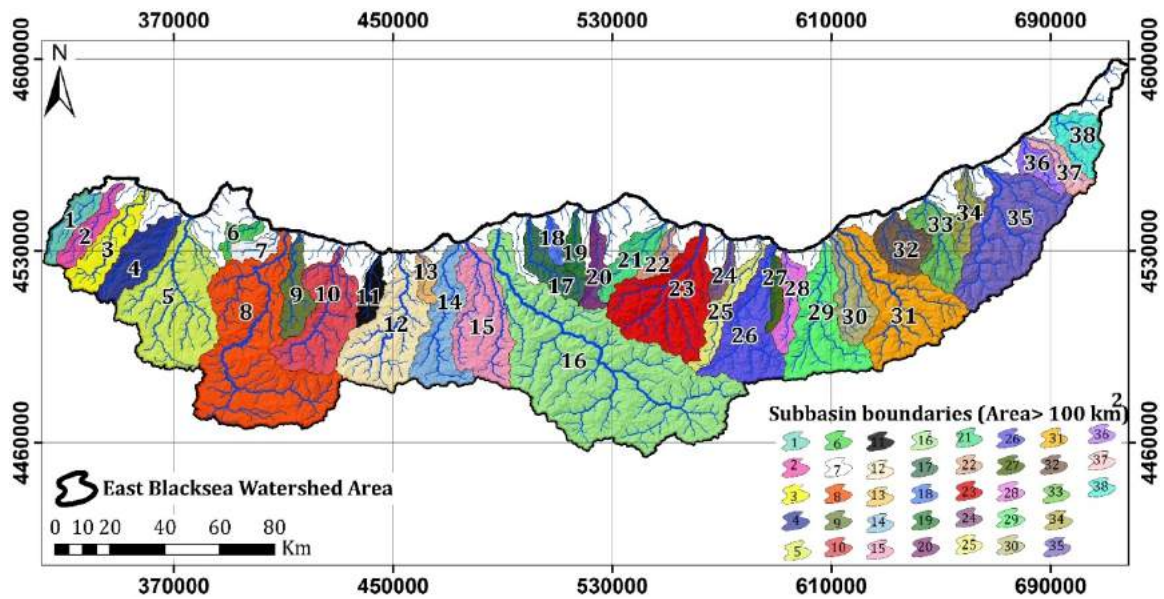
Figure 7. Rivers and sub-basin boundaries of the Eastern Black Sea basin.

4.1. Linear Morphometric Evaluations of the Eastern Black Sea Sub-Basins

Linear morphometric parameters consist of numerical examination of the river systems forming the basins (Ritter et al., 1995; Özdemir, 2011; Hajam et al., 2013). The basis of linear parameters is based on the number of river tributaries obtained by stream grading and their relations with each other. Linear morphometric evaluations of the Eastern Black Sea sub-basins were evaluated with bifurcation ratio (Rb), Average river length (Lum) and river length ratio (Rl) and Texture ratio parameters. Inbetween the 38 sub-basins of the Eastern Black Sea basin, 15 are composed of 2-grade river systems (Table 2). Among these basins, it is seen that the 1st index of the 6th basin has the lowest average river length, and the 2nd series of the 20th basin has the highest. The forking ratio (Rb) values range from 1.13 to 2.00 and present relatively low values. It can be interpreted as having a high drainage density. The basin with the highest average river length is basin 18. The number of basins formed by the 3-grade river system is 15, and the average river length of these basins has been calculated as 4.44. The lowest average river length was calculated as 2.37 in the basin numbered 26, while the second index of the basin no. 30 was calculated as 19.24. According to the average bifurcation rate parameter of the basins; It is seen that it varies between 1.53-7.08 (Table 3). Among the sub-basins of the Eastern Black Sea basin, the basins 8, 12, 15, 23, 31 and 35 consist of 4 series. The average river length varies between 3.51-5.87 (Table 4), the 1st Series of the 8th basin of these basins has a total length of 621.96 km. The bifurcation rate parameter varies between 1.64 and 2.64, and the basin no. 31 has the highest bifurcation rate. Inbetween the sub-basins in the Eastern Black Sea basin, only the basin no. 16 consists of 5 series. Each index has 136, 66, 22, 14 and 32, respectively. Looking at the lengths of the indexes, it is seen that the lowest 4th Index is (47.83 km) and the highest 1st Index is 441.62 km in length. The average bifurcation ratio of the basin no. 16 was calculated as 1.77. The texture ratio (T) is calculated as the ratio between the total number of indexes belonging to the 1st index and the perimeter of the basin from the indexes created according to the Strahler method. Accordingly, it varies between 0.03-0.37 for the Eastern Black Sea basin.

Table 2. Bifurcation ratio (Rb), Average river length (Lum) and river length ratio (Rl) parameter values of basins with 2 indexes.

Havza Number	index	L	L_u (km)	L_{um} (km)	R_b	R_l
1	1	6	60.86	10.14	-	-
	2	5	18.30	3.66	1.20	3.33
2	1	8	34.32	4.29	-	-
	2	7	36.60	5.23	1.14	0.94
6	1	5	8.45	1.69	-	-
	2	3	26.10	8.70	1.67	0.32
7	1	5	20.38	4.08	-	-
	2	4	20.94	5.23	1.25	0.97
11	1	4	21.91	5.48	-	-
	2	3	23.92	7.97	1.33	0.92
13	1	4	14.53	3.63	-	-
	2	3	15.21	5.07	1.33	0.96
18	1	3	34.09	11.36	-	-
	2	2	5.68	2.84	1.50	6.00
19	1	5	15.21	3.04	-	-
	2	4	21.74	5.44	1.25	0.70
20	1	3	12.94	4.31	-	-
	2	2	35.31	17.66	1.50	0.37
24	1	4	8.11	2.03	-	-
	2	2	17.87	8.93	2.00	0.45
25	1	7	25.53	3.65	-	-
	2	6	53.02	8.84	1.17	0.48
27	1	2	18.22	9.11	-	-
	2	1	14.10	14.10	2.00	1.29
28	1	8	24.16	3.02	-	-
	2	7	36.82	5.26	1.14	0.66
34	1	9	34.43	3.83	-	-
	2	8	33.75	4.22	1.13	1.02
37	1	7	15.81	2.26	-	-
	2	6	31.27	5.21	1.17	0.51

Tablo 3. 3 dizine sahip havzaların çatallanma oranı (Rb), Ortalama akarsu uzunluğu (L_{um}) ve akarsu uzunluk oranı (R_l) parametre değerleri.

Havza Number	index	L	Lu (km)	Lum (km)	Rb	Rl
3	1	16	55.30	3.46	-	-
	2	5	16.09	3.22	3.20	3.44
	3	9	52.15	5.79	0.56	0.31
4	1	11	66.33	6.03	-	-
	2	5	54.36	10.87	2.20	1.22
	3	4	16.72	4.18	1.25	3.25
9	1	12	32.23	2.69	-	-
	2	6	22.47	3.75	2.00	1.43
	3	5	37.86	7.57	1.20	0.59
10	1	31	96.74	3.12	-	-
	2	15	64.74	4.32	2.07	1.49
	3	15	65.80	4.39	1.00	0.98
14	1	26	63.66	2.45	-	-
	2	7	36.06	5.15	3.71	1.77
	3	18	62.08	3.45	0.39	0.58
17	1	12	38.25	3.19	-	-
	2	5	18.16	3.63	2.40	2.11
	3	6	30.46	5.08	0.83	0.60
21	1	12	31.13	2.59	-	-
	2	9	29.79	3.31	1.33	1.05
	3	2	10.88	5.44	4.50	2.74
22	1	12	31.13	2.59	-	-
	2	9	29.79	3.31	1.33	1.05

[1] Adiyaman University, Mining and Mineral Extraction Department, School of Technical Sciences, Adıyaman, Turkey.
[2] Çukurova University, Department of Geology Engineering, Adana, Turkey
* Corresponding author: senemtekin@adiyaman.edu.tr

Havza No	Dizin	L	Lu (km)	Lum (km)	Rb	Rl
	3	2	10.88	5.44	4.50	2.74
26	1	34	80.73	2.37	-	-
	2	18	69.43	3.86	1.89	1.16
	3	15	53.52	3.57	1.20	1.30
29	1	37	104.58	2.83	-	-
	2	22	62.51	2.84	1.68	1.67
	3	14	42.99	3.07	1.57	1.45
30	1	11	31.67	2.88	-	-
	2	2	38.48	19.24	5.50	0.82
	3	5	42.33	8.47	0.40	0.91
32	1	15	70.74	4.72	-	-
	2	13	38.52	2.96	1.15	1.84
	3	1	2.84	2.84	13.00	13.57
33	1	16	48.09	3.01	-	-
	2	11	36.73	3.34	1.45	1.31
	3	4	22.39	5.60	2.75	1.64
36	1	8	23.89	2.99	-	-
	2	5	21.60	4.32	1.60	1.11
	3	2	7.25	3.62	2.50	2.98
38	1	11	42.72	3.88	-	-
	2	7	28.81	4.12	1.5´	1.48
	3	3	12.39	4.13	2.33	2.32

Table 4. Bifurcation ratio (Rb), Average river length (Lum) and river length ratio (Rl) parameter values of basins with 4 indexes.

Havza No	Dizin	L	Lu (km)	Lum (km)	Rb	Rl
8	1	90	326.07	3.62	-	-
	2	37	123.96	3.35	2.43	2.63
	3	20	64.63	3.23	1.85	1.92

	4	32	107.30	3.35	0.63	0.60
12	1	36	129.41	3.59	-	-
	2	17	62.87	3.70	2.12	2.06
	3	5	16.95	3.39	3.40	3.71
	4	13	55.42	4.26	0.38	0.31
15	1	25	78.71	3.15	-	-
	2	15	92.01	6.13	1.67	0.86
	3	7	57.30	8.19	2.14	1.61
	4	2	12.00	6.00	3.50	4.78
23	1	39	124.32	3.19	-	-
	2	19	97.00	5.11	2.05	1.28
	3	10	29.41	2.94	1.90	3.30
	4	9	30.29	3.37	1.11	0.97
31	1	44	139.05	3.16	-	-
	2	23	83.59	3.63	1.91	1.66
	3	4	15.20	3.80	5.75	5.50
	4	16	55.09	3.44	0.25	0.28
35	1	43	144.49	3.36	-	-
	2	21	82.71	3.94	2.05	1.75
	3	17	63.13	3.71	1.24	1.31
	4	4	21.47	5.37	4.25	2.94

Table 5. Bifurcation ratio (Rb), Average river length (Lum) and river length ratio (Rl) parameter values of basins with 5 indexes.

Havza Number	index	L	Lu (km)	Lum (km)	Rb	Rl
16	1	136	441.62	3.25	-	-
	2	66	235.24	3.56	2.06	1.88
	3	22	67.48	3.07	3.00	3.49
	4	14	47.83	3.42	1.57	1.41
	5	32	92.43	2.89	0.44	0.52

4.2. Areal Morphometric Evaluations of the Eastern Black Sea Sub-Basins

The morphometric parameters formed by the spatial characteristics of the basins have a very important feature in terms of the collection of precipitation falling into the basin and the accumulation of surface runoff. In the Eastern Black Sea basin, the circumferential lengths of 38 sub-basins, which are larger than 100 km^2 in area, vary between 50-370. The basin numbered 16, which has the largest areal size, is 3306.46 km^2. Drainage density (Dd), which expresses the degree of fragmentation of the basins by the rivers, varies between 0.2-0.6 according to the parameter calculations. It may vary with the relations of more than one factor with each other, and it itself gives clues about the water and sediment transport of the streams. Among the factors that determine the drainage density are climate, vegetation, soil and rock structure, surface features, erosion and deposition processes (Malik et al., 2011, Elbaşı and Özdemir, 2018). The drainage density values of the sub-basins of the Eastern Black Sea basin are in the class range that is considered to be low. It shows that the basin has a high infiltration capacity with its vegetation and soil structure. According to the river frequency analysis, the frequency of the rivers varying between 0 and 0.3 in 38 basins was calculated. It is seen that the sub-basins of the Eastern Black Sea basin have low river frequency according to the river frequency values that present similar characteristics with the drainage density parameter. It is known that as the value in the circularity ratio parameter calculations approaches 1, the basin displays a longitudinal basin shape.

4.3. Surface Morphometric Evaluations of the Eastern Black Sea Sub-Basins

The hypsometric curve and the hypsometric integral indicate the erosional state of the basin and the stage of youth, maturity and old age (Strahler, 1952, Ritter et al., 2002). According to the hypsometric curve and integral results, it is seen that 13 basins are in the maturity stage and have completed their erosion processes (Figure 9a). On the other hand, it is seen that 18 basins approach the maturity stage and in general, more than 60% of these basins are eroded by erosional processes, and erosion continues in the regions towards the bottom of the basins (Figure 9b). It is observed that erosion continues in the remaining basins 9, 16, 22, 23, 26, 30 and 31 (Figure 9c). It was determined according to the hypsometric curve and integral values that the youngest basin among the sub-basins of the Eastern Black Sea basin was the 26th basin.

5. Results

In this study, geomorphometric evaluations were carried out as linear, areal and surface morphometric features for the basins located in the Eastern Black Sea basin and larger than 100 km^2 in area. According to the linear morphometric parameter results, similar results were obtained in 38 basins and it was calculated that they generally have low bifurcation degrees. Bifurcation ratio values lower than 3 show us that almost all of the basins have high drainage density and that they have no effect of any tectonic activity in the basins, and they also have geologically heterogeneous features. According to the areal morphometric properties; low stream frequency and similar low drainage density values were calculated. These results show that units in lithology with high infiltration capacity outcrop throughout the basin. According to the results of superficial morphometric analysis; Among these basins, where erosion still continues in 7 of 38 sub-basins, it is seen that the youngest one is basin 26.

[1] Maltepe University, Faculty of Engineering and Natural Science, Department of Electrical and Electronics Engineering, Istanbul, Turkey
[2] Fatih Sultan Mehmet Vakıf University, Faculty of Engineering, Department of Electrical and Electronics Engineering, Istanbul, Turkey
* Corresponding author: cihatmumcu@maltepe.edu.tr
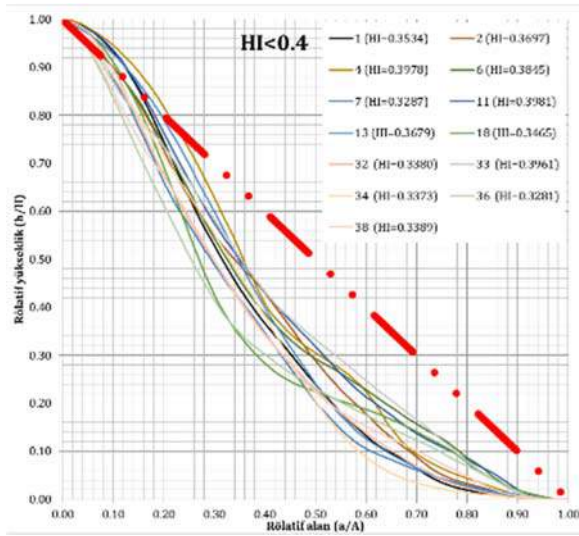
(a)
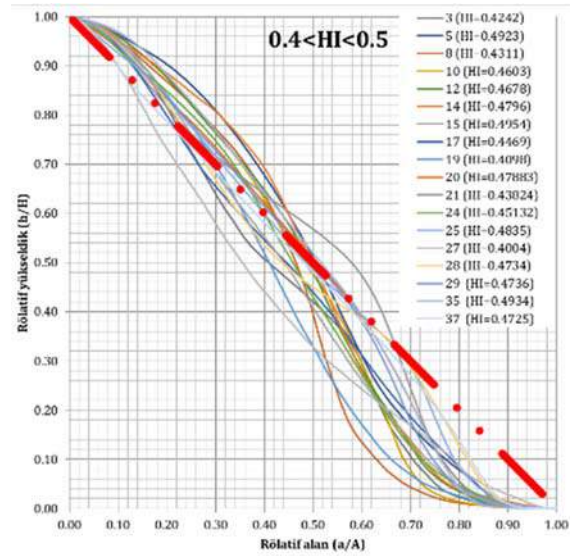
(b)
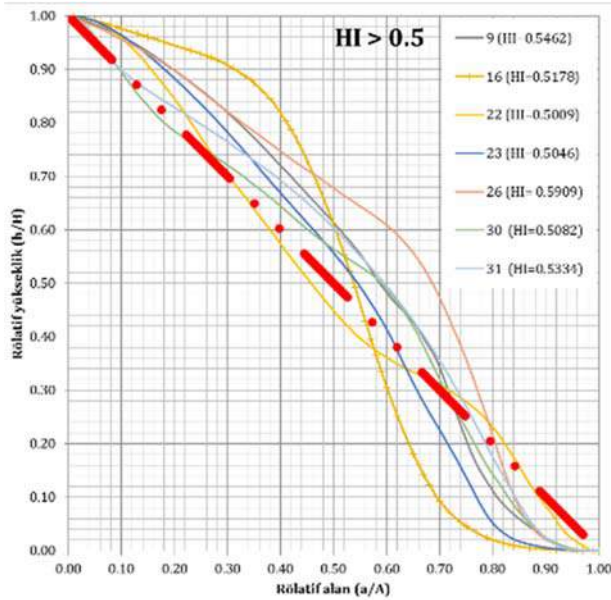
(c)

Figure 10. Distribution of sub-basins in the Eastern Black Sea basin according to mature (a), old (b) and young (c) stages.

References

Chorley, R. J. (1957)., Climate And Morphometry. The Journal Of Geology, 65(6), 627–638.

CORINE, (2006). (Coordination of Information on the Environment), http://www.corine.itu.edu.tr/typography.html.

Elbaşı, E., Ozdemir, H., (2018). Morphometric Analysis of the Marmara Sea River Basins. Journal of Geography. 63-84. 10.26650/JGEOG418790.

Fryirs, K.A. and Brierley, G.J., (2013). Geomorphic Analysis of River Systems: An Approach to Reading the Landscape, Blackwell Publishing Ltd. 360p.

Hajam, R.A. Hamid, A., Bhat, S., (2013). Application of morphometric analysis for geo-hydrological studies using geo-spatial technology-A case study of Vishav Drainage Basin. Hydrol Current Res. 4. 1-12.

Horton, R. E., (1932). Drainage basin characteristics. American Geophysics Union, 13(1), 350–361.

Horton, R. E., (1945). Erosional development of streams and their drainage basins; Hydrophysical approach to quantitative morphology. Bulletin of The Geological Society of America, 56, 275–330.

Keller, E. A., and Pinter, N., (1996). Active tectonics: Earthquakes, uplift and landscape. London, UK: Pearson.

Özdemir, H., (2011). Havza morfometrisi ve taşkınlar. D. Ekinci (Ed.), Fiziki coğrafya araştırmaları: Sistematik ve bölgesel içinde (s. 507–526). İstanbul: Babil.

Patton, P. C., and Baker, V.R., (1976). Morphometry and floods in small drainage basins subject to diverse hydrogeomorphic controls. Water Resources Research, 12(5), 941–952.

Pike, R., Evans, I., and Hengl, T. (2009). Geomorphometry: A brief guide. In T. Hengl and H. I. Reuter (Eds.), Geomorphometry: Concepts, software, applications (pp. 3–30). New York, NY: Elsevier.

Pike, S., (2002). Destination image analysis: A review of 142 papers from 1973-2000. Tourism Management. 23(5): 541-549.

Ritter, D.F., Kochel, R.C., and Miller, J.R., (1995). Process geomorphology. Dubuque, IA: William C. Brown.

Malik, M.I., Bhat, M.S., Kuchay, N.A. (2011). Watershed based drianage morphometric analysis of Lidder Catchment in Kashmir Valley Usin Geographical İnformation System. Recent Research in Science And Technology, 3(4), 118–126.

Schumm, S. A., (1956). Evolution of drainage systems and slopes in badlands at Perth Amboy, New Jersey. GSA Bulletin, 67, 597–646. https://doi.org/10.1130/0016-7606(1956)67[597:EODSAS]2.0. CO;2.

Strahler, A. N., (1952). Quantitative analysis of watershed geomorphology. Transamer Geophys Union, 38, 913–920.

Worldclim (http://www.worldclim.org/version1).

Influence of Cell Transportation Microchannel Wall Quality on Cell Deposition Risk: a DPM Analysis

Daver ALİ[1*]

Abstract: The dynamic cell culture process has been used in tissue engineering. Like other microfluidics systems, these devices always run the risk of particles deposition and eventually clogging up. Since the use of microchannels, one of the difficulties has been producing microchannels with ideal surface smoothness. In this study, the movement of stem cells through a microchannel with roughness was investigated theoretically using discrete phase computational fluid dynamics. The surface waviness was modeled using sinusoidal equations in different severity. Also, four sizes of 10, 15, 20, and 30 μm were selected for cell discreet phase modeling. The analysis results showed that surface roughness of 5 μm in the microchannel could increase the risk of its obstruction with more cell sedimentation. This phenomenon was more severe in models with more large cells or a lower fluid flow rate. This study further elucidates the effect of a microchannel surface quality on dynamic cell culture success.

Keywords: Microchannel, Surface Roughness, Cell Culture, Stem-cells, DPM Analysis,

1. Introduction

Microfluidic devices are highly integrated, multidisciplinary applied science that has been in development for over 30 years (Whitesides, 2006). One of the areas where micro-devices are widely used in biology and cellular studies. Dynamic cell culture is a modern method of obtaining tissue containing living cells and is widely used by tissue engineers (Kato et al., 2018). Many parameters, including the transfer rate and the number of healthy cells delivered to the destination from the bioreactor (Lee et al., 2021). Dynamic cell culture is performed on a small scale, and therefore the equipment used in such a process is minimal. For example, cells are transported by tiny connection pipes to scaffolds at very low speeds. Immediate success in cells' migration to their destination (usually a three-dimensional scaffold) is the key to success in the later stages of such a process (Campos Marin et al., 2017). An effective cell transfer will require a meticulous design of the microchannels and the inherent quality of its surface. Like other microchannels, one of the risks in cell transfer is the risk of cells settling on the microchannel wall, which potentially depends on medium flow boundary conditions. This problem can be caused by several factors (Zhou et al., 2021, Li et al., 2021). Microchannel studies have already shown the effect of the surface roughness o the modality of fluid flow within microchannels. For example, the relationship between phenomena such as pressure drop or heat transfer rate from a microchannel to its surface roughness has been shown. Therefore, it is conceivable that the surface roughness affects cell migration dynamics within them (Yuan et al., 2016). Because it is difficult and expensive to obtain microchannels with perfectly smooth surfaces, understanding microchannel surface quality on cell culture efficiency can be valuable in optimizing the time and cost in dynamic cell culture systems. In

[1] Karabuk University, Faculty of Engineering, Department of Medical Engineering, Karabuk, Turkey
* Corresponding author: daverali@karabuk.edu.tr

this study, the effect of surface roughness of one of the walls of a cell transfer microchannel (bottom wall) on cell deposition was theoretically investigated using discrete cell modeling.

2. Material and Method

The surface roughness of microchannels can vary between 1-10 μm depending on the production techniques (Weaver et al., 2011). There are different approaches to model surface roughness in microchannels. One of them is modeling surface irregularity with sinusoidal curves (Dharaiya and Kandlikar, 2013). In this work, a microchannel with a rectangular cross-sectional area of 3000×1000 μm and a length of 40 mm (Marin et al., 2017) and a roughness of and a roughness of 5 μm was created on the bottom surface using sinusoidal curves. Based on Torres et al study result (Cámara-Torres et al., 2020), the density and related viscosity were assigned to the culture media as 1024 (kg/m^3) and 0.025 Pa.s, respectively. Also, four different inlet flow rates of 20, 50, 90, and 180 μl/min were selected to investigate the effect of fluid velocity on the fate of cells within the microchannel. The governing equations for CFD and DPM analysis of models can be found elsewhere (Ali, 2019).
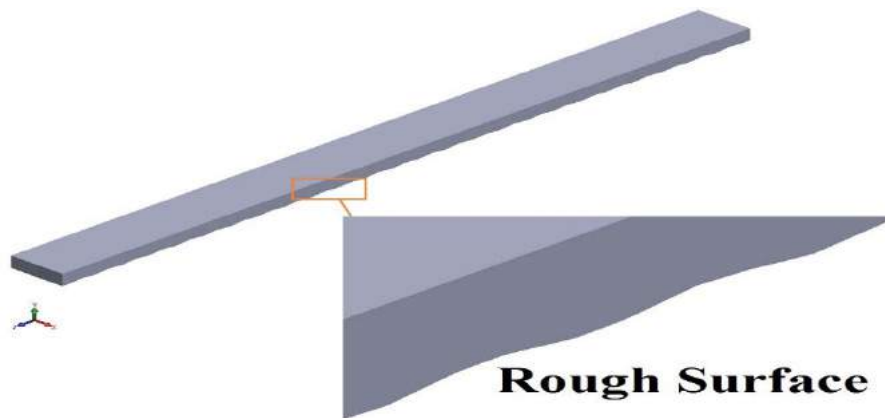
Figure 1. The microchannel model with a rough surface was used in this study.

3. Results

To understand the effect of surface roughness on the number of cells that failed to exit the microchannel, the percentage of cells trapped in a similar microchannel with a smooth surface was compared and shown in Figure 2.
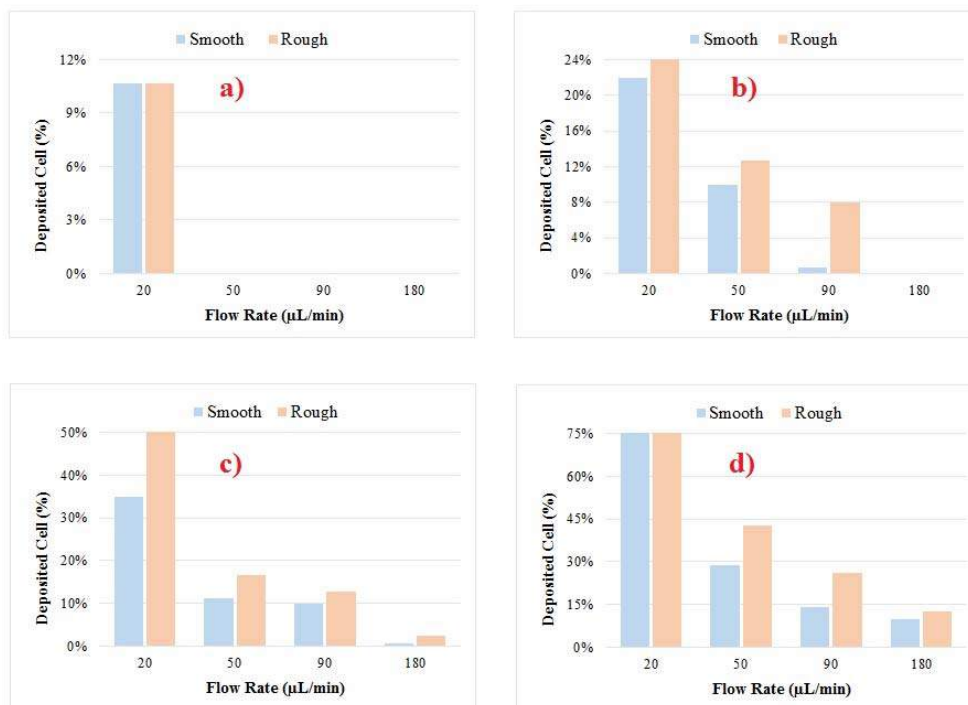
Figure 2. The number of sedimented cells was normalized with the total number of injected cells for a cell size of a) 10 µm, b) 15 µm, c) 20 µm, and d) 30 µm, respectively.

As can be seen, three factors of fluid flow rate, cell size, and surface roughness were effective in the number of sedimented cells. Fluid flow rate of 20 in all models, regardless of cell size or microchannel surface roughness, carries a high risk of sedimentation. Except for the first group with a cell size of 10 µm in all groups, surface roughness increased cell deposition.

4. Discussion and Conclusions

What can be deduced from the results of this theoretical work is that many parameters, including the fluid flow rate and the size of the cells themselves, are more involved in the design and regulation of a dynamic cell culture system. However, the quality of the microchannel, including its surface quality and the mentioned factors, can be the determining factor in the smooth and unobstructed transfer of cells to the destination.

References

ALI, D. 2019. Effect of scaffold architecture on cell seeding efficiency: A discrete phase model CFD analysis. *Computers in biology and medicine,* 109**,** 62-69.

CÁMARA-TORRES, M., SINHA, R., MOTA, C. & MORONI, L. 2020. Improving cell distribution on 3D additive manufactured scaffolds through engineered seeding media density and viscosity. *Acta Biomaterialia,* 101**,** 183-195.

CAMPOS MARIN, A., GROSSI, T., BIANCHI, E., DUBINI, G. & LACROIX, D. 2017. 2D µ-Particle Image Velocimetry and Computational Fluid Dynamics Study Within a 3D Porous Scaffold. *Annals of Biomedical Engineering,* 45**,** 1341-1351.

DHARAIYA, V. V. & KANDLIKAR, S. G. 2013. A numerical study on the effects of 2d structured sinusoidal elements on fluid flow and heat transfer at microscale. *International Journal of Heat and Mass Transfer,* 57**,** 190-201.

KATO, Y., KIM, M.-H. & KINO-OKA, M. 2018. Comparison of growth kinetics between static and dynamic cultures of human induced pluripotent stem cells. *Journal of Bioscience and Bioengineering,* 125**,** 736-740.

LEE, H., MARIN-ARAUJO, A. E., AOKI, F. G., HAYKAL, S., WADDELL, T. K., AMON, C. H., ROMERO, D. A. & KAROUBI, G. 2021. Computational fluid dynamics for enhanced tracheal bioreactor design and long-segment graft recellularization. *Scientific Reports,* 11**,** 1187.

LI, C., KUSS, M., KONG, Y., NIE, F., LIU, X., LIU, B., DUNAEVSKY, A., FAYAD, P., DUAN, B. & LI, X. 2021. 3D Printed Hydrogels with Aligned Microchannels to Guide Neural Stem Cell Migration. *ACS Biomaterials Science & Engineering,* 7**,** 690-700.

MARIN, A. C., GROSSI, T., BIANCHI, E., DUBINI, G. & LACROIX, D. 2017. μ-Particle tracking velocimetry and computational fluid dynamics study of cell seeding within a 3D porous scaffold. *Journal of the Mechanical Behavior of Biomedical Materials,* 75**,** 463-469.

WEAVER, S. A., BARRINGER, M. D. & THOLE, K. A. 2011. Microchannels With Manufacturing Roughness Levels. *Journal of Turbomachinery-Transactions of the Asme,* 133**,** 8.

WHITESIDES, G. M. 2006. The origins and the future of microfluidics. *Nature,* 442**,** 368-373.

YUAN, X., TAO, Z., LI, H. & TIAN, Y. 2016. Experimental investigation of surface roughness effects on flow behavior and heat transfer characteristics for circular microchannels. *Chinese Journal of Aeronautics,* 29**,** 1575-1581.

ZHOU, Z., CUI, F., WEN, Q. & ZHOU, H. S. 2021. Effect of vimentin on cell migration in collagen-coated microchannels: A mimetic physiological confined environment. *Biomicrofluidics,* 15**,** 034105.

Processing of Seismic Signals on base of AI during Oil Exploration

Ramziyya Garazade[1*], Naila Allahverdiyeva[2]

Abstract: Preprosessing of seismic data is one of the most widely used methods in oil and gas exploration which is providing comprehensive information about various layers and rock properties underneath the Earth without any expensive drilling operations. The accuracy and efficiency of the seismic data analysis mainly depend on the quality and the quantity the seismic receivers - geophones or hydrophones located on the Earth or marine surface. Furthermore, the choice of the seismic source energy is also important factor in the reliability of the acquired seismic data. Unfortunately, such seismic data analysis usually appears with an excessive amount of noise generated by various sources and erratically missing information due to inaccessible points in the field. The attenuation or suppression of random noise is of great importance for geologists to achieve high quality and precise seismic data in oil and gas exploration. According to this data, the potential oil or gas resources can be found out, even an approximate capacity of the reservoir can be estimated by expert geoscientists and engineers. Many methods have been investigated for random noise attenuation and each of them has certain advantages and disadvantages. The selection of the appropriate method depends upon the preferred criteria on the acquired results in the seismic data analysis. In this paper is considered the application of Artificial Neural Network (ANN) in seismic data analysis using MATLAB. As result ANN filter is designed. While comparing with other classical filters this method has showed his efficiency.

Keywords: Seismic data, preprocessing, Artificial Neural Network, root-mean-square error, seismic signals, filter, signal-to-noise ratio.

1. Introduction

In recent years, major improvements and innovations have been developed in energy exploration. Oil and gas exploration is one of the most expensive processes in fuel energy acquisition. Millions of dollars are being spent to find out if there is a potential petroleum reservoir to continue drilling and complete the well. Seismic surveys have become one of the most efficient methods applied in energy exploration providing huge return on investment. Seismic technique is a remarkable option to analyze the subsurface structure in advance of drilling and to determine the design of the well trajectories in order to achieve the reservoir in the safest and most effective way. Obtaining a detailed record of the geological formations, which is known as well logging, allows the geologists to gather comprehensive information about different layers of rock formations. This contributes greater certainty about whether or not the hydrocarbons exist beneath Earth's surface. If there is not any latent petroleum reservoir, the drilling process needs to be stopped and the well should be abandoned to prevent incurring

[1] Baku Higher Oil School, Informatics and Control in Technical Systems, Process Automation Engineering, Baku, Azerbaijan
[2] Baku Higher Oil School, Process Automation Engineering, Baku, Azerbaijan
* Corresponding author: ramziyya.garazade.std@@bhos.edu.az

higher costs of completing a well. In consequence, seismic data analysis leads to a more profitable hydrocarbon extraction with fewer wells drilling.

Seismic data with high quality is very crucial in seismic exploration to accurately analyze the subsurface structure. However, in real industrial experiments, the seismic signals are usually obtained with high frequency noise which could cause losing useful information about the rock formations underneath the Earth. So that, noise attenuation is one of the important stages in seismic signal analysis. Although a number of methods have been suggested to attenuate the seismic noise signal, the efficiency of these methods is evaluated with the preservation of the original signal amplitude. Traditional attenuation algorithms, such as transform domain algorithms (V. Oropeza and M. Sacchi, (2011), Y. Chen, H. Chen, K. Xiang, and X. Chen, (2017), W. Chen, M. Bai, and H. Song, (2019)), spatial domain algorithms (A. Stumpf, N. Lachiche, J.-P. Malet, N. Kerle, and A. Puissant, (2014)), curvelet transform (H. Zhang, S. Diao, H. Yang, G. Huang, X. Chen, and L. Li, (2018)), comprehensive types denoising algorithms (Y. Chen and S. Fomel, (2015), Q. Zhao, Q. Du, X. Gong, and Y. Chen, (2018), W. Liu, S. Cao, Z. Jin, Z. Wang, and Y. Chen, (2018), et.al) can manage to eliminate the noise to some extent, they usually appear with some drawbacks such as inaccurate design assumptions and problems in estimating parameter values (M. Bai, J. Wu, S. Zu, and W. Chen, (2018), R. Anvari, A. R. Kahoo, M. Mohammadi, N. A. Khan, and Y. Chen, (2019), D. Zhang, D. J. Verschuur, S. Qu, and Y. Chen, (2020)). Furthermore, a comprehensive experience and knowledge about the noise are required before the traditional methods applied in seismic noise attenuation. As the random noise is obscure in the real exploration process, it needs to be tested at different variances which contributes to time-consuming and inefficient process. Considering the drawbacks of the traditional methods. contemporary science and industry demand more effective and intelligent denoising methods. In recent years, deep learning or ANN has rapidly and extensively developed, consequently it has also applied in seismic exploration field.

2. Experimental Data Preparation and Artificial Neural Network Application

The suggested method for preprocessing of raw seismic signal learns the difference between noisy and clean data. The data representation and noise cancellation will be performed using MATLAB software. MATLAB has a range of features for filtering the noisy signal and its Neural Network Toolbox – "*nntool*" enables to design an Artificial Neural Network structure with desired number of layers and flexible parameters. There are mainly five steps in the method described in this paper:
1. Generate a clean - ideal output signal using traditional filtering methods.
2. Design a neural network framework.
3. Train the network and test the network performance.
4. Compare the denoising results of neural network and traditional methods.
5. Calculate the signal-to-noise ratio to check the efficiency of the result.

2.1. Experimental data representation

The input data is represented as a tabular data which shows the measurements of seismic sensors on 513 traces of the Earth. When the seismic sources – air guns are fired and send acoustic waves to the lower layers of the Earth surface, seismic receivers or hydrophones towed behind the seismic ship collect the depth values of the rocks according to the time duration between sent and received signals. As a result of multitude bombing actions from air guns, a table of data in the size of 886 x 513 is obtained. Each column in the table depicts one trace or layer in the Earth subsurface and each raw shows a time at which the sample is acquired from the

sensors. Considering the acoustic signal speed (v_s) in the water and two sequential depth samples (s_1, s_2) the data parameters are initialized in **Table 1** below:

Table 1. Acoustic signal parameters

v_s	$1500 \frac{m}{s}$
$s1$	$-2.385\ m$
$s2$	$-1.803\ m$

Using the known signal parameters represented above, the sampling time ($T_{samplig}$) and sampling frequency ($F_{sampling}$) parameters can also be easily calculated as shown below:

$$T_{sampling} = \frac{|s2 - s1|}{v_s} = 0.388\ ms$$

$$F_{sampling} = \frac{1}{T_{sampling}} = 2.577\ kHz$$

Each trace – column consists of error measurements due to sensor accuracy or environmental noises. Therefore, the experimental raw data obtained directly from hydrophones or geophones is not helpful for geologists and geoscientists to predict the potential of hydrocarbon resource. The noise interference on the pure signal is apparently observed in the 2D representation of the original experimental data in time and frequency domains (**Figure 1**):
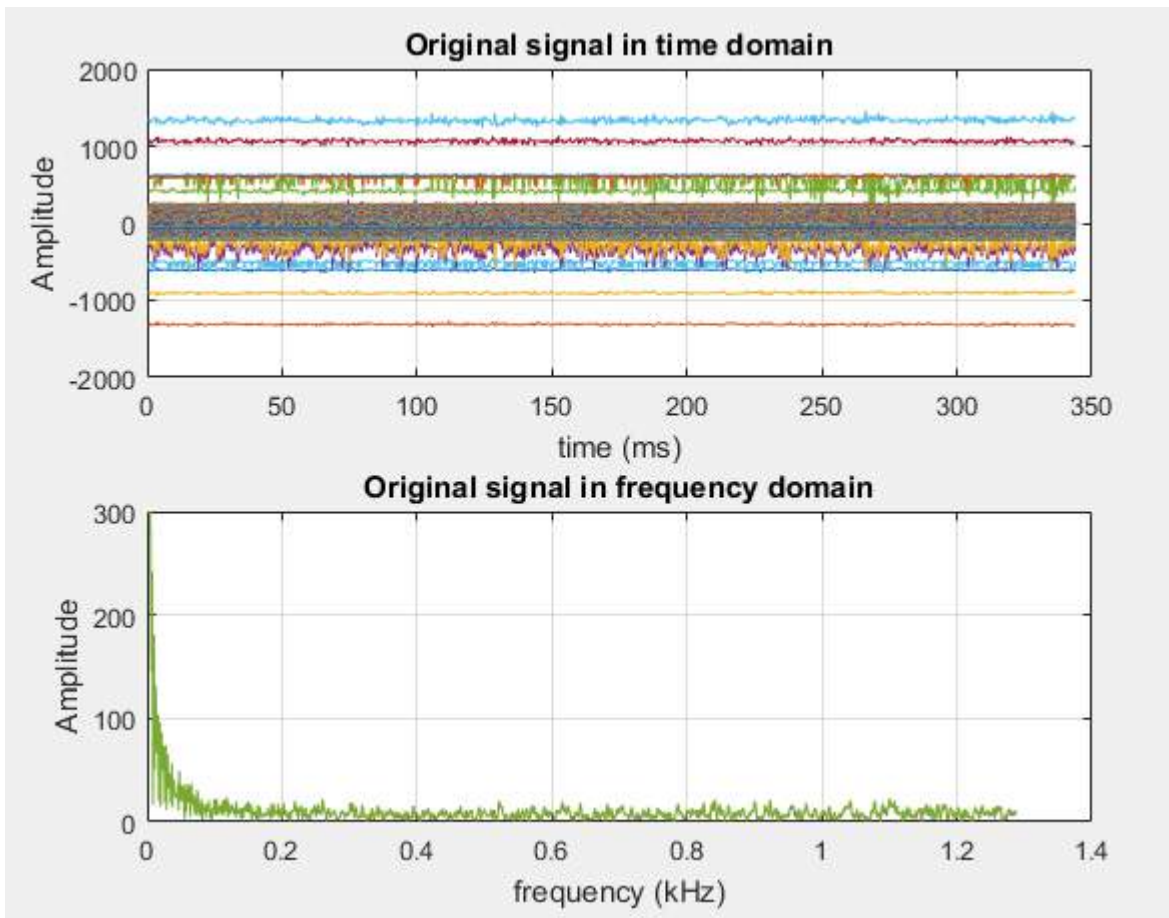
Figure 1. 2D representation of original seismic data

2.2 Noise attenuation using lowpass filter

Prior to neural network design, we need a target data to train the network. This target data can be obtained by applying traditional filters on the input data in MATLAB. As the random noise signals are generally high frequency signals, we need a lowpass filter to vanish the noise from the signal.

While designing the low-pass filter, the choice of cutoff frequency at which the signal is sufficiently cleaned is very important. Based on the noisy signal frequency response, the cutoff frequency has been chosen 0.02 kHz approximately in order to minimize the amplitude of the noise on the seismic signal. Furthermore, the passband and stopband frequencies should be less than Nyquist frequency, which is half of sampling frequency. The low-pass Butterworth filter with minimum order was designed using MATLAB $filterDesigner$ tool (**Figure 2**):
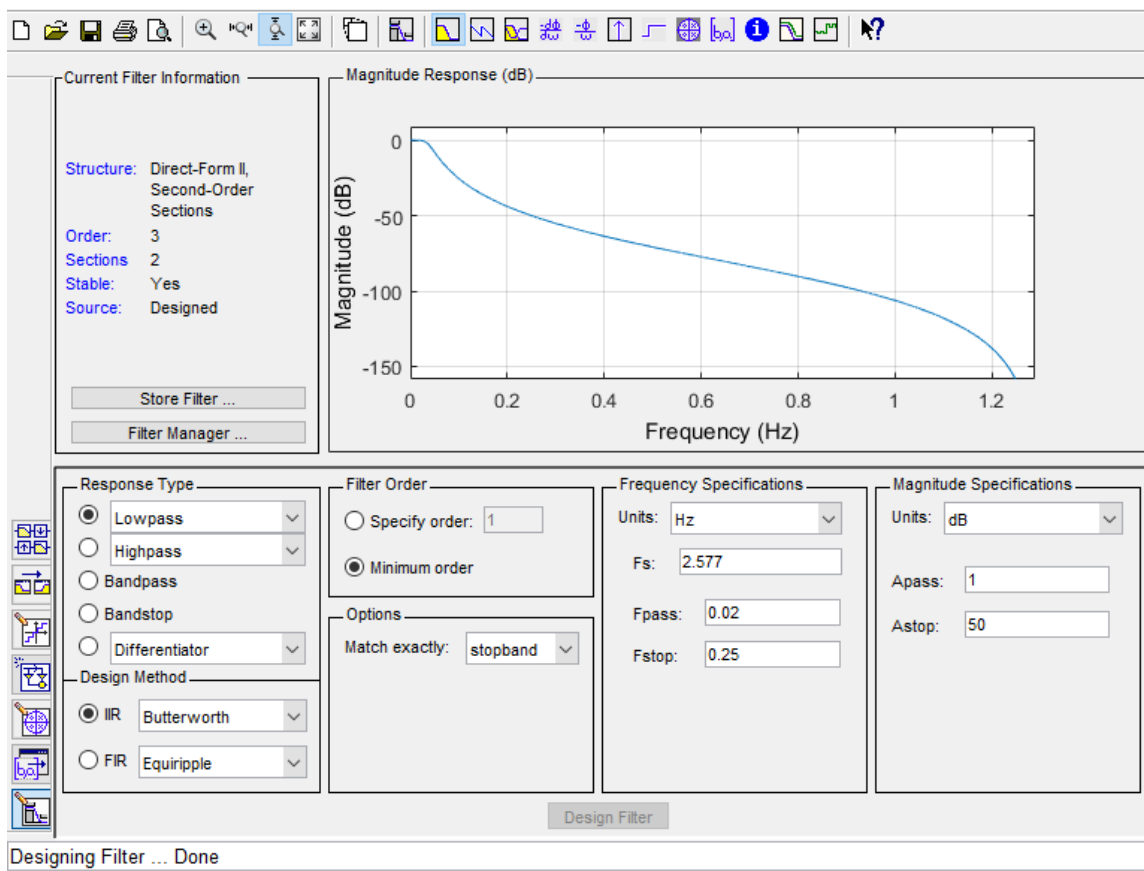
Figure 2. Low-pass filter design

After applying the designed low-pass Butterworth filter on the original noisy seismic signal, the noise was attenuated and an ideal – noise-free signal was obtained (**Figure 3** & **Figure 4**):
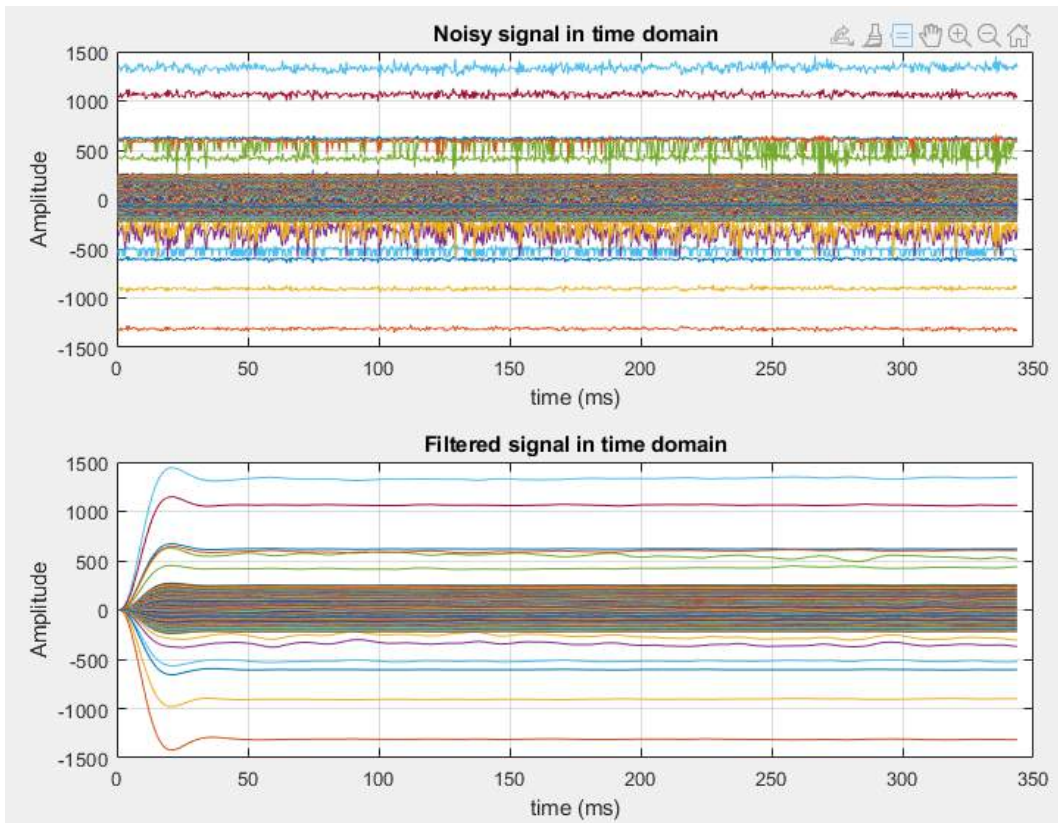
Figure 3. Noisy and Filtered signal in time domain
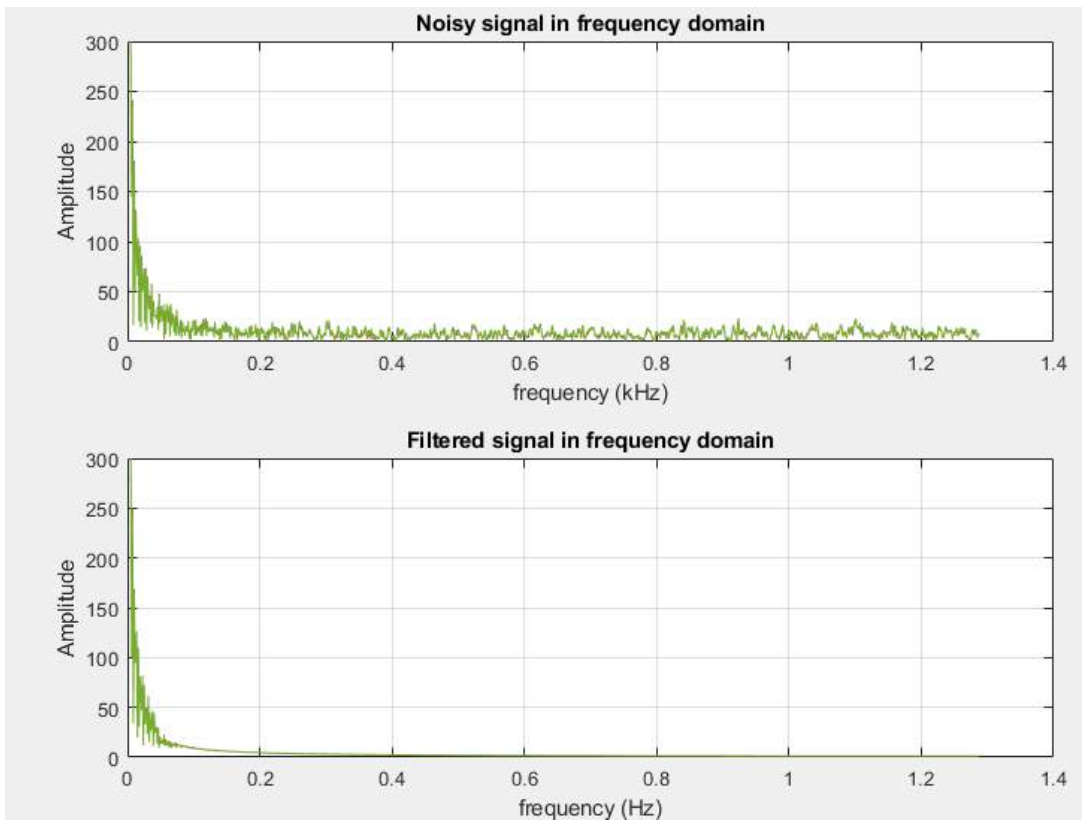
Figure 4. Noisy and Filtered signal in frequency domain

Comparing with original noisy signals, the acquired results are much smoother and ideal both in time and frequency domain representation. There are some ripples in time domain as demonstrated in **Figure 3**, this is because of the allowable passband attenuation indicated in magnitude specifications of the filter.

In summary, the obtained signal will be the target data for the neural network to learn the system and will be used to validate the acquired results.

2.3. Noise attenuation using Artificial Neural Network

ANN learns how ideally the system performs and implements it on the other samples in the same manner, afterwards. As discussed in the previous subsection, the input data was filtered using traditional low-pass filter firstly. The input signal together with the ideal filtered signal are two main inputs of the neural network to be able to calculate the respective weights of the hidden layers. Since the provided seismic signal data is quite big, only some portion of the data is used to train the system. In this instance, 200 samples of traces obtained in $100 \, ms$ time were used for learning purpose of the neural network and the next 200 samples were used to test and validate the results. MATLAB has *nntool* function which opens Neural Network/Data Manager window in order to import the input data, create a neural network with desired parameters and to export the neural network results.

After input and target data were imported, a neural network structure is designed. The neural network design used in this work is a 7 layers (6 hidden, 1 output) network with 10 neurons at each hidden layer. The hidden layers have a hyperbolic tangent activation function which is more successful than sigmoid function and is applied in many neural network problems. As it is regression type prediction problem, Linear activation function has been selected for the output layer. After creating the neural network, it needs to be trained with the imported input and target data. Training parameters are specified as represented in **Figure 5**:
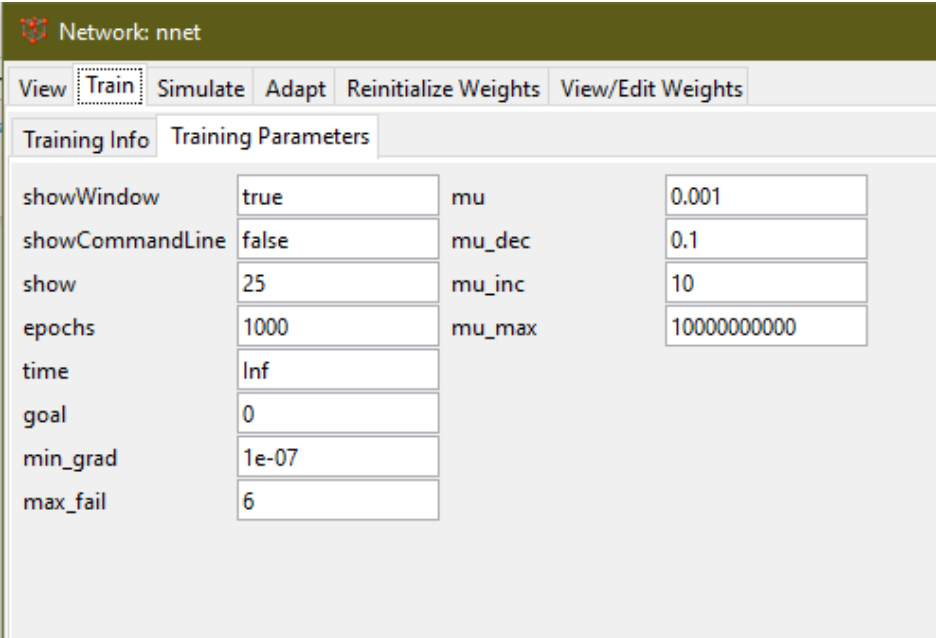
Figure 5. Training parameters of neural network

The training process lasted for 13 minutes approximately, and after 57 iterations the goal was achieved (**Figure 6**):

Figure 6. Neural network training GUI

The performance of the training and error histogram as represented in **Figure 7,** also validates the neural network successful results:
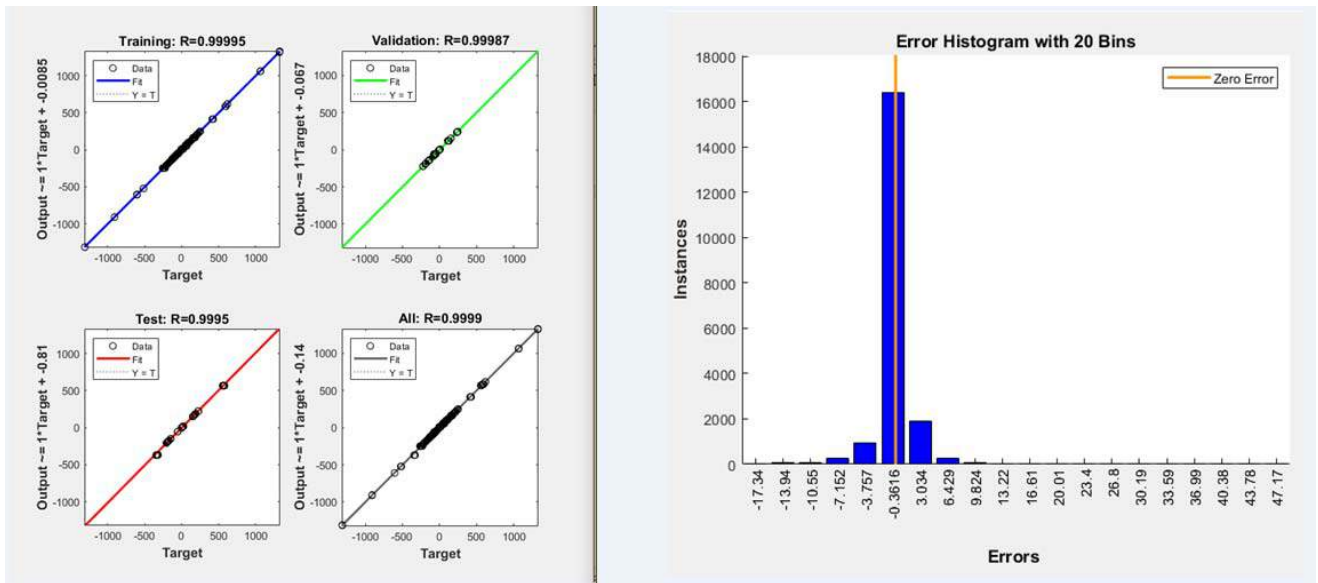
Figure 7. Regression performance and Error histogram of the neural network

3. Results

As mentioned above, 200 samples different from the trained data were used to check and validate the neural network performance. When the testing data was initiated as an input to the trained network model the obtained result was compared with the desired output in time (**Figure 8**) and frequency domain (**Figure 9**):
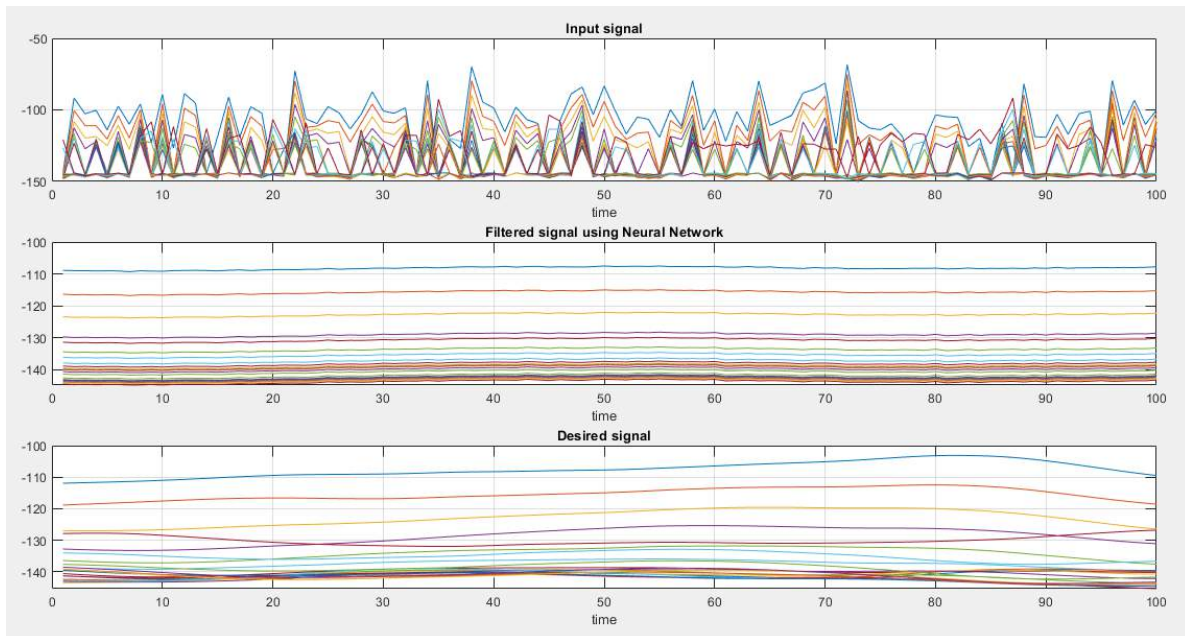
Figure 8. Signal comparison in time domain
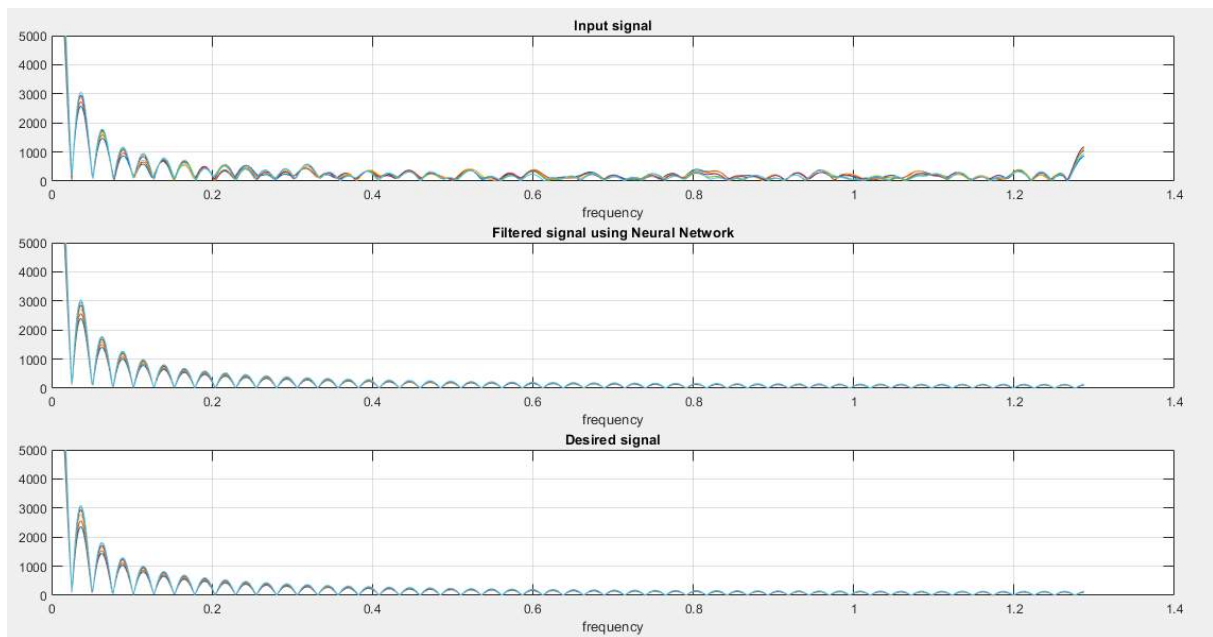
Figure 9. Signal comparison in frequency domain

As can be seen from the figures above, the results are very close to the desired ones and the noise on the signal has considerably been attenuated. Different sets of data were tested with the designed network and all results were the satisfying as represented in **Figure 8** and **Figure 9**.

Furthermore, the statistical properties of the input and output signals were also calculated to verify the model efficiency (**Table 2**):

$mean$ ($input$)	-81.1607
$mean$ ($output$)	-82.3470
$variance$ ($input$)	275.7967
$variance$ ($output$)	0.1800
$RMSE$ ($training$)	0.2050
$RMSE$ ($testing$)	0.4444
SNR ($input$)	0.9054
SNR ($output$)	8.8955

The derived values show that the signal has been cleaned from the noise successfully as its *mean* and *variance* have decreased as expected. Another important parameter, root-mean-square-error ($RMSE$) is almost the same for the training and testing data. Finally, the most essential parameter to confirm the noise attenuation in the signal is the Signal-to-noise ratio (SNR). A significant increase in the signal-to-noise ratio value also implies the noise reduction in the output signal.

4. Discussion and Conclusions

In conclusion, as implemented in many areas of industry, a neural network can successfully be applied in oil and gas exploration to achieve a desired result in a more efficient and eco-friendly way. A detailed and systematic analysis of seismic data can guide the geologists to decide the

potential capability of the reservoir and can save millions of dollars for oil and gas companies if the well does not worth to drill. Moreover, a careful preprocessing and interpretation of seismic signals can result in an accurate drilling direction and depth due to precise assumptions about rock formations. Although the preprocessing of seismic signals using ANN model is time consuming, it can deal with the seismic signal without requiring any prior knowledge or comprehensive analysis of the signal. Despite the fact that the traditional methods are more accurate and reliable, Artificial Intelligence (AI) or Machine Learning has become main focus of industry due to its convenience and flexibility.

This paper mainly discusses the AI application in noise cancellation in seismic signals which is known as preprocessing of seismic signals. A future work could be to apply a CNN in seismic signal processing and improve the processing of seismic signals in order to make a judgement about reservoir capability and to identify the rock properties. Certainly, it requires a deep knowledge about various rock formations and their characteristics, afterwards, a neural network can be trained to be implemented in seismic signal processing.

References

V. Oropeza and M. Sacchi, (2011). ''Simultaneous seismic de-noising and reconstruction via multichannel singular spectrum analysis (MSSA),'' Geophysics, vol. 76, no. 3, pp. V25–V32, 2011

W. Chen, M. Bai, and H. Song, (2019). ''Seismic noise attenuation based on waveform classification,'' J. Appl. Geophys., vol. 167, pp. 118–127, Aug. 2019.

Y. Chen, H. Chen, K. Xiang, and X. Chen, (2017). ''Preserving the discontinuities in least-squares reverse time migration of simultaneous-source data,'' Geophysics, vol. 82, no. 3, pp. S185–S196, May 2017.

A. Stumpf, N. Lachiche, J.-P. Malet, N. Kerle, and A. Puissant, (2014). ''Active learning in the spatial domain for remote sensing image classification,'' IEEE Trans. Geosci. Remote Sens., vol. 52, no. 5, pp. 2492–2507, May 2014

H. Zhang, S. Diao, H. Yang, G. Huang, X. Chen, and L. Li, (2018). ''Reconstruction of 3D non-uniformly sampled seismic data along two spatial coordinates using non-equispaced

curvelet transform,'' Explor. Geophys., vol. 49, no. 6, pp. 906–921, Nov. 2018.

Y. Chen and S. Fomel, (2015). ''Random noise attenuation using local signaland-noise orthogonalization,'' Geophysics, vol. 80, no. 6, pp. WD1–WD9, Nov. 2015.

Q. Zhao, Q. Du, X. Gong, and Y. Chen, (2018). ''Signal-preserving erratic noise attenuation via iterative robust sparsity-promoting filter,'' IEEE Trans. Geosci. Remote Sens., vol. 56, no. 6, pp. 3547–3560, Jun. 2018.

W. Liu, S. Cao, Z. Jin, Z. Wang, and Y. Chen, (2018). ''A novel hydrocarbon detection approach via high-resolution frequency-dependent AVO inversion based on variational mode decomposition,'' IEEE Trans. Geosci. Remote Sens., vol. 56, no. 4, pp. 2007–2024, Apr. 2018

W. Huang, D. Feng, and Y. Chen, (2018). ''De-aliased and de-noise Cadzow filtering for seismic data reconstruction,'' Geophys. Prospecting, vol. 68, pp. 553–571, 2018

D. Zhang, D. J. Verschuur, S. Qu, and Y. Chen, (2020). ''Surface-related multiple leakage extraction using local primary-and-multiple orthogonalization,'' Geophysics, vol. 85, no. 1, pp. V81–V97, Jan. 2020.

R. Anvari, A. R. Kahoo, M. Mohammadi, N. A. Khan, and Y. Chen, (2019). ''Seismic random noise attenuation using sparse low-rank estimation of the signal in the time–frequency domain,'' IEEE J. Sel. Topics Appl. Earth Observ. Remote Sens., vol. 12, no. 5, pp. 1612–1618, Apr. 2019.

The effect of holding time on the mechanical properties of TFP produced thermoplastic matrix composites under compression molding process

Hasan KARA[1*], Mustafa Özgür BORA[2*], Emine BAŞ[3*]

Abstract: The purpose of this study is to characterize, optimize and manufacture glass fiber reinforced thermoplastic composites using the compression molding process for the application of producing improved automotive parts. Composites offer many benefits; the key among them are corrosion, design flexibility, durability, light weight, and specific strength. Thermoplastic composites offer some interesting advantages over their thermoset counterparts like a higher toughness, faster manufacturing and their recyclable nature. In this study, the woven glass fiber/Nylon6 (PA6) was produced by using Tailored Fiber Placement (TFP). TFP is an embroidery-based technology that allows the fibre tows to be placed exactly where they are most needed for structural performance and stitched into position on a compatible textile or polymer substrate. After this production, compression molding process was applied for obtaining the final composite materials. During the compression molding process, various holding time values were selected for determining the mechanical properties (tensile strength, tensile modulus, flexural strength and flexural modulus) of the woven glass fiber reinforced PA6 composites. The aim of the study is to investigate the influence of holding time parameters on the mechanical properties of the woven glass fiber reinforced PA6 composites. Tensile and 3 point bending tests were applied the thermoplastic matrix composites which were produced and manufactured by TFP and compression molding process. Tensile strength, tensile modulus, flexural strength and flexural modulus values were determined. It was determined that holding time parameters were slightly affected the composite materials' mechanical properties.

Keywords: Tailored Fiber Placement (TFP), Thermoplastic Matrix Composites, Compression Molding, Mechanical Properties.

1. Introduction

Firstly, the material selection is the most important for the automotive sector once the product development process has been well recognized in recent years. There are two main reasons why materials selection is required: firstly, to design an existing product for better performance, lower cost, increasing reliability and reduced weight and secondly, to select a material for a new product [1]. The car manufacturing companies are competed an extremely strong among leading to larger model variety, and shorter model cycles. Application of lightweight design principles is one of the most important trends to meet above requirements.

[1] Plascam A.Ş, Maden Caddesi No:22 Pelitli Köyü, Gebze 41480, Kocaeli, Turkey
[2] Aviation Material Research and Development Laboratory, Faculty of Aeronautics and Astronautics, Kocaeli University, Kocaeli, Turkey
* Corresponding author: hasankaraial@hotmail.com

As such the new design concepts are needed new materials [2]. Government regulations in the world continue to demand for tighter restrictions on vehicle emissions. Among these are lightweight materials such as plastics and composites. Also, there are interesting to see that as fuel economy standards increase, total vehicle mass and steel content decreases and are replaced by composite materials. Actually, the transport sector notably accounts for about 25% of worldwide production of glass fiber and, cars produced in the United States can contain as much as 100 kilograms of composite samples, compared with slightly less than 30 kilograms for cars built in Europe [3].

The polymeric materials are selected because they are replacing traditional materials in many engineering applications due to their attractive properties such as excellent strength, stiffness to weight ratio, chemical resistance, corrosion resistance, impact resistance, fatigue resistance, thermal resistance, wear resistance and low processing cost [4]. The automotive composite samples, reinforced plastics and polymers are among widely preferred alternatives for light weighting of the automobile as they offer enhanced properties such as impact strength, easy mold-ability, improved aesthetics, and reduced weight as compared to conventional automotive components. The main advantages, which offer opportunities in the automotive industry, are their potential for maximum mass reduction of automobile and carbon emission reduction potential by light weighting of the vehicle. All material industries plastics and polymer composites, as well as steel, aluminum, and magnesium, are operating to respond to the automotive industry changing needs. Since start of the using, advanced plastics and polymer, composites have been helped the improvement of appearance, functionality, and safety of automobiles while reducing vehicle weight and delivering superior value to customers at the same time [5].

Polymer matrix composites divided into main group for matrix material; thermoset and thermoplastic. Although thermoset and thermoplastics sound similar, they have very different properties and applications. The thermoplastic materials are processed with heat. When enough heat is added to bring the temperature of the plastic above its melting point, the plastic melts, liquefies, or softens enough to be processed. Thermoplastics tend to be tougher or less brittle than thermoset. They can have better chemical resistance, do not need refrigeration as uncured thermosets (prepreg materials) frequently do, and can be more easily recycled and repaired. Table 1 presents a comparison between thermoset and thermoplastic materials [6].

The thermoplastic composites (TPCs) are the most advantages than thermosets in terms of reduced cycle times, improved toughness and potential for re-cycling. Finally, TPCs is used to product within the automotive industry, including battery trays, seat structures, front end modules and load floors. Most current applications utilize glass mat thermoplastic (GMT), based usually on random fibres within a polypropylene matrix. If it is requested to achieve higher mechanical properties, materials will be based on aligned fibres, usually in the form of woven fabrics, have been developed. Actually, the problem of main here is to reduce the required consolidation pressure to achieve a high fibre volume fraction. The problem can be solved to achieve by minimising the required flow distanced for the matrix. A number of approaches have been developed, usually involving the development and matrix at the tow level. As with GMTs, this is undertaken in a separate oven, as the mold temperature is below the melt temperature of the matrix [7].

Table 1: Presents a comparison between thermoset and thermoplastic materials [6]

	Thermoset	Thermoplastic
Processing	The product remelting when heat is applied, making thermosets ideal for high-heat applications such as electronics and appliances	This characteristic allows thermoplastics to be remolded and recycled without negatively affecting the material's physical properties
Features and benefits	Thermoset are often used for sealed products due to their resistance to deformation	Commonly offer high strength, shrink resistance, and easy bendability.
	Cannot be recycled	Highly recyclable
	Cannot be remolded or reshaped (not melt if heat)	Can melt if heated, remolding / reshaping capabilities
	Easy to wet the reinforcing fibers and fillers	More difficult to wet the reinforcing fibers and fillers
	More resistant to high temperatures than thermoplastics	High-impact resistance
	Highly flexible design	Chemical resistant
	Thick to thin wall capabilities	Hard crystalline or rubbery surface options
	Excellent aesthetic appearance	Aesthetically superior finishes
	High levels of dimensional stability	Eco-friendly manufacturing
	More difficult to surface finish	Generally, more expensive than thermoset
	Cost-effective	

By way of Tailored Fiber Placement (TFP) is solved that this is problem that how to affordably, reliably and quickly fabricate the resulting complex shapes that depend for their performance in the finished part on minimal quantities of precisely oriented fibers. (TFP) is a unique stitched preforming process that has the potential to answer and eliminate most of the limitations of drilling/machining holes in composites [8]. Compared with other textile preforming methods, TFP reinforcement fibres can be orientated in any direction and can also be curved in a radius allowing the fibre structure to align with the load paths in the material taking full advantage of the anisotropic properties of fibre reinforced plastics [9].

E.Richter et al. [10] investigated the effect of short or continuous glass fiber reinforcement on the mechanical properties of polyamide 6.6 (PA 6.6) material. They produced short and continuous glass fiber reinforced PA 6.6 materials by using TFP method. The results showed that by using continuous glass fiber, failure load values under tension and compression loading increased about 120% compared to short fibre reinforcement. K.Gliesche et al. [11] investigated that the influence of open-hole tension plate on the mechanical properties of carbon/epoxy laminated composites which were produced by using TFP technology. The test layer parts were included the hole in the center. They were found that the stress-field aligned local reinforcement on an open hole tensile plate. The reference plate from textile MAG preforms without hole reached a specific failure load of 90 kN. Due to the hole, this value decreased to 55 kN. Applying the TFP reinforcement, the value increased to 85kN. In addition, it was shown that the TFP technology is an advanced technique to design

reinforcements with only little weight increase of the tool due to the fact that the fiber alignment only takes place corresponding to the major stress trajectories.

Compression molding offers some specific properties such as low cost, high efficiency, low internal stress, small buckling deformation, good mechanical stability, and excellent product repeatability for producing composite samples. The production volume is increasing for the requirement part quantities thus the molding method boasts a strong competitive advantage in industrial. However, the process parameters of compression molding (e.g., preheating temperature, molding temperature, molding pressure, pressure holding time, cooling rate, exhaust pressure, exhaust times, and blank holder force) directly affect the flow of the matrix material, the impregnation effect of the reinforcing fibers and also mechanical properties of the composite samples. This effect exerts an impact on both the quality and mechanical performance of the material once coupled with the interaction between process parameters. Consequence, the best process parameters of compression molding are provided to optimize the mechanical performance of the material, it is critical to analyze the interaction between various process parameters and mechanical properties of the manufactured material [12]. G. Başer et al. [13] developed a new process to produce non crimp glass fabric (NCGF) reinforced Poly buthyleneterephtalate (PBT) matrix composites. Isothermal and semi-isothermal processing of NCGF reinforced IPCBT composites via in-situ polymerisation of cylic buthyleneterephtalate (CBT)/glass fiber prepregs has been successfully performed by means of compression molding technique. The results showed that the prepreg production temperature which gave highest mechanical property was identified as 160 °C. The optimum compression parameters which gave highest mechanical properties were identified as 200 °C compression temperature, 30 minutes compression time and 1.6 MPa compression pressure for isothermal process. Semi-isothermal process with 180 °C demolding temperature gave higher tensile and flexural properties than isothermal process. To enhance the quality and mechanical performance of a carbon fiber–reinforced polymer (CFRP) workpiece, J.Xie et al. [12] prepared a polyacrylonitrile (PAN)-based carbon fiber–reinforced thermosetting polymer (CFRTP) laminated board through compression molding, and carried out orthogonal tests and single-factor tests to disclose the effects of different process parameters (i.e., compression temperature, compression pressure, pressure-holding time, and cooling rate) on the mechanical performance of the CFRTP workpieces. The results showed that the optimal process parameters for compression molding included a compression temperature of 150 °C, a pressure-holding time of 20 min, a compression pressure of 50 T, a cooling rate of 3.5 °C/min, and a mold-opening temperature of 80 °C. Under this parameter combination, the tensile strength, bending strength, and the interlaminar shear strength (ILSS) of the samples were, respectively, 785.28, 680.36, and 66.15 MPa.

From literature surveys, there was not easily found an article which was investigated the effect of holding time parameters on the mechanical properties of the woven glass fiber/Nylon6 (PA6) composite samples which were produced by using both TFP and compression molding technology. By this way, in this study, the woven glass fiber/Nylon6 (PA6) was produced by using TFP. After TFP production, compression molding process was applied to produce composite samples under various holding time parameters (for tensile test 1.0 mm thickness composite samples – 3.30 min., 4.00 min., 4.30 min.) (for bending test 2.0 mm thickness composite samples – 4.00 min., 4.30 min., 5.00 min.). Tensile and three point bending tests were applied the composite samples. Tensile strength, tensile modulus, flexural strength and flexural modulus values were determined.

2. Materials and Methods

2.1. Materials

In this study, Polyamide 6 (PA6) [14] and E-glass fibre were supplied from Universal Fibers from USA and Owen Corning, respectively. E-glass fibre is SE1200 Type 30 Single [15] end roving which is designed for excellent processing for knitting and weaving in polyester, vinyl ester, and epoxy resins. E-glass fibre is also suitable for Long Fiber Thermoplastic (LFTP) PA compounding applications.

2.2. Tailored Fiber Placement (TFP)

In this study, unidirectional (UD) E-glass fabrics were produced by using Tailored Fiber Placement (TFP) technology which was an invention of the Institute for Polymer Research Dresden. We used this production method for producing fiber preforms with stress field-aligned fiber orientations. This is based on the well-known embroidery technique used for fabrics. The principle of TFP technology was showed at Fig. 1. The process is that by stitching with a needle yarn a roving is fixed on a base material. As you can see in Fig. 1 which in between the stitches the base material is moved in both X and Y-direction. This process is working in this way how the roving is fixed with zigzag stitches on either side of the roving. Also, the roving can be made of carbon, glass, or other types of fiber. The TFP technology advantage, compared to common textile technologies, is the ability to arrange reinforcing fibers in every direction of the reinforcing area from an angle of 00 to 3600 [16].
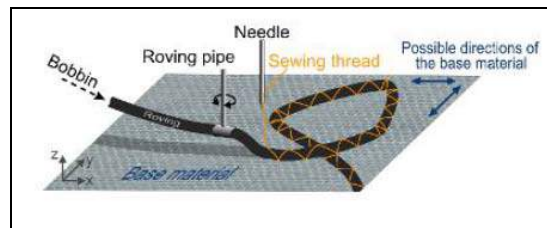
Figure 1: The principle of TFP technology

The system is ideally suited for series production because the highly automated production process allows good reproducibility. The other advantage is almost no fiber waste. Because the near-net-shape preforms are made using the material [16].
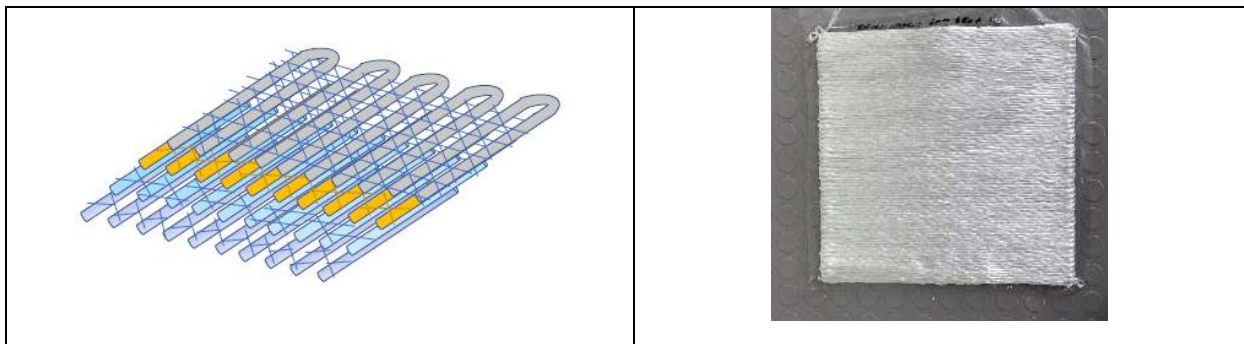
Figure 2: The manufactured of UD E-glass/PA6 fabrics by using TFP

For the produced fabrics, 2 3 Michelamn PA845H was used for improving thermal stability of the material. The UD E-glass/PA6 fabrics were produced by Coats in Bursa (Fig.2). The fabrics were produced different thicknesses such as 1mm and 2 mm for tensile and bending tests. The size of fabrics was 305 mm x 305 mm.

2.3. Compression molding process

100 tonne Hydraulic hot press was used in the study with Roctool equipment (Fig.3). By using Roctool equipment thermoplastic matrix composite samples produced faster in the compression molding process. Thus, this process is suitable for a wide range of industrial, commercial, and consumer parts and products ranging from very small to large automobile panels. After the TFP production of GF-PA6 fabrics, materials were manufactured by using a compression molding process with Roctool equipment.
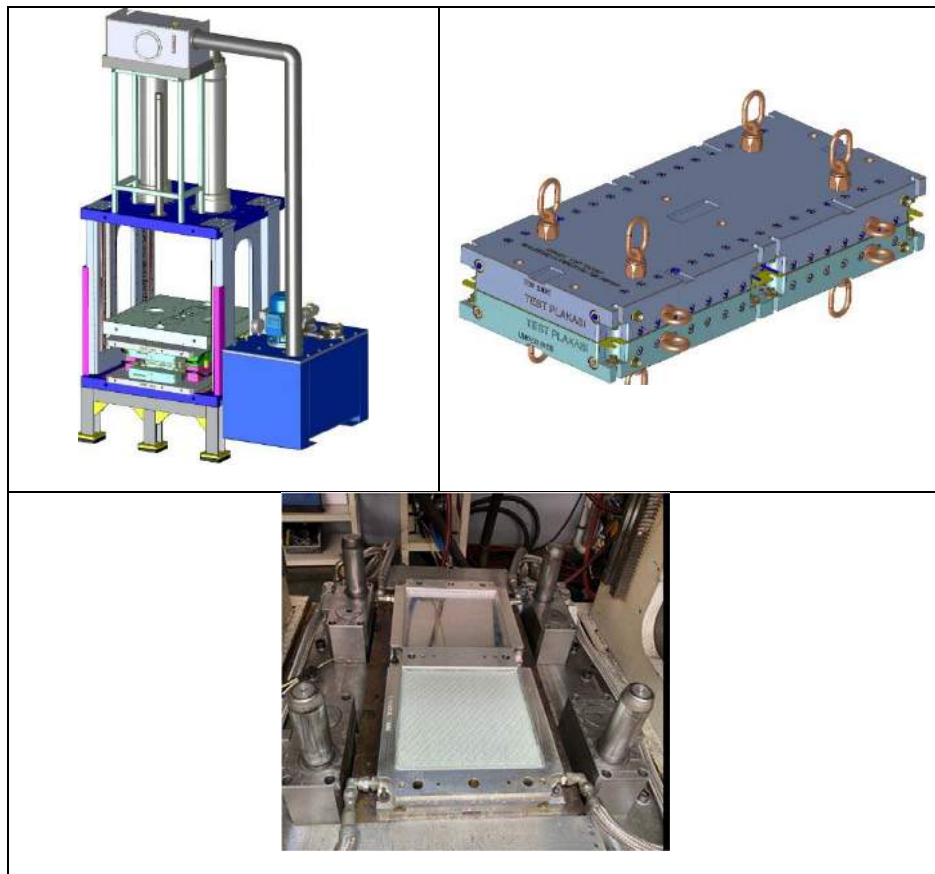
Figure 3: Compression molding process and used molds

The GF-PA6 fabrics were pressed into the molds under 160 bars with 300 ºC. The cooling system also placed for suitable cooling of composite samples to the molds. The mold dimension is 830 mm x 380 mm x 145 mm as has 2 cavities which are 1.00 mm and 2.00 mm. Each cavity dimension is 305mm x 305 mm. In the study both cavities were used for producing 1mm and 2mm thick composite samples. For 1.00 mm and 2.00 mm thickness composite samples, the weight of GF-PA6 fabrics was measured as 185 gr. and 367 gr., respectively. In this study, composite samples with different thickness were produced at compression molding process under various holding times. The holding times were 3.30 min. / 4.00 min. / 4.30 min. for 1.00 mm thickness of composite samples. For the 2.00 mm of composite samples, holding times were 4.30 min. / 5.00 min. / 5.30 min. After the production, water jet system was used for cutting the composite samples according to the standards for tensile and 3 point bending tests. Then the specimens put on the dehumidifier machine along 24 hours due to moisture effect for PA6.

2.4. Mechanical tests

2.4.1 Tensile Test

ISO 527 test standard was used for determining the maximum tensile strength and tensile modulus of GF-PA6 composite samples which were produced under various holding times (3.30 min. / 4.00 min. / 4.30 min.). In this study that Fig. 4, Type A test specimen was used. The dimension of the specimen was 250 mm x 15 mm x 1 mm. The sides of each individual specimen were parallel to within 0.2 mm. The tensile tests were done at 1 mm/min. at Shimadzu AGS-X series test device. Tensile modulus and tensile strength values were determined under various holding times. The standard is allowed the used alternatives include tabs made from the material under test, mechanically fastened tabs, unbonded tabs made of rough materials (such as emery paper or sandpaper, and the use of roughened grip faces.). Sandpaper was used for tabs. Also, all specimens were scratch before they had started test tabs location point. And the scratch points had been controlled and reviewing during the test keep going.
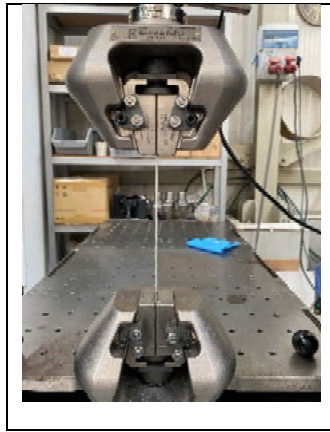
Figure 4: In this study, Type A test specimen was used. The dimension of the specimen was 250 mm x 15 mm x 1 mm.

2.4.2. 3-Point Bending Test

ASTM D 7264/D 7246 test standard was used for determining flexural modulus and flexural strength values of GF-PA6 composite samples (2.00 mm thickness) which were manufactured under various holding times (4.30 min. / 5.00 min. / 5.30 min.). The test method determines the flexural stiffness and strength properties of polymer matrix composites. This test method was developed for optimum use with continuous-fiber-reinforced polymer matrix composites. In this study, span-to-thickness ratio of 32:1 was selected. The standard specimen thickness is 2.00 mm, and the standard specimen width is 13.00 mm with the specimen length being about 20% longer than the support span. 3-point bending test was done at 1 mm/min. at Shimadzu AGS-X series test device which is Fig. 5.

Figure 5: The support span. 3-point bending test was done at 1mm/min. at Shimadzu AGS-X series test device

3.Results and Discussion

3.1 Tensile Test

In this work, the effect of holding time on tensile properties of GF-PA6 composites was investigated. Tensile test results according to holding time values of manufactured composite samples having 1 mm thickness were given in Fig. 6. As can be seen from Fig. 6, as a result of the increase in holding time, tensile modulus and tensile strength values were increased. If we compared these obtained results, tensile modulus showed close values at both 3.30 min. and 4.00 min. Beside this, because of increasing the holding times at 4.30 min. the tensile modulus values improved to nearly 20 GPa. In addition, tensile strength values increasing significantly due to increasing of holding time values from 3.30 min. to 4.00 min. As manufactured composite samples at 4.30 min. holding time, flexural strength value was determined as 577 MPa. The ideal duration holding time was achieved for both tensile modulus and strength values at 4.30 min. holding time. Xie et al. [19] investigated the effect of compression molding parameters (compression temperature, compression pressure, pressure-holding time, and cooling rate) on the mechanical properties of polyacrylonitrile (PAN)-based carbon fiber–reinforced thermosetting polymer (CFRTP). In this study, the authors selected pressure holding times from 10 min. to 25 min. From test results, the mechanical performance of the test material gradually increased with the elapse of the pressure-holding time, before the time reached a certain threshold. The mechanical performance remained constant after the threshold because the resin flow and impregnation both improve with the extension of the pressure-holding time, but the flow ceases after the resin is fully impregnated. Taking tensile strength as the main criterion, the optimal pressure-holding time was determined as 20 min. for the mechanical properties of the samples. With respect to the effect of holding times, it was clear that the tensile strength increased with increasing holding times from 3.30 to around 4.30 minutes as stated in Ref. [20].
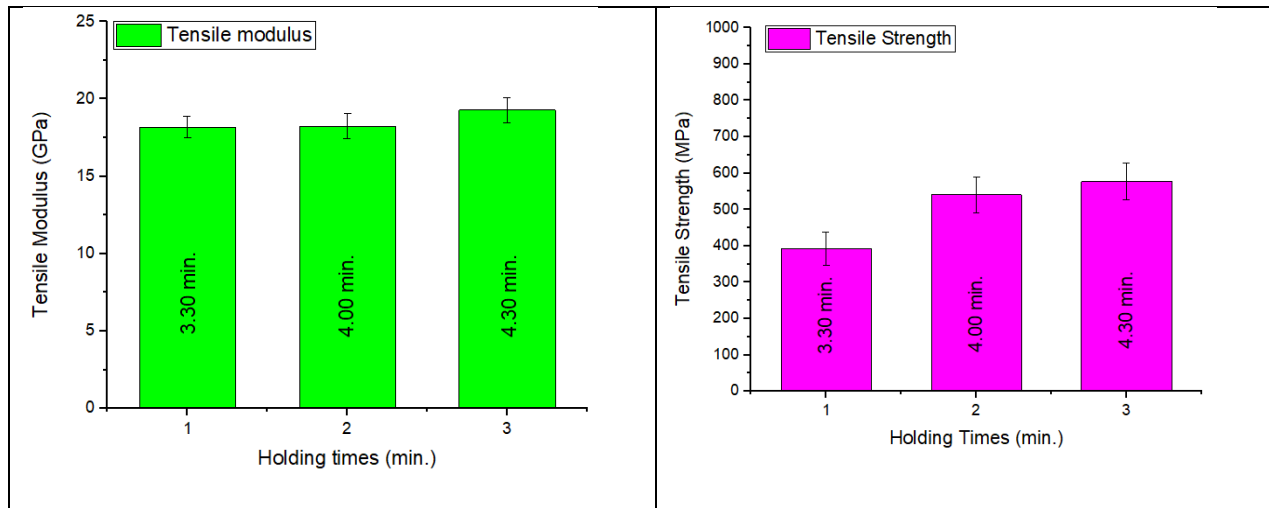
Figure 6: Tensile test results according to holding time values of manufactured composite samples having 1.00 mm thickness

3.2 Three Point Bending Test

Figure 7 summarized three point bending test results according to holding time values of manufactured composite samples having 2 mm thickness. From Fig. 7, flexural modulus and flexural strength values decreased in order to the holding time values increased. As you can see from Fig. 5, the maximum flexural modulus value reached 28.77 GPa at 4.30 min. Also, we compared the other holding times realized, there wasn't a significantly change for flexural modulus values when the applied holding times at both 4.30 min. and 5.00 min. However, when the other holding time was compared the 5.00 min. and 5.30 min., the flexural modulus value was decreased. In addition, the maximum flexural strength was obtained at 4.30 min. as 689 MPa compared to other composite samples which were manufactured at 5.00 min. and 5.30 min. holding times. The flexural strength values were also determined as 672 MPa (5.00 min.) and 608 MPa (5.30 min). Xu et al. [20] investigated bending properties of the unidirectional continuous glass fiber-reinforced poly (ether ether ketone). They held composite materials at the mold temperature for a certain time as 10 min. – 150 min. Bending strength and modulus values were determined under various molding times with the same molding temperature of 400 ℃ and the same cooling rate of 10 ℃/min. The results showed that the bending strength and modulus increased as the holding time increased. This is because the matrix was gradually penetrated into the GFs under pressure, and the dispersibility of the GFs was improved. In addition, when the holding time was increased to 120 min, the bending strength and modulus reached its maximum, at 941.1 MPa and 38.3 GPa, respectively. This indicates that a sufficient holding time was critical to improving the bending performance of the composites based on the cowrapped yarns method. From another study, Fujihara et al. [21] achieved an optimum fabrication for the continuous carbon fiber reinforced PEEK matrix composites. So, they selected three processing temperatures (380, 410, and 440 ℃) and three holding time (20, 40 and 60 min.). The result showed that the bending modulus was not changed with increasing the holding times from 20 min. to 60 min. for the specimens fabricated at 380 and 410 ℃, which was around 95 GPa. It was noted that a slight modulus drop was seen in the case of 440 ℃. A similar tendency was also seen in the bending strength showed around 1300 MPa, in the case of 380 and 410 ℃ indicated that the bending strength dropped about 200 MPa from the 40 to 60 min. holding time.
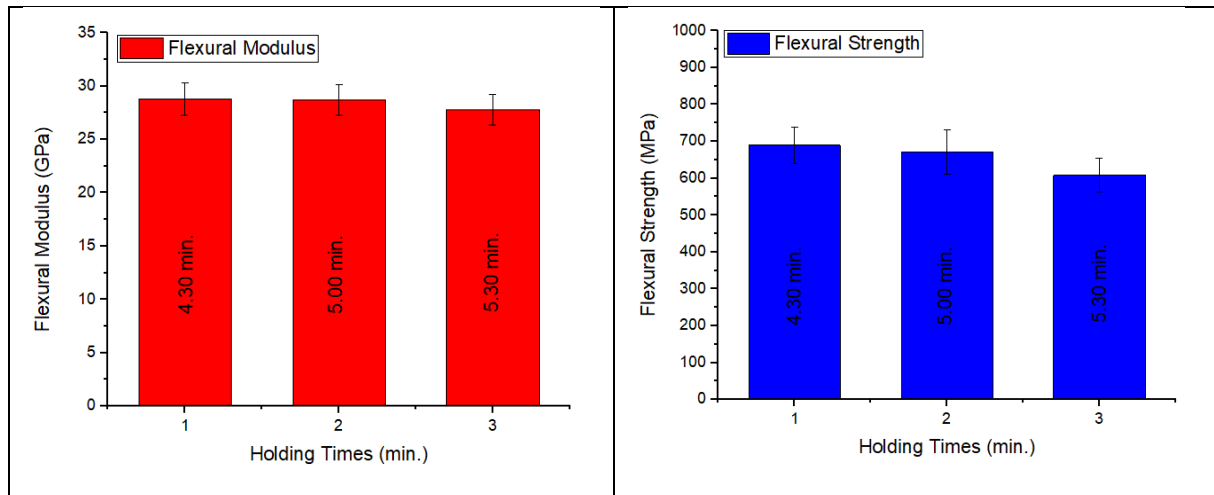
Figure 7: Three point bending test results according to holding time values of manufactured composite samples having 2.00 mm thickness

4.Conclusion

In this study, it was aimed to determine the mechanical properties of thermoplastic matrix composite materials (GF-PA6) produced via TFP then compression molding process. Tensile and 3 point bending tests were applied the thermoplastic matrix composites which were produced and manufactured by TFP and compression molding process. Tensile strength, tensile modulus, flexural strength and flexural modulus values were determined.

➢ Tensile modulus showed close values at both 3.30 min. and 4.00 min. Beside this, because of increasing the holding times at 4.30 min. the tensile modulus values improved to nearly 20 GPa. As manufactured composite samples at 4.30 min. holding time, flexural strength value was determined as 577 MPa. The ideal duration holding time was achieved for both tensile modulus and strength values at 4.30 min. holding time.

➢ Flexural modulus and flexural strength values decreased in order to the holding time values increased. The maximum flexural modulus value reached 28.77 GPa at 4.30 min. The maximum flexural strength was obtained at 4.30 min. as 689 MPa compared to other composite samples which were manufactured at 5.00 min. and 5.30 min. holding times.

➢ No correlation was found between sample thickness and holding time. For both tensile and flexural composite samples, optimum holding time was found as 4.30 min.

Acknowledgement

References

1. Campbell F.C. (2010). Structural Composite Materials, ASM International.
2. Ngo, T.-D. (2020). Introduction to Composite Materials. Composite and Nanocomposite Materials – From Knowledge to Industrial Applications.
3. William D. Cllister, Jr. and David G. Rethwisch, Materials Science and Engineering an Introduction. 8th ed.p.cm.
4. Biron M. Thermoplastics and Thermoplastics Composites.

5. Mazumdar, Sanjay K. (2001). Composite Manufacturing: Materials, Product, and Process Engineering.
6. Park C.H. and Lee W.I. Compression Molding in Polymer Matrix Composites, University of Le Havre, France and Seoul National University, Korea.
7. Long, A. C., Wilks, C. E., & Rudd, C. D. (2001). Experimental characterisation of the consolidation of a commingled glass/polypropylene composite. Composites Science and Technology, 61(11), 1591–1603. doi:10.1016/s0266-3538(01)00059-8
8. Koricho, E. G., Khomenko, A., Fristedt, T., & Haq, M. (2015). Innovative tailored fiber placement technique for enhanced damage resistance in notched composite laminate. Composite Structures, 120, 378–385. doi: 10.1016/j.compstruct.2014.10.016
9. Crothers, P. J., Drechsler, K., Feltin, D., Herszberg, I., & Kruckenberg, T. (1997). Tailored fibre placement to minimise stress concentrations. Composites Part A: Applied Science and Manufacturing, 28(7), 619–625. doi:10.1016/s1359-835x (97)00022-5
10. E.Richter, K. Uhlig, A.Spickenheuer, L.Bittrich, E.Mader,G.Heinrich, Thermoplastic Composite Parts Based on Online Spun Commingled Hybrid Yarns With Continuous Curvilinear Fibre Patterns, ECCM16-16th European Conference on Composite Materials, Seville, Spain, 22-26 June 2014
11. Gliesche, K. (2003). Application of the tailored fibre placement (TFP) process for a local reinforcement on an "open-hole" tension plate from carbon/epoxy laminates. Composites Science and Technology, 63(1), 81–88. doi:10.1016/s0266-3538(02)00178-1
12. J.Xie,S.Wang,Z.Cui and J.Wu, Process Optimization for Compression Molding of Carbon Fiber-Reinforced Thermosetting Polymer, MDPI, Materials 2019, 12(15), 2430
13. G.Başer, Production of Fiber Reinforced Thermoplastic Composites, ITU, Department of Polymer Science and Technology Polymer Science and Technology Programme, October 2012
14. Universal Fibers, – 1000D PA6
15. Owens Corning, SE1200 TYPE30 Single-End Roving
16. Mattheij, P., Gliesche, K., Feltin, D. (1998). Tailored Fiber Placement-Mechanical Properties and Applications. Journal of Reinforced Plastics and Composites, 17(9), 774–786.
17. EN ISO 527-5, Plastics – Determination of tensile properties
18. D 7264/D 7264M – 07 – Standard Test Method for Flexural Properties of Polymer Matrix Composite Materials.
19. Xie, J., Wang, S., Cui, Z., & Wu, J. (2019). Process Optimization for Compression Molding of Carbon Fiber–Reinforced Thermosetting Polymer. Materials, 12(15), 2430. doi:10.3390/ma12152430
20. Tharazi, I., Sulong, A. B., Muhamad, N., Haron, C. H. C., Tholibon, D., Ismail, N. F., … Razak, Z. (2017). Optimization of Hot Press Parameters on Tensile Strength for Unidirectional Long Kenaf Fiber Reinforced Polylactic-Acid Composite. Procedia Engineering, 184, 478–485. doi: 10.1016/j.proeng.2017.04.150
21. Xu, Z., Zhang, M., Wang, G., & Luan, J. (2018). Bending property and fracture behavior of continuous glass fiber-reinforced PEEK composites fabricated by the wrapped yarn method. High Performance Polymers, 095400831876750. doi:10.1177/0954008318767500
22. Fujihara, K., Huang, Z.-M., Ramakrishna, S., & Hamada, H. (2004). Influence of processing conditions on bending property of continuous carbon fiber reinforced PEEK composites. Composites Science and Technology, 64(16), 2525–2534. doi: 10.1016/j.compscitech.2004.05.014

Image Data Augmentation Techniques for Fracture Detection of Dogs

Gülnur Begum ERGÜN[1*], Selda GÜNEY[2]

Abstract: Image collection and preparation phases are very costly for machine learning algorithms. They require a lot of labeled data, especially deep learning algorithms. Hence, the image pre-processing method, data augmentation, is commonly used. Since there are so many proposed methods for this task, this comparison study is presented to be a supporting guide for the researchers working in this field. In addition, the scarcity of studies with animal-based data sets makes this study more valuable. The study is investigated on a comprehensive medical image data set consists X-ray images of many different dogs. The goal is to determine the fracture of the long bones in dogs. Three traditional augmentation methods are employed on the data set: flipping, rotating, and changing brightness of the images. The experimental work shows that flipping and changing the brightness of the image methods are more successful than the rotation.

Keywords: biomedical image processing; bone fractures; data augmentation; preprocessing.

1. INTRODUCTION

Great advances have been made in the use of deep learning models. They have found a place in many application areas. One of the most used area is biomedical field [1]. In orthopedics, these deep architectures are utilized for fracture and bone disease detection [2].

Despite of all advances, deep architectures require lots of labeled data. That problem leads us to one of the most preferred pre-processing method, data augmentation. Data augmentation is a transition from limited data to more data [3]. On one hand, it helps to reduce overfitting problem, on the other hand, it equalizes unbalanced data sets.

In order to prevent the overfitting, it is possible to modify the network structure. Batch normalization and drop-out can be given as examples of the modifications. Data augmentation techniques are different from them, as they are basically a pre-processing step [4].

In a work, authors explored and compared the data augmentation methods in image classification. They applied simple techniques, such as cropping, rotating, and flipping the images. Also, they experimented Generative Adversarial Neural Networks (GANNs), and a proposing method named neural augmentation. Their experiments show that the traditional augmentation methods are more effective than the others [5].

[1,2] Department of Electrical and Electronic Engineering, Başkent University, Ankara, Turkey
* Corresponding author: gbcangoz@baskent.edu.tr

In another research paper, a variety of augmentation strategies, horizontal flips, random crops, and principal component analysis (PCA) are investigated. Their work shows that augmentation strategy greatly affects classification performance [6].

Shijie et. al. used some data augmentation methods in their paper include: GAN/WGAN, flipping, cropping, shifting, PCA jittering, color jittering, noise, rotation, and some combinations. According to the results of the study, the four individual methods (Cropping, Flipping, WGAN, Rotation) perform generally better than the others, and some appropriate combination methods are slightly more effective than the individuals [7].

In the recent years, GANNs have become very popular for synthesizing images [8-10]. The works which related traditional methods can be exemplified further [11-15]. Nevertheless, these methods can be highly impacted by data sets, and it is difficult to find studies in the literature using comprehensive data sets of X-Ray images of dogs.

In this work, a comprehensive data set created from dogs is employed. The aim is to detect long bone fractures in dogs. Since it needs a lot of labeled data to do this task, three data augmentation techniques are investigated: flipping, rotating, and changing brightness of the images. These traditional methods can positively affect classification performance. Additionally, they are easy to apply. After realizing the pre-processing step, deep neural model, CNN is performed for detection of the long bone fractures.

2. MATERIAL AND METHODS

A. Data set

The data set consists of 2027 X-Ray images of long bones of many different dogs taken from Ankara Metropolitan Municipality Stray Animals Temporary Nursing Home. 479 images of the data set were labeled as fractured, and the remaining 1548 images were labeled as no fracture. For more detail about the data set, readers can be referred in our previous study [16]. The .png extension images have a size of 227x227x3. For better understanding, an example is given Fig.1. Both images in the figure belong to radius-ulna.

a)   b)
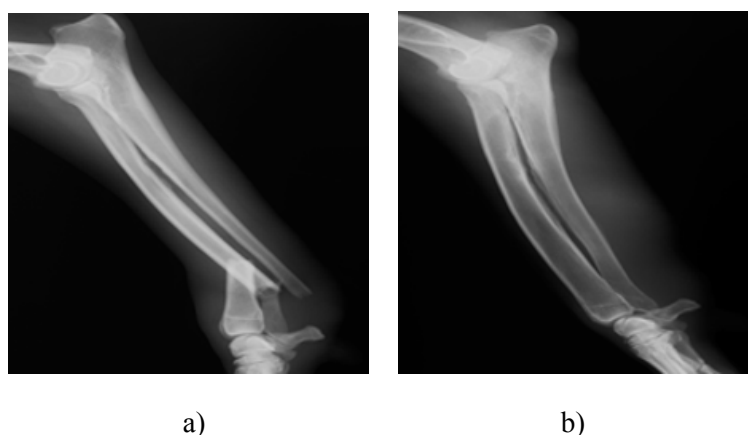
Figure 1. A visual example of the data set
a) fractured, b) no fracture

B. Methods for Data Augmentation

Some of image data augmentation techniques can be divided into two classes. These are:

a. Position augmentation: Cropping, Flipping, Padding, Rotation.

b. Color augmentation: Brightness, Contrast, Saturation, Hue.

Although, there are various methods for augmentation, because of the simplicity, three common data augmentation methods are investigated in this study.

1. Flipping: For augmentation, images can flip horizontally and vertically. In this study, three flipping options are applied: horizontally, vertically, and both horizontally and vertically.

2. Rotation: Rotating the images at specific angles. But after the rationing process, the image dimensions are not the same, so after the application, the images are resized to the original dimensions again. In this study, three different angles are applied: +30, -30 and +45 degrees.

3. Brightness: Another way for augmentation is changing the brightness of the image. The resultant images become lighter or darker. In this study, three brightness settings are applied.

After the process, size of the data set increased from 2027 (479 broken, 1548 non-broken bones) to 8108 (1916 broken, 6192 non-broken bones) for each technique. After augmentation process, the outputs from all techniques are given in Fig.2.

C. Methods for Classification

In this study, convolutional neural network (CNN) is used for train and test phases because of its success in image processing [17]. A convolutional neural network consists of 5 primary layers: An input layer, convolution layers, pooling layers, fully connected layers and an output layer [18]. The purpose of the convolution layer is to extract features from the input image by performing a dot product between images and filters. After the convolution layer, pooling layer is used to reduce the dimensions of the featured matrix. Finally, the output from network matrix is flattened and ready for classification process in the fully connected layer [16].

For the classification, a CNN network is created. The network has 7 layers (6 convolutional layers, all of them followed by max-pooling layers, and 1 fully connected layer).

The filter sizes used in convolutional layers are selected as 3x3 and in pooling layers, maximum pooling method is preferred. Adam optimizer is implemented, and batch number of the network is chosen as 32. The training and test sets are randomly selected 0.8 and 0.2 from the data set, respectively.

| a) | b) | c) |
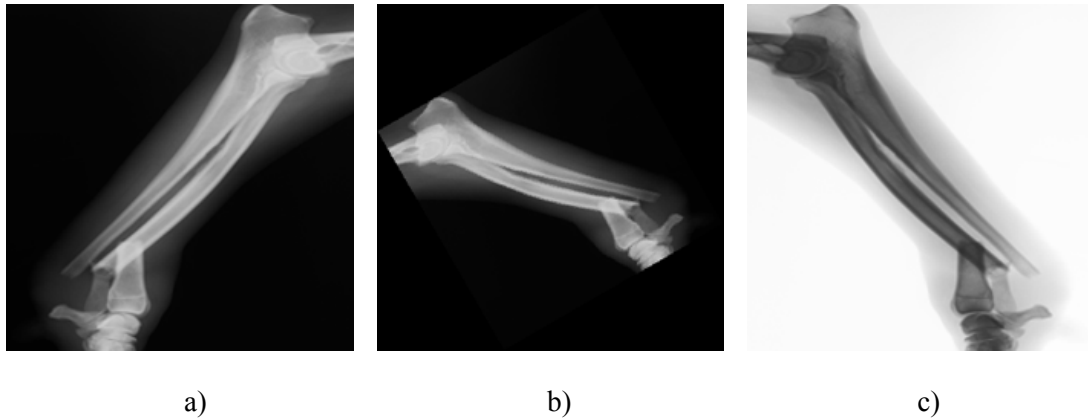
Figure 2. Outputs after the augmentation process
a) after flipping, b) after rotating 30 degrees, c) after changing the brightness

3. RESULTS AND DISSCUSSION

The objective is to classify the images into their classes which are fractured or no fracture. In order to achieve this goal, CNN is utilized, and the results are given in Table 1.

Despite the diversity of the augmentation techniques, in this study three of them were studied. It is because, these methods are very easy to be implementation and they have very low cost.

From Table 1, it can be seen that the classification accuracy of the raw data is only 77.57%. On the other side, after the augmentation methods, the accuracy is increased. The most effective method is changing the brightness of the images in data set, as it has 89.34% classification success. Therefore, the outcomes of the study confirm the prediction that it will increase the success. However, the rotation method did not make much of a change. The essential problem of the situation might be that the image size changes after the rotation process, and it resized again. During these stages, data loss has occurred.

Table I. Classification Results for the Fracture Detection

Augmentation Technique	Accuracy (%)	Selectivity
Raw Data	77,57	0,7807
Flipping	85,13	0,8095
Rotation	79,49	0,6915
Brightness	89,34	0,8952

4. CONCLUSION

This paper tries to present a basic solution with comparison for the problem of overfitting seeing the veterinary medicine. Since, deep architectures need big data sets, data augmentation is a very powerful technique for creating bigger data sets.

Lots of related work in the literature exists, but all of these methods depend on the data sets. For this reason, we wanted to contribute to the literature with a data set containing canine (dogs) X-rays images. The results of the study are promising for future works.

REFERENCES

[1]   J.Schmidhuber, "Deep learning in neural networks: An overview", Neural Networks, 2015, vol. 61, pp. 85-117.

[2]   Adams M, Chen W, Holcdorf D, McCusker M W, Howe P D, Gaillard F., "Computer vs human: deep learning versus perceptual training for the detection of neck of femur fractures," J Med Imaging Radiat Oncol; vol.63, pp. 27–32, 2019.

[3]   Raúl de la Fuente Lopes, "Wild Data Part 1: Augmentation", https://blog.stratio.com/wild-data-part-one-augmentation-2/ access: 19.04.2021, 18.56.

[4]   Shorten, C., Khoshgoftaar, T.M. "A survey on Image Data Augmentation for Deep Learning," J Big Data 6, 60, 2019. https://doi.org/10.1186/s40537-019-0197-0

[5]   Luis Perez, Jason Wang, "The Effectiveness of Data Augmentation in Image Classification using Deep Learning," Computer Vision and Pattern Recognition, 2017.

[6]   Hussain Z, Gimenez F, Yi D, Rubin D. "Differential Data Augmentation Techniques for Medical Imaging Classification Tasks," AMIA Annu Symp Proc. pp. 979-984, 2018.

[7]   J. Shijie, W. Ping, J. Peiyi and H. Siping, "Research on data augmentation for image classification based on convolution neural networks," Chinese Automation Congress (CAC), pp. 4165-4170, 2017.

[8]   Calimeri F., Marzullo A., Stamile C., Terracina G. "Biomedical Data Augmentation Using Generative Adversarial Neural Networks." Artificial Neural Networks and Machine Learning – ICANN 2017. Lecture Notes in Computer Science, vol 10614. Springer, Cham. https://doi.org/10.1007/978-3-319-68612-7_71,

[9]   M. Frid-Adar, E. Klang, M. Amitai, J. Goldberger and H. Greenspan, "Synthetic data augmentation using GAN for improved liver lesion classification," 2018 IEEE 15th International Symposium on Biomedical Imaging (ISBI 2018), 2018, pp. 289-293, doi: 10.1109/ISBI.2018.8363576

[10]   Shin HC. et al. "Medical Image Synthesis for Data Augmentation and Anonymization Using Generative Adversarial Networks," Simulation and Synthesis in Medical Imaging. SASHIMI 2018. Lecture Notes in Computer Science, vol 11037. Springer, Cham. https://doi.org/10.1007/978-3-030-00536-8_1

[11]   Jia S, Wang P, Jia P, Hu S. "Research on data augmentation for image classification based on convolutional neural networks" Chinese automation congress, 2017. p. 4165–70.

[12]   Shunjiro Noguchi Mizuho Nishio Masahiro Yakami Keita Nakagomi Kaori Togashi, "Bone segmentation on whole-body CT using convolutional neural network with novel data augmentation techniques," Computers in Biology and Medicine, vol. 121, 2020.

[13]   Hernández-García A., König P. "Further Advantages of Data Augmentation on Convolutional Neural Networks," Artificial Neural Networks and Machine Learning ICANN 2018. Lecture Notes in Computer Science, vol 11139. Springer, Cham. https://doi.org/10.1007/978-3-030-01418-6_10.

[14]   Sajjad M. et. al. "Multi-grade brain tumor classification using deep CNN with extensive data augmentation," Journal OF Computational Science, vol. 30, pp.174-182, 2019.

[15]   Abdollahi B., Tomita N., Hassanpour S. (2020) "Data Augmentation in Training Deep Learning Models for Medical Image Analysis," Deep Learners and Deep Learner Descriptors for Medical Applications. Intelligent Systems Reference Library, vol 186. Springer, Cham. https://doi.org/10.1007/978-3-030-42750-4_6.

[16]   Ergün G. B. , Güney S., Ergün T.G., Köpeklerdeki Uzun Kemiklerin Evrişimsel Sinir Ağları Kullanılarak Sınıflandırılması, Fırat Üniversitesi Fen Bilimleri Dergisi, vol. 33, pp. 125-132, 2021.

[17]   K. Guo et al., "Angel-Eye: A Complete Design Flow for Mapping CNN onto Customized Hardware," 2016 IEEE Computer Society Annual Symposium on VLSI (ISVLSI), Pittsburgh, PA, 2016, pp. 24-29.

[18]   LeCun, Y.; Boser, B.; Denker, J. S.; Henderson, D.; Howard, R. E.; Hubbard, W.; Jackel, L. D. (December 1989). "Backpropagation Applied to Handwritten Zip Code Recognition". Neural Computation. 1 (4): 541–551.

Sürdürülebilir- Eko Köy Olarak Inşaat Yapıları Ve Tasarım Planlaması Örneği Akbaş Köyü İncelemesi

An Example of Construction Structures and Design Planning as a Sustainable-Eco-Village Akbaş Village Analysis

Ayse Arıcı[1]*

Özet: Araştırma alanı olarak, Akbaş köyü sahip olduğu doğal güzellikler ve yöresel konut tipi, kültürel değerleri ile eko turizm potansiyeli açısından önemli bir yerleşim yeri olan Antalya İli Serik İlçesi'ne bağlı Akbaş Köyü seçilmiştir. Akbaş Köyü'nün Türkiye'modern besi-süt işletmeleri tarımsal turizm- eko turizm- örnek sürdürülebilir köy çalışmalarına örnek teşkil etmesi, alanın seçilmesinde etkili olmuştur. Bu çalışmada, "Akbaş Köyü, kırsal planlama çerçevesinde mevcut konut tipleri-kullanılan yapı malzemeleri incelenerek sürdürülebilir mimari için kullanılması gereken yapı malzemeleri belirlenmelidir. Mevcut konutların kullanılabilmesi için nasıl yapı malzemeleri ile restorasyon yapılmalıdır? Yörede nasıl amaçlara hizmet edecek yapılar gerekmektedir? Yapıların nasıl bir konfor sağlanması beklenmektedir? Yörede ekonomik ve kültürel sürdürülebilirliğin sağlanması için neler gereklidir" sorularına yanıt aranmıştır. Araştırmada yörede ki mevcut durumu incelenmiş ve yerel halkın görüşleri alınmıştır. Bu kapsamda, yöre halkına bu sorular yöneltilerek araştırmada anket çalışması yapılmıştır. Yörede fotoğraf çekilerek yerinde inceleme yapılmıştır. Nitel ve nicel veriler toplanarak değerlendirilmiştir. Bu kapsamda Akbaş Köyü için kırsal kalkınma ve yerel kimlik açısından önemli bir potansiyele sahip olduğu görülmüştür. Sonuç olarak, kırsal alanlarda mevcut doğal- kültürel kimliği ve iklimsel değerleri- tarım-hayvancılık faaliyetleri-turizm çalışmalarına ve çalışma alanında mevcut kültürel değerlere sahip olan konutların uygun yapı malzemeleri kullanılarak yaşatılması ve yeni planlanacak konutlar ve yapılar için yöreye uyumlu yeni yapı malzemeleri ile geleneksel yapı malzemelerinin harmanlanarak sürdürülebilirliği bağlamında sonuç ve önerilere yer verilmiştir.

Anahtar Kelimeler: Sürdürülebilir yapılar, eko köy, yapı malzemeleri, kırsal sürdürülebilirlik, fonksiyonel yapı malzemeleri.

Abstract:

Akbaş Village of Antalya Province Serik District, which is an important settlement in terms of its natural beauties, local housing type, cultural values and eco-tourism potential, was chosen as the research area. The fact that Akbaş Village sets an example for modern fattening-dairy farms, agricultural tourism-eco-tourism-exemplary sustainable village studies in Turkey has been influential in the selection of the area. In this study, "Akbaş Village, within the

[1] International Vizyon University, Faculty of Engineering and Architecture, Department of Civil Engineering, Gostivar, Northern Macedonia.
* Corresponding author: aysearici.iut@gmail.com

framework of rural planning, existing housing types-used building materials should be examined and the building materials that should be used for sustainable architecture should be determined. What kind of building materials should be restored so that the existing houses can be used? What kind of buildings are needed in the region to serve what purposes? What kind of comfort is expected from the buildings? Answers were sought to the questions "What is necessary to ensure economic and cultural sustainability in the region". In the research, the current situation in the region was examined and the opinions of the local people were taken. In this context, a survey was conducted in the research by asking these questions to the local people. Photographs were taken in the region and an on-site examination was carried out. Qualitative and quantitative data were collected and evaluated. In this context, it has been seen that Akbaş Village has an important potential in terms of rural development and local identity. As a result, the existing natural-cultural identity and climatic values-agricultural-livestock activities-tourism studies in rural areas and the existing cultural values in the study area should be kept alive by using appropriate building materials, and new building materials and traditional building compatible with the region for the newly planned houses and structures. The results and suggestions are included in the context of sustainability by blending the materials.

Keywords: Sustainable buildings, eco village, building materials, rural sustainability, functional building materials.

1. Giriş

Kırsal kalkınma, kırsal alanlarda ekonomik ve sosyal alanlarda gelişme ve büyümeyi sağlamak için yapılan faaliyetleri kapsamaktadır. Kırsal kalkınma projeleri denildiği zaman genellikle tarımsal ürünlerin işlenmesi, değerlendirilmesi ve pazarlanmasına yönelik ekonomik faaliyetleri ve yatırımları ve üretime teşvik etmek olarak programlanmaktadır. Kırsal kalkınmada tarımsal üretim- hayvansal üretim kadar turizm faktörü de göz önünde bulundurulmalıdır.

Sürdürülebilir kalkınma yaklaşımının temel vurgusu ekonomik büyüme değil, sosyal bir varlık olarak insan ve çevre konuları üzerinedir. Söz konusu yaklaşımda kalkınma salt bir ekonomik büyümedir. Ekonomik büyüme tek başına çoğunluğun yaşam standardının yükselmesine neden olmaz. Salt ekonomik büyüme için önemli olan olgular; doğal kaynakların verimli kullanılması- alt yapının kurulması- dünden bugüne aktarılan değerlerin bundan sonrası içinde aktarılması gereken değerlerin verimli ve sürdürülebilir hale getirilmesi- mevcut yapıların restorasyona sokularak fonksiyonel ve sağlıklı bir hale getirilmesi çok önemlidir. Doğal kaynakların dengesiz kullanımı, kısa vadeli amaçlar için kaynakların yok edilmesi gelecek nesiller için oldukça tehlikelidir.

Dolayısı ile sürdürülebilir kalkınmanın temel hedefi yoksulluğu ve yoksulluğa yol açan nedenleri ortadan kaldırmaktır (Gülçubuk, 2007).

Sürdürülebilir kalkınma sosyal gereklilik, eşitlik, katılım ve insan kaynaklarının geliştirilmesi birbiriyle ilişkili ilkelerdir. Bunların tamamının gerçekleştirilmiş olması toplumun güçlenmesiyle sonuçlanır ki, bu durum kalkınmanın temel hedeflerindendir. Güçlenmiş bir toplum doğal kaynakları tahrip etmeden koruyarak onlardan sürekli yararlanabilme yollarını

bulmalıdır. Kırsal alanın kendi sorunlarını tanımlayıp, dışsal müdahaleye gerek kalmadan bunların çözüm yollarını geliştirebilir (Mutlu, 2002).

Sürdürülebilir Yapılar- Sürdürülebilir Planlama – Sürdürülebilir Kalkınma

Şekil 1 Sürdürülebilir Örnek Köy Modeli İçin Tasarım Önerisi

Çevresel sürdürülebilirlik kavramı, kaynakların özellikle de yenilenemeyen kaynakların korunması ve yönetilmesini içermektedir. Sosyal sürdürülebilirlik kavramı ise; toplumdaki herkes için eşit fırsat yaratarak insan haklarına saygı duymak anlamına gelmektedir. Ekonomik sürdürülebilirlik kavramı, farklı toplum seviyelerinde refah düzeyini ve tüm ekonomik faaliyetlerin maliyet etkinliğini ele alınması anlamına gelmektedir (UNEP/ WTO, 2005; Gurung, 2012).

2. Materyal ve Yöntem

Çalışma evreni olarak Antalya ilinin Serik İlçesi'ne bağlı Akbaş köyü seçilmiştir. Akbaş köyü'nde mevcut konutların durum incelemeleri yapılmıştır. Köyde ki inşaat yapıları tipleri incelenmiştir. Köyde ki mevcut ticari faaliyet türleri ve faaliyetlerin gerçekleştiği inşaatlar tespit edilmiştir. Söz konusu yapıların yöre halkının ihtiyaçlarını karşılayıp karşılamadığı ve beklentileri tespit edilmiştir. Araştırma için yöre halkının görüşleri ve tecrübeleri önemli kaynak olarak değerlendirilmiştir.

Literatür, haritalar, uydu görüntüleri incelenmiştir ve yörede fotoğraf çekimleri yapılmıştır. Yörede yaşayan yerli halkından bilgiler alınmıştır. Köy yönetiminde bulunan muhtardan bilgiler alınmıştır. Ayrıca, yerel halk ve yöneticilerle sorunlar ve çözüm önerileri hakkında görüşmeler yapılmıştır. Yörede geçmişten günümüze kadar olan değişimler hakkında nitel ve nicel bilgiler toplanmıştır. Yörede fotoğraf çekimleri yapılmıştır. Yörede mevcut durum için yerinde inceleme ve kontrol sağlanmıştır. Arazi çalışmaları ile arazi kullanım özellikleri incelenmiştir. Yörede sürdürülebilir mimari ve sürdürülebilir yapı malzemeleri ile sürdürülebilir ekolojik köy önerisi oluşturulacaktır. Yöre mimarisinde inşaat yapılarında modern ve konforlu yapı malzemeleri ile çözüm önerileri sunulmuştur.

Örnek sürdürülebilir köy planlaması için bir sistem yaklaşımı kapsamında model köylerincelenerek yeni ve özgün yapılarla yeni sürdürülebilir köy örneği oluşturulmaya çalışıldı. Yaklaşım kapsamında öncelikle köyün ileri gelenleri ile birlikte köy gezilir, köyde yaşayanlarla görüşülerek ve bazı ailelere konuk olunarak köyün sorunlarının, koşullarının, beklentilerinin ne olduğu, köy halkının gelişimi, iş olanakları, uğraş alanları ve kendine yeterliliği konusunda gözlemler yapılarak köy hakkında ön değerlendirmeler yapılır. Köyde bulunan konutların mevcut durumları tespit edilerek köy halkının ihtiyaçlarını ne derece karşıladığı nelerden rahatsız oldukları ve nasıl yapılar istedikleri konusunda araştırma yapılarak bilgi toplandı. Çalışma kapsamı çerçevesinde köyü temsil edecek bir grup oluşturularak SWOT analizi yapıldı. Yörede fotoğraf çalışmaları yapılarak nitel ve nicel gözlemlemeler yapıldı.

3. Bulgular

SWOT analizi kapsamında saptanan sorunları daha geniş tabana yaymak gerekmektedir. Yöre halkından gelen önerileri geliştirmek, yöre halkı ile birlikte ortak çözümler üretmek için belirlenen başlıklarda çalışma grupları (konforlu inşaatlar- konforlu kullanışlı yapılar - altyapı - donanım, tarımsal işletmecilik, turizm, eko köy çalışmaları, ortak geçmiş ve kültür, tarımsal yapılar, yerleşim inşaat alanları ve yeni inşaat malzemeleri ile konforlu yap kültürü, çevre, kırsal görünüm vb.) oluşturulur. Oluşturulan çalışma gruplarında beklentilere dayalı çözüm önerilerinin hayata geçirilmesi ile yöre de nasıl etkiler beklenildiğine dair görüşler alındı.

Kırsal bölgelere çağdaş bir görünüme kavuşmak amacıyla örnek sürdürülebilir köy oluşturulmalıdır. Ancak örnek sürdürülebilir köylerin kuruluşunda ve yaşam alanlarının oluşturulmasında köy kültürünün beklentilerinin karşılaması çok önemlidir. Mevcut durumda ihtiyaçların karşılanamadığı gözlemlenmiştir. Gözlemlenen eksikliklerin giderilmesi ve beklentilere cevap verebilmek açısından örnek sürdürülebilir köy tasarımları için proje geliştirilebilir. Farklı projeler üreterek farklı bakış açılarını inceleyerek en verimli çalışmayı seçebilmek adına proje yarışması yapılabilir. Söz konusu tasarım yarışmasının ana teması köylüyü ve köyü inşaat bakımından iyi etüt ederek yapılacak olan masrafların en verimli şekilde değerlendirilmesidir. Bu bağlamda Akbaş Köyü için oluşturulması gereken inşaat alanları üniteler şeklinde tasarım sıralamasına göre;

1.Eğitim Yapıları Ve Uygulama Bahçesi
2.Öğretmen evi
3. Konuk odası
4.Kütüphane – Bilgi Merkezleri- Okuma Odası
5.Konferans salonu
6.0tel-Bungalov Evler
7.Çocuk bahçesi
8.Köy parkı
9.Sağlık kuruluşları
10.Hayvan sağlık korucusu
11.Sosyal kurumlar
12.Tarım ve köy el işleri müzesi
13.Gençler kulübü
14. Hamam
15.Dini İbadethane-Cami
16. Rekreasyon Alanları
17.Kooperatifler
18.Köy dükkânları
19.Spor alanı
20.Damızlık Tavuk, Tavşan, Arı istasyonları
21.Damızlık ahırı
22.Kesimhane
23. Mandıra
24.Asri mezarlık
25.Hayvan Mezarlığı
26.Yem bitkileri arazisi
27.Koruluk
28.Köy hayvan gübreliği
29.Modern ağıl

30.Pazar yeri
31.Panayır- şenlik- festival yeri'dir

Örnek köy uygulamalarında fiziksel planlama olarak köydeki diğer sosyo-kültürel donatılarla birlikte 4 - 5 kişilik ailenin barınabileceği konut ile ona bitişik ahır ve yem depoları tesis edilmiştir. Oluşturulan bu ideal köylerin birer model olarak eski ve geri kalmış köy tipinin yerini alması amaçlanmıştır (Anonymous, 1934).

Turizmin çeşitlendirilmesi ile birlikte yörenin potansiyel özellikleri; doğal güzellikleri dağları, gölet, tarihi özellikleri, bungalov evler yapılarak yörenin doğasında şehir yaşamından uzak doğasına uyumlu uygun konutlar yapılarak turistleri ağırlayabilecektir, çok önemli değere sahip olan mağarası, safari turları ile doğada özel geziler planlanarak ülke genelinde ve yurtdışından gelen turistlere tüm yıla yaygınlaştırılan etkinliklerle pek çok alternatif türler geliştirilmeye çalışılmıştır. Çevrenin korunmasında turizmin fiziksel planlamasının önemi oldukça büyüktür. Sürdürülebilir turizmin geliştirilmesi için turizmin fiziksel planlamasında mekanın rasyonel şekilde kullanılması gerekmektedir.

Köy yerleşimini yeniden düzenlemeye yönelik planlamalar kapsamında yani turizm köyleri oluşturmaya yönelik çalışmalarda köyün kültürü, gelenek ve görenekleri ile mimari biçimi korunmalıdır yeni konforlu yapı malzemeleri ile mimarisine uygun olarak restorasyon yapılmalıdır. Yeni yapılacak olan yapıların eski mimariye uygun olarak tasarlanması ve uygun yapı malzemeleri seçimi tapılarak sürdürülebilirlik sağlanması gerekmektedir.

Akbaş köyünde konut kullanımı tarım ve hayvancılık faaliyetleri için konut tipleri ve kullanılan yapı malzemeleri;

Köyde 200 konut bulunmaktadır. Köyde bulunan en yaslı ev 80-100 yas aralığında 50 adet ev bulunmaktadır. Bu eski kevler- konutlar ayakta olmasına rağmen terk edilmiştir. 20-25 yıldır bu konutlarda yaşam sürdürülmemektedir. Taş duvar örgü yöntemi kullanılmıştır. Bu konutların üst kısmı ahşap çatı şeklinde yapılmıştır. Değişik konut planları olmasına rağmen en yaygın görülen konut tipleri 2 odalı ve 4 odalı olanlarıdır. 2 odalı ev tipinde; 1 oda gündüzleri oturmak geceleri yatmak amacı ile dizayn edilir gömme dolaplar bulunmaktadır. Bu gömme dolaplar el işçiliği ile oyularak ve boyanarak yapılmış özel üretimlerdir. Diğer oda ise ekmek pişirmek için mutfak niteliğinde dizayn edilmiştir fakat ihtiyaca göre zaman zaman yatak odası olarak ta kullanılabilmektedir. Wc ve banyo ev dışında bahçede konumlandırılmıştır. Bunun sebebi ise evde temizlenme ve arınma mekanlarının bulunmaması gerektiği düşüncesidir.1990'lı yıllardan itibaren bu görüş değişerek wc ve banyolar ev içerisine dahil edilmeye başlanmıştır. (Arıcı, 2021)

Şekil 2'de geleneksel konut tipinde tek katlı ev tipine ait görseller bulunmaktadır. Wc nin dışarıda konumlandırıldığı üçüncü resimde görülmektedir.

Geleneksel Köy Evi Tek Katlı

Şekil 2 Geleneksel Köy Evi Tek Katlı (Arıcı,2021)

Diğer geleneksel konut tipi;4 odalı ev tipinde ise genellikle 2 aile birlikte yaşamaktadır. 3 oda gündüz zaman diliminde oturmak için kullanılırken geceleri yatak yapılarak yatak odası şeklinde kullanılmaktadır. Yine 1 oda ekmek pişirmek için ve ateşte yemek pişirmek için, ısınma amaçlıda kullanılmamaktadır. Wc ve banyo dışarıda bahçede konumlandırılmış. Bu konutların ön kısmında konuta bitişik şekilde 20m2 ve 40m2 lik arasında değişen köşk şekilde adlandırılan geniş ferah oturma alanları tasarlanmıştır. Bu köşk adı verilen oturma alanında yaz aylarında yataklar ile uyumak içinde kullanılabilirken yemek yeme, oturma gibi fonksiyonel amaçlar içinde kullanılırdı. Her evde muhakkak büyük yada küçük bir adet hayvan ahırı bulunmaktadır. Kışları ısınma ihtiyacı konutlarda soba kullanılır. 200 adet hayvan ahırı bulunmaktadır. Aşşağıda (şekil 3'de) geleneksel konut tasarımını görmekteyiz yöresel malzemeler kullanılmıştır. Zamanla terk edilerek kullanım dışı kalmasına rağmen köy dokusunda köy kimliği hakkında bilgi veren önemli bir kültürel değer olarak kalmıştır. Söz konusu yapıda geleneksel yapı malzemelerinin yöre halkında ki kullanım talebine kendi imkanları ile tasarlanarak kendi işçilikleri ile yöresel malzemelerin harmanlanarak hizmete sunulmuş olması köy kimliğini tanımak için farklı bir değer daha kazanmasına yardımcı olmaktadır. Söz konusu yapının artık hangi amaçlara hizmet etmediğinin belirlenerek yöre halkının konutlardan beklentilerini tespit edilmesi içinde önem arz ettiğini görmekteyiz.

Geleneksel Köy Evi 2 Katlı

Şekil 3 Geleneksel Köy Evi 2 Katlı (Arıcı,2021)

Geleneksel köy evinde zaman içerisinde yetersiz kalması sonucu ile konuta ekleme yapılmıştır. Fakat bu yapılan ekleme konutun kendi geleneksel malzemeleri ile yapılmadığı için konutun kimliğini kaybetmesine neden oluştur. (şekil 4) Söz konusu durumlar için bilinç oluşturulmalıdır. Kültürel değerin korunarak geleneksel konut tiplerinde uygun yapı malzemesi seçilmesi uygun işçilik kullanılması çok önemlidir. Geleneksel konut tiplerinde yapının dokusu ve tasarımına uygun restorasyon yapılmalıdır. Yapılacak olan eklemelerde uygun prosedürler sonucunda uygulamaya geçirilmelidir.

Geleneksel Köy Evi

Şekil 4 Geleneksel Köy Evine Sonradan Betonarme Ekleme Yapılmıştır(Arıcı,2021)

Köyde bulunan 100 yıldan daha uzun bir geçmişe sahip olan köy camiisi restorasyon çalışmaları yapılmamıştır. Mevcut durumda şadırvanlar yetersiz kalmıştır. Dini ibadethane yetersiz kalmaktadır. Camiide yalıtım bulunmamaktadır. Yazın oldukça sıcaktır. Termal konfor bulunmamaktadır. Kış şartlarında ılık bir iklim olmasına rağmen termal konfor bulunmaması kullanıcılar için olumsuz etki yaratmaktadır. Camii içerisinde uygun restorasyon çalışmaları yapılmalıdır. Camii dışında avluda ise daha fonksiyonel bir ortam tasarlanmalı uygun yapı malzemeler kullanılmalıdır.

Köy Camii

Şekil 5 Köy Camiisi Görüntüleri (Arıcı,2021)

Köyde bulunan Zeytintaşı mağarasının oluşumunun yaklaşık olarak 14 milyon yılda tamamlandığını belirlendiğini belirtti mağaranın tanıtımını yapan yetkililer. Mağara içerisinde karbondioksit oranının belirli düzeyde kalması gerekmektedir. Karbondioksit oranı arttığı zaman mağara içersinde deformasyonlar oluşmaktadır. Bu nedenden dolayı belirli süre içersinde belirli ziyaretçileri ağırlayabilmektedir. Mağara içersinde kamera ve dijital çekimlere izin verilmemektedir. Mağara için gelen ziyaretçilerin bekleme sırasında rahat ve konforlu bir ortamda zaman geçirebilmeleri için uygun cafe restoran ve bekleme salonları bulunan yapılar inşaa edilmelidir. Mevcut durumda ziyaretçilerin kaliteli zaman geçirebileceği ortamlar bulunmamaktadır. Söz konusu eksiklik köyün sürdürülebilirliğini etkileyen önemli bir eksikl iktir.(Şekil 6)

Zeytintaşı Mağarası

Şekil 6 Zeytintaşı Mağarası Dış Görünüşleri (Arıcı,2021)

4. Tartışmalar ve Sonuçlar

Akbaş köyü'nde sürdürülebilir ekolojik köy olarak planlama yapılabilir ve ekolojik turizm, doğa ile iç içe ve atıksız bir yaşam elde edilebilir.

Şehir yaşamından uzaklaşarak doğa ile iç içe sağlıklı bir yaşam sürmek isteyenler için özel bir altarnatif sunabilecek potansiyele sahiptir. Söz konusu özelliği ön plana çıkartacak tasarımlar ile sürdürülebilir eko köy örneği teşkil edecek tasarımlar geliştirilmelidir.

En önemli doğal kaynaklarımızdan birisi olan tarım topraklarımızın amaç dışı kullanımı kesinlikle önlenmeli, bu konuda arazi sahipleri bilinçlendirilmeli, tarım dışı yatırım ve hizmet girişimlerinin verimli arazi dışındaki alanlarda konumlandırılması teşvik edilmelidir.

Sürdürülebilir ekolojik köy kapsamında otel ve bungalov evlerin eğlence ve aktivitelerini gerçekleştirerek sosyalleşebilecekleri cafe-restoran ve eğlence alanları, dini ibadethaneler, sağlık kuruluşları, kamu yapıları, eğitim yapıları, kütüphane gibi bilgi merkezleri, spor ve rekreasyon alanları yürüme ve erişim mesafesinde özgün ve sürdürülebilir tasarımlar yapılarak uygun yapı malzemeleri kullanılmalıdır. Kullanılacak olan yapı malzemelerinde ısı yalıtım ve nem yalıtımına özellikle dikkat edilmesi gerekmektedir. Akdeniz bölgesi ve Antalya ilinin nemli hava koşullarında yapıyı güvende ve konforda uzun süre kalmasını sağlayacak şekilde dizayn edilmelidir.

Doğa ile uyumlu, sürdürülebilir ve ekolojik yaklaşım için uygun temalar seçilmelidir.

Söz konusu çalışmada önerilen eko-köy yorumlarının günümüzün ekolojik ve toplumsal sorunlarına bir çözüm modeli olarak, Türkiye'de eko-köy uygulamalarına örnek teşkil edileceği ve eko- köy bilincinin gelişesine katkı sağlayacak nitelikte olmalıdır.

-İnsan kaynaklarının geliştirilmesi açısından özellikle teknolojik altyapı hizmetleri ile birlikte kırsal alan fiziksel altyapı hizmetleri etkinliği arttırılmalıdır. Bu bağlamda örnek köy modelleri oluşturulmalıdır.

- Köyün mimari kültürü korunarak gerekli restorasyonlar çalışmaları yapılmalıdır.
- Köyün alt yapısı (içme ve kullanma suyu, kanalizasyon sistemi, ulaşım ağları) sistemleri planlanmalı, geliştirilmelidir.
- Köyün kültürü ve mimarisine yönelik yeme içme ve de konaklama tesisleri oluşturulmalıdır.
- Köyün ilçe ve il merkezleri ile ulaşımı düzenlenmeli ve çevre ilişkileri geliştirilmelidir.
- Mağara çevresinde uygun cafe- restoran ve bekleme alanları inşaa edilmelidir. Yapılacak olan inşaatlarda yalıtım özelliği ve fonksiyonel kullanım özelliğine dikkat edilmelidir.

Teşekkürler

Referanslar

Ayşe ARICI,(2021antalya- Serik-Akbas Köyü'nün Yeniden İşlevlendirilerek Post Covıd Veya Salgın Hastalıklar Döneminde Sosyal Mesafeli Sürdürülebilir Konaklama Amaçlı Ekolojik Köy Önerisi 13- 14 Temmuz-2021 Uluslararası Fen Ve Uygulamalı Bilimler Kongresi Adıyaman-Türkiye

Anonymous, 1934. 2510 Sayılı İskân Kanunu.

Gülçubuk, B., (2007.) Uluslararası Tarım Politikalarının Kırsal Yoksulluk Üzerine Etkileri. Ulusal Tarım Kurultayı, 15–17 Kasım 2006, Adana.

Gurung L. (2012). Exploring Links between Tourism and Agriculture in Sustainable Development: A Case Study of Kagbeni VDC, Nepal. Master thesis (unpublished), Lincoln University, Faculty of Environment, Society and Design Department of Social Sciences, Parks, Recreation, Tourism and Sport Christchurch, Canterbury, New Zealand, 138 p

Mutlu, N.,2002. Avrupa Birliği ve Türkiye'de Kırsal Kalkınma Politikaları. Güneydoğu Anadolu Projesi Bölge Kalkınma İdaresi Başkanlığı. Ankara.

Şahinkaya, S., 2008. İdeal Cumhuriyet Köyü "Cumhuriyeti Kuranların Tahayyülüne Bir Örnek''.Mülkiye Dergisi, Cilt:XXIV, Sayı:225, Ankara.

Moving Towards Sustainable Construction: A primitive transitional guide

Hagar Ali LABIB[1*], Gökhan GELISEN[2*]

Abstract: This research clearly defines the concept of sustainability and its historical traces as it highlights the significance of sustainability, sustainable development, and sustainable construction. Furthermore, this research aims to provide solutions and alternatives that aid in transitioning towards sustainable construction through gradual and progressive alterations that act as a primitive guide to help achieve the purpose of recognizing the environment and its exhaustible resources.

Keywords: Sustainability, Sustainable development, Sustainable construction, Environment, Construction, Renewable energy, Recycling, Energy efficiency.

Introduction

The definition of sustainability is not as relatively straightforward as it might seem, likewise with the definition of sustainable development. The fact that there are hundreds of distinct definitions for what defines sustainability and sustainable development is a good illustration of this. The indefinite ability to persist substantially throughout many realms of life is referred to as sustainability. It refers to the capacity of the Earth's ecosystem and human civilization to coexist in the twenty-first century.

On the other hand, Sustainable Development has been the current development catchphrase during the last few years. It has been adopted as the new development paradigm by a wide variety of nonprofit and governmental organizations. Sustainable development is a framework for achieving human development goals while also preserving natural systems' ability to supply the natural resources and ecosystem services that the economy and society rely on.

In simple words, the key to the survival of all human beings on this planet is sustainability. At the same time, sustainable development is the development that satisfies current demands without jeopardizing future generations' capacity to meet their own. Sustainability refers to the Earth's inherent life-supporting system's capacity to adapt to changing conditions. Human activities have a significant impact on the Earth's natural environment and ecosystem.

[1] Bahcesehir University, Faculty of Engineering and Natural Sciences, Civil Engineering Department, Construction Management Program, Istanbul, Turkey

[2] Bahcesehir University, Faculty of Engineering and Natural Sciences, Civil Engineering Department, Istanbul, Turkey

* Corresponding author: hagar.alilabib@bahcesehir.edu.tr_gokhan.gelisen@eng.bau.edu.tr

Therefore, these activities should be conducted without deteriorating or degrading the quality or function of the biological system.

In civil engineering and construction management, the concept of sustainability is becoming more prevalent. Construction engineering and management encompass all stages of a building's life cycle, such as design, construction planning and management, construction works, maintenance, and rehabilitation of structures or infrastructure items.

When it comes to new constructions, sustainable construction involves the use of renewable and recyclable materials while also decreasing energy usage and wastage. Thus, the main objective of sustainable building is to mitigate the industry's environmental effect. This research aims to provide steps and solutions for moving towards sustainable construction through gradual and progressive alterations to achieve the purpose of recognizing the environment and its definite resources.

Sustainability Traces and Background

From the dawn of civilization to the present, the history of sustainability tracks human-dominated ecological systems. This history is marked by a society's growing regional prosperity, followed by crises that were either addressed, resulting in sustainability, or not, resulting in decline.

Since the 18th century, interest has been increasing in the environment. The conception of the idea of "sustainability," or "Nachhaltigkeit" in German, can be traced back to Hans Carl von Carlowitz between 1645–1714. Carlowitz suggested proposals for the forest's "sustainable use." His belief that just as much wood should be harvested as can be regrown through planned or organized reforestation initiatives became a guiding concept in contemporary forestry.

Coal was utilized to power increasingly efficient engines and, eventually, to create electricity. In the mid-twentieth century, a growing environmental movement highlighted that the numerous material gains that were now being experienced had ecological consequences. The energy crises of 1973 and 1979 revealed how reliant the global society had become on nonrenewable energy supplies.

The threat presented by the human-induced increased greenhouse effect, primarily caused by forest clearance and the combustion of fossil fuels, is becoming more widely recognized in the twenty-first century.

Sustainable Construction

The technique of building a healthy environment based on ecological principles is known as sustainable construction. According to Professor Charles J. Kibert, sustainable building is based on six principles: "conserve, reuse, recycle/renew, protect nature, develop non-toxic and high-quality materials." Furthermore, sustainable construction should not cease once construction is over; the structure should have a lower environmental effect during its lifecycle. This indicates that components in the building design should have a long-term positive impact on the building's ecological impact. Proper insulation to minimize heat loss, solar panels to reduce energy use, and long-lasting building materials are just a few examples.

The objective of sustainable construction is to decrease the industry's environmental effect by implementing sustainable development methods, increasing energy efficiency, and deploying green technologies. Although many various business sectors are striving to become far more sustainable, the construction industry is unique. It could have a substantial impact on how these practices are implemented. This is due to the industry's enormous use of resources and energy. Below are few methods that can be followed or taken as a guide towards transitioning into sustainable construction.

Training Employees

Sustainability starts with proper awareness and education. Construction companies must invest in staff training to keep up with new methodologies, insights, and strategies used on their projects. In addition, employee skills must be improved in concert with technology and procedures as the sector moves towards a digital future. Not only will this boost employee productivity and performance, but it will also upsurge job satisfaction and workplace contentment.

Embodied Carbon Mitigation

Embodied carbon is the total influence of a material's greenhouse gas emissions across its entire life cycle. Embodied carbon contributes to more than 10% of total global greenhouse gas emissions. Embodied carbon is estimated to account for nearly half of all new construction emissions between now and 2050. Concrete, steel, and ceramics are the materials that consume the most embodied carbon. As a result, substituting concrete with fly ash on a construction site can reduce embodied carbon.

Modernized construction methods

Modern construction methods aim to be more sustainable since they are dedicated to saving money, increasing delivery and construction speed, and avoiding budget overruns. On a project, there is a range of approaches that may be used. Floors, walls, and roofs, for example, can be manufactured in factories and delivered to the job site. Modular construction is comparable to traditional construction, except it entails fabricating prefabricated rooms in a factory environment that may be joined to make a complete structure. This could possibly mitigate above 50% of the wastage generated by conventional methods.

Management and Waste Reduction

Construction organizations can still save money and materials by employing prefabricated parts since components are manufactured off-site and, in an environment, where leftover materials can be readily recycled. In addition, companies will pay less for waste services as a result of this method.

Additionally, Incineration is another option for getting rid of wastage. This is especially beneficial for hazardous chemicals since it eliminates the risk of contamination in the surrounding area. While Incineration can result in CO2 emissions, the gas can be stored in subterranean spaces, and the heat generated by burning can be utilized to generate power or heat water. Finally, the resulting or the end product fly-ash can be used for manufacturing purposes. In fact, fly-ash has been proven to act as an excellent cement substitute in concrete.

Renewable and Recyclable materials

Sourcing environmentally friendly materials might be challenging; however, it is not impossible. Timber and recyclable materials such as concrete, metals, plastics, rubbers, and composites are among these materials. In addition, several forms of renewable materials are employed in various end-use applications to decrease the detrimental impacts on the environment.

Insulation materials, light structural walls, natural paints and finishes, thatch, and geotextiles are all made from crop-based renewable resources. As all-natural, renewable, and efficient insulating materials, various sustainable materials such as Rockwool, sheep's wool, and recycled paper are employed. For example, Rockwool, produced from molten stone, saves 100 times the amount of CO_2, SO_2, and NO_2 emitted during its manufacture.

Virtual meetings, data and video sharing between stakeholders

The current COVID-19 pandemic has caused many people to work from home and use video conferencing services to communicate. Continuing to participate in virtual meetings after returning to work can help decrease carbon emissions by reducing travel. Of course, some site visits will inevitably be necessary, but for those who aren't, virtual meetings can assist in minimizing carbon emissions while also saving time when sharing information. In addition, without needing to travel to the project site, video conferencing may be utilized to view the equipment or the data as a team.

Utility Usage Tracking

Utility usage tracking is critical for identifying essential cost sinks and carbon sources on a building site. Furthermore, documenting information regarding gasoline and gas is crucial since it has a more significant impact on a job site than other utilities. Several online tools, such as Green Badger, may be used to track water, energy, and trash across multiple building sites to see where substantial improvements might be made.

Discouraging the Use of Paper Blueprints Drawings and Specs

Although it may appear trivial, avoiding the usage of paper blueprints, drawings, and specifications may save a significant number of trees. But, most significantly, it will save a lot of time, cut down on material waste, and speed up the completion of the project. It is highly recommending to invest in construction management software instead of utilizing paper. Users may use this software to arrange the entire construction project, calculate and regulate various costs, manage the portfolio and documents, assess risk, and follow the project's progress, among other things. Most businesses provide cloud-based solutions that allow on-site and off-site employees to communicate in real-time. The project will undoubtedly have a beneficial influence on the environment due to greater on-site productivity and decreased waste.

Encouraging the use of Energy-Efficient Construction and Material Handling Equipment

Using energy-efficient construction and material-handling equipment is yet another method to assure sustainability. Reduce energy waste by using the appropriate equipment. You may prevent squandering fuel, for example, by using a suitable on-site generator. Similarly, energy-efficient overhead cranes and other construction equipment may be used. However, repairing and maintaining energy-efficient construction equipment can be challenging. In

addition, handling such equipment may need further training for the employees. That is why you should always purchase equipment from local suppliers familiar with local rules, weather conditions, and material handling needs.

Monitoring Transportation

One of the most critical on-site construction operations is transportation. A transportation management system may be implemented to decrease the transportation fleet's carbon impact. It will allow tracking drivers and their driving habits, setting speed limits, planning the optimal routes, and doing real-time preventive maintenance. All of these elements will aid in the reduction of air pollution.

Conclusion

The significance of sustainability, sustainable development, and sustainable building is highlighted in this research, which clearly explains the concept of sustainability, sustainable development, and its historical origins. Furthermore, the objectives of this research were to offer solutions and alternatives that will assist in the transition to sustainable construction through gradual and incremental changes that can positively impact the environment. Sustainability refers to the Earth's inherent life-supporting system's capacity to adapt to changing conditions, and the key to the survival of all human beings on this planet is sustainability. At the same time, sustainable development is basically the development that satisfies current demands without jeopardizing future generations' capacity to meet their own.

In civil engineering and construction management, the concept of sustainability has been becoming more prevalent. The technique of building a healthy environment based on ecological principles is known as sustainable construction. The objective of sustainable construction is to decrease the industry's environmental effect by implementing sustainable development methods, increasing energy efficiency, and deploying green technologies.

Several methods can be followed or taken as a guide towards transitioning into sustainable construction. This includes employee training, mitigating embodied carbon through the replacement of cement with a byproduct such as fly-ash, following modernized construction methods, managing and reducing waste, usage of recyclable and renewable materials, tracking utility, **discouraging the use of paper blueprints drawings and specs, encouraging virtual meetings and the** use of Energy-Efficient Construction and Material Handling Equipment and finally, monitoring transportation to enhance time and waste management. Historically, the construction sector has been seen as a major polluter of the environment. The construction sector, on the other hand, is striving to develop more sustainable building methods. As a result, construction trucks, equipment, and building materials are becoming more energy-efficient and environmentally friendly.

References

10 Ways to Green Up Your Construction Site. Sustainable Investment Group. (2020, April 30). https://sigearth.com/10-ways-to-green-up-your-construction-site/.

10 ways to make construction more sustainable. List secondary lists page | Construction Global. (n.d.). https://constructionglobal.com/top10/10-ways-make-construction-more-sustainable/modern-construction-methods.

BigRentz, I. (2021, April 19). HOME. BigRentz. https://www.bigrentz.com/blog/sustainable-construction.

Glick, V. (2019, May 20). Building a Better Tomorrow: 6 Ways to Create a More Sustainable Construction Site. construction21.org. https://www.construction21.org/articles/h/building-a-better-tomorrow-6-ways-to-create-a-more-sustainable-construction-site.html.

Hans Carl von Carlowitz and "Sustainability." Environment & Society Portal. (n.d.). http://www.environmentandsociety.org/tools/keywords/hans-carl-von-carlowitz-and-sustainability.

Lélé, S. M. (1991). Sustainable development: a critical review. World Development, 19(6), 607-621.

Sustainability and Sustainable Development. Circular Ecology. (2020, May 17). sustainable construction. British. (n.d.). https://www.british-assessment.co.uk/insights/what-is-sustainable-construction-and-why-is-it-important/.

Sustainable Development. International Institute for Sustainable Development. (2013, January 6). https://www.iisd.org/about-iisd/sustainable-development

https://circularecology.com/sustainability-and-sustainable-development.html.

What is sustainability? What is biomimicry? Explain why learning from the earth is a key to learning how to live more sustainably. Bartleby learns. (n.d.). https://www.bartleby.com/

Why Is Sustainability Important?: BluGlacier - Top-quality salmon producer. BluGlacier. (2021, March 11). https://bluglacier.com/why-is-sustainability-important/.

Wikimedia Foundation. (2021, May 10). History of sustainability. Wikipedia. https://en.wikipedia.org/wiki/History_of_sustainability.

Wikimedia Foundation. (2021, June 14). Sustainability. Wikipedia. https://en.wikipedia.org/wiki/Sustainability.

Zavadskas, E. K., Šaparauskas, J., & Antucheviciene, J. (2018). Sustainability in construction engineering.

Relationship and Differences Between Leadership and Management in Construction

Hagar Ali LABIB[1*], Gökhan GELISEN[2*]

Abstract: This research clearly defines leadership and management in construction management as it investigates the relationship, attributes, and differences and the link that binds them both. The goal of this research is to convey a fundamental comprehension of the contrasts between managers and leaders while examining the characteristics of an ideal leader in order to achieve success in construction management.

Keywords: Leadership, Management, Construction, Motivation, Delegation.

Introduction

What is leadership? This is a quite simple question that, despite its simplicity, it continues to be a source of consternation for both experts and non-experts.

It is prevalent to encounter the misconception between a leader and a boss. It mainly refers to seniority or a particular person's position in the hierarchy of a company or an organization. When the word "leader" is mentioned, it is typical for people's first thoughts to divert towards a domineering, bossy, or senior executive kind of individual. However, this is not the case because there is quite a difference between a manager and a leader. In simple words, according to the Oxford Languages dictionary, it can be agreed that a leader is said to be someone who leads a specific group or an organization.

Whereas leadership is best described as a process of social influence, which maximizes the efforts of others towards the achievement of a goal (Kruse, April 2013). Nevertheless, a 'leader' or 'leadership' has several definitions that will be discussed later in depth in this research. On the other hand, a manager, by definition, is said to be an individual who is in charge of a worker, group of people, or organization according to Oxford Languages. To elaborate, a manager is a person who is usually responsible for other staff members, commands or gives orders, and is held accountable for company goals and developing employees. Basically, a manager manages their employees, while a leader inspires them to innovate, think creatively, and strive for perfection. The ability to properly lead and manage in the construction business is vital as it aids in evading negative issues that may arise during a project's life cycle. This research intends to deliver a genuine understanding of the differences between a boss and a leader while discussing an ideal leader's attributes to achieve success in construction management.

[1] Bahcesehir University, Faculty of Engineering and Natural Sciences, Civil Engineering Department, Construction Management Program, Istanbul, Turkey
[2] Bahcesehir University, Faculty of Engineering and Natural Sciences, Civil Engineering Department, Istanbul, Turkey
* Corresponding author: hagar.alilabib@bahcesehir.edu.tr_gokhan.gelisen@eng.bau.edu.tr

Management in Construction

Management is the coordination and organization of assignments to accomplish an objective. The management activities include determining corporate strategy and coordinating the efforts of employees to achieve these goals with the help of available resources. Additionally, in a company or an organization, management could also refer to the seniority structure of employees.

Construction management is a branch of civil engineering known as a profoundly proficient framework intended to work with planning, coordinating, and controlling a construction project from commencement to completion. It is the role of the construction manager to work as a leader throughout the life of the construction project. This is because working as a leader allows the construction manager to efficiently and effectively plan, monitor, and control the progression of a construction project.

A construction manager's need for leadership ability depends on the tasks, teams, organizational environment, manager's capabilities, project resources, available time, and budget.

Leaders versus Managers

Over the past decades, one of the reoccurring questions has been the difference between managers and leaders. There is no direct straight-line answer for that; however, this research intends to compare and contrast management versus leadership skills by exploring their similarities and differences to provide a clear picture to the reader. It's important to note that there is no such thing as a hundred percent manager or a hundred percent leader. It's the job of the construction manager to do a little bit of both.

Managers are clearly in managerial positions since they are tied to an official position, whereas leaders can lead anywhere. A leader should lead by example by motivating their team and inspiring them to move forward towards the set goals. Managers tend to have more of a controlled mindset, and they tend to focus more on the administration of processes, the structure, the resources of the organization. They are very much into maintaining their status quo as maintenance plays a crucial part in their work. They also tend to be very task-focused. So overall, managers work on day-to-day tasks and making sure all the activities get accomplished in an orderly fashion. Leaders, however, can be slightly different since their approach to pursuing goals can vary from managers. Leaders can be inclined to have a more persuasive approach to communication rather than controlling.

According to Bill Hybels, leaders are also focused on taking the organization from 'here' to 'there.' This basically means casting a vision by setting goals for the team members to get from point A to point B for the betterment of the organization. Leaders are also known for taking risks; instead of maintaining their status quo and keeping the working environment running under steady conditions, they try to stretch the organization past what its currently doing, which usually involves taking risks. Additionally, Leaders are inclined to be people or relationship-focused as they mentor, coach, and teach. It can be noticed that most of the leadership skills mentioned above, such as persuasive communication, take the organization from 'here' to 'there' through casting a vision well as relationship-focused approach are all communication-centric, which means that a leader must have outstanding and sophisticated

communication skills to practice those leadership functions well. As mentioned above, nowadays, it's quite essential to be a good manager as a good leader.

Managerial and Leadership Skills

In simple words, leadership is the process or the action of leading a group of people towards a common goal. Being a leader means one is required to inspire, motivate and encourage. Some of the top leadership skills that leaders are required to have will be discussed below.

Leaders tend to communicate with any group effectively as they have outstanding communication skills. They are inclined to motivate and inspire their team members towards the success of the organization. Leaders have proficient delegation skills as they tend to delegate certain activities best suited or done best by someone else. They encourage a positive environment even at the worst times since positivity leads to measurable performance improvement. They represent trustworthiness since trust is the glue that binds the leader to their team members or followers as it brings forth the capacity for organizational and leadership success.

 Additionally, one of the crucial characteristics of an effective leader is promoting creativity. It fosters a prosperous and healthy workplace environment. It opens up opportunities in problem-solving, achieving goals, and inspiring teams to be creative and find unlikely perspectives. One of the advantages of being a leader over a manager is that leaders are more likely to feed the behavior of giving constructive feedback rather than destructive feedback without offending any team members. Moreover, leaders take responsibility for actions and performance. A responsible behavior combined with a responsible attitude gives the leader powerful influence and accelerates their leadership growth.

Last but not least, leaders are quite committed to their team, work, and the organization. This is because commitment is a trait of leadership that motivates and draws others. It demonstrates that the leader is committed to the cause and believes in it. Before they believe in the vision, a team will believe in the team leader. Commitment is a heart issue. Finally, leaders are flexible and adaptable. This is because leaders with an elastic cognitive style can employ various thinking processes and mental frameworks. Leaders may better understand how their team thinks and feels and how their customers believe by increasing their awareness and perspective.

On the other hand, while leadership is the process or the action of leading a group of people towards a common goal, management is the process of dealing with or controlling things or people. And while it's the leader's job to inspire, motivate and encourage, it's the manager's job to plan, organize and coordinate. Some of the top managerial skills would start with interpersonal skills. Interpersonal communication skills are quite vital since they could help the manager become more productive at work, create solid and constructive connections with coworkers, and execute team tasks efficiently. Strong interpersonal skills could significantly affect the confidence and efficiency of the entire team or department.

Like leaders, managers are expected to communicate, motivate, and delegate effectively with their team members. Managers are expected to forward a plan by thinking ahead and the organization's path to ensure it's on the right track towards achieving its next goal. Besides, managers are supposed to have efficient organizational skills such as time management, scheduling, prioritization through to-do and to-don't lists, project management skills,

continuous communication, multi-tasking, and flexibility and adaptation are all examples of organizational abilities. Mangers are more likely to adopt a strategic thinking behavior. It aims to identify and create unique possibilities to generate value by facilitating a provocative and innovative debate among those who could influence its performance, such as the board of directors and management.

Furthermore, managers are expected to have analytical and robust problem-solving skills since the managerial problem-solving operation is a non-stop cycle of planning, doing, checking, and acting while keeping an eye on the issue and the results. Managers alter their plans as required so that the team may continue to work toward a solution that will lead to improved company results. Last but not least, managers tend to have commercial awareness. Commercial awareness is the capacity to comprehend what makes a company or organization prosperous, whether via the purchase or sale of goods or the provision of services to a market.

Business awareness or organizational awareness are other terms for commercial awareness. Lastly, a good manager is required to be a mentor since mentoring is essential in management. It is mainly about assisting team members in becoming more productive. It's a mentoring relationship that aims to provide the mentee/team member the confidence and support they need to take charge of their growth and job.

Conclusion

This research intends to deliver a genuine understanding of the differences between a boss and a leader while discussing an ideal leader's attributes to achieve success in construction management. The ability to properly lead and manage in the construction business is vital as it aids in evading negative issues that may arise during a project's life cycle. Leadership is the act of leading a group of people by inspiring, motivating, and encouraging them. In contrast, on the other hand, managing focuses on planning, organizing, and coordinating people. Managers are clearly in managerial positions since they are tied to an official position, whereas leaders can lead anywhere. Managers and leaders have several skills that they share in common: motivation, delegation, and effective communication. Finally, a leader is required to have outdating leadership and managerial skills. Leadership and management can't replace one another, and in today's world, it is crucial to find the proper combination of being a little bit both.

"Leadership is the art of getting someone else to do something you want to be done because he wants to do it" Eisenhower, D. D. (2012)

"Management is doing things right; leadership is doing the right things." Peter, D. (2009)

References

2011-2021, (c) C. skillsyouneed.com. (n.d.). Developing Commercial Awareness. SkillsYouNeed. https://www.skillsyouneed.com/general/commercial-awareness.html.

6 Essential Organizational Skills for Leadership Success - mysimpleshow. simpleshow video maker. (2018, April 17). https://videomaker.simpleshow.com/6-essential-organizational-skills-leadership

Drucker, P. (2009). Management is doing things right; leadership is doing the right things. In US Naval Institute Proceedings (Vol. 135, No. 4, p. 96).

Everything You Need To Know About the Importance of Interpersonal Communication at Work. Indeed Career Guide. (n.d.). https://www.indeed.com/career-advice/career-development/importance-of-interpersonal-communication.

Eisenhower, D. D. (2012). Leadership: the art of getting someone else to do something you want to be done because he wants to do it. Leadership.

Gharehbaghi, K., & McManus, K. (2003). The construction manager is a leader. Leadership and management in engineering, 3(1), 56-58.

Kruse, K. (2015, September 2). What Is Leadership? Forbes. https://www.forbes.com/sites/kevinkruse/2013/04/09/what-is-leadership/?sh=685c3cc45b90.

Keating, K. (2021, March 10). 3 Traits of Adaptable Leaders. Main. https://www.td.org/insights/3-traits-of-adaptable-leaders.

Lyon, A. (2017). Management vs. Leadership. YouTube. YouTube. https://www.youtube.com/watch?v=Tddlkly1cC0.

Managers Must Be Effective Problem-Solvers. CMOE. (2019, November 18). https://cmoe.com/blog/managers-must-effective-problem-solvers/#:~:text=The%20managerial%20problem%2Dsolving%20process,them%20to%20better%20business%20results.

Oxford Languages and Google - English. Oxford Languages. (n.d.). https://languages.oup.com/google-dictionary-en/.

Peck, A., Roddy, S., & Clark, E. (n.d.). The Importance of Creative Leadership. The Importance of Creative Leadership | Clutch. co. https://clutch.co/hr/resources/importance-of-creative-leadership.

What is a Boss? Three Types of Bosses. Job Search. (n.d.). https://www.indeed.com/hire/c/info/types-of-bosses.

What is Construction Management? (And Why It Matters): Stonemark. Stonemark Construction Management. (2021, May 24). https://stonemarkcm.com/blog/what-is-construction-management/.

What Is Management? Definitions and Functions. Indeed Career Guide. (n.d.). https://www.indeed.com/career-advice/career-development/what-is-management.

What is 'strategic thinking'? Effective Governance. (n.d.). https://www.effectivegovernance.com.au/page/knowledge-centre/news-articles/what-is-strategic-thinking.

Zenger, J. (2015, July 16). Taking Responsibility Is The Highest Mark Of Great Leaders. Forbes. https://www.forbes.com/sites/jackzenger/2015/07/16/taking-responsibility-is-the-highest-mark-of-great-leaders/?sh=65d3738448f2.

Thermodynamic Assessment of Solar-Driven Rankine Cycle for Supercritical Working Fluids

Serpil ÇELİK TOKER[1*], Gamze SOYTÜRK[1], Hiroshi YAMAGUCHİ[2], Önder KIZILKAN[1]

Abstract: In this study, thermodynamic analysis of transcritical Rankine cycle integrated with evacuated solar collectors operating by various supercritical working fluid types is conducted. In order to examine the performance of the integrated system, the energy and exergy analyses are first made, followed by a parametric study for determining the effect of turbine inlet temperature, solar irradiation, and working fluid on the system performance. Using the meteorological data of Isparta province, the performance of the integrated system has been examined. The results indicate that when the working fluid is taken as N_2O, the performance of the system gets better compared to that based on other types of working fluids. Also, that the highest power generation is calculated for the cycle using R170 with a net power generation of 0.2479 kW, followed by R744. Results show that the highest exergy efficiency is calculated for the system using N_2O as 10.1%.

Keywords: Evacuated U-tube, transcritical Rankine cycle, supercritical fluids, energy.

1. Introduction

An important rise in the world population and technological advances has significantly increased the energy demand. However, fossil fuels used to generate energy are consumed rapidly, and environmental pollution due to this usage rises. In this context, renewable energy resources and innovations are seen to be the primary solution. Solar energy, which is one of the renewable energy sources, has become important due to its features such as sustainability, abundance, and environmental friendliness. Researchers have focused on studies on electricity generation from solar energy in recent years. Within these workings low- temperature solar energy application has been widely developed. There are many thermodynamic cycles such as Organic Rankine, transcritical CO_2 Rankine, and Kalina cycle that operate using low-temperature sources (Mehran et al., 2019).

Work is increasing on transcritical Rankine cycles to improve the performance of energy conversion at low temperatures. The first step when designing a transcritical Rankine cycle is the choice of the appropriate working fluid. Working fluids with relatively low critical temperatures and pressures can be compressed directly to their supercritical pressures and heated to their supercritical state before expansion so as to obtain a better thermal match with the heat source (Kizilkan, 2019). In a transcritical Rankine cycle, the working fluid is heated directly from the liquid state into the supercritical state after passing the two-phase region, which allows it to have a better thermal match with the heat source, resulting in less exergy

[1] Isparta University of Applied Sciences, Department of Mechanical Engineering, Isparta/Turkey
[2] Doshisha University, Department of Mechanical Engineering, Kyoto/Japan
* Corresponding author: serpilcelik@isparta.edu.tr

loss. Furthermore, by avoiding the boiling process, the configuration of the heating system is potentially simplified. Sometimes if condensation temperature is near to critical temperature, then the smaller fraction of heat rejection occurs due to condensation, and the cycle is called as condensation cycle. In this case, sometimes, both pump and compressor are used for the compression process (Dostal, 2006).

There are several general criteria, including physical and chemical characteristics, personal, environmental and operational safeties, design, and economy, that the working fluid should ideally satisfy to be used in power cycle. Several working fluids have been proposed within the last decade (Sarkar, 2015). Various organic working fluids including R23, R32, R125, R143a, R227ea, R234, R236fa, R245fa, R134a, R218, isobutene, propane, propylene, and R170 have been used in the transcritical Rankine cycle (Karellas and Schuster, 2008). Cayer et al. (2010), used CO_2, ethane, R125 as working fluids in the transcritical Rankine cycle. Among various working fluids, CO_2 is a non-flammable and non-toxic fluid and has less influence on the environment and personal safeties than other working fluids (Zhang et al., 2007). Nitrous oxide is another working fluid that has a very similar molecular weight, critical pressure, and temperature causes nearly the similar behavior to CO_2 with respect to system temperature and pressure, properties, and compactness, but it remains largely unexplored (Sarkar, 2015).

Chen et al. (2010), Chen (2010) and Gao et al. (2010) reviewed various working fluids for transcritical Rankine cycle and used various selection criteria such as physical and thermodynamic properties, efficiencies, turbine shape factor, stability of the fluid and compatibility with materials. Zhang et al. (2007), have also conducted research on the supercritical CO_2 power cycle. Their experiments revealed that the power generation efficiency was 8.78% to 9.45%, and the COP for the overall outputs from the cycle was 0.548 and 0.406, respectively, on a typical summer and winter day in Japan. Karellas and Schuster (2008), organic fluids like isobutene, propane, propylene, difluoromethane, and R-245fa have been suggested for the supercritical Rankine cycle. They concluded that supercritical fluids could maximize the efficiency of the system. Gu and Sato (2001), used propane, R125 and R134a as the working fluids in the transcritical power cycle and showed that propane and R-134a are appropriate working fluids of supercritical cycles for geothermal binary design. Various working fluids, including R23, R32, R125, R143a, R227ea, R234, R236fa, R245fa, R134a, R218, isobutene, propane, propylene, and R170 have been used in the transcritical Rankine cycle.

In this study, thermodynamic analysis of a transcritical Rankine cycle integrated with evacuated tube solar collectors operating by various working fluid types is conducted. In order to examine the performance of the integrated system, the energy and exergy analyses of the system are conducted. After that, parametric analysis is performed to examine the variation of system performance with solar radiation values and turbine inlet temperature using various working fluids. In addition, the monthly performance of the evacuated tube solar collector with the meteorological data of Isparta province is analyzed.

2. Transcritical Rankine Cycle with Regenerator

The layout of the transcritical Rankine cycle with regenerator is shown in Figure 1. In the transcritical Rankine cycle, working fluid is pumped above its critical pressure (1–2) and then heated to supercritical steam in an evacuated tube solar collector (3-4). The supercritical fluid is expanded to generate work in the turbine (3–4). After expansion, the fluid condenses in the

condenser (6-1), and the condensed liquid is then pumped back to high pressure; thus the cycle is completed. As seen in the figure, the regenerator is used to recover the turbine exhaust heat (5-6) and to preheat the liquid entering the vacuum tube solar collector (3-2).
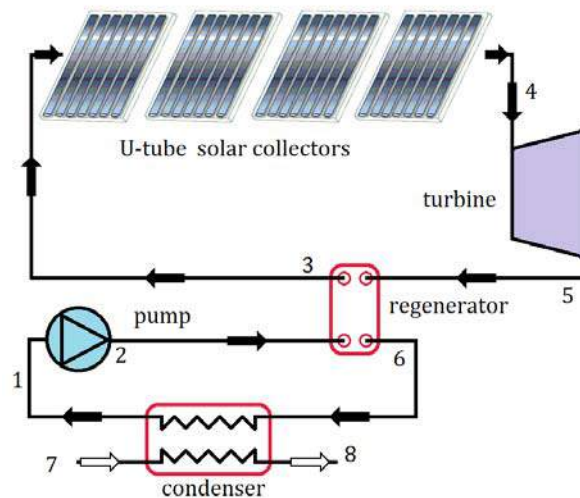
Figure 1. Transcritical Rankine cycle with regenerator

The selection of working fluid is one of the essential factors influencing the system performance and also has an effect on the environment. Generally, an appropriate working fluid should have suitable thermodynamic properties and low environmental impacts. The choice of the cycle fluid in this study is performed, taking into account mostly used the type of cycle fluid in the literature. Six different supercritical fluid types are chosen, namely R774, R125, R41, SF_6, R170, and N_2O. Table 1 shows the basic features of the selected supercritical fluids.

Table 1. Thermophysical properties of supercritical working fluids (Kizilkan, 2019; Sarkar, 2015)

Chemical Name	Refrigerant Number	Molecular Mass (kg/kmol)	ODP	GWP	Critical Temperature (°C)	Critical Pressure (kPa)
Carbon dioxide	R744	44.01	0	1	30.97	7377.3
Pentafluoroethane	R125	120	0	3500	66.023	3617.7
Fluor methane	R41	34.03	0	92	44.13	5897
Sulfurhexafluoride	SF_6	146.1	0	22800	45.57	3755
Ethane	R170	30.07	0	3	32.2	4872
Nitrous Oxide	N_2O	44.01	0.017	298	36.4	7245

Abbreviations: GWP, global warming potential; ODP, ozone depletion potential

For the performance analysis of the evacuated tube solar collector assisted transcritical Rankine cycle for different supercritical fluids, the design parameters are given in Table 2.

Table 2. Operating parameters of transcritical Rankine cycle (Kizilkan, 2020)

Parameter	Value
Turbine inlet temperature, °C	200
Turbine outlet pressure, kPa	$P_{crit} \times 1.13$
Pressure ratio	1.5
Turbine isentropic efficiency, %	92
Pump isentropic efficiency, %	85
Heat exchanger effectiveness, %	65

3. Thermodynamic Analysis

A thermodynamic model is constructed using Engineering Equation Solver (EES) software (Klein, 2020) in order to evaluate the energetic and exergetic performance of the solar-powered transcritical Rankine cycle for different supercritical working fluids. The main assumptions of the model are given as:

- The system operates at steady-state conditions.
- Kinetic and potential energies and exergy changes are ignored.
- Pressure is constant in the heat exchangers.
- There are no heat losses in the heat exchangers.
- The turbine and pump operations are assumed to be adiabatic.
- The reference state properties are 22°C and 101.325 kPa.

In order to calculate absorbed solar energy by the evacuated tube solar collector, the relations developed in reference (Kalogirou, 2009) are utilized. The useful absorbed energy from the sun is calculated as:

$$\dot{Q}_u = F_R A[S - U_L(T_{in} - T_a)] \tag{1}$$

where S is the solar irradiance, F_R is the heat removal factor, U_L is the overall heat loss coefficient, A is the collector area, T_a is the temperature air, and T_{in} is the inlet CO_2 temperature. For determining the CO_2 temperature at the collector exit, the useful solar energy collected by evacuated solar tubes can also be written as:

$$\dot{Q}_u = \dot{m}C_p(T_{out} - T_{in}) \tag{2}$$

The mass balance equation for steady-state and steady-flow processes can be written as (Cengel and Boles, 2006):

$$\sum \dot{m}_{in} = \sum \dot{m}_{out} \tag{3}$$

In the above equation, m˙ is the mass flow rate, and the subscripts in and out stand for inlet and outlet, respectively. The energy balance equation can be written as:

$$\dot{Q} + \sum \dot{m}_{in}h_{in} = \dot{W} + \sum \dot{m}_{out}h_{out} \tag{4}$$

Here, $\dot{Q}$ is the rate of heat, $\dot{W}$ is the rate of work, and h is the specific enthalpy. For the exergy analysis, the balance equation is defined as (Dincer and Rosen, 2007):

$$\dot{Ex}_Q - \dot{Ex}_W = \sum \dot{Ex}_{in} - \sum \dot{Ex}_{out} + \dot{Ex}_{dest} \tag{5}$$

where the first and the second terms are exergy of heat and work respectively, $\dot{Ex}$ is the rate of flow exergy, $\dot{Ex}_{dest}$ is exergy destruction. In the above equation, each term is defined as follows:

$$\dot{Ex}_Q = \dot{Q}\left(\frac{T - T_0}{T}\right) \tag{6}$$

$$\dot{Ex}_W = \dot{W} \tag{7}$$

$$\dot{Ex} = \dot{m}\,ex \tag{8}$$

$$\dot{Ex}_{dest} = T_0 \dot{S}_{gen} \tag{9}$$

In equation (8), ex is the specific flow exergy and can be calculated using the equation below:

$$e = (h - h_0) - T_0(s - s_0) \tag{10}$$

Applying the above mentioned by applying the thermodynamic equilibrium equations to each system element, the capacities, and exergy destruction rate equations for each system component can be obtained as follows.

Evacuated Tube Solar Collector:

$$\dot{Q}_{Col} = \dot{m}_3\,(h_4 - h_3) \tag{11}$$

$$\dot{Ex}_{dest,Col} = \dot{Ex}_{solar} + \dot{Ex}_3 - \dot{Ex}_4 \tag{12}$$

Turbine:

$$\dot{W}_T = \dot{m}_4(h_4 - h_5) \tag{13}$$

$$\dot{Ex}_{dest,T} = \dot{Ex}_4 - \dot{Ex}_5 - \dot{W}_T \tag{14}$$

Regenerator:

$$\dot{Q}_R = \dot{m}_2(h_3 - h_2) = \dot{m}_5(h_5 - h_6) \tag{15}$$

$$\dot{Ex}_{dest,R} = \dot{Ex}_2 + \dot{Ex}_5 - \dot{Ex}_3 - \dot{Ex}_6 \tag{16}$$

Condenser:

$$\dot{Q}_C = \dot{m}_6(h_6 - h_1) \tag{17}$$

$$\dot{Ex}_{dest,C} = \dot{Ex}_6 + \dot{Ex}_7 - \dot{Ex}_1 - \dot{Ex}_8 \qquad (18)$$

Pump:

$$\dot{W}_P = \dot{m}_1(h_2 - h_1) \qquad (19)$$

$$\dot{Ex}_{dest,P} = \dot{Ex}_1 - \dot{Ex}_2 + \dot{W}_P \qquad (20)$$

The energy efficiency of the solar-assisted transcritical Rankine cycle with regenerator is expressed as:

$$\eta_{en} = \frac{\dot{W}_T - \dot{W}_P}{\dot{Q}_{Col}} \qquad (21)$$

3. Results and Discussion

The solar-assisted Rankine Cycle was analyzed in terms of the first and second laws of thermodynamics in order to determine the thermodynamic performance characteristics of the system. The Engineering Equation Software was used for determining the thermodynamic properties of the working fluid.

In Figure 2, the variation of mean solar radiation for the months of the year according to the meteorological data of Isparta was given. It is clear from the figure that the mean solar radiation increases gradually from January to August and reaches a maximum value of 974 W/m^2 in August for Isparta. In addition, the lowest solar radiation is reported for January as 497 W/m^2.
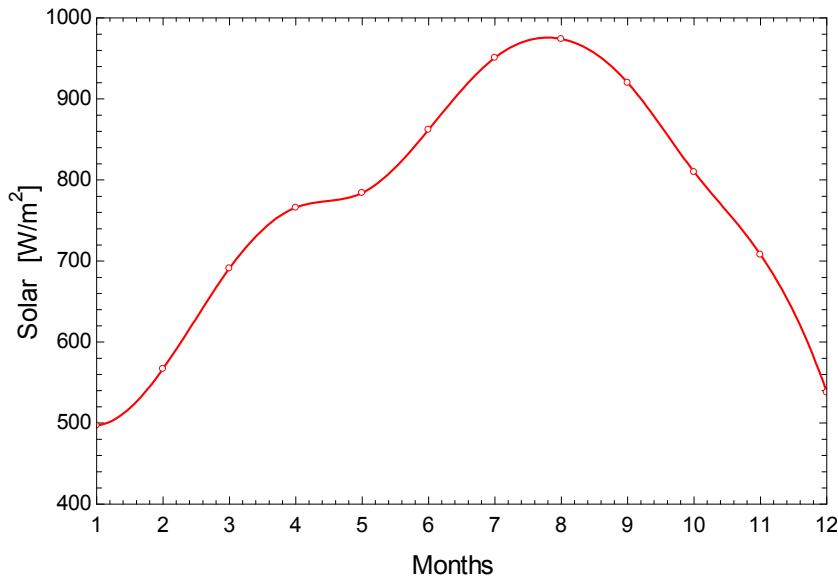
Figure 2. Monthly solar radiation data of Isparta

Figure 3 shows the variation of temperature at the exit of the evacuated solar collectors in terms of the solar irradiation for different working fluid types (R744, R125, R41, SF$_6$, R170, and N$_2$O). This figure indicates that temperature at the exit of the evacuated tube solar collectors for various cycle fluid types increases with increasing solar irradiation. It can be

seen that when the solar irradiation rises, the temperature of the fluid at the evacuated solar collector outlet increases, which in turn causes a rise in the enthalpy and temperature of the inlet of the turbine.
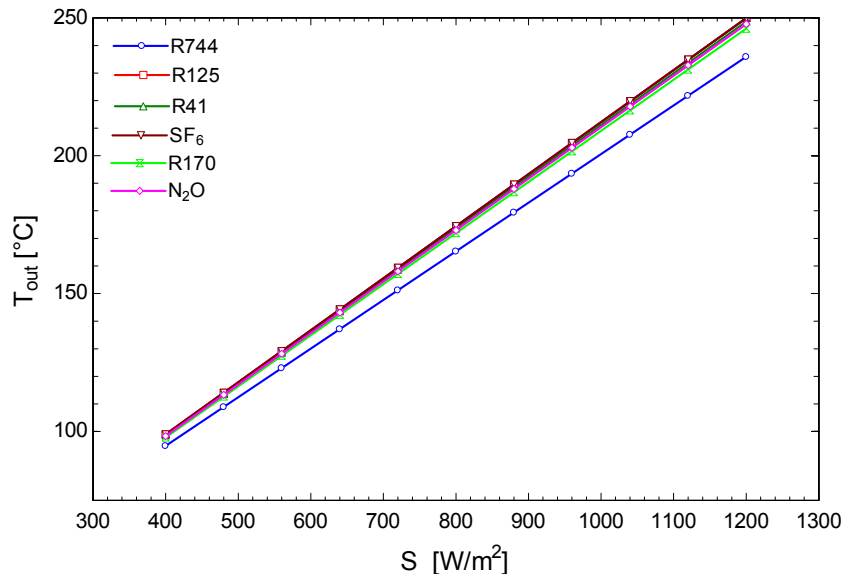
Figure 3. Variation of different supercritical working fluids temperature at the exit of solar collector

Figure 4 shows the monthly averaged variation of collector energy efficiency for different working fluid types. It was obtained that, if R744 is used as the cycle fluid for the study conducted, the collector efficiency has the highest value among the other fluids.
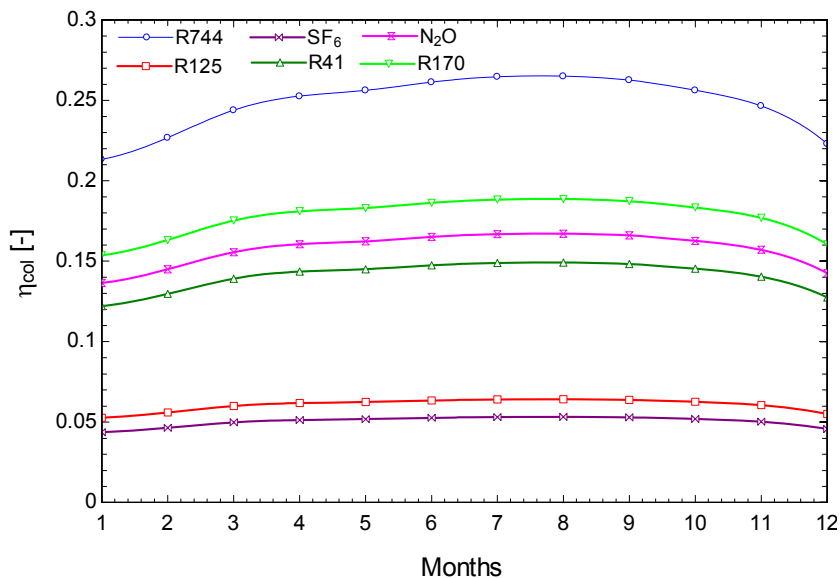
Figure 4. The monthly averaged variation of collector efficiency for different cycle fluid types

For the investigation of the effects of system characteristics on system performance, parametrical analyses were conducted. Figure 5 shows the effect of the turbine inlet temperature on the net power generation. During the analysis, turbine inlet temperature was

varied between 120°C and 220°C, and it was observed that net power generation was increased for all supercritical fluids. As seen from the figure, R125 has the lowest power generation, whereas N_2O has the highest amount of net power generations.
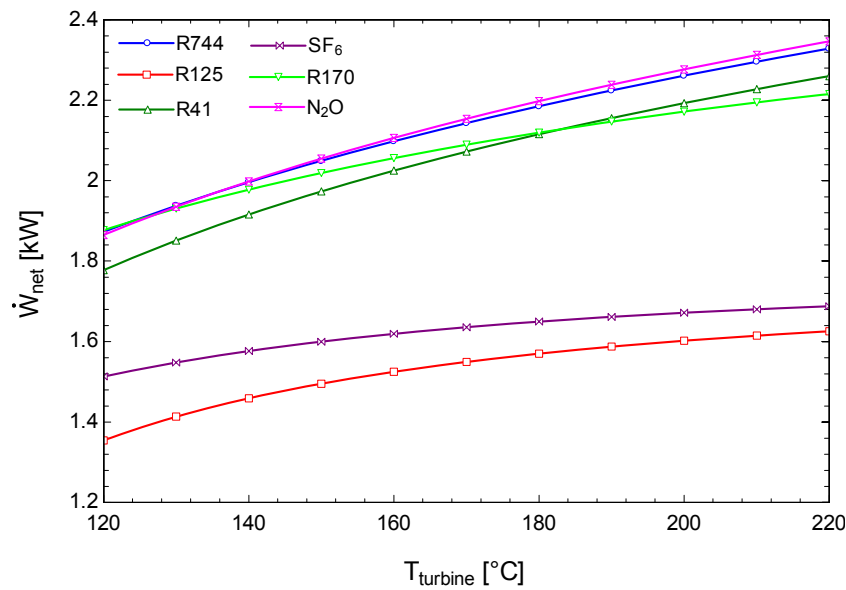
Figure 5. Variation of net power generation with the turbine inlet temperature

In Figure 6, energy efficiencies were given as a function of turbine inlet temperature. From the figure, it can be seen that energy efficiencies are increasing with the turbine inlet temperature for all working fluids. However, the increment slope for R744 and R41 is nearly constant. The energy efficiency of the integrated system for R744 and N_2O is almost equal to each other and has the highest efficiency.
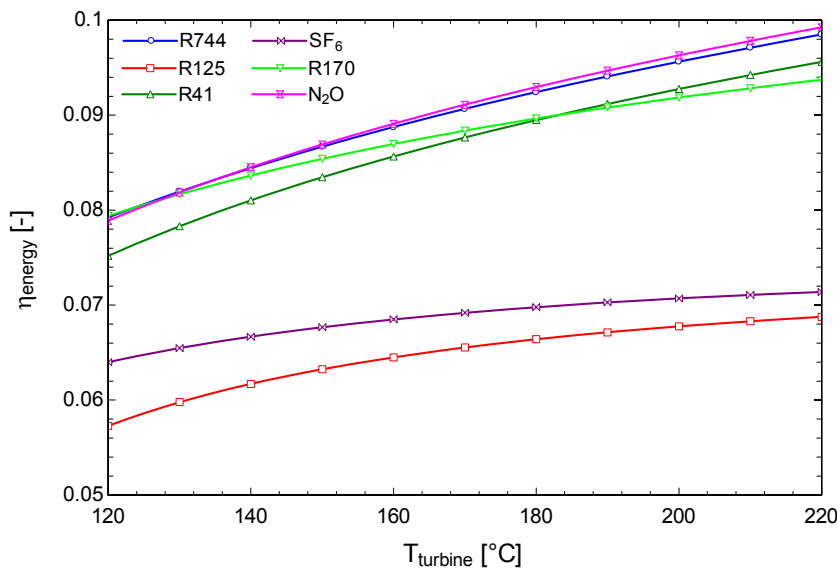
Figure 6. Variation of energy efficiencies with the turbine inlet temperature

The net work generated in the cycle for different supercritical fluids with reference to July is given in Figure 7. As seen from the figure, the highest net electricity production was obtained for R170 with a value of 0.24 kW.
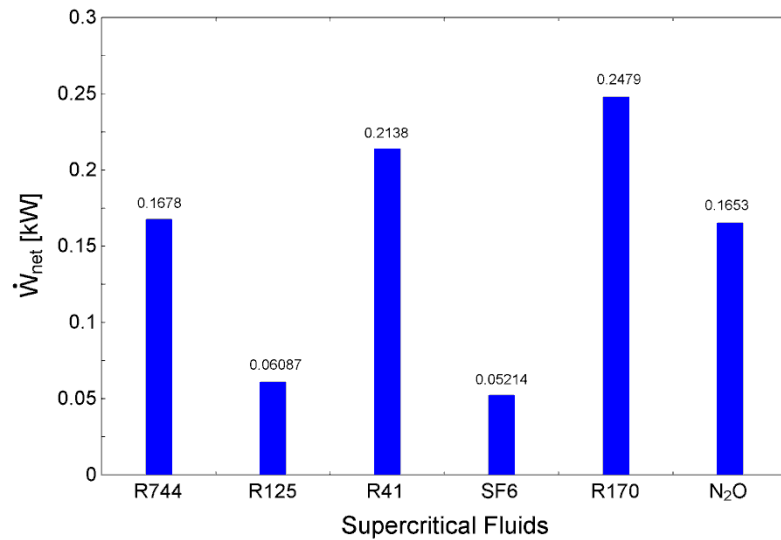
Figure 7. Comparison of net work produced in the cycle with respect to supercritical fluids

In Figure 8, the energy and exergy results of the solar-assisted transcritical Rankine cycle are given comparatively. According to the results of the analyses, the best performance for the transcritical Rankine cycle is obtained using CO_2 and N_2O, followed by R41, R170, SF_6, and R125, respectively. N_2O is another working fluid that has a very similar molecular weight, critical pressure, and temperature causes nearly the similar behavior to CO_2 with respect to system temperature and pressure, properties, and compactness. But the GWP value of N_2O supercritical fluid is higher than CO_2.
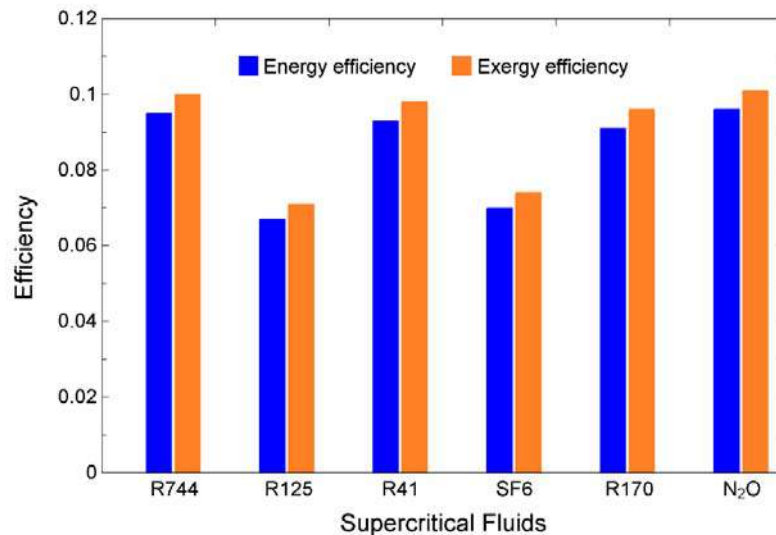
Figure 8. Comparison of energy and exergy efficiency of cycle with respect to supercritical fluids

4. Conclusions

In this study, the thermodynamic performance of a system including transcritical Rankine Cycle and evacuated solar collector is assessed using 6 different supercritical working fluids. For this purpose, energy and exergy analyses were carried out for determining the system performance indicators such as net power generation and energy and exergy efficiencies. In addition, comprehensive parametric analyses were conducted for transcritical Rankine cycle using different supercritical working fluids. According to the results of the study, the important findings are summarized as follows:

- The solar energy potential of Isparta was found to be relatively high. According to the solar data, the maximum solar radiation was 974 W/m^2 for Isparta for August.

- Among the supercritical working fluids examined in this study, it was observed that the maximum outlet temperature (202.9°C) from the evacuated tube collector was reached when R125 and SF_6 were used.

- It was found from the study that the highest and lowest amount of net power generations are found as 0.2479 kW and 0.05214 for R170 and SF_6, respectively.

- According to the results of the comparative analyses for the transcritical Rankine Cycle using supercritical fluids, the best performance was obtained using N_2O, followed by R744, R41, R170, SF_6, and R125 with the energy efficiencies of 9.6%, 9.5%, 9.3%, 9.1%, 7%, and 6.7%, respectively.

- The results of the parametrical analyses showed that the turbine inlet temperature has significant effects on system performance. For all supercritical fluids, the energy efficiencies increased with the turbine inlet temperature.

- The exergy analysis, according to the input parameters given in Table 1. Showed that the lowest and the highest exergy efficiency are 0.101 and 0.071 for N_2O and R125, respectively.

- According to the performance analysis results of the cycle, among the supercritical working fluids investigated in the present study, N_2O and R744 have great potential for transcritical power generation applications utilizing low-grade thermal energy. The critical temperature and pressure values of N_2O and CO_2 are similar, but the GWP value of N_2O is very high. Due to the fact that CO_2 has a relatively lower environmental impact and low cost, it is more preferred in low-temperature applications in recent years.

References

Cayer, E., Galanis, N., Nesreddine, H., (2010). Parametric study and optimization of a transcritical power cycle using a low temperature source. Applied Energy, 87(4), 1349–1357.

Cengel, Y.A., Boles, M.A., (2006). Thermodynamics: an engineering approach. McGraw-Hill, New York.

Chen, H., Goswami, D.Y., Stefanakos, E.K., (2010). A review of thermodynamic cycles and working fluids for the conversion of low-grade heat. Renewable Sustainable Energy Reviews, 14(9), 3059–3067.

Chen, H., (2010). The conversion of low-grade heat into power using supercritical Rankine cycles (PhD Thesis). University of South Florida.

Dincer, I., Rosen, M.A., (2007). Exergy: Energy, Environment and Sustainable Development. Elsevier Science.

Dostal, V., (2006). A supercritical carbondioxide cycle for next generation nuclear reactors (PhD Thesis). Department of Nuclear Engineering, Massachusetts Institute of Technology.

Gao, H., Liu, C., He, C., Xu, X., Wu, S., Li, Y., (2012). Performance analysis and working fluid selection of a supercritical organic Rankine cycle for low grade waste heat recovery. Energies, 5, 3233–3247.

Gu, Z.L., Sato, H., (2001). Optimization of cyclic parameters of a supercritical cycle for geothermal power generation. Energy Conversion and Management, 42, 1409–1416.

Kalogirou, SA., (2009). Solar Energy Engineering: Processes and Systems. Academic Press: Oxford.

Karellas, S., Schuster, A., (2008). Supercritical fluid parameters inorganic Rankine cycle applications. International Journal of Thermodynamics, 11(3), 101–108.

Kizilkan, O., (2019). Evaluation of transcritical Rankine cycle driven by low-temperature geothermal source for different supercritical working fluids. International Journal of Technological Sciences, 11(3), 155-169.

Kizilkan, O., (2020). Performance assessment of steam Rankine cycle and sCO_2 Brayton cycle for waste heat recovery in a cement plant: A comparative study for supercritical fluids. International Journal of Energy Research, 44, 12329-12343.

Klein, S.A., (2020). Engineering Equation Solver (EES). F-Chart.

Mehran, A., Shahram, K., Samad, J., (2019). Exergoeconomic analysis of a novel integrated transcritical CO_2 and Kalina 11 cycles from Sabalan geothermal power plant. Energy Conversion and Management, 195, 420-435.

Sarkar, J., (2015). Review and future trends of supercritical CO_2 Rankine cycle for low-grade heat conversion. Renewable and Sustainable Energy Reviews, 48, 434-451.

Zhang, X.R., Yamaguchi, H., Uneno, D., (2007). Thermodynamic analysis of the CO_2- based Rankine cycle powered by solar energy. International Journal of Research, 31(14), 1414–1424.

Zhang, X., Yamaguchi, H., Uneno, D., (2007). Experimental study on the performance of solar Rankine system using supercritical CO_2. Renewable Energy, 32, 2617–2628.

Comparative Thermodynamic Investigation of Ground Coupled Refrigeration System for Supercritical Refrigerants

Gamze SOYTÜRK[1*], Serpil ÇELİK TOKER[1], Önder KIZILKAN[1]

Abstract: The purpose of this study is to examine the thermodynamic performance of the ground-coupled refrigeration system using different supercritical refrigerants. For this purpose, six different supercritical refrigerants are analyzed in terms of the first and second laws of thermodynamics. The analyses are made for a refrigeration capacity of 75 kW and cold room temperature of -5 °C. The energy performance indicator COP and exergy performance indicator exergy efficiency and destruction rates of the system are determined. Results showed that the best COP value and exergy efficiency were obtained using R125. Besides, the highest exergy destruction was found to be 13.49 kW for R170, followed by R744 with a value of 13.44 kW. A parametric study was carried out to examine the effect of ground and cold room temperatures on the energy and exergy efficiency of the system. According to the parametric studies, COP values decreased with the increase of ground temperature for all refrigerants, while they increased with the increase of evaporator temperature.

Keywords: Supercritical refrigerant, ground-coupled, refrigeration, energy, exergy.

1. Introduction

The rapid growth of the population and accelerating process of urban modernization give rise to a greater demand for energy consumption. Compared with the year 1990, it was predicted that the energy consumption of 2050 could increase by up to 275% (Fridleifsson, 2001). However, a great portion of the energy used for space heating/cooling and electricity generation comes in the form of burning fossil fuels (Aresti et al. 2018), which are limited available and harmful to the environment (Atam and Helsen, 2016). A reduction of fossil fuel use and an improvement in the global energy structure to include more sustainable energy is required (Mohammadi et al. 2017). Nguyen and Eslami-Nejad (2019), were proposed the concept of a "ground source heat pump" (GSHP), which uses soil as an environmentally friendly and sustainable source for heating and cooling. In cold climates, ground source heat pump (GSHP) systems are increasingly deployed for heating, cooling, and air-conditioning in residential, commercial, and institutional buildings. These systems rely on a relatively constant ground temperature throughout the year to operate with higher efficiencies than conventional air-source heat pump systems.

The refrigerants used in the ground-coupled refrigeration system must have a low global warming potential (GWP) and zero ozone depletion potential (ODP) since these two major environmental concerns are important for the future development of refrigeration industries. ODP and GWP have become one of the most important criteria in analyzing new alternatives

[1] Isparta University of Applied Sciences, Department of Mechanical Engineering, Isparta/Turkey
* Corresponding author: gamzeyildirim@isparta.edu.tr

to chlorofluorocarbon (CFC) and hydrochlorofluorocarbon (HCFC) refrigerants in vapor-compression refrigeration systems. CFC and HCFC-type refrigerants have been used predominantly in refrigeration systems for the past few decades. HCFCs have both ODP and high GWP and may not be produced or imported after 2030 in developed nations and 2040 in developing countries. The Kigali Amendment to Montreal Protocol (UNEP, 2016) requires the participating parties to gradually reduce HFCs use by 80–85% by the late 2040s.

There have been many publications on ground-coupled heat pumps and refrigeration systems in the literature for heating and cooling applications. Sakulpipatsin et al. (2010), presented a method for exergy analysis of buildings and Heating Ventilation Air Conditioning systems. They illustrated an office building equipped with low-temperature heating and high-temperature cooling systems situated in the Netherlands. They found the overall exergy efficiencies of the system to be 17.15% and 6.81%. They also noted that the thermal energy emission and control system and the energy conversion system were the main causes of the exergy inefficiencies in the heating and cooling cases. Healy et al. (1997), researched the effect of system parameters, such as the depth of ground heat exchanger, brine flow rate, the length between pipes, on the performance of ground heat exchanger in Canada. The researcher also concluded that ground source heat pumps were more advantageous than the other traditional heating and cooling systems. Esen et al. (2007), have reported a detailed techno-economic analysis of a ground source heat pump system and six conventional heating systems for the climate conditions of Turkey in a heating season of 2002–2003. In hot climates such as in Turkey, ground source heat pump systems represent a viable alternative to air source heat pump systems and conventional space cooling and heating systems because of their higher operating efficiency, especially during the cooling season. Coskun et al. (2008), and Pulat et al. (2009), studied the effect of experimental COPs on ground source heat pumps constructed in Bursa, Turkey for heating and cooling. Using ANSYS computer program, the same researchers obtained temperature distributions near the GSHE by using inlet and outlet temperatures of brine temperatures. Jin et al. (2016), introduced a concept of a CO_2 hybrid source coupled heat pumping system for a warm climate. This hybrid system utilized the heat sink by combining city water, ground, and ambient air in cooling mode, while the ground is used as the only heat source in heating mode. Alkan et al. (2014), examined the thermodynamic analysis of the system by using different alternative refrigerants in the ground source heat pump. They chose R22, R404a, R410a, R407c, R134a, and R600 fluids as refrigerants in their studies.

They found that R600 fluid had the best performance among other refrigerants. Xu et al. (2013), were compared the performance of R410a and R32 refrigerants used in heat pump systems. They said that the use of the R32 coolant, which has a lower global warming potential, is 10% and 9% better in terms of capacity and COP, respectively, than the use of the R410a coolant. Li et al. (2014), investigated the energy and exergy performance of secondary loop systems using R152a and R290 in automotive air-conditioning systems. They found that the COP was increased by 8% to 15% with the use of R290 instead of R134a. Cho et al. (2016), compared the heating and cooling performance of a heat pump system with R32 or R410a. Cheng et al. 2014, replaced R22 and R410a with R32 and R290 as heat pump refrigerants respectively and studied their cycle performance. Nawaz et al. (2017), focused on the substitution of R290 for R134a, and they also analyzed the cycle performance of 13 low global warming potential (GWP) refrigerants in their follow-up studies (Nawaz and Ally, 2019). Joybari et al. (2013), carried out exergy analysis to investigate the performance of a domestic refrigerator for R134a and R600a. They also applied the Taguchi method to design experiments to minimize exergy destruction while using R600a.

In this study, the performance of the ground-coupled refrigeration system is investigated for six supercritical fluids. These supercritical fluids are pentafluoroethane (R125), methyl fluoride (R41), sulfur hexafluoride (SF$_6$), ethane (R170), nitrous oxide (R744A), and carbon dioxide (R744). In order to determine the energetic and exergetic performance of the ground-coupled refrigeration system, the first and second laws of thermodynamics are applied to the system. The highest energy and exergy efficiency of the ground-coupled refrigeration system is found for R125 fluid, while the lowest energy and exergy efficiency is found for R170 fluid. A parametric study is carried out to examine the effect of ground and cold room temperature on the energy and exergy efficiency of the system.

2. System Description

The system consists of the ground-coupled refrigeration system, a cold room to be maintained at -5°C, and a ground source for the heat rejection process from the condenser (Figure 1). The refrigerant circulating in the vapor compression refrigeration cycle evaporates by extracting heat from the room air in the evaporator and then enters the compressor. In the compressor, the temperature and pressure of the refrigerant are increased, and the fluid is sent to the condenser. The refrigerant, whose heat has been taken by the ground in the condenser, passes through the throttling valve, and its pressure is reduced and sent to the evaporator; thus, the cycle is completed. The T-s diagram of the ground-coupled sub-critical refrigeration system is given in Figure 2.
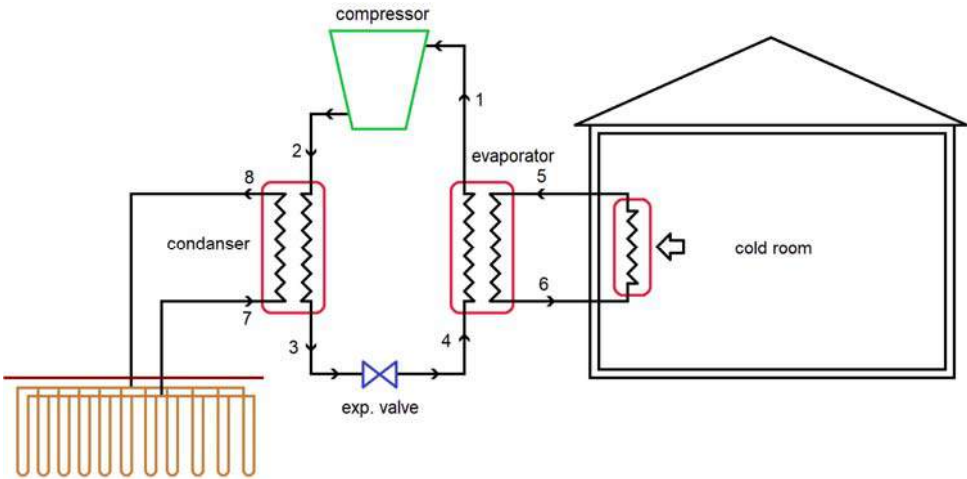
Figure 1. Schematic representation of the ground-coupled sub-critical refrigeration system
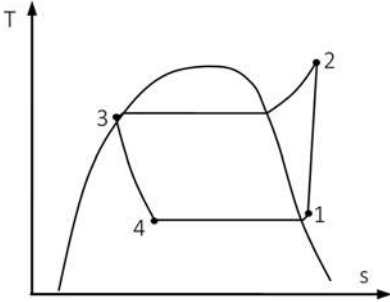
Figure 2. T-s diagram of the sub-critical refrigeration cycle

The selection of working fluid is one of the essential factors influencing the system performance and also has an effect on the environment. Generally, an appropriate working fluid should have suitable thermodynamic properties and low environmental impacts. The analyses are made for six supercritical refrigerants with low ODP values. The general properties of these refrigerants are tabulated in Table 1, and T-s diagrams are given in Figure 3.

Table 1. Thermophysical and environmental properties of supercritical working fluids (ASHRAE 2004; Restrepo et al., 2008; Calm and Hourahan, 2011)

Name	Refrigerant Number	Chemical formula	Molecular Mass, kg/kmol)	Critical pressure, kPa	Critical temperature, °C	ODP[a]	GWP[b]
Pentafluoroethane	R125	CHF_2CF_3	120.02	3617.5	66.02	0	3500
Methyl fluoride	R41	CH_3F	34.03	5897	44.13	0	92
Sulfurhexafluoride	SF_6	SF6	146.5	3755	45.57	0	22800
Ethane	R170	CH_3CH_3	30.07	4872.2	32.17	0	3
Nitrous oxide	R744A	N_2O	44.01	7245	36.37	0.017	298
Carbon dioxide	R744	CO_2	44.01	7377.3	30.98	0	1

[a] relative to R11 [b] relative to CO_2
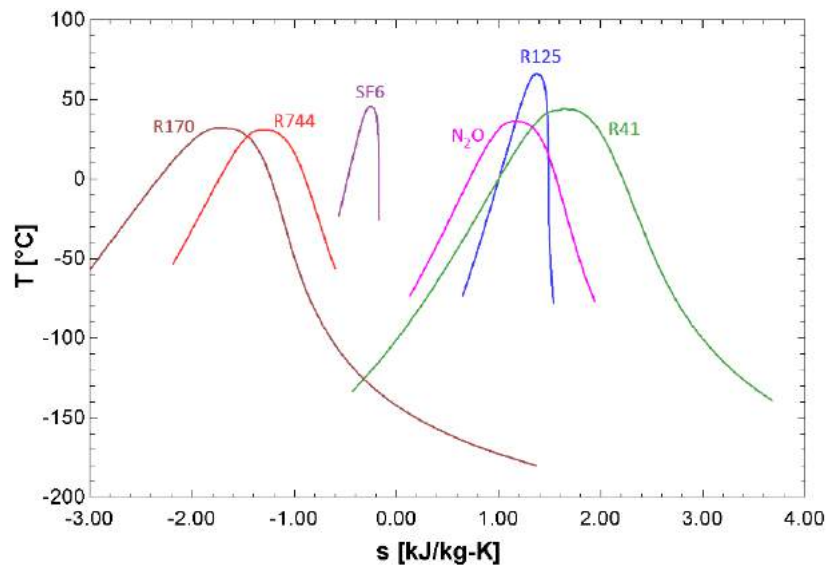
Figure 3. T-s diagram of the supercritical refrigerants

The refrigeration load from the cold room is absorbed by a secondary fluid, which is ethylene glycol (EG), and selected in order to prevent the freezing problem. The freezing point of EG is -18.84 °C for the specified concentration. Also, the condenser heat load is absorbed by cooling water, and the water is cooled down by means of the ground-coupled heat exchangers. In order to determine the performance analysis of the system for different supercritical refrigerants, the operating parameters are tabulated in Table 2.

Table 2. Design parameters of the ground-coupled sub-critical refrigeration system

Refrigeration capacity, $\dot{Q}_{CR}$	75 kW
Cold room temperature, T_{CR}	-5 °C
Ground temperature, T_G	14 °C
Evaporator temperature, T_E	T_{CR} - 5°C
Condenser temperature, T_C	T_G + 12°C
Superheating temperature, ΔT_{SH}	0.1 °C
Subcooling temperature, ΔT_{Sc}	0.1 °C
Isentropic efficiency of compressor, η_{is}	0.88
Mechanical efficiency of compressor, η_{mec}	0.92
Electrical efficiency of compressor, η_{elec}	0.86
Ethylene -glycol concentration	0.30

3. Thermodynamic Balance Equations

The performance characteristics of the ground-coupled refrigeration system are assessed by applying first and second law analysis of thermodynamics. The balance equations are used to determine the work and heat interactions, energy and exergy efficiencies, and exergy destruction rates for each system component. The general mass balance equation for steady-state and steady-flow processes can be written as (Cengel and Boles, 2006):

$$\sum \dot{m}_{in} = \sum \dot{m}_{out} \tag{1}$$

The energy balance equation is defined as:

$$\sum \dot{E}_{in} = \sum \dot{E}_{out} \tag{2}$$

Equation (2) can be written in the form given below:

$$\dot{Q} + \sum \dot{m}_{in}h_{in} = \dot{W} + \sum \dot{m}_{out}h_{out} \tag{3}$$

In the above equations, $\dot{m}$ is the mass flow rate, $\dot{E}$ is the rate of net energy, $\dot{Q}$ is the rate of net heat, $\dot{W}$ is the rate of net work, and h is the specific enthalpy. The subscripts in and out stand for inlet and outlet, respectively.

The second law of thermodynamics overcomes with concepts of entropy and exergy. Exergy analysis of systems allows determining irreversibility and available energy (exergy) in the system. These analyses reveal the efficiency of the systems in terms of the First and Second Law of Thermodynamics (Göktürk et al., 2013). For a steady-state operation, the general exergy balance equation can be defined as (Dincer and Rosen, 2007):

$$\sum \dot{Ex}_{in} = \sum \dot{Ex}_{out} + \sum \dot{Ex}_{dest} \tag{4}$$

The exergy balance equation can also be written more explicitly as:

$$\dot{Ex}_Q - \dot{Ex}_W = \sum \dot{m}_{in}e_{in} - \sum \dot{m}_{out}e_{out} + T_0\dot{S}_{gen} \tag{5}$$

where, $\dot{E}x_Q$ and $\dot{E}x_W$ are the exergies of heat and work, respectively, e is the specific exergy, T_0 is the reference state temperature and $\dot{S}_{gen}$ is the entropy generation rate. In the above equation, exergies of heat and work and entropy generation rate are given below (Kotas, 1985).

$$\dot{E}x_{dest} = T_0\dot{S}_{gen} \tag{6}$$

$$\dot{E}x_Q = \dot{Q}\left(\frac{T-T_0}{T}\right) \tag{7}$$
$$\dot{E}x_W = \dot{W} \tag{8}$$

The specific exergy is expressed relative to the environmental conditions as:

$$e = (h - h_0) - T_0(s - s_0) \tag{9}$$

where s is entropy, P is the pressure, and the subscript 0 indicates properties at the reference state.

The performance of the ground-coupled refrigeration system can be determined using energy and exergy efficiency definitions:

$$COP = \frac{\dot{Q}_{CR}}{\dot{W}_{Comp,el}} \tag{10}$$

$$\eta_{ex} = \frac{\dot{E}x_{\dot{Q}_{CR}}}{\dot{E}x_{\dot{W}_{Comp,el}}} \tag{11}$$

where $\dot{Q}_{CR}$ represents refrigeration capacity and $\dot{W}_{Comp,el}$ represents compressor's electric consumption.

3. Results and Discussion

The performance of the ground-coupled refrigeration system is compared for six supercritical refrigerants in this study. In order to analyze the ground-coupled sub-critical refrigeration system for supercritical refrigerants the several assumptions have to be made:

- ✓ The system operates at the steady-state.
- ✓ Kinetic and potential energies and exergy changes are ignored.
- ✓ Pressure losses through pipelines are neglected.
- ✓ The pump operations are assumed to be adiabatic.
- ✓ The directions of heat transfer to the system and work transfer from the system are taken positive.
- ✓ Heat losses and heat gains from or to the system are neglected.

Using the balance equations and under the assumptions given above, the analyses are performed for different supercritical refrigerants by EES software. In Figure 4, the COP value is given for all supercritical refrigerants. It can be seen from the figure that the best COP value is obtained using R125, followed by R41, SF$_6$, and N$_2$O.
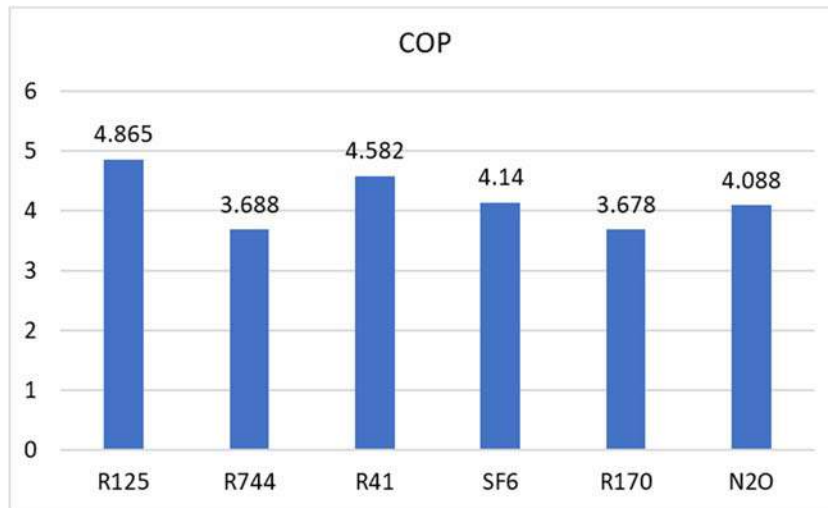
Figure 4. COP values for different supercritical refrigerants

Figure 5 shows the exergy efficiency of the ground-coupled refrigeration system for different supercritical fluids. The exergy efficiency trend is the same as COP. As can be seen from the figure, the best exergy efficiency is occurred using R125, while the lowest exergy efficiency was obtained when using R744.
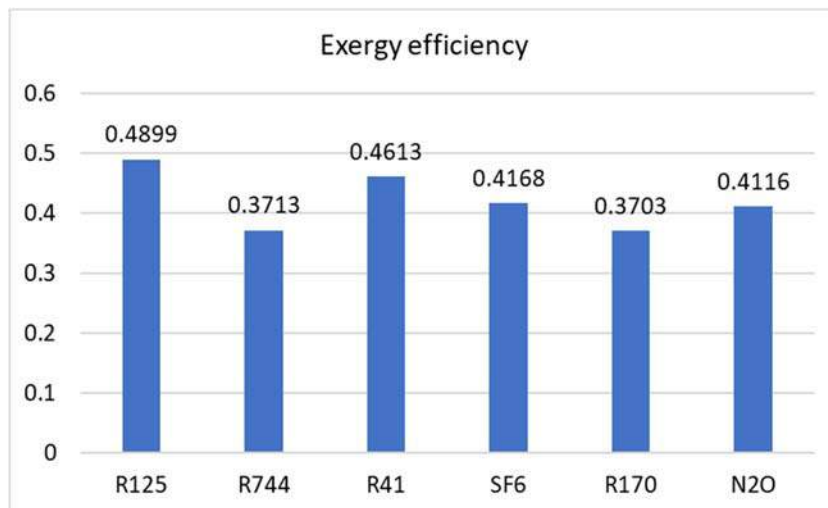
Figure 5. Exergy efficiency of the system for different supercritical fluids.

In Figure 6, exergy destruction of the system is given in the case of using different supercritical fluids. The highest exergy destruction is obtained using when R170 and R744 are using in the system.
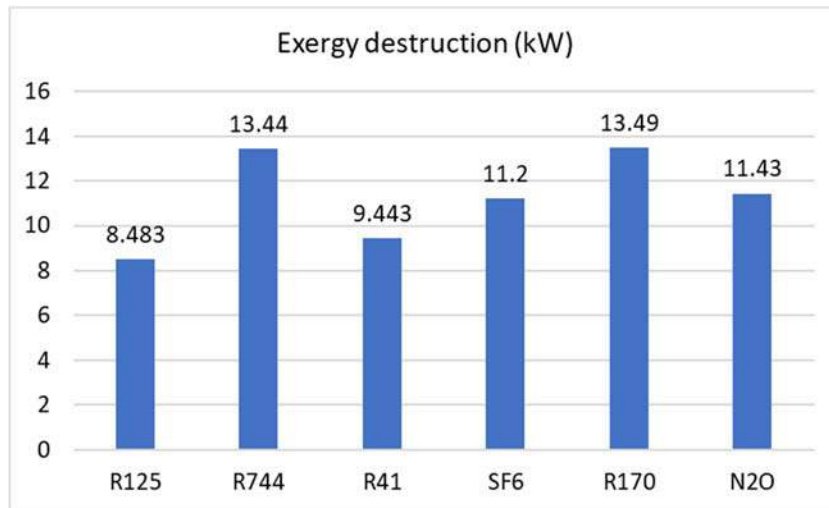
Figure 6. Exergy destruction of the system for different supercritical fluids.

In Figures 7 to 9, the variations of COP, exergy efficiency, and exergy destruction rates are given with the variation ground temperature. As can be seen from the figures, with the increase of ground temperature, COP and exergy efficiency values decrease for all refrigerants. The exergy destruction rates increase with ground temperature, contrary to COP.
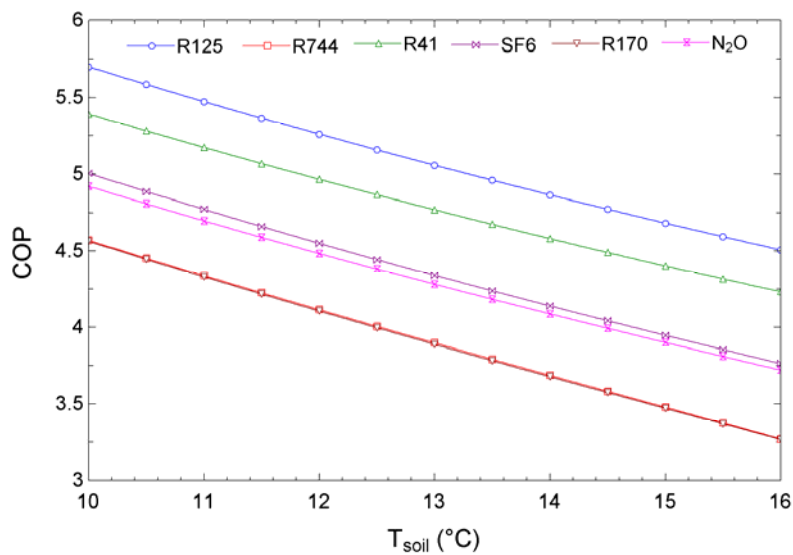
Figure 7. Variation of COP with ground temperature
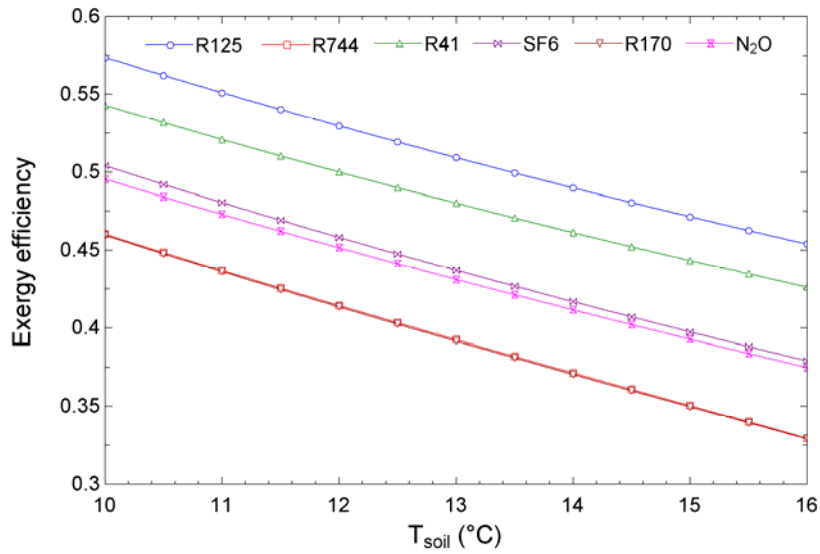
Figure 8. Variation of exergy efficiency with ground temperature
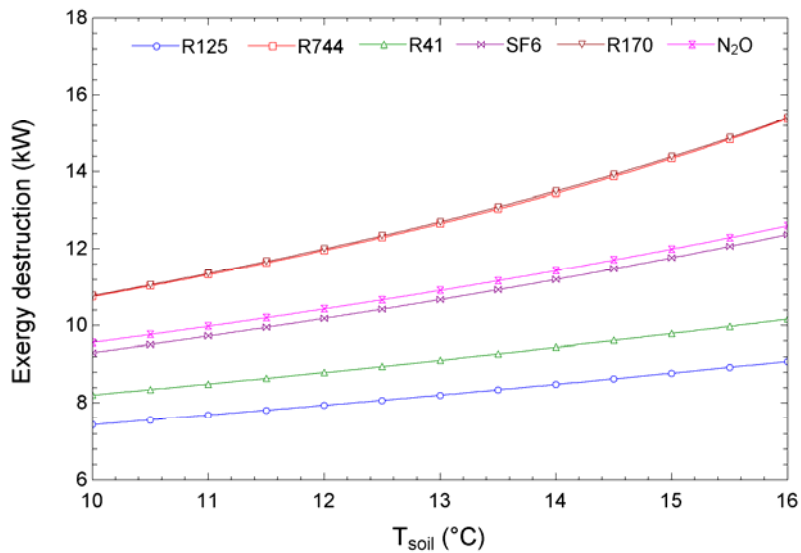
Figure 9. Variation of exergy destruction with ground temperature

Figure 10 shows the variation of COP with evaporator temperature. As expected, while the COP increases with evaporator temperature, exergy efficiency and exergy destruction rates decrease for all refrigerants (Figure 11 and 12).
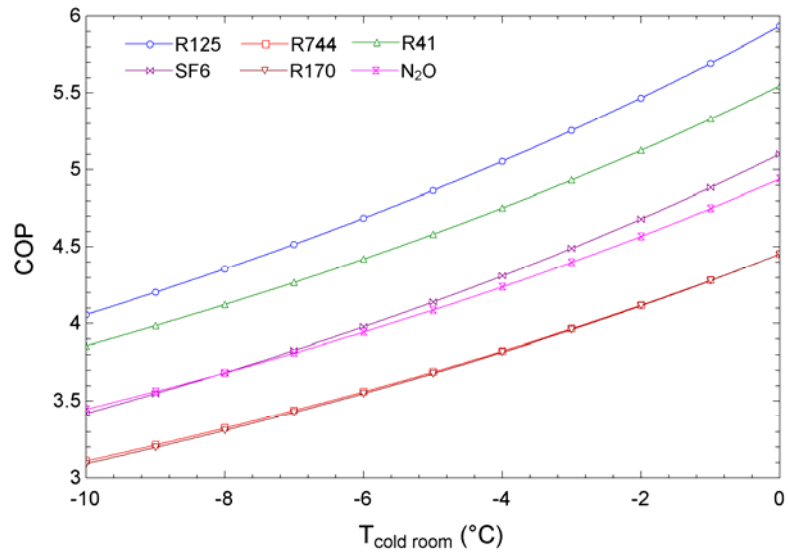
Figure 10. Variation of COP with evaporator temperature
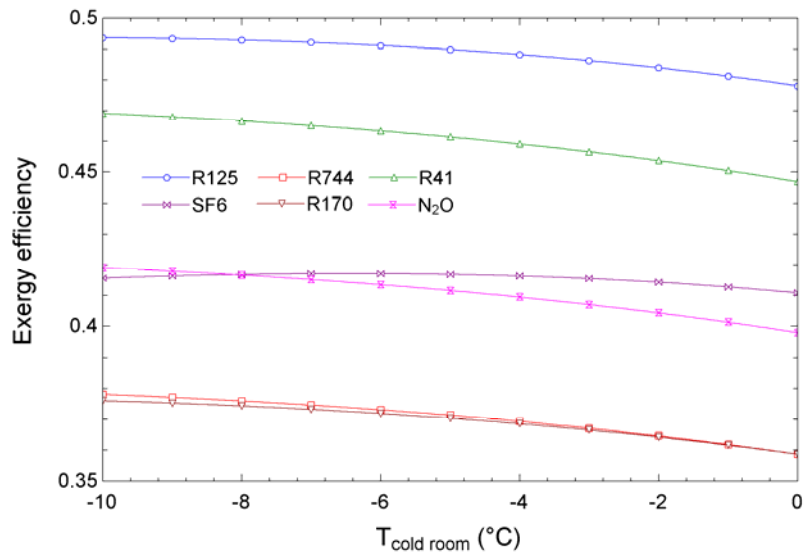
Figure 11. Variation of exergy efficiency with evaporator temperature
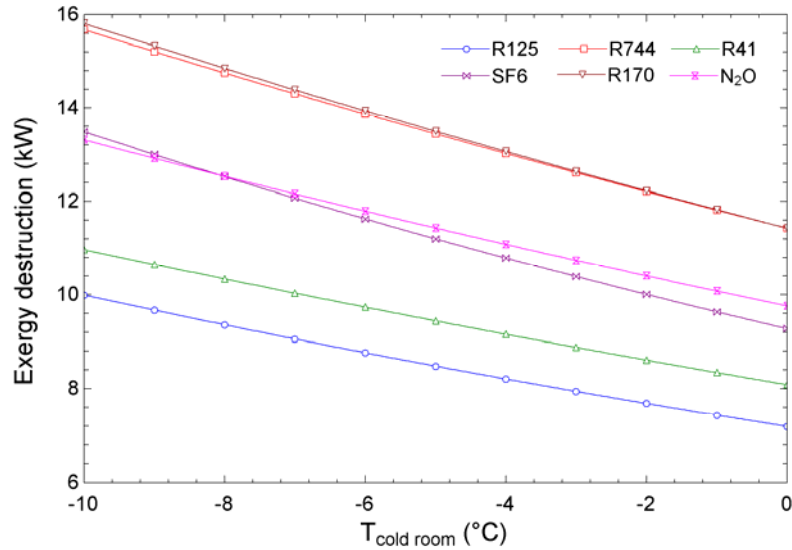
Figure 12. Variation of exergy destruction with evaporator temperature

4. Conclusions

In this study, the performance of the ground-coupled refrigeration system using different supercritical refrigerants has been investigated. Analyses were made for six different supercritical refrigerants. The results of the analyses were showed that the best COP was obtained by using R125 followed by R41, SF$_6$, and N$_2$O. The best exergy efficiency is obtained using R125, while the lowest exergy efficiency was obtained when using R744. Parametric studies have been done to see the effect of ground temperature and evaporator temperature on the system performance. The results of parametric studies showed that the increase of evaporator temperature had a positive effect on the coefficient of performance, exergy efficiency, and exergy destruction of the system, while the increase of ground temperature had a negative effect.

References

Alkan, R., Kabul, A., Kızılkan, Ö., (2014). Thermodynamic analysis of a ground source heat pump for different refrigerants. Journal of Thermal Science and Technology, 34(1), 27-34 (In Turkish).

Aresti, L., Christodoulides, P., Florides, G., (2018). A review of the design aspects of ground heat exchangers. Renewable Sustainable Energy Reviews, 92, 757–763.

ASHRAE, (2004). Designation and safety classification of refrigerants. ANSI/ASHRAE Standard 34-2001, Atlanta, GA, USA.

Atam, E., Helsen, L., (2015). Ground-coupled heat pumps: part 1 – literature review and research challenges in modeling and optimal control. Renewable Sustainable Energy Reviews, 54, 1653–1667.

Calm, J.M., Hourahan, G.C., (2011). Physical, safety, and environmental data summary for current and alternative refrigerants. Proceedings of the 23rd International Congress of Refrigeration, Prague, Czech Republic, 21-26.08.2011.

Cengel, Y.A., Boles, M.A. (2006). Thermodynamics: an engineering approach. 5th ed., McGraw-Hill, New York, USA.

Cheng, S., Wang, S., Liu, Z., (2014). Cycle performance of alternative refrigerants for domestic air-conditioning system based on a small finned tube heat exchanger. Applied Thermal Engineering, 64, 83–92.

Cho, I.Y., Seo, H.J., Kim, D., (2016). Performance comparison between R410A and R32 multi-heat pumps with a sub-cooler vapor injection in the heating and cool- ing modes. Energy 112, 179–187.

Coskun, S., Pulat, E., Unlu, K., Yamankaradeniz. R., (2008). Experimental performance investigation of a horizontal ground source compression refrigeration machine. International Journal Energy Research, 32, 44-56.

Dincer, I., Rosen, M.A., (2007). Exergy: Energy, environment and sustainable development. 1st ed., Elsevier Science; Oxford, UK.

Esen, H., Inalli, M., Esen, M., (2007). A techno-economic comparison of ground-coupled and air-coupled heat pump system for space cooling. Building and Environment, 42, 1955-1965.

Fridleifsson, IB., (2001). Geothermal energy for the benefit of the people. Renewable Sustainable Energy Reviews, 299–312.

Göktürk, M., Oztop, H.F., Hepbaslı, A., (2013). Energy and exergy assessments of a perlite expansion furnace in a plaster plant. Energy Conversion and Management, 75, 488–497.

Healy, PF., Ugursal, VI., (1997). Performance and economic feasibility of ground source heat pumps in cold climate. International Journal Energy Research, 21, 857-870.

Jin, Z., Eikevik, T.M., Nekså, P., (2016). Investigation on CO2 hybrid ground coupled heat pumping system under warm climate. International Journal of Refrigeration, 62, 145-152.

Joybari, M.M., Hatamipour, M.S., Rahimi, A., Modarres, F.G., (2013). Exergy analysis and optimization of R600a as a replacement of R134a in a domestic refrigerator system. International Journal of Refrigeration, 36, 1233-1242.

Kotas, T.J., (1985). The exergy method of thermal plant analysis. Butter-Worths, London, UK.

Li, G., Eisele, M., Lee, H., Hwang, Y., Radermacher, R., (2014). Experimental investigation of energy and exergy performance of secondary loop automotive air-conditioning systems using low-GWP (global warming potential) refrigerants. Energy, 68, 819-831.

Nawaz, K., Shen, B., Elatar, A., Baxter, V., Abdelaziz, O., (2017). R290 (propane) and R600a(isobutane) as natural refrigerants for residential heat pump water heaters. Applied Thermal Engineering, 127, 870-883.

Nawaz, K., Ally, M., (2019). Options for low-global-warming-potential and natural refrigerants Part 2: Performance of refrigerants and systemic irreversibilities. International Journal of Refrigeration, 106, 213-224.

Nguyen, A., Eslami-Nejad, P. A., (2019). Transient coupled model of a variable speed transcritical CO2 direct expansion ground source heat pump for space heating and cooling. Renewable Energy, 140, 1012-1021.

Pulat, E., Coskun, S., Unlu, K., Yamankaradeniz, N., (2009). Experimental study of horizontal ground source heat pump performance for mild climate in Turkey. Energy, 34(9), 1284-1295.

Restrepo, G., Weckert, M., Brüggemann, R., Gerstmann, S., Frank, H., (2008). Ranking of Refrigerants. Environmental Science & Technology, 42, 2925–2930.

Sakulpipatsin, P., Itard, L.C.M., Kooi, H.J., Boelman, E.C., Luscuere, P.G., (2010). An exergy application for analysis of buildings and HVAC systems. Energy and Buildings, 42, 90–99.,

UNEP, (2016). Amendment to the Montreal Protocol on Substances that Deplete the Ozone Layer, Kigali. (Date of Access: 25.04.2021).

Xu, X., Hwang, Y., Radermacher, R., (2013). Performance comparison of R410A and R32 in vapor injection cycles. International Journal of Refrigeration, 36(3), 892–903.

Modelling the Color Removal Efficiency of an Electrochemical Process from Organic Wastewater by Response Surface Method

Bir Elektrokimyasal Prosesin Organik Atıksudan Renk Giderim Etkinliğinin Yanıt Yüzey Metodu ile Modellenmesi

Oğuz ŞAHİNER[1]*, Murat SOLAK[2]

Abstract: European Union member countries use the spectral absorption coefficient (SAC) method within the framework of the standards set in EN ISO 7887 in the analysis of the color parameter in industrial wastewaters. In the study, the color removal efficiency of the discharge wastewater of the yeast production industry was investigated as SAC unit by electrochemical process using titanium and stainless steel electrodes. The effects of operating parameters such as pH, current density and electrolysis time on the removal of SAC436, SAC525 and SAC620 color parameters were optimized by the Response Surface Method (RSM).

Keywords: Yeast industry discharge wastewater, electrochemical treatment, titanium electrode, stainless steel electrode, optimization

Özet:

Avrupa Birliği üyesi ülkeler endüstriyel atıksularda renk parametresinin analizinde EN ISO 7887'de belirlenen standartlar çerçevesinde renklilik sayısı (RES) yöntemini kullanmaktadır. Çalışmada, maya üreten işletmenin deşarj atıksuyunun RES birimi olarak titanyum ve paslanmaz çelik elektrotlar kullanılarak elektrokimyasal prosesle renk giderim verimi araştırılmıştır. pH, akım yoğunluğu ve elektroliz süresi gibi işletme parametrelerinin RES436, RES525 ve RES620 renk parametrelerinin giderimi üzerindeki etkileri Yanıt Yüzey Metodu (YYM) ile optimize edilmiştir.

Anahtar Kelimeler: Maya endüstrisi deşarj atıksuyu, elektrokimyasal arıtma, titanyum elektrot, paslanmaz çelik elektrot, optimizasyon.

1. Giriş

Gıda endüstrisi, artan temel ihtiyaçların karşılanması için stratejik öneme sahip, üretimin her aşamasında yüksek miktarlarda su ihtiyacı olan ve buna bağlı olarak da atıksu üretimi oldukça yüksek olan endüstriyel üretim alanlarından biridir. Gıda endüstrisi alanında faaliyet gösteren maya üretim tesisleri dünyada ve ülkemizde önemli bir yere sahiptir (Balcıoğlu, 2013). Ekmek mayası üretiminde, şeker fabrikalarının yan ürünü olan melas, endüstriyel

[1] Düzce Üniversitesi, Yapı İşleri ve Teknik Daire Başkanlığı, Düzce/Türkiye
[2] Düzce Üniversitesi, Çevre Mühendisliği Bölümü, Mühendislik Fakültesi, Düzce/Türkiye
* Sorumlu Yazar: oguzsahiner@duzce.edu.tr

sürdürülebilirlik yaklaşımlarından biri olan endüstriyel simbiyoz örneği olarak maya endüstrisinin hammaddesi olarak kullanılmaktadır.

Maya endüstrisi atıksuları, kimyasal oksijen ihtiyacı (KOİ), biyokimyasal oksijen ihtiyacı (BOİ), toplam organik karbon (TOK), azot, fosfor, renk gibi yüksek konsantrasyonlarda kirletici içeriğe sahiptir (Balcıoğlu, 2013). Maya üretimi süreçlerinde ortaya çıkan atıksulardaki yoğun renk (koyu kahverengi) içeriği, biyopolimer kompleksi olan, biyokimyasal reaksiyonlar sonucu oluşan melanoidden kaynaklanmaktadır. Bu içeriklerin parçalanması oldukça zordur (Alkan, 2010). Bu tür atıksuların arıtımında biyolojik, kimyasal arıtma teknikleri kullanılmaktadır. Biyolojik prosesler, atıksudaki organik maddeleri parçalayan mikroorganizma yumaklarının çöktürme havuzunda çöktürerek giderimi üzerine tasarlanmıştır. Konvansiyonel biyolojik prosesler; Aktif çamur prosesleri, damlatmalı filtreler ve döner biyolojik disklerdir (Aydın, 2020). Ayrıca kimyasal koagülasyon, kimyasal çöktürme, elektrokoagülasyon ve fenton prosesi gibi prosesler de organik içerikli kirleticilerden renk gideriminde kullanılan proseslerdir (Haksevenler vd. 2014). Elektrokimyasal prosesler, kimyasal proseslere ve çeşitli kirleticilerin gideriminde kullanılan proseslere alternatif olabilecek ve son dönemlerde önemi artmış olan bir arıtma tekniğidir (Cansu, 2018). Elektrokimyasal arıtım prosesleri içerdikleri mekanizma anlamında koagülasyon, adsorbsiyon, absorbsiyon, çöktürme flotasyon, oksidasyon gibi proseslerin bir ya da bir kaçını kapsayabilmektedir (Ihara vd, 2004; İlhan vd. 2007). Elektrooksidasyon (EO) prosesi çözünmeyen bir anot malzeme kullanılarak organik maddelerin oksitlenmesini sağlamaktadır (Fil, 2004; Kul, 2005). EO prosesinde yaygın şekilde kullanılan elektrotlar grafit (Kannan vd. 1995), titanyum (Xion vd. 2003), paslanmaz çelik (Bejankiwar vd. 2005), bor kaplı elmas (Martínez-Huitle vd. 2008) gibi çözünmeyen elektrotlardır. EO prosesi temel olarak doğrudan veya dolaylı oksidasyon olmak üzere 2 farklı proses olarak gerçekleşebilir. Doğrudan oksidasyon (Anodik oksidasyon) prosesinde; kirleticiler anot yüzeyinde adsorbe edilir ve daha sonra anodik elektron transfer reaksiyonu ile ayrıştırılır. Dolaylı oksidasyon prosesinde reaksiyon hipoklorit / klor, ozon ve hidrojen peroksit gibi güçlü oksidantlar ile gerçekleşir (Alfredo vd. 2014).

Bu çalışmada titanyum ve paslanmaz çelik elektrotların kullanıldığı EO prosesi ile maya üretimi süreçlerinde ortaya çıkan, işletmenin arıtma tesislerinde arıtılarak deşarj standartlarına getirdiği ve alıcı ortama deşarj edilen atıksu alınarak, renk parametresi açısından tekrar kazanılabilirliğinin belirlenmesi için RES parametresi olarak renk giderim verimleri incelenmiştir.

2. Materyal ve Metod

2.1. Atıksu Karakterizasyonu

Deneysel çalışmalarda kullanılan atıksu maya üretim fabrikasının arıtma tesisi çıkışından alınmıştır (deşarj suyu). Ham atıksu karakterizasyonu Tablo 1'de görülmektedir.

Tablo 1. Ham atıksu karakterizasyonu

Parametre	Değer/ Konsantrasyon	Parametre	Değer/ Konsantrasyon
pH	7,66±0,2	Renk (m^{-1})	
İletkenlik(mS/cm)	6,43	RES436 (m^{-1})	6,81
TDS (mg/L)	3,97	RES525 (m^{-1})	5,21
KOİ (mg/L)	300±10	RES620 (m^{-1})	4,14

2.2. Optimizasyon Çalışmaları

Çalışmada model reaktör ile maya üretimi yapan ve SKKY kapsamındaki Yönetmelik değerlerini sağlayan bir işletmenin deşarj noktasında alınan atıksudan renk giderimi üzerine pH, akım yoğunluğu ve elektroliz süresi gibi işletme parametrelerinin etkisi araştırılmıştır. Araştırmalarda parametre aralıkları literatür taraması ve ön deneysel çalışmalar ile belirlenmiştir. Parametrelerin etkin giderim aralıklarını belirlemek amacıyla, pH 4,5-10,5, akım yoğunluğu 90-150 A/m^2 ve elektroliz süresi 30-60 dk. aralığında olacak şekilde istatistiksel analize göre hazırlanan deney serisi uygulanmıştır (Tablo 2). Optimizasyon çalışmalarında Yanıt Yüzey Metodu kullanılmıştır. 3D grafikler ve ANOVA analizi Design Expert programı ile hazırlanmıştır.

Tablo 2. Farklı elektrot türleri için aralıklar

Faktörler	Titanyum	Paslanmaz Çelik
pH	4,5-9,5	4,5-9,5
Akım Yoğunluğu (A/m^2)	80-140	60-120
Elektroliz Süresi (dk.)	30-60	15-75

2.3. Deney Düzeneği

Elektrokimyasal proses ile renk gideriminin yapıldığı deneysel çalışmalarda, akım ve voltaj kontrolü DC güç kaynağı ile sağlanmıştır. Deneylerde kullanılan model reaktörün hacmi 500 ml'dir. Elektrotların boyutları 50*80*0.5 mm olup, su içerisinde elektroliz işleminin gerçekleştiği bölümün boyutları 50*55 mm'dir (165 cm^2 aktif yüzey alanına sahip elektrotlar için 90, 120 ve 150 A/m^2 akım yoğunlukları için hesaplanan ve sisteme verilen akım sırasıyla, 1,5A, 2A ve 2,5 A'dir).

Elektrokimyasal proses ile maya endüstrisi deşarj atıksularından renk giderimi çalışmasında kullanılan prosesin şematik gösterimi Şekil 1'de verilmiştir.
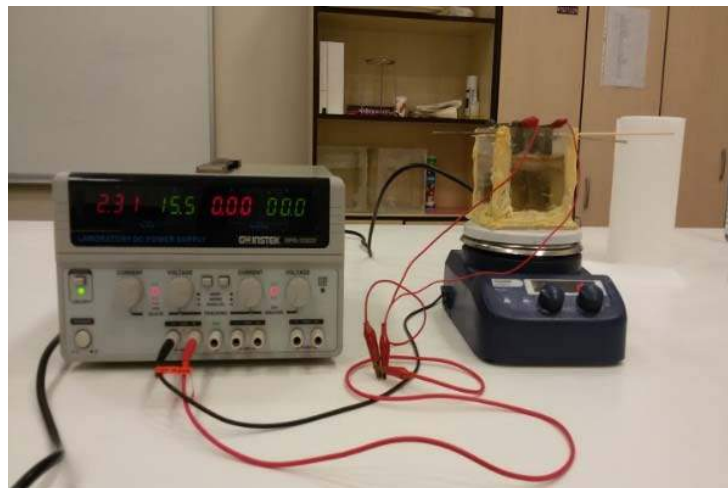
Şekil 1. EO prosesinin şematik gösterimi

2.4. Metot

2.4.1. Renk Tayini

Maya endüstrisi arıtma sonrası deşarj sularından renk giderim veriminin belirlenmesi amacıyla RES metodu kullanılmıştır. EN ISO 7887'ye göre renk parametresinin RES metodu ile ölçülmesi 3 farklı renk analizine (Remazol Yellow RR gran için 436 nm, Remazol Red RR gran için 525 nm, Remazol Blue RR gran için 620 nm dalga boylarında ölçüm yapılır) ayrılmaktadır ve m^{-1} biriminde RES-436, RES-525 ve RES-620 şeklinde renk değerleri belirlenmektedir [EPA].

Hach Lange DR6000 model spektrofotometrede sırasıyla 436, 525, 620 nm dalga boylarında numunenin absorbans değerler okunarak, bu absorbans değerleri Denklem 1'de yerine konulmuş ve RES 436, RES 525, RES 636 değerleri hesaplanmıştır.

$$RES = \frac{A}{d} \cdot f \tag{1}$$

A	: λ dalga boyunda çözeltinin absorbans değeri (cm^{-1})
d	: Küvet kalınlığı (mm)
f	: Spektral absorbans değerini m^{-1} biriminde elde etmek için faktör, f=1000
RES(λ)	: λ dalga boyundaki renklilik sayısı (RES) değeri (m^{-1})

2.4.2. KOİ, pH, İletkenlik Tayini

KOİ analizi SM 5220-D metoduna göre Hach DR6000 model spektrofotometre kullanılarak, pH ve iletkenlik ölçümleri elektrometrik metoda (Standard Metod 4500-H^+) göre Hanna model cihaz ile belirlenmiştir (APHA, 2005).

3. Sonuçlar

Titanyum Elektrot bağlı Elektrokimyasal Proses için optimizasyon çalışmalarında elde edilen RES436, RES525 ve RES620 renk parametreleri için ANOVA analizi sonuçları Tablo 3'te verilmiştir.

ANOVA analizinde, p değerlerine bakıldığında, RES436 renk değeri için pH ve akım yoğunluğu parametrelerinin elektroliz süresine göre daha etkin olduğu söylenebilir (p<0,05). RES525 renk değeri için sadece pH değerinin etkin olduğu, RES620 renk değeri için de pH ve akım yoğunluğu parametrelerinin prosesi etkileyen parametreler olduğu belirlenmiştir. 3D grafiklerde de bu tespitler görülmektedir.

Quadratik modele uyumlu olduğu belirlenen istatistiksel analiz sonucunda R^2 değerleri RES436, RES525 ve RES620 için sırasıyla 0.99, 0.99 ve 0.98'dir.

Tablo 3. Titanyum için ANOVA analizi sonuçları

Source	Sum of Squares	df	Mean Square	F Value	p-value Prob > F
RES 436					
Model	0.59	9	0.066	49.66	0.0002
A-pH	0.25	1	0.25	189.51	< 0.0001
B-A.Y	0.054	1	0.054	40.94	0.0014
C-E.S.	2.000E-004	1	2.000E-004	0.15	0.7141
AB	9.025E-003	1	9.025E-003	6.79	0.0480
AC	2.500E-005	1	2.500E-005	0.019	0.8963
BC	0.021	1	0.021	15.81	0.0106
A^2	0.024	1	0.024	18.33	0.0079
B^2	1.442E-004	1	1.442E-004	0.11	0.7553
C^2	0.24	1	0.24	182.29	< 0.0001
Residual	6.650E-003	5	1.330E-003		
Lack of Fit	6.650E-003	3	2.217E-003		
Pure Error	0.000	2	0.000		
Cor Total	0.60	14			
R^2	0.99				
Adj R^2	0.97				
RES 525					
Model	1.11	9	0.12	53.39	0.0002
A-pH	0.37	1	0.37	159.86	< 0.0001
B-A.Y	4.050E-003	1	4.050E-003	1.75	0.2431
C-E.S.	0.011	1	0.011	4.86	0.0786
AB	9.000E-004	1	9.000E-004	0.39	0.5601
AC	3.600E-003	1	3.600E-003	1.56	0.2675
BC	0.096	1	0.096	41.54	0.0013
A^2	1.641E-004	1	1.641E-004	0.071	0.8006
B^2	0.093	1	0.093	40.01	0.0015
C^2	0.56	1	0.56	240.70	< 0.0001
Residual	0.012	5	2.313E-003		
Lack of Fit	0.011	3	3.833E-003	115.00	0.0086
Pure Error	6.667E-005	2	3.333E-005		
Cor Total	1.12	14			
R^2	0.99				
Adj R^2	0.97				
RES 620					
Model	0.66	9	0.073	33.10	0.0006
A-pH	0.44	1	0.44	197.34	< 0.0001
B-A.Y	0.017	1	0.017	7.73	0.0389
C-E.S.	2.000E-004	1	2.000E-004	0.090	0.7759
AB	0.026	1	0.026	11.56	0.0193
AC	2.500E-005	1	2.500E-005	0.011	0.9195
BC	6.250E-004	1	6.250E-004	0.28	0.6180
A^2	0.17	1	0.17	78.86	0.0003
B^2	1.131E-003	1	1.131E-003	0.51	0.5069
C^2	3.692E-004	1	3.692E-004	0.17	0.7000
Residual	0.011	5	2.215E-003		
Lack of Fit	0.011	3	3.692E-003		
Pure Error	0.000	2	0.000		
Cor Total	0.67	14			
R^2	0.98				
Adj R^2	0.95				

Şekil 2'de RES436, RES525 ve RES620 renk giderim verimleri için pH ve akım yoğunluğu parametrelerinin etkisi görülmektedir. Buna göre, pH değerinin tüm renk parametreleri gideriminde etkin olduğu görülmüştür. Akım yoğunluğunun artması bir noktaya kadar RES525 renk giderim verim artışı ile paralel hareket etmiş yaklaşık 100 A/m² akımdan sonra giderim verimi duraklamıştır. RES436 ve RES620 renk gideriminde akım yoğunluğunun artması ANOVA analizinde de görüldüğü üzere giderim verimini olumsuz yönde etkilemiştir. Titanyum elektrot ile tekstil endüstrisi atıksuyunun elektrokimyasal yöntem ile arıtılmasının incelenmiş olduğu bir çalışmada, 18 dakikalık elektroliz süresinden sonra KOİ, BOİ ve renk parametreleri için giderim verimi %80'in üzerinde olduğu belirlenmiştir (Kocaer vd. 2002; Vlyssides vd. 2000).
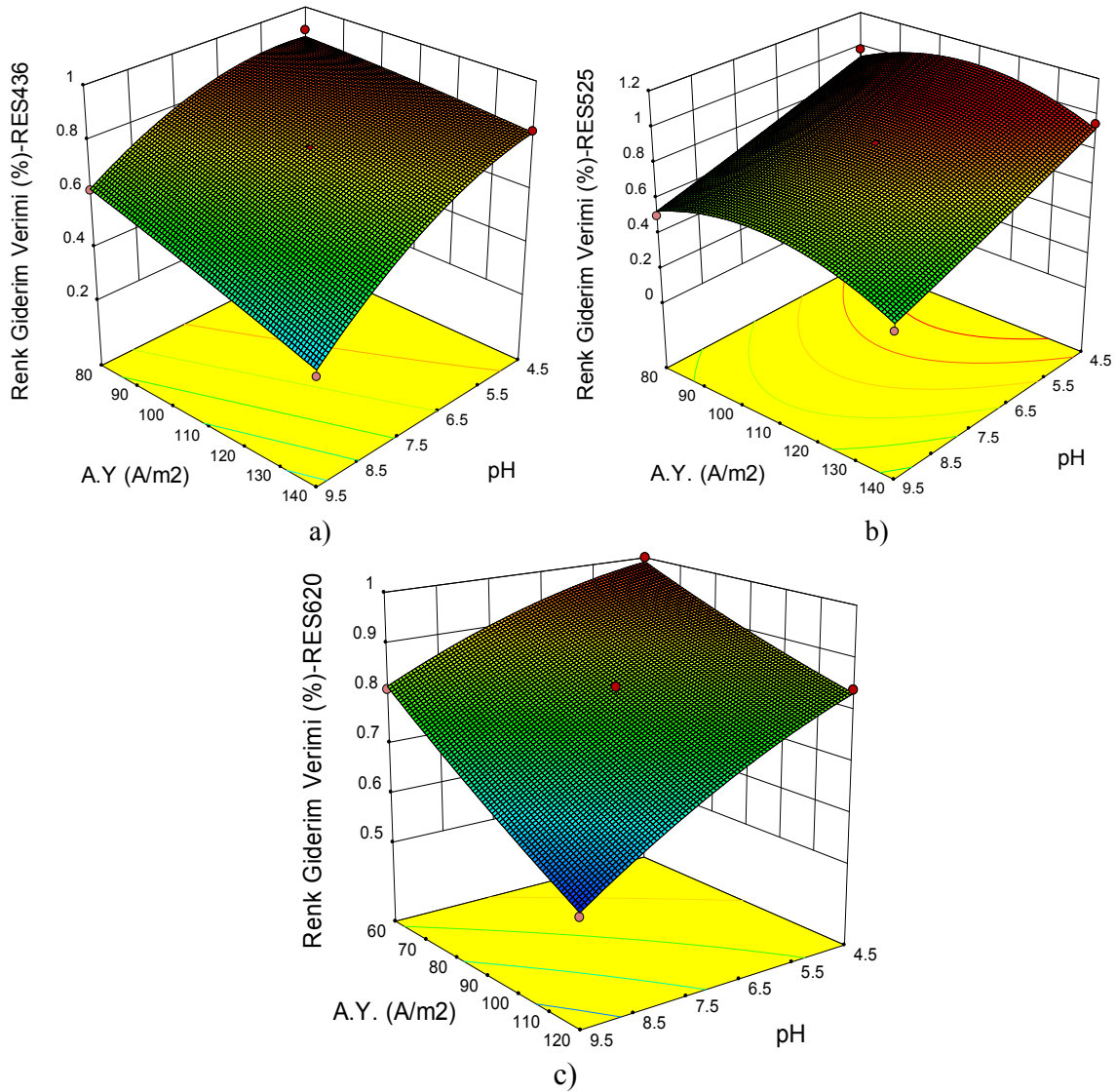
Şekil 2. Titanyum elektrotların kullanıldığı EO prosesinde pH - akım yoğunluğu
parametrelerinin renk giderim verimine etkisi
a) RES 436 b) RES 525 c) RES 620
(Elektroliz Süresi: 45 dk.)

Yapılan çalışma sonucunda elde edilen denklemler Tablo 4'te verilmiştir.

Tablo 4. Farklı renk değerleri için belirlenen eşitlikler

RES436		RES525		RES620	
+0.76		+0.87		+0.98	
-0.18	* A	-0.21	* A	-0.23	* A
-0.083	* B	-0.023	* B	+0.046	* B
-5.000E-003	* C	+0.037	* C	+5.000E-003	* C
-0.047	* AB	-0.015	* AB	+0.080	* AB
+2.500E-003	* AC	-0.030	* AC	-2.500E-003	* AC
+0.072	* BC	+0.16	* BC	-0.013	* BC
-0.081	* A^2	+6.667E-003	* A^2	-0.22	* A^2
-6.250E-003	* B^2	-0.16	* B^2	+0.018	* B^2
-0.26	* C^2	-0.39	* C^2	-0.010	* C^2

Şekil 3'te maksimum RES436, RES525 ve RES620 renk giderim verimi için optimum pH değeri 4.57, akım yoğunluğu 139.84 A/m^2, elektroliz süresi 58 dk. olarak tespit edilmiştir. Optimum koşullarda RES436 giderim verimi yaklaşık % 97, RES525 ve RES620 renk giderim verimleri >%99.99 olarak belirlenmiştir.
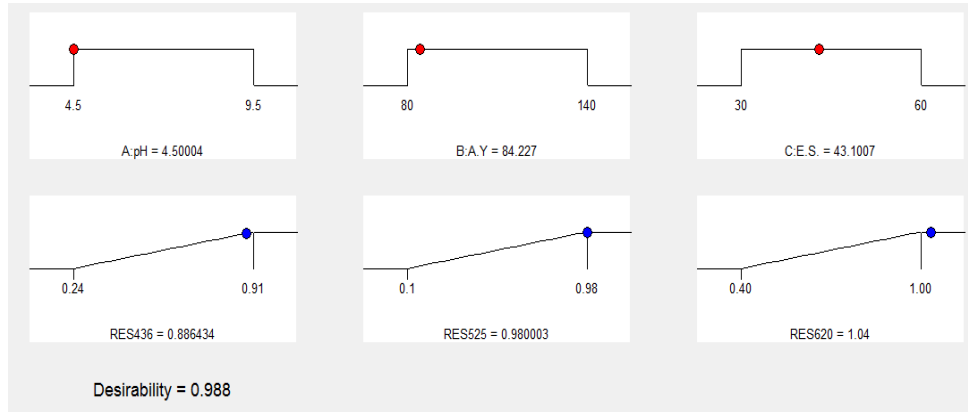
Şekil 3. Renk giderim verimlerini maksimize eden optimum değerler

Paslanmaz çelik elektrot bağlı elektrokimyasal proses için deneysel çalışma sonucunda elde edilen RES436, RES525 ve RES620 renk parametreleri için ANOVA analizi sonuçları Tablo 5'te görülmektedir. Quadratik modele uyumlu olarak belirlenen istatistiksel analiz sonucunda R^2 değerleri RES436, RES525 ve RES620 için sırasıyla 0.99, 0.97 ve 0.99 olarak tespit edilmiştir.

ANOVA analizinde, RES436 renk değeri için, pH, akım yoğunluğu ve elektroliz süresi parametrelerinin p değerlerine bakıldığında, pH ve akım yoğunluğu parametrelerinin elektroliz süresine göre daha etkin olduğu görülmektedir (p<0,05). RES525 renk değeri için sadece pH değerinin etkin olduğu, RES620 renk değeri için de pH ve akım yoğunluğu parametrelerinin prosesi etkileyen parametreler olduğu belirlenmiştir. 3D grafiklerde de bu tespitler görülmektedir.

Şekil 4'te RES436, RES525 ve RES620 renk giderim verimleri için pH ve akım yoğunluğu parametrelerinin etkisi görülmektedir. Buna göre, pH değerinin tüm renk parametreleri gideriminde etkin olduğu, özellikle pH <5 olması durumunda renk giderim verimleri >%80 olarak tespit edilmiştir. RES436, RES525 ve RES620 renk giderim verimleri için akım

yoğunluğu parametrelerinin artması giderim verimini olumsuz etkilemiştir. Çeliğin katot olarak, alüminyum ve demirin anot olarak kullanıldığı bir elektrokimyasal proseste tekstil endüstrisinde kullanılan boyar madde bulunan numuneden renk giderimi üzerine yapılan çalışmada; pH, akım yoğunluğu ve elektroliz süresi gibi değişken parametrelerin renk giderim verimi üzerine etkileri araştırılmıştır. Akım yoğunluğu 2,5 mA/cm² olduğunda renk giderimi %20 iken, akım yoğunluğu 12.5 mA/cm² olduğunda renk giderimi %98 olarak gerçekleşmiştir. Bu proses için optimum akım yoğunluğu 11,25 mA/cm² olarak belirlenmiştir. pH'ın <2 olması durumunda en düşük giderim verimi elde edilmiştir. 5-9 arası renk giderim veriminde bir değişiklik olmazken, ph 9 dan sonra giderim verimi artmıştır (Daneshvar vd. 2007).
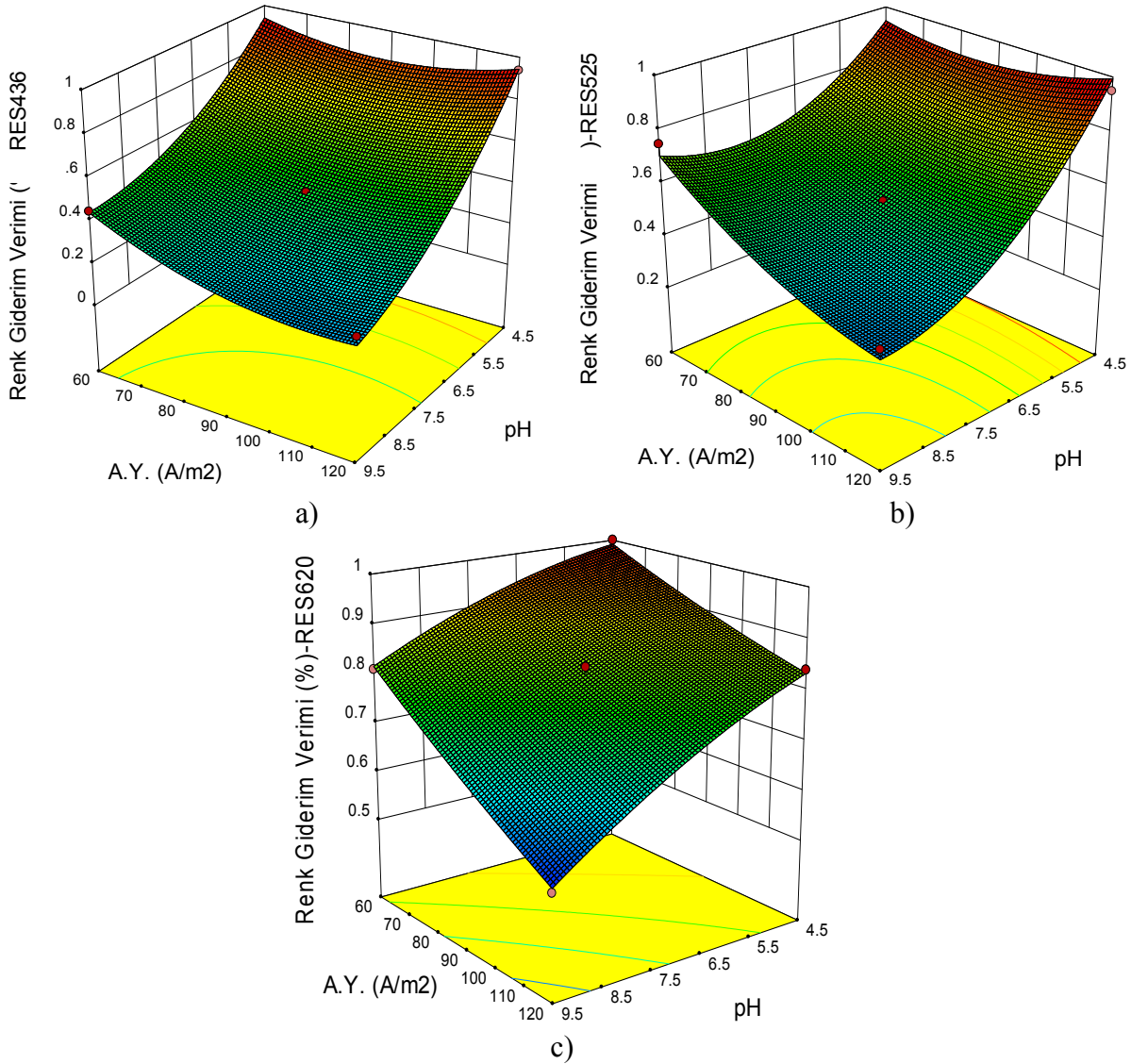
Şekil 4. Paslanmaz çelik elektrotların kullanıldığı EO prosesinde pH - akım yoğunluğu parametrelerinin renk giderim verimine etkisi.
a) RES 436 b) RES 525 c) RES 620
(Elektroliz Süresi: 30 dk.)

Tablo 5. Paslanmaz Çelik için ANOVA analizi sonuçları

Source	Sum of Squares	df	Mean Square	F Value	p-value Prob
RES 436					
Model	0.59	9	0.066	49.66	0.0002
A-pH	0.25	1	0.25	189.51	<
B-A.Y	0.054	1	0.054	40.94	0.0014
C-E.S.	2.000E-004	1	2.000E-	0.15	0.7141
AB	9.025E-003	1	9.025E-	6.79	0.0480
AC	2.500E-005	1	2.500E-	0.019	0.8963
BC	0.021	1	0.021	15.81	0.0106
A^2	0.024	1	0.024	18.33	0.0079
B^2	1.442E-004	1	1.442E-	0.11	0.7553
C^2	0.24	1	0.24	182.29	<
Residual	6.650E-003	5	1.330E-		
Lack of Fit	6.650E-003	3	2.217E-		
Pure Error	0.000	2	0.000		
Cor Total	0.60	14			
R^2	0.99				
Adj R^2	0.97				
RES 525					
Model	1.11	9	0.12	53.39	0.0002
A-pH	0.37	1	0.37	159.86	<
B-A.Y	4.050E-003	1	4.050E-	1.75	0.2431
C-E.S.	0.011	1	0.011	4.86	0.0786
AB	9.000E-004	1	9.000E-	0.39	0.5601
AC	3.600E-003	1	3.600E-	1.56	0.2675
BC	0.096	1	0.096	41.54	0.0013
A^2	1.641E-004	1	1.641E-	0.071	0.8006
B^2	0.093	1	0.093	40.01	0.0015
C^2	0.56	1	0.56	240.70	<
Residual	0.012	5	2.313E-		
Lack of Fit	0.011	3	3.833E-	115.00	0.0086
Pure Error	6.667E-005	2	3.333E-		
Cor Total	1.12	14			
R^2	0.99				
Adj R^2	0.97				
RES 620					
Model	0.66	9	0.073	33.10	0.0006
A-pH	0.44	1	0.44	197.34	<
B-A.Y	0.017	1	0.017	7.73	0.0389
C-E.S.	2.000E-004	1	2.000E-	0.090	0.7759
AB	0.026	1	0.026	11.56	0.0193
AC	2.500E-005	1	2.500E-	0.011	0.9195
BC	6.250E-004	1	6.250E-	0.28	0.6180
A^2	0.17	1	0.17	78.86	0.0003
B^2	1.131E-003	1	1.131E-	0.51	0.5069
C^2	3.692E-004	1	3.692E-	0.17	0.7000
Residual	0.011	5	2.215E-		
Lack of Fit	0.011	3	3.692E-		
Pure Error	0.000	2	0.000		
Cor Total	0.67	14			
R^2	0.98				
Adj R^2	0.95				

Yapılan çalışma sonucunda elde edilen denklemler Tablo 6'da görülmektedir.

Tablo 6. Farklı renk değerleri için belirlenen eşitlikler

RES436		RES525		RES620	
+0.44		+0.53		+0.81	
-0.31	* A	-0.22	* A	-0.11	* A
-0.058	* B	-0.079	* B	-0.11	* B
+0.12	* C	+0.12	* C	+0.034	* C
-0.060	* AB	-0.10	* AB	-0.028	* AB
+0.035	* AC	+0.073	* AC	-7.500E-003	* AC
-0.035	* BC	-0.030	* BC	+0.015	* BC
+0.11	* A^2	+0.16	* A^2	-0.024	* A^2
+0.084	* B^2	+0.062	* B^2	+8.333E-003	* B^2
-0.026	* C^2	-0.023	* C^2	+0.048	* C^2

Şekil 5'te maksimum RES436, RES525 ve RES620 renk giderim verimi için optimum pH değeri 4,84, akım yoğunluğu 60,15 A/m², elektroliz süresi 44 dk. olarak tespit edilmiştir. Optimum koşullarda RES436 giderim verimi yaklaşık %97, RES525 giderim verimi yaklaşık % 95 ve RES620 renk giderim verimi > %99.99 olarak belirlenmiştir.
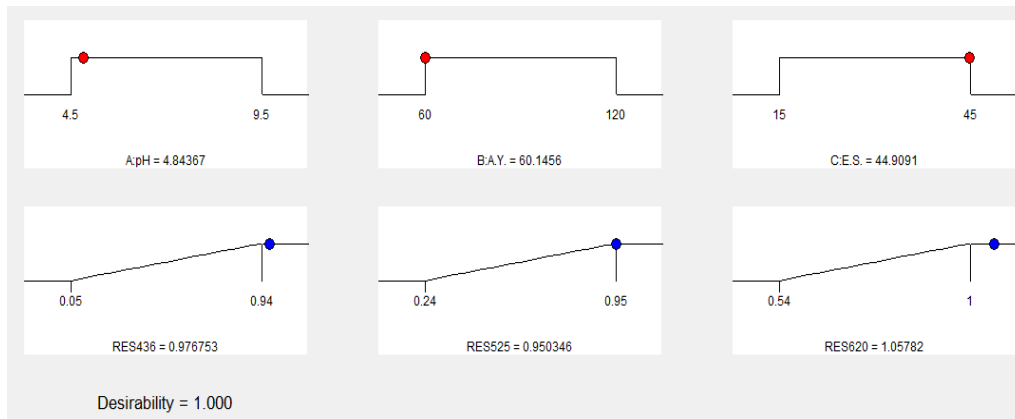
Şekil 5. Renk giderim verimlerini maksimize eden optimum değerler.

Optimize edilen koşullarda maya endüstrisi arıtım sonrası deşarj suyunun (deneysel çalışmalarda kullanılan ham atıksu) ve EO prosesi sonrası atıksudaki renk değişimi Şekil 6'da görülmektedir.

Şekil 6. İşletmenin deşarj atıksuyu ve EO prosesi ile arıtılmış su

4. Tartışma ve Sonuçlar

Yanıt yüzey metodu ile yapılan elektrokimyasal proseslerin optimizasyon çalışmalarında titanyum elektrot için pH değerinin 4.55, akım yoğunluğunun 84.23 A/m^2 ve elektroliz süresinin 43 dk. olduğu optimum şartlarda RES436, RES525, RES620 renk giderim verimleri sırasıyla % 89, % 98, % 99,99 olarak tespit edilmiştir. Paslanmaz çelik elektrot için pH değerinin 4.84, akım yoğunluğu 60.15 A/m^2, elektroliz süresi 45 dk. olduğu optimum şartlarda RES436, RES525, RES620 renk giderim verimleri sırasıyla % 98, % 95, % 99,99 olarak tespit edilmiştir.

İstatistiksel analiz sonucunda quadratik modele uyumlu olduğu belirlenen modelin, R^2 değerleri titanyum için RES436, RES525 ve RES620 için sırasıyla 0.99, 0.99 ve 0.98 olarak, paslanmaz çelik için RES436, RES525 ve RES620 için sırasıyla 0.99, 0.97 ve 0.99 olarak bulunmuştur. Akım yoğunluklarına bağlı olarak prosesin enerji tüketimleri ise sırasıyla, 34,2-122,2 kWsa/m^3 ve 4,64-42,86 kWsa/m^3 aralığında değişim göstermiştir. Aynı giderim verimleri için paslanmaz çelik elektrodunun kullanımının, titanyum elektrot kullanımına göre enerji maliyeti açısından daha uygun olacağı düşünülmektedir.

Titanyum ve paslanmaz çelik elektrotların kullanıldığı elektrokimyasal proseslerin maya endüstrisi deşarj sularındaki rengi oluşturan ve giderimi oldukça kompleks olan melanoidlerin parçalanarak giderilmesinde oldukça etkin olduğu belirlenmiştir. Özellikle, deşarj suyunun tüm renk parametreleri için giderim verimi > %89'dur. Bu durumda işletme tarafından arıtıldıktan sonra deşarj edilen suyun elektrokimyasal prosesler ile tekrar kullanım açısından arıtılabileceği ve arıtılan suyun işletmede tekrar kullanımı için uygulanan prosesler üzerine renk haricinde farklı parametreler ile de değerlendirmeler yapılması gerektiği düşünülmektedir.

Referanslar

Alfredo G., Veronica M., Ivan G. M.,Perla T. A., Monserrat C., Ivonne L. (2014). Industrial wastewater treatment by electrocoagulation–electrooxidation processes powered by solar cells, Fuel 149 (2015) 46–54.

Alkan R., 2010, Melanoidin içeren atık suların renginin mikroorganizmalarla giderilmesi, Ankara Üniversitesi Çevre Bilimleri Dergisi, 2, 89-94.

APHA. (2005). American Public Health Association (APHA), Standard Methods for the Examination of Waste and Wastewater (19th ed.), Washington.

Aydın S., (2020). Erzurum biyolojik atıksu arıtma tesisi arıtma çamuru yönetiminin incelenmesi, Yüksek Lisans Tezi, Atatürk Üniversitesi Fen Bilimleri Enstitüsü, Erzurum, Türkiye.

Balcıoğlu G., (2013). Biyolojik olarak arıtılmış ekmek mayası endüstrisi atıksularının ileri arıtım alternatiflerinin incelenmesi, Yüksek Lisans Tezi, İstanbul Üniversitesi Fen Bilimleri Enstitüsü, İstanbul, Türkiye.

Bejankiwar R., Lalman J., A., Seth R., Biswas N., (2005). Electrochemical degradation of 1,2-dichloroethane (DCA) in a synthetic groundwater medium using stainless-steel electrodes, Water Research, 39, 4715–4724.

Cansu E., (2018). Atık aktif çamurun elektrooksidasyon yöntemi ile ön arıtımının incelenmesi, Yüksek Lisans Tezi, Atatürk Üniversitesi Fen Bilimleri Enstitüsü, Erzurum, Türkiye.

Chen G., (2004). Electrochemical technologies in wastewater treatment, Separation and Purification Technology, 38 (1), 11-41.

Daneshvar N., Khataee A., R., Amani G., A., R., Rasoulifard M., H., (2007). Decolorization of C.I. Acid Yellow 23 solution by electrocoagulation process: Investigation of operational parameters and evaluation of specific electrical energy consumption (SEEC), Journal of Hazardous Materials, 148, pp. 566–572.

Demir N., M., (2012). İleri biyolojik arıtma proseslerinde nütrient giderimi ve mikroorganizme türlerinin incelenmesi, Doktora Tezi, Yıldız Teknik Üniversitesi Fen Bilimleri Enstitüsü, İstanbul Türkiye.

EPA (2009). http://water.epa.gov/drink/contaminants/upload/mcl-2.pdf Europa Norm, 1994. EN ISO 7887.(Erişim Tarihi:02.06.2021).

Haksevenler G., B., H., Doğruel S., Alaton A., İ., 2019. Kimyasal arıtma proseslerinin karasuyun boyutsal dağılımı üzerindeki etkilerinin incelenmesi, Uludağ Üniversitesi Mühendislik Fakültesi Dergisi, Cilt 24, Sayı 3.

Ihara I., Kanamura K., Shimada E., et.al., (2004). High gradient magnetic separation combined with electrocoagulation and electrochemical oxidation for the treatment of landfill leachate, Ieee Transactions On Applied Superconductivity, 14-2, 1558-1560.

İlhan F., Kurt U., Apaydın Ö., Arslankaya E., Gönüllü M., T., (2007). Elektrokimyasal arıtım ve uygulamaları" TÜRKAY 2007 AB sürecinde Türkiye'de katı atık yönetimi ve çevre sorunları sempozyumu.

Kannan K., Sivadurai S., N., John Brechmans, L., Vijayavalli R., 1995. Removal of phenolic compounds by electrooxidation method, J. Environ. Sci. Health, A 30, 2185.

Karaoğlu M., H., (2007). Sulu çözeltilerden bazı boyarmaddelerin fizikokimyasal yöntemlerle giderimi, Doktora Tezi, Balıkesir Üniversitesi Fen Bilimleri Enstitüsü, Balıkesir, Türkiye.

Kocaer F., O., Alkan U., (2002). Boyar madde içeren tekstil atıksularının arıtım alternatifleri, Uludağ Üniversitesi Mühendislik-Mimarlık Fakültesi Dergisi, Cilt 7, Sayı 1.

Kul S., (2005). Zeytin karasuyunun elektrooksidasyon yöntemi ile arıtımının incelenmesi, Doktora Tezi, Atatürk Üniversitesi Fen Bilimleri Enstitüsü, Erzurum, Türkiye.

Martínez-Huitle C., A., Alfaro M., A., Q., (2008). Elmas elektrodun son çevresel uygulamaları: Kritik inceleme, J. Environ. Eng. Manage., 18 (3), 155-172.

Stone C., (1998). Yeast Products in the Feed Industry , Diamond V Mills, Inc. Cedar Rapids, Iowa, 3-15.

Ünal T, (2011). Ekmek mayası endüstrisi seperasyon prosesi atıksularında ozon ve ozon/hidrojen peroksit oksidasyonu ile renk giderimi. Yüksek Lisans Tezi, İstanbul Teknik Üniversitesi Fen Bilimleri Enstitüsü, İstanbul, Türkiye.

Xion Y., He C., Karlsson H., T., Zhu X., (2003). Performance of three-phase three-dimensional electrode reactor for the reduction of COD in simulated wastewater-containing phenol, Chemosphere, 50, 131–136.

Vardar B.,(2006). Tekstil endüstrisi reaktif boya banyolarının elektrokimyasal yöntemler ile arıtımı, Yüksek Lisans Tezi, İstanbul Üniversitesi Fen Bilimleri Enstitüsü, İstanbul, Türkiye.

Vlyssides A., G., Papaioannou D., Loizidoy M., Karlis P., K., Zorpas A., A., (2000). Testing an electrochemical method for treatment of textile dye wastewater, waste management, 20, 569-574.

Yılmaz E., (2014). Maya endüstrisi atıksuyunun ses ötesi dalgalarla arıtılması, Yüksek Lisans Tezi, Hitit Üniversitesi Fen Bilimleri Enstitüsü, Çorum, Türkiye.

Description of 7.5KW Plant Pollution in PV System

Vehebi Sofiu[1*]; Sami Gashi[2*], Besa Veseli[3*]; Shkelzim Ukaj[4*]; Muhaxherin Sofiu[5*]

Abstract: Particles with aerosol pollution based on radiation efficiency, slope angle validity, based on solar panel specification models are used in a residential residence in Prizren. As a result, it has been concluded that aerosol pollution has a direct impact on the efficiency and effectiveness of sunlight taking into account all climatic conditions, including the degree of validity of the slope of the solar panels and the pollution contained on the surface of the panels. Particles found in solar panels resulting from the effects of fossil fuels $CO2$ emissions, as follows from the monitoring of the electronic station located in Prizren. of PM10, PM2.5, SO_2, NO_2, CO, O_3 and NOx. The optimal angle of inclination when satisfactory use of renewable energy is made at 33^0, especially the solar energy source with zero emissions balance. The inclination rate of the solar panel in the Prizren region is 35.5^0 which is close to the optimal value of the analytical measurements of the solar panel placement. Based on the results made with this study for solar radiation, it was concluded that Prizren has the best conditions for the use of sunlight with 12. 15 hours / day of sunshine or 2015 hours / year. From the electronic measurements performed in the 7.5 kW plant in Prizren, it has resulted that the solar radiation is 1580 kWh / m² / year, therefore Prizren has good climatic conditions for the production of solar energy.

Keywords: Radiation efficiency, aerosol particles, electronic station, slope angle.

1. Introduction

The generating plant with photovoltaic system 7.5 kW is composed of modules and connections of solar panels in the form of strings connected in series, divided into groups of inverter connection which are considered as the basic group of the plant, depending on the installation power in converting PV energy. Impacts of pollution from fossil fuels whether from greenhouse gas emissions, dust pollution, burning of old cars, or even from rainfall coming from the atmosphere. Such aerosol pollution is in the form of smog and sticks in the form of a stick on the surface of solar panels, therefore creating many dilemmas of what should actually be done in the future to eliminate these obstacles to the efficiency of solar radiation. Common and simple solar panel models have been developed and integrated into many engineering programs including data simulation on the Matlab platform. However, these models in the case of this research have turned out to be inadequate for the application of the hybrid power system as they need to adapt to certain atmospheric parameters, depending on the locations where the solar plants are installed. Therefore, this study presents a step-by-step procedure for simulating PV cells / modules / arrays with the Matlab / Simulator Tag tools. A DS-100M solar panel is used as the reference model. Characteristics of operation of PV group with large or medium systems and in some cases even small PV

[1] UBT- Higher Education Institution

* Corresponding author: vehebi.sofiu@ubt-uni.net; sami.gashi@ubt-uni.net; besa.veseli@ubt-uni.net; shkelzim.ukaj@ubt-uni.net; muhaxherin.sofiu@ubt-uni.net

systems in case of study for aerosol rainfall, from which convincing results have been obtained that aerosol pollution affects the efficiency of the converting rays of the sun (V. Sofiu, 2019).

1.1. Reflection of sunlight by aerosol particles in space

Aerosol particles are formed by fossil fuels with CO2 which are distributed in the atmosphere in the form of black clouds clustered in appearance as puddles concentrated in different forms which are reflected in the ozone layer envelope where at the same time it affects the direct equilibrium of climate change and also changes the flow of the sun's radiant energy into the atmosphere and the Earth's surface. The distribution of sunlight in the atmosphere by the presence of aerosol particles on the surface of solar panels directly changes the intensity properties in the conductivity flows of radiation cells. Figure 1 shows how to measure aerosol particles in the atmosphere.
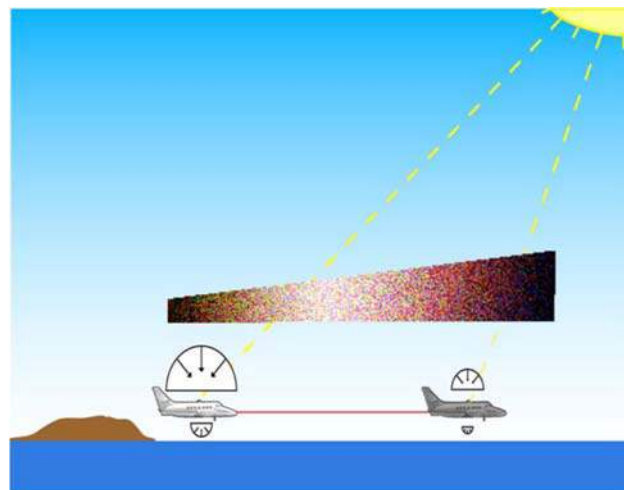
Figure 1: Measurement of aerosol particles in air

Aerosol particles are extraordinarily different depending on the sources they have natural or artificial (driving cars, industry, or power plants) directly affecting climate change which is one of the most important and most pressing challenges facing atmospheric science today globally. Figure 1 illustrates the aerosol particles in the atmosphere with the help of two airplanes in which two measuring instruments are placed in different positions to see to what extent the variety of aerosol according to the flight paths including different amounts (Sofiu.V, 2018).

1.2**. Climate change from aerosol particles**

Particles suspended in the atmosphere in small quantities at cooling points affect the climate of sunlight by changing the flow of radiant energy from the sun to the earth's surface and inside the atmosphere. The effect is to raise the temperature at the earth's surface as a result of the warm energy trapped between the gases in space. This effect occurs directly with the scattering of rays and absorption of sunlight, indirectly affecting the formation of clouds and changing their properties from rain and snow creating the atmospheric mixture, so the atmospheric particles of the aerosol are extremely different because their sources are of artificial and natural composition. To understand in reality the phenomenon of aerosol particles how much they affect climate change, the greenhouse effect is considered to be one

of the most difficult challenges of technological science that the world is facing today from the presence of Global Warming. The change of solar energy flux according to AOD is an important change with aerosol effects which enables climate change called the Forced efficiency of solar radiation (Sofiu.V, 2013).
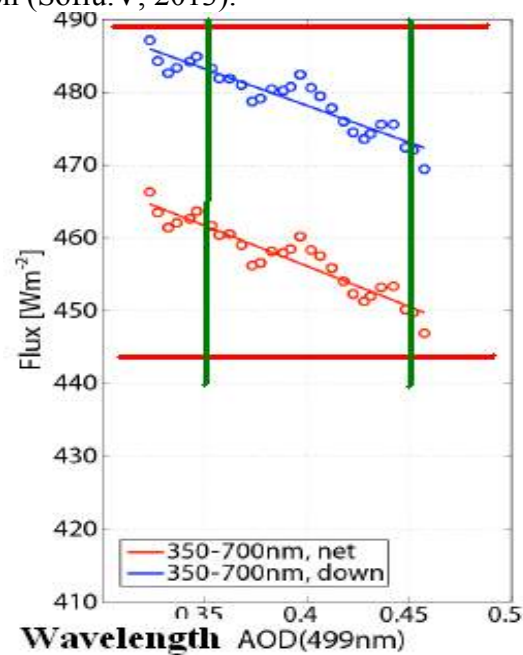
Figure 2. Flux of solar radiation

Figure 2 shows the reduction of sunlight on the surface of space affected by the effect of the aerosol; the flux of solar radiation according to the measured values reaches from 350-700 nm wavelengths with radiant visibility of the sun. (J. Redemann, P.Pileweskie, 2006)

1.3.   Discussion of results

Electronic monitoring stations of KHMI in Prizren with altitudes above 400 m with Latitude 42 ° N and Longitude 20 ° E, in the case of our study are taken in elaboration the data measured in the 7.5 kV system with the generated data planned in the period one year from the commissioning of the PV plant. This analyzes in detail the impact of air polluted with aerosol particles on solar panels, the presence of which affects the intensity of radiation for electricity generation. The average hourly values of Irradiance Global Horizontal (GHI) for these days (23 and 24 April 2019) are presented in Table 1. It From this it is observed that 1 MJ / m2 = 225 Watt-h / m2. As expected, the GHI value has dropped during the storm of rain with aerosol pollution. In fact the average daily values of GHI has decreased from 250 W / m2 on April 23, 2019 to 225W / m2 on April 24, 2019 (reduction of 10% from the previous day). The peak value was reduced from 300 W / m2 to 250 W / m2 (Reduction of 16% from the previous day) (KHMI, 2019).

x	y	z
0.5	8	0.6
2	10	1.9
2.75	12	3.1
2.8	13	2.9
2.7	14	2.8
1.7	16	1.8
0.2	18	0.3

The main reason why a detailed study of solar radiation has been done in this research is analyzing external factors as a benefit or even an obstacle to electricity generation by the PV system with the effect of aerosol pollution on the solar surface where it has resulted in energy loss in case of study .

A cautious role is also the approach of placing the solar panels or the steep slope with orientation at a suitable angle to maximize the solar energy of the incident. In such situations it is necessary to calculate the Global Tilted Irradiance (GTI or IT). The averages of the global tilt, global irradiance, horizontal irradiance and horizontal distribution, irradiances are denoted by It, Id, Ig respectively are related to the following equation (Solar Energy, 2015):

$$\frac{I_t}{I_g} = r_b \left[1 - \frac{I_d}{I_g} \right] + r_d \left[\left[\frac{I_r}{I_g} \right] \right] + r_r \tag{1}$$

Bending factors for radiation, diffuse radiation and reflected radiation:

$$r_b = \left[\frac{\cos(\theta)}{\cos(\theta)_z} \right] = \left[\frac{\sin(\delta)\sin(\emptyset - \beta) + \cos(\delta)\cos(\omega)\cos(\emptyset - \beta)}{\sin(\emptyset)\sin(\delta) + \cos(\emptyset)\cos(\delta)\cos(\omega)} \right] \tag{2}$$

$$r_d = \frac{1 + \cos(\beta)}{2} \tag{3}$$

$$r_r = \rho \frac{1 - \cos(\beta)}{2} \tag{4}$$

Where: latitude (φ), clock angle (ω), declination angle (δ) and solar zenith angle (θz) depend on the location of the place, time and day of the year (T. Hill, 2013).
The tilt angle (β) of the PV panel is taken to be 275 W and the ground reflection (ρ) is assumed to be 0.2. It can be observed that the slope factor for scattered radiation is based on the assumption that the sky is an isotropic source. There are other models that account for the anisotropy of diffuse radiation scattering. The isotropy assumption may be sufficient to predict the yield of the PV plant (S. Kaligirou, 2015).

Table 2: Estimated value of GTI (or TI)

GTI	100	200	300	400	500	600	700	800	900	1000
time	6	8	10	12	14	16	18	20	22	24

It is clear that due to the large decrease in DHI efficiency, the GTI value is significantly reduced when compared to the GHI shown in Table 35. Thus, it is necessary to consider the value of the tilted radiation as a change of the scattered component which reflects in total solar radiation table 2 available for electricity generation (Sofiu.V, 2019).

Table 3 Optimal angle and solar energy per year per m2 for the Prizren region

Month	Ugao(^{0})	Solar energy kWh/m^2/d	No. day	Solar energy kWh/m^2
January	68.5	2.03	31	152.6
February	49.1	3.33	28	93.24
Mart	38.9	4.55	31	136.5
April	25.2	25.2	30	166.5
Maj	5.9	5.9	31	222
June	4.6	4.6	30	299.9
July	1.5	1.5	31	296
August	17.3	17.3	31	186.6
September	32.1	32.1	30	116.6
October	49.3	49.3	31	91.8
November	59.5	59.5	30	99
Decembar	73.4	73.4	31	62.4
Year	**35.5**	**3.14**	**365**	**152.6**

Looking at the graph of monthly and annual data of Table 3, it is concluded that the optimal average angle for the whole year for which we use the maximum solar energy in the solar collector 35, 5 °.

Therefore, the decrease in power due to aerosol particles is expected to be of the same order. (B. Ravindra, 2011)

Conclusion

Particles found in solar panels derived from the effects of fossil combustion pollution based on mathematical modules, simulations on radiation efficiency, slope angle validity, based on the model specifications of the solar panels used for the study and as an intermediate consequence it has been concluded that aerosol pollution has a direct impact on the efficiency and effectiveness of sunlight.

Orientation of the solar panels in the adequate direction in the south-east position, the angle of inclination in the optimal degree is as follows: The angle of validity of the extension of the solar panel for Prizren is 33.5^0 and 35^0 which is close to the optimal value of the analytical analysis solar in 7.5 kV PV system.

Polluted particles with exceeded values are PM 10 and PM 2.5 particles and pollution with fossil fuels and greenhouse gas emissions. Based on the available air quality data, emission data and other statistical data, it can be assessed that the air in Kosovo is of unsatisfactory quality and is outside the allowed limits.

The correlation coefficients of the dependence factor of the intensity of solar radiation falling on the earth's surface fluctuate from the relative humidity of the air, and range from 0.150 to

about 0.440. Formed analytical equations in empirical with the hierarchical communication system are used to make the necessary corrections according to the built algorithmic schemes. Therefore, we will look at the possibilities of finding a way to eliminate these atmospheric obstacles by replacing a new technology including SMART equipment for monitoring particulate matter and at the same time automatic cleaning of solar panels through sensors in the installed plant.

References

Mathematical modelling of aerosols in solar panels; Vehebi Sofiu; 2019.

Impact of aerosol optical depth on seasonal temperatures in Kosovo; V. Sofiu, 2018.

Global access to living environmental protection, V. Sofiu, 2013.

Airborne measurements of spectral direct aerosol radiative forcing in the Intercontinental chemical Transport Experiment/Intercontinental Transport and Chemical Transformation of anthropogenic pollution, 2004.(J Redemann; P.Pileweskie, 2006)

Ames tracking Airboume, AOD (aerosol optical depth - Global Monitoring Laboratory, 2018.

IHMK – Hidrometerological institute, Pristina, 2019

Solar irradiance forecast using aerosols measurements; Solar Energy vol. 122, no. 1158, 2015.

Mathematical modeling of the effect of aerosols on solar panels and climate conditions in order to support the use of alternative energy sources (V.Sofiu, 2019).

Solar Energy, Principles of Thermal Collection and Storage, S.P. Sukhatme and J.K. Nayak, Third ed. New Delhi: Tata McGraw Hill, 2013.

Solar Energy Engineering, Soteris A. Kaligirou, 2015

Performance of a crystalline silicon photovoltaic power plant during sandstorms. B. Ravindra, 2011.

Diagnostic expert systems

Rahimova N.A[1]*, Abdullayev V.H.[2]*

Abstract: The object of the research is expert diagnostic systems. The natural field of application of diagnostic expert systems is medicine. This article considers the expert system "System of diagnosis and programming of treatment of acute surgical abdominal diseases, pancreatic diseases and ophthalmology." Relevant issues were considered for the implementation of this system. The features of expert systems are also discussed here. This article focuses on the characteristics and symptoms of many eye diseases and their grouping into special categories. In addition, the conceptual model of the database, which was implemented in DBASE IV. After that, the structure and phases of the diagnostic expert system for determining the disease were discussed.

Keywords: expert systems; diagnostics; information systems; artificial intelligence; diagnostic expert systems.

1. Introductıon

The medical field is considered more natural for diagnostics, which is why diagnostic systems are more widely used in this field. However, there are still many issues to be investigated in this area. The system of facts characterizing the diagnostics for the application area, the relevant description of the knowledge, the correct estimation of the facts and the validity of the results in the rules, and the adaptation of the diagnostic strategy to the real situation can be considered. [1] In this regard, the medical diagnostic systems developed by the scientists of the Department of Computer Science and Programming at the Azerbaijan State Oil Academy and the Department of Surgery and Ophthalmology of the Azerbaijan Medical University - "Acute surgical diseases of the abdominal cavity", Diagnostics and treatment programming systems for diseases of the pancreas and ophthalmology may be considered relevant. The following issues were investigated and solved for the purpose of each system:

- Investigation of expert systems related to the subject area and the findings and drawbacks in this area;
- Investigation of the subject area, determination of its main objects and relationships between objects;
- Diagnostic decision-making strategy and its main factors;
- Determine the structure of the data base and knowledge base and develop a conceptual model based on the study of the subject area;
- Design and formal description of rules and metadata;
- Creation of logical output mechanism;
- Development of software for expert system implementation;
- System setup and implementation. [2, 3]

The modern level of development of computer technology, mass production of high-performance and wide range of hardware, the emergence of a wide range of software

[1] ASOIU, Baku, Azerbaijan
* Corresponding author: abdulvugar@mail.ru

packages have facilitated the implementation and expansion of intelligent systems, including expert systems. [4] Expert systems are currently used in many areas (planning, forecasting, management, diagnostics, etc.). The most effective of these is diagnostics (failure of complex technical devices and systems, diagnosis of disease in humans), because the solution of diagnostic problems by humans in the usual way often does not give the desired result. [5] There are many reasons for this:

- Lack of complete and accurate information about the object that is diagnosing the condition
- The greater the volume of information, the more difficult it is to analyze and make logical conclusions and to make mistakes;
- Human factor - poor experience, fatigue, memory impairment, etc. [6]

Let's look "Eye Diseases" system created at the City Clinical Hospital I with the help of scientists-ophthalmologists of the Department of Ophthalmology of AMU.

The clinical history of outpatients is collected in the admission department, complaints are studied and clarified, objective examinations in a special sequence (visual acuity, visual field, examination of the eyeball by focal light, reverse and direct aphthamoscopy, determination of eye refraction, biomicroscopy and intraocular pressure palpator) binocular vision examination) and based on the results of these examinations, informative information about the functional condition of each patient's eyes is obtained. Preliminary data are listed in the following order:

- Patient's passport data;
- Doctor's indications;
- Patient's medical history;
- Complaints (local complaints of the patient, general complaints of the patient). [7]
  - Examinations:
  - Stage I (objective examination);
  - Stage II (visual acuity, atropinization, etc.);
  - Stage III (ophthalmolmoscopy);
  - Stage IV (visual field, intraocular pressure, USM). [8]

The study included a total of 150 eye diseases and about 1,000 symptoms associated with those diseases in the 10 most common groups of diseases that cover ophthalmology. [9, 10]

2. Materials and Methods

Before compiling the conceptual scheme of the database, the structure, boundaries of the data and the queries that can be submitted to the system were analyzed. When creating a conceptual scheme, not only the information interests of the user, but also the information needs of the subject area are taken into account for structuring the subject area. All requirements are summarized in a conceptual model that allows you to see the full information content of the subject area. A conceptual diagram showing the structure of the data stored in the database and the relationships between the sections of the subject area is shown in Table 1 to 9.

The conceptual scheme of the system database is based on the relational model of DB. The relational model is based on the description of data structures in the form of ratios and tables. Based on the developed conceptual scheme, the DBASE IV environment was selected to build the physical model of DB.

3. Research results and discussion

According to the conceptual scheme, the database is composed of nine linked tables. PATIENT, DOCTOR, LOCAL COMPLAINTS, GENERAL COMPLAINTS, HISTORY, EXAMINATIONS (STAGES I, II, III, AND IV). Their structure is described in the order from Table 1 to 9.

Table 1. Table of Patient

Field name	Type	Size
Id	N	15
First_Name	C	15
Last_Name	C	15
Second_Name	C	15
Date	D	
Sex	C	8
Age	C	45
Family_status	C	10
Education	C	35
Workplace	C	250
Address	C	250
Diagnosis	M	
Phone	C	10
Have_you_been_examined?	C	5
Where_was_examined?	C	200

Table 2. Table of Doctor

Field name	Type	Size
Id	N	15
D_First_Name	C	15
D_Last_Name	C	15
D_Second_Name	C	15

Table 3. Table of Local Complaints

Field name	Type	Size
Id	N	15

Cipher	C	15
Local_Complaints	C	55
OD	C	15
OS	C	15
OU	C	15

Table 4. Table of General Complaints

Field name	Type	Size
Id	N	15
Cipher	C	15
General_complaints	C	60

Table 5. Table of Anamnesis

Field name	Type	Size
Id	N	15
Cipher	C	50
Anamnesis	C	100
OD	C	25
OS	C	25
OU	C	25

Table 6. Table of Phase I

Field name	Type	Size
Id	N	15
Cipher	C	50
Phase_I	C	100
OD	C	25
OS	C	25
OU	C	25

Table 7. Table of Phase II

Field name	Type	Size
Id	N	15
Cipher	C	50

Field name	Type	Size
Phase_II	C	100
OD	C	15
OS	C	15
OU	C	15

Table 8. Table of Phase III

Field name	Type	Size
Id	N	15
Cipher	C	15
Phase_III	C	100
OD	C	15
OS	C	15
OU	C	15

Table 9. Table of Phase IV

Field name	Type	Size
Id	N	15
Cipher	C	55
Phase_IV	C	100
OD	C	25
OS	C	25
OU	C	25

For example, glaucoma is described as follows:

Q.1. Congenital glaucoma

Q.2.Primary glaucoma

    Q.2.1. Primary glaucoma (by angle)

        Q.2.1.1. Primary open glaucoma

        Q.2.1.2. Primary closed-angle glaucoma

        Q.2.1.3. Primary mixed angle glaucoma

        Q.2.1.4. Suspicion of primary glaucoma

    Q.2.2. Primary glaucoma (by stage)

        Q.2.2.1. Phase I primary glaucoma

        Q.2.2.2. Phase II primary glaucoma

        Q.2.2.3. Phase III primary glaucoma

        Q.2.2.4. Phase IV primary glaucoma

Q.3. Secondary glaucoma

    Q.3.1. secondary glaucoma uveitis

    Q.3.2. Phacogenic secondary glaucoma

Q.3.3. After secondary glaucoma retinal thrombosis

Q.3.4. Secondary glaucoma is neoplastic

Q.4. Intraocular pressure is normal

Q.5.Glaucoma operations

The knowledge base formed in the system consists of about 400 heuristic rules. The rule reflects the decision-making decision of the expert doctor. These rules are constantly changing in the research process. Compilation of rules

Common symptoms and symptom weights appropriate for eye diseases were used in the study. Prices are heuristic and are divided into three conditional groups:

- 0.9- pathognomic;
- 0.8¸0.7 total;
- 0.5¸0.3 according to differential indicators and some medical data.

The pathognomonic (0.9) symptoms accepted in the diagnosis of the disease play an important role in the correct diagnosis. For example, the main pathognymic symptoms of glaucoma selected by a physician are structured in the following sequence:

- 1.4.1. Newborn-1-6 months old babies
- 1.4.2. Child-6 months-12 years;
- 2.30.1. Fear of light (weak) - photophobia;
- 2.31. Irritation of the eyes;
- 5.4.2. The volume of the eyeball is larger than normal (macrophthalmia);
- 5.4.4. Buftalm;
- 6.8.1. Nausea in the cornea;
- 6.12.3. Front camera depth;
- 6.15.1.3. Dilation of the baby (mydriasis).

While these are the main symptoms of congenital glaucoma, they only allow the diagnosis of one type of glaucoma. Using this structure, a knowledge base is created on the principle of "IF THEN" rules. For example,

IF the patient	is a newborn (1-6 months old) {1.4.1.},
OR	is 6 months-12 years old {1.4.2.},
AND	you are not afraid of light {2.30.},
AND	the eye is irritated {2.31.},
AND	the volume of the eyeball is larger than normal (macrophthalmia) {5.4.2.},
OR	the volume of the eyeball is buffalo {5.4.4.},
AND	in the cornea, which is the optic system of the eye
If	there is nausea {6.8.1.},
AND	the front camera is deep {6.12.3.},
AND	the size of the pupil of the eye is gendered (mydriasis) {6.15.1.3.},
THEN	The patient was diagnosed with congenital glaucoma (Q.1.)

The extraction mechanism in the system depends on the state of the working memory and the composition of the knowledge base. At the selection stage, the active collection of

data and rules (modules) is selected. After all the information is collected in the database and the rules knowledge base, the patient's complaints and symptoms collected in the database on the doctor's examination are displayed in turn, and the answers are collected in the computer's memory block.

The activation phase determines which active modules are ready for use in which active data. Performs comparison of all rules and data at each stage of the extract mechanism for the diagnosis of the disease. The facts collected in the memory block are compared to the diseases collected in the knowledge base. The structure of the disease is defined as a tree-like hierarchical scheme. Figure 1.
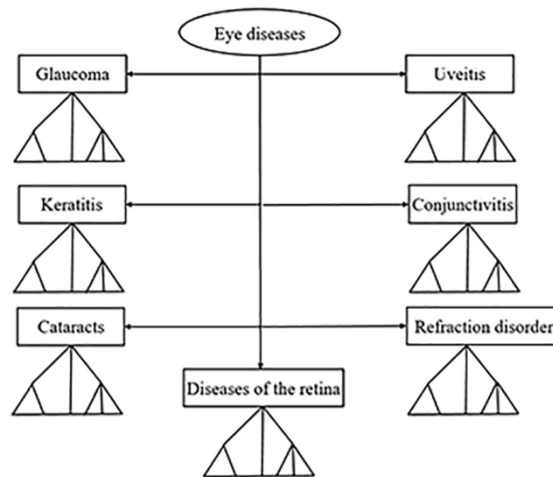
Figure 1. Classification scheme of eye diseases

The woody structure is of great importance for testing hypotheses. This structure, on the one hand, reflects the possible relationships between diseases, and on the other hand, determines the strategy of the diagnostic search process. The main goal is to search for the right data. There are high-level group diseases, low-level diseases, and intermediate diseases, which combine diseases that are not so different from each other. The purpose of the diagnostic system is to detect the disease. Second-level diseases include several diseases that have a certain amount of common properties, and if the system cannot identify the disease, it responds to the user with a corresponding second-level disease. The first level of diseases is pathologically common and is called a group disease.

In the dispute resolution phase, the extract mechanism evaluates these rules for their relevance to the current goal.

At the execution stage, the description of the rules (modules) selected during the dispute resolution stage is performed, and finally, the result of the operation period of the extraction mechanism is output to the user.

The algorithm for selecting the operating mode of the system is described in Figure 2.

The software is organized in modules. These modules allow you to receive information about the patient at any time, enter the patient's symptoms, diagnose, edit the information, quickly search for the necessary information from the database, make a decision, print a medical history, and more allows.
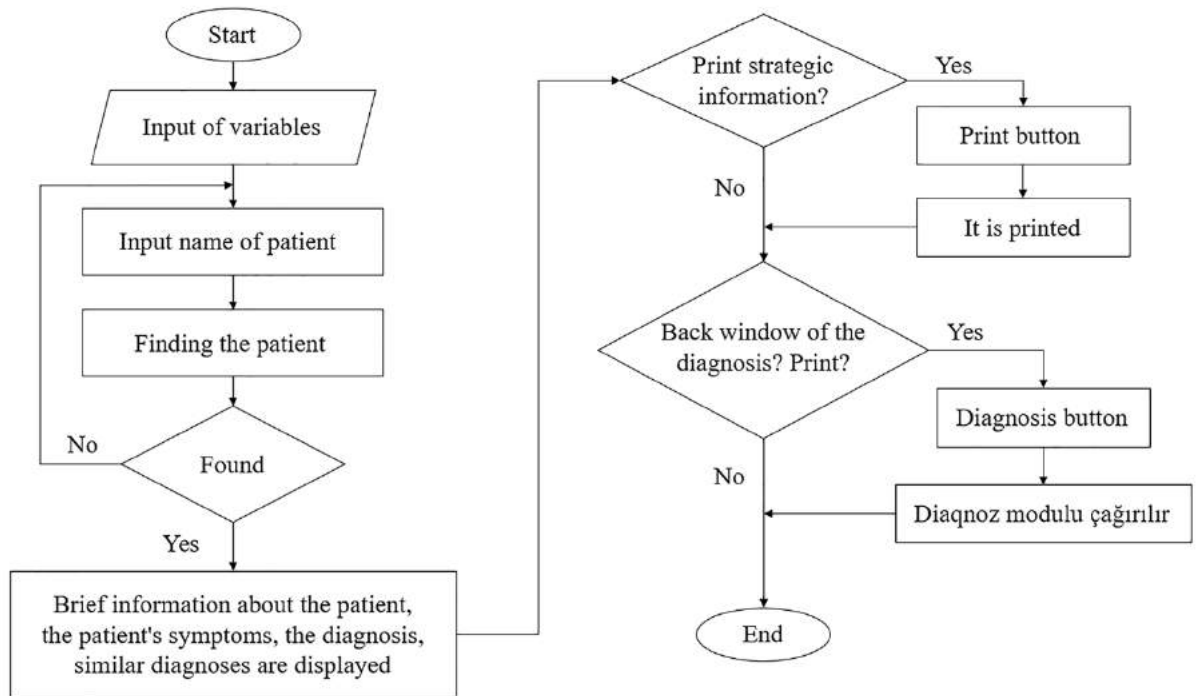
Figure 2. Search module algorithm

This tree-like structure contains information about all the modules, allows you to look at the sub-branches to get acquainted with the working principle of other modules.

The facts section describes the working principles of the modules, which ensure that the patient's symptoms are included in the program. These modules are mainly:
- anamnesis;
- examinations;
- complaints.

The anamnesis module provides input of the patient's anamnesis data into the program.

The "Examinations" module provides for the inclusion in the program of the patient's data, i. e. symptoms identified as a result of examinations. The admission process is carried out according to the following examination stages:
- Stage I (objective examination);
- Stage II (visual acuity, atropinization, etc.);
- Stage III (ophthalmoscopy);
- Stage IV (visual field, intraocular pressure, USM).

The "Complaints" module provides for the inclusion in the program of the data identified as a result of the patient's complaints, i. e. symptoms. The admission process is conducted in accordance with the following types of complaints
- local complaints;
- common complaints.

In the "Diagnosis" module, the diagnosis is made by including the main symptoms of both patients with a permanent medical history and those with a history of illness. Diagnosis is made according to the following modules:
- diagnosis made with constant maintenance of medical history;
- Diagnosis of non-permanent or operative history of the disease.
- Optics;
- Teaching part;
- Part of public service.

The "Help" module informs the user about the program, the author, as well as the working principles of the individual modules of the program. This module also explains the working principle of the Inquiry Book. This module consists of 4 parts:

- About medicines;
- Optics;
- Teaching part;
- Part of public service.

The research materials included 500 patients admitted to the "Eye Diseases" department of Baku Clinical Hospital No. 1 with eye diseases.

4. Conclusions

Expert Systems, which play a special role in the field of artificial intelligence, are very important for the development of technology and their future achievements.
With the help of Diagnostic Expert Systems, a type of expert system, great advances have been made in both the technology and the medical world. With the correct use of these systems, it is possible to conduct accurate diagnostic assessments.

References

[1] J. Yanase, E. Triantaphyllou, "A Systematic Survey of Computer-Aided Diagnosis in Medicine: Past and Present Developments". Expert Systems with Applications 138, 2019
[2] S. Jabeen, G. Zhai, "A Prototype Design for Medical Diagnosis by an Expert System". 7th International Workshop on Computer Science and Engineering (WCSE 2017)
[3] P. Patra, D. Sahu, I. Mandal, "An Expert System for Diagnosis Of Human Diseases". International Journal of Computer Applications 1(13), 2010
[4] J. Singla, D. Grover, A. Bhandari, "Medical Expert Systems for Diagnosis of Various Diseases". International Journal of Computer Applications 93(7), 2014.
[5] D. Matthias, O. Udo, "Expert System for Medical Diagnosis of Hypertension and Anaemia". MA YFEB Journal of Enviromental Science 3, 2017.
[6] S. Abu-Naser, R. Aldahdooh, A. Mushtaha, M. El-Naffar, "Knowledge Management in ESMDA: Expert System for Medical Diagnostic Assistance". ICGST-AIML Journal 10(1), 2010.
[7] I. Abundez, E. Rendon, C. Estrada, S. Zagal, "Diagnosis of Medical Images Using an Expert System".
https://www.researchgate.net/publication/220942958_Diagnosis_of_Medical_Images_Using_an_Expert_System
[8] S. Abu-Naser, Abu Zaiter O., "AN EXPERT SYSTEM FOR DIAGNOSING EYE DISEASES USING CLIPS". Journal of Theoretical and Applied Information Technology 4(10), 2008.
[9] S. Sikchi, S. Sikchi, M. S. Ali, "Artificial intelligence in medical diagnosis". International Journal of Applied Engineering Research 7(11), 2012.
[10] A. Oluwafemi J., I. A Jimoh, "Expert System for Diagnosis Neurodegenerative Diseases". International Journal of Computer and Information Technology 4(4), 2015.

Investigation of the Relationship Between Bridge Equipment Location, Fatigue and Mental Workload by Using Piper Fatigue Scale and NASA-TLX

Leyla Tavacıoğlu[1*], Bayram Barış Kızılsaç[2*], Neslihan Gökmen İnan[3*], Özge Eski[4*], Can Tanguç[5*]

Abstract: Fatigue is the decrease in the level of physical and mental data received by the individual in connection with many reasons such as the individual's work. Fatigue also takes an important place by negatively affecting the individual herself, her/his relations with her environment and her working life. Maritime trade, which has a great place in the growing world trade day by day, is indisputably affected by these situations. Thanks to the developing technology, the quality of the equipment used becomes better and more efficient over time. However, despite these, due to the increasing workload, the fatigue on the employees gradually increases and this causes some negativities in individuals. In this study, it is aimed to investigate the relationship between bridge equipment position, mental workload and fatigue. In this context, 42 ship's people who have worked/worked on the ships are participated and answered NASA-TLX and Piper Fatigue Scale. NASA-TLX measures performance, effort, frustration, mental, physical and temporal demand. Piper Fatigue Scale have four subdimensions such as behavior, affective, sensory and cognitive mood. This study reveals that there is statistically significant positive correlation between fatigue and mental workload ($p < 0.05$). In addition, mental workload and fatigue are found to be associated with bending status and the degree of eye strain from the bridge equipment in the use of ECDIS and RADAR. In the following studies, mental workload assessment can be made for different operational processes by increasing the number of samples.

Keywords: piper fatigue scale, NASA-TLX, bridge equipment location, maritime transportation

1. Introduction

Approximately 90% of global trade is carried out by maritime transport. In case of the slightest interruption of this trade, it deeply affects the world markets from the largest to the smallest. The safe handling and management of ships is a responsibility of the ship's people. For this reason, the health and well-being of seafarers is known as an important building block for the flow of trade to continue undisturbed (Kinchington, 2020).

Maritime is one of the most dangerous occupations compared to other occupations. It is also seen that the stress is high. Considering the working environment on the ship, it includes

[1] Istanbul Technical University, Maritime Faculty, Basic Sciences, Istanbul, Turkey
* Corresponding author: tavaciog@itu.edu.tr

sound pollution, vibration effect, intense work tempo, hot and cold weather conditions (Öztürk, 2021).

Fatigue is a common denominator in the maritime sector, as in many other sectors, and is an important problem. In general, it is stated that 70-80% of the accidents that occur in the sea are caused entirely by human error. Fatigue is shown as the main cause of the majority of these accidents (Reyner&Baulk, 1998).

With the increase in the level of fatigue of the ship's people, which are frequently encountered in the maritime community, disasters with high costs occur. The decrease in performance caused by fatigue in individuals causes health problems, damages to the environment and a decrease in the working time of individuals on board (Smith et al., 2001).

In this study, the relationship between bridge equipment position, fatigue and mental workload is investigated. During this study, the Piper Fatigue Scale (PFC) and NASA-TLX's rating and weighting models are handled and a seafarer's attitude-based survey is conducted. The sub-dimensions of PFC and the rating part of NASA-TLX are analyzed among themselves and it was also examined whether there was a correlation between them.

2. Material ve Method

The research is carried out to measure the relationship between the position of bridge equipment, mental workload and fatigue. The content of the research is conducted in the form of data collection on a survey basis. The survey consists of three parts. First of all, 6 questions are asked within demographic characteristics, such as the gender, age, education status of the participants, their duties on the ship, the length of time they worked at sea, and the types of ships they mostly worked with. Following the demographic data, questions about the Piper Fatigue Scale and the bridge related questions are added. Finally, NASA-TLX rating and weighting questionnaires are asked and the questions. The questionnaire is completely created on the online platform and send to the people via the Google Forms. To investigate the correlation between two normally distributed variable Pearson correlation analysis is used. IBM SPSS Statistics for Windows, Version 24.0. is used and the significance level is determined as 5%.

2.1. Piper fatigue scale (PFC)

A comprehensive measurement model for fatigue, the Integrated Fatigue Model, was created by Piper et al. in 1987 to evaluate. When the scale was first made, it consisted of 42 items and with the changes made over time, each question is 0-10 points in the present time and is evaluated in four sub-sections at the point of fatigue levels of the patients, which consists of 22 items in total evaluated based on the VAS (Visual Analog Scale). These parts are: violence and behavior sub-dimension that evaluates the effect and severity of fatigue (2-7 items), affective sub-dimension (8-12 items), which includes the emotional state that is the source of fatigue, and sensory sub-dimension that reflects mental and mental symptoms of fatigue (13-17 items) and the mental sub-dimension (18-23 items) that shows the level of cognitive effect of fatigue on symptoms and mood. In addition, there are 5 items (1st and 24-27 items) that are not active at the point of calculating the fatigue score in the scale, but are important for the evaluation of the data related to fatigue. Out of these 5 items, item 1 deals with the process of fatigue, while item 24-27 is for individuals who are sick to express their thoughts on fatigue (Clark et al., 2006).

According to the mean scores of the Piper scale, they are ranked as follows:
0 points: No fatigue
1-3 points: Mild feeling of fatigue
4-6 points: Moderate fatigue
7-10 points: Extreme level of fatigue

2.2. NASA-TLX

Although the definition of workload is gradually increasing its effectiveness in the academic community, there has not been a clear consensus on the definition point. Generally used in the existing definitions; It is done on the basis of three variables, namely the amount of work, duration and the individual's psychological experience. When the definition of workload was first made, the focus was on physical workload, however, with the advancement of technology over time, the use of machines more efficiently instead of the work that is physically engaged in, the workload of workload began to be focused on the issue of workload in a mental rather than physical sense (Taç, 2018).

NASA-TLX (NASA Task Load Index) is a subjective and multidimensional workload assessment scale created by Hart and Staveland in order to evaluate the degree of mental workload of individuals. NASA-TLX Since it was originally designed for use in the aviation industry, most of the work has been done on air traffic control, civil or military cockpits. Recently, studies on portable technological devices such as automobile drivers, clinical research, computers or mobile phones are increasing day by day (Taç, 2018).

NASA TLX is a multidimensional assessment-based procedure that looks at the rating averages of six subscales and creates an overall score for a workload. These dimensions are as follows;
performance, effort, frustration, mental, physical and temporal demand. Individuals define the contribution rate made by each of the six dimensions in order to make the determined workload intensity clear.

NASA-TLX evaluates the workload scale in two stages as rating and weighting. In the first stage, each dimension describing the workload consists of a comparative evaluation of its contribution to the workload. NASA-TLX weighting form is used for this. Based on the preference made by the person, how much each factor is marked is calculated, and weights (from 0 to 5) are assigned to the six factors. In the second stage, it consists of grading the six dimensions that make up the definition of the workload separately on a numerical basis. For this reason, NASA-TLX rating form is used, based on independent scoring of all six workload factors. The person completes the form by giving a score between 0 (low) and 20 (high) for the dimensions of the workload in the specified jobs. Finally, the person's total mental workload rating averages (between 0 and 100) are obtained (Taç, 2018; Hart, 2006).

3. Results

42 ship's people who have worked/worked on the ships are participated and answered demographic questions, NASA-TLX and Piper Fatigue Scale. NASA-TLX measures performance, effort, frustration, mental, physical and temporal demand. Piper Fatigue Scale have four subdimensions such as behavior, affective, sensory and cognitive mood.

Table 1. Distribution of Demographics

		N	%
Age	20 ve altı	4	12
	21-30	33	79
	31-40	5	9
Education	Faculty	40	95
	Vocational School	2	5
Position	Deck Intern	23	55
	Watch Officer	14	33
	First Officer	4	10
	Captain	1	2
Working at sea	Up to 2 years	29	69
	2-4 years	11	27
	4-8 years	1	2
	8-12 years	1	2
Type of vessel	Tanker	23	55
	Dry cargo	6	14
	Container	6	14
	Ro-Ro	3	7
	Other	4	10

A significant part of the participants consists of male ship people. The main reason for this is that women have not worked at sea for many years. However, this perception has started to be broken and women's employment in the sector continues to increase. It can be said that the majority of those who participated in the survey were young. Most of the people who participated in the survey are either a faculty graduate or a faculty member. More than half of the respondents are deck trainees. The number of deck trainees is followed by the watch officers. It is seen that the majority of the participants have up to 2 years of sea experience. It is seen that more than half of the participants mostly worked as a tanker type of ship (Table 1).

Table 2. Distribution of Bridge Related Questions

		Mean	SD
The degree of eye strain from bridge equipment lights.	00.00-04.00	5.45	1.316
	04.00-08.00	6.5	2.057
	08.00-12.00	4.97	1.494
	12.00-16.00	4.85	1.197
	16.00-20.00	5.64	1.686
	20.00-24.00	5.16	1.229
		N	%
How the chart table affects the bow view	Yes	30	71.4
	No	12	28.6
Color distribution in which Radar is used in general at night time	White	5	11.9
	Blue	14	33.3
	Green	18	42.9
	Orange	5	11.9
Body bending distribution in the use of RADAR and	Yes	30	71.4

ECDIS.	No	12	28.6
Presence of any obstacle that may affect the viewpoint of the captain and pilot's seat at the bow point of view	Yes	7	16.7
	No	35	83.3
Eye disease	Yes	24	57.1
	No	18	42.9
If there is an eye disease, whether or not it occurred while working on board.	Yes	2	4.8
	No	16	38.1

SD: Standard Deviation

According to Table 2, while the shift in which fatigue is felt more is seen as 04.00-08.00, the shift in which fatigue is felt less is reflected to the values between 12.00-16.00. 71.4% of the participants stated that chart table affects the bow view, they are bending their body in the use of RADAR and ECDIS and 42.9% of them answered that green color is used in Radar in general at night time. 4.8% of them have eye disease and it occurred while working on board.

Table 3. Distribution of PFC and NASA-TLX

		Mean	SD
PFC	Behavior/severity	5.658	2.035
	Affective/meaning	5.971	1.943
	Sensory	5.523	2.065
	Cognitive mood	5.13	1.928
NASA-TLX	Mental demand	7.26	2.26
	Physical demand	6.93	2.37
	Temporal demand	7.5	2.2
	Performance	8.07	1.28
	Effort	6.43	2.42
	Frustration	6.07	2.9

Since the general average of the total 4 sub-dimensions remained in the 4-6 points band, an analysis can be made that the individuals participating in the study felt moderately fatigued. In the NASA-TLX form each dimension are changing between 0-20 points (very low-very high). The results show that, the participants have medium level mental workload which is close to 10.

Table 4. Correlation analysis between PFC and NASA-TLX

		PFC			
	r, p	Behavior/ severity	Affective/ meaning	Sensory	Cognitive mood
NASA-TLX	Mental demand	0.116,0.464	**0.339, 0.028**	0.070, 0.659	0.298, 0.055
	Physical demand	**0.477, 0.001**	**0.566, <0.001**	**0.350, 0.023**	**0.439, 0.004**
	Temporal demand	0.284, 0.068	**0.392, 0.010**	0.222, 0.157	0.293, 0.060
	Performance	0.157, 0.322	0.180, 0.255	0.032, 0.842	-0.006, 0.972
	Effort	**0.380, 0.013**	0.293, 0.060	0.234, 0.134	**0.460, 0.002**
	Frustration	**0.512, 0.001**	**0.488, 0.001**	**0.509, 0.001**	**0.527, <0.001**

Pearson correlation coefficient

According to Table 4, there is statistically significant positive moderate correlation between behavior/severity and physical demand, effort and frustration. There is statistically significant positive moderate correlation between affective/meaning and frustration, physical, mental and temporal demand. There is statistically significant positive moderate correlation between sensory and physical demand, frustration. In addition, the significant positive correlation is found between cognitive mood and physical demand, effort and frustration.

4. Discussion and Conclusions

In this study, the relationship between the effects of bridge device positions on the people of the ship and the Piper fatigue scale and NASA-TLX were examined. First of all, it consists of the distribution of gender, age, education level, task distribution on the ship, working time at sea and finally the ship types they mostly worked in.

Participants showed that fatigue was felt more at the end of the 04.00-08.00 shift on the bridge. (10/6.5) Bridge 12.00-16.00 shift was recorded as the shift in which fatigue was felt the least compared to other shifts (10/4.5).

According to the 1st sub-dimension scale of the Piper fatigue scale, the value of the dimension evaluating the effect and severity of fatigue was approximately 5.65 points out of 10. This shows that the effect is felt moderately. According to the data of the 2nd sub-dimension, the affective sub-dimension data covering the emotional meaning attributed to fatigue is 5.97 points out of 10, which is the highest score among the dimensions. It is seen that the effect part is moderate. In the data presented by the 3rd sub-dimension, the emotional sub-dimension score of fatigue, which reflects mental, physical and emotional symptoms, emerged as 5.52 out of 10. Accordingly, the degree to which it is felt is medium in size. Finally, according to the data of the 4th sub-dimension, the psychological sub-dimension value, which reflects the effect of fatigue on cognitive functions and mental state, is 5.13 points out of 10 and has the lowest value among the four dimensions.

In general, when the average value of all the sub-dimensions of the Piper fatigue scale is taken, it is clearly seen that the participants feel moderately fatigued because they are at the level of 4-6 points.

In the correlation analysis of PFC and NASA-TLX rating, 4 sub-dimensions of Piper and 6 titles from NASA-TLX rating were taken and a total of 24 pairwise relationships are evaluated. 11 of these have significant positive moderate correlation. Frustration and physical demand have significant correlation with all PFC sub-dimensions. It can be said that as the fruition and physical demand increase, fatigue increases and vice versa. In addition, mental workload and fatigue can be associated with bending status and the degree of eye strain from the bridge equipment in the use of ECDIS and RADAR due to having large part of sample.

In the following studies, mental workload assessment can be made for different operational processes by increasing the number of samples.

References

Carrieri-Kohlman, V., Lindsey, A. M., & West, C. M. (2003). Pathophysiological phenomena in nursing: Human responses to illness (p. 640). Philadelphia, PA: Saunders.

Clark, P. C., Ashford, S., Burt, R., Aycock, D. M., & Kimble, L. P. (2006). Factor analysis of the Revised Piper Fatigue Scale in a caregiver sample. Journal of nursing measurement, 14(2), 71-78.

Hart, S. G. (2006, October). NASA-task load index (NASA-TLX); 20 years later. In Proceedings of the human factors and ergonomics society annual meeting (Vol. 50, No. 9, pp. 904-908). Sage CA: Los Angeles, CA: Sage publications.

IBM Corp. Released 2016. IBM SPSS Statistics for Windows, Version 24.0. Armonk, NY: IBM Corp.

Kinchington, F. Under whose flag? The race to dominate natural resources: an examination of the evolving power dynamics of superpowers and flag protectionism on global trade and maritime security.

Reyner, L., & Baulk, S. (1998). Fatigue in ferry crews: a pilot study (p. 34). Cardiff: Seafarers International Research Centre.

Smith, A. P., Lane, T., & Bloor, M. (2001). Fatigue offshore: A comparison of offshore oil support shipping and the offshore oil industry. Seafarers International research Centre/Centre for Occupational and health Psychology, Cardiff University, Cardiff.

Taç, Umut. (2018). Gemiadamlarının Bilişsel Yeteneklerinin Durumsal Farkındalık Açısından Modellenmesi, İstanbul Teknik Üniversitesi, Fen Bilimleri Enstitüsü.

The Developing Automation and Applications in Maritime Transformation Process of Freights

Leyla Tavacıoğlu[1*], Bayram Barış Kızılsaç[2*], Özge Eski[3*], Neslihan Gökmen İnan[4*], Mehmet Mert Dalyan[5*], Ercan Emre Erköse[6*]

Abstract: Due to a variety of facilities created by the globalized world trade, the products and services have recently been able to meet the relevant consumers in a geographically wide scope of the area. The trade implemented in the global scope does naturally involve trade activities with global features wherein transportation plays a critical role. In meeting any products, particularly low-cost ones, with the consumers, one of the highest cost items is transportation. In this context, supply chain management involves not only supplying the goods but also comprises planning, implementing, monitoring, and controlling the whole process including transportation from the supply point to the final consumer in a manner that could yield minimum cost and maximum utility. The ever-increasing severe competition has made it inevitable for ports to get operated efficiently and ceaselessly providing customers with added value. Regarding this, providing ceaseless and efficient port services requires a performance measuring device. There are mainly four logistical processes carried out at container terminals. Those are ship operations, moving containers, warehousing, and handling containers. The efficient and effective operation of these four basic processes increases the competitive power of ports, which means that the mentioned processes are necessary to optimize. Such optimization requires thorough analyses of the contribution to the system made by any aspects affecting the basic processes and where needed, the system operations must be interfered with.

The purpose of this research is to review a logistical oriented decision supporting model as a decision support instrument for port management aims to contribute to such basic topics as comprehending analyzing and evaluating the logistical structure of ports as well as port performance indicator, planning port capacity, increasing port efficiency, developing internal port logistical processes and predicting the needs of the port in the future. Eight specific trends, that will have a combined impact on the port industry's outlook in 2030 are explained in this study. This research also examines how the major maritime trends are affected by the various factors, as well as what this means for the port business in the future.

Keywords: automation, maritime transportation, freights, logistics

1. Introduction

Ports, which constitute the nodal point in the fulfillment of many activities in the transportation chain; In addition to their basic functions such as loading/unloading, towage, and storage, they are in contact with many organizations or individuals such as shippers,

[1] Istanbul Technical University, Maritime Faculty, Basic Sciences, Istanbul, Turkey
* Corresponding author: tavaciog@itu.edu.tr

exporters, importers, logistics companies, state authorities, banks, insurance companies. With this feature, ports provide important contributions to the country's economy by providing the coordination of many commercial and legal transactions as well as the transfer of cargo. Ports have very different and important functions in terms of micro and macro aspects. In the fulfillment of national and international marketing functions, these functions must be carried out effectively and economically (Esmer, 2009).

A well-functioning freight transportation infrastructure is critical for the economy and for maintaining a good standard of living. Intelligent transportation systems aspire to enhance the utilization of current transportation systems, capacity from existing physical infrastructure, safety, and security, while lowering the negative environmental consequences of freight transportation (Ranaiefar, 2012). Innovative solutions may assist operators in the organization of freight management and handling operations at freight terminals, promoting intermodal transport by lowering terminal handling times and costs. Driven by mechanization of manufacturing, automated guided transport systems and vehicles for commercial purposes were developed in the early 1950s in the United States and about 10 years later in Europe, with the goal of optimizing material flows and decreasing labor demands. Automation was first utilized in manufacturing and warehousing (Flämig, 2016), but automated freight transport systems have yet to be used in public open space because they require specialized infrastructure and laws. With autonomous driving hitting the market, (Neuweiler &Riedel, 2017) discovered a research gap in finding competitive advantages. In terms of 'technology,' there has been a lot of work put into researching new technologies for transportation systems, and there has been significant development in recent years. However, research on the microeconomic and macroeconomic advantages and costs of these advances has been minimal, and further study is needed. The purpose of this research is to revies a logistical oriented decision supporting model as a decision support instrument for port management aims to contribute to such basic topics as comprehending analyzing and evaluating the logistical structure of ports as well as port performance indicator, planning port capacity, increasing port efficiency, developing internal port logistical processes and predicting the needs of the port in the future.

2. Material ve Method

In this study, the importance of ports in the supply chain is emphasized, and the relationship between cargo handling systems in ports and logistics is emphasized.

Two separate and simultaneous techniques were used to perform the review:

• finding relevant material published internationally on the review subjects, including academic papers, reports, trials and experiences, and any other evidence on the issue by contacting a pool of experts
• using online web search engines like Google and Google scholar to find relevant materials
The status of technical progress, its implications to date, and its application to various operational settings were all taken into account for each new technology (defined in relation to modes of transport and location in the supply chain). A two-stage filtering and ranking procedure was used to find, select, and prioritize candidate source documents for inclusion. The first phase examined the evidence's relevance and transferability, followed by a second evaluation based on the source's perceived importance.

a. At ports and depots, automated loading methods are used. A container port is a point when the supply chain breaks down (Franke, 2008). As an intermodal transshipment point, it is vulnerable to variations in arrival and departure times, as well as a lack of information that leads to inefficiencies in lead times. Automation in a container port can help solve problems caused by space constraints. According to Tavasszy (2016), automation can increase the productivity of a container port: if the order of truck arrivals at a terminal is known ahead of time, yard design can be more effective. As a result, port terminals must have a part-ashore efficient marine terminal and an inland intermodal interface center (Franke, 2008). The efficient marine port and multimodal interface center are connected by a dedicated railway line in this Agile Port System ideal concept (Franke, 2008). The main principle of the Agile Port System is as follows:

• move containers quickly between the terminal and the intermodal interface center by train
• sort containers between trains according to their final destination
• handle as many containers as possible between vessels and trains, avoiding terminal storage
• load and unload vehicles that serve the surrounding area at the intermodal interface facility

b. The Agile Port idea is based on a mix of enhanced semi-automated equipment that allows for direct container transshipment from vessel to train and vice versa at the quay without sacrificing performance. In effect, instead of being stored at the port terminal, load units may be kept near to the client (Franke, 2008). The Port of Hamburg is a good example of how Noell9 improved on the original efficient marine terminal concept by developing the 'Mega Hub' concept, which allowed 360 boxes to be transshipped between trains in less than 100 minutes. Due to the redundancy of yard transfer trucks, the efficient marine terminal's major benefit is a decrease in machinery and personnel expenses. The system includes improved semi-automated ship-to-shore cranes, semi-automated cantilevered and rail-mounted gantry cranes, and a box mover based on rail-mounted, automated shuttle cars powered by linear motor technology.

3. Results

3.1. The importance of ports in the supply chain and port-related dynamics

Supply chain management is the integration of essential business activities from the end user to the initial supplier in order to provide consumers and partners with value-added goods, services, and information (Stock&Lambert, 2001).

In order to obtain a competitive edge, businesses are reorganizing their relationships with their suppliers and consumers. Particularly noteworthy is the tight collaboration created with suppliers; it is clear that they contribute significantly to issues such as enhancing product quality, lowering purchasing costs, boosting production and distribution flexibility, and raising customer satisfaction. In order to obtain a competitive edge, businesses are reorganizing their relationships with their suppliers and consumers. Particularly noteworthy is the tight collaboration created with suppliers; it is clear that they contribute significantly to issues such as enhancing product quality, lowering purchasing costs, boosting production and distribution flexibility, and raising customer satisfaction. Since the 1990s, the logistics concept aimed at creating an integrated structure inside a single company has begun to spread along the distribution route, which is situated towards both supply sources and customers. This method, known as "supply chain," attempts to adopt an integrated approach not only

inside the framework of a single company, but also across the distribution channel process at all suppliers, manufacturers, wholesalers, retailers, and even customers (Tuna, 2001).

All parties participating in the fulfillment of client needs, whether directly or indirectly, are included in the supply chain. Not only manufacturers and suppliers are part of the supply chain, but so are transportation, warehouses, retailers, and even customers. Any function in a firm that fulfills consumer needs is included in the supply chain. New product creation, marketing, operations, distribution, financing, and customer support are some of these functions (Chopra&Meindhl, 2007).

Supply chain management is a larger notion than logistics in that it manages both the materials in the process from the raw material source necessary for manufacturing to the ultimate customers, as well as the relationships between the distribution channel's intermediaries (Johnson et al., 1998). Beyond being mere transit hubs in the conventional sense, ports play an essential role in the supply chain, evolving to become logistics centers. Without a doubt, changes in the dynamics influencing the port business have influenced this progress. Mangan et al. (2008) explain these processes and their consequences as follows; Under the topic, there are sections on the consequences of marine transport, developments in the port sector, rivalry between global port operators and inter-port competition, economic contribution of ports, and port-based logistics and supply chain strategies. These topics are covered in depth farther down.

3.1.1 Port operators around the world

Operators of Major Container Terminals Around the World ten worldwide container terminal operators, which handle about 37% of all container handling at the world's ports (UNCTAD, 2014). Mediterranean Shipping Company (MSC), APM Terminals, and Mitsui O.S.K. are all global container terminal operators.It has a tight relationship with shipping firms like Lines. According to the Drewry Research Company's Global Container Operators 2014 Annual Report, as of the end of 2013, PSA International (8.2 percent) was the container terminal operator with the most TEU handling in the world, followed by Hutchison Port Holdings (7.0 percent), APM Terminals (5.5 percent), DP World (5 percent), and China Merchants Holdings International (CMHI) (3.6 percent). The top five container operators handled around 41% of all containers handled globally in 2014 (Table 1).

Table 1. Major Global Container Terminal Operators Handling Quantities and Market Share (UNCTAD, 2014)

Port Name	Handling Quantities (Million TEU)	Market Share (%)
The Port of Singapore Authority (PSA)	50,9	8,2
Hutchison Port Holdings (HPH)	44,8	7,2
APM Terminals (APMT)	33,7	5,4
Dubai Ports World (DP World)	33,4	5,4
China – Ocean Shipping (Group) Company (Cosco)	17	2,7
Terminal Investment Ltd.	13,5	2,2
China Shipping Terminal Development	8,6	1,4
Hanjin	7,8	1,3
Evergreen	7,5	1,2
Eurogate	6,5	1

3.1.2. Economic development and ports

Global growth is expected to stay stable in 2018-19, at the same pace as in 2017. Global growth is expected to be 3.7 percent in 2018-19, down from (-) 0.2 percent in 2017-2018. The downward revision reflects unexpectedly weak activity in some major advanced economies in early 2018, as well as the negative effects of trade measures implemented or approved between April and mid-September, and a weaker outlook for some key emerging market and developing economies due to country-specific factors, tighter financial conditions, geopolitical tensions, and higher oil prices, as well as a weaker outlook for some key emerging market and developing economies due to country-specific factors, tighter financial conditions, geopolitical tensions, and higher oil prices (WTO, 2018). The high pace of GDP change in emerging nations caused a 5% increase in global GDP between 2004 and 2008. However, the Economic (Financial) Crises of 2008 experienced a sharp decline. After 2008, the negative impacts of the crisis began to fade, and the GDP growth rate has been steady at above 3%. This GDP change has been 3.8 percent since 2008, and by 2023, this value is anticipated to remain unchanged.
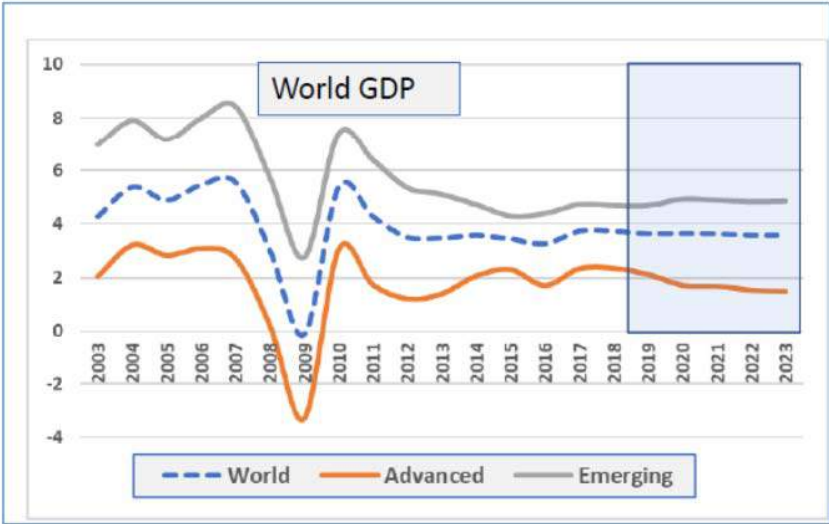
Figure 1. Change of World GDP (UNCTAD, 2018)

The global seaborne commerce is performing well, aided by the world economy's recovery in 2017. Global marine trade grew at a rate of 4%, the fastest in five years, gaining traction and boosting confidence in the shipping sector. Total volumes reached 10.7 billion tons, up 411 million tons from the previous year, with dry bulk commodities accounting for roughly half of the total (UNCTAD, 2018). As crude oil slows to 2.4 percent, there is a considerable increase in containerized commerce (6.4 percent) and dry bulk freight (4%). The outlook for seaborne commerce is bright; UNCTAD (2018) forecasts a 4% rise in volume in 2018, which is similar to 2017. UNCTAD forecasts a 3.8 percent compound annual growth rate between 2018 and 2023, assuming or continuing favorable global economic trends.
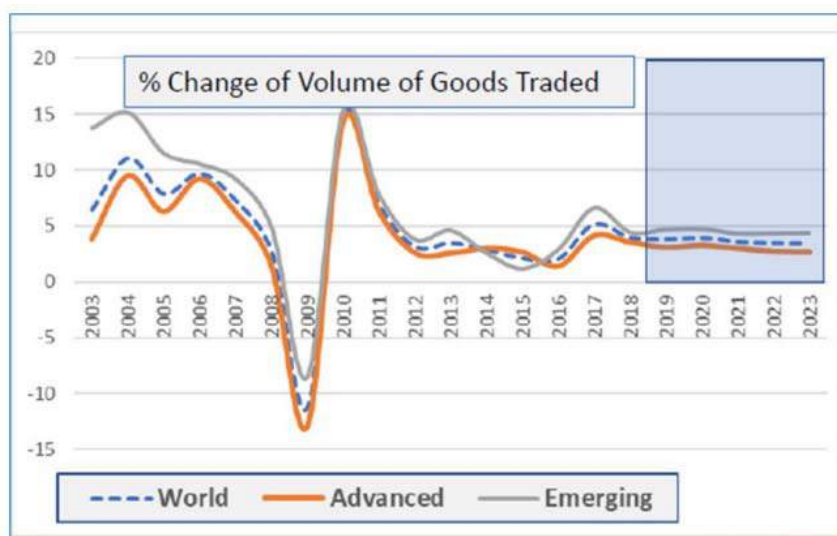
Figure 2. Change of Volume of Goods Traded (UNCTAD, 2018)

Martin Stopford proposed a relationship between freight rates, ship building, and sales, in which freight rates rise for four years and then fall when the other two drops. And this pattern has been in place for a long time. However, during the 1990s, when global economic growth surged from 2% to 4%, this scenario has altered appropriately. The freight rates, which began to rise in earnest in the early 2000s and peaked in 2008, have been steadily increasing since then. As a result of this deceptive scenario, shipbuilding investments have grown, and second-hand ship values have climbed, making it hard to locate a new shipyard. With the commencement of the financial / economic crisis in 2008, freight rates dropped to rock bottom. Many marine firms were forced to shut as a result of this scenario. Stopford's tendency has never been reversed, and the uncertainty and stability have persisted for the past ten years.

As a result of this circumstance, maritime operators are looking for new ways to operate. Conducting scientific study on a new trend in marine transportation is necessary in order for individuals to develop a new idea for forecasting improvements and making long-term plans.

The idea is to develop a system for estimating maritime transportation growth based on global commerce and economic growth based on credible data. This application will help to better characterize the supply-demand curve in order to forecast freight rates, as well as future ship building and sales expectations. After, deleting two years due to crises, the average increase of world trade is 5.29 percent, while global GDP growth is 2.14 percent. That indicates that the growth of global trade is almost 2.5 times greater than the increase of global GDP. The average growth rate of seaborne trade is 4,154 percent, whereas the global GDP growth rate is 2.14 percent. As a result, the growth of seaborne trade is around 2.17 times greater than the increase of global GDP. Between GDP and Seaborne Trade, there is a smooth rate connection. As a result, the expansion of the global economy may be utilized to forecast the rise of seaborne trade.

3.2. Automated loading systems at ports, depots and technology's role

A mathematical model that can be assessed analytically cannot adequately explain most complicated real-world systems containing stochastic aspects. As a result, simulation is

sometimes the only form of inquiry available (Law, 1982). Simulation may be used to verify the accuracy of assumptions and a specific model. An analytic model, on the other hand, might offer acceptable options to test in a simulation. The concept of a system is central to every simulation research (Graybeal, 1980). A system is more than just a collection of physical things and their interactions. A container port terminal is viewed as a system, with its activities and interactions viewed as a collection of objects in our example. One of the benefits of simulating a system's performance, such as a container terminal, is that it allows you to assess alternatives capable of meeting the design criteria before they are implemented. It also calculates the operating costs of such design configurations, which may be compared to the prices of alternative changes. Proposed operational enhancements and port developments can be integrated gradually into the simulation model to assess local terminal performance while keeping the global viewpoint in mind (Seeley&Griffiths, 1992). It also gives you a way to make sure you're working on the most productive project at any given time. Ships generally arrive in a random manner that is characterized by some sort of statistical distribution. The most common estimate is a negative exponential distribution of inter-arrival periods (and hence a Poisson arrival rate). The arrival of ships and the length of time a berth is occupied are included in the ship turn-around time (service time). With vessel arrivals, single or multiple service(s), and limitless lines at an anchorage, ports or, more accurately, ship-to-berth linkages are called queuing systems (Radmilovich, 1992). Only operational improvements are included in the models created for comparison in this article. They encompass actions that take place within the terminal, namely ship-to-shore operations and container transfer from the ship to the stacking area. The models do not include events that take place outside of the terminal gates (e.g., land transport). A quick description of the two terminals is provided in order to have a good grasp of the systems and sequences.

3.3. Self-Driving or remote-controlled units and stacking equipment

Vehicle automation is based on a number of technologies that provide varying degrees of functionality and capacity. The technologies most often linked with autonomous cars are described in the following section.

Radar uses a variety of radio frequencies to offer continuous distance (and, to a lesser extent, object size) monitoring by measuring the time it takes radio waves to travel to and back from an object. Radar sensors, which use both long and short-range radar, are mounted on the front bumper region of a truck in a transportation application. 13 Long-range radar was used to focus further down the road (820', 18°), whereas short-range radar had a tighter and broader field of vision (230', 130°). 14

LIDAR is a radar-like concept that collects information about the surroundings using lasers rather than radio waves. While LIDAR provides unique benefits over radar, adoption has been hampered by the equipment's "size, weight, cost, and power consumption." 15 According to Google, its self-driving car has a roof-mounted LIDAR with "64 lasers spinning at roughly 900 rpm to provide a 360-degree view." 16 This technique is estimated to cost $75,000. 17 Due to the trailer and the additional height requirements for a rooftop installation, a 360° vision in a trucking scenario would be difficult with a comparable arrangement (Figure 1).

Signs, highway striping, and other characteristics of the surrounding transportation infrastructure and environment are read using video camera systems. Currently available video camera apps assist truck drivers in maintaining lanes and alerting them to potential collisions with cars and pedestrians. 18 The same functions may be available through the video camera in an autonomous truck, but they would be automated.

Figure 3. Location of Technologies that Enable Automation (Url-1)

The Federal Communications Commission (FCC) designated 5.9 DSRC (Dedicated Short-Band Communications) as a particular range of the 75 MHz spectrum for use in intelligent transportation systems in 1999. 20 When "coupled with accurate vehicle location," this range has been intensively researched in safety applications to determine if DSRC might improve autonomous car-based safety systems or enable new communication-based safety applications. 21 Due of the short range of 5.9 DSRC, embedded DSRC transceivers are required every quarter mile or so to sustain connection. The 5.9 GHz frequency enables for exceptionally fast data transfer rates, despite the DSRC range being limited. LTE (Long-Term Evolution) is a high-speed wireless communications technology used most often by smartphones. 5G LTE is the name given to the next iteration of this terrestrial infrastructure. The 5G technology is projected to be "10-100 times quicker than today's typical 4G LTE connections," allowing enabling accident avoidance and vehicle platooning via cellular communications. 23 4G wireless communications, while capable of functioning over a significantly wider range than 5.9 DSRC, have a slower data transmission rate.

The Differential Global Positioning System (DGPS) expands on the Global Positioning System (GPS) by incorporating ground-based correction stations that serve as a third point of reference between the vehicle and a GPS satellite. This improves precision from a few meters to a few millimeters. When used in real time, such precision might assist preserve a driving lane when markers are lacking.

Combinations of these technologies are now being utilized to create autonomous systems. Radar and video camera technologies are used in the Freightliner L3 truck mentioned previously. 24 OTTO employs the same technological categories as 24 OTTO, but adds three LIDAR units and precise mapping data, bringing the system to L4.25 It's likely that linked vehicle technologies (e.g., 5.9 DSRC), often known as V2X or vehicle-to-everything, will improve and allow L3-L5 technologies. When two V2X devices come within range of each

other, V2X communicates directly between them using wireless local area network (WLAN) technology.

Table 2. V2X Categories

V2X Technology	Functionality
Vehicle-to-Infrastructure (V2I)	Enables vehicles to communicate with and gain awareness of infrastructure such as traffic signals.
Vehicle-to-Vehicle (V2V)	Enables vehicles to communicate with and gain awareness of other vehicles.
Vehicle-to-Pedestrian (V2P)	Enables vehicles to communicate with and gain awareness of pedestrians, bicyclists and others.

These technologies may enable cars to monitor and respond to their environment more quickly and accurately than a human driver. V2I, for example, may enable a vehicle to anticipate traffic light changes or to travel at various speeds as it crosses different roads. As long as the signal is not blocked, V2V may allow a car to quickly detect and respond to another vehicle ahead of it that is suddenly stopping, or to spot a vehicle around an urban
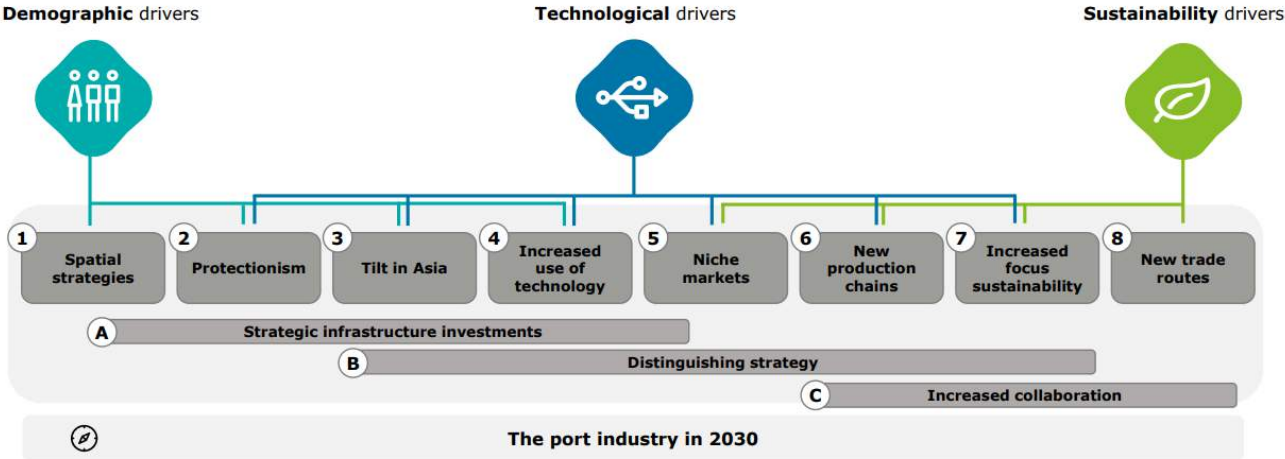
street corner (Table 2).

Figure 4. The Port Industry in 2030 (Url-2)

Today's port isn't the port of tomorrow. Several major developments are predicted to influence the marine sector as a result of demographic, technological, and sustainability forces. We've identified eight specific trends, as well as three that reflect wider trends, that will have a combined impact on the port industry's outlook in 2030. This research will examine how the major maritime trends are influenced by the various factors, as well as what this means for the port business in the future.

Ports are progressively using a variety of technology to execute improvements across the whole value chain.

More technical solutions are required.

• To boost productivity, technological solutions like as robots and the Internet of Things are required. As a consequence, supply networks would become more automated, digitalized, and linked, requiring less physical labor.

• It assists in the transformation of the port ecosystem from a basic logistics and transportation node to an open and efficient community capable of participating in the global landscape of integrated international trade.

Increased susceptibility to cyber attacks

• The increased usage of automated, digitalized, and linked supply chains increases the vulnerability to cyber assaults.

• Ports have traditionally been key infrastructure and must be secured against cyber-attacks that may shut them down or steal data.

There is a lesser emphasis on physical infrastructure investments.

• On the one hand, upgrades to the port's supply chains will necessitate investments in digitization and automation. To safeguard this new supply chain, however, investments in cyber security are required.

• Physical port infrastructure investments are projected to diminish as a result of a shift in investment priorities toward more technology alternatives. The Impact of Workforce Aging on Productivity, IMF 4

Case example;

• From the Hamburg-Le Havre range to the main Middle East hubs, from Chinese mega-terminals to South African IOT pilots, 5g networks in Antwerp, smart port platforms in Rotterdam, unique track and trace in Vancouver, and so on, terminal automation is taking place all over the world.

4. Discussion and Conclusions

In this study, automation systems at ports are explained. An agile port is defined as an interface that can act as a 10G port or cover a predefined set of 10G interfaces to create an interface with higher speed capabilities. The set of interfaces that can be combined to create a higher speed port is limited by the hardware configuration. The importance of ports in supple chain and port-related dynamics are mentioned. Without a doubt, changes in the dynamics influencing the port business have influenced this progress. Mangan et al. (2008) explain these processes and their consequences as follows; the consequences of marine transport, developments in the port sector, rivalry between global port operators and inter-port competition, economic contribution of ports, and port-based logistics and supply chain strategies.

The economic situation is evaluated from 2003 to 2023. According to UCTAD (2018), it can be seen that World GDP and % change of volume of goods traded have similar pattern among the time period. Both of them decreased in 2009 and started to increase after 2009. The stable pattern follows after 2018 both for World GDP and % change of volume of goods traded. Consequently, freight and economic development are related to each other. Therefore, the development of the port industry has significant importance.

In this study, eight specific trends identified as well as three that reflect wider trends, that will have a combined impact on the port industry's outlook in 2030. The future of the global ports and shipping industry is still uncertain, but four important aspects are expected to change: trade routes, the competitive position of ports, ecosystems, and cargo distribution. Each affected by underlying trends.

Automation systems can be examined in more detail in future studies and economic factors can be investigated to show the relationships between port operations and percentage of volume of goods traded.

References

Chopra, S., Meindl, P. (2007). Supply Chain Management, Strategy, Planning, and Operation, 3rd edition, Pearson Prentice Hall, 130.

Dülger, M. C. (2006). Denizcilik Gücünün Geleceği. Yüksek Lisans Tezi. Gebze İleri teknoloji Enstitüsü, Sosyal Bilimler Enstitüsü, Gebze.

Esmer S., Yıldız G., Tuna O., (2008) Konteyner terminallerinde gemi-rıhtım bağlantısının benzetim yöntemi ile modellenmesi. Yöneylem Araştırması ve Endüstri Mühendisliği XXVII. Ulusal Kongresi,İzmir.

Esmer, S., (2009). Konteyner Terminallerinde Lojistik Süreçlerin Optimizasyonu ve Bir Simülasyon Modeli., Doktora Tezi, Dokuz Eylül Üniversitesi. Sosyal Bilimler Enstitüsü. İzmir.

Flämig, H. (2016). Autonomous vehicles and autonomous driving in freight transport. In Autonomous driving (pp. 365-385). Springer, Berlin, Heidelberg.

Graybeal, W.J. (1980), Concept of a System: Simulation, Principles and Methods, p.3.

Johnson, James C., Wood, Donald F., Wardlow, Daniel L. et. al. (1998). Contemporary Logistics. Seventh Edition. Prentice Hall, Inc: New Jersey.

Law, A. (1982), Advantages and disadvantages of simulation", Simulation Modeling and Analysis, p. 8.

Mangan, J., Lalwani, C., Fynes, B. (2008) Port centric logistics. The internatioal journal of logistics management. Vol:19. No: 1. Sayfa: 29-41.

Neuweiler, L., Riedel, P. V. (2017). Autonomous Driving in the Logistics Industry: A multi-perspective view on self-driving trucks, changesin competitive advantages and their implications.

Radmilovich, Z.R. (1992). Ship-berth link as bulk queuing system in ports. Journal of Waterway, Port Coastal, and Ocean Engineering.

Ranaiefar, F. (2012). Intelligent Freight Transportation Systems. Institute of Transportation Studies.

Review of Maritime Transport (2008) UNCTAD.

Seeley, D., Griffith, T. (1992), Objects used in Simview. Understanding Systems with Simview.

Stock, J.R. ve D. M. Lambert (2001) Strategic Logistics Management, 4. Baskı, 2001, McGraw-Hill Higher Education.

Tuna, O. (2001) Türkiye İçin Lojistik ve Denizcilik Stratejileri: Uluslararası ve Bölgesel Belirleyiciler. Dokuz Eylül Üniversitesi Sosyal Bilimler Enstitüsü Dergisi,Cilt 3, Sayı:2, 2001

UNCTAD (2005) Free Trade Zone and Port Hinterland Development, Research report of the Economic and Social Commission for Asia and the Pacific, New York.

Url-1. "Safer, More Efficient Commercial Trucks." Accessed October 25, 2016. http://www.freightlinerinspiration.com/technology/

Url-2. "The Port Industry in 2030." Accessed October 25, 2016. https://www2.deloitte.com/content/dam/Deloitte/nl/Documents/consumer-business/deloitte-nl-cb-global-port-trends-2030.pdf

Identification of Defective Cherries Using Convolutional Neural Network

Halil KAYGISIZ[1]*, Abdulkadir ÇAKIR[2]*

Abstract: Worldwide, 2.45 million tons of cherries were produced in 2017, 2.57 million tons in 2018 and 2.59 million tons in 2019. It is very important to sort defective sweet cherries to ensure that the export capacity of sweet cherry producing countries is high. Because defects in fruits are contagious. A single rotten sweet cherry can cause all sweet cherries to rot. Therefore, a model was proposed in the present study to prevent the spread of decay. Defective and non-defective sweet cherry images are classified in the proposed model.

In developing countries, defective fruits are sorted manually during or after harvest of fruits. Checking defective fruits during harvest requires a special effort and is time consuming. This, in turn, increases the cost of labor. The cost of labor are reduced with the proposed model.

A data set consisting of 1,050 images with a resolution of 224x224 pixels was created in the study. Convolutional Neural Network (CNN) was used for the extraction of characteristics and SOFMAX was used for classification. Other methods were also examined using the transfer learning approach to compare the performance of the proposed system. The highest success rate in the classification of sweet cherries was achieved with the proposed method.

Keywords: Chery Defect Detection, Convolutional Neural Network, Transfer Learning, Deep Learning

1. Introduction

Approximately 3 million tonnes of sweet cherries are produced annually (Wordatlas, 2020). The data for sweet cherry production reveal the size of the sweet cherry market in the world. It is very important for countries to export for creating added value. The removal of defective products in the export of fruits needs to be performed much more carefully. Because, a rotten fruit may cause all fruits to rot. The defective fruits are generally sorted by manpower. Using manpower increases both the error rate and labor cost. Sorting defective fruits by a system increases efficiency, while reducing error rate and labor costs.

Recently, machine learning and deep learning have become widespread in computer vision applications and successful results have been obtained. Such companies as Unitec, Compac, Greefa, Buhler and GpGraders have systems that can perform fruit classification and defect analysis. However, those systems cost millions of dollars. Thus, apart from those systems, there is a need for new systems with low cost and high success rate.

[1] Korkuteli Vocational School, Akdeniz University, Antalya, Turkey.
[2] Faculty of Technology, Isparta University of Applied Sciences, Isparta, Turkey.
* Corresponding author: halilkaygisiz@akdeniz.edu.tr

2. Related Work

Arango et al. conducted a study to perform the quality control of apples. They primarily took infrared and color images of the apple in their study. Then, they attempted to classify the data set by creating a Convolutional Neural Network model. It was stated that the success rate of the model was 97% (Arango et al., 2021).

Jana et al. studied on the classification of rotten fruits. They created a Convolutional Neural Network model for a data set consisting of 1,200 apple, banana and orange images in the size of 64x64 pixels. The success rate of the model with four convolutional layers was reported to be 97.7% in average for all fruits (Jana et al., 2021).

Bongulwar tried to classify defective fruits in a dataset consisting of apple, banana, grape, litchi and mango images. The model uses Convolutional Neural Networks to identify fruits from images. The accuracy obtained is 92.23% (Bongulwar, 2021).

An automatic detection method is proposed by Wu et al. for apple defects based on laser-induced light backscattering imaging and convolutional neural network (CNN) algorithm. Laser backscattering spectroscopic images of apples are obtained using semiconductor laser. An AlexNet model with an 11-layer structure is established and trained to identify apple defects. We analyze how well the model does with the recognition effects of apple defects. The proposed CNN model for the detection of apple defects achieves a higher recognition rate of 92.5%, and the accuracy is better than conventional machine learning algorithms (Wu et al., 2020).

The method proposed by Nur Allam et al. is based on a deep learning approach using SqueezeNet architecture. However, the apple images are extracted and fed into a deep network for training and testing. The proposed SqueezeNet architecture utilizes convolution neural network to regress a bypass connection between the fire modules across the images. It has been evaluated our own created dataset. The excremental result shows that our proposed methods are efficient and effective. The general detection rate was 92.23% (Nur Allam et al., 2021).

3. Material and Methods

3.1. Dataset acquisition and pre-processing

First of all, the dataset was created in the study. The data set comprised of 1,050 images. Figure 1 shows some image samples from the data set created. The resolution of the images was 224x224 pixels. The convolution process is applied to all images in the data set in the Convolutional Neural Network model. This is a long process with a lot of processing overhead. The images are converted to 224x224x3 numpy array for faster access in the convolution process to be applied on the images in RGB format. Then, all images are labelled classifying into two group as defective and non-defective. Whereas, when training the dataset using transfer learning the image augmentation is applied, validation is done in parallel while training and tested upon the test set (Figure 1).

Figure 1. Sample Images from the dataset

3.2. Convolutional neural networks

The deep learning is very widely used in machine learning applications since it produces very successful results across different types of data. In the classification of images in the Convolutional Neural Network model, the deep learning approach is used (Hussain et al., 2018). The main structure of Convolutional Neural Network model is presented in Figure 2.
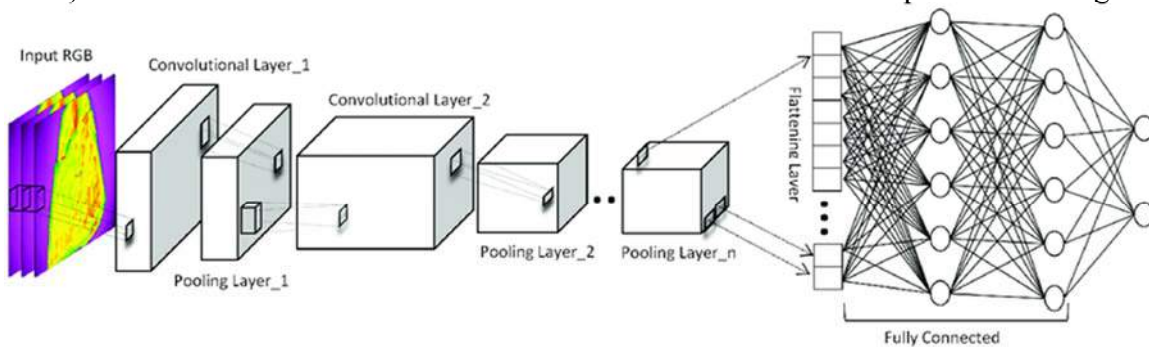
Figure 2. Convolutional neural network architecture

The collection of pixels that constitutes the images can represent different patterns such as edge and shadow in various images. Convolution is a process used to define the patterns. The image is converted to a matrix before the convolution process. The size of the matrix changes depending on the resolution of the image. A matrix in the size of 500x300x3 is created for an image having the resolution of 500x300 in RGB format. The patterns can be determined by the multiplication of the image matrix with the filter matrix. Although the size of the filter matrix may vary, 3x3 filters are widely used. The convolution process is performed starting from the first pixel of the image to the last pixel by shifting. The new matrix obtained at the end of the convolution process is indeed a feature map to be passed to the next layer (Krizhevsky et al., 2012; Yang et al., 2021).

A pooling layer is used after the convolution layer in the CNN model. This layer reduces the size of our feature map. The pool size was determined to be 2x2. The last layer of the CNN model is a fully-connected layer. The matrix is preprocessed by flattening to obtain the fully connected matrix and converted into a single vector. Then, this single vector is transmitted to the fully connected layer (Thenmozhi et al., 2019).

3.3. Proposed model for classification of fresh and rotten fruits

In the present study, a CNN model shown in Figure 3 is proposed for the classification of defective and non-defective sweet cherries. Sixteen filters are applied in the first convolution

layer, which is the first layer of the model. The size of these filters is 3x3. The keyword arguments used for passing initializers to layers depends on the layer. Usually, it is simply kernel_initializer and bias_initializer. Kernel regularizer, and bias regularizer of 0.05. The initial weights in the neural network are randomly determined, then the weights are updated with the values that give better results. Random_uniform minimum value is -0.05 and the maximum value of 0.05. In the model, a regularizer is used as a penalty mechanism in the optimization of the layer. These penalties are utilized to optimize the loss function in the neural network. A normalization is applied to each convolution layer before passing the max-pooling layer By means of the process, the activation function approaches 0 and the activation standard deviation approaches 1. Rectified linear units (RELU), which is a linear function, are used in the normalization. RELU produces outputs at positive value, otherwise produces 0 for the output. Max-Pooling layer reduces number the parameters by down-sampling. Since this layer reduces the size of the data set, efficient use of hardware resources and time savings are achieved. Thus, the features required for classification are retained while getting rid of the excess data irrelevant to classification. Sixteen filters were used in the second convolution layer as in the first layer. The size of the filters used was 3x3. After the convolution layer, RELU was used for the normalization and max-pooling layer for data reduction. Sixteen 3x3 filters were also used in the third convolution layer. After the third layers of RELU and Max-pooling, there is the fully connected layer. In this layer, first of all, the feature map obtained from the the third Convolution layer should be converted into a one-dimensional array. This process is called as flattening. In this study, the loss function used is categorical cross-entropy and Adam optimizer with a learning rate of 0.0001. The architecture of the proposed CNN model is shown in Figure 3.
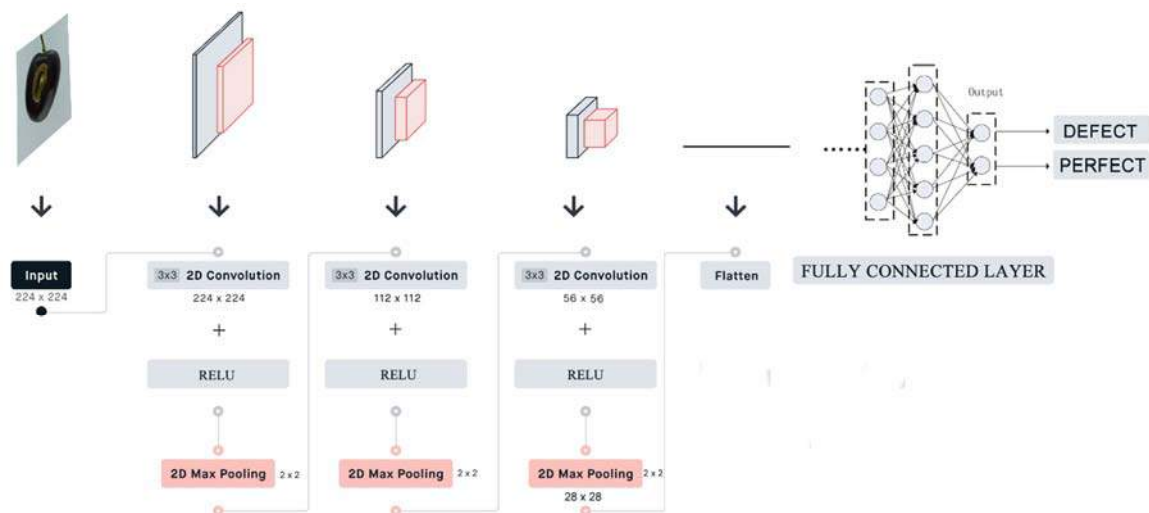
Figure 3. Architecture of proposed model

3.4. Cherry classification using transfer learning

Transfer learning, a research problem in machine learning, focuses on retaining the knowledge gained during solving a problem and then applying it to a different but related problem. It can be also defined as adapting and applying a model that gives successful results in solving a problem to other problems. With transfer learning, we only perform neural network training when applying another model to our dataset. For feature extraction, we

adjust the fully connected layer according to our own data set and perform classification without changing the weights obtained in the convolution layer of different models. Thus, we are able to use the feature maps without running the convolution layer, which requires serious hardware and takes a long time (Pardede et al., 2021).

The proposed model were compared with AlexNet, GoogleNet, Vgg19 and ResNet50 transfer learning models in the study.

3.4.1. Alexnet

Although it is said that the application of deep learning was first appeared in the article published by LeCun in 1998 (Lecun et al., 1998), its worldwide recognition occurred in 2012. The AlexNet model designed with deep learning architecture won the Imagenet competition held in the same year. The study was published as an article with the title of "ImageNet Classification with Deep Convolutional Networks"(Krizhevsky et al., 2012) and received 16,227 citations as of October 2017. This architecture allowed the computerized object identification error rate to decrease from 26.2% to 15.4%. The architecture given in Figure 4 is compromised of five convolution layers and three fully connected layers. The architecture has been designed to classify 1,000 objects. The filters are 11x11 in size and the number of step shifts is four in the AlexNet model.
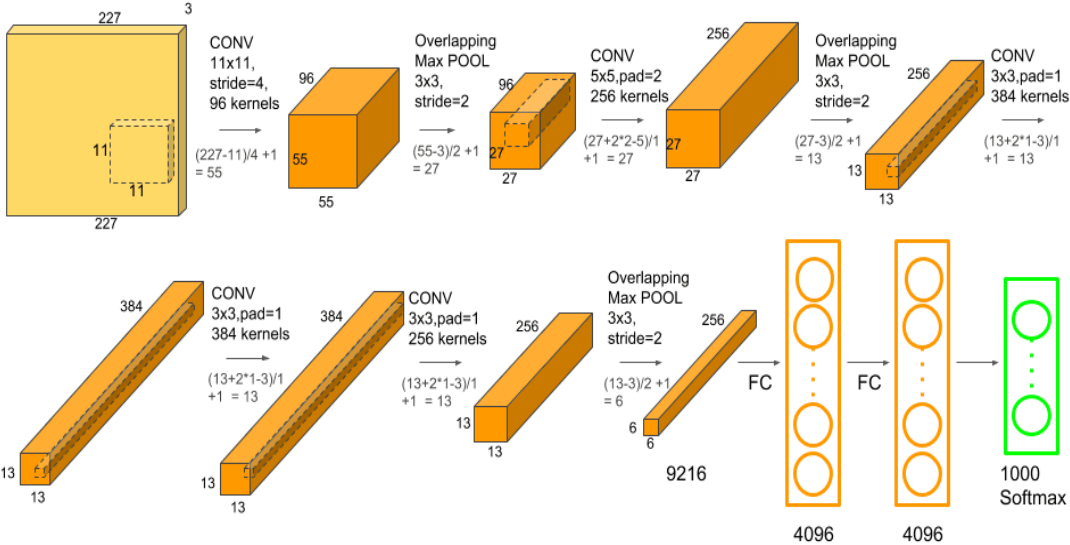
Figure 4. AlexNet architecture

3.4.2. GoogLeNet

The GoogLeNet is a complicated architecture because of the inception modules in its structure. The GoogLeNet with 22 layers is the winner of the ImageNet competition in 2014 with its error rate of 5.7%. Its architecture is among the first CNN architectures that avoided to stack convolution and pooling layers on top of each other in a sequential structure. In addition, this new model has an important place in terms of memory and power usage. Because stacking all layers together and adding lots of filters bring about a calculation and memory cost and increases the possibility of overfitting. The modules connected in parallel have been used in the GoogLeNet to overcome this situation (Mohammed, 2018).

3.4.3. Vgg19

The main layers of the VGG-19 architecture comprise of 16 convolutional, five pooling and three fully connected layers. This architecture has a total of 24 main layers. The filters used in the convolutional layers are used to decrease the numbers of parameters since the VGG-19 has a deep network structure. The filter size selected in this structure is 3x3 pixels. The VGG-19 architecture consists of approximately 138 million parameters (Pardede et al., 2021).

3.4.4. ResNet50

The ResNet model is an architecture designed deeper than any other architectures so far. It consists of 152 layers. The Resnet is also the winner of the ImageNet competition in 2015 with its 3.6% error rate (People typically have an error rate of 5-10%, depending on their skills and expertise) (Tran et al., 2019).

4. RESULTS AND DISCUSSIONS

In the study, we first classified the data set we created, which includes the images of defective and non-defective sweet cherries. Sixty percent of the data set was randomly selected for training, 10% for validation and 30% for testing. The effects of the parameters used during training were examined, and necessary changes were made so that the model proposed in the present study can give the best results. Python library "Keras" is used to implement this deep CNN model on google colab which uses NVIDIA Tesla K80 GPU, 12.72GB RAM, and 68.40GB of disk space.

4.1. The model parameters of the proposed CNN model and Effects of hyper-parameters of the proposed model

This model uses Adam optimizer with 0.0001, learning rates, batch size 16 and epochs 32. The accuracy rate of the models were calculated with the test data.

4.1.1. Effect of Batch Size

Convolutional neural networks are sensitive against batch size. Small changes in batch size may cause large effects in the success of the model (Houlsby et al., 2019). A small batch size creates a regularization effect. In the batch process, the data set is divided into parts based on the value determined as the batch size, and the model is trained on this part in each iteration. However, in some cases, the data may become grouped within themselves. This situation creates a correlation within the data set and also provides to give a high success rate in the test set selected from the data set, so there will be an overfitting. Before training starts and the data set was divided into parts, the data set should be shuffled to prevent overfitting to occur (Salman, et al., 2019). The random selection of the data is important in choosing the batch size. The batch size is generally selected from the values that are multiples of 2 between 64 and 512. The accuracy rates of the model with the batch sizes of 8, 16, 32 and 64 in the present study are given in Table 1. The highest success rate has been achieved for the batch size of 16.

Table 1. Effect of Batch Size

Effect of Batch Size:
- 64: 68
- 32: 96
- 16: 97
- 8: 93
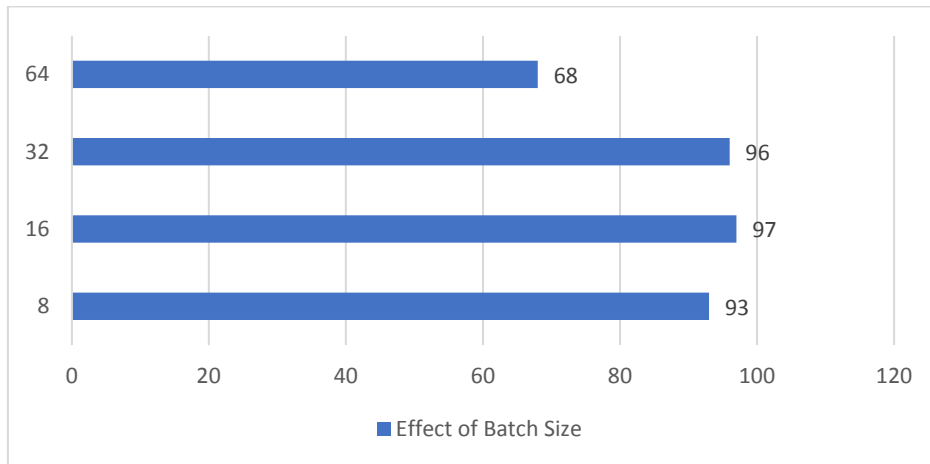
4.1.2. Effect of Number of epochs

Not all data are included in the training process simultaneously while the model is being trained. They take part in the training in certain numbers of pieces. The first part is trained, the success of the model is tested, and the backpropagation and weights are updated based on the success rate. Then, the model is re-trained with the new training set and the weights are updated again The optimal weight values are calculated for the model by repeating this process in each training step (Kishore et al., 2021). Each of these training steps is called "epoch" The success is low in the first epochs in deep learning since the optimum weight values to solve the problem are calculated step by step. However, the success of the model increases with increasing number of epoch. Table 2 presents the change in accuracy rate depending on the number of epoch.

Table 2. Effect of Number of epochs

Effect of Number of epochs:
- 32: 97
- 16: 87
- 8: 83
- 4: 58
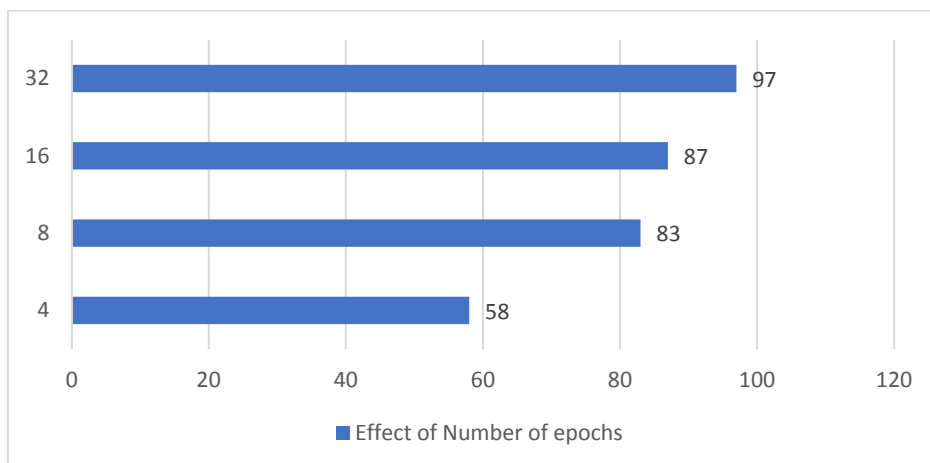
4.1.3. Effect of optimizers

In deep learning applications, the absolute minimum value of the error function must be determined for the learning process to be optimally concluded (Onishi et al., 2019). This process is performed by using optimization methods. Optimization is the methods used to

minimize the error which is the difference between the output value produced by the network and the actual value. There are various algorithms available for the optimization of artificial neural networks. The accuracy rates of Rmsprop, Adagrad, Adam and Nadam optimization algorithms used for testing in the study are provided in Table 3.

Table 3. Effect of optimizers
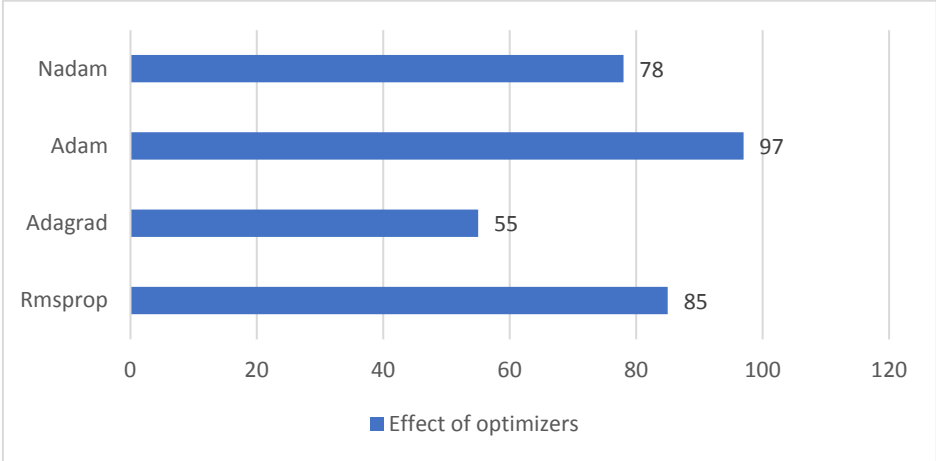
4.1.4. Effect of learning rates

In the training of neural networks, the calculated weights are updated to a certain extent. The update amount of the weights is expressed as learning rates. This parameter, which takes a value between 0 and 1, is an important hyperparameter for the CNN model. In the study, four learning rates were used and their effect on the accuracy rate was examined. Table 4 shows the learning rates used and their corresponding success rates.

Table 4. Effect of learning rates
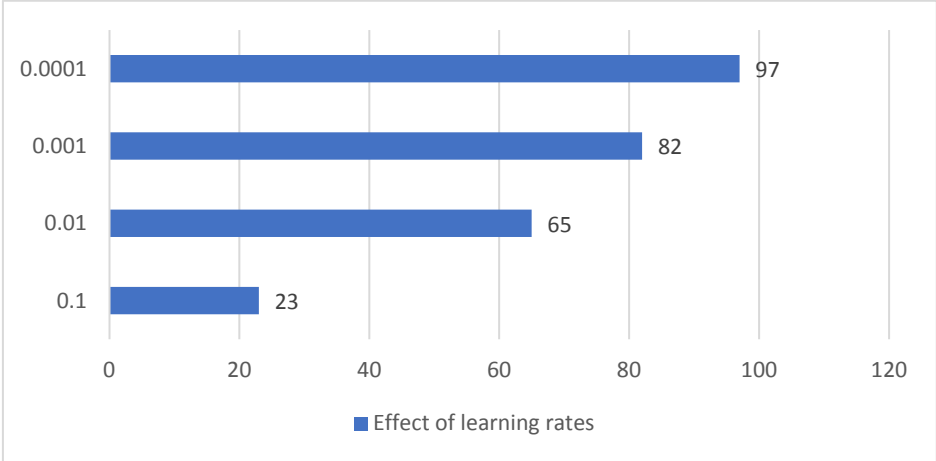
4.2. Comparison of classification accuracies of the proposed and transfer learning models

The best result in the training process of the neural network was achieved with the following combination of hyperparameters: batch size = 16, number of epochs = 32, optimizer = Adam, and learning-rate = 0.0001. The test procedure was performed using the test data set after the

training conducted with the selected parameters. The accuracy rate of 97,9 was obtained at the end of the test. The same data set was also tested on AlexNet, GoogleNet, Vgg19 and ResNet50 models using the transfer learning. The accuracy rates obtained are given in Table 5. The Vgg19 model produced the highest accuracy rate with 88.32% compared to the other models tested. The accuracy rates of Vgg19 and resnet50 were appeared to be similar. The model proposed in the study saved time with the use of fewer filters. In addition, the model is able to operate with less hardware requirement. As seen in Figure 3, with the appropriate combination of convolution and pooling layers created and appropriate hyperparameters determined during training, the proposed model produced the highest accuracy rate. The normalization conducted with RELU function between the convolution layer and max-pooling layers has reduced the overfitting that will occur during training. The regularizers are used as a penalty mechanism during the optimization. The error loss has been reduced by the Adam optimization function. Table 5 shows the detection rates of defective and non-defective sweet cherries of the model proposed in the present study. In addition, the comparison with the studies in the literature is shown in Table 6.

Table 5. Accuracy of pre-trained and proposed model
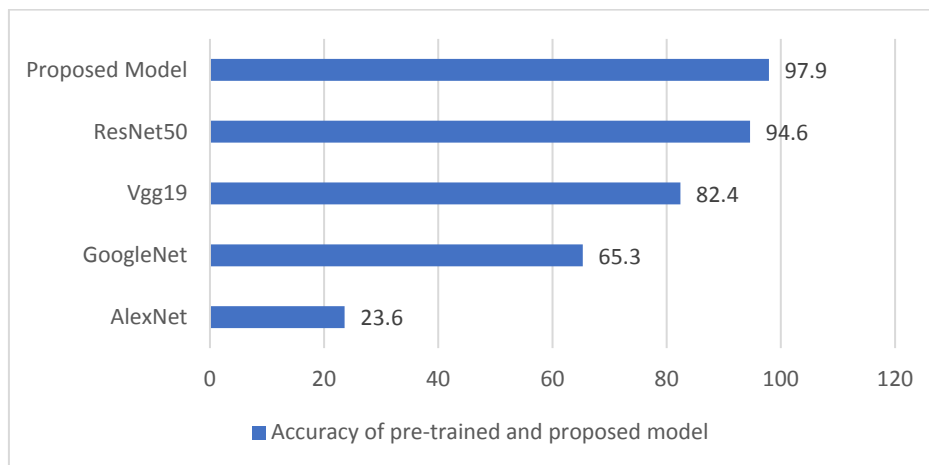
Table 6. Comparison of proposed CNN model with state of art methods

Author	Accuracy
Arango et al.	%97
Jana et al.	%97,7
Bongulwar et al.	%92,23
Wu et al.	%92,5
Nur Allam et al.	%92,23
Proposed CNN model	%97,9

5. CONCLUSION

Detecting and sorting defective fruits is of great importance for the agricultural economy. Performing this process by an automated system will make a significant contribution to the agricultural economy. In the present study, the data set consisting of a total of 1050 defective and non-defective sweet cherry images was attempted to be classified by creating a CNN model. The effects of different hyper-parameters i.e. batch-size, number of epochs, optimizer,

and learning rate are interrogated in this work. In addition, AlexNet, GoogleNet, Vgg19 and ResNet50 models were also applied to the same data set using the transfer learning. The model proposed in the study produced the highest success rate with 97.9% compared to the other models. Thus, the proposed CNN model with high success rate proved that an automated system can successfully detect defective sweet cherries.

References

Arango J. D., Staar B., Baig A. M., Freitagac M., (2021). Quality control of apples by means of convolutional neural networks-Comparison of bruise detection by color images and near-infrared images. Procedia CIRP, Volume 99, 2021, Pages 290-294. https://doi.org/10.1016/j.procir.2021.03.043

Bongulwar D. M., (2021). Identification of Fruits Using Deep Learning Approach, IOP Conf. Series: Materials Science and Engineering. doi:10.1088/1757-899X/1049/1/012004

Houlsby N., Giurgiu A., Jastrzebski S., Morrone B., (2019). "Parameter-Efficient Transfer Learning for NLP", Machine Learning, arXiv: 1902.00751

Hussain M., Bird J.J., Faria D.R., (2018). "A Study on CNN Transfer Learning for Image Classification", Advances in Intelligent Systems and Computing, vol. 840. Springer, Cham

Jana S., Parekh R., Sarkar B., (2021). Detection of Rotten Fruits and Vegetables using Deep learning, Computer Vision and machine learning in agriculture, Algorithms for intelligent systems, https://doi.org/10.1007/978-981-33-6424-0_3

Kishore M., Kulkarni S. B., Babu K. S., (2021). Fruits and Vegetables Classification using Progressive Resizing and Transfer Learning, Journal of University of Shanghai for Science and Technology, Volume 23, Issue 1, 489-498

Krizhevsky A., Sutskever I., Hinton G., (2012). "ImageNet classification with deep convolutional neural networks." In NIPS'2012. 23, 24, 27, 100, 200, 371, 456, 460

Lecun Y., Bottou L., Bengio Y., Haffner P., (1998). "Gradient-based learning applied to document recognition." Proceedings of the IEEE 86(11): 2278–2324.

Mohammed N.A., (2018). Evaluation of CNN, Alexnet and GoogleNet for fruit recognition Indonesian. J. Electr. Eng. Comput. Sci. **12**(2), 468–475

Nur Alam M. D., Ullah I., Al-Absi A. A. (2021). Deep Learning-Based Apple Defect Detection with Residual SqueezeNet, Proceedings of International Conference on Smart Computing and Cyber Security, Lecture Notes in Networks and Systems 149, https://doi.org/10.1007/978-981-15-7990-5_12

Onishi Y., Yoshida T., Kurita K., (2019). "An automated fruit harvesting robot by using deep learning". Robomech J 6, 13 doi:10.1186/s40648-019-0141-2

Pardede J., Sitohang B., Akbar S., Khodra M. L., (2021). Implementation of Transfer Learning Using VGG16 on Fruit Ripeness Detection, I.J. Intelligent Systems and Applications, 2021, 2, 52-61

Salman S., Liu X., (2019). "Overfitting Mechanism and Avoidance in Deep Neural Networks", Machine Learning, arXiv: 1901.06566

Thenmozhi K., Reddy U.S. (2019). Crop pest classification based on deep convolutional neural network and transfer learning. Computers and Electronics in Agriculture, 164: 104906. https://doi.org/10.1016/j.compag.2019.104906

Tran T. T., Choi J. W., Le T. T. H., Kim J. W., (2019). A comparative study of deep CNN in forecasting and classifying the macronutrient deficiencies on development of tomato plant. Applied Sciences, 9(8), 1601.

Worldatlas (2020). World cherry production, https://www.worldatlas.com/articles/the-world-leaders-in-cherry-production.html, (Accessed 20 October 2020)

Wu A., Zhu J., Ren T. (2020). Detection of apple defect using laser-induced light backscattering imaging and convolutional neural network. Computers & Electrical Engineering, 81: 106454. https://doi.org/10.1016/j.compeleceng.2019.106454

Yang X., Zhang Z., Qiu C., Wang L., (2021). Study On Feature Layer Of Adaptive Selection Pyramid For Small Object Detection In Complex Environments, Fresenius Environmental Bulletin, Volume 30– No. 01/2021 pages 474-483.

Estimation of the NiTi alloy corrosion rate dependence on the percentage of oxygen in three different seawater environments

Nataša Kovač[1], Špiro Ivošević [2*], Radmila Gagić[3*]

Abstract: This research is based on the analysis of empirical data obtained in a real experiment which included monitoring the corrosion behaviour of NiTi shape memory alloy created under the influence of three different seawater environments. In their work so far, the authors have conducted extensive research on the analysis of the rate of corrosion processes of specific alloys subjected to real experiments and the influence of various external influences and modelling of these complex processes by linear and nonlinear probabilistic analysis. However, now the corrosion process is viewed from the standpoint of changes in the chemical composition of the alloy. The empirical database was formed based on measurements obtained based on Energy Dispersive X-Ray Analysis, so that data were systematically collected after 6, 12, and 18 months of exposure of samples to the influence of the seawater environment. The conducted statistical analysis is performed with an aim to establish a correlation between the corrosion rate and the percentage of oxygen in the sample.

Keywords: corrosion, oxygen, SMA, statistical analysis

1. Introduction

In recent decades, the use of smart materials, such as shape memory materials, has attracted special attention from researchers. Various families of alloys based on Cu, Al, Ni, Ti, Fe are used in various branches of industry, such as medicine, transport, robotics, aviation, traffic, etc. (Jani et. al., 2014; Huang, 1998). To enable the application of these alloys in the maritime industry, numerous studies are performed in the laboratory and real conditions.

Under the influence of external and complex environmental factors in which metallic materials are located, physical changes in the metal are manifested through a decrease in the thickness of the metal and its weight. These influences will also affect the change of metal surface and chemical composition of metals, predominantly through the process of oxidation and reduction of the share of less noble metals. Changes in the material's physical shape and chemical composition are the product of a corrosion process that increases with time, both in terms of volume and depth of the material.

The decrease in metal weight and the increase in corrosion rate increase with time and according to previous research, there are different linear and nonlinear models of corrosion. Linear model is developed in (Guedas Soares and Garbatov, 1998), while non-linear models are presented in (Yamamoto and Ikegami, 1998; Paik et. al., 1998; Paik, 2003; Paik, 2004; Melchers, 1999a; Melcher, 2003) and in the work of some other researchers.

[1] University of Donja Gorica, Faculty of Applied Sciences, Mathematical Department, Podgorica, Montenegro
[2] University of Montenegro, Maritime Faculty, Kotor, Montenegro
* Corresponding author: spiroi@ucg.ac.me

Basically, all models developed so far are based on exposure time while some more advanced models take into account other parameters such as salinity, pH, seawater temperature and flow rate, the content of oxygen dissolved, sulfur pollution, and fouling (Melchers, 1999a; Melchers, 1999b).

Considering the above, through the realization of the experiment in real conditions of the marine environment, in this paper we analyze the influence of the different marine environments in which the materials are located (atmosphere, tide, and sea), elapsed times and changes in the chemical composition of alloys surface over the time. Specifically, depending on the three environmental conditions, we consider the dependence of the corrosion depth (expressed in nm of alloy wear) on the change in the percentage of oxygen during the exposure time of 6, 12, and 18 months.

The paper is structured through 4 chapters. The second chapter discusses materials and methods, the third presents research results, while the fourth chapter presents discussion and conclusion remarks.

2. Materials and methods

2.1. Materials

Pure metals were used to produce NiTi alloys by the classical casting process. Ni (99.99 wt.%) and Ti (99.99 wt.%) were delivered by Zlatarna Celje d.o.o. Slovenia. Totally 9 disks samples with a diameter of 42.3 mm and thickness of 3.4 mm were used in this research (Figure 1). Three samples were located in the atmosphere (close to shore), three samples were located in the tide area, and three were located in the sea three meters below the sea surface.

Figure 1. Sample of NiTi alloy disk

2.2. Methods

All samples posted in real sea water environment were analyzed in period of 18 months. Three samples were checked upon 6 months, 3 samples upon 12 months and 3 samples upon 18 months of exposure in each analyzed areas. Upon every 6 months test samples were monitored and measured in way to calculate depth of corrosion in nm and monitor chemical composition of samples.

2.1.1 Collecting data methods

In this article, two methods for collecting data were used. The first method was used for measuring the depth of corrosion and the second was used for calculating the percentage of oxygen contents in the alloy.

Material characterization by the FIB method (Focused Ion Beam on a scanning electron microscope) is used as a method for measuring the depth of corrosion (Ivošević et. al., 2021). This method was used to measuring the depth of corrosion (in nm) of NiTi alloys after 6, 12, and 18 months of exposure on the surface and image of the samples below surfaces.

For calculating the percentage content of oxygen in NiTi allow we use semi-quantitative analyses. More precisely, the chemical composition of the selected NiTi alloy was determined through the use of a high-resolution Field Emission SEM Sirion 400 NC (FEI, USA). The microscope contains an Energy Dispersive Spectrometer (EDS) - Oxford INCA 350 - for microchemical analysis (Ivošević et. al., 2020). This EDX semi-quantitative analysis determined the chemical composition of the materials after corrosion, as well as the content of oxygen on the surface of the examined samples which were used for future comparison.

2.1.2 Multivariate linear regression

In the process of studying the behavior of a physical phenomenon, it is often necessary to have a tool that will enable the prediction of future quantities that characterize the observed phenomenon. Therefore, one of the requirements of the statistical analysis of empirical data is the formation of a model on the basis of which a general conclusion can be drawn about measured values. For this purpose, one or more dependent variables are selected whose values are to be predicted as functions of other explanatory input variables, and whose all values are known in advance.

One of the basic ways to build a predictive model is linear regression. In the first phase of linear regression, the independent variables that will participate in the formation of the model are defined, as well as the dependent variables that will represent the response of the model. The next phase involves estimating the values of the model parameters to minimize errors in predicting the dependent variable. The final step should include tests to show whether the model adequately monitors the behavior of the dependent variable.

There are two basic types of linear regression. If the model has only one independent variable, we are talking about a simple linear regression. In the case that the model is built from several independent variables, it is a multivariate linear regression (Heckler, 2005).

If the dependent variable is denoted by Y, and X represents the vector of independent variables of dimension $N + 1$, then the linear regression model can be written in the following way:

$$Y = \beta_0 + \beta_1 x_1 + \beta_2 x_2 + \cdots + \beta_N x_N \tag{1}$$

The common name for Y is the response variable, while X is known as the predictor (Willard, 2020). The coefficient β_0 represents the fixed value of the model, i.e., the expected mean value of Y when $X=0$ and it is known as intercept. The coefficients values $\beta_0, \beta_1, \beta_2, \dots, \beta_N$ are unknown and need to be estimated in such a way that the linear dependence of Y on X is best captured. Once the model parameters are determined, the model can be further used to predict the value of Y for a given value of the vector X.

3. Results

The main goal of statistical analysis performed in this paper is to establish a relationship between NiTi alloy corrosion rate and the observed process of oxygen development on the material surface caused by seawater environment influence and time of exposure. To predict NiTi alloy corrosion rate degree (measured in nm/month) in three different seawater environments, regression analysis was used to form appropriate prediction models. Oxygen levels expressed in percentage and samples exposure time, expressed in months, were used as explanatory variables in each model.

At the beginning of the experiment (zero month), there were no traces of corrosive processes on the NiTi samples. in addition, the samples used in this experiment were not treated with anti-corrosion coatings or any other technique that could further affect the surface structure and behavior of the alloy during the experiment. Alloy samples were placed in three different seawater environments (air, tide, sea) and changes were monitored at 6, 12, and 18 months. Each sample was subjected to FIB and EDX methods, after 6, 12, and 18 months of exposure to one of the observed marine influences, and then the values of corrosion depth, percentage of oxygen in the alloy, and months of environmental exposure were detected. In this way, a comprehensive empirical database was formed, which was the subject of this statistical analysis.

Table 2. shows the basic descriptive statistics of the formed empirical database. The values related to the percentage of oxygen representation as well as the corresponding values of the corrosion rate that was manifested on the NiTi alloy samples are presented.

Table 2. Descriptive statistics of input data

Environment	Variable	N	Mean	StD	Min	Q1	Median	Q3	Max
air	oxygen	31	11.41	10.15	0.00	2.02	8.28	19.34	30.00
	corr. depth	31	43.36	8.84	30.00	37.50	40.00	50.00	58.33
tide	oxygen	41	29.90	8.68	9.14	24.77	28.57	35.61	48.41
	corr. depth	41	38.78	10.86	22.50	30.00	37.50	45.83	66.67
sea	oxygen	49	26.67	13.16	0.00	15.04	29.82	37.63	52.48
	corr. depth	49	281.3	158.5	41.7	168.8	308.3	414.6	575.0

Figure 2. graphically shows the corrosion rate dependence of the observed NiTi alloy and visualizes the empirical database. The data are grouped with respect to the three seawater environments, so that Figure 2. shows the empirical data for the corrosion rate generated by air, tides, and sea. Corrosion rate values are shown on a color scale with the lowest values assigned in blue, while the highest values are shown in red. In all three images, the corrosion rate is shown as a function of two independent variables that are the basis of the future regression model (oxygen percentage and exposure time).
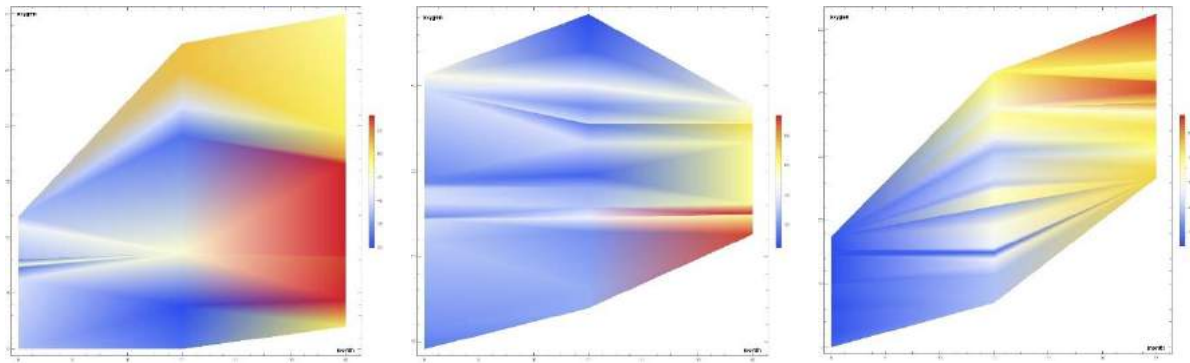
Figure 2. Visualization of NiTi alloy corrosion data measured under the influence of air, tide, and sea

Changes in the values of one variable can affect changes in the values of another variable. Understanding this causal relationship is especially important in creating models that aim to predict and estimate the future values of a dependent variable. The correlation can reflect these changes from the point of view of the trend and the strength of the joint changes of the two variables. Various types of correlation are represented in the statistical analysis. In this paper, one of the most common correlation coefficients, the so-called Pearson correlation coefficient, is used (Lee Rodgers et. al., 1988).

Figure 3. shows the results of the correlation analysis between the corrosion rate, the percentage of oxygen, the elapsed time since the beginning of the experiment, as well as the mutual simultaneous influence of oxygen and the time of exposure of the sample to the environmental influences. Correlation analysis is given here in the form of a correlation matrix.
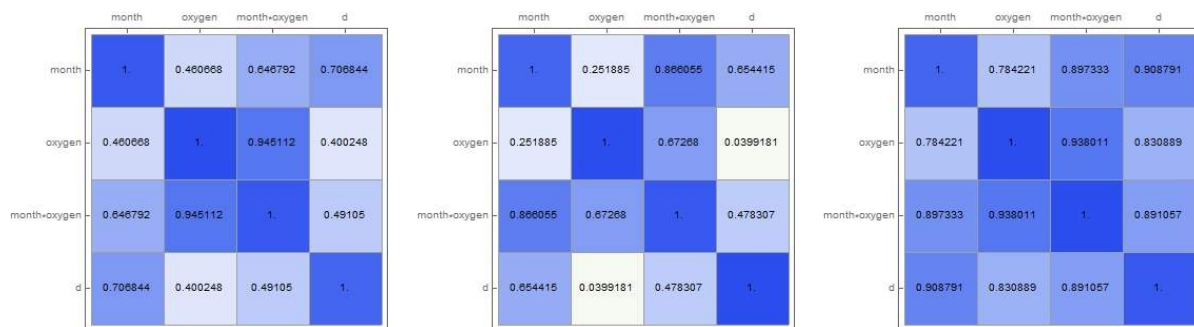
Figure 3. Correlation analysis

A Pearson's correlation coefficient can take values between -1 and 1. Negative values also indicate a negative correlation, while positive values of the correlation coefficient indicate a positive correlation between the two observed variables. As can be seen in Figure 3., in all three observed environments, only positive correlation effects occur. This means that an increase in one value of the observed variable affects the increase in the value of the other observed variable. The degree of correlation may be high, moderate, low, or no correlation. These degrees of correlation are characterized by the values of the coefficients between ± 0.50 and ± 1, ± 0.30 and ± 0.49, respectively, below ± 0.29, and the correlation is said to be strong, moderate, or small. If the correlation coefficient is zero, then it is said that there is no correlation. On the correlation matrices shown in Figure 3., the correlation degrees were additionally plotted through the color intensity assigned to each cell of the matrix.

One correlation matrix is given for each observed seawater environment, on the basis of which positive values of Pearson's correlation coefficient can be observed for all considered variables, but with different degrees of correlation, whose values are shown in the cells of the matrix. As expected, the corrosion rate increases with increasing exposure time to the environment, as well as with an increase in the percentage of oxygen, in all three seawater environments.

The generalized regression model presented in formula (1) was applied to an empirical database of NiTi alloys and measured values of corrosion rate and percentage of oxygen for 6, 12, and 18 months of exposure to three seawater environments, i.e., air, tide, and sea. At the beginning of the experiment, the oxygen content was zero, and the corrosion rate for all samples and all observed seawater environments. As a result, the intercept was set to zero in all models in the regression analysis, i.e., $\beta_0 = 0$ in all three regression models. The corrosion rate in a given seawater environment was considered as a dependent variable, so that three regression models were obtained, which we refer to as d_A, d_T, and d_S, respectively. As explanatory variables, the time elapsed since the beginning of the experiment, the percentage of oxygen in the alloy, and the simultaneous interaction of oxygen and elapsed time (which was obtained by multiplying these two values) were observed. These three independent variables are denoted by x_1, x_2, and x_3, respectively, in each produced regression model. The results of the regression analysis are shown in Table 3.

Table 3. Table of parameters for the three formed models of corrosion for air, tide, and sea

Environment	Coefficient	Estimate	Std. error	t-statistics	p-value
air	β_1	3.4271	0.228483	14.9993	6.534×10^{-15}
	β_2	2.28241	0.451786	5.05198	0.0000240593
	β_3	-0.157748	0.0296944	-5.31239	0.0000118121
tide	β_1	4.00726	0.439707	9.11348	4.2203×10^{-11}
	β_2	0.71392	0.119184	5.99005	5.87456×10^{-7}
	β_3	-0.0814676	0.0158206	-5.14946	8.31654×10^{-6}
sea	β_1	12.086	2.5077	4.81956	0.0000160634
	β_2	-0.212609	1.68564	-0.126129	0.900179
	β_3	0.347143	0.0952672	3.64388	0.000680433

The third column of Table 3. shows the values of the coefficients of the three independent variables in the case of the regression model under the influence of air, tide, and sea. In the last column of Table 3., the corresponding values for p-value are given. As the significance level in the regression analysis was set to 95%, i.e., $\alpha = 0.05$, all values for p-value that are less than 0.05 indicate the fact that the observed model parameters have a significant effect on the corrosion rate in the observed environment. From this, it follows that all three independent variables (environmental exposure time, oxygen percentage, and interacting oxygen interaction and exposure time) have a significant share in describing corrosive processes in the air and tide environment.

Under the influence of sea, the regression model showed small difference in terms of corrosion rate behavior. Namely, the coefficient β_2 has a high value for p-value, which indicates that single oxygen observation does not have a significant share in the corrosion rate modeling. Despite the fact that initial research has shown that the percentage of oxygen has an impact on the formation of corrosive processes in the sea environment, regression analysis

shows that combining the influence of oxygen percentage with other factors significantly reduces the degree of oxygen influence as a separate factor. Based on this, it can be concluded that it is necessary to further calibrate the model for corrosion rates under the influence of sea, due to very complex factors that can affect the corrosive processes in that environment.

By including obtained specific values of regression coefficients for the considered empirical data related to the NiTi alloy in three different seawater environments, three regression linear models were formed whose patterns are given in formulas (2) - (4).

$$d_A = 3.4271x_1 + 2.28241x_2 - 0.157748x_3 \qquad (2)$$
$$d_T = 4.00726x_1 + 0.71392x_2 - 0.0814676x_3 \qquad (3)$$
$$d_S = 12.086x_1 - 0.212609x_2 + 0.347143x_3 \qquad (4)$$

The coefficient of determination, i.e., R^2 statistics were used to estimate the goodness of fit for the three formed regression models represented by expressions (2) - (4). This statistic shows how much proportion of variation in the dependent variable can be explained by the independent variables. The corresponding values of R^2 for the three formed regression models da, dt, and ds, are respectively 0.959489, 0.961901, and 0.962615. This means that approximately 95.95%, 96.19%, and 96.26% of the variation in the corrosion rate can be explained by the obtained linear models (2) - (4).

To test variability within a regression model and to address the model significance, Analysis of Variance (ANOVA) is used (Miller, 1997). Simultaneous and individual effects of the percentage of oxygen and the elapsed time of exposure to the influence of the seawater environment on the corrosion rate of NiTi alloys were verified by ANOVA test with a 95% confidence level. ANOVA results are summarized in Table 4.

Table 4. Regression Analysis of Variance for three observed seawater environment

Environment	Source	DF	AdjSS	AdjMS	F-Value	P-Value
	Regression	3	58169.5	19389.8	221.06	0.000
air	Error	28	2456.0	87.7		
	Total	31	60625.5			
	Regression	3	63852.8	21284.3	319.80	0.000
tide	Error	38	2529.1	66.6		
	Total	41	66381.9			
	Regression	3	4891817	1630606	394.81	0.000
sea	Error	46	189984	4130		
	Total	49	5081800			

The F-test belongs to the group of statistical tests on the basis of which the conclusion is drawn whether the regression model better describes the data than the model in which the explanatory variables would not be included (Bingham and Fry, 2010). For each value of F statistics, the corresponding p-value is calculated. As the significance level in this paper is set at 0.05, all p-values less than 0.05 provide sufficient evidence to conclude that the formed regression model corresponds well to the empirical data for the corrosion rate. In all three seawater environments, the calculated p-values for F statistics are close to zero. Based on this, it is concluded that the regression models presented in expressions (2) - (4) well represent the values of NiTi alloy corrosion rate in the observed seawater environments. More specifically, these models can be used to predict future corrosion rate values generated under the influence of oxygen and the time of exposure of the sample to the seawater environment. It can be

noticed that these values are in accordance with the obtained values for R^2 and the conclusions that these values impose.

As another way of checking the quality of the regression model, a residual normality plot can be used (Anscombe, 1973). These graphs are shown in Figure 4. for all three considered seawater environments. If the regression model follows well the changes in the dependent variable, the residual plot should show that the residuals follow the normal distribution, i.e., that the graph of the normal probability of the residual lies approximately on a straight line extending along the main diagonal of the graph. It is evident that in all three regression models corresponding to the influence of air, tide, and sea, the graphs approximately follow a straight line, so it is concluded that there are no deviations, unexpected behaviors, or evident existence of some unidentified variable.
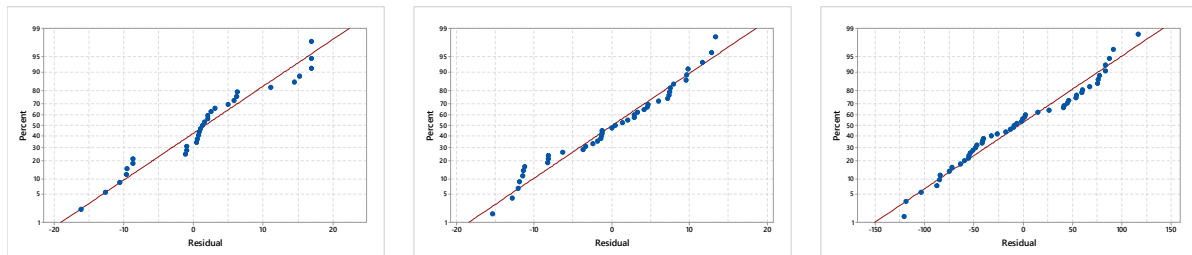
Figure 4. Normal probability plot of residuals for corrosion depth under air, tide, and sea influence

Statistical analysis shows that the formed regression models with three explanatory variables that indicate the time of exposure of the sample to the environment, the percentage of formed oxygen on the sample surface, and the joint impact of the previous two variables, adequately monitor changes in the corrosion rate of NiTi alloy in all three seawater environments. Therefore, the formed models (2) - (4) can be used as a tool for predicting the value of corrosion rate as a function of the described independent variables. Predicted values for corrosion rates caused by air, tides, and sea are shown in Figures 5-7. These figures clearly show the different behavior of corrosion rates in the three observed seawater environments. The values for the corrosion rate are shown in these figures by a scale on which the lowest values are assigned blue dots while the higher highest values correspond to red dots.

Figure 5. Predicted corrosion rate values based on regression model for air

Figure 6. Predicted corrosion rate values based on regression model for tide

Figure 7. Predicted corrosion rate values based on regression model for sea

4. Discussion and Conclusions

In this paper, the authors have dealt with the development of regression models that will adequately describe the corrosion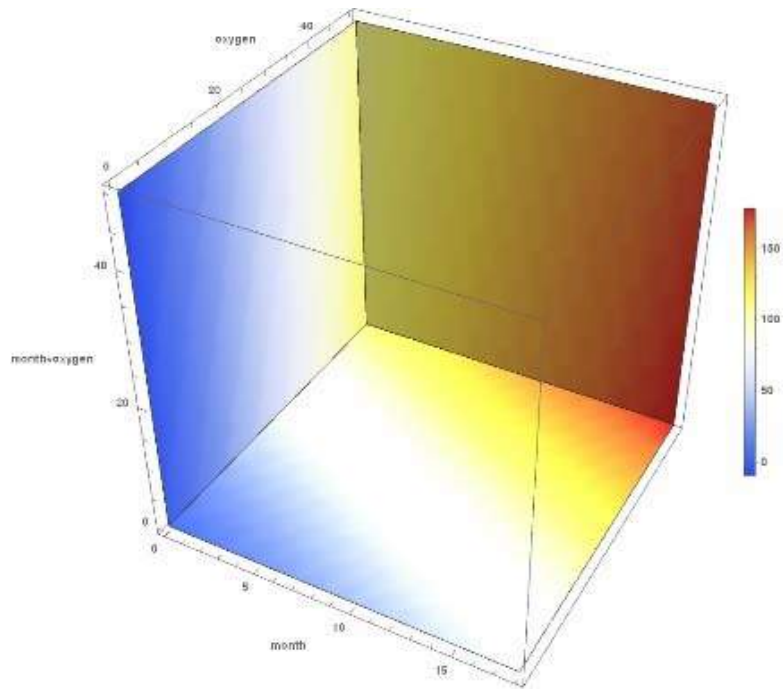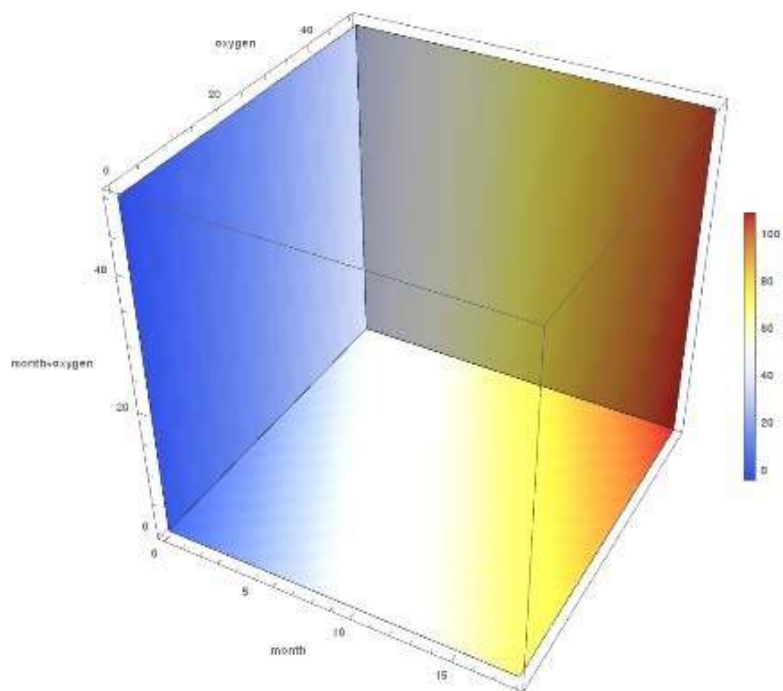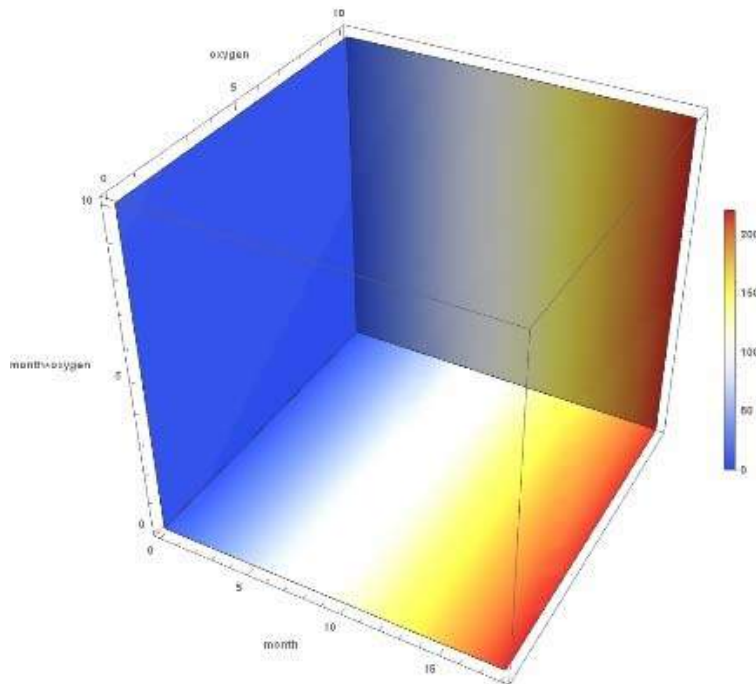 rate behavior for NiTi alloy formed under the influence of air, tide, and sea. For the explanatory variables of the model, the time of exposure to the influence of the environment, the percentage of formed oxygen on the sample surface, and the joint simultaneous influence of both variables were selected. The conducted statistical analysis provides sufficient evidence that the selected model parameters are valid for describing the corrosion rate as a dependent variable, and that the formed regression models can be further used to predict the corrosion rate of NiTi alloy in all three observed environments.

Despite the fact that preliminary research has shown that the influence of oxygen on the formation of corrosion of NiTi alloy under the influence of the sea is noticeable, a more detailed statistical analysis revealed an interesting fact. Namely, oxygen as a standalone factor of the regression model is not statistically significant, but in interaction with other factors, it has shown that it is an unavoidable factor of regression analysis. Based on this, it can be concluded that it is necessary to make an effort and form even more complex regression models, which will include a larger number of variables and their mutual interactions in the formation of regression models for corrosion rate.

A more detailed insight into the correlation coefficients given in the correlation matrices (Figure 3.) can also show the effects of multicollinearity. Multicollinearity is not an aggravating factor if the main goal of regression analysis is only to predict the value of the dependent variable, as is the goal of statistical analysis in this paper. However, based on this multicollinearity, it is possible to define future research directions that could also have a stricter relationship between explanatory variables and corrosion rate as output variables. Therefore, this research can be extended with principal component analysis or partial least squares regression.

References

Anscombe, F. J. (1973). Graphs in statistical analysis. *The american statistician*, *27*(1), 17-21.

Heckler, C. E. (2005). Applied multivariate statistical analysis.

Bingham, N. H., & Fry, J. M. (2010). *Regression: Linear models in statistics*. Springer Science & Business Media.

Huang, W. (1998). Shape memory alloys and their application to actuators for deployable structures. University of Cambridge Department of Engineering.

Ivošević, Š., Vastag, G., Majerič, P., Kovač, D., & Rudolf, R. (2020). Analysis of the Corrosion Resistance of Different Metal Materials Exposed to Varied Conditions of the Environment in the Bay of Kotor.

Ivošević, Š., Kovač, N., Vastag, G., Majerič, P., & Rudolf, R. (2021). A Probabilistic Method for Estimating the Influence of Corrosion on the CuAlNi Shape Memory Alloy in Different Marine Environments. *Crystals*, *11*(3), 274.

Jani, J. M., Leary, M., Subic, A., & Gibson, M. A. (2014). A review of shape memory alloy research, applications and opportunities. *Materials & Design (1980-2015)*, *56*, 1078-1113.

Lee Rodgers, J., & Nicewander, W. A. (1988). Thirteen ways to look at the correlation coefficient. *The American Statistician*, *42*(1), 59-66.

Melchers, R. E. (1999a). Corrosion uncertainty modelling for steel structures. *Journal of Constructional Steel Research*, *52*(1), 3-19.

Melchers, R. E. (1999b). Factors Influencing the Immersion Corrosion of Steels in Marine Water. In *Proceedings of the 14th International Corrosion Congress, Cape Town, South Africa*.

Melchers, R. E. (2003). Probabilistic model for marine corrosion of steel for structural reliability assessment. *Journal of Structural Engineering*, *129*(11), 1484-1493.

Miller Jr, R. G. (1997). *Beyond ANOVA: basics of applied statistics*. CRC press.

Paik, J. K., Kim, S. K., & Lee, S. K. (1998). Probabilistic corrosion rate estimation model for longitudinal strength members of bulk carriers. *Ocean Engineering*, *25*(10), 837-860.

Paik, J. K. (2003). A time-dependent corrosion wastage model for bulk carrier structures. *Int J Marit Eng R Just Naval Arch*, *145*(2), 61-87.

Paik, J. K. (2004). Corrosion analysis of seawater ballast tank structures. *International Journal of Maritime Engineering*, *146*(A1), 1-12.

Soares, C. G., & Garbatov, Y. (1999). Reliability of maintained, corrosion protected plates subjected to non-linear corrosion and compressive loads. *Marine Structures*, *12*(6), 425-445.

Willard, C. A. (2020). *Statistical Methods: An Introduction to Basic Statistical Concepts and Analysis*. Routledge.

Yamamoto, N., & Ikegami, K. (1998). A study on the degradation of coating and corrosion of ship's hull based on the probabilistic approach.

Estimation Forest Cover Map with Fusion Lidar And Sentinel Data

Nuray Bas[1]*

Abstract: With the development of remote sensing technology, the information about the surface and the changes can be determined more precisely and more accurately. In this contex, forest cover density is one of the important froest structural parameter in forest management. This extremely important issue in forest management is determined with the help of various satellite images. A wide variety of satellite images are used for this purpose depending on the study. The forest cover map can be derived from the spectral properties of optical images and also derived from 3D point cloud data such as LiDAR data with high accuracy. In this study, point cloud forest cover map was determined using Sentinel-2 optical image and 3D LiDAR data in Turkey located in the wooded area in the province of Adapazarı. The benefits and shortcomings were revealed in terms of utilization possibilities and forest management in both studies. Then, the values of Forest Index (FI) and Normalized Difference Vegetation Index (NDVI), Enhanged Vegetation Index (EVI), Red Edge Ratio Vegetation Index (RERVI) were calculated and the results were compared in forest area. At the end of the study, user accuracy for forest cover density for LiDAR data and Sentinel data is very high with 76% and 85%.

Keywords: NDVI, 3D LiDAR Sentinel-2, EVI, RERVI

1. INTRUDUCTION

Forestry monitoring plays an important role in sustainable forest management (Foody 2002), (Tucker et al.. 1985). It is possible to determine the amount of biomass as well as the spatial determination of forest information with remote sensing techniques (Sinha et al.. 2015), (Lu, et al.. 2014), (Eisfelder, et al.. 2012), (Li, et al.. 2020). Forest information is frequently used in environmental, biomass and biodiversity applications as well as forest inventory studies (Li et al. 2014), (Wulder et al. 2012), (Hansen et al. 2010).

Forest maps are crucial for global environmental change assessment and local forest management planning (Waser et. al. 2015). It has been discussed as a research topic in many subjects such as agriculture, environment and sustainable forest management (Ampadu et al. 2020), (Boyd et al. 2002), (Hansen et al. 2013). However, the cost of measurement of large area, need high accuracy map and the limited area coverage make monitoring problematic (Shimizu et al. 2020). Therefore, optical data can be combined with synthetic data (Sánchez et al. 2018).

Another important consideration is the need to produce high-level cover maps when the production of forest maps requires spatial accuracy and detailed content information (Ganz et al. 2020). Obtaining spatial information about the forested area on-site measurement work.

[1] Sivas Cumhuriyet University, Engineering Faculty, Geomatic Engineering Department, Sivas/Turkey
* Corresponding author: nuraybas@gmail.com

This is possible in local area studies. However, it is very difficult to produce a map of forest areas by measuring with a total station or Global Positioning System (GPS) at the world scale and especially in large and hard-to-reach areas.

Consequently, their development is time-consuming and therefore limited to relatively small areas (Naesset, 1997), (McRoberts 2007). In this case, we come across the Airborne Light Detection and Ranging (LiDAR) technique, which has been popular in the science of remote sensing in recent years. With this technique, both positional information and canopy height information are determined with high accuracy (Wulder et al. 2012), (Li et al. 2020).

The fact that LiDAR provides height information as well as spatial information to users is an important advantage especially in tree height determination and biomass calculation studies. For this reason, it is widely used in operations such as individual tree height, volume and biomass determination. (Yao et al. 2012), (Stereńczak et al. 2020).

However, in some cases, optical and synthetic data may also need to be considered. In addition to LiDAR, Optic and SAR (Sentetic Aparture Radar) data are also widely used in forestry studies. Long observation time, temporal data caracteristics wide spatial coverage and multiple bands can provide abundant information about forest structure (Mc Cue et al. 1971), (Gao et al. 2014), (Fagua et al. 2019). Sensor selection, spatial variations, radiometric and temporal resolutions are also of great importance in land cover classification studies (Lu and Weng 2007).

Various satellite images can be used by evaluating effects such as the study area and the precision of the study. Low-resolution images such as Landsat, (Gao and Zhang 2009), (Manandharet al. al 2009), SPOT, (Gxumisa, and Breytenbach 2017), MODIS (Aredehey, et al. (2017), ASTER (Zhao et al. 2019) can be used or classification can be made with QuickBird (Lu et al. (2010), WorldView, (Ranaie et al. (2018) images on a more local scale. Multispectral sensors are used for issues such as vegetation character, species determination, and plant health (Lu et al. 2016).

In this study, we used a multisensory fusion approach involving both LiDAR data and Sentinel-2 data. The applied methods are almost completely automated land use classification. Therefore suitable for area-wide forest mapping using Optic data and high resolution LiDAR data. We showed that the forest cover map could be derived by Sentinel-2 data with combination LiDAR data. In addition this result adding Forest index such as Enhanged Vegetation İndex (EVI), Normalized Vegetation Index (NDVI), and Red Edge Vegetation Index (RERVI).

2. DATA AND METHODS

2.1. Study Area

The study area is located in the Karasu region of Sakarya in Turkey which has 1.311 km^2 area. Sakarya Province is very rich in terms of natural vegetation. The mountains, which are extensions of the northern Anatolian coastal mountains are covered with dense forests. There are abundant ash forests in the east of Adapazarı. Here, elm and alder trees are mixed among the ash trees. There are settlement areas, cultivated areas and forest areas in places. Vegetation weakens around the lower Sakarya valley in the plains. The climate in Karasu, where the study area is located, is classified as warm and temperate. The average temperature

of the province is 14.1 °C. Even in the driest months, the amount of precipitation is quite high. The study area is at a min elevation of 34.79 m above sea level and max elevation is 594.44 meter.

Figure 1: Study Area

2.2 Data Acquisition and Pre-Processing

In this study, three different data sets were used, namely LiDAR, Sentinel-2 and Google Earth data. LiDAR data is 5.1 samples/m^2 and point spacing is 0.44 m. First, second last, first of many and last return and Scan angle 26°. Riegl VQ580 LiDAR sensor was used as the sensor. Flight altitude is an average of 450-500 m. above ground level. Average Helicopter Speed was purchased as 75-80 km\h. Data has UTM zone 36 WGS 84 coordinate system. Since LiDAR data was obtained in October, The Sentinel-2 image was acquired on 10 October 2020. The European Space Agency was selected by determining the time interval with minimum cloudiness. Ten bands were used for analysis as shown in Table 1. The Sentinel-2 image was atmospherically corrected using QGIS software. Since the Sentinel-2 image was acquired at level-1 C orthorectification was already.

Table 1: Sentinel-2 bands used for analysis

Bands	Central wave length(µm)	Resolution (m)	Bandwith (nm)
Band 2- Blue	0.490	10	65
Band 3-Green	0.560	10	35
Band 4-Red	0.665	10	30
Band 5-Vegetation Red Edge	0.705	20	15
Band 6- Vegetation Red Edge	0.740	20	15
Band 7- Vegetation Red Edge	0.783	20	20
Band 8- NIR	0.842	10	115
Band 8A- Narrow NIR	0.865	20	20
Band 11- Swır	1.610	20	90
Band 12- Swır	2.190	20	180

3. LiDAR DATA PROCESS

Forest canopy density is frequently used in applications such as biomass estimation biodiversity determination in environmental and forestry applications. Canopy density or canopy cover ratios in vegetation cover can be viewed by aerial acquisition with the help of

LiDAR data. In order to calculate the canopy cover ratio with the help of LiDAR data, it is necessary to first make the raw LiDAR data that has been classified into ground returns (bare earth) versus non-ground returns.

In this study, Cloth Simulation Filter (CSF) filtering method was used in the classification of LiDAR data (Zhang et al. 2016). The CSF method first inverts the original point cloud by creating a DTM process. As a second step, rigid cloth is used to cover the inverted level formed in the first step. At the end of the process, the ground surface is obtained. In the final step, the original point cloud and the final shape of the simulated cloth are compared with each other.

In the LiDAR data classification process, ground and nonground classification were obtained at the end of the classification process. Since the altitude values are the altitudes obtained from sea level in the flight data, the altitude values were normalized to obtain local altitude values.
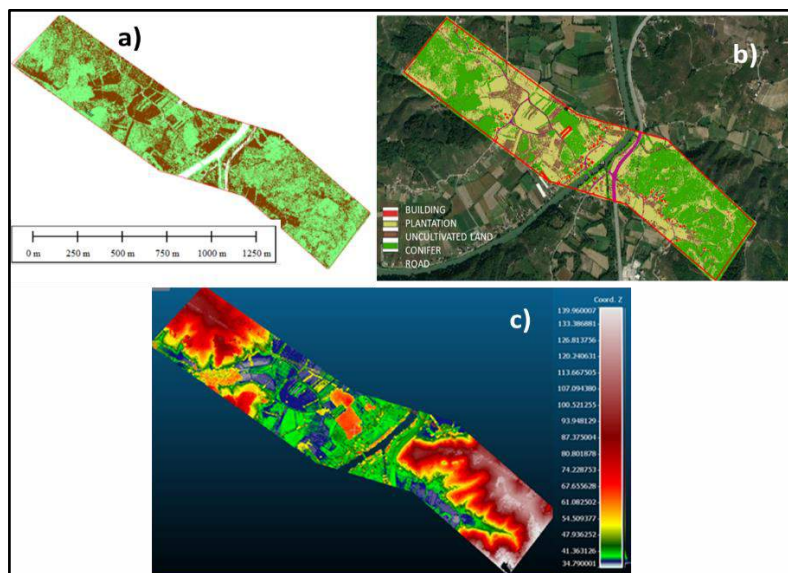
Figure 2 : LiDAR Data Classification Results **a)** Unclassified Data**, b)** Classified Data, **c)** Normalized hight value

4. RESULTS

4.1. LULC Land Classification Using Sentinel-2 Data

In Remote Sensing management, the concept of Land use and land cover (LULC) classification can be defined as the determination of socioeconomic and environmental changes at local, regional and global scales (Li et al. (2014), (Forkuor et. al. 2017).

Region of Interest (ROI) polygons were created in the classification process to define the spectral characteristics of the land classes. ROIs are polygons drawn over homogeneous areas of the image that overlay pixels belonging to the same land cover class. The image is segmented around a pixel seed including spectrally homogeneous pixels using region growing algorithm. ROI polygons were stored as training input. It is worth pointing out that classification is always based on spectral signatures. In the algorithm used, the spectral signatures of the fields determined as training input are used and the program assigns a

microclass ID to each class. Spectral Angle Mapping (SAM) method was used as a method in the classification process.

The Spectral Angle Mapping calculates the spectral angle between spectral signatures of image pixels and training spectral signatures. The spectral angle θ is defined as (Kruse et al.., 1993) Eq (1), where,

$$\theta(x,y) = \cos^{-1}\left(\frac{\sum_{i=1}^{n} xi, yi}{(\sum_{i=1}^{n} X_i^2)^{1/2} * (\sum_{i=1}^{n} y_i^2)^{1/2}}\right) \tag{1}$$

   x = spectral signature vector of an image pixel,
   y = spectral signature vector of a training area,
   n = number of image bands.
Therefore a pixel belongs to the class having the lowest angle, that is Eq(2).

$$x \in C_k \Leftrightarrow \theta(x, y_k) < \theta(x, yj) \forall k \neq j \tag{2}$$

 Where,
 Ck = land cover class k,
 yk = spectral signature of class k,
 yj = spectral signature of class j.

BUILDING
CONIFER
CONIFER
BUILDING
UNCULTIVATED AREA

Figure 3 : Sentinel 2 data Spectral Engine Mapping Classification Results

4.2.Forest Index Based on NDVI, EVI and RERVI Index

NDVI is a simple but widely used index for determining the amount of green vegetation. This index normalizes green leaf scattering at near Infrared wavelengths with chlorophyll absorption at red wavelengths. The value range of NDVI is -1 to 1. Values close to zero (-0.1 to 0.1) generally correspond to barren rocky areas, sand or snow areas with the least vegetation. Low, positive values represent shrubs and grasslands (approximately 0.2 to 0.4), while high values represent high wooded areas (values approaching 1), such as tropical rainforests with the densest vegetation. NDVI is defined as Eq (3) , (Rouse Jr. et al.1974).

$$NDVI = \text{index (NIR,RED)} = \frac{NIR\text{-}RED}{NIR\text{+}RED} \tag{3}$$

The Enhanced Vegetation Index (EVI) is an index designed to monitor the amount of biomass in improved vegetation with reduced atmospheric effect (Huete et al.. 1997), (Eq.4). NDVI is sensitive to chlorophyll, while the EVI leaf area index (LAI) is more sensitive to canopy structural variations, including canopy type, plant physiognomy, and canopy architecture. The two vegetation indices complement each other in global vegetation studies and improve upon detection of vegetation changes and extraction of canopy biophysical parameters. Another difference between the NDVI and EVI is that NDVI decreases in the presence of snow, whereas EVI increases (Huete, 2002).

$$EVI = 2.5 \ \frac{NIR\text{-}RED}{NIR + C_1 * RED - C_2 * BLUE + L} \qquad (4)$$

Where NIR, RED and Blue are atmospherically- corrected surface reflectance and C1,C2, and L are coefficients to correct atmospheric conditions . Fort he standart MODIS EVI product L=1 , C1=6 and C2= 7.5 . The range of values for EVI is -1 to 1, with healthy vegetation generally around 0.20 to 0.80. Red-edge ratio vegetation index (RERVI) (Cao et al.., 2013) is calculated three visible bands (B2, B3, B4), two red-edge bands (B5, B6), and three NIR bands (B7, B8, and B8a). To improve the saturation problem of NDVI, the red-edge ratio is considered. Among the red-edge bands in Sentinel-2, the B5 and B6 band are selected, because they have similar reflectance values at low vegetation densities, and because there is a gradual increase in the difference between the two bands in relation to increased biomass. Finally, we propose the Red Edge Ratio NDVI (RERNDVI) which is formed by multiplying the red-edge ratio and NDVI as Eq.5.

$$RERNDVI = NDVI \times sqrt(B6/B5) \qquad (5)$$

As a result s a result, NDVI, EVI, RERVI indices were calculated as shown in the figure to calculate vegetation rates in the study area. When these indexes calculated according to the classification results obtained in high resolution LiDAR data are compared, it is seen that there is a similarity. Namely, the conifer area seen in the LiDAR data is seen as the closest value to 1 in the NDVI, EVI and RERVI index maps. Similarly, Sentinel Data index map corresponding to the area in LiDAR data classified as uncultivated area is seen as a value closer to zero. Thus, with the help of plant indexes, the classification accuracy can be increased with the help of both the calculated index values and the corresponding fields in the LiDAR data of the classified areas in the sentinel data
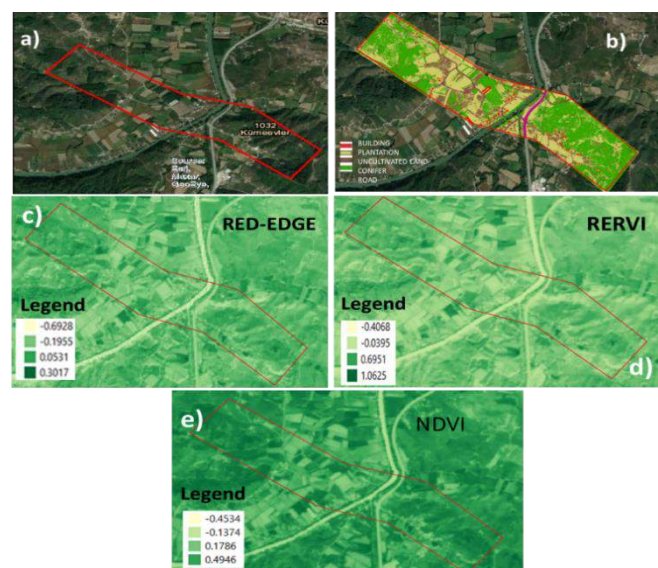
Figure 4 : a) Google earth İmage , **b)** LiDAR forest cover map , **c)** NDVI map **, d)** RERVI map , **e)** EVI map

4.3.Accuracy Assestment

Reference points were determined in Google Earth software as a reference data set for accuracy. For each land class, 50 reference points were determined randomly distributed throughout the image. In this way, the reference point file was created (Figure 5).
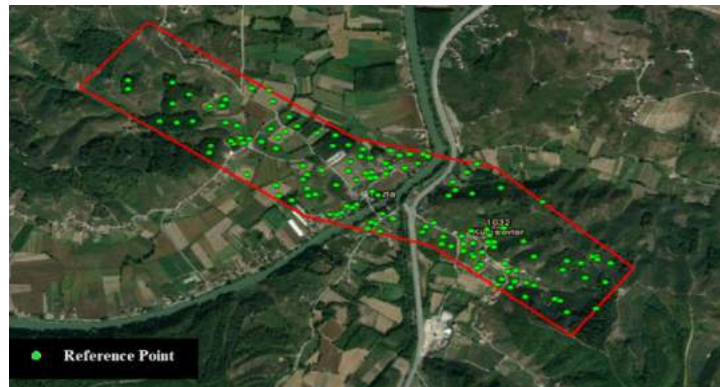
Figure 5: Study Area Reference Points

In the second step an error matrix was created for accuracy management. The error matrix allows us to calculate various or accuracy metrics from our data. This matrix consists of n x n arrays and "n" number of data classes. The columns in the error matrix represent the reference data. Rows are mapped classes created from remotely sensed data. 50 samples were created from each class for building, plantation, uncultivated area, conifer and road classes. These sample areas were then compared with the classified data. As a result, the error matrix in the figure was created.

Table 2 :Relationship between reference data and classified data obtained error matrix report for samples

Reference		Building	Plantation	Uncultivated	Conifer	Road	Total	Correct Sampled	PA (%)	UA (%)
Classification	Building	**32**	2	3	3	4	44	32	0.78	0.73
	Plantation	2	**35**	4	3	2	46	35	0.78	0. 76
	Uncultivated	3	2	**39**	2	3	49	39	0.74	0.80
	Conifer	2	3	4	**38**	5	52	38	0.76	0.73
	Road	2	3	3	4	**47**	59	47	0.77	0.80
	Total	41	45	53	50	61	250	191		
	OE(%)	22	22	26	24	30				
	CE(%)	37	24	20	27	20				
	Overall Accuracy			%76			Kappa Statistics: 0.75			

Highlighted diagonal items in the error matrix represent correctly classified areas. These diagonal values show the accuracy of our classification process. The accuracy is determined with the help of the following equation (Eq.6).

The overall classification accuracy = No. of correct points/total number of point (6)

In the example above, 32 of the 50 building reference points, 35 of the Plantation class, 39 of the Uncultivated class, 38 of the Conifer field and 47 of the Road zones are correctly identified on the classified Sentinel-2 map

At the end of the process, Ommission Error (OE) and Commission Error (CE) percentages were calculated. OE show false positives. So the pixels are assigned to the wrong class. CE indicates false negatives. That is pixels of a known class are classified as something other than that class. Also, the non-diagonal elements in the rows of the confusion matrix are divided by the total number of pixels assigned to the Sentinel image class corresponding to the row, and the resulting value shows CE. CE defines the probability that a pixel assigned to a particular class actually belongs to one of the other classes.

Errors of omission are also known as user's accuracy or Type -1 error. The producer's accuracy column shows false negatives, or errors of commission. The Total column shows the number of points that were identified as a given class, according to the classified map. Kappa statistic of agreement gives an overall assessment of the accuracy of the classification of commission are also known as producer's accuracy or Type-II error. Overall accuracy, on the other hand, shows how accurately the classification is made according to the reference data. The diagonal values in the table show the correctly classified values. Overall accuracy was calculated as 76% according to the classification result.

5. CONCLUSIONS

In this study, forest indices were calculated for forest areas and a land classification map was created using Sentinel-2 and LiDAR data. Thus, the densely forested area, cultivated areas, uncultivated areas and the settlement areas in the region were determined by automatic classification algorithms. In addition, spectral range values obtained from NDVI, EVI, RERVI indices obtained from Sentinel-2 data were compared with LiDAR classification results. The Vegetation Index (VI) is a mathematical combination of bands with spectral features in green plants as a factor that affects and supports the classification result. In conclusion, conifer, Red Edge , NDVI, EVI indices of forest and cultivated areas were calculated for uncultivated area, plantation, road. The relationship between these vegetation indices and classification results has been revealed. When the relationship obtained was examined, it was concluded that there was a positive relationship. Vegetation indices were found to be high in areas with high conopy biomass. In the study, it was concluded that we should decide which remote sensing data to choose depending on the target we want to achieve results. using Sentinel-2 data in the classification process is an option for very high accuracy undesired targets. Another option is the result that we can obtain a more accurate terrain map with LiDAR data for areas that require high sensitivity or for more localized areas. In addition, since LiDAR data allows viewing in areas that are difficult to reach from the air, it will be possible to classify it in wide areas as well as high accuracy. Another result is that it is possible to obtain a terrain map with the combination of Sentinel and LiDAR data fusion. Thus, a more accurate classification map will be obtained. Interpreting the results obtained from Sentinel data and LiDAR data combination together with spectral index values

will increase the accuracy of the classification map to be obtained. In general, higher resolution additional data is required in studies with low resolution data in the imaging of agricultural areas and forest areas with remote sensing data. In this case, LiDAR data becomes an important resource. This study has shown that Sentinel-2 and LiDAR data can be used to generate accurate irrigation. As a result of the process, 76% overall accuracy was obtained with Sentinel data and 85% with Lidar data.

ACKNOWLEDGE

REFERENCES

Aredehey, G., Mezgebu, A., and Girma, A. (2017). Land-use land-cover classification analysis of Giba catchment using hyper temporal MODIS NDVI satellite images. International Journal of Remote Sensing, 39(3), 810–821. doi:10.1080/01431161.2017.1392639

Boyd, D., Foody, G. And Ripple, W. (2002). Evaluation of approaches for forest cover estimation in the Pacific Northwest, USA, using remote sensing. Applied Geography, 22(4), 375–392. doi:10.1016/s0143-6228(02)00048-6

Cao, Q., Miao, Y. , Wang, H., Huang, S., Cheng, S., Khosla, R., Jiang, R. (2013). Non-destructive estimation of rice plant nitrogen status with Crop Circle multispectral active canopy sensor. Field Crops Research 154, 133–144. doi:10.1016

Eisfelder, C., Kuenzer, C., and Dech, S. (2012). Derivation of biomass information for semi-arid areas using remote-sensing data. International Journal of Remote Sensing, 33(9), 2937–2984. doi:10.1080/01431161.2011.620034

Fagua, J.C., Jantz, P., Rodriguez-Buritica, S.,Duncanson, L., Goetz, S.J. (2019). Integrating LiDAR, Multispectral and SAR Data to Estimate and Map Canopy Height in Tropical Forests. Remote Sens. 11, 2697.

Foody, G. M. (2002). Status of land cover classification accuracy assessment. Remote Sensing of Environment, 80(1), 185–201. doi:10.1016/s0034-4257(01)00295-4

Forkuor, G., Dimobe, K., Serme, I., and Tondoh, J. E. (2017). Landsat-8 vs. Sentinel-2: examining the added value of sentinel-2's red-edge bands to land-use and land-cover mapping in Burkina Faso. GIScience & Remote Sensing, 55(3), 331–354. doi:10.1080/15481603.2017.1370169

Gao, Y., and Zhang, W. (2009). LULC Classification and Topographic Correction of Landsat-7 ETM+ Imagery in the Yangjia River Watershed: the Influence of DEM Resolution. Sensors, 9(3), 1980–1995. doi:10.3390/s90301980

Gao, M.L., Zhao, W.J., Gong, Z.N., Gong, H.L., Chen, Z., Tang, X.M. (2014). Topographic correction of ZY-3 satellite images and its effects on estimation of shrub leaf biomass in mountainous areas. Remote Sens. 6, 2745–2764.

Ganz, S., Adler, P., and Kändler, G. (2020). Forest Cover Mapping Based on a Combination of Aerial Images and Sentinel-2 Satellite Data Compared to National Forest Inventory Data. Forests, 11(12), 1322. doi:10.3390/f11121322

Gxumisa, A., and Breytenbach, A. (2017). Evaluating pixel vs. segmentation based classifiers with height differentiation on SPOT 6 imagery for urban land cover mapping. South African Journal of Geomatics, 6(3), 436. doi:10.4314/sajg.v6i3.12

Gyamfi-Ampadu, E., Gebreslasie, M., and Mendoza-Ponce, A. (2020). Mapping natural forest cover using satellite imagery of Nkandla forest reserve, KwaZulu-Natal, South Africa. Remote Sensing Applications: Society and Environment, 18, 100302. doi:10.1016/j.rsase.2020.10030 2

Hansen, M. C., Stehman, S. V., and Potapov, P. V. (2010). Quantification of global gross forest cover loss. Proceedings of the National Academy of Sciences, 107(19), 8650–8655. doi:10.1073/pnas.0912668107

Hansen, M. C., Potapov, P. V., Moore, R., Hancher, M., Turubanova, S. A., Tyukavina, A., Townshend, J. R. G. (2013). High-Resolution Global Maps of 21st-Century Forest Cover Change. Science, 342(6160), 850–853. doi:10.1126/science.1244693

Huete, K. Didan, T. Miura, E. P. Rodriguez, X. Gao, L. G. Ferreira. (2002). Overview of the radiometric and biophysical performance of the MODIS vegetation indices. Remote Sensing of Environment 83195-213 doi:10.1016/S0034-4257(02)00096-2.

Kruse, F. A., Lefkoff, A. B., Boardman, J. W., Heidebrecht, K. B., Shapiro, A. T., Barloon, P. J., and Goetz, A. F. H. (1993). The spectral image processing system (SIPS)—Interactive visualization and analysis of imaging spectrometer data. Remote Sensing of Environment, 44(2-3), 145–163. doi:10.1016/0034-4257(93)90013-n.

Li, Y., Li, M., Li, C., and Liu, Z. (2020). Forest aboveground biomass estimation using Landsat 8 and Sentinel-1A data with machine learning algorithms. Scientific Reports, 10(1). doi:10.1038/s41598-020-67024-3

Li M, Zang S, Zhang B, Li S, Wu C. (2014). A review of remote sensing image classification techniques: The role of spatio-contextual information. European Journal of Remote Sensing. 47(1):389-411. Doi: 10.5721/EuJRS20144723

Li, W., Niu, Z., Shang, R., Qin, Y., Wang, L., and Chen, H. (2020). High-resolution mapping of forest canopy height using machine learning by coupling ICESat-2 LiDAR with Sentinel-1, Sentinel-2 and Landsat-8 data. International Journal of Applied Earth Observation and Geoinformation, 92, 102163. doi:10.1016/j.jag.2020.102163

Li, M., Im, J., Quackenbush, L. J., & Liu, T. (2014). Forest Biomass and Carbon Stock Quantification Using Airborne LiDAR Data: A Case Study Over Huntington Wildlife Forest in the Adirondack Park. IEEE Journal of Selected Topics in Applied Earth Observations and Remote Sensing, 7(7), 3143–3156. doi:10.1109/jstars.2014.2304642

Lu, D., Chen, Q., Wang, G., Liu, L., Li, G., and Moran, E. (2014). A survey of remote sensing-based aboveground biomass estimation methods in forest ecosystems. International Journal of Digital Earth, 9(1), 63–105. doi:10.1080/17538947.2014.990

Lu D, Weng Q . (2007). A survey of image classification methods and techniques for improving classification performance. International Journal of Remote Sensing. 28(5):823-870. Doi: 10.1080/01431160600746456

Lu D, Chen Q , Wang G, Liu L, Li G. and Moran E. (2016). A survey of remote sensing-based aboveground biomass estimation methods in forest ecosystems. International Journal of Digital Earth ,9(1):63-105. Doi: 10.1080/17538947.2014.990526

Lu, D., Hetrick, S., & Moran, E. (2010). Land Cover Classification in a Complex Urban-Rural Landscape with QuickBird Imagery. Photogrammetric Engineering & Remote Sensing, 76(10), 1159–1168. doi:10.14358/pers.76.10.1159

Manandhar, R., Odeh, I., and Ancev, T. (2009). Improving the Accuracy of Land Use and Land Cover Classification of Landsat Data Using Post-Classification Enhancement. Remote Sensing, 1(3), 330–344. doi:10.3390/rs1030330

McCue, G. A., Williams, J. G., and Morford, J. M. (1971). Optical characteristics of artificial satellites. Planetary and Space Science, 19(8), 851–868. doi:10.1016/0032-0633(71)90137-1

McRoberts, R.E., and Tomppo, E.O. (2007). Remote sensing support for national forest inventories. Remote Sens. Environ. 110, 412–419.

Naesset, E., (1997). Determination of mean tree height of forest stands using airborne laserscanner data. ISPRS J. Photogramm. Remote. Sens. 52, 49–56.

Ranaie, M., Soffianian, A., Pourmanafi, S., Mirghaffari, N., and Tarkesh, M. (2018). Evaluating the statistical performance of less applied algorithms in classification of worldview-3 imagery data in an urbanized landscape. Advances in Space Research, 61(6), 1558–1572. doi:10.1016/j.asr.2018.01.004

Rouse, J. W., Haas, R. H., Schell, J. A. And Deering, D. W. (1974) . Monitoring vegetation systems in the great plains with ERTS. in: Proceedings of the Third Earth Resources Technology Satellite-1 Symposium, NASA SP-351 (pp. 309-317).

Shimizu, K., Ota, T., Mizoue, N. and Saito, H. (2020). Comparison of Multi-Temporal PlanetScope Data with Landsat 8 and Sentinel-2 Data for Estimating Airborne LiDAR Derived Canopy Height in Temperate Forests. Remote Sensing, 12(11), 1876. doi:10.3390/rs12111876

Stereńczak, K., Kraszewski, B., Mielcarek, M., Piasecka, Ż., Lisiewicz, M. and Heurich, M. (2020). Mapping individual trees with airborne laser scanning data in an European lowland forest using a self-calibration algorithm. International Journal of Applied Earth Observation and Geoinformation, 93, 102191. doi:10.1016/j.jag.2020.102191

Sánchez Sánchez, Y., Martínez-Graña, A., Santos Francés, F.and Mateos Picado, M. (2018). Mapping Wildfire Ignition Probability Using Sentinel 2 and LiDAR (Jerte Valley, Cáceres, Spain). Sensors, 18(3), 826. doi:10.3390/s18030826

Sinha, S., Jeganathan, C., Sharma, L. K. and Nathawat, M. S. (2015). A review of radar remote sensing for biomass estimation. International Journal of Environmental Science and Technology, 12(5), 1779–1792. doi:10.1007/s13762-015-0750-0

Tucker, C. J., Townshend, J. R. And Goff, T. E. (1985). African Land-Cover Classification Using Satellite Data. Science, 227(4685), 369–375. doi:10.1126/science.227.4685.369

Waser, L., Fischer, C., Wang, Z. and Ginzler, C. (2015). Wall-to-Wall Forest Mapping Based on Digital Surface Models from Image-Based Point Clouds and a NFI Forest Definition. Forests, 6(12), 4510–4528. doi:10.3390/f6124386

Wulder, M. A., White, J. C., Nelson, R. F., Næsset, E., Ørka, H. O., Coops, N. C.,Gobakken, T. (2012). LiDAR sampling for large-area forest characterization: A review. Remote Sensing of Environment, 121, 196–209. doi:10.1016/j.rse.2012.02.001 143–3156.

Yao, W., Krull, J., Krzystek, P., Heurich, M. (2014). Sensitivity analysis of 3D individualtree detection from LiDAR point clouds of temperate forests. Forests 5, 1122–1142.K. Stereńczak, et al..Int J Appl Earth Obs Geoinformation 93 (2020) 10219112

Zhang W, Qi J, Wan P, Wang H, Xie D, Wang X, Yan G. (2016). An Easy-to-Use Airborne LiDAR Data Filtering Method Based on Cloth Simulation. Remote Sensing., 8(6):501.

Zhao, B., Yang, F., Zhang, R., Shen, J., Pilz, J., and Zhang, D. (2019). Application of unsupervised learning of finite mixture models in ASTER VNIR data-driven land use classification. Journal of Spatial Science, 1–24. doi:10.1080/14498596.2019.1570478

Observations on public space in the city: the Town Hall Square of Vigonza (Italy)

Enrico Pietrogrande[1*], Alessandro Dalla Caneva[1]

Abstract: This contribution examines the building complex planned and constructed in Vigonza, a populous town situated to the north-east of Padua, between 1937 and 1939. The almost exclusive use of exposed terracotta brickwork and the abstract sinusoidal design of the main façade make the architecture scenario characteristic and crystalised, a fundamental element in the identity of Vigonza although its inhabitants are not aware, today, of the issues that produced it.

The authors of this article are deeply convinced that the public quality of life in the city is connected with the formal choices made by the project plan. They think that it is possible to trace a close relationship of identification between the community and the architectural forms that create a sense of belonging in those places. One of the identifying forms of the city is certainly provided by the piazza, the place par excellence throughout history in which the community recognises itself.

From the city of classical times to the medieval city followed by the Renaissance city and continuing up to the present day, the piazza persists as a space of identity with continuity in the layout of the urban structure. Its maximum expression is seen in the Renaissance where the project of the city was planned as a place of the representation of civil life and its institutions were recognisable in the form of the places.

Keywords: Vigonza, public space, reuse of built heritage, functional conversion

1. Introduction

Vigonza is a town situated in the province of Padua in the region of Veneto. In Vigonza a very large urban transformation was initiated at the end of the 1930s, designed by the thirty-year-old architect Quirino De Giorgio (1907-1997). The transformation was centred on the town hall which stood in an isolated position, outside the populated area historically secluded around the parish church of Saint Margaret. The intention was to define a new lay centre, a town hall square that would be bordered on all sides by a series of new buildings in only a few months: the House of the Fascist Party (Casa del fascio), the theatre, rural houses, and residential blocks for the employees.

The town hall square or piazza in Vigonza, with its evident metaphysical character, nowadays constitutes the back-drop of most local shows and events. The naturally non-monumental approach De Giorgio used in all his work [Monti, 2006], the full trust of the

[1] University of Padua, Department of Civil, Environmental and Architectural Engineering, Padua, Italy
* Corresponding author: enrico.pietrogrannde@unipd.it

client, the almost exclusive use of terracotta brickwork, the sinusoidal design of the façade facing the town hall make this a very particular place. It survived intact the Second World War and recently underwent a restoration that contributed to valorise its urban presence.

Figure 1. View of un unhealthy house burned and substituted by new rural houses promoted by Fascist Party at the end of the the Thirties.
Figure 2. Quirino De Giorgio, general planimetry of the transformation implemented in Vigonza between 1937 and 1939 where the town hall had been built a long way from the centre of the town. At the time the centre was secluded around the parish church. Please note: North is the opposite direction to that stated on the layout.

The construction of ordered housing in five buildings in sequence for the rural population was one of the policies of the fascist regime to improve the living conditions of this poor people (fig. 1). A comment in the "Padua" magazine reveals that thirteen accommodation units were built, "inhabited by one hundred and four people. (…). There was a seventeen thousand square metre piazza in front of the houses for which sixteen thousand cubic metres of soil was transported in two thousand working days. The piazza is adorned by green lawns, with a flagpole for raising a flag and an artistic well" [Rigamo 1938].

The wave of rural houses concluded to the west in the architecture of the theatre. This building presents a convex front on the piazza that together with the concave profile of the adjacent covered market, gave rise to a second sinusoid that was in a very close relationship with the first. The high entrance portico opens into the central part of the theatre façade, corniced by the compact stonework and divided by five columns, these also made of exposed terracotta bricks.

The joints between the courses of bricks in the columns of the façade of the theatre are cancelled by the peculiar shape of the pieces whose bases are inclined so as to contain the binder in the internal part: this results in the smooth surfaces of the cylinders and their shiny

bright response to the light contrasting with the shade of the portico. If, on the one hand, there is no evidence of representations held in the theatre by 1943, that is, before the fall of the fascist regime, on the other hand, it is certain that the Padua Federation of the National Fascist Party quickly but vainly attempted to rid itself of the building, considered to be too large for Vigonza and too onerous to maintain.

Figure 3. The House of the Fascist Party (casa del fascio) in the Town Hall Square of Vigonza. The picture was taken in 1940.
Figure 4. The same building in the post-war period, after the partial demolition of the façade.
Figure 5. The current condition after the repair and restoration in the image of House of the Fascist Party completed in 1995 with De Giorgio present as consultant.

The adjacent covered market is composed of an oblong portico, open towards the piazza and to the back through a series of completely curved arches obtained in the composition of the brickwork. The concave arch in plan of the covered market concludes, on the part opposite the theatre, with a celebrative element, that is, a stylised pillar on which the motto "believe, obey, fight" is inscribed. This is also made in brickwork and was meant to support a sculpture that was never made.

The architecture of the House of the Fascist Party was obtained by covering the façades facing the public space of a pre-existing building originally used as a school.

The general planimetry of the transformation presented by De Giorgio in the propaganda publication "Three years of marches by Paduan fascism" (fig. 2) also includes the prismatic buildings planned for the employees. The planning methods of De Giorgio in this period can be seen here: volumetric layout in blocks, exposed brick masonry, hidden guttering, slots all of the same size and shape and open with regularity [De Giorgio 1940].

2. The latest restyling of the building that once hosted the House of the Fascist Party in the Town Hall Square (1995)

After the fall of fascism in Vigonza, as everywhere else in the Kingdom of Italy [Mangione 2003], evidence of the regime was removed [Lenci and Segato, 1996] including the covering of the old school buildings that De Giorgio had studied in order to change the building into the office of the local Fascist Party (fig. 3). Consequently, after the fall of the regime, the House of the Fascist Party in Vigonza, having only operated for a few years, shared the fate of many buildings that hosted the structures of fascism and marked its presence in the territory.

No substantial variation affected the side along the road apart from the fitting of in the slots in the portico with glass while the stylised Fascist tower on the side facing the piazza was knocked down and the changing concave wall was demolished. The mystic value precisely assigned to the façade on the piazza by De Giorgio (fig. 4) explains how the determination to erase evidence of the National Fascist Party was concentrated here, bringing the school façade back to light.

Above all, the case of this building in the national panorama in recent times is distinct. In 1995 the characterisation in exposed terracotta brickwork planned in 1938 by De Giorgio was restored (fig. 5), not giving any consideration to the opinions of the antifascist associations.

The work involved rebuilding the concave wing-wall from top to bottom without any other opening except the small door in the middle, giving meaning to the building construction again that is now no longer only an answer to a function but once again represents the ideal value. The symbolic Fascist tower was also rebuilt. Consultant to the work was Quirino De Giorgio himself, by now almost ninety years old, who had been thirty years old when he planned the new lay centre in Vigonza developed around the Town Hall.

3. The theatre in the piazza

The architecture of the theatre closes the piazza to the west and the planner solved this by almost completely using exposed brickwork thereby contributing to the alienating character of the square generated by the same material apart from modest exceptions (fig. 6).

The characterisation by using exposed terracotta brickwork is particularly intense in the space of the portico that opens onto the piazza beyond the columns (fig. 7): the walls on the two sides, the ceiling and the floor are finished in brick. The only plasterwork used is on the bottom wall, on which the four doors of the entrance are arranged and above which are the round windows of the room that leads to the gallery. The covered market branches out from the theatre in the form of a concave portico facing the piazza, entirely built in exposed terracotta brickwork too.

Completed in 1939, the theatre was never used before the fall of fascism in 1943. In fact, from the very start the Padua Federation of the National Fascist Party tried to disassociate itself from the building, considering it to be excessively large for Vigonza and also too expensive to maintain.

The theatre has undergone various modifications since the post-war period that do not respect either the plan or building site work of De Giorgio. In particular, the parish transformed it into an orphanage in the 1960s. After this, the communal management promoted its return to its original function while the entrance hall was converted into a library. Regarding the outside, later additions were built, part of the arches of the lateral porticoes and all of those of the covered market had cladding put on them, new window openings were made, the round slots of the entrance portico were increased in number, like the doors beneath. A recent building operation corrected the main alterations suffered by the building [Zanella, 1996-1997].

Figures 6, 7. Quirino De Giorgio, theatre in the new piazza in Vigonza (1938-1939), photographed by the architect De Giorgio himself in 1940. General view and detail of the colonnaded portico.

4. Restoration of the rural houses

The rural houses (fig. 8) were restored from the autumn of 2012. The method used was very conservative and replaced a previous transformative approach, which was also due to the work of the Superintendency for Architectural and Landscape Heritage.

The transformation involved the five buildings arranged according to the sinusoidal line. The land use designation given to the rooms on the first floor was as habitation while the premises on the ground floor were expected to see the installation of craft workshops. Therefore, a series of samples were taken from the building to see how much of the original finishing was still there even if concealed from view, to document the construction process even after seventy years of the environments being used. Furthermore, traces of the original openings in the most altered façades were found, those facing the countryside. In fact, no drawings of the original situation exist, not a single copy of the architectural plan has been found in the archive of the architect nor in those of public administrations, and furthermore, the rich archive of the construction company Grassetto which carried out the work has always been inaccessible.

The rural houses of Vigonza constitute an above all fortunate case in that they belong to the State Property Office, which has maintained the unitariness of the building complex. In the case of a twin transformation carried out by De Giorgio in the period, the plan and the construction of rural houses in Candiana [Longhin, 2009], the breaking of the property passed to the individual occupants generated the almost complete loss of the original structure and layout of the architecture and the image the village.

Therefore, the original floor made of terracotta tiles was identified a few centimetres under the existing floor in nearly all of the ground floor rooms (fig. 9), confirming that the heightened tendency of De Georgio in those years was to use one material as much as possible in developing an architectural project.

Figure 8. Quirino De Giorgio, the rural houses that close off the southern side of the new piazza in Vigonza (1937-1938). General view photographed by De Giorgio in 1940.

Figures 9, 10. The rural houses that close off the southern side of the new piazza in Vigonza (1937-1938). Ground floor, the original floor of terracotta square tiles, laid without joints simulating continuous flooring (preliminary phase of the restoration, 2012-2013).

As at other times the planner preferred using travertine stone, here adopting terracotta bricks not only for the façades on the piazza but also for the floors on the ground, made using square shaped tiles. The laying of tiles without joints served to simulate a continuous surface throughout the whole room (fig. 10). The restoration of the tiles unfortunately turned out to be impossible since the cement-based mortar used for bedding was so firmly attached to the pieces that they could not be re-used once the new insulation screed had been supplied.

The intermediate floors are made of wood with beams of a modest cross-section, sometimes with a square cross-section, often put in place at varying distances. On top of these 2.5

centimetre-thick planking functioned as the floor. The joists were fixed to the beams to support the trellis to which the plasterwork of the ceiling of the floor below was fixed (fig, 11).

According to the choice De Giorgio often made, these houses are covered with single-pitched rooves, descending towards the back. Consequently, he obtains greater height for the main façade and eliminates from the most significant view of the architectural scene those functional accidents such as the drainpipes and the guttering that can dissipate the metaphysical aura he focused on. As his own photographs show, he looks for a pure and strong contrast between light and shade. The demolition of the ceilings on the first floor facilitated the discovery of the technique De Giorgio used to put the single-pitched solution into effect and at the same time make an appreciable saving in the cost of the construction: the masonry of the façade on the piazza above the ceilings was raised 12 centimetre-thick, instead of 24, with small support pilasters under each roof beam (fig. 12).

This is an example of how the planner applied himself to reduce the cost to the Paduan Federation of the Fascist Party to whom he answered for his actions, aiming at coexistence with the greater expressive strength to capture the attention of the head of state, Benito Mussolini. Mussolini was expected in Padua on the 24 September 1938 [Bertolini, 1938], but did not go to Vigonza perhaps because the work had not been completed in time [Pietrogrande, 2011].

During the restoration work on the houses, the 12 centimetre-thick brickwork that concluded the façades in the part above the first floor was strengthened from the inside using a second brick course so that the framework of the building guarantees the building is safe and will remain so in the future.

The openings in these buildings, the doors and windows, were provided for by De Giorgio without external shutters (fig. 13). In such a way another accident of a practical nature did not question the ideal and everlasting destiny of his architecture and the shadows were to strongly mark the composition of the façades (fig. 14).

Figures 11, 12, 13. The rural houses that close off the southern side of the new piazza in Vigonza (1937-1938). Details of the original situation: the wooden intermediate floors, the masonry that supports the beams of the single-pitched roof, the doors and windows made of wood and painted white.

The windows had frames of a significant size and were painted white to generate the chromatic relationship between the white and the colour of the terracotta bricks that

characterises most historic buildings in the Venetian area – but where the white is that of the stone.

In general, the transformation also involved the demolition of several additions constructed at the back of the buildings so as to reduce the volumes to the initial stereometry desired by the planner. Upon the restoration of the original appearance, other initiatives were activated such as the modification of the terrace on the portico behind the convex building with a pitched roof.

5. General considerations. The piazza as a place of community identity

In general, two ideas of piazza can be recognised. They refer to two different urban models: the closed city and the open city. The piazza in the idea of the closed city has a distinctive form protected from the surrounding territory and has its own size. The buildings that extend along the sides of the piazza are arranged so that they give the empty space form.


Figure 14. The rural houses in Vigonza at the end of the restoration transformation, view of the first buildings from the east (November 2015). The façades on the piazza are made of exposed brick with the exclusion of the corresponding portion on the upper floor of the building with convex trend (on the right, partially off).

This idea of piazza is the opposite of the open piazza in which the empty space becomes even more determining since it constitutes the motivation for the relationships that the main elements of the city establish between themselves. The idea of the piazza proposed by Le Corbusier still recognises the compositional elements of the project such as the transport network, the building fabric, and the public buildings but assembled more freely as a consequence of a new element that enters the composition: the surrounding open space offered by nature.

The piazza is the archetypal element in the form of the city, recurring in and identifying the city. It appears in the architecture of classical times as the result of two or more stoas (porticoes in ancient Greece). The arrangement of the volumes generates a public space surrounded by porticoes that is the origin of the forum or the agora. In this case the portico defines an introverted space that can be read as being the precursor of the construction of the public piazza in the city. The Greek agora signals a starting point, a real and true invention. Thanks to it, the social life and the relationships between human beings take on a new form, more socially and culturally evolved.

The orthogonality of the axes in the Roman foundation city piazza, the cardo and decumanus, is at the origin of the structure of the urban spaces. The axes are necessary to identify at their crossing a symbolic centre and boundary, the mundus and the terminus or pomerium. The first act of an architect in the planning phase is to draw the layout of the city which then shows the division of the city into areas inside it, obtained from the framework of the urban fabric with the main and minor roads being delineated. Then he traces the space where both the residential buildings and the public ones with a religious or political function have to be positioned. The succession of phases in the transformation is given by the erection of the city wall that surrounds it and delimits the internal area and then by the subdivision of the open spaces, roads, and piazzas. The public buildings are arranged around the symbolic empty space of the forum composing a scenic urban wing-wall representative of the collective place in the city. The Roman city of Timgad belongs to a settlement model typical of a closed city surrounded by walls (fig. 15).

The forum in Pompei and the imperial forums in Rome are constructed where the cardo and decumanus form a crossroads and the regular empty space of the civil space is defined by colonnaded porticoes that unify the representative buildings according to precise relationships of axiality. The piazza constitutes one of the urban spaces of the Roman city that, by virtue of their introverted character, conform by starting from the principle of the limit.
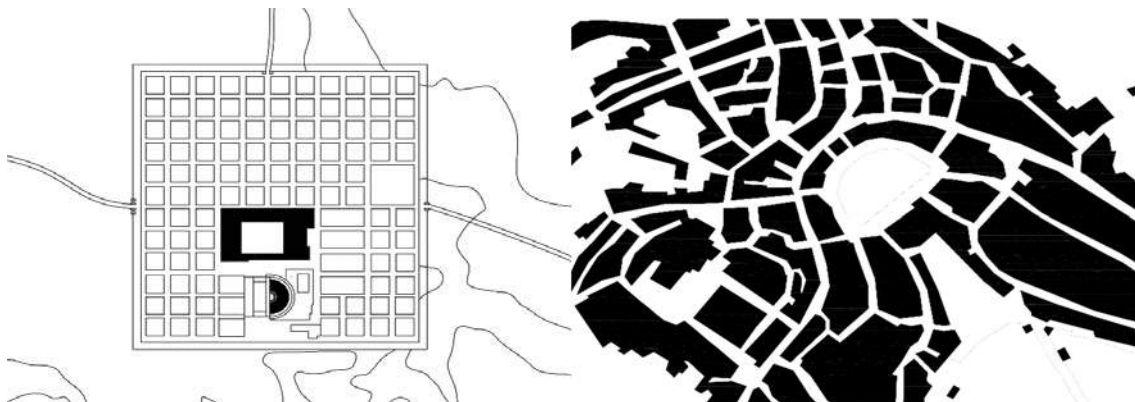
Figures 15, 16. Alessandro Dalla Caneva, graphic restoration of the city of Timgad with identification of the piazza (on the left), the city of Siena and identification of the Piazza del Campo.

Figures 17, 18. Alessandro Dalla Caneva, the city of Pienza with identification of the piazza (on the left), partial graphic restoration of the city of Paris and identification of the Place Vendome.

The act of delimiting the space belongs to a way of thinking in the founding and construction of the Roman city. On the other hand, the theme of the limit has its origin in identifying and delimiting one space through religious rites, a dimension that has assumed civil values with the passing of the centuries.

The medieval city (fig. 16) was superimposed on the ancient city giving shape to the space according to analogous principles. The space in the civic and religious piazza is analogously limited and protected by urban wing-walls that configure the space by giving it an identity. The relationship between empty and filled spaces constitutes the reason for a picturesque composition of the parts between volumes that are related according to an apparently free arrangement of the parts giving life to irregular but unitary spaces. The medieval roads and piazzas break the orthogonal grid of the city founded by the Romans into pieces but also constitute the texture of continuous change alongside which the buildings of the city stand that are recognised by role and position within a wider and general urban framework. The founding principles of the medieval city always arose from the same idea that considers the relationships between the house and road, the public buildings and the piazza as invariable elements.

In the sixteenth century the space of the piazza assumed a unitary layout, aimed at urban decorum in line with the theories developed on the idea of the ideal city. Starting from Leon Battista Alberti the idea of the ordered city is reflected in the design of the piazza recognised by its symmetrical shape, which the experience of urban planners in developing piazzas such as the piazzas in the cities of Pienza (fig. 17) and Vigevano attempt to emulate.

The eighteenth and nineteenth centuries saw general ideas on the modernisation of spaces in large cities proliferate. This is the case with the Paris plan by urban planner Pierre Patte (fig. 18). The collage of piazzas inside historic Paris redesigned the look of the city by re-ordering the spaces using a new order in form that copied the same principles of construction as the historic city. Road and piazza always have the same role generator but change their dimensions. Piazzas represent the fulcrum of a series of relationships and routes that unify the individual piazza with a unitary urban spatial system. A hierarchical order can be recognised in the size of piazzas from the exceptional dimensions to the small ones. It represents the celebrative role of the public space very well and through which real power manifests its own meaning and role.

The idea of the piazza thought of like this for millennia enclosed inside a symbolic enclosure representing the values identifying a community was in crisis at the start of the twentieth century because of the emergence of a new ideal of the city and spatiality.
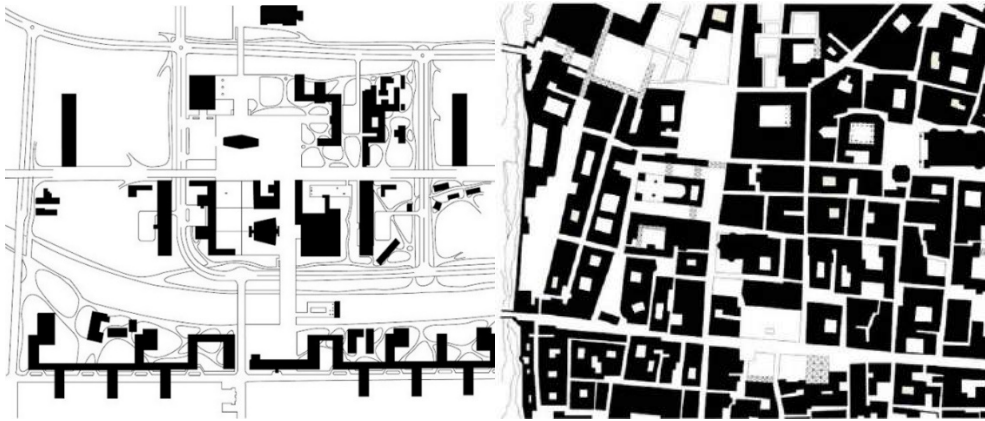
Figures 19, 20. Le Corbusier, planimetry of the civic centre of Saint Dié, 1945. On the right plan of the city of Parma. The two planimetries identify the two models of historical city, the open city and the closed city, to which correspond the open piazza and the closed piazza.

The end of the traditional piazza is found in the unrealised project Le Corbusier developed for the city of Saint Dié in which free volumes in close visual relationship constitute the meaning of the new urban piazza (figg. 19, 20).

Arranging autonomous volumes in space in close interdependent relationship so that they form spatial harmony constitutes what the architectural historian Siegfried Giedion defined as the first design conception in space: architecture understood as sculpture. This principle of composing by relationships between individual and autonomous buildings, this perception of the spatial effect that volumes, as plastic figures, produce in their close relationship, are carried over in twentieth century architecture.

The idea of the ancient piazza is still valid today at least in the historic city. This model becomes invalid with the removal of the ancient walls that affirms an urban form constructed on the relationship between urban elements and natural context. Saint Dié is therefore constructed on a specific principle: the form of the place results from the system of the relationships that are established between distinct urban elements and the surrounding nature. An analogous principle is stated by the organisation of two places: the system of the architectures in the Athenian Acropolis (the Parthenon in relationship with the Propylaea and the Erechtheion, and with the slopes of Mount Pentelicus) and the relationships that the distinct volumes of the Baptistry, the Cathedral, and the leaning tower establish in the empty space of the Field of Miracles in Pisa.

6. Conclusions

Quirino De Giorgio's urban project rejects the model of the open city and is in continuity with the ways of composing the traditional city that conceives space by arranging the volumes around a void with a recognizable shape. The close relationship between the street and the houses, typical of the way of composing the ancient city, is still evident, as is the scenographic position of the theater which makes its hierarchical role within the square recognizable.

De Giorgio gave form to the piazza of the town hall of Vigonza by interweaving curvilinear forms, and subdivided the piazza into specific functional areas. A green area in front of the theatre was initially enclosed in a circular flower bed with a tree in the middle, alluding to the theme of the garden. Opposite on the far side was the area with the well, with the well-head

made of terracotta bricks raised on three small concentric steps placed on trachyte stone paving. The red bricks of the yard extended in the middle. This tricolour, like the Italian flag, was probably a symbolic reference that De Giorgio made to represent the large scale of the village of Vigonza. All of this was progressively removed in the second half of the last century until largely reduced by the invasion of a homogeneous tarmac surface good for parking and the weekly market. Together with the restoration of the houses was the transformation of the piazza for which the covering of tarmac was removed leaving a continuously paved space now not used for parking vehicles.

The monumental complex planned by De Giorgio nowadays constitutes one of the most important references in the life of the population of Vigonza, also because of the marked characterisation influenced by the metaphysical poetry. At first sight not identifiable as a work of the fascist regime [Portoghesi, Mangione, Soffitta, 2006], the piazza is also one of the most complete examples of how fascism, through its provincial federations, intervened in the transformation of villages on an urban scale. It is also because of the lack of a grandiloquent and rhetorical character of the square that the inhabitants of Vigonza live in this space happily as a useful resource for the life of the community, regardless of its origins and ignoring them in many cases.

In conclusion, it should be noted that the corresponding author has followed the restoration of the first two rural houses in the framework of the agreement between the Commune of Vigonza and the Department of Civil, Environmental, and Architectural Engineering of the University of Padua.

References

Bertolini, A., (1938). La grande giornata, in «Padova», n. 10, 10.

De Giorgio, Q., (1940). Tre anni di marcia del fascismo padovano, Padua.

Lenci, G., Segato, G., (Eds., 1996), Padova nel 1943, dalla crisi del regime fascista alla resistenza, Padua.

Longhin, S., (2009). Quirino De Giorgio a Candiana. Il Borgo del Littorio, in «Quaderni di storia Candianese», n. 5, 9-35.

Mangione, F., (2003). Le case del fascio in Italia e nelle terre d'oltremare, Rome.

Monti, G., (2006). Quirino De Giorgio, in «Territorio e ambiente veneti», n. 2, 71-79.

Pietrogrande, E., (2011). L'opera di Quirino De Giorgio (1937-1940). Architettura e classicismo nell'Italia dell'impero, Milan.

Portoghesi, P., Mangione, F., Soffitta, A., (Eds., 2006), L'architettura delle case del fascio, Florence.

Rigamo, R., (1938). Vasta opera rigeneratrice nelle campagne padovane. Dal casone alla ridente casa rurale, in «Padova», n. 10, 44.

Zanella, M., (1996-1997). I borghi rurali di Candiana e Vigonza progettati da Quirino De Giorgio, degree thesis, Institute of Architecture and Urbanism, University of Padua (supervisor Vittorio Dal Piaz).

Crease-Resistance Treatments of Cotton Fabrics by Electrostatic Self-Assembly

Buse Sağgün[1*], Şule Sultan Uğur[2*], Okan Ayvacık[3*]

Abstract: Cotton fabrics, especially during use, washing and drying operations due to their tendency to wrinkle are subjected to non-wrinkle finishing processes. Although many different chemical finishing agents and innovative methods have been proposed for this purpose, solutions that can provide a wide range of uses are still needed for reasons such as whether they are not economically suitable or damage the physical properties of the fabric while providing wrinkling. In this study, it was aimed to give the cotton fabric a wrinkle-free property by using layer by layer coating technique. It is aimed to minimize the loss of strength, color change and cost in cotton fabric with laboratory studies carried out for this purpose. In this way, layer by layer coating method, a nanofabrication method, will be used commercially without additional investment costs, to gain new functional features with both the wrinkle-free feature and the nanoparticles to be used.

Keywords: crease-resisance, electrostatic self-assembly, cotton.

1. Introduction

Cellulose-based fibers have been one of the most preferred textile materials in years, due to its natural origin, biodegradable, sustainable, renewable properties and superior wearing comfort. But a common and undesirable condition in cellulose-based fabrics, wrinkles are defined as a form-breaking and cause significant user discomfort. Wrinkles occur in cellulose fibers because of the presence of free hydroxyl groups, and when any force is applied to the fabric, these groups form new hydrogen bonds with the adjacent polymer chain, and affect the appearance on the fabric, causing lines and fold marks (Yuen et.al, 2007). Anti-wrinkle chemical finishing process is applied to fabrics to prevent wrinkle. With the chemical finishing process, the effect of functional groups is limited and crease-proof is gained by the formation of cross-links between neighboring cellulose molecules. But functional groups whose movement is restricted are known to cause loss of strength in the fabric and hardening in attitude. In addition, some chemicals used in wrinkle finishing processes release formaldehyde, a carcinogenic substance that has a negative effect on human health, causing color changes or yellowing in the fabric. In recent years, intensive efforts have been made to develop formaldehyde-free cross-linking agents for cotton to replace formaldehyde-based reagents due to the negative effects of formaldehyde-based cross-linkers on human health. Especially many studies have been done with polycarboxylic acids such as citric acid (CA), maleic acid (MA) and 1,2,3,4-butane tetracarboxylic acid (BTCA). According to the literature, BTCA (1,2,3,4-butane tetracarboxylic acid) may be the most promising to replace other crosslinkers, but it is not suitable for commercial use due to its high cost (Lam et al.

[1,2] Süleyman Demirel University, Engineering Faculty, Textile Engineering Department, Isparta, Turkey
[3] Söktaş Textile Industry and Trade Inc., Aydın, Turkey
* Corresponding author: suleugur@sdu.edu.tr

2011; Hebeish et al. 2011; Sarwar et al. 2019).

In the study, the applicability of commercially used anti-wrinkle chemicals with ionic charges in the electrostatic self-assembly coating method was investigated and compared with the proposed metal oxide nanoparticles. The fact that it will be possible to use both a new method and new chemical groups to improve the easy-care properties of cotton fabrics will allow this work to be evaluated commercially.

2. Material ve Method

100% cotton fabric with 50/1 yarn and 215 gr/m^2 weight was purchased from Söktaş Textile Industry and Trade Inc. and used for obtaining nanofilm coated fabrics. Before multilayer film coating process, cotton fabric surfaces were pretreated with Polyethylenimine (PEI, 0.1 g/l, PH: 10, dip-coating method) for obtaining cationic surface charges. Anatase titanium oxide (TiO_2) nanoparticle, Silicon dioxide (SiO_2) nanoparticle, Poly(sodium 4-styrene sulfonate) (PSS) and Poly(diallyldimethylammonium chloride) (PDDA) were purchased from Aldrich and used as received. Aqueous solutions of the polyelectrolytes were prepared at concentrations of 3 mM l^{-1} with using deionized water. 1 g/l nanoparticle suspensions were prepared at 50 W for 1 h by Sonics Vibra-Cell Ultrasonic Homogenizer. Knittex FA crosslinking agent (FA) was purchased from Hunstman and used as commercial agent. In the electrostatic self-assembly process, cotton fabrics were deposited with 20 multilayer films by using a laboratory type padding machine for continuous process. Air permeability, DP rating, crease recovery angle and tensile strength analyses were performed to examine the electrostatic self-assembly process effect on the cotton textile fabric properties.

3. Results

The wrinkling which is the major disadvantage of cotton fabric may handle the situation by crease-resistant finishing processes. The results of the DP rating and wrinkle recovery angle analysis were used to examine the crease resistance process on the cotton fabrics are shown in Table 1. The test results proved that the applied electrostatic-self assembly processes, especially with FA content are very effective in improving the wrinkling properties. For DP rating test results minimum 3 value were obtained.

Table 1. DP rating and crease recovery angle of different types of fabrics

	Samples	Durable Press (DP) Rating	Wrinkle Recovery Angle WRA(^{o})	% Differnce
1	Untreated fabric	1	151,04	-
2	PSS/PDDA (20°C)	3	190,2	25,9
3	TiO_2/TiO_2 (20°C)	3,5	220,2	45,7
4	TiO_2/TiO_2 (50°C)	3	216	43
5	SiO_2/TiO_2 (20°C)	3	221,2	46,4
6	SiO_2/TiO_2 (50°C)	3	215	42,3
7	$SiO_2/PDDA$ (20°C)	3	217,5	44
8	$SiO_2/PDDA$ (50°C)	3	220,5	45,9
9	FA/PPDA (20°C)	3	211,5	40
10	FA/PPDA (50°C)	3	228	50,9

The mechanical tests were performed on electronic tensile strength machine according to EN ISO 2062 Standard. The breaking strength of warp and weft yarns that are extracted from the untreated and multilayer films deposited fabrics was tested at fracture and all the test results are given in the Table 2. It was observed that the tensile strength values of the cotton fabrics also decreased after multilayer film deposition both warp and weft directions.

Table 2. Strength evaluation results of different types of fabrics

	Samples	**Warp Tear Strength**	**Weft Tear Strength**
1	Untreated fabric	2138,5	1741
2	PSS/PDDA (20°C)	1239	522
3	TiO_2/TiO_2 (20°C)	1370	587
4	TiO_2/TiO_2 (50°C)	913	391
5	SiO_2/TiO_2 (20°C)	1174	587
6	SiO_2/TiO_2 (50°C)	913	652
7	$SiO_2/PDDA$ (20°C)	1109	652
8	$SiO_2/PDDA$ (50°C)	978	456
9	FA/PPDA (20°C)	1109	848
10	FA/PPDA (50°C)	1370	913

TexTest Instruments FX 3300 Air Permeability Tester III instrument was used to obtain the air permeability values of the untreated and multilayer films deposited on cotton fabrics according to EN ISO 9237 Standard. Fabric air permeability tests were performed 10 times at 100 Pa pressure for all the samples. Table 3 shows air permeability values of untreated and multilayer films deposited fabrics. After multilayer film deposition on the cotton fibers, air permeability values are decreased. These results verified the presence of the deposited layers on the cotton fiber.

	Samples	**Aır Permeabılıty**	**% Difference**
1	Untreated fabric	410,3	-
2	PSS/PDDA (20°C)	350,3	-14,6
3	TiO_2/TiO_2 (20°C)	277	-32,4
4	TiO_2/TiO_2 (50°C)	253,3	-38,2
5	SiO_2/TiO_2 (20°C)	323	-21,2
6	SiO_2/TiO_2 (50°C)	241,6	-41,11
7	$SiO_2/PDDA$ (20°C)	316	-22,9
8	$SiO_2/PDDA$ (50°C)	260	-36,6
9	FA/PPDA (20°C)	314,3	-23,3
10	FA/PPDA (50°C)	333,7	-18,6

Table 3. Air permeability and percentage differences of different types of fabrics

4. Discussion and Conclusions

In the study, the applicability of commercially used anti-wrinkle chemicals with ionic charges in the electrostatic self-assembly coating method was investigated and compared with the proposed metal oxide nanoparticles. The fact that it will be possible to use both a new method

and new chemical groups to improve the easy-care properties of cotton fabrics will allow this work to be evaluated commercially.

Acknowledgements

References

Yuen C.W.M., Ku S.K.A., Kan C.W., Cheng Y.F., Choi P.S.R., Lam Y.L., (2007). Using nano-TiO$_2$ as co-catalyst for improving wrinkle-resistant of cotton fabric. Surf Rev Lett, 14(4), 571–575.

Lam Y, Kan C, Yuen C., (2011). Wrinkle-resistant finishing of cotton fabric with BTCA - the effect of co-catalyst. Textile Research Journal, 81(5), 482-493.

Hebeish A., Moustafa F.A., Fouda M. G., Elsaid Z., Essam S., Tammam G. H., Drees E. A., (2011). Green synthesis of easy care and antimicrobial cotton fabrics. Carbohydrate Polymers, 86, 4, 1684-1691.

Sarwar N., Ashraf M., Mohsin M., Rehman A., Younus A., Jayid A., Iqbal K., Raz S., (2019). Multifunctional Formaldehyde Free Finishing of Cotton by Using Metal Oxide Nanoparticles and Ecofriendly Cross-Linkers. Fibers and Polymers, 20, 2326–2333.

All Optical Gate Based on Photonic Crystal Ring Resonator

**Lila Mokhtari*[1], Hadjira Badaoui, Mehadji Abri, Rahmi bachir ,
Lallam Farah, Moungar Abdelbasset**

Abstract: The aim of this paper was to propose and design a photonic crystal drop filter based on ring resonators and study its properties numerically. This structure is constituted in a two-dimensional square lattice. The resonant wavelengths of the PCRR proposed are λ = 1.553 µm, the extraction efficiency exceeds 99% with a quality factor of 5177. To study the all-optical OR and XOR logic gate function, we calculated the electric field distribution of the 2D photonic crystal for the 1.553 µm signal light.

Keywords: photonic crystals ; filter ; ring resonators ; logic gates ; OR ; XOR .

1. Introduction

PCs are periodic optical nanostructures composed of two different materials with low and high dielectric constant [1-2]. As a result of this periodicity, it owns photonic band gap (PBG), where the transmission of light in certain frequency range is absolutely zero [3]. Depending on the geometry of the structure, PCs can be divided into three broad categories, namely one-dimensional (1D), two-dimensional (2D) and three-dimensional (3D) structures. 2D PCs due to their complete PBG and ease of design and fabrication attract more attention than 1D structures [4].

In this study, we propose a new design of PCRR based on square photonic crystal ring resonator with flower shaped. The COMSOL Multiphysics based on the finite element method FEM is used for simulate the distribution and transmission of electromagnetic wave. In our design, 100% dropping efficiency with quality factor of 5177 is achievable at wavelength λ=1.553 µm, which is a satisfactory result in comparison with other T-shaped channel drop filters based on photonic crystal ring resonators.

Optical logic gates are essential components required for optical signal processing and optical communication networks Saidani [5] proposed a multifunctional logic gate in a 2D PCs waveguide structure using multimode interference concept. By switching optical signal to different input waveguides, different functions such as XOR, OR, NOR and NOT gates have been obtained. An all optical NOR gate have been proposed by Isfahani [16]. We used the PCRR presented to realize the gate logic for OR and XOR function, there are presented by studying the electric distribution of the 2D photonic crystal for the 1.553 µm signal light.

[1] STIC Laboratory, Faculty of Technology, University of Tlemcen, Algeria.
* Corresponding author: l_benseddik2003@yahoo.fr

Structural characteristics

2.1. Band gap structure

To determine the physical parameters of the filter, it is necessary to calculate the band gap diagram of the design. This last is traced using the plane wave expansion method PWE under COMSOL Multiphysics software [7]. The dielectric rod radius $r=0.188 \times a$, and background constant are taken $a=0.64$ μm. As shown in Fig.1, the PCs structure supports a photonic band gap in the region $0 < wa/2\pi c < 0.455$, $0.525 < wa/2\pi c < 0.545$ and $0.675 < wa/2\pi c < 0.750$ for TE mode.

The resonant frequency is chosen such that there will not be a propagative mode in a photonic structure without defect as shown in Fig. 1. At the wavelength 1.553 μm ($wa/2\pi c=0.412$), we observe the absence of modes in these regions. The electric field is reflected back because of the existence of the PBG as show in Fig. 1.
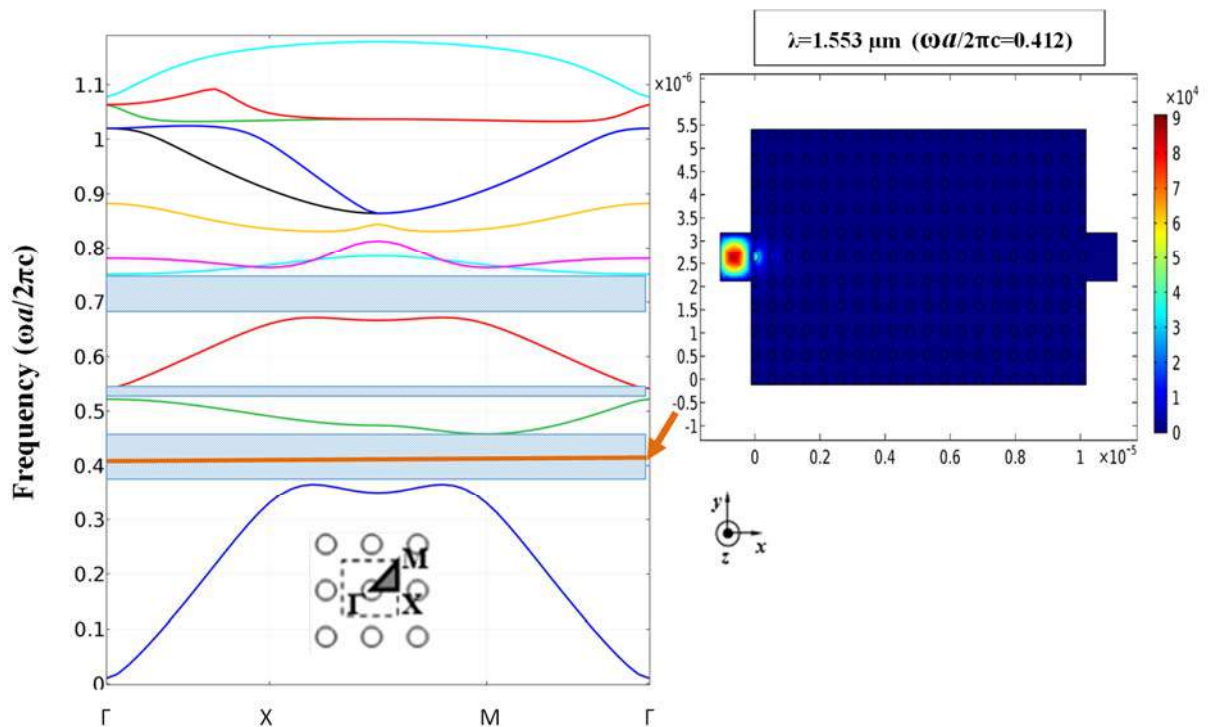

Figure 1. Schematic of photonic band gap

2.2. Field formulation
Use the Helmholtz field eaqution and starting from the frequency-domain governing equation:

$$\nabla \times (\mu^{-1} \nabla \times \mathbf{E}) - \omega^2 \varepsilon_c \mathbf{E} = 0$$

(1)

The total electric field, E, can be decomposed into two components:

$$E = E_{total} = E_{background} + E_{relative}$$

(2)

In mode analysis and the boundary mode analysis COMSOL Multiphysics solve equation (1), the electric field in spectral domain is given by:

$$\mathbf{E}(\mathbf{r}, t) = \mathrm{Re}(\tilde{\mathbf{E}}(\mathbf{r}_T) e^{j\omega t - j\beta z}) = \mathrm{Re}(\tilde{\mathbf{E}}(\mathbf{r}) e^{j\omega t - \alpha z})$$

(3)

The spatial parameter, $\alpha = \delta z + j\beta$

- β : Propagation constant
- δz : Attenuation constant

Use the scattering boundary conditionto make a boundary transparent for a scattered wave. The boundary condition is also transparent for an incoming plane wave.

$$\mathbf{E} = \mathbf{E}_{sc}e^{-jk(\mathbf{n}\cdot\mathbf{r})} + \mathbf{E}_0e^{-jk(\mathbf{k}\cdot\mathbf{r})} \qquad \text{Plane scattered wave}$$

(4)

2.3. Design of the channel drop filter

In this study, the structure of the two-dimensional photonic crystal considered is formed by a square lattice of dielectric cylindrical rods of GaAs embedded in an air background. The numerical simulations are based on finite element method exploiting the commercial software COMSOL. Rods have a refractive index value of $n=3.28$, and a radius of $r=0.188\times a$, $a=640$ nm being the lattice of the photonic crystal structure which is defined as the distance between centers of two adjacent rods, and a resolution of 20 rods horizontally and 20 rods vertically. Fig.2 shows the schematic structure of a Channel-Drop Filter CDF based on a PCRR. In this structure the ring resonator is created by removing a 7×7 square of dielectric rods and then replacing it with four flowers with height holes each separated by a hole the radii $r_1=0.2356\times a$. In this study the used mesh is non-uniform and the type of sequence used is physics-controlled mesh with scattering boundary condition.
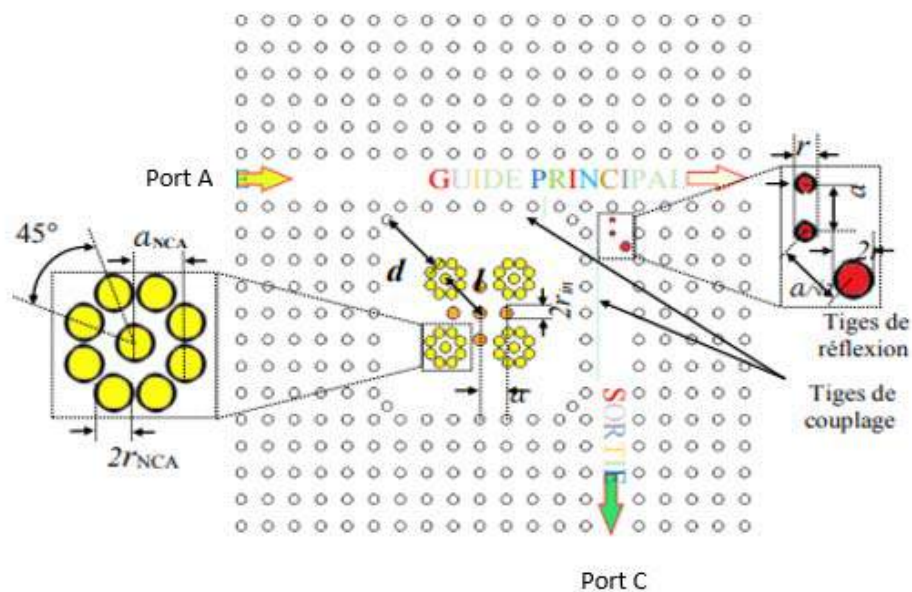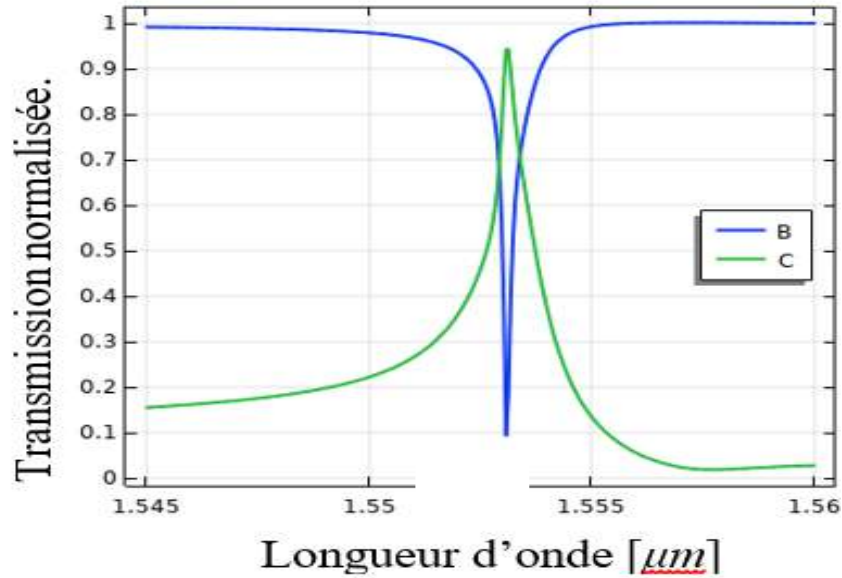
Fig. 2. (a) Single ring PCRR. (b) Normalized transmission spectra at two output ports 2 and 3 for PCRR. The designing parameters of the proposed NRC-QSRR : a= 640 nm, r=120.32 nm, r_{in} = 151.3 nm, a_{NRC}=551.36 nm, r_{NRC} =130.34nm, d= 1608.36 nm, l= 1169.61 nm.

The optical waves enter the structure through port 1 and exit through port 2, but during resonance, the optical wavelengths will be transferred to the drop guide via the resonant ring and exit through port 3. At the resonance wavelength λ = **1.553 μm**, the extraction efficiency exceeds 99% with a quality factor of 1411.
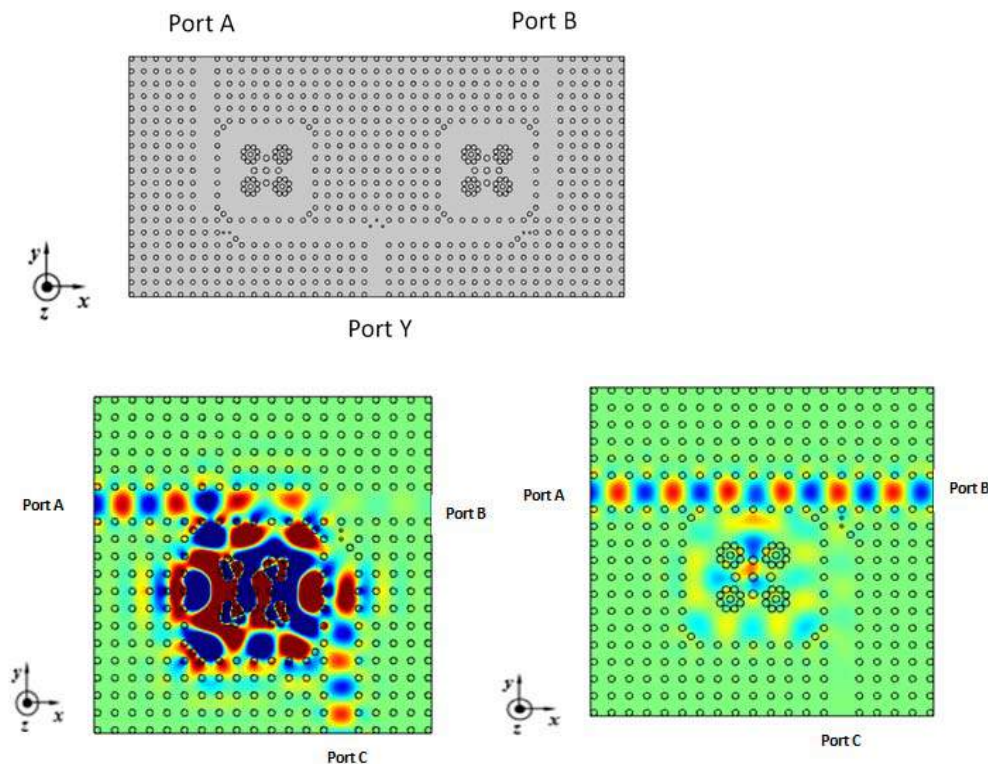

Fig.3. Electric field pattern of the ring resonator at a) λ = 1.553 μm (the resonant wavelength). b) λ = 1.556 μm (the off-resonance)

The electromagnetic wave transverse component Ez is presented around the wavelengths λ=1.553 μm and λ=1.556 μm where the positive pulses are in red and the negative pulses are in blue.

3.2. OR gate

The proposed OR gate structure is formed from two waveguides and two ring resonators with a resolution of 38 rods horizontally and 23 rods vertically. Two symmetrical optical waveguides AY and BY were formed along the Γ–M direction by removing two rows of GaAs rods, and put two ring resonators between them. The refractive index, radius and lattice constant of the structure are the same as the PRCC structure. The final schematic of our proposed OR gate structure is shown Fig.4.

The all-optical OR logic gate operation is presented by studying the electric field distribution of the 2D photonic crystal for the 1.553 μm signal light, and the calculated results are shown in Fig.4. If a signal is injected into input port A, then the signal light can transmit through the optical waveguide AY and be output from port Y, as shown in Fig.4 (b). If a single beam is injected into input port B, then the signal light can transmit through the optical waveguide BY and be output from port Y, as shown in Fig.4 (c). If two beams are injected into input ports A and B simultaneously, then the signal light can transmit through optical waveguides AY and BY, as shown in Fig4. (d). Thus, an all-optical OR logic gate can be achieved very easily.
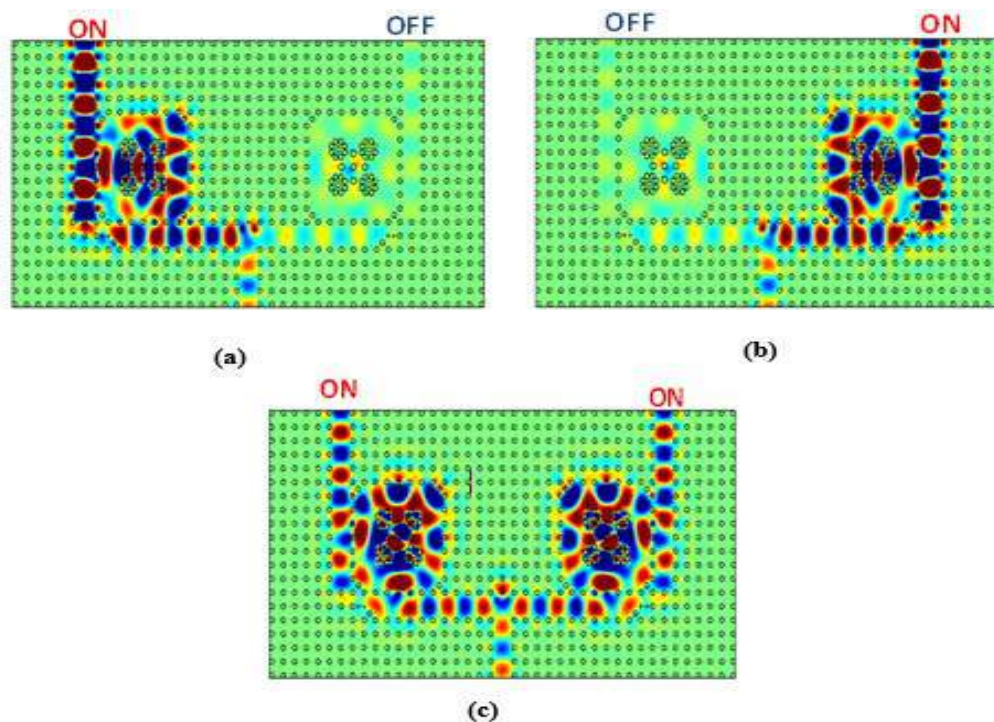

Fig.4 (a) OR gate structure. (b) 1 OR 0 = 1. (c) 0 OR 1 = 1. (d) 1 OR 1 = 1. The OR gate structure parameters are set such as: n=3.28, r=0.188×a and a=640 nm.

3.3. XOR gate

To study the all-optical XOR logic gate function, the same structure of OR gate 2D photonic structure is used adding one column of rods after the first ring resonator and is presented in

Fig.5. The optical XOR logic gate operation is presented by studying the electric field distribution of the 2D PCRR device for a particular wavelength λ=1.553 μm.

First, we insert a signal light into only port A of the input waveguide. A large part of this signal travels to the port Y through the ring resonator waveguide. This is identified as the logic phenomenon "1 XOR 0 gives 1" and it is shown in Fig.5 (b).

The similar situation occurs, when the signal is incident to the B port only, and we get output as 1.This corresponds of the logic operation "0 XOR 1 gives1" as shown in Fig.5 (c).

When the signals given to the input ports A and B simultaneously, there occurs a phase difference between these two signals due to path difference, and we get a destructive interference. As a result of this, there is approximately zero output at the port Y. This corresponds to the logic operation "1 XOR 1 gives 0" as shown in Fig. 5 (d).

When the both input signals are same ("0", "0" or "1", "1") the output of XOR gate is zero "0" and both are different ("0", "1" or "1", "0") the output is one "1".)
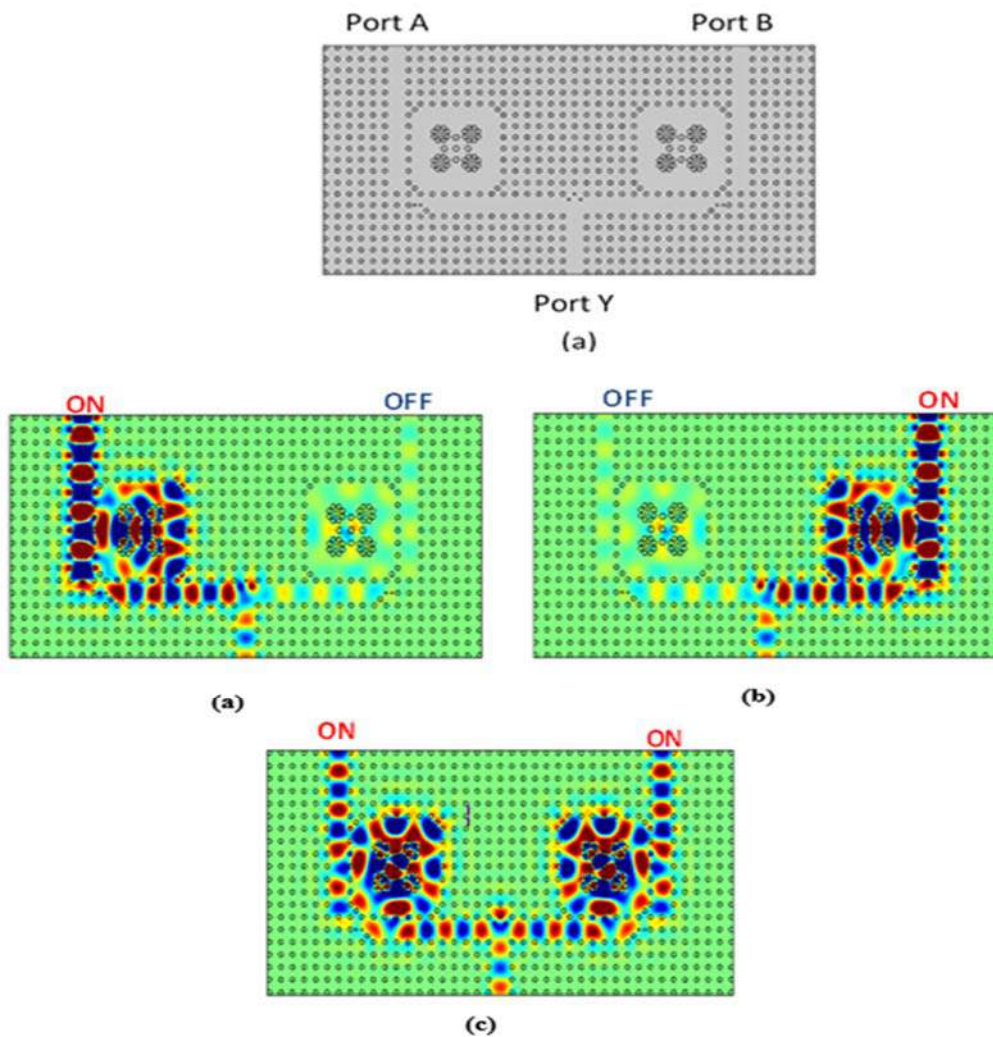

Fig. 5. (a) XOR gate structure. (b)1 XOR 0 = 1. (c) 0 XOR 1 = 1. (d) 1XOR 1 = 0. The XOR gate structure parameters are set such as: *n*=3.28, *r*=0.188×*a* and *a*=640 nm.

4. Conclusion

In this article, photonic crystal ring resonator based Channel-Drop Filter is designed and investigated. First we designed a flower shaped PCRR based on only one photonic crystal ring resonator. By combining two ring resonators, we proposed OR and XOR gates operating with TE mode optical signals.. Photonic crystal manufacturing is one of the main inconvenient that can be confronted where is expensive in production. Sub 100 nm dimensions need generally employing of high resolution electron beam lithography (EBL).

References

[1] S.H. Kim, H.Y. Ryu, H.G. Park, G.H. Kim, Y.S. Choi, Y.H. Lee, 'Two-dimensional photonic crystal hexagonal waveguide ring laser', Appl. Phys. Lett. 81 PP.2499–2501, 2002.

[2] V. Dinesh Kumar, T. Srinivas, A. Selvarajan,' Investigation of ring resonators in photonic crystal circuits', Photon. Nanostruct. 2 pp.199–206, 2004.

[3] Z. Qiang, W. Zhou, R.A. Soref, Optical add-drop filters based on photonic crystal ring resonators, Opt. Express 15 pp.1823–1831, 2007.

[4] S. Robinson, R. Nakkeeran, 'Investigation on two dimensional photonic crystal resonant cavity based band pass filter', Optik, Volume 123, pp.451–457, 2012.

[5] H.Alipour Banaeia, S.Seraj mohammadib,F.Mehdizadehc,Alloptical NOR and NAND gate based on nonlinear photonic crystal ring resonators,Optik Volume 125 pp.5701–5704, 2014.

[6] Mahmoud M Y, Bassou G, Taalbi A, Chekroun Z M. Optical channel drop filter based on photonic crystal ring resonators. Optics communications 2012; 285:368-372.

[7] M. A. M. Birjandi, and M. R. Rakhshani, " Anew design of tunable four-port wavelength demultiplexer by photonic crystal ring resonators" Optik (2013), http://dx.doi.org/10.1016/j.ijleo.2013.04.128.

[8] L. Mokhtari, H. A. Badaoui, M. Abri, M. Abdelbasset, F. Lallam, and B. Rahmi, "Proposal of a New Efficient or/Xor Logic Gates and All-Optical Nonlinear Switch in 2D Photonic Crystal Lattices," Progress In Electromagnetics Research C, Vol. 106, 187-197, 2020. doi:10.2528/PIERC20051501 http://www.jpier.org/pierc/pier.php?paper=20051501 (scopus)

[8] Saidani N, Belhadj W, Abdel Malek F. 'Novel all-optical logic gates based photonic crystal waveguide using self imaging phenomena'. Optical Quantum Electron 47:1829–46, 2015.

[9] Isfahani BM, AhamdiTameh T, Granpayeh N, Javan AM.' All optical NOR gate based on nonlinear photonic crystal microring resonators'. Optical Society of America, volume 26,pp.1097–102,May 2009.

[10]   Moungar A, Badaoui H, Abri M, '16-Channels Wavelength Efficient Demultiplexing around   1.31/1.55   μm   in   2D   Photonic   Crystal   Slab',   Optik   (2019), https://doi.org/10.1016/j.ijleo.2019.04.032

[11]   T. Skauli, P. S. Kuo, K. L. Vodopyanov, T. J. Pinguet, O. Levi, L. A. Eyres, J. S. Harris and M. M. Fejer, B. Gerard, L. Becouarn, and E. Lallier 'Improved dispersion relations for GaAs and applications to nonlinear optics', Journal of Applied Physics, Vol. 94, N. 10, pp 6447-6455, 2003.

Air Pollution Prediction Based on LSTM Neural Network: Sample of Isparta Province

Mahmut TOKMAK[1*]

Abstract: In recent years, air pollution has become an important problem as a result of the increase in population, the advancement of technology, the growth of developing industries and cities. Especially, pollutants such as PM10 (Particulate Matter) and SO2 have been shown to threaten human health. Therefore, the detection and prediction of PM10 air pollution is an important issue. The Province of Isparta, Turkey, is among the Provinces with the risk of 1st degree pollution due to its geographical location. For this reason, the Province of Isparta has been taken as an example.

In this work, we propose an approach to forecast PM10 concentration using Recurrent Neural Network (RNN) with Long Short- Term Memory (LSTM). In the estimation of air pollution, hourly temperature, pressure, humidity, wind speed, wind direction meteorological parameters and PM10 concentration obtained between 2016-2021 were used. The data were trained and tested with the established LSTM model. In assessing the accuracy of model predictions, we used Explanatory Coefficient (R^2), Root-Mean-Square Error (RMSE) and Mean Absolute Error (MAE). The predicted values of R^2, RMSE, MAE were 0.90, 9.43, 5.99 respectively. The result shows that the proposed approach can effectively forecast the value of PM10.

Keywords: Air pollution, Deep Learning, RNN, LSTM

1. Introduction

With the rapid development of urbanization, air pollution is becoming an increasingly serious environmental problem affecting human health and sustainable development worldwide (D.-R. Liu et al., 2021). The rapid development of industrial technology has caused many negative environmental impacts. Air pollution is one of them (Chang et al., 2020).

Typical sources of air pollution include industrial emission and traffic emission, and the main pollutants are PM2.5, PM10, NO2, SO2, O3 etc. The correlation between health risk and the concentration of air pollutants have been studied (J. Fan et al., 2017). In order to decide on the level of air pollution in a region by the World Health Organization (WHO), it was found sufficient to determine the sulfur dioxide (SO2) and particulate matter (PM) values, which are pollutants that change the natural composition of the air and give it the characteristic of polluted air, and it has been suggested to measure it in every country (Özel, 2019; Tsai et al., 2018). Isparta Province in Turkey is among the ones with the highest pollution risk (*ICSİM*, 2021). In order to prevent or reduce the harmful effects of air pollution on human health and the

---

[1] Isparta University of Applied Sciences, Gelendost Vocational School, Gelendost, Isparta, Turkey
* Corresponding author: mahmuttokmak@isparta.edu.tr

environment, it is aimed by the authorities to achieve the determined air quality targets. Therefore, to effectively monitor and forecast PM concentration is an important issue.

When the studies in the literature for the estimation of air quality parameters are examined, various studies have been carried out on air pollution using data sets from different cities in different countries and various machine learning methods. These methods can be basically divided into two groups as traditional classification algorithms and deep learning methods. Traditional classification algorithms refer to classification algorithms developed to perform data mining tasks. Examples of these algorithms are Support Vector Machines (SVM) (Zhu et al., 2018), Random Forest (Kumar, 2018), k Nearest Neighbor algorithms (KNN) (Y. Fan et al., 2018) Artificial Neural Network (ANN) (Maleki et al., 2019). The methods used as deep learning methods are Deep Neural Networks (DNN) (Eslami et al., 2020), Convolutional Neural Networks (CNN) (Park et al., 2020; Zhang et al., 2020) and RNN (J. Fan et al., 2017; Krishan et al., 2019; D. Liu et al., 2020; D.-R. Liu et al., 2021; Tsai et al., 2018).

Air pollution is also affected by meteorological factors such as wind speed, direction, temperature, pressure and humidity. The most important role of meteorology in atmospheric air pollution is to be effective in the stages of distribution, transport and separation from the atmosphere (Özel, 2019). Therefore, in this study, an LSTM model was established by combining meteorological parameters with pollutant parameters. The data used in the model is retrieved from the General Directorate of Meteorology and Turkey Ministry of Environment and Urbanisation from year 2016 to 2021 and is combined into 7 dimensions dataset. The performance of the established model was evaluated with R^2, RMSE and MAE criteria.

2. Material and Method

2.1. Data Preprocessing and Experiments Design

The meteorological data used in this study were obtained from the General Directorate of Meteorology for the Province of Isparta. These data consist of hourly temperature, humidity, pressure, wind direction and wind speed information for the years 2016-2021. PM10 and SO_2 data was obtained from Turkey Ministry of Environment and Urbanisation, air quality station data web page (*RTMEU*, 2021).

Table 1. Dataset Statistics

	Pressure	Wind direction	Humidity	Temperature	Wind speed	SO₂	PM10
count	43844	43841	43844	43845	43841	41651	41725
mean	902.21	179.91	60.67	13.42	1.66	11.74	53.79
std	4.43	115.92	22.25	9.43	1.27	12.60	52.51
min	878.80	0.00	7.00	-13.70	0.00	0.00	0.02
max	918.20	360	99	37.40	20.90	201.62	1646.03

First of all, meteorological parameters and pollutant parameters were combined. When there are missing values in the all data, we used the average value to fill in the all data. And Min-Max Normalization (1) is used to limit values in each dimension between 0 and 1. Min-Max Normalization is used to avoid multiple iterations of the neural network and decrease in accuracy.

$$z = \frac{x - \min(x)}{\max(x) - \min(x)} \tag{1}$$

2.2. RNN and LSTM

RNN is a variation of feed-forward neural network (FNN): FNN consists of layers stacked on top of each other, where each layer is composed of neurons, and all connections between layers follow the same direction. RNN present cyclic structure into the neural network, which is implemented by self-connection of each node (neuron). By using self-connected each node, historical inputs can be memorized by RNN (J. Fan et al., 2017; Tsai et al., 2018). Training of FNN is done with back propagation. While RNN sequence data and takes the transfer of 'memory' into account, for that reason its training process should stack back propagation results over time dimension, resulting in the back propagation through time algorithm (J. Fan et al., 2017).

The LSTM deep learning algorithm is known as a recurrent neural network introduced by Hochreiter and Schmidhuber in 1997 to overcome the disadvantages of RNN architecture (Hochreiter & Schmidhuber, 1997). The difference between LSTM and traditional RNN is that each node in LSTM is a memory cell. The LSTM links the previous data information to the current nodes. Each nodes contains three gates: input gate, forget gate, and output gate (Tsai et al., 2018).
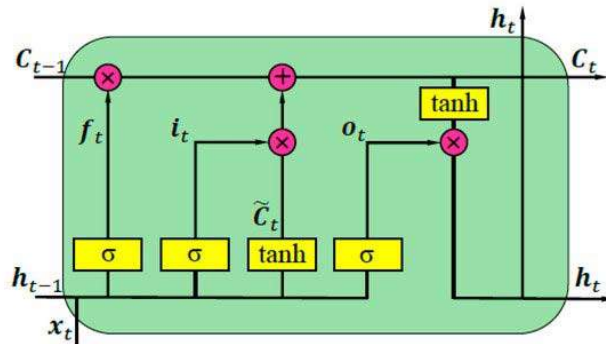

Figure 2. LSTM Unit (Xiao & Yin, 2019)

In the LSTM architecture (Figure 2), first of all, X_t and h_{t-1} information are used as inputs, and it is decided which information to delete. These operations are done in the forget layer (f_t) using Equation (2) and sigmoid is used as the activation function. Secondly, the input layer, where new information will be determined, comes into play and firstly (i_t) the information is updated with the sigmoid function using Equation (3). Then, the candidate information that will form the new information with Equation (4) is determined by the tanh function. New information is created by equation (5). Finally, the output data is obtained by using Equation (6) and (7) in the output layer. Weight parameters (W) and bias parameters (b) are learned by the model in a way that minimizes the difference between actual training values and LSTM output values (Xiao & Yin, 2019).

$$f_t = \sigma(W_f \cdot [h_{t-1}, x_t] + b_f) \tag{2}$$

$$i_t = \sigma(W_i \cdot [h_{t-1}, x_t] + b_i) \tag{3}$$

$$\tilde{C}_t = \tanh(W_C \cdot [h_{t-1}, x_t] + b_C) \tag{4}$$

$$C_t = f_t * C_{t-1} + i_t * \tilde{C} \tag{5}$$

$$o_t = \sigma(W_o[h_{t-1}, x_t] + b_o) \tag{6}$$

$$h_t = o_t * \tanh(C_t) \tag{7}$$

Three different statistical evaluation criteria were used to evaluate the prediction performance of the proposed LSTM model. These criteria are: R^2, RMSE and MAE. R^2 (8), RMSE (9) and MAE (10) are commonly used as a measure of the difference between predicted and observed values (Delavar et al., 2019; D. Liu et al., 2020).

$$R^2 = 1 - \frac{\sum_{i=1}^{n}(y_i - \hat{y}_i)^2}{\sum_{i=1}^{n}(\hat{y}_i - \overline{y_i})^2} \tag{8}$$

$$RMSE = \sqrt{\frac{\sum_{i=1}^{n}(y_i - \hat{y}_i)^2}{n}} \tag{9}$$

$$MAE = \frac{1}{n}\sum_{i=1}^{n}|y_i - \hat{y}| \tag{10}$$

n number of samples in Equation (8) - (10) used for statistical evaluation criteria, y_i i. the true value of the observation, $\hat{y}_i$ i. is the estimated value of the observation and $\overline{y_i}$ represents the average of the actual observation values.

3. Results

The proposed models and baseline models are implemented using Python, Theano, Keras and Scikit-learn, and executed on a computer with Intel Core i5-4200 CPU 2.50 GHz, 16 GB RAM. The dataset was divided into two groups for training 90% and testing 10% approximately. The training and test data of PM10 are shown in Figure 2.
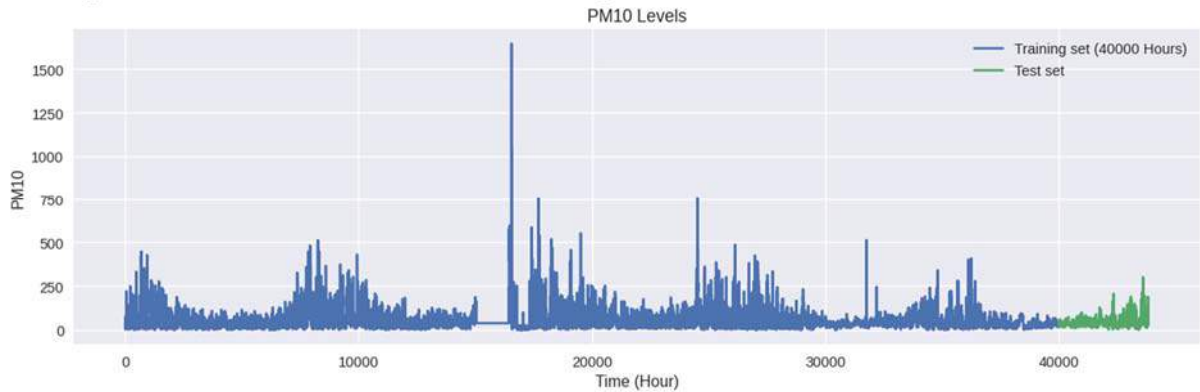

Figure 2. PM10 Training Set and Test Set

The established LSTM network consists of 3 layers and there are 120 neurons in each layer. The dropout rate is set to 0.2. The parameters used for the LSTM network are given in Table 2.

Table 2. LSTM Model Parameters

Structures of LSTM Model	Value
Number of Records	43849
Inputs	7
Neuron	120
Layers	3
Dropout	0.2
Outputs	1
Batch Size	64
Epoch	50
Loss Function	Mean Square Error
Optimizer	Adam

After the model was trained, as a result of the test; R2, RMSE and MAE scores of 0.90, 9.43 and 5.99 were obtained, respectively (Table 3).

Table 3. Test Results

	R2	RMSE	MAE
Test Results	0.90	9.43	5.99

The representation of the estimated values and the actual values on the graph is given in Figure 3. Forecast data and actual data for the last 100 hours are shown in Figure 4.
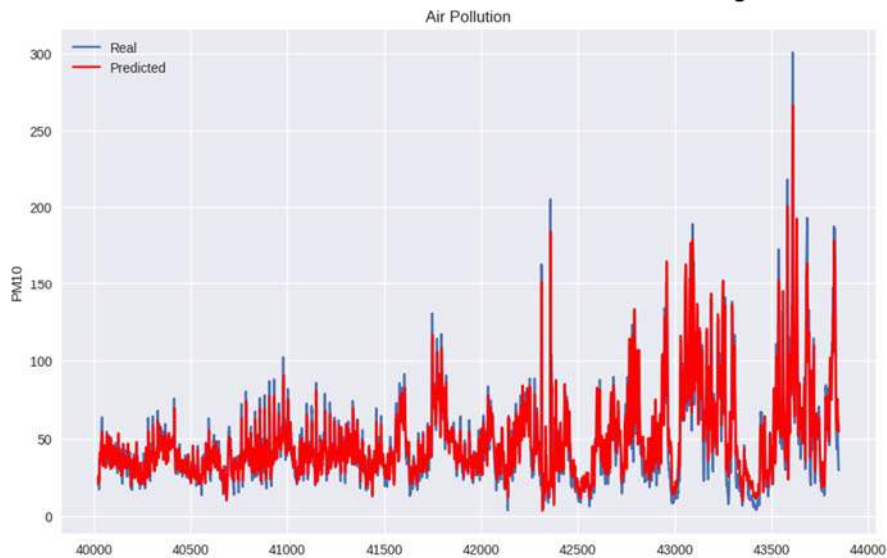

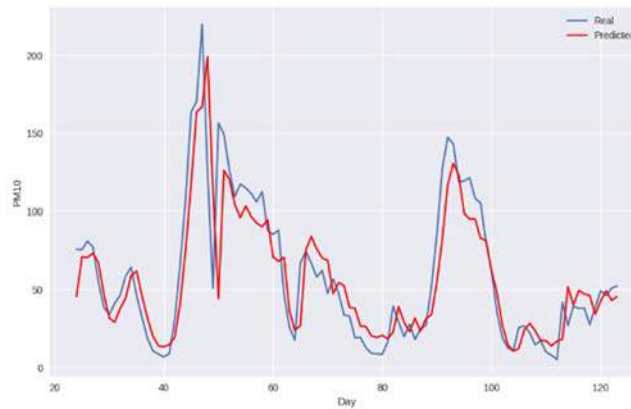**Figure 3.** Hourly Timestep on Test Set

Figure 4. Last 100 Hours on Test Set

4. Discussion and Conclusions

Forecasting air pollution is a significant issue for human health. Measures to be taken as a result of correct predictions will have positive results. Countries, administrators, non-governmental organizations and scientists are doing various studies on this subject.

In this study, the LSTM model, which is a deep learning approach, is proposed to predict air pollutant values. Hourly meteorological parameter and pollutant parameter data of Isparta Province of Turkey between 2016 and December-2020 were used to train the proposed model and evaluate its performance. These data were divided into two groups as training and test sets. While the training data was used only in the learning process of the model, the test data were not used in the learning process. After the learning process of the model was completed, the test data were used while evaluating the performance of the algorithm. Three different statistical evaluation criteria were used to evaluate the prediction performance of the proposed LSTM model. These criteria are: R^2, RMSE and MAE. As a result of the test, very high predictive values were obtained. It is concluded that improving air pollution forecast accuracy will have significant positive effects on public health and environmental policy making.

References

Chang, Y.-S., Chiao, H.-T., Abimannan, S., Huang, Y.-P., Tsai, Y.-T., & Lin, K.-M. (2020). An LSTM-based aggregated model for air pollution forecasting. Atmospheric Pollution Research, 11(8), 1451–1463. https://doi.org/10.1016/j.apr.2020.05.015

Delavar, M., Gholami, A., Shiran, G., Rashidi, Y., Nakhaeizadeh, G., Fedra, K., & Hatefi Afshar, S. (2019). A Novel Method for Improving Air Pollution Prediction Based on Machine Learning Approaches: A Case Study Applied to the Capital City of Tehran. ISPRS International Journal of Geo-Information, 8(2), 99. https://doi.org/10.3390/ijgi8020099

Eslami, E., Salman, A. K., Choi, Y., Sayeed, A., & Lops, Y. (2020). A data ensemble approach for real-time air quality forecasting using extremely randomized trees and deep neural networks. Neural Computing and Applications, 32(11), 7563–7579.

Fan, J., Li, Q., Hou, J., Feng, X., Karimian, H., & Lin, S. (2017). A Spatiotemporal Prediction Framework for Air Pollution Based on Deep RNN. ISPRS Annals of the Photogrammetry, Remote Sensing and Spatial Information Sciences, IV-4/W2, 15–22. https://doi.org/10.5194/isprs-annals-IV-4-W2-15-2017

Fan, Y., Hou, L., & Yan, K. X. (2018). On the density estimation of air pollution in Beijing. Economics Letters, 163, 110–113.

Hochreiter, S., & Schmidhuber, J. (1997). Long Short-Term Memory. Neural Computation, 9(8), 1735–1780. https://doi.org/10.1162/neco.1997.9.8.1735

Isparta Çevre ve Şehircilik İl Müdürlüğü. (2021). Isparta Çevre ve Şehircilik İl Müdürlüğü. https://isparta.csb.gov.tr/ilimiz-hava-kirliligi-degerlendirmesi-haber-257500, (Access Date: 01.07.2021)

Krishan, M., Jha, S., Das, J., Singh, A., Goyal, M. K., & Sekar, C. (2019). Air quality modelling using long short-term memory (LSTM) over NCT-Delhi, India. Air Quality, Atmosphere & Health, 12(8), 899–908. https://doi.org/10.1007/s11869-019-00696-7

Kumar, D. (2018). Evolving Differential evolution method with random forest for prediction of Air Pollution. Procedia Computer Science, 132, 824–833.

Liu, D., Lee, S., Huang, Y., & Chiu, C. (2020). Air pollution forecasting based on attention-based LSTM neural network and ensemble learning. Expert Systems, 37(3). https://doi.org/10.1111/exsy.12511

Liu, D.-R., Hsu, Y.-K., Chen, H.-Y., & Jau, H.-J. (2021). Air pollution prediction based on factory-aware attentional LSTM neural network. Computing, 103(1), 75–98. https://doi.org/10.1007/s00607-020-00849-y

Maleki, H., Sorooshian, A., Goudarzi, G., Baboli, Z., Tahmasebi Birgani, Y., & Rahmati, M. (2019). Air pollution prediction by using an artificial neural network model. Clean Technologies and Environmental Policy, 21(6), 1341–1352. https://doi.org/10.1007/s10098-019-01709-w

Özel, G. (2019). Markov Zinciri Kullanarak Ankara İli İçin Hava Kirliliği Tahmini. 3(2), 144–151. https://doi.org/10.30516/bilgesci.546317

Park, Y., Kwon, B., Heo, J., Hu, X., Liu, Y., & Moon, T. (2020). Estimating PM2. 5 concentration of the conterminous United States via interpretable convolutional neural networks. Environmental Pollution, 256, 113395.

Republic of Turkey Ministry of Environment and Urbanisation. (2021). Republic of Turkey Ministry of Environment and Urbanisation. https://sim.csb.gov.tr/STN/STN_Report/StationDataDownloadNew, (Access Date: 07.04.2021)

Tsai, Y.-T., Zeng, Y.-R., & Chang, Y.-S. (2018). Air Pollution Forecasting Using RNN with LSTM. 2018 IEEE 16th Intl Conf on Dependable, Autonomic and Secure Computing, 16th Intl Conf on Pervasive Intelligence and Computing, 4th Intl Conf on Big Data Intelligence and Computing and Cyber Science and Technology Congress (DASC/PiCom/DataCom/CyberSciTech), 1074–1079. https://doi.org/10.1109/DASC/PiCom/DataCom/CyberSciTec.2018.00178

Xiao, Y., & Yin, Y. (2019). Hybrid LSTM neural network for short-term traffic flow prediction. Information, 10(3), 105.

Zhang, Q., Lam, J. C., Li, V. O., & Han, Y. (2020). Deep-AIR: A Hybrid CNN-LSTM Framework forFine-Grained Air Pollution Forecast. ArXiv:2001.11957 [Eess]. http://arxiv.org/abs/2001.11957

Zhu, S., Lian, X., Wei, L., Che, J., Shen, X., Yang, L., Qiu, X., Liu, X., Gao, W., & Ren, X. (2018). PM2. 5 forecasting using SVR with PSOGSA algorithm based on CEEMD, GRNN and GCA considering meteorological factors. Atmospheric Environment, 183, 20–32.

Pro and Contra for Self-Driving Car: Public Opinion in Serbia

Livija Cveticanin[1*], Ivona Ninkov[2]

Abstract: Self-driving car (SDC), considered in this paper, is a cyber-physical system i.e. a fully autonomous vehicle without human driver. All activities of the vehicle are expected to be done automatically. Based on data obtained from the sensors for perception and navigation and those given by passengers the decision for SDC would be done by the system with artificial intelligence. Such SDC is expected to be on public roads very soon. In spite of the fact that the first manufactured SDCs have been already tested in some cities of the world, the result of investigation of the public opinion in more than 150 countries of the world show some doubts and distrust in their application. The aim of this paper is to present the results of queries done in Serbia among the wide range of population. The questionnaire is extended in comparison to already used and is modelled as the tripartite with cognitive, affective and behavior components. It is obtained that the replies dependent on gender, age, professional orientation, living place. The persons under interview express their opinion about technical, social, economic, safety and security aspects of SDC. It is concluded that the results of interview obtained in Serbia differ significantly to those obtained in highly developed countries with high level of traffic in cities and highways. As the most of people is Serbia is skeptical with SDC, certain education and dissemination of knowledge on the topic is necessary.

Keywords: autonomous vehicle, questionnaire, benefits of self-driving car, barriers for self-driving car

1. Introduction

Currently, one of the most investigated transport innovation is in the so called 'self-driving car' (SDC). There are many definitions to SDC, but the most widely spread is that 'it is an autonomous car without human driver' (SAE, 2018). Namely, SAE gives the classification of cars in six groups depending on the level of automation. SDC is believed that represents the most sophisticated version where riding do not need human driver to operate or to supervise the vehicle. SDC represents a cyber-physical system where all activities of mechanical parts are directed with computers i.e. hardware and software. For the function and making decision the algorithms need data obtained from various sensors, but also from passengers of the car. The project of SDC is multidisciplinary. Besides mechanical and electro engineering, IT, architecture and civil engineering, traffic engineering the aspects of environmental protection, economics, social sciences etc. have to be considered in realization but also application of SDC. The scholars believe that SDCs will change the world (Myrick, 2019). The major benefit of SDCs would be to eliminate many car accidents and to save tens of thousands of lives per year and to prevent hundreds of thousands of injuries and their associated economic toll. Nowadays, human errors are recognized as a major factor to traffic crashes. More than 90% of traffic

[1] University of Novi Sad, Faculty of Technical Sciences, Novi Sad, Serbia
[2] Obuda University, Doctoral School of Safety and Security Sciences, Budapest, Hungary
* Corresponding author: cveticanin@uns.ac.rs

crashes can be tied to a human error or human choice (NHTSA, 2016). SDCs, replacing fallible human drivers, are expected to largely reduce traffic crashes. In addition, adoption of SDCs in traffic will promise to (Liu & Xu, 2020): reduce traffic congestion, air pollution and transportation emissions, and to increase the mobility of those who currently are unable to drive, to improve the fuel efficiency, space utilization and productivity, increase human mobility, and to decrease risks and challenges related to safety, security, legal liability, and regulation issues (Penmetsa et al, 2019; Anderson et al, 2016; Fagnant and Kockelman, 2015; NHTSA, 2016).

As the analysts predict that completely autonomous cars will be for sale by 2025-2030 (Ilkova & Ilka, 2017) it is necessary to know if the SDC will be accepted from population. Namely, the SDCs are technically almost prepared for testing and application on public roads and their inclusion in the everyday transportation seems is necessary. For realization of the process, the users need to accept the SDC. But, are people really ready for autonomous vehicles? To obtain the answer the population is worldwide interviewed about SDC.

According to online survey in 2011 on two thousand persons from USA and UK it is found that even 49% of them were ready to use SDC. Due to Reiss & Pitts (2021) the confidence in the future of the SDC continued to grow in spite of the fact that the global pandemic gripped the world.

In a 2012 survey of about thousand German drivers by automotive researcher Puls, 22% of the respondents had a positive attitude towards these cars, 10% were undecided, 44% were skeptical and 24% were hostile (Floridi, 2020). Similar results gives the survey made in the USA, the UK and Australia (Schoettle & Sirak, 2014).

In 2015 a questionnaire survey by Delft University of Technology explored the opinion of five thousand people from 109 countries on automated driving (Kyriakidis et al, 2015). Results showed that respondents, on average, found manual driving the most enjoyable mode of driving. 22% of the respondents did not want to spend any money for a fully automated driving system. Respondents were found to be most concerned about software hacking/misuse, and were also concerned about legal issues and safety. Finally, respondents from more developed countries (in terms of lower accident statistics, higher education, and higher income) were less comfortable with their vehicle transmitting data. The survey also gave results on potential consumer opinion on interest of purchasing an automated car, stating that 37% of surveyed current owners were either "definitely" or "probably" interested in purchasing an automated car.

57% of 1500 interviewed persons in China in 2018 stated that "they would be likely to ride in a car controlled entirely by technology that does not require a human driver" (Qu et al, 2019). The most are willing to trust automated technology.

A Pew Research Center (Smith & Anderson, 2017) surveyed more than four thousand adults from USA and found that 94% of them have heard about SDC and even 44% are ready to ride it. The reasons against riding the SDC are: no trust into the control (42%), no trust in the safety (30%), enjoy of driving is eliminated (9%), feeling that the technology is not ready for everyday use (3%), fear to be hacked (2%) and other (8%). The reasons to accept the ride of SDC are: "cool" experience 37%, safer drive 17%, can do other things 15%, less stresses 13%, greater independence 4%, convenience 4% and others 11%.

In 2019 a new standardized questionnaire about the autonomous vehicle acceptance or decline is introduced. The questionnaire includes the additional description which helps respondents better to understand the implications of different automation levels (Montoro et al, 2019). Using this questions the public opinion on SDCs among various groups of respondents was analyzed (Kyriakidis et al, 2015). Results showed that partial automation (regardless of level) which requires higher driver engagement (usage of hands, feet and eyes) was more supported by population than SDC with full autonomy. The perceived and predicted safety give the level of intention to use highly autonomous SDCs.

The questionnaire used in the aforementioned was used as the basis for forming of the corresponding one for Serbia in Serbian language. The questionnaire is extended to be of tripartite type with cognitive, affective and behavior components.

The aim of this paper is to analyze the opinion of population on SDC in Serbia and to compare with that obtained in other countries. It will be suggest how to improv the knowledge in population in Serbia with the aim to increas the acceptence level and to destroy the barriers for accepting SDC.

2. Investigation Method

Most of studies on attitudes toward SDCs, mentioned in the previous section of this paper, are made through the traditional view with one - dimensional bipolar scales (Eagly and Chaiken, 1993; Marletto, 2019) which implies answers in questionnaire to be positive, negative (Nielsen & Haustein, 2018), or neutral i.e. uncertain (Hulse et al, 2018). However, we think that this approach is very simply and is not enough sophisticated to include ambivalent and indifferent opinions. To overcome the lack in our investigation the model for estimation is conceptualized as a tripartite (Rosenberg and Hovland, 1960) with cognitive, affective and behavior components. Cognitive components define the object by perceptions and beliefs and also thoughts. Affective components describe the feelings and emotions which are linked to the object. The behavioral components include the behavior intention and verbal statements. So, the gradation on answer is, for example, very likely – somewhat likely – somewhat unlikely – very unlikely.

The questionnaire is given in Appendix. In the questionnaire the short description of SDC is given. After that the question are divided into two parts: Personal questions and Questions according to SDC. The personal questions concern the gender, age, level of education and living place. The second group of questions have to give the conclusion about level of knowledge about SDC and its acceptance or rejection.

The interview involved 150 persons: 75 males and 75 females. (The percent of persons in the interview is equal to that in the already done interview in other countries and reported in the section before.)

3. Results

Distribution of persons in interview due to education and living location is plotted in Fig.1 and due to age in Fig.2.
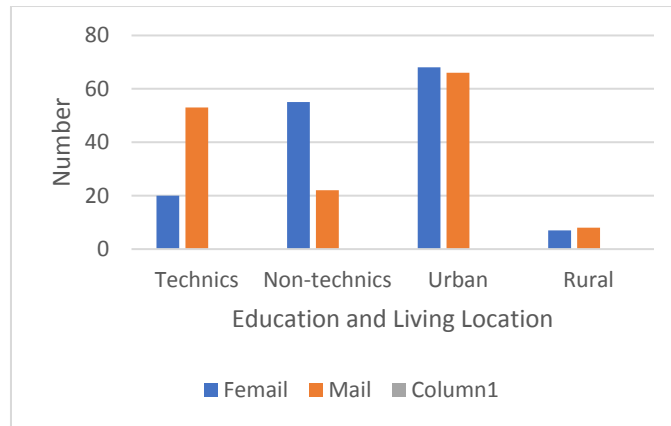
Figure 1. Education and Living Location
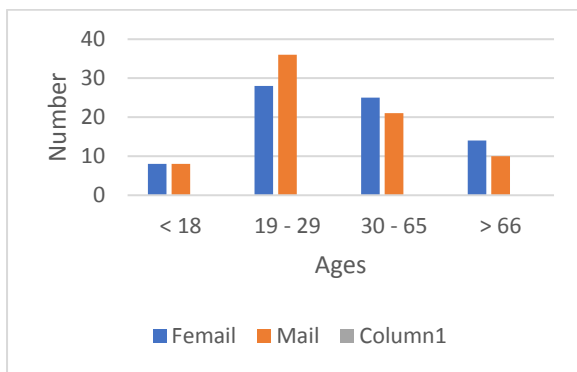
Figure 2. Age distribution
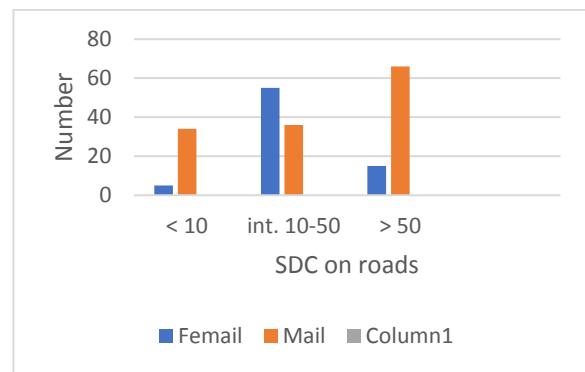
Figure 3. Education and Living Location

Only 24 female and 58 male have heard of SDC. Only one female and 25 males who have not the technical education know something about SDC.

In Fig.3 the expectation of SDC on public roads is shown. The opinion regarding SDC is plotted in Fig.4.
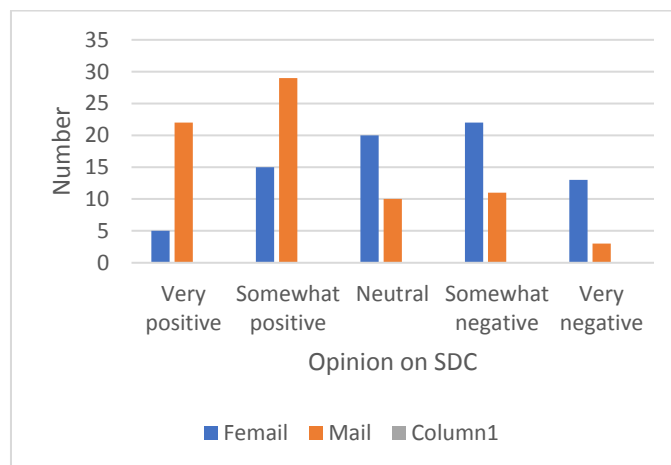
Figure 4. Opinion regarding SDC

Even 29 female and 68 male would like to be the part of the SDC project as designer, manufacturer or owner. In Fig.5 the expected crashes with SDC in comparing with conventional car is shown.
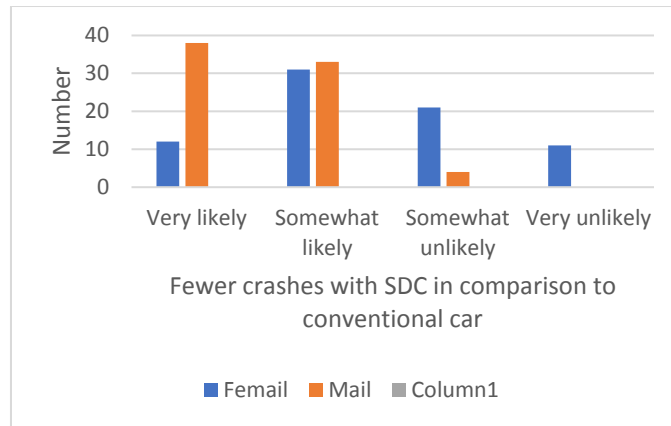
Figure 5. Decrease of crashes with SDC in comparing with conventional car

15 of the female population expect very likely, 27 somewhat likely, 20 somewhat unlikely and 13 very unlikely the crashes of SDC with mortal would be reduced in comparison to the case with conventional car. In the male population the replies are: 25 very likely, 34 somewhat likely, 12 somewhat unlikely and 4 very unlikely.
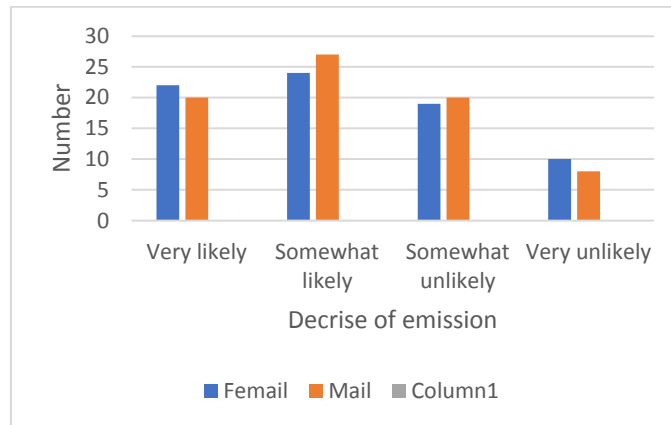
Figure 6. Decrease of emission

In Fig.6 the opinion about emission decrease is plotted. The statement about reduction of fuel consumption is shown in Fig.7.
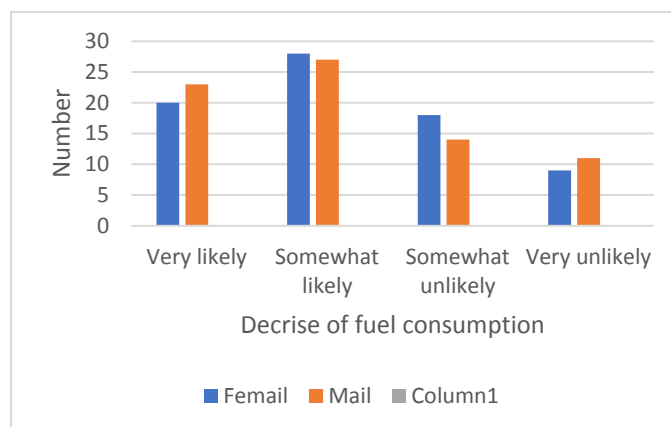
Figure 7. Decrease of fuel consumption

59 females and only 22 males said that they would worry during driving in SDC.
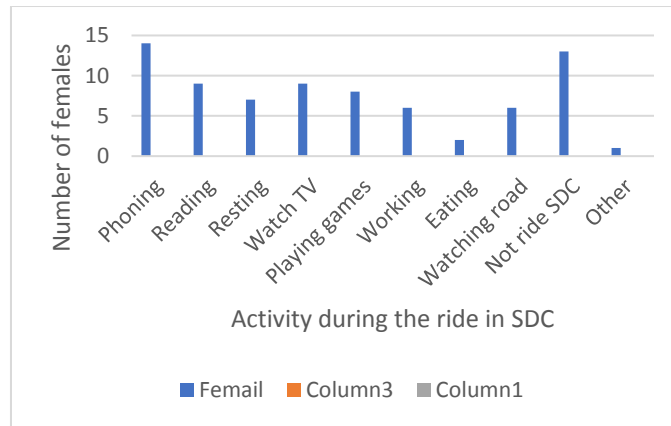
Figure 7. Activity of females during driving in SDC
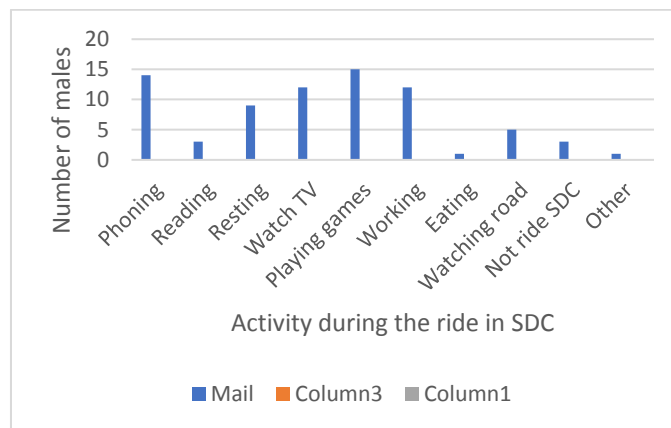
Figure 8. Activity of males during driving in SDC

In Fig.7 and Fig.8 the activity during driving in SDC of females and males, respectively, are presented.
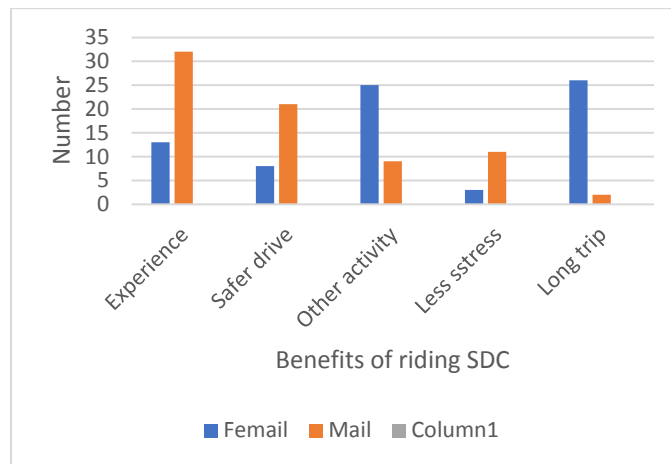
Figure 9. Benefits of riding SDC

In Fig.9 the benefits and in Fig.10 the barriers of riding SDC are given.
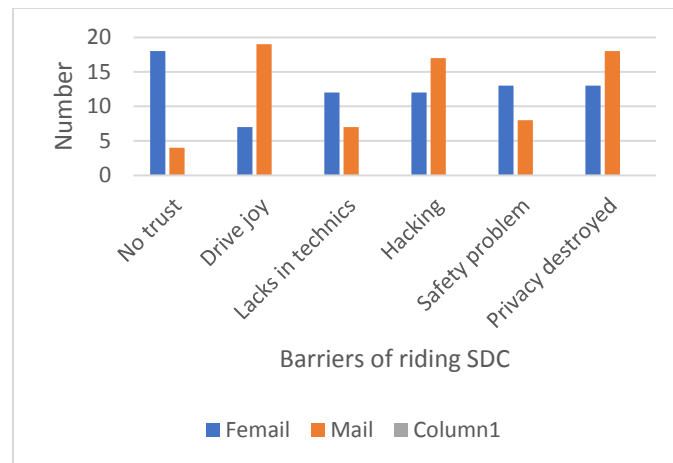
Figure 10. Barriers of riding SDC

4. Discussion and Conclusions

In general, based on results of interview the following is concluded:

1. Analysing the results of the interview it is concluded that the population in Serbia gives the support to SDC acceptance. This support is in the ration 55% to 45%. The support of application of SDC is based on the assumption the number of crashes will decrease. The special influence on the decision is the expecting that the mortality in accidents will be smaller. The result agrees with that published in Liu et al (2019a).
2. Other benefits of SDC in opinion of respondents it connected with comfortable long-time trip, faster trip in cities, cheaper transportation costs, available the ride for older and disabled, application of the time in car for another activities like work, rest, etc., but with 'healthy life' in the environment with decreased pollution i.e. life outside areas with polluted air.
3. The opinion is that SDC would decrease the environmental pollution and conventional fuel consumption, too. Respondents believe that SDC would increase the efficiency in reducing carbon emissions more than conventional vehicles. Population expects the manufacturer to place a greater emphasis on emission reductions and conventional fuel consumption (Liu et al, 2019b).
4. When SDCs can be used throughout the day the traffic will be optimally organized and many parking spaces in cities and towns may be eliminated in the future.
5. Population in Serbia is fearful about cyber-security and privacy in SDC. All the population is worried that SDCs will be easily hacked because of the abundance of digital infrastructure required for them to work. The population agree that the cybersecurity in SDC has to be increased before inclusion of vehicle into the traffic. The population is afraid that criminals will use the data that they retrieve, hacking the vehicle and getting it to perform actions the user is unaware of, unable to undo, and maliciously causing harm to persons in the car. The similar consequences of cyber-attack are mention by Stevens (2018). If cyber-criminals take over a vehicle, they can cause minor nuisances (closing or opening windows), or they can create greater threats (disable the functionality of car to read stop signs, causing crash of vehicles, harm passengers), or they can use SDCs for terrorist purposes (transporting and detonating bombs).

These positive, neutral or negative opinions on inclusion of SDC on roads in Serbia are independent on the gender, aging or education of respondent. There is the group of questions

where answers differ if they are given by males or females, younger or older persons, technically or non-technically educated persons or those living in urban or rural ambient.

1. The persons from urban give higher support to SDC than those from rural ambient. Namely, the last are mainly indifferent and not interested in SDC. The reason for urban inhabitants to accept SDC is based on the problem of traffic jams, not enough parking space, sparing driving time, better use of the time during driving and at last there is also an economic aspect. Living in the suburbs or in rural area and working in cities gives the benefits not to pay expensive flats in the downtown and living in more ecological environment. Individuals would be able to rent further away from the centres of towns and cities because of the ease of commuting with SDC and, in addition, reduced costs. It would be the new stream in living way: reduction in urbanisation and spread out of population throughout the region (Lim & Taeihagh, 2018). People would be less of a need to live in cities. The importance of this item is seen in this pandemic situation, when the human activity was possible only in fields and inside the houses. It is worth to say, that in Serbia the urban population lives mainly in flats.

2. The interview highlighted that there is a difference in perceptions about SDCs between men and women. Men are ready to accept SDC on public roads, but women have serious worry. Males thrust in SDC and consider SDC to be safer than conventional cars. Men are ready to ride SDC because experience and have less stress and fear in comparison to females. Females are less enthusiastic and more fearful about their safety in SDC. As the advantage of SDC the females mentioned the long-time trip and the possibility to have other activities during riding.

3. Females and males opinion about the joy of driving differs, too. As it is known, the joy of driving is one of the primary pleasure of the vehicle (Kemp, 2018). The interview shows that the most of men are not ready to waive the joy of driving. In contrary, it is not the case for women. For significant number of female driving is a necessary activity for fulfilling the everyday duties, but for most of men it is a form of pleasure: a connection with surroundings, a sense of adventure and control, a relaxation form etc. Males think that SDCs would threat this joy.

4. Female have higher affinity to doing other things than driving in comparison to males. Female are primary ready to phone, read, to sleep or watch the road. Male spend time in phoning, playing games, working and watching films.

5. The interview shows that there is the fear during riding SDC. The stress and fear in driving is significantly higher in female than in male population. In addition, the fear is stronger than in driving conventional car. It is interesting to note, that females are afraid to ride in the SDC independently on ages. Similar result is reported by Johnsen et al. (2017) and Naughton (2019).

6. The age of the respondents proved to be a significant factor in decision making. This conclusion is already presented in some publication (see for example, Rahman et al. 2019). In general, younger people are ready to accept the SDC. There is also a group of older persons, non-drivers and disabled who see the benefits of SDC in their inclusion into the normal life. They consider SDC to potentially reduce the inequality in population and have the positive opinion in accepting SDC (Abraham et al, 2017; Lee et al, 2017) It is worth to be said that school children where included into the interview. Namely, they would be most likely the users of this technical innovation in the future.

7. The persons with technical education have much more information about SDC than others. However, their knowledge is insufficient. Both, males and females, are ready to be included into the projects considering this autonomous vehicle. The population need education in this segment of life. Popular and informative lectures on the topic are necessary on all levels and for various aging (from those for children up to old persons).

> Scholars have to disseminate the knowledge in SDC while manufacturers and sellers have to invest in SDC advertising.

Finally, based on interview a new, quite unexpected aspect of SDC appears. There is an additional lack in using SDC due to pandemic situation with Covid-19. Namely, car-sharing which is a fundamental property of SDC ride, is prohibited for persons who are not from one family. This argument is mentioned in the interview against SDC. At the moment, the solution of the problem is not evident.

Acknowledgement

References

Abraham, H., Lee, C., Brady, S., Fitzgerald, C., Mehler, B., Reimer, B. & Conghlin, J.F., (2017). Autonomous vehicles and alternatives to driving: trust, preferences, and effects of age. Transportation Research Board, Conference paper, pages 17.

Anderson, J.M., Kalra, N., Stanley, K.D>, Sorensen, P., Samaras, C. & Oluwatola, T., (2016). Autonomous vehicle technology: A guide for policymakers. RAND Corporation, 9780833083982.

Eagly, A.H. & Chaiken, S., (1993). The psychology of attitudes. New York, Harcourt Brace Jovanovich College Publisher.

Fagnant, D.J. & Kockelman K., (2015). Preparing a nation for autonomous vehicles: opportunities, barriers and policy recommendations. Transportation Research Part A 77, 167-181.

Floridi, L., (2020). The pulse of autonomous driving. Puls, pages 52, audi-study-autonomous-driving.pdf

Hulse, L., Xie, H, & Galea, E.R., (2018). Perceptions of autonomous vehicles: Relationships with road users, risk, gender and age. Safety Science, 102, 1-13.

Ilkova, V. & Ilka, A., (2017). Legal aspects of autonomous vehicles – an overview. Proceedings of the 2017, 21st International Conference on Process Control, Strbsko Pleso, Slovakica, June 6-9 2014, 428-433.

Johnsen, A., Strand, N., Andersson, J., Patten, C, Kraetsch, C. & Takman, J, (2017). Literature review in the acceptance and road safety, ethical, legal, social and economic implications of automated vehicles. BRAVE No. 723021, pages 76.

Kemp, R., (2018). Autonomous vehicles – who will be liable for accidents. Digital Evidence and Electronic Signature Law Review, 15, 33-47.

Kyriakidis, M. Happee, R. & De Winter, J.C.F., (2015). Public opinion on automated driving: Results of an international questionnaire among 5000 respondents. Transportation Research Part F: Traffic Psychology and Behaviour 32, 127–140.

Lee, C., Ward, C., Raue, M., D'Ambrosio, L. & Coughlin, J.F., (2017). Age differences in acceptance of self-driving cars: a survey of perceptions and attitudes. In: Zhou J, Salvendy G, (eds) Human aspects of it for the aged population, Aging, design and user experience, London, Springer, 3–13.

Lim, H.S.M. & Taeihagh, A., (2018). Autonomous vehicles for smart and sustainable cities: An in-depth exploration of privacy and cybersecurity implications. Energies, 11(5), pages 24.

Liu, P., Zhang, Y. & He, Z., (2019a). The effect of population age on the acceptable safety of self-driving vehicles. Reliability, Engineering & System Safety, 185, 341-347.

Liu, P., Ma, Y. & Zuo, Y., (2019b). Self-driving vehicles: Are people willing to trade risks for environmental benefits? Transportation Research Part A Policy and Practice, 125, 139-149.

Liu, P. & Xu, Z., (2020). Public attitude toward self-driving vehicles on public roads: Direct experience changed ambivalent people to be more positive. Technological Forecasting and Social Change, 151, 119827.

Marletto, G., (2019). Who will drive the transition to self-driving? A socio-technical analysis of the future impact of automated vehicles. Technological Forecasting & Social Change 139, 221-234.

National Highway Traffic Safety Administration (NHTSA) (2016) ODI Resume – Investigation: PE 16-007, Office of Defects Investigations

Montoro, L., Useche, S.A., Alonso, F., Lijarcio, I., Boso-Segni, P. & Marti-Belda, A., (2019). Perceived safety and attitude value as predictors of the intention to use autonomous vehicles: A national study with Spanish drivers. Safety Science 120, 865-876.

Myrick, J.G., Ahern, L., Shao, R. & Conlin, J., (2019). Technology name and celebrity endorsement effects of autonomous vehicle promotional messages: mechanisms and moderators. Science Communication, 41(1), 38-65.

Naughton, K., (2019) Americans still fear self-driving cars. BLOOMBERG, March 13, 2019, https:// www.bloomberg.com/news/articles/2019-03-14/americans-still-fear-self-driving-cars.

Nielsen, T.A.S. & Haustein, S., (2018). On sceptics and enthusiastics: What are the expectations towards self-driving cars? Transport Policy, 66, 49-55.

Penmetsa, P., Adanu, E., Wood, D., Wang, T. & Jones, S., (2019). Perceptions and expections of autonomous vehicles - snapshot of vulnerable road user opinion. Technological Forecasting and Social Change, 143, 9-13.

Qu, W., Xu. J., Ge, Y., Sun, X. & Zhang, K. (2019) Development and validation of a questionnaire to assess public receptivity toward autonomous vehicles and its relation with the traffic safety climate in China, Accident Analysis and Prevention 128, 78-86.

Rahman, M.M., Deb, S., Strawderman, L., Burch, R. & Smith, B., (2019). How the older population perceives self-driving vehicles, Transportation Research Part F, Traffic Psychology ad Behavior, 65(8), pages 12.

Reiss, M. & Pitts, B., (2021). Accenture on operations: Objects may be closer than they appear. Modern Materials Handling, 3 pages, https://www.mmh.com/article/accenture_on_operations_ objects_may_be_closer_than_they_appear

Rosenberg, M.J. & Hovlan, C.I., (1960). Cognitive, affective and behavioral components of attitudes. In: Rosenberg, M.J. & Hovlan, C.I., Eds., Attiture Organization and Change: An Analysis of Consistency among Attitude Components. Yale University Press, New Haven.

Schoettle, B. & Sirak, M., (2014). A survey of public opinion about autonomous and self-driving vehicles in the U.S., the U.K., and Australia. UMTRI Report No–2014-021, University of Mechigen, Transportation Research Institute, pages 42.

Smith, A. & Anderson, M., (2017). American attitudes toward driverless vehicles. Pew Research Center, https://www.pewresearch.org/internet/2017/10/04/americans-attitudes-toward-driver less -vehicles/

Society of Automotive Engineers (SAE), (2018). International: Taxonomy and definitions for terms related to driving automation systems for on-road motor vehicles. Standard J3016_201806, USA, https://www.sae.org/standards/content/j3016_201806/

Stevens, T., (2018). Global cybersecurity: New directions in theory and methods. Politics and Governance, 5(2), 1-4.

Appendix: QUESTIONNAIRE ABOUT SELF-DRIVING CAR (SDC)

(SDC is an autonomous vehicle which need not the human-driver. Receiving your call the SDC would pick you up and transport you to the willing location in the shortest time, along optimal path and in the most comfortable way.)
Remark: *Circle only one answer at a time*!

Personal questions:
1. What kind of vehicle you use most often for transportation?
   a) Pedestrian   b)Personal car   c)Bicycle   d) Motorcycle
   e) Public transportation

2. What is your gender?
   a) Female   b) Male

3. What is your age?
   a) Under 18   b) 19 to 29   c) 30 to 49   d) 50 to 64   e) 65 or older

4. What is your level and type of education?
   a) Student in non-technics
   b) Student in technics

c) Undergraduate in non-technics
d) Undergraduate in technics
e) Graduate in non-technics
f) Graduate in technics

5. Living place
a) Urban   b) Rural

Questions in acceptance of SDC
1. Had you ever heard of SDC before participation in this survey?
a) Yes   b) No

2. What is your opinion regarding SDC?
a) Very positive b)Somewhat positive c)Neutral d)Somewhat negative e)Very negative

3. In how many years do you believe the SDC will be on roads?
a) Less than 10 years   b) 10 to 50 years   c) More than 50 years

4. Would you like to be the part of the SDC project (designer, producer, owner)?
a) Yes   b) No

5. Would you be ready to study engineering considering the SDC?
a) Yes   b) No

6. How likely do you think that fewer crashes would occur with SDC?
a) Very likely   b) Somewhat likely   c) Somewhat unlikely   d)Very unlikely

7. How likely do you think the reduction of sever crashes with mortal would occur?
a) Very likely   b) Somewhat likely   c) Somewhat unlikely   d)Very unlikely

8. How likely do you think that lower emission would occur with SDC?
a) Very likely   b) Somewhat likely   c) Somewhat unlikely   d)Very unlikely

9. How likely do you think the reduction of fuel consumption would occur?
a) Very likely   b) Somewhat likely   c) Somewhat unlikely   d)Very unlikely

10. If you were to ride in a SDC what do you think you would use the extra time doing instead of driving?
a) Phoning and mailing   b)Read   c)Resting and sleeping
d)Watch movies/TV   e)Playing games   f)Working
g)Eating   h)Watching road   i)Not ride in SDC   j)Other (please specify)

11. Would you be worried during driving in SDC?
a) Yes   b) No

12. I would ride in SDC because:
a) Experience   b)Safer than conventional car   c)Can do other things
d) Less stress   e)Long-time trip convenience

13. I would not ride in SDC because:

a) Do not trust   b)Enjoy of driving   c)Feel technology is not ready
d) Hacking   e) Safety concerns   f)Worry of privacy

Thank you for completing this survey about SDC.

Effects of Activated Carbon on Medium Density Fiber Board Properties

Ayşe Ebru Akın[1*], Mustafa Karaboyacı[1]

Abstract: There is a growing concern all over the world on the health effect of the formaldehyde emission coming from the adhesive used in the MDF production. In this work, we investigated the effect of activated carbon addition into urea-formadehyde resin on the total emitted formaldehyde from MDF plates produced using the resin modified as such.

First, the gel time behavior of the resin was studied by monitoring the pH, gelation time, solid content, flow time and viscosity of the modified resin in comparison to the reference resin with no exist activated carbon. The dosing of the activated charcoal in the dry resin was kept at 1wt%, 3wt% and 5wt%. After that modified resin was used in the production of 40x40 cm MDF samples by using laboratory scale press line with full automation system. İnternal bonding strength, surface soundness, screw holding resistance, water absorption and thickness swelling were also measured in addition to the main interested parameter formaldehyde emission level which is determined via spectrometric technique following an extraction procedure.

Threshold values for activated carbon were determined to be 1wt%. Formaldehyde emission level was observed where addition of 1wt% activated carbon into the urea formaldehyde adhesive decreased the formaldehyde emission 52% comparison to reference whereas addition of activated carbon at above its threshold level provided 47% decreasing**.**

Keywords: activated carbon, formaldehyde emission, MDF, adsorbent

1. Introduction

The increase in diseases in the world has increased the awareness of the chemical hazards that will come from the products used. For this reason, it has become an important issue to reduce the chemicals released over time from the products that are constantly used in furniture industry. Medium density fiber boards (MDF) that are used different areas school, home, etc. is an important wood panel industry composite material consisting urea formaldehyde. Urea formaldehyde resin has an important use in wood panel industry. This resin is preferred because it is cheap and transparent but ıt has disadvantages. These disadvantages are low water resistance and high formaldehyde emission that is measured from MDF. As it known, formaldehyde has many negative effects on human health. One important among these is the increasing risk of cancer. In 2004 the Internal Agency for Research on Cancer (IARC) classified formaldehyde as harmful chemical for human body (Pizzi 1994).

[1] Süleyman Demirel University, Engineering Faculty, Chemical Eng. Department, Isparta, Turkey
* Corresponding author: a.ebru.0714@gmail.com

Formaldehyde is used in the production of urea formaldehyde resins used in the MDF industry and depending on the reaction conditions between urea and formaldehyde, some amount formaldehyde can remain in the environment without reacting. In addition this, some formaldehyde is released due to bond formation in the condensation stage of the resin, which develops during the pressing stage of the MDF production. Due to these reasons, some formaldehyde which is called free formaldehyde remains in the fiber board plate produced (Pizzi 1989).

Consequently, the use of formaldehyde on wood panels currently has been reduced to particular levels, regarded as not harmful to human health. Formaldehyde emission can be lowered by several methods. Several methods for producing low formaldehyde emission MDF panels have been studied, such as reducing formaldehyde to urea mol ratio and addition of formaldehyde scavengers in to resin. However mostly mechanical and physical properties of wood based panels have been affected badly. In addition to this, decreasing formaldehyde mol ratio causes to spread of curing time at MDF production. In this situation requires more energy and time. In the 21st century, where energy and time are important, this is an undesirable situation. The other factors affecting formaldehyde emission are wood type, resin type, type of hardeners, press conditions, amount of resin used in MDF production and storage time. Moreover, modifications of the resin with different amine containing chemicals are also important to reduce formaldehyde emission.

Activated carbons have been used as adsorbents in various fields, for instance, solvent recovery, gas separation, and deodorization. The activated carbon is characterized by a strong adsorption capacity which is attributed to its large internal surface area, porosity and high degree of surface reactivity. In related to this the use of activated carbon is one of the possible method to reduce formaldehyde emission (Kumar et al., 2013).

The use of activated carbon as formaldehyde absorbent has been analyzed by many researchers rayon based activated carbon as formaldehyde absorbent and activated charcoal have been used as bio-scavenger for decreasing formaldehyde emission from melamine formaldehyde resin.

As the relevance, in this work aimed to investigate the effect of activated carbon addition in to urea formaldehyde resin properties, formaldehyde emission values of MDF, mechanical and physical properties of MDF.

2. Materials and Methods

2.1. Materials

Urea and formaldehyde to be used in the resin synthesis was provided from AGT AĞAÇ SAN.TİC.A.Ş. Mixed wood fibers which contain of soft and hardwood fibers that were be used in the MDF productions were provided by AGT. The activated carbon powders that have 200 mesh particle size, 900-950 m^2/g surface area, iodine number greater than 900 and pH 8-10 were procured from ECS KİMYA.

2.2. Synthesis of urea formaldehyde resin

Urea formaldehyde resin synthesis basically; it is dived into two stages: an alkaline condensation stage in which mono-, di- and trimethylolureas forms are formed, and a condensation stage of the formed methylolureas in acid environment.

In the synthesis process, 45% industrial type aqueous formaldehyde solution and powdered urea have been used. The mol ration of formaldehyde/urea was taken as 1.04/1.00. Pure water was added by weighing powder urea in the appropriate mole ratio into three-necked glass reaction ballon flask assembly, then placed in heated magnetic stirrer unit and set to heat at 40 ºC. At this stage, the appropriate molar ratio of formaldehyde was added gradually and the pH of the reaction media was adjusted to 8.20 with 20% NaOH solution by weight. Reaction was continued at 40°C for 30 minutes. Then, for polycondensation, the pH was arranged with ~4.5 with formic acid. The reaction was continued at 90 ºC for 100 – 120 minutes by controlling flow time of resin with DIN Cup 4. Finally, while the resin was cooled to 70 ºC, its pH was adjusted to 8.5 and the reaction was continued for a while. Finally, vacuum drying was applied to the solution and resin was cooled to 40 °C, and the solid content of resin was reduced to 58% from %60 by weight.

In order for the synthesized 1.04 mol urea formaldehyde resin to cure sufficiently in the plate press stage, it must be used with a hardener. As the hardener 20% by weight aqueous ammonium chloride was used, constituting 4% by weight based on the resin solid content.

Table 1. Resin manufacturing parameters

Resin manufacturing parameters	
Parameters	**Values**
pH	8.20 ±10
Viscosity (cP@ 25°C)	160 cP±10 at 30 rpm
Flow time (second @ 25°C)	25±5
Gelation time (second)	60±5
Solid content (%)	58±1

2.3. Mixing of activated carbon with urea formaldehyde resin

To obtain a uniform dispersion of activated carbon powder in the urea formaldehyde resin, mechanical stirring with YOKEŞ VBR-600 high shear disperser mixer was done for 30 min at 1200 rpm by using cowls type blade. Activated carbon was added to the urea formaldehyde resin at 1%, 3% and 5% by weight according to the resin solid weight. The modified resin was named based on percent added as AC1, AC3 and AC5. AC0 indicates reference resin. AC0 shows that absence of activated carbon powder in the resin.

2.4. Characterization of physical properties of activated carbon containing urea formaldehyde resins

Viscosity measurements were done by Brookfield LV DV2T viscometer by using spindle no 1 at 30 rpm 25°C. Flow time measurements were done by DIN cup 4mm. Gelation time tests were done by using water bath at 100 °C with stirring according to related standard test method.

2.5. Preparation of medium density fiberboard and physical and mechanical testing

The resin free wood fibers (a mixture of 15% beech wood fiber + 85% pine wood fiber) with an average moisture content of 30% were dried in an ındustrial oven for approximately 6 hours until 2% - 4% humidity was achieved. Theoretically the amount of dry fiber was calculated and activated carbon added urea formaldehyde resin was weighed as 12% according to dry fiber amount. Activated carbon added resin was sprayed onto the wood fibers with the help of a mixer with a nozzle system, and a homogenous glue fiber mixture was tried to be obtained. After a 3 g of fiber sample taken from the resinated wood fiber mixture and analyzed in a moisture analyzer and, it was determined that it had an average moisture content of 9% - 10%, and this value was appropriate for pressing. The glued fibers that activated carbon added resin were transferred into a 40x40 cm mold with the help of a vacuum suction unit and the preform was formed before the press. Then, it was transferred to the IMAL PAL laboratory press unit and pressed with a pressure of 120 N/cm^2 for 326 seconds. Table 3 shows all the details of the MDF that contains activated carbon added resin and for reference MDF. The boards were then conditioned to attain uniform moisture content in panels. After that, the boards were cutted and tested according to related standard test method for determining of internal bond strength (EN 319), Edge screw holding resistance (EN 320), and surface soundness (EN 311). Physical tests of samples as thickness swelling and water absorption (EN 317), moisture content determination were done (EN 322). The mechanical properties of MDF panels were evaluated according to TS EN 622-5. Internal bonding tests and other mechanical tests were done with universal testing machine (IMAL IB800 Board property tester)

Table 2. MDF manufacturing parameters with different loading activated carbon

MDF manufacturing parameters	
Parameters	**Values**
Size	400*400 mm
Thickness	17 mm ± 1
Target density	740±20 kg/m^3
Press Pressure	120 N/cm^2
Pressing Time	326 seconds
Press temperature (for both top and bottom plate)	190 °C
UF resin wt % of dry wood fibers	12wt%
Activated carbon wt % of solid resin content	1%, 3% and 5%
Number of boards for each type of concentrations	4

2.6. Formaldehyde emission testing

The formaldehyde emissions from MDF panels were evaluated using the EN-120 (perforator method). 100 g sample were put in a round bottomed flask that contain the 600 ml of toluene. The 1000 ml of distilled water was poured into the perforator attachment. The samples were boiled with the toluene for 2 hours. In this test method the distilled water absorbs the formaldehyde and the volatile organic compounds captured by the boiling toluene. Formaldehyde trapped by the water is then quantitatively determined using UV spectrophotometer.

3. Results

3.1. Effect of activated carbon on the resin physical properties

As shown in the table 3, increasing with amount of activated carbon increases the viscosity of urea formaldehyde resin and extended the gelation time period.

Table 3. Resin properties with addition activated carbon

Sample	pH	Flow Time (second @ 25°C)	Gelation Time (second)	Viscosity (cP@ 25°C)	Solid Content (%)
Reference	8.15	20.00	53	164	58,76
AC1	8.30	20.12	66	174	59,12
AC3	8.52	23.91	88	197	59,69
AC5	8.63	25.13	96	227	60,15

The reactivity of the UF resin depends on the amount of free formaldehyde which produces more acidic during the curing process when the hardener is added (Moslemi 2020). The pH values in Table 3 are the values measured only with the activated carbon, without the addition of hardener. Gelation time test were done with adding the hardener ammonium chloride solution. Since the pH of the resin medium is high, we expect the gel time to be extended. This situation was parallel to the literature. The high pH value of the activated carbon increased the pH value of the resin and extended the gel time period even after the addition of hardener, since the environment was not acidic enough with the increasing concentration of activated carbon.

Resin flow time, viscosity and solid content increased with the addition of activated carbon. Increasing the resin viscosity and flow time will decrease the resin fluidity and cause a decrease in the adhesive property. This situation may cause weakening of the mechanical strength of MDF (Anjum 2020).

3.2. Physical and mechanical properties of MDF panels

Physical tests were done as water absorption and thickness swelling for 24h. For the water absorption tests, the test results for the MDF samples coded as AC0, AC1, AC3 and AC5 are respectively; it is 48.13%, 49.19%, 45.92% and 53.1%. The results are shown that in figure1.
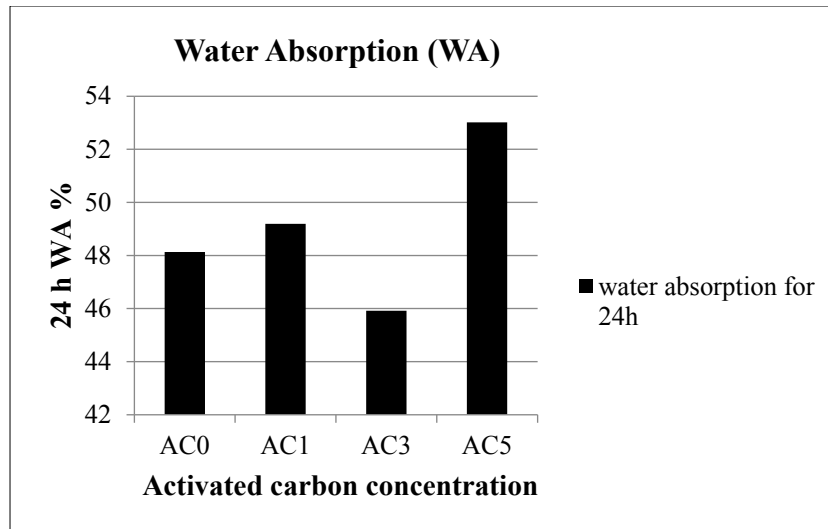
Figure 1. Water Absorption results of MDF panels

For the thickness swelling tests, the results for the MDF samples coded as AC0, AC1, AC3 and AC5 are respectively; as shown in figure 2, it is 19.48, 19.66%, 19.46% and 22.01%.
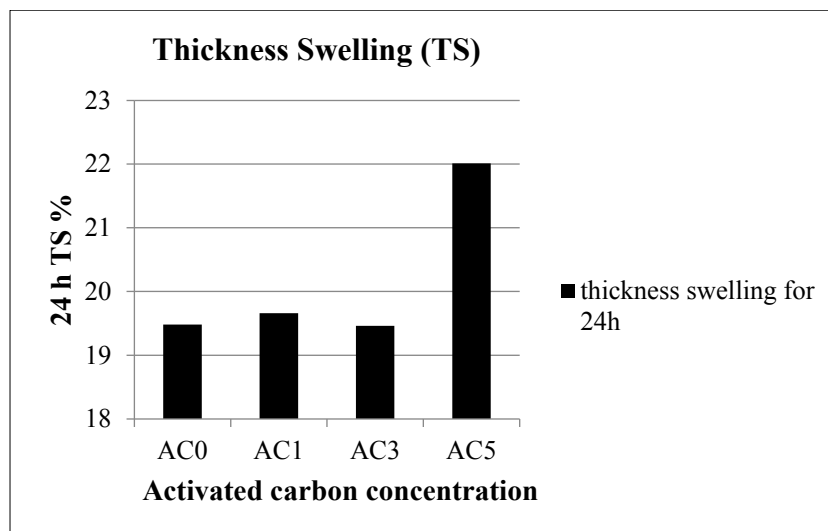
Figure 2. Thickness swelling results of MDF panel

When the results of MDF samples were evaluated, there was an increase of 0.91% in swelling value compared to the reference at 24 hours swelling tests with the addition of 1% activated carbon. There was a 10% decrease and 13% increase for the 3% and 5% concentrations respectively. Based on the results, it was observed that the addition of 1% activated carbon did not cause a significant increase in swelling value. Addition of 3% active carbon caused a decrease in swelling value. When all concentrations are evaluated ıt can be stated that the threshold value is 3% for the swelling test because the addition of 5% activated carbon negatively affected the swelling value of the system within increase of 13%. With the addition of activated carbon, the change in water absorption values at increasing values at increasing rates compared to the reference is an increase of 2.2%, a decrease of 4.6% and an increase of 10.4% respectively.

Table 4. Thickness swelling and water absorption values of MDF panels

Sample	Density kg/m^3	Moisture %	24 h TS %	24 h WA %
Reference	756.64	4.93	19.48	48.13
AC1	753.48	4.99	19.66	49.19
AC3	758.37	4.63	19.46	45.92
AC5	755.34	4.90	22.01	53.01

According to table 4 thickness swelling (TS) and water absorption (WA), activated carbon particle addition did not affect the moisture and density values of the MDF panels, and did not cause a significant change in TS and WA values. This was also observed in the study of in a literature (Kumar et al, 2013).

Mechanical tests were done as internal bonding resistance, surface soundness and screw holding resistance. For the internal bonding tests, the results for MDF samples coded as AC0, AC1, AC3 and AC5 are respectively it is 0.32 N/mm2, 0.34 N/mm2, 0.32 N/mm2 and 0.30 N/mm2. The results are shown in figure 3. The results for surface soundness tests are respectively 0.80 N/mm^2, 0.69 N/mm^2, 0.75 N/mm^2, and 0.84 N/mm^2. The results are shown in figure 4. For the screw holding resistance tests, the results for MDF samples coded as AC0, AC1, AC3 and AC5 are respectively it is 690.00 N, 737.50 N, 668.50 N and 660.75 N. The results are shown in figure 5.
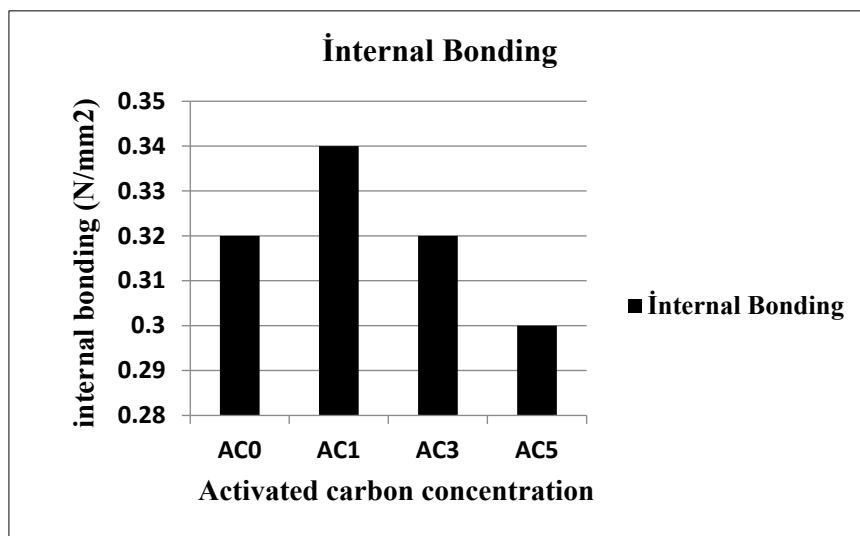

Figure 3. İnternal bonding results of MDF panels
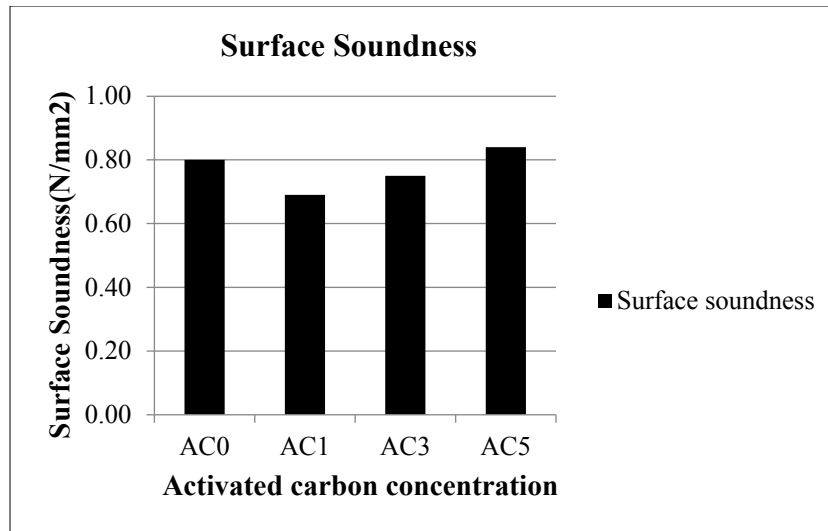
Figure 4. Surface soundness results of MDF panels
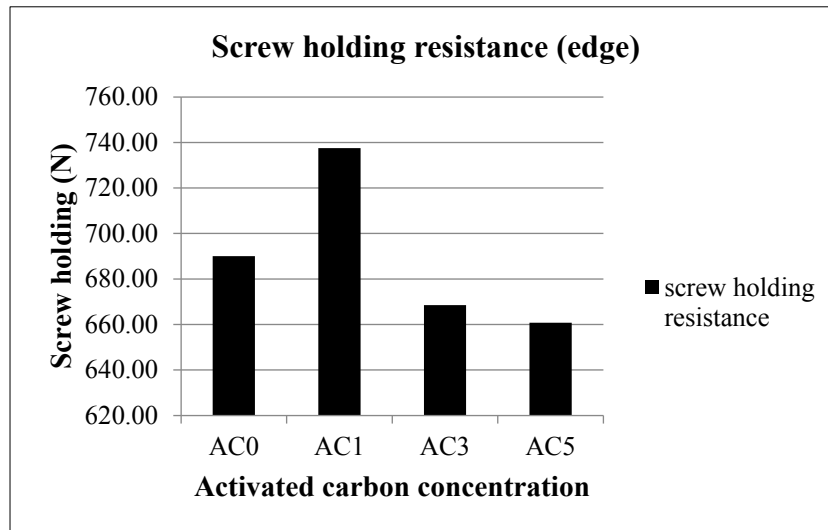
Figure 5. Screw holding resistance results of MDF panels

Mechanical tests were examined; there was a 6.25% increase in internal bonding values for the 1% concentration. With the addition of activated carbon at increasing concentrations for the 3% and 5% ratios, there was a 5.9% decrease and a 12.5% decrease in the internal bonding values, respectively. The screw holding resistance values are analyzed, an increase of 6.4%, a decrease of 3.1% and a decrease of 4.2% were observed, respectively compared to the reference at increasing concentrations. When the surface soundness test results are examined, it is 12.5% decrease, 6.25% decrease, 5% increase compared to reference at increasing rates respectively.

Based on the test results of MDF internal bonding strength, it can be deduced that MDF with less active carbon added mostly exhibits higher strength than control MDF. This can be explained by the fact that the incorporation of activated carbon in MDF fills the space between the fibers in the MDF, thereby intensifying the close contact of the fiber-carbon-fiber system, thereby strengthening the hydrogen bond and Van Der Waals forces. (Darmawan et al., 2010)

By holding the formaldehyde by the activated carbon, the free formaldehyde in the resin is prevented from escaping from the reaction medium during the curing of the formaldehyde. This strengthens cross-linking. However, the higher activated carbon loading (above 1%), results in less effective retention of formaldehyde due to the agglomeration of the activated carbon particles, the internal bonding strength is reduced. (Resmi et al., 2017)

3.2. Formaldehyde emission tests of MDF panels

Figure 6 shows the formaldehyde emission testing results by the perforator method. The formaldehyde emission tests were done with samples that having 5% moisture content. The value of formaldehyde emission of samples that are named as AC0, AC1, AC3 and AC5 are respectively 22.33, 10.60, 10.67 and 11.78 mg/100g board.
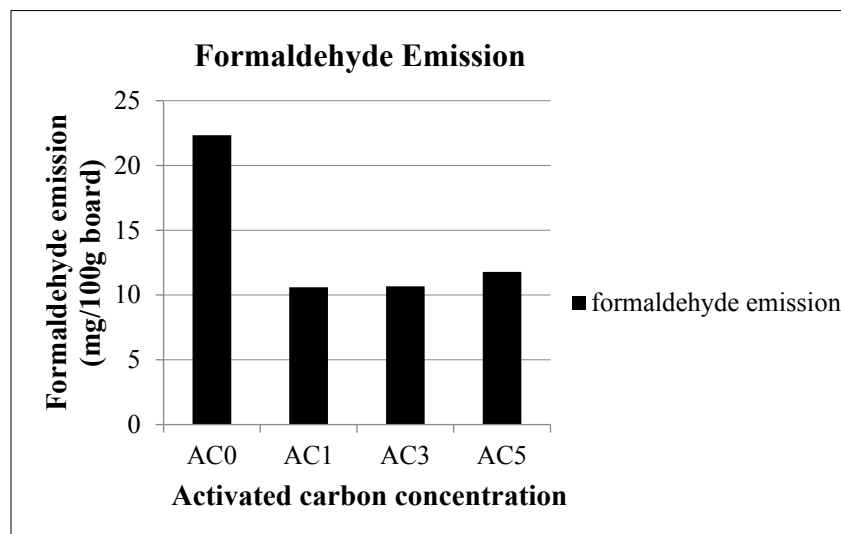
Figure 6. Formaldehyde emission results of MDF panels

According to formaldehyde emission test results, with the addition of activated carbon, a decrease of 52.5%, 52.2% and 47.2% was observed in the emission values, respectively.

That the addition of activated carbon into the resin system reduces the formaldehyde emission values for all concentrations was detected. Such lowering was caused by the capability of the microstructure of the activated charcoal to adsorb formaldehyde in the MDF (Rong et al., 2002; Pari et al., 2006). Further, the porous structure afforded greater surface area of the adsorbent (activated carbon) and the holding of the adsorbate (formaldehyde) by activated charcoal through the secondary force of hydrogen bonding as well as Van Der Waals type. This enhanced the intimate take-up of adsorbate on the surface of adsorbent, thereby intensifying the adsorption of formaldehyde by the activated carbon incorporated MDF.
Since the activated carbon used has an iodine number value of over 900 and surface area high that its adsorption capacity to be high based on the information in the literature was expected situation (Medek 2006)

4. Discussion and Conclusions

The main purpose of this study is to produce MDF panels that are sensitive to the environment and human health by reducing formaldehyde emission. For this reason, activated carbon, which is a good adsorbent due to its surface area and porous structure, was used as filler in the urea formaldehyde resin system. The study also aimed to protect the mechanical

and physical strength values while reducing the emission values. For this reason, the threshold value for the addition of activated carbon into the resin system has been tried to be determined.

In addition to the emission tests, when all mechanical and physical strength tests were examined, it was decided that the optimum activated carbon concentration was 1%. With the addition of 1% active carbon, the emission value was reduced, while the internal bonding strength, screw holding resistance were increased and a value close to the reference was obtained in surface soundness tests. For thickness swelling and water absorption values, we see that the addition of activated carbon does not cause a significant change compared to the reference.

References

Anjum A., Khan G.M.A.(2020) Effect of synthesis of conditions on the molecular weight and activation energy of urea formaldehyde prepolymer and their relationship. Journal of Eng. Advancements, 01(04), 123-129.

Darmawan S, Sofyan K, Pari G, Sugiyanto K (2010) Effect of activated charcoal addition on formaldehyde emission of medium density fiberboard. J For Res 7(2):100–111.

Kim S, Kim HJ, Kim HS, Lee HH (2006) Effect of bio-scavengers on the curing behavior and bonding properties of melamine–formaldehyde resins. Macromol Mater. Eng., 291(9):1027–1034.

Kumar A, Gupta A, Sharma K, Nasir M, Khan TA (2013) Influence of activated charcoal as filler on the properties of wood composites. Int J Adhesive, (46), 34–39.

Liu C., Luo J., Li X., Gao Q., Li J. (2018) Effects of compounded curing agents on properties and performance of urea formaldehyde resin. J. Polym. Environ. 26:158–165.

Medek J., Weishauptova Z., Kovar L., Micropor. Mesopor. Mater., 89, 276.

Moslemi A., K. Mohsen, Behzad T., Pizzi A. (2020) Addition of cellulose nanofibers extracted from rice straw to urea formaldehyde resin; effect on the adhesive characteristics and medium density fiberboard properties, International journal of adhesion and adhesives, 99(10), 25-82.

Pari G., S. Kurnia, S. Wasrin. (2006) Tectona grandis activated charcoal as catching agent of formaldehyde on plywood glued with urea formaldehyde. Proceedings of the 8th pacific rim bio-based composites symposium. Kuala Lumpur. Malaysia.

Pizzi A. (1983), Aminoresin Wood Adhesives in Wood Adhesives, Chemistry and Technology 59-104.

Pizzi A. (1994), Advanced Wood Adhesives Technology.

Resmi V.C., Narayanankutty S.K. (2017) Effect of charcoal on formaldehyde emission, mechanical, thermal and dynamic properties of resol resin. Int J Plast Technol 21(1):55–69.

EN 120, 1992. Wood based panels determination of formaldehyde content-extraction method called perforator method. European standard.

EN 317, 1993. Particleboards and fiberboards, Determination of swelling in thickness after immersion in water, CEN, Brussels.

EN 319, 1993. Particleboards and fiberboards. Determination of Tensile Strength Perpendicular to the Plane of the Board.

EN 322, 1993. Wood based panels, Determination of density, Brussels.

EN 311, 2002. Wood based panels, Surface soundness test method.

EN 320, 2011. Particleboards and fiberboards, Determination of resistance to axial withdrawal of screws test method.

Performance Analysis of FBMC-OFDM Waveform in Multipath Fading Channels

Halil Alptug Diver[1*], Kubilay Tasdelen[1*]

Abstract: In Fifth Generation (5G) wireless communication, in order to support different requirements, more flexile resource distribution is needed. To enable flexible resource distributions, different Orthogonal Frequency Division Multiplexing (OFDM) techniques are proposed such as, Filter Bank Multicarrier (FBMC), rather than conventional OFDM. FBMC techniques gives much more flexible resource distribution on time-frequency domain because in OFDM systems, through all used spectrum, the subcarrier spacing must be fixed. In this study, a new waveform of OFDM, which is FBMC, used in Wi-Fi and 4G technologies, which are the most common usage systems of communication technologies, and their usage areas are examined. In addition to the existing communication methods, there are researches on 5th generation communication systems and technologies beyond these and new waveforms for these systems. The study also includes simulations for doubly-selective channels and Bit Error Rate (BER) performance and Peak-to-Average Power Ratio (PAPR) analysis of conventional OFDM and FBMC waveforms in doubly-selective channel.

Keywords: OFDM, FBMC, PAPR, 5G and Beyond

1. Introduction

With the development of digital technology, the techniques used in communication technologies have begun to be developed to increase the speed values, as well as to keep the accuracy rates in data transfer high. In today's communication systems, OFDM modulation techniques in use have started to be used in Wi-Fi and 4G systems, which are the most popular systems, as well as being the subject of many researches. Since the OFDM waveform used in the aforementioned systems could not meet the demands for 5G and beyond, new waveforms have become one of the popular topics of current research. Within the scope of this study; The new waveforms in the literature and their comparison with the current OFDM waveform are presented with computer simulated studies.

Orthogonal waveforms used in 4G and LTE standards are called Cyclic Prefix-OFDM (CP-OFDM). In these waveforms, the last portion of the OFDM signal is placed at the beginning of the OFDM symbols, longer than the channel's delay spread, to avoid inter-symbol interference. However, repetition of the same data in this way reduces the efficiency. For example, a ¼ cyclic prefix (CP) length is used in Wi-Fi signals. This reduces the efficiency of the system by ¼, and waveforms such as Universal Filtered Multicarrier (UFMC) and Filter Bank Multicarrier (FBMC) are planned to be used in order to prevent this.

[one] Isparta University of Applied Sciences, Faculty of Technology, Electrical and Electronics Engineering, Isparta, Turkey
* Related Author: halildalgic@gmail.com

The current 4G multi-carrier technology, CP-OFDM, has many problems. The cyclic prefix in OFDM modulation technique is used to reduce multipath effects and hence inter-symbol interference (ISI) and inter-carrier interference (ICI), but the cyclic prefix reduces efficient spectral utilization. In addition, CP-OFDM has higher Out-of-Band (OOB) emission and higher PAPR than adjacent sidebands. Hence, two 5G waveforms UFMC and FBMC-OQAM are discussed here, which do not use circular prefixes and increase spectral efficiency. UFMC and FBMC systems consist of additional filtration that can reduce OOB emission. In addition, system performance is analyzed across different fading channels (Ravindran and Viswakumar, 2019).

To support high data rates in 5G and beyond, high-order modulations are intended to be used, so how the 256 and 1024 QAM modulations perform has also been studied in FBMC waveforms (Kamurthi, 2020). In the aforementioned study, it is aimed that new waveforms show the same bit error rate as existing OFDM waveforms. In this way, it is expected to exhibit the same performance as normal OFDM systems, eliminating the problems of different subcarrier lengths, PAPR, OOB emission and cyclic prefix.

In order to meet more flexible resource allocation in 5G and beyond communication techniques, the existing OFDM modulation technique is not sufficient. For this reason, an alternative technology called UFMC technique has emerged. In UFMC technique, Quadruple Amplitude Modulation (QAM) is used to avoid an orthogonality and is also suitable for Multiple Input Multiple Output (MIMO) technology. In his study, Kamurthi describes the performance of the UFMC modulation technique. In this article, 256 and 1024 QAM Mapping techniques were selected and PAPR values of 256-QAM and 1024-QAM techniques were observed in the simulation results, and PAPR values in the 1024-QAM technique were found to have low PAPR values. Therefore, 1024-QAM is the best mapping technique in the UFMC technique. In the article, the performance of the UFMC technique based on PAPR and spectrum usage was also evaluated. All PAPR and BER values for both 256-QAM and 1024-QAM are also included. Systems based on OFDM technique are vulnerable to high power amplifiers (HPA). Also, due to multi-carrier signal overlap, the 4G OFDM technique suffers from high PAPR. High PAPR causes non-linear distortion in high power amplifiers and it is concluded that UFMC multi-carrier technique also has high PAPR values, which indicates high power consumption. (Kamurthi, 2020) However, FBMC waveforms have a more complex structure than normal CP-OFDM systems, where various filters are used to give the same performance as CP-OFDM signals, these filters are also included in the Filter Bank. In the studies in the literature, it is aimed to reduce the complexity of FBMC systems and to create suitable filter banks.

FBMC/OQAM (Filterbank Multicarrier/Offset QAM) systems attract the attention of researchers due to their advantages over the classical CP-OFDM system. In this paper, a processing and synchronization scheme is developed for the promising FBMC/OQAM system. The proposed scheme is simulated, a plot of the dependence of the probability of a bit error on the signal-to-noise ratio is obtained. (An, Kim and Ryu, 2016, Doré, Gerzaguet, Cassiau and Ktenas, 2017, Abenov, 2019).

FBMC is one of the candidate modulation techniques for 5G and beyond communication systems due to the disadvantages of OFDM signals using cyclic prefix, OOB emission shortage etc. It was created as an alternative to the standard w-OFDM (windowed OFDM) waveforms used in current communication systems such as 4G, LTE and Wi-Fi. FBMC is provided to be used for more specific purposes by using different filters, for example, the

OOB emission problem can be solved in this way. It is a technique of filtering subcarriers. As with the normal OFDM technique, the cyclic prefix is not used and provides a better spectrum utilization. In the FBMC modulation technique, each subcarrier is filtered separately.

In this study, channel estimations and bit error rates of FBMC modulation technique in multipath fading channels were investigated and their BER performances were compared with normal OFDM systems. Similar bit error rates and PAPR results were obtained in the simulations. However, the filters used in FBMC modulation create more complexity in the receiver and transmitter than the OFDM technique.

2nd. FBMC-OQAM Modulation
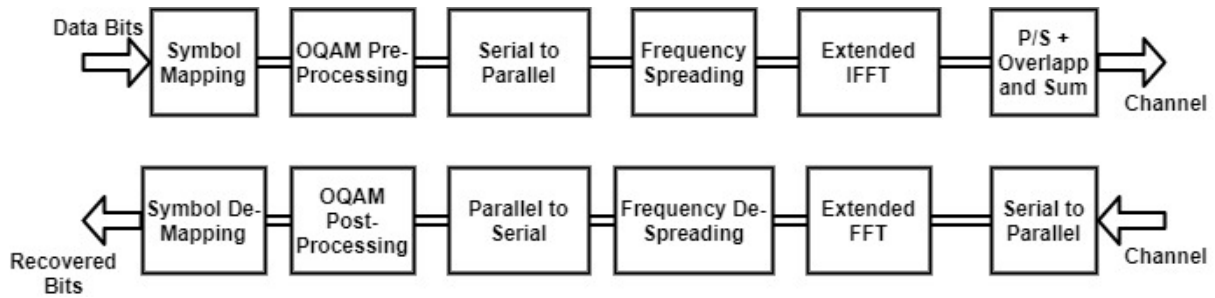
Fig. 1. Transmitter and Receiver Block Diagram of FBMC-OQAM Modulation

The fact that OFDM-OQAM modulation does not require the use of cyclic prefix provides an advantage in terms of spectral efficiency compared to CP-OFDM. Increasing the spectral efficiency can be achieved by modulating each subcarrier with a prototype filter/function without the need to add redundant shielding fields. Good localization of the prototype filter/function to modulate the subcarriers is important for the robustness/robustness of the channel variations. While the filter/function localization in time aims to limit the intersymbol interference, the localization in frequency aims to limit the intercarrier interference caused by the Doppler effect.

It is important that the orthogonality between subcarriers is preserved after modulation. OFDM modulation using localized filters/functions that only guarantee orthogonality over the real values is called OFDM-OQAM.

Each subcarrier in the OFDM-OQAM method carries real-valued symbols part $(a_{m,n})$ corresponding to the real or imaginary part $(s_{m,n})$ in a complex OFDM symbol; m is the frequency index, n is the time index. (El Tabach, Javaudin and Hélard, 2007)

Mathematically, FBMC signals can be expressed as the following equations. (1)(2)

$$s(t) = \sum_{n=-\infty}^{+\infty} \sum_{m=0}^{M-1} a_{m,n} i^{m+n} e^{2i\pi\Delta Ft} g(t - n\tau_0) \tag{1}$$

$$s(t) = \sum_{n=-\infty}^{+\infty} \sum_{m=0}^{M-1} a_{m,n} g_{m,n}(t) \tag{2}$$

Here $g(t)$, is defined as the pulse shape filter in the transmitter and must satisfy the underlying equation for orthogonality (3).

$$Re\left(\int g_{m,n}(t)g^*_{m_0,n_0}(t)\,dt\right) = \delta_{m,m_0}\delta_{n,n_0} \tag{3}$$

$$g_{l,k} = p(t - kT)e^{j2\pi lF(t-kT)}e^{j\frac{\pi}{2}(l+k)} \tag{4}$$

In Equation (4), $g_{l,k}$ is a time and frequency shifted filter of $p(t)$. Time shift in here is T, the shift in frequency is F. $p(t)$, the prototype filter was derived from Hermite polynomials (Haas, Belfiore, 1997)

$$p(t) = \frac{1}{\sqrt{T_0}}e^{-2\pi\left(\frac{t}{T_0}\right)^2}\sum_{i=\{0,4,8,12,16,20\}}c_iH_i(2\sqrt{\pi}\frac{t}{T_0}) \tag{5}$$

In Equation (5) $p(t)$ filter, c_i values that will provide orthogonality at $T = T_0$ in and $F = 2/T_0$, were obtained.

2.1. System Model

To test the FBMC and OFDM modulations in doubly-selective multipath and Gaussian noise channels, a simulation model was established. The parameters of this Model are given in Table 1.(Chiavaccini and Vitetta, 2000)

Table 1. Simulation Model Channel Parameters

Carrier Spacing	15kHz
SNR Range	10: 5: 40
Number of Sampling	2940000
Number of Subcarriers	196
Number of Active Subcarriers	24
FBMC Prototype Filter	Hermite
Doppler Frequency	Hazrat
Channel Model	Pedestrian A
Carrier Frequency	2.5GHz
OFDM Symbol Count	14
FBMC Symbol Count	30

A single-input and single-output channel is modeled. The channel parameters used in the simulation are shown in Table 1. For this channel model, both BER performances and PAPR analyzes of FBMC and OFDM signal structures were performed (Al-Jawhar, Ramli, Taher, et al, 2021). It is assumed that the receiver knows the channel and one-tap channel equalization is done in the receiver.

3. Results

3.1 BER Results in Multipath Channel

In this chapter, FBMC and OFDM signals are tested for 16, 64 and 256 QAM modulations and channel estimation is made by performing one-tap channel equalization on the receivers. The Pedestrian A channel model was used as the channel type and it was assumed that the receiver and transmitter were fixed, that is, the Doppler frequency was zero.
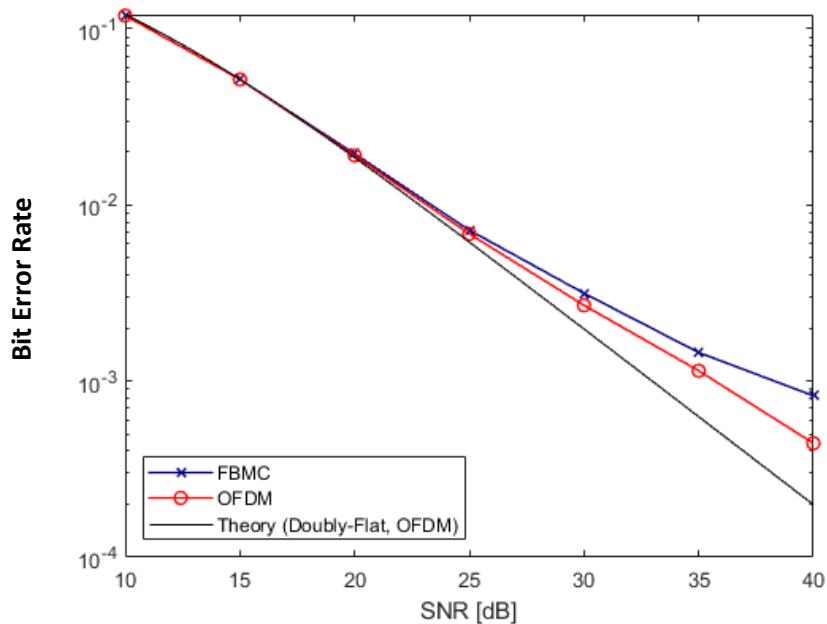
Figure 2. OFDM vs FBMC 16-QAM BER Performances
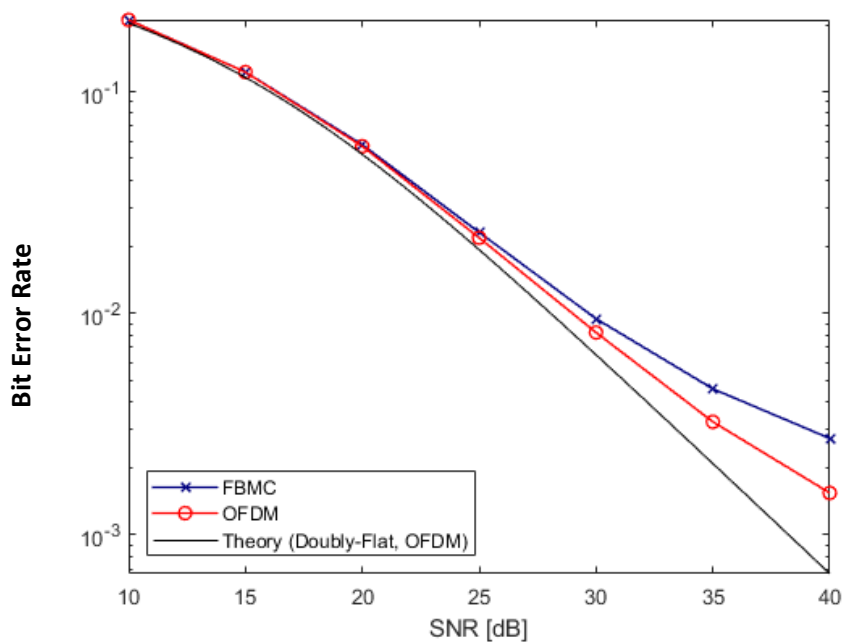
Figure 3. OFDM vs FBMC 64-QAM BER Performances
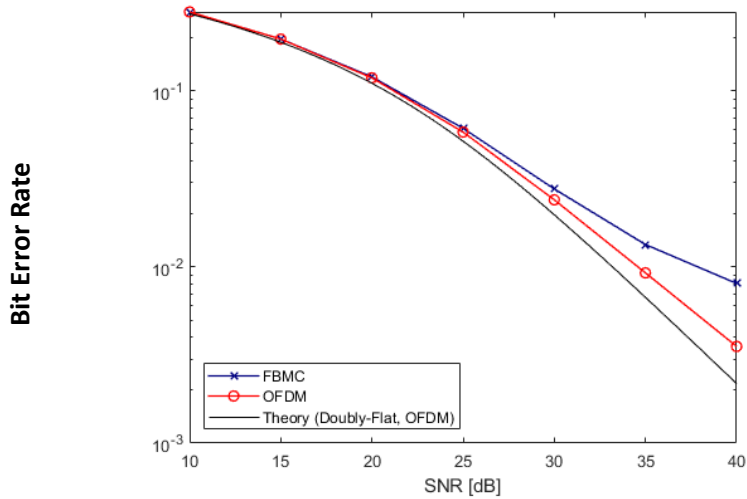
Figure 4. OFDM vs FBMC 256-QAM BER Performances

As seen in Figure 2, Figure 3 and Figure 4, FBMC waveforms performed very closely with OFDM waveforms. By not using circular prefixes, a greater resource usage is achieved. Since channel codes are used in traditional communication systems, this small BER difference between them can be eliminated by channel coding.

3.2 FMBC and OFDM PAPR Analysis
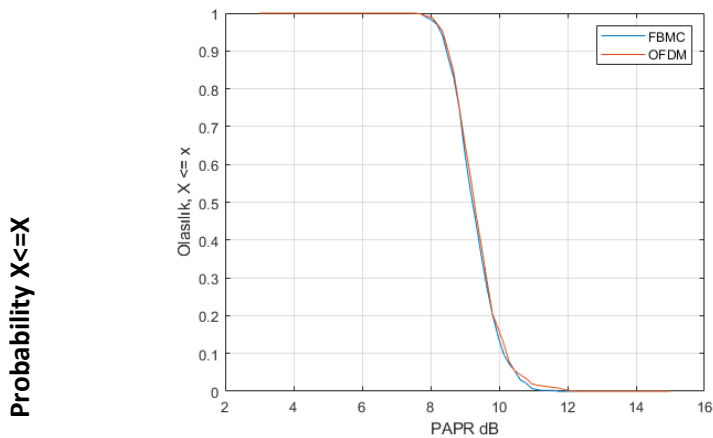
Figure 5. OFDM vs FBMC 16-QAM PAPR
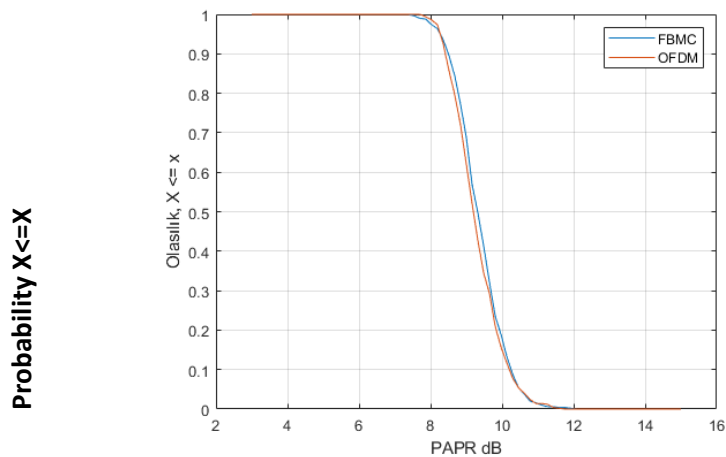
Figure 6. OFDM vs FBMC 64-QAM PAPR
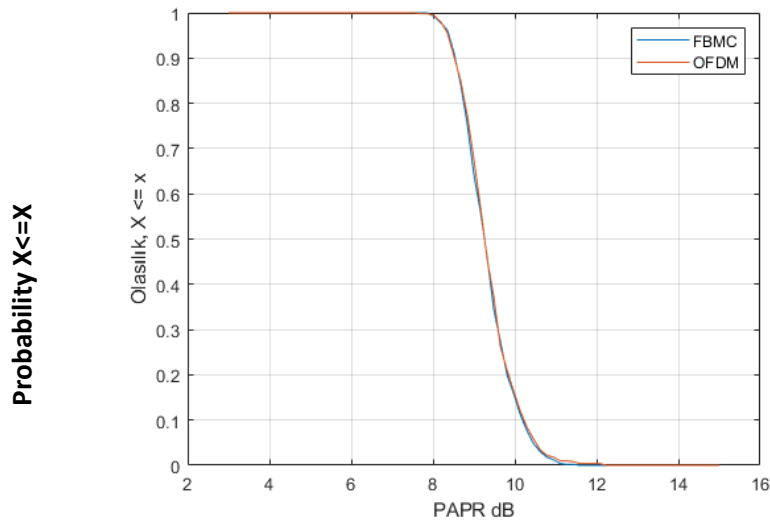
Figure 7. OFDM vs FBMC 256-QAM PAPR

In Figure 5, Figure 6 and Figure 7, PAPR analyzes of OFDM and FBMC waveforms were performed with CCDF (Complementary Cumulative Distribution Function) graphs. In these graphs, the PAPR performance of both waveforms is observed to be the same. This means that both waveforms will perform similarly when using a non-ideal amplifier.

4. Evaluation And Conclusion

For Doubly-Selective channels, FBMC can provide almost the same performance as normal OFDM. It seems appropriate that different wave models can be used, especially in the middle SNR region, according to their intended use. Considering the sector needs and complex structures, it will already be the subject of researches of future communication technologies since the new waveforms can be used in different channel models as OFDM alternatives in different areas. In the selected channel model, the scenario chosen is one of the most realistic scenarios in terms of the time resolution of the channel impulse responses. In this context, considering that the study is performed in 64-QAM OFDM sub-modulation, 10^{-1} BER performance around 15 dB is sufficient. In future studies, real-time performances of low-subcarrier OFDM systems such as Wi-Fi protocols with the help of SDR should be examined with FBMC waveforms.

References

Abenov, R. R., Pokamestov, D. A., Rogozhnikov, E. V., Anatoliy, D. Y., & Kryukov, Y. V. (2019, October). FBMC/OQAM Equalization Scheme with Linear Interpolation. In 2019 International Multi-Conference on Engineering, Computer and Information Sciences (SIBIRCON) (pp. 0130-0133). IEEE.

Al-Jawhar, Y. A., Ramli, K. N., Taher, M. A., Shah, N. S. M., Mostafa, S. A., & Khalaf, B. A. (2021). Improving PAPR performance of filtered OFDM for 5G communications using PTS. ETRI Journal, 43(2), 209-220.

An, C., Kim, B., & Ryu, H. G. (2016, December). Waveform comparison and nonlinearity sensitivities of FBMC, UFMC and W-OFDM systems. In 8 th International Conference on Networks & Communications (pp. 83-90).

Chiavaccini, E., & Vitetta, G. M. (2000). Error performance of OFDM signaling over doubly-selective Rayleigh fading channels. IEEE communications letters, 4(11), 328-330.

Doré, J. B., Gerzaguet, R., Cassiau, N., & Ktenas, D. (2017). Waveform contenders for 5G: Description, analysis and comparison. Physical communication, 24, 46-61.

El Tabach, M., Javaudin, J. P., & Hélard, M. (2007, June). Spatial data multiplexing over OFDM/OQAM modulations. In 2007 IEEE International Conference on Communications (pp. 4201-4206). IEEE.

Haas, R., Belfiore, J. C. (1997). A time-frequency well-localized pulse for multiple carrier transmission. Wireless personal communications, 5(1), 1-18.

Kamurthi, R. T., Chopra, S. R., & Gupta, A. (2020, March). Higher Order QAM Schemes in 5G UFMC system. In 2020 International Conference on Emerging Smart Computing and Informatics (ESCI) (pp. 198-202). IEEE.

Ravindran, R., & Viswakumar, A. (2019, November). Performance evaluation of 5G waveforms: UFMC and FBMC-OQAM with Cyclic Prefix-OFDM System. In 2019 9th International Conference on Advances in Computing and Communication (ICACC) (pp. 6-10). IEEE.

The normative regulations, legislation and standards on the control and preservation of electronic records in the northern countries of Europe

Lana Žaja[1]*

The northern countries of Europe, namely: Iceland, Norway, Sweden, Finland, Denmark, Lithuania, Latvia and Estonia, have taken the lead in developing their own standards and thus carry significant weight in the development of archival legislation and other similar normative regulations. Normative frameworks are key elements in the safeguarding of electronic records. Within this framework, archives are faced with the issue of record control, as well as the construction of an IT infrastructure that must preserve downloaded electronic records in the long run. The Open Information Archive System (OAIS) reference model and international ISO standards provide solutions to the presented tasks and are the major models that underpin the development of record architecture in northern Europe. The aforementioned digital archives are developed in a modular fashion to allow the development of each IT section separately. For example, sections such as: receiving digital records, the physical storage of records, record management and access to records, must be modularly separated to ensure long-term usability and the possibility of implementing technological upgrades. By adapting their own standards to legal requirements and international standards, these countries continuously create and maintain the ideal conditions for long-term archival record keeping.

Keywords: electronic records, standards, norms, legislation, northern European countries.

1. Introduction

Governments around the world, with the help of archives, increasingly scrutinize private, public and governmental bodies through normative regulations, legislation and standards. Electronic data laws are a growing challenge and they must comply with various legal and enforcement rules. Understanding and complying with regulations can be a challenging task, like treading through a minefield while harmonizing regulations with standards. The northern countries of Europe have a regulatory regime in which various stakeholders are required to deliver information on a variety of media, while following standardized instructions. Data and content standards set out requirements with which public authorities must comply. This poses a challenge for long-term access to information. Compliance with laws and standards is the focus of data control and archives are now facing the task of constructing an IT infrastructure that preserves downloaded electronic records for long-term periods. In the specific Croatian example, Vlatka Lemić presented the experiences of Scandinavian countries with regard to electronic records,[1] because their example is an interesting and advanced system in terms of

---

[1] Lemić, V. (2003). *Archives and electronic records – experiences of Scandinavian countries.* Croatia. Bulletin d'archives. 46(1), pp. 179-207. URL: https://hrcak.srce.hr/7378. (09.12.2019.)

[1] Croatian State Archives, Zagreb, Croatia
* Corresponding author: lanazaja@gmail.com

drafting laws and standards tailored to the needs of their own state apparatus. A similar paper, authored by L. Žaja in 2019, included research into the establishment of digital archives and the policy of long-term preservation of digital records in selected national archives of EU countries. The aim was to investigate the policies and practices of digital preservation of all types of records in publicly available data and strategic documents in the archives of Austria, Belgium, France, Croatia, Italy, Germany, Poland, Slovenia and the United Kingdom.[2] Using relevant standards helps digital archives harmonize different electronic systems inter-institutionally. Compliance with standards also enables digital archives to continuously audit the certification for managing digital information systems. Standardization and certification contributes to competitiveness, as well as enhancing the image of archives in the sense of a reliable and organized partner. It is beneficial from a marketing standpoint and provides a guarantee for the safe handling of records and sensitive (classified) data within precisely defined responsibilities and authorities. David Giaretta,[3] was chairman of the panel that produced the reference model OAIS (ISO 14721),[4] accepted today as the de facto standard for building digital archives, on which most northern European countries rely. His organization also leads a group that has developed an ISO standard for auditing and certifying digital repositories ISO 16363: 2012.[5] At the Faculty of Humanities and Social Sciences of the University of Zagreb (Croatia), the scholarship on digital archives is being refined and continuously developing under the leadership of Professor Hrvoje Stančić, PhD – Head of the Department of archival and documentation sciences,[6] Department of Information and Communication Sciences.[7] Although northern European countries are leading the development of their own standards, they rely heavily on internationally proven standards to ensure the best possible quality, which they then further develop with their own scientific and information resources. This is particularly evident in the example of the National Estonian Archives, which uses the OAIS reference model for its records architecture and the National Archives of Latvia, whose original standards are based on international ISO standards.

Iceland

The Icelandic Public Archives Act[8] (2014) prescribes the obligation to transfer all types of records and the right to make information accessible. Records covered by the transfer obligation must be submitted to the public archive when they reach the age of 30 years.

---

[2] Žaja, L. (2019). *Digital preservation policy in publicly available data and strategic documents on the websites of selected national archives of European Union countries.* 51. Counseling of the Croatian Archivist Society: Management of Electronic Material and Contemporary Archival Practice. Croatia. Slavonski Brod., pp. 147-169.

[3] Giaretta Associates Ltd. URL: http://giaretta.org/digital-preservation/standards/. (09.12.2019.)

[4] Reference Model for an Open Information Archival System OAIS. URL: https://public.ccsds.org/pubs/650x0m2.pdf. (09.12.2020.)

[5] Space data and information transfer systems — Audit and certification of trustworthy digital repositories. ISO 16363: 2012. URL: https://www.iso.org/standard/56510.html. (09.12.2020.)

[6] Stančić, H. (2005*). A theoretical model of the persistent preservation of the authenticity of electronic information objects.* Doctoral thesis. University of Zagreb. Faculty of Philosophy. Croatia. URL: https://bib.irb.hr/datoteka/244465.Ocuvanje_autenticnosti_e-informacijskih_objekata.pdf. (10.12.2020.)

[7] Lectures of Prof. Stančić at graduate studies level: Digital Archives, Archival Legislation, Digitization and Migration of Documents, Digitization of 3D Objects and Spaces, Planning and Design of Material Management Systems, Management and Business in Archives and Protection of Electronic Material. Lectures of prof. Stančić at postgraduate study: Disruptive technologies and long-term preservation of e-content and Preservation of digital record authentication. URL: https://inf.ffzg.unizg.hr/index.php/hr/odsjek/katedre/arhivistika-i-dokumentalistika. (10.12.2020.)

[8] Icelandic Public Archives Act. URL: https://skjalasafn.is/files/docs/ThePublicArchivesAct-in-Iceland-No-77-2014.pdf. (27.11.2019.)

However, electronic and digital records are generally submitted no later than 5 years. In both cases, the date of the reference is the date of the last metadata entered or last entered in the closed case. The „Rules on Electronic Public Data and Data Delivery"[9] comprise a set of rules on electronic data systems used by institutions which are obligated to provide their data. Government bodies that intend to store their information in electronic form must comply with these rules, including notifying all electronic systems in which the data are stored. The brief instructions on electronic archiving outline two basic rules that a provider must report to the electronic archive data system. Archival electronic data systems are defined by the electronic institution filing system described in the first rule and submitted to the archive together with the electronic files / databases as defined in the second rule. The notification of data submission must be sent to the archive in electronic form according to the attached forms. The archives must receive the submitted documentation within one month after notification. The documentation is described in the electronic filing systems with a description of how the data is searched, the rules for using the electronic system, and a technical description of the data structure in that system. If the system will not be used as a relational database, the notice must also include a statement that the submitted version can be transformed into a relational database in accordance with the rules of the National Archives of Iceland,[10] which provide information on the electronic data systems of those institutions subject to the delivery data.

Norway

The Norwegian Archives Act,[11] in force since 1999, together with additional regulations, provides a complete legal framework for all issues related to archival affairs in public administration from the original creation of records to the operational documentation of day-to-day business. The differences in regulations for paper and electronic records relate to differences in the management and transfer to storage. The Rulebook on Supplementary Technical and Archival Regulations for the Treatment of Public Archival and Documentary Materials[12] (archival regulation of the Norwegian Archives) states the requirements for the system of archiving and electronic processing of archival records in Chapter 3. These requirements are in fact instructions describing the responsibilities, protocols and legal rights associated with the creation, receipt, exchange, maintenance and use of archives. They describe the following responsibilities and procedures: responsibility for assigning and updating user rights; special rights for processing archival material granted to system users with assigned roles, types of authentication and signatures for documents, as well as rules and procedures for signing documents, including the use of a digital signature; responsibilities and procedures for secured quality filing and responsibilities and procedures for recording the sending and receiving of archived documents. With regard to the requirements for document formats and functions for export to the electronic archive system, it indicates that electronic archive documents are stored in one or more document formats that are specified in separate chapters. This does not apply to documents that can be destroyed after 10 years or less. After completing the process, the institution must confirm that the conversion to the default archive format has been completed correctly and that the documents are legible. The National

---

[9] Icelandic electronic documentation. URL: https://skjalasafn.is/rafraen_skjalavarsla. (27.11.2020)

[10] Iceland National Archives. URL: https://skjalasafn.is/. (10.10.2020.)

[11] Norwegian Archives Act. URL: https://www.arkivverket.no/forvaltning-og-utvikling/regelverk-og-standarder/lover-og-forskrifter-for-arkiv/arkivloven. (7.11.2020.)

[12] Norwegian Ordinance on Supplementary Technical and Archival Regulations for the Treatment of Public Archival and Documentary Records. URL: https://lovdata.no/dokument/SF/forskrift/2017-12-19-2286#KAPITTEL_3. (27.11.2020.)

Archives of Norway[13] provide that systems that store electronic archival documents have such export functions that ensure that the stored electronic records can be transferred to another system or submitted to the archive. When exporting data for delivery or storage, this system must comply with the requirements set by the archive. This provision does not apply if all records in the system are allowed to be extracted after 10 years or less, in accordance with the Archives Act. Regarding the storage and safe preservation of records, protocols have been drawn up with the following guidelines: the storage media and formats for use have been specified for the types of records to be submitted electronically, as well as the statutory forms for those records. These must be submitted in paper form. Responsibilities and procedures for converting records to the default format include conversion times, guidelines for the disposal of archived paper and electronically digitized records. Furthermore, the plan includes the preparation of records, which should be transferred to the archives by implementing protocols and safeguards that include information security. Noark[14] is the name for the Norwegian Document Management Standard. This standard was developed by the Norwegian State and its National Archives. All government agencies must use Noark approved systems for record keeping and electronic filing. Noark 5 is the latest release of the Noark standard and was officially released in 2008. Noark 5 is a conceptual standard where its technical application is left to the open market, and the quality of individual solutions in various sectors is not controlled by the archive itself. This standard specifies the type of information that should be processed, but does not specify any technical specifications. Therefore, when public authorities procure new records management systems, it is important to differentiate what the archive approval system includes and what the company must control in the procurement process. Noark 5 archive approval is displayed so that the system is logged in and that further updates to the standard are granted. Final approval is based on a vendor statement, which is ultimately the most important document when purchasing an electronic database system. The buyer of this solution must then determine which requirements he wants and test them so that they fulfill all the specified functions of the electronic system.

Sweden

The Swedish National Archives regulations[15] are binding for all government bodies which hold various types of records. With the support of the Archives Act and other segments of archival regulation, the regulations regulate, among other things, how records are created, organized, evaluated, processed, stored, protected and submitted to the archive. General regulations and general advice of the National Archives of Sweden[16] have been published in the National Archives Collection RA-FS.[17] The regulations are generally applied by all government agencies, including individual bodies that hold public records and documents, but there are several regulations in the series RA-FS intended only for a specific group of authorities and this is stated in the title of the regulation. The rules are set out in the following way:
1.   Rules specific to procedures in different types of media. This applies to electronic, digital, paper or microfilmed records.

---

[13] National Archives of Norway. URL: https://www.arkivverket.no/. (10.10.2020.)

[14] NOARK – Norwegian Document Management Standard. URL: https://www.arkivverket.no/forvaltning-og-utvikling/noark-standarden. (27.11.2020.)

[15] Swedish Archival Regulations RA-FS i RA-MS. URL https://riksarkivet.se/offentlig-forvaltning. (28.11. 2020.)

[16] National Archives of Sweden. URL: https://riksarkivet.se/startpage. (10.10.2020.)

[17] Swedish General Regulations RA-FS. URL: https://riksarkivet.se/generella-foreskrifter. (28.11.2020.)

2. Technical regulations pertaining to requirements for different media, such as requirements for formats for keeping electronic records or for hard-copy archives. These regulations should always be read in conjunction with specific media practices.

3. Regulations on archival repositories can be found in a separate section of the RA-FS on the planning, execution and operation of archival repositories (RA-FS 2013: 4).

4. The general regulations for the extraction and destruction of records in the RA-FS series deal with the operational or current documentary material available to all or most state agencies. Much of this regulation concerns the elimination of documentary material with specific retention periods for financial, personnel, procurement and application documents. The basis of this regulation is the records of universities and colleges on research and project cooperation with the EU. By applying general rules, public authorities in their activities must document the actions of, for example, an internal implementation decision.

Regulations on the management of archives relating to competent archival data are included in a separate series of titles RA-MS.[18] So, this is a series that involves administrative powers related to both managing, extracting and destroying records. These decisions are for a specific body or group of authorities. The structure of the RA-MS regulation is used in the following cases:

1. Reducing the scope („thinning") of material that is not covered by the RA-FS General regulations. The most common case of such treatment is the return of records to the applicant as an alternative to disposal.

2. Exceptions to the General Rules (i.e. exceptions to the RA-FS) apply to the design of archival repositories or formats for electronic documents. In certain cases, the National Archives may prescribe exceptions for "thinning out", i.e. keeping those records that would otherwise be extracted in accordance with the recommendations of the Constitutional Register.

3. Lending or depositing of records to the competent archives (instead of handover).

The Technical Committee of the Archives participated in the work with the International Organization for Standardization ISO,[19] as well as with special professional bodies such as the International Council on Archives ICA,[20] the Society of American Archivists SAA,[21] the Document lifecycle management DLM,[22] and Research Libraries Group RLG.[23] RLG has developed guidelines for Trustworthy Repositories,[24] where the idea is that institutions which meet the high standardized requirements for advanced digital storage have the ability to audit with a trusted storage certificate, while the National Archives is still exploring options for certification. ICA has developed de facto standards for describing archival records. Furthermore, these de facto standards were developed in order to address everything from questions about the structure of an electronic system to the interconnection of metadata and digital preservation objects. SAA develops its work on standardization by working with some de facto standards that have proved useful for inter-archival cooperation. Once a year, a meeting is held at which relevant working groups share experiences about what the annual reports should cover. The Technical Committee participates and develops international and national standards relating to many aspects of business information management such as:

---

[18] Swedish General Regulations RA-MS. URL: https://riksarkivet.se/ansok-om-gallring. (28.11.2020.)

[19] International Organization for Standardization ISO. URL: https://www.iso.org/home.html. (27.11.2020.)

[20] International Council on Archives ICA. URL: https://www.ica.org/en. (8.11.2020)

[21] Society of American Archivists SAA. URL: https://www2.archivists.org/. (28.11.2020.)

[22] Document lifecycle management DLM. URL. https://www.webpdf.de/blog/en/dlm-document-lifecycle-management/. (18.11. 2020.)

[23] Research Libraries Group RLG. URL: http://www.rlg.org/. (28.11.2020.)

[24] Giaretta, D. (2011). *Advanced Digital Preservation*. ISBN 9783642168086.

archive records, preservation, archiving, metadata, conversion formats, the migration of information, digitization and security risk management, accountability, copying and designing work processes. This Committee also works to ensure that standards are applied to their full extent in Sweden, for example by authorizing public bodies to process inquiries in a way that is then usable for certification.

Finland

The implementation of comprehensive reform of archival legislation was crucial in reforming the National Archives Service.[25] The following laws are currently in force in Finland: The Archives Act[26] (1994), the Electronic Communications Act[27] (2003), the State and Private Archives Act[28] (2006), the Act on State Aid to Private Archives[29] (2006), the National Archives Act[30] (2016), and the Government Ordinance on State Archives[31] (2017). In accordance with the new National Archives Act and the Government Ordinance, the name of the National Archives was changed to the State Archives (in Helsinki), and the regional archives are the offices of the State Archives. The name Arhiva Sámija was retained, it being a part of the National Archives, and whose special duty is to be the „keeper of the documentary cultural heritage of Sam". These regulations removed the outdated model of the county administration and the inefficient use of the resources of the National Archival Office in a situation where appropriations were being reduced. The proposed legislation on private archives would make cooperation between the National Archives of Finland and private archives funded from the national budget more efficient as the regulation of functions has been specified and this fosters development that is mutually beneficial.[32] The decision to build a joint central archival facility, as well as the right to reasonably destroy the digitized documents, enables the storage of analogue records. The implementation of the comprehensive digitization project for permanent records eliminated the need to build more archival facilities suitable for permanent storage after the completion of the central archive. The achievement of strategic goals was evaluated by the self-assessment conducted in 2017 and 2018. Based on these evaluations, an international assessment for the remaining strategic period was the basis for recommendations and guidelines which will be used in the planning of the forthcoming strategy leading up to the year 2025. The permanent storage of records relating to the screening strategy is ensured by various sufficiently standardized processes that are conditionally controlled according to the research stages. The goal of record management is to ensure lasting preservation, usability and availability, and the primary focus is on managing the entire record life cycle in an electronic operating environment. The structured data included in information systems is also available separately, in line with the goals of

---

[25] Strategy of the National Archives of Finland 2020. URL: https://www.arkisto.fi/en/the-national-archives-2/copy-of-strategy-2020. (2.10.2020.)

[26] Law on the Archives of Finland. URL: http://www.finlex.fi/fi/laki/ajantasa/1994/19940831 (2.11.2020.)

[27] Electronic Communications Act of Finland. http://www.finlex.fi/fi/laki/ajantasa/1994/19940831. (02.12.2020.)

[28] Law on the Private and National Archives of Finland. URL: http://www.finlex.fi/fi/laki/ajantasa/2006/20061006. (2.11.2020.)

[29] Law on state aid to the private archives of Finland. URL: http://www.finlex.fi/fi/laki/ajantasa/2006/20061006. (2.10.2020.)

[30] Law on the National Archives of Finland. URL: http://www.finlex.fi/fi/laki/alkup/2016/20161145. (2.10.2020.)

[31] Government Ordinance on the National Archives of Finland. URL: http://www.finlex.fi/fi/laki/ajantasa/2017/20170039. (2.11. 2020.)

[32] National Archives of Finland. URL: https://www.arkisto.fi/. (10.10.2020.)

open public information. The Finnish Archives promote electronic archiving within public administration by determining which records are of lasting importance. The contents of records relating to basic administrative functions shall be permanently stored in digital form. The amount of permanently stored analogue records in the possession of the public administration is evaluated in such a way as to allow the transmission cycle to be transferred to new media. The final point is that analogue records transferred to permanent storage must be digitized as part of the process of the transfer itself. Institutions responsible for the transfer of records are also responsible for the costs of digitization. At the same time, the proportion of documentation stored in analogue format is evaluated. Digitization, in addition to improved record accessibility, leveled the functional bridge between the analogue and the original digital record. An international survey is currently underway for evaluating the criteria for the disposal or preservation of digitized records and records of permanent value in analogue form, which is part of the international practice of preserving and permanently storing analogue records. Analog records will not be destroyed before the completion of the survey and the preparation of the final report. The ultimate goal is to have 80-90% of the records transferred to new media, to be disposed of in permanent storage or destroyed in accordance with the retention periods.

Denmark

The Danish Ministry of Culture manages the National Archives. The powers of the Minister in connection with the archiving activity of public authorities are defined by the Archives Act of 1992,[33] which has been modified three times, in 1997, 2000 and 2007. The provisions of the Act on Management of Records of State Bodies apply to all activities carried out by public administration bodies and the judiciary. However, rules and regulations differ from one type of government to another. Therefore, only state bodies, courts and categorized institutions are required to submit records to the National Archives of Denmark.[34] The law further authorizes the Minister of Culture to determine the rules and regulations relating to the handover of records to archives. Finally, the Minister of Culture is empowered to determine that in certain circumstances the rules and regulations governing archives may apply to certain private companies, institutions and associations that are not considered as part of the public administration. Specific provisions relating to the activities of the Danish National Archives are laid down in the Executive Order on Archives signed by the Minister of Culture. This order stipulates that the State Archivist has the authority to issue further rules, guidelines and regulations on the following: the downloading of records by state bodies, including approval and entry into the archiving system; installation, design, restriction and operation of the filing system; measures to ensure that electronic filing systems are independent; technical requirements for archival records in various media relating to the storage of records; evaluation of government bills; time limits for the transfer of records of government bodies, including the transfer of electronic systems to the archive; lending of records to a state body which was transferred by the same body to the archive, and evaluation and handing over of municipal records. The Executive Order on Archives also stipulates that the National Archives of Denmark may require the submission of the necessary information by public authorities for expert review and archiving. If a public authority neglects such archival considerations, the archives may issue an order to take the necessary measures to comply with the relevant archival regulations. National authorities are obliged to inform the archives of

---

[33] Danish Archives Act. URL: https://www.sa.dk/wp-content/uploads/2014/12/Danish-Archives-Act.pdf. (6.11.2020.)

[34] National Archives of Denmark. URL: https://www.sa.dk/en/. (10.10. 2020.)

their electronic filing systems prior to their application, followed by the evaluation of the system and, if it meets the set standards, to set a time limit for the transfer of electronic records to the archive system. This process usually takes place after a period of approximately five years. The electronic file management systems that need to be preserved must be further professionally monitored for approval (certification). To this end, the Danish National Archives shall determine whether the system fulfills the requirements laid down for public authorities with regard to the management of their documentation. The expert review focuses on the organizational and technical aspects of the electronic system. The legal requirement for information on electronic filing systems means that an archive must, in principle, have information on all electronic filing systems used in the Danish Central Administration. However, decisions regarding long-term digital preservation or storage may, in some cases, be made in collaboration with local archives. All public authorities must adhere to the national standard for the submission of electronic system data. The "Executive Order on Submission Information Packages – Danish National Standard"[35] gives an overview of the elements and structure in the information packages. The handover of the information packet of data and all documents in the IT system contains: general rules on information packets for submission, data structure, data content, and information on the packet to be submitted to the archive. The data structure contains general rules for data structure, the location of folders and files, index folders, tables, record contexts, schemas, and documents. The data content relates to table content along with data type, conversion of table content to digital archive, audio, video or other file formats, text formatting, digital records, audio and video, geographic features, compression and optimization without degradation (without deterioration). This is followed by the Handover Data Package Information, which contains the archive descriptive file, context documentation, content information in the handover information packet tables, and SQL queries. Lastly, we find the choice of media for the transmission of information packages.

Lithuania

The Republic of Lithuania law on documents and archives[36] currently in force, uses the professional term "official electronic record", which denotes those records created by the Lithuanian public and state sectors and various non-governmental organizations. Electronic records shall be prepared in accordance with the specifications on electronic documents approved by the Central Archives of Lithuania.[37] It should be noted that the professional term "official electronic record" is defined in response to the application of the 2011 Regulation and Council of the European Parliament. Its specification is defined to basically describe the contents of the record, that is, the main components of official email, such as metadata and electronic signatures. The Lithuanian Chief archivist approved the ADOC-V1.0 (current version)[38] specification for electronic records with electronic signatures. The application of this specification for electronic documents is further defined by the 2017 Order of the

---

[35] Executive Order on Information Packages and Submission – Danish National Standard. URL: https://www.sa.dk/wp-content/uploads/2014/12/Executive-Order-on-Submission-Information-Packages-Danish-national-standard.pdf. (7.10.2020.)

[36] Laws of the Lithuanian Archives Office. URL: http://www.archyvai.lt/lt/teisine-informacija_51/teisesaktai/el_specifikacijos.html. (6.12.2020.)

[37] Central Archive of Lithuania. URL: http://www.archyvai.lt/lt/lvat.html. (10.10.2020.)

[38] Specification ADOC-V1.0 for an electronic record with the electronic signature of the Lithuanian Archives Office. URL: https://www.e-tar.lt/portal/lt/legalAct/TAR.11EFBB8DA962/tgLnzGXfEL. (6.10.2020.)

Archives of Lithuania specification for official electronic records,[39] which currently requires institutions to accept official electronic records, equivalent to analogue records, prepared in accordance with ADOC-V1.0. The Archives adhere to Regulation (EC) No. 1049/2001 of the European Parliament and of the Council No. 910/2014 eIDAS[40] on electronic identification and trust services for electronic transactions in the internal market, and efforts are being made to increase confidence in electronic transactions. This applies in particular to providing a common basis for secure electronic interaction between citizens, businesses and public authorities, simpler and more secure transactions, and facilitates mutual recognition of electronic identification. The electronic signature has already been previously regulated by Directive 1999/93/EC, and the eIDAS regulation removes existing obstacles to the cross-border use of electronic identification used in member states for authentication to access online public services. The Regulation defines which means of electronic identification must be recognized, establishes the conditions under which Member States recognize the means of electronic identification of natural and legal persons covered by another Member State's notified electronic identification system, establishes rules for trust services, in particular for electronic transactions, and establishes a legal framework for electronic signatures, electronic stamps, electronic timestamps, electronic documents, electronically registered delivery services and certification services for web site authentication. One of the key activities in establishing a digital single market and promoting its values for the digital economy of the future is to create the appropriate conditions for the mutual recognition of key cross-border factors such as electronic identification, electronic documents, electronic signatures and electronic delivery services, and conditions for interoperable services of eGovernment across the European Union. Building trust in the online environment is crucial to economic and social development because consumers, businesses and public authorities are often reluctant to conduct transactions electronically and find issues with the introduction of new services. With regard to standards, the Lithuanian Archives adhere to the following international standards for electronic records: ISO 19005-1: 2008; ISO 12234-2: 2008; ISO / IEC 29500-1: 2009; ISO / IEC 29500-2: 2009; ISO / IEC 29500-3: 2009; ISO / IEC 29500-4: 2009 and ETSI TS 119 101 V1.1.1.

Latvia

The work of the National Archives of Latvia[41] is based on the Archives Act[42] of 2011. It defines the basic principles for the collection, preservation, accessibility and management of the national documentary heritage. The archive implements the following regulations: lists with time limits for the storage of archival and documentary material and model nomenclature,[43] procedures for using archives in the reading room of the Latvian Archives,[44]

---

[39] Specification for official electronic records of the Lithuanian Archives Office. URL: https://www.e-tar.lt/portal/lt/legalAct/a79ba6a0f29a11e692c5977c7316c9b5. (6.10.2020.)

[40] REGULATION (EU) NO. 910/2014 EUROPEAN PARLIAMENT AND COUNCIL. URL: https://eur-lex.europa.eu/legal-content/HR/TXT/HTML/?uri=OJ:JOL_2014_257_R_0002&from=EN. (6.10.2020.)

[41] National Archives of Latvia. URL: https://www.arhivi.gov.lv/. (accessed 10 December 2019)

[42] Law on Archives of the Republic of Latvia. URL: http://likumi.lv/doc.php?id=205971#p20. (6.10.2020.)

[43] Latvian Lists with deadlines for archival and documentary storage and model nomenclature URL: https://www.arhivi.gov.lv/content.aspx?id=466&mainId=127 (6.10.2020.)

[44] Procedures for Using Documents in the Reading Room of the Latvian Archives. URL: https://www.arhivi.gov.lv/files/files/Ieksejie%20normativie%20akti/Groz_lasitavas%20darbibas%20noteikumos_1.pdf. (6.10.2020.)

the ethical codex,[45] rules of the Latvian National Archives,[46] statute of the Commission for the Accreditation of Private Archives,[47] guidelines for the digitization of archives and documents in public archives,[48] guidelines for the application of criminal offenses in administrative offenses,[49] terms of use of the common information system of the State Archives,[50] terms of use of the portal of the common state archival information system[51] and guidelines on conditional partial immunity from fines in cases of administrative violations of the law.[52] In addition to the aforementioned laws, the Latvian Archives has developed seven of its own standards based on the international ISAD (G)[53] standard, accredited by the International Council on Archives ICA.[54] The first Latvian standard AA (VP)[55] provides general guidance on how to make an archival description. The AA (VP) standard is based on generally accepted theoretical principles of archiving and provides intellectual control over the authenticity and availability of all types of records described throughout their life cycle. This standard is primarily concerned with the preparation of descriptions of archival records after they have been selected for permanent retention, but its provisions can also be applied at an earlier stage of the record lifecycle, which is of particular relevance to electronic records. Its policies apply regardless of medium or format, but do not include instructions for describing specific types of records, such as audio tracks or maps or postage stamps. The second Latvian standard LVS ISO 11108[56] it is identical to the international standard ISO 11108: 1999. „Information and documentation – Requirements for persistence and durability". This standard establishes requirements for the preservation of original archives that have not yet been published, as well as publications that are frequently used but also

---

[45] Code of Ethics for the Latvian Archives. URL:
https://www.arhivi.gov.lv/files/files/Ieksejie%20normativie%20akti/LNA%20Etikas%20kodekss.pdf. (6.10.2020.)

[46] Rules of the Latvian National Archives. URL:
https://www.arhivi.gov.lv/files/files/LNA_reglaments_08_01_19__grozjijumi-1.pdf (6.10.2020.)

[47] Statute of the Commission for Accreditation of Private Latvian Archives. URL:
https://www.arhivi.gov.lv/files/files/Ieksejie%20normativie%20akti/Privatu_arhivu_akreditacijas_komisijas_nolikums.pdf. (6.10.2020.)

[48] Guidelines for the digitization of archival and documentary material in Latvian public archives. URL:
https://www.arhivi.gov.lv/files/files/Vadlinijas%20digitalizacijai%20arhivos.pdf. (6.10.2020.)

[49] Guidelines for the application of criminal offenses in administrative offenses in Latvia.URL:
https://www.arhivi.gov.lv/files/files/Ieksejie%20normativie%20akti/Vadlinijas_adm_parkapumu_lieatas.pdf. (6.10.2020.)

[50] Terms of use of the common information system of the Latvian State Archives. URL:
https://www.arhivi.gov.lv/files/files/Ieksejie%20normativie%20akti/VVAIS_Lietosanas_noteikumi.pdf. (6.10.2020.)

[51] Terms of use of the portal of the common Latvian state archival information system. URL:
https://www.arhivi.gov.lv/files/files/Ieksejie%20normativie%20akti/VVAIS_Portala_Lietosanas_noteikumi.pdf. (6.10.2020.)

[52] Guidelines on conditional partial immunity from fines in cases of administrative breach of law in Latvia. URL:
https://www.arhivi.gov.lv/files/files/Vadl%C4%ABnijas.pdf. (6.10.2020.)

[53] ISAD(G): General International Standard Archival Description – Second edition 2011. URL:
https://www.ica.org/en/isadg-general-international-standard-archival-description-second-edition. (6.10.2020.)

[54] International Council on Archives ICA. URL: https://www.ica.org/en. (6.10.2020.)

[55] The first Latvian standard LVS 369: 2004. „Archive description. General principles: aa (vp) ".

[56] The second Latvian standard LVS ISO 11108. „Information and Records – Archival Paper – Requirements for Persistence and Long Term".

permanently stored. The third Latvian standard LVS ISO 11798[57] it is identical to the international standard ISO 11798: 1999. „Information and documentation – Durability and authenticity of written, printed and copied paper records – Requirements and test methods". This international standard lists libraries, archives and museums according to stability requirements, which means that special test methods evaluate the durability and authenticity of paper, printed or copied records over a long period in a protected environment. The fourth Latvian standard LVS ISO 11800: 2003[58] is identical to the international standard ISO 11800: 1999. „Information and documentation – Requirements for materials and methods". This international standard specifies the production methods and materials to be used in the commercial production of hard and soft-bound books. This does not apply to hand-binding, individual sewing or collecting archives, nor to works of art that are movable cultural heritage. The basic purpose of this standard is not to have a permanent protection function, for example, it cannot provide guidance for carved artwork on a book cover. This International Standard has two prescribed annexes and one supplement with a set of guidelines. Each of them places requirements for a specific category of publication production. The fifth Latvian standard Latvian standard LVS EN 1047-2: 2006[59] is identical to the international standard „Secure storage units – Classification and test methods for fire resistance – Part 2: Metadata and storage depository". A part of this norm EN 1047 defines the requirements and includes test methods to determine the capability of the storage facilities for data storage and the storage containers for serving content protection. The parameters of sensitivity to humidity and temperature, as well as protection against the effects of fire outside and inside the storage depository, are specifically defined. A test method has also been defined to measure the resilience of data storage spaces and data containers to this effect. The sixth Latvian standard LVS ISO 14416: 2005[60] is identical to the international standard ISO 14416: 2003 „Information and documentation – Requirements for binding books, periodicals, serials and other paper records – Methods and materials." This International Standard applies to the binding of books, periodicals and archival records with special requirements for permanent preservation. The frequency of use, as well as the extraction of libraries from archival records, varies significantly. The choice of binding method is based on the specific requirements of the library or archive. This standard does not apply to those records which the expert has valued as high artistic or historical values or because of their physical characteristics, records cannot and should not be imported in accordance with this standard. Special treatment of specific species must be carried out separately. The standard was prepared as part of the project „National Unified Library Information System". The seventh Latvian standard LVS ISO 11799[61] is identical to the international standard ISO 11700: 2003 (E), „Requests for information and records of archives and books". This international standard specifies the characteristics of universal repositories for the long-term storage of archives and library material. This includes the location and construction of the facility as well as the necessary installations and equipment. It does not include special requirements for long-term

[57] Third Latvian standard LVS ISO 11798. „Information and documentation – Durability and authenticity of analogue, printed and copied records – Requirements and test methods".

[58] The fourth Latvian standard LVS ISO 11800: 2003. „Information and Documentation – Material and Method Requirements for Book.

[59] The fifth Latvian standard Latvian standard LVS EN 1047-2: 2006. „Safe repositories: Classification and test methods for fire resistance. Part 2: Storage areas and data containers".

[60] The sixth Latvian Standard LVS ISO 14416: 2005. „Information and documentation. Requirements for binding books, periodicals, serials and other paper records for archives and libraries. Methods and materials".

[61] The seventh Latvian standard LVS ISO 11799. "Information and documentation. Requirements for the preservation of records of archives and library material".

preservation of records or specific types of records, such as parchment or photographic records. It also does not include repository management procedures. In a number of areas, national or local building codes may include issues of construction and safety of public buildings or buildings containing valuable items related to natural disasters, robberies or terrorist attacks. These include professional furnishing services such as alarms and security doors. Therefore, this international standard avoids detailed rules regarding those that have been listed here, unless the guidelines supplement those requirements.

Estonia

The work of the State Archives of Estonia[62] is based on the Archives Act[63] and the Archives Policy,[64] the main document that lays down the general requirements for archival file formats. The activities of the archives are within the purview of the Ministry of Education and Research, and are based on the archiving program, which requires that all state records which are entered in the archives, are kept stored in a publicly accessible register of records. The archive implementing regulations are structured as follows: the Statute of the State Archives,[65] the Statutes of the Archival Departments,[66] the Statute of Digital Archives,[67] the Statutes of the Office of Research and Publications,[68] the Statute of the Law Office,[69] the Statute of the Film Archive[70] and the Film Archive Policy.[71] This archive uses a migration strategy for long-term preservation of digital records, which means that digital records are always stored in a format that is easy to manage with current hardware and software. An analysis of the various file formats has compiled a list of so-called "archive formats" containing recommended file formats suitable for long-term storage, and all files uploaded to the digital archive are migrated to the default formats. At the same time, international support for these file formats is being monitored, and the list of "archive formats" is updated as necessary and the files are moved to the new format. Digital record descriptions or metadata also play an important role, so that all digital records are easily searchable and manageable. Physically, the digital records are stored as equivalent copies in different places. This also ensures that records are preserved even if the data is lost in one place. Similar to file formats, new storage solutions for analyzing the most appropriate media are utilized, as well as the hardware needed to read them. Currently, the archive simultaneously stores digital records in

---

[62] National Archives of Estonia. URL: http://www.ra.ee/. (10.12.2020.)

[63] Estonian Law on Archives. URL: https://www.riigiteataja.ee/akt/106012016006?leiaKehtiv. (10.12.2020.)

[64] Estonian Archive Policy. URL: https://www.riigiteataja.ee/akt/131052017011?leiaKehtiv. (10.12.2020.)

[65] Statute of the State Archives of Estonia. URL: https://www.riigiteataja.ee/akt/130112011009?leiaKehtiv. (10.12.2020.)

[66] Statute of the archival departments of the Estonian Archives.URL: http://www.ra.ee/wp-content/uploads/2019/11/ra_osakondade_p%C3%B5him%C3%A4%C3%A4rus_2019.pdf. (10.12.2020.)

[67] Statute of the Estonian Digital Archives. URL: http://www.ra.ee/wp-content/uploads/2018/01/Digitaalarhiivi-p%C3%B5him%C3%A4%C3%A4rus.pdf. (10.12.2020.)

[68] Statute of the Estonian Research and Publications Office. URL: http://www.ra.ee/wp-content/uploads/2018/01/Teadus-ja-publitseerimisb%C3%BCroo-p%C3%B5him%C3%A4%C3%A4rus.pdf. (10.12.2020.)

[69] Statute of the Estonian Law Office. URL: http://www.ra.ee/wp-content/uploads/2018/01/Haldusb%C3%BCroo-p%C3%B5him%C3%A4%C3%A4rus.pdf. (10.12.2020.)

[70] Statute of the Estonian Film Archive. URL: http://www.ra.ee/wp-content/uploads/2016/11/fa_pm.pdf. (accessed 8 December 2019)

[71] Politics of the Estonian Film Archive. URL: http://www.ra.ee/wp-content/uploads/2019/01/Filmiarhiivi.tegevuspohimotted_vers.1.1.pdf. (10.12.2020.)

a network array of disks and magnetic tapes. The digital archive is being developed modularly, which means that digital archive modules such as digital record reception, physical storage, content management and access to the record are mutually separate modules, thus ensuring long-term digital preservation of records. Estonian standards for information and document management are mainly prepared by the Technical Board for Standardization[72] EVS / TC 22 for information and documentation. The main activity of this committee is to cooperate with European and international standards, primarily because Estonia is required to adopt all European standards as Estonian standards in their unaltered state. Participation in work on European and international standardization is key to promoting the best practices, as well as, among other things, avoiding requirements that are not appropriate to the set objectives.

The number of valid Estonian standards in December 2020:

	Number of valid Estonian standards	Available in Estonian
Original Estonian standards[73]	**280**	**280**
Implemented European standards[74]	**26555**	**1238**
CEN	15.637	1030
CLC	6222	193
ETSI	4696	15
Implemented international standards	**343**	**222**
ISO	293	178
IEC	50	44
Total number of valid Estonian standards	**27.178**	**1740**

In absence of an appropriate European or international standard, the drafting of an original Estonian standard may be initiated. It must be observed that the standard to be drafted should not present requirements that contradict any European or international standard (differences from a European standard must be introduced as a special national condition into the European standard).

An Estonian standard may be:

1) an original standard.

2) an implemented international or European standard:

a) endorsement method;

b) reprint method;

c) translation method.

It is designed in such a way as to ensure that it does not conflict with the law or European or international standard or its draft. The elements of the description of the archives of the Estonian archive are based on ISAD(G) and ISAAR(CPF) standards developed under the

---

[72] Estonian Technical Committee for Standardization EVS / TC 22. Information and documentation. URL: https://www.evs.ee/Standardimine/Tehnilisedkomiteed/EVSTK22/tabid/218/Default.aspx. (10.12.2020.)

[73] The original Estonian standards are drafted in Estonian and are not available in other languages, generally.

[74] The implemented European standards are generally available in English and some of them in Estonian. Other languages are available depending on the existence of official texts.

auspices of the International Council on Archives. The digital archive is based on the ISO 14721: 2003 referent OAIS[75] model. Within the scope of information and documentation description, the Estonian Committee has developed nine standards of its own: CEN / SS F17 – Administrative records; CEN / TC 346 – Preservation of cultural heritage; ISO / TC 171 – Records management applications; ISO / TC 46 – Information and records; ISO / TC 46 / SC 10 – Record storage requirements and conditions for long-term preservation; ISO / TC 46 / SC 11 – Archive / records management; ISO / TC 46 / SC 4 – Technical interoperability; ISO / TC 46 / SC 8 – Quality – Statistics and performance appraisal and ISO / TC 46 / SC 9 – Quality – Statistics and performance appraisal.

Conclusion

International standards and archival legislation are open working categories for upgrading the architecture of records in archives worldwide. The countries of northern Europe involved in the evolution of the standard thus gain access to relevant knowledge, resources and experience, and have the opportunity to network with a worldwide community of experts in this field. This enables them to develop these professions, to gain the recognition of the global archival community and to establish inter-institutional professional cooperation. No matter what storage strategy and standardized digital preservation security strategy they use, the makers of these lessons shall still face these remaining questions:

Can it be said with certainty that the stored content will remain unchanged within the set time frame of record preservation?
How will this technology be updated to ensure long-term record availability?
Does this technology make it easier for institutions to hand over records to respond to a legal request within the time limit that is set?
Can this technology be developed with regular operating business and legal requirements?
Can standards-based and model-based technology be used with other content generation applications?
How will this technology architecture for record storage handle the ongoing workflows and challenges of understanding for archival professionals?

In order to meet regulatory compliance requirements, archives must focus on collecting, safe-keeping and easily retrieving key records. After knowing which electronic data laws and standards affect them, archives must follow the best practices and build an IT architecture that will support all legal requirements. However, due to their complex nature, most regulations still do not provide a clear map of protocols for compliance. The best practice often proves to be the highlight of any record management project. Archives should by no means disregard regulations, but should adjust the standards to a mutually acceptable outcome for private, state and public institutions. On the other hand, institutions that have to comply with electronic data laws have all questions regarding the issue of handover of records have been answered, including questions on standardized processes, people and technology for the efficient management, as well as the maintenance of electronic records. Certainly, by investing adequate time in the development of record architecture and thinking strategically about the best practices for archiving and protecting records, northern European countries can satisfy the legal requirements and thus continuously create and maintain the ideal conditions for long-term preservation of archival records.

---

[75] See under fn 4.

Bibliography:

Giaretta, D. (2011). Advanced Digital Preservation. ISBN 9783642168086.

Lemić, V. (2003). Archives and electronic records - experiences of Scandinavian countries. Croatia. Bulletin d'archives, 46(1), pp. 179-207. URL: https://hrcak.srce.hr/7378. (09.12.2020.)

Stančić, H. (2005). A theoretical model of the persistent preservation of the authenticity of electronic information objects. Doctoral thesis. University of Zagreb. Faculty of Philosophy. Croatia. URL: https://bib.irb.hr/datoteka/244465.Ocuvanje_autenticnosti_e-informacijskih_objekata.pdf. (10.12. 2020.)

Žaja, L. (2019). Digital preservation policy in publicly available data and strategic documents on the websites of selected national archives of European Union countries. 51. Counseling of the Croatian Archivist Society: Management of Electronic Material and Contemporary Archival Practice. Croatia. Slavonski Brod., pp. 147-169.

Sources:

Central Archive of Lithuania. URL: http://www.archyvai.lt/lt/lvat.html. (10.12.2020.)

Code of Ethics for the Latvian Archives. URL: https://www.arhivi.gov.lv/files/files/Ieksejie%20normativie%20akti/LNA%20Etikas%20kodekss.pdf. (10.12.2020.)

Danish Law on Archives. URL: https://www.sa.dk/wp-content/uploads/2014/12/Danish-Archives-Act.pdf. (10.12.2020.)

Document lifecycle management DLM. URL. https://www.webpdf.de/blog/en/dlm-document-lifecycle-management/. (10.12.2020.)

Electronic Communications Act of Finland. URL: http://www.finlex.fi/fi/laki/ajantasa/1994/19940831. (10.12.2020.)

Estonian Archive Policy. URL: https://www.riigiteataja.ee/akt/131052017011?leiaKehtiv. (10.12.2020.)

Estonian Law on Archives. URL: https://www.riigiteataja.ee/akt/106012016006?leiaKehtiv. (10.12.2020.)

Estonian Technical Committee for Standardization EVS / TC 22. Information and documentation. URL: https://www.evs.ee/Standardimine/Tehnilisedkomiteed/EVSTK22/tabid/218/Default.aspx. (10.12.2020.)

Executive Order on Information Packages and Submission – Danish National Standard. URL: https://www.sa.dk/wp-content/uploads/2014/12/Executive-Order-on-Submission-Information-Packages-Danish-national-standard.pdf. (10.12.2020.)

Giaretta Associates Ltd. URL: http://giaretta.org/digital-preservation/standards/. (10.12.2020.)

Government Decree on the National Archives of Finland. URL: http://www.finlex.fi/fi/laki/ajantasa/2017/20170039. (10.12.2020.)

Guidelines for the application of criminal offenses in administrative offenses in Latvia. URL: https://www.arhivi.gov.lv/files/files/Ieksejie%20normativie%20akti/Vadlinijas_adm_parkapumu_lieatas.pdf. (10.12.2020.)

Guidelines for the digitization of archival and documentary material in Latvian public archives. URL: https://www.arhivi.gov.lv/files/files/Vadlinijas%20digitalizacijai%20arhivos.pdf. (10.12.2020.)

Guidelines on conditional partial immunity of fines in cases of administrative breach of law in Latvia. URL: https://www.arhivi.gov.lv/files/files/Vadl%C4%ABnijas.pdf. (10.12.2020.)

Iceland National Archives. URL: https://skjalasafn.is/. (10.12.2020.)

Icelandic electronic documentation. URL: https://skjalasafn.is/rafraen_skjalavarsla. (10.12.2020.)

Icelandic Law on Public Archives. URL: https://skjalasafn.is/files/docs/ThePublicArchivesAct-in-Iceland-No-77-2014.pdf. (10.12.2020.)

International Council on Archives ICA. URL: https://www.ica.org/en. (10.12.2020.)

International Organization for Standardization ISO. URL: https://www.iso.org/home.html. (10.12.2020.)

ISAAR (CPF): International Standard Archival Authority Record for Corporate Bodies, Persons and Families, 2nd Edition. URL: https://www.ica.org/en/isaar-cpf-international-standard-archival-authority-record-corporate-bodies-persons-and-families-2nd. (10.12.2020.)

ISAD (G): General International Standard Archival Description - Second edition 2011. URL: https://www.ica.org/en/isadg-general-international-standard-archival-description-second-edition. (10.12.2020.)

Latvian Lists with deadlines for archival and documentary storage and model nomenclature. URL: https://www.arhivi.gov.lv/content.aspx?id=466&mainId=127. (10.12.2020.)

Law on Archives of the Republic of Latvia. URL: http://likumi.lv/doc.php?id=205971#p20. (10.12.2020.)

Law on state aid to the private archives of Finland. URL: http://www.finlex.fi/fi/laki/ajantasa/2006/20061006. (10.12.2020.)

Law on the Archives of Finland. URL: http://www.finlex.fi/fi/laki/ajantasa/1994/19940831

Law on the National Archives of Finland. URL: http://www.finlex.fi/fi/laki/alkup/2016/20161145. (12.12.2020.)

Law on the Private and National Archives of Finland. URL: http://www.finlex.fi/fi/laki/ajantasa/2006/20061006. (12.12.2020.)

Laws of the Lithuanian Archives Office. URL: http://www.archyvai.lt/lt/teisine-informacija_51/teisesaktai/el_specifikacijos.html. (12.12.2020.)

National Archives of Denmark.URL: https://www.sa.dk/en/. (12.12.2020.)

National Archives of Estonia. URL: http://www.ra.ee/. (12.12.2020.)

National Archives of Finland. URL: https://www.arkisto.fi/. (12.12.2020.)

National Archives of Latvia. URL: https://www.arhivi.gov.lv/. (12.12.2020.)

National Archives of Norway. URL: https://www.arkivverket.no/. (12.12.2020.)

National Archives of Sweden. URL: https://riksarkivet.se/startpage. (12.12.2020.)

NOARK – Norwegian Document Management Standard. URL: https://www.arkivverket.no/forvaltning-og-utvikling/noark-standarden. (12.12.2020.)

Norwegian Law on Archives. URL: https://www.arkivverket.no/forvaltning-og-utvikling/regelverk-og-standarder/lover-og-forskrifter-for-arkiv/arkivloven. (12.12.2020.)

Norwegian Ordinance on Supplementary Technical and Archival Regulations for the Handling of Public Archival and Documentary Materials. URL: https://lovdata.no/dokument/SF/forskrift/2017-12-19-2286#KAPITTEL_3. (12.12.2020.)

Politics of the Estonian Film Archive. URL: http://www.ra.ee/wp-content/uploads/2019/01/Filmiarhiivi.tegevuspohimotted_vers.1.1.pdf. (14.12.2020.)

Procedures for Using Documents in the Reading Room of the Latvian Archives. URL: https://www.arhivi.gov.lv/files/files/Ieksejie%20normativie%20akti/Groz_lasitavas%20darbibas%20noteikumos_1.pdf. (14.12.2020.)

Reference Model for an Open Information Archival System. URL: https://public.ccsds.org/pubs/650x0m2.pdf. REGULATION (EU) NO. 910/2014

EUROPEAN PARLIAMENT AND COUNCIL. URL: https://eur-lex.europa.eu/legal-content/HR/TXT/HTML/?uri=OJ:JOL_2014_257_R_0002&from=EN. (14.12.2020.)

Research Libraries Group RLG. URL: http://www.rlg.org/. (14.12.2020.)

Rules of the Latvian National Archives. URL: https://www.arhivi.gov.lv/files/files/LNA_reglaments_08_01_19__grozjijumi-1.pdf. (14.12.2020.)

Society of American Archivists SAA. URL: https://www2.archivists.org/. (14.12.2020.)

Space data and data transmission systems - Audit and certification of trusted digital repositories. ISO 16363: 2012. URL: https://www.iso.org/standard/56510.html. (14.12.2020.)

Specification for official electronic records of the Lithuanian Archives Office. URL: https://www.e-tar.lt/portal/lt/legalAct/a79ba6a0f29a11e692c5977c7316c9b5. (14.12.2020.)

Specification of ADOC-V1.0 for electronic record with electronic signature of the Lithuanian Archives Office. URL: https://www.etar.lt/portal/lt/legalAct/TAR.11EFBB8DA962/tgLnzGXfEL. (14.12.2020.)

Statute of the Archival Departments of the Estonian Archives. URL: http://www.ra.ee/wp-content/uploads/2019/11/ra_osakondade_p%C3%B5him%C3%A4%C3%A4rus_2019.pdf. (14.12.2020.)

Statute of the Commission for Accreditation of Private Latvian Archives. URL: https://www.arhivi.gov.lv/files/files/Ieksejie%20normativie%20akti/Privatu_arhivu_akreditacijas_komisijas_nolikums.pdf. (14.12.2020.)

Statute of the Estonian Digital Archives. URL: http://www.ra.ee/wp-content/uploads/2018/01/Digitaalarhiivi-p%C3%B5him%C3%A4%C3%A4rus.pdf. (14.12.2020.)

Statute of the Estonian Film Archive. URL: http://www.ra.ee/wp-content/uploads/2016/11/fa_pm.pdf. (14.12.2020.)

Statute of the Estonian Law Office. URL: http://www.ra.ee/wp-content/uploads/2018/01/Haldusb%C3%BCroo-p%C3%B5him%C3%A4%C3%A4rus.pdf. (15.12.2020.)

Statute of the Estonian Research and Publications Office. URL: http://www.ra.ee/wp-content/uploads/2018/01/Teadus-ja-publitseerimisb%C3%BCroo-p%C3%B5him%C3%A4%C3%A4rus.pdf. (15.12.2020.)

Statute of the State Archives of Estonia. URL: https://www.riigiteataja.ee/akt/130112011009?leiaKehtiv.

Strategy of the National Archives of Finland 2020. URL: https://www.arkisto.fi/en/the-national-archives-2/copy-of-strategy-2020. (15.12.2020.)

Swedish Archival Regulations RA-FS i RA-MS. URL https://riksarkivet.se/offentlig-forvaltning. (15.12.2020.)

Swedish General Regulations RA-FS. URL: https://riksarkivet.se/generella-foreskrifter. (15.12.2020.)

Swedish General Regulations RA-MS. URL: https://riksarkivet.se/ansok-om-gallring. (15.12.2020.)

Swedish International Standardization. URL: https://riksarkivet.se/Standardisering. (15.12.2020.)

Terms of use of the joint information system of the Latvian State Archives. URL: https://www.arhivi.gov.lv/files/files/Ieksejie%20normativie%20akti/VVAIS_Lietosanas_noteikumi.pdf. (15.12.2020.)

Terms of use of the portal of the common Latvian state archival information system. URL: https://www.arhivi.gov.lv/files/files/Ieksejie%20normativie%20akti/VVAIS_Portala_Lietosanas_noteikumi.pdf. (15.12.2020.)

University of Zagreb. Faculty of Philosophy. Department of Information and Communication Sciences. Chair of Archival and Documentary Studies. URL: https://inf.ffzg.unizg.hr/index.php/hr/odsjek/katedre/arhivistika-i-dokumentalistika. (15.12.2020.)

E-learning Technology in Higher Education: A Review

Faton Kabashi[1*], Zamir Dika [2*], Lamir Shkurti[3*] and Vehbi Sofiu[4*]

Abstract: Nowadays e-learning is a way of learning in higher education, which includes electronic media in the field of education. The rapid development of technology has had a great impact on the field of education. E-learning is now a day one the most important tool of learning & becoming a core part of today's education system and open new avenues to higher education. Today, almost all institutions of higher education deliver programs that incorporate digital media into an online environment to provide versatile learning opportunities, regardless of time and location. A major issue for faculty and educational developers in higher education is to determine which e-learning technology is most appropriate to support their particular teaching needs and provide optimum learning opportunities for students. Many Higher Education Institutions are now relying on various technological advances and changing their pedagogical practices, teaching methods, and implementing various e-learning strategies such as the Flipped Classroom (FC), Blended Learning & MOOCs, Open Educational Resources (OER), etc. In this paper, a review of e-learning technology in Higher education has been presented. Fifty relevant papers, published between 2009 and 2021, were reviewed and analyzed. This paper provides a background for e-learning in Higher Education Institutions, characteristics, advantages and disadvantages of e-learning, its requirements, and the various strategies of e-learning, in Higher Education Institutions.

Keywords: E-learning, Higher Education, Open Educational Resources (OERs), Blended Learning, Flipped Classroom, Massive Open Online Courses (MOOCs)

1. Introduction

E-learning is the use of electronic tools, information technologies and communication in education. E-learning is broadly inclusive of all forms of educational technology in learning and teaching [1]. E-learning is characterized as the use of information and communication technology in various educational processes to support and enhance learning in higher education institutions, which includes the use of information and communication technology as a complement to traditional classrooms, online learning or a combination of the two modes [2].

E-leaning focuses on usage of technology in the field of education and learning. E-learning refers to the use of advanced technology of information communication in the learning process where the advanced technology comprises of electronic media [3]. Another way of defining, e-learning can be defined as learning without using paper instructional material and the use of technology to teach [4]. Therefore, it is seen as opposite of classroom instruction,

1UBT- Higher Education Institution, Pristina, Kosovo
* Corresponding author: vehebi.sofiu@ubt-uni.net

traditional teaching or face to face teaching. Several terms are used to cover E-learning such as online learning, virtual learning, network, and web-based learning [4].

ICTs is a diverse set of technological tools and resources used to communicate and to create, disseminate, store and manage information [5]. This broad definition of ICT includes technologies as radio, television, video, DVD, telephone, satellite systems, computer and network hardware and software; as well as the equipment and services associated with these technologies, such as videoconferencing and electronic mail [5]. Success of ICT-based education depends upon the teacher's ability to keep pace with the developments since teachers are responsible for quality control, improvement of learning and the aggregate effectiveness of the learning process [6].

The introduction of ICT in the higher education has profound implications for the whole education process ranging from investment to the use of technologies in dealing with key issues of access, equity, management, efficiency, pedagogy and quality [7].

1. Student-centered Learning: ICT provides a technology that has the capacity to promote and encourage the transformation of education from a teacher directed enterprise towards student-centered models. As more and more students use computers as information sources and cognitive tools, the influence of the technology will increase to support their studies [8][9][10][11].

2. Supporting Knowledge Construction: Learning approaches using contemporary ICTs provide many opportunities for constructivist learning and support for resource-based, student centered settings by enabling learning to be related to context and to practice [5].

3. Anyplace Learning: With the help of ICT, educational institutions can offer programs at a distance mode. Today many students can use this facility through technology-facilitated learning settings [5].

4. Anytime Learning: Technology-facilitated educational programs remove the geographical barriers. Students are able to undertake education anywhere, anytime and at any place. This flexibility has provided learning opportunities for many more learners who previously were constrained by other commitments [5].

5. Information Literacy: The growing use of ICT as tools of everyday life have seen the pool of generic skills expanded in recent years to include information literacy. It is highly probable that due to the future developments and growth in technology, it will help further for information literacy [5].

Information technology (IT) is considered as one of the most fundamental forces for change in the all sectors of our lives [12]. Today many students want to learn online and in turn get degrees from worldwide colleges and universities, but still cannot go anywhere as they live in isolated areas without proper communication systems [13][14]. Consequently, many researchers encourage learning courses under the e-learning system as it saves time and energy of those students staying at any far-off distant regions from the universities or colleges they have enrolled [15] [16]. Indeed, e-learning adoption is increasing in most universities and institutions of higher learning all around the world. E-learning which is also known as web-based learning, is defined as the delivery of education in a flexible and easy way through the use of internet to support individual learning or organizational performance goals [17][18]. Furthermore, there are different kinds of e-learning system such as blackboard and second

life. Both of blackboard and the second life systems are used for attended lecturers, do homework and so many services.

As IT becomes more robust and easier to use, it increasingly infiltrates academic activities in higher education. Course management systems let teachers easily integrate technology into their instruction. Online communication and information access expand a course's range to wherever and whenever a professor or student logs on. Higher network bandwidth provides a quick and efficient conduit to accomplish these activities [19]. As an increasing number of institutions adopt e-learning strategies, their successes depend not only on the availability of technology but also on the extent to which faculty and students are supported as they explore and develop innovative ways to integrate technology into the learning experience. Pedagogical practices must be adapted, technical proficiency becomes more important, and a reliable and robust technical infrastructure must be maintained in order to use e-learning effectively. These demands are translated into a host of new professor and student support requirements that institutions must address [20]. The use of technology in education, commonly defined as e-learning, has become a standard component in many courses. Technology applications are not limited to the classroom – they are also placing some classroom sessions with virtual sessions or fully replacing classroom courses with online courses.

As institutions adopt e-learning, some important new issues arise:

- institutions must provide an adequate and reliable technical infrastructure to support e-learning activities;
- teachers and students must possess the technical skills to use e-learning tools;
- professors must redesign their courses to incorporate e-learning effectively into their pedagogy [21].

E-learning is an educational process, using information and communication technologies to create courses, to distribute a study content, to enable communication between students and teachers and the study management. However, the success of an e-learning system depends on the understanding of certain antecedent factors that influence the students' acceptance and usage of such e-learning systems.

This paper is organized as follows. The second section, shows the history of e-learning, in the third section is shown the research methodology, in the fourth section, the characteristics, advantages, and disadvantages are given. Further, the fifth section is shown e-learning technology. Finally, the sixth section will be summarized the conclusion.

2. History of e-learning

A revolution in the information technology and the emergence of web has made the human society take a huge leap. The focus of society is shifted from industry to information. The appearance of information technology has been the most important event at the start of this century. Information technology suddenly became an important element of every aspect of our society. Education is no exception. The use of multimedia and networking is welcomed by the field of education [22]. Historically, distance education can be traced back to the 18th century, to the beginning of print-based correspondence study in the United States. In the mid-19th century correspondence education started to develop and spread in Europe (Great Britain, France, and Germany) and the United States. Isaac Pitman, the English inventor of shorthand, is generally recognized as the first person to use correspondence courses [23]. Some experts refer to the education in 21st century as a multimedia network education.

Educational information is being accepted and promoted by all the nations around the world. A fact stated by the National Centre for Education Statistics that in 2008, there were 18 million students, who were enrolled in some online program worldwide, which was a 1.6% increase from 2002 [22].

ICT supported education quickly became the hot topic in the 1990s due to spreading use of the World Wide Web and its fast developing applications. These new technologies have opened up new opportunities for the non-traditional learner as well as for the traditional training institutions [23].

The education system and the teaching methods and many other things related to the education field are changing. And this transformation has given birth to e-learning. Nowadays, almost all available ICT developments are being used for distance education, or – with today's more popular term – for e-Learning.

3. Methodology

In this paper review, are taken into consideration the studies published between 2009 and 2021 in major online scientific databases, including Google Scholar, IEEE Xplore, Web of Science, Scopus, Elsevier and Research Gate. The key words used were e-learning, High Education, and e-learning technology. Thus, 49 documents including articles, books and web pages were finally selected based on specific inclusion/exclusion criteria.

4. Characteristics, advantages and disadvantages of e-learning

E-Learning is the use of ICT to deliver information for education where instructors and learners are separated by distance, time, or both in order to enhance the learner's learning experience and performance [24] [25]. The promise of e-Learning is that it brings powerful new tools for improving competency and capability, speed, and performance whether an organization operates at one geographical location or at many. Just as the rise of ICTs fundamentally changed the nature of how work and communication gets done, the emergence of e-Learning technologies is fundamentally changing the nature of how people learn. People are more and more encouraged to learn by themselves and to only learn what they really need to know to perform their task optimally [23]. The major part of the effective e-learning is interactive. Because one should also possess a good portion of self regulation skills, in most cases a coach is also provided to support the learners throughout their learning path. In terms of greater flexibility and timeliness, e-Learning can suit training needs 24 hours-a-day, 7 days-a-week, where traditional classroom-based training initiatives are quite disruptive. Rather than having to wait due to making up a class of students, e-Learning allows training to be conducted for individuals at their own convenience.

The adoption of e-learning in education, especially for higher educational institutions has several benefits, and given its several advantages and benefits, e-learning is considered among the best methods of education. Several studies and authors have provided benefits and advantages derived from the adoption of e-learning technologies into schools [26].

These are some advantages of adoption of e-learning in education obtained from review of literature:
- Class work can be scheduled around work and family
- Reduces travel time and travel costs for off-campus students
- Students may have the option to select learning materials that meets their level of knowledge and interest

- Students can study anywhere they have access to a computer and Internet connection
- Self-paced learning modules allow students to work at their own pace
- Flexibility to join discussions in the bulletin board threaded discussion areas at any hour, or visit with classmates and instructors remotely in chat rooms
- Instructors and students both report eLearning fosters more interaction among students and instructors than in large lecture courses [27].

E-learning, in spite of advantages it has when adopted in education, also has some disadvantages. regardless of all the disadvantages of e-learning, there are a lot of benefits that inspire its use and encourage search for ways to reduce its disadvantages. Disadvantages of e-learning listed in various studies include.

E-learning also has several disadvantages:
- Learners with low motivation or bad study habits may fall behind
- Without the routine structures of a traditional class, students may get lost or confused about course activities and deadlines
- Students may feel isolated from the instructor and classmates
- Instructor may not always be available when students are studying or need help
- Slow Internet connections or older computers may make accessing course materials frustrating
- Managing computer files and online learning software can sometimes seem complex for students with beginner-level computer skills
- Hands-on or lab work is difficult to simulate in a virtual classroom [27].

5. E-learning Technology

To deliver and manage their learning processes, establishments are using learning platforms. A learning platform could be a set of interactive online services that give learners access to data, tools, and resources to support instructional delivery and management. Learning platforms exist as proprietary or open-source software systems. They are distributed as closed-source programs with learning management systems (LMS) license prices supported a per-user fee. Open-source programs, work under the terms of the General Public License (GNU), which is meant to ensure the liberty to share and alter the program and make sure that it remains free for all users.

The e-learning necessities are:

- Comprehensive infrastructure, quick communication tools, and trendy pc labs.
- Training academics to use technology.
- Building enticing instructional curricula and materials.
- An effective program for the academic method of student registration, follow up, and analysis
- Providing these instructional materials round the clock.
- Reducing prices [28].

E-learning is the use of technology to connect teachers and students who are physically apart. The training can be delivered by a number of means. Many teachers in schools, colleges or universities are already relying on different technological advancements and changing their pedagogical practices and teaching methods. Some of the technologies that are being used for

e-learning in higher education are: the Flipped Classroom (FC), Blended Learning (BL), Open Educational Resources (OERs), Massive Open Online Courses (MOOC).

5.1 The Flipped Classroom

A Flipped Classroom (FC) is an instructional strategy and a type of blended learning, which aims to increase student engagement and learning by having students complete readings at their home and work on live problem-solving during class time [29]. In a FC approach, students see online lectures, work together as a team in online discussions and perform research at home and employ the concepts in the classroom with the guidance of a teacher or a mentor [30]. In FC, students see lesson videos at any time convenient to them. In getting to know the learning process, actively they arrive in the classroom with their homework and participate [31].

In a Traditional Classroom, students are typically given projects where they would research their topic at home, watch a lecture/presentation in school, and then given homework to carry out at home, based on the information they have gathered. In a FC, students are given information about their topic, along with a presentation/lecture prior to class. In class, students discuss the information they have received with their peers and teachers and then carry out homework at home based on their classmate's and their own findings. The differences between the Traditional Classroom and the FC are shown in Figure 1.
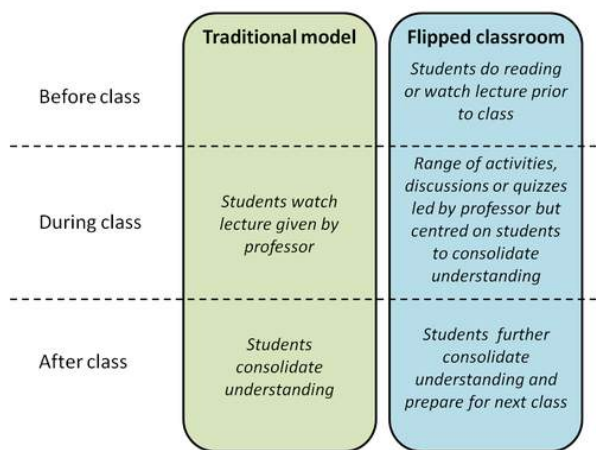

Figure 1. Differences between the Traditional Classroom and the Flipped Classroom

Figure 2 summarizes the core components of the FC model discussed above separately for in-class and out-of-class learning [32].
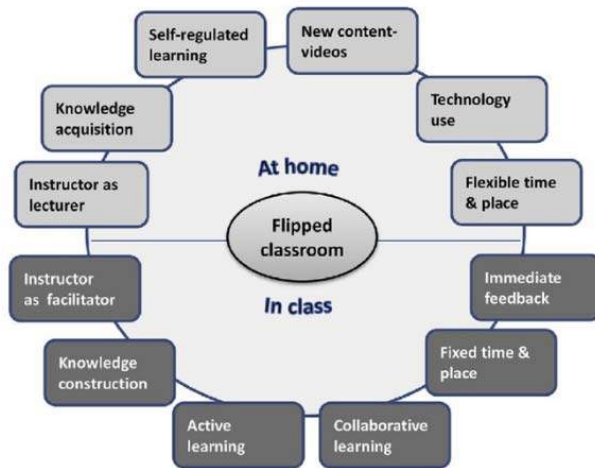
Figure 2: The components of the traditional Flipped Classroom model

The advantage of FC is that students can see the e-content or the videos as per their convenience. Thus a student can learn at his own pace. Secondly, the teacher can get a lot of time to fulfill the learning & emotional demands of students. Thirdly, students get ample coverage and new perceptions of the course material and are capable to spend more time with scientific tools that can be only used in the classroom & this will motivate the students to perform the work they want to do.

The disadvantage of the FC mode is that students may come to class without preparation. Secondly, it may be that students are lack of smart phones, tablets or computers, and may have internet problems [33].

5.2   Blended Learning

Blended Learning (BL) is a novel model of learning which combines the benefits of both traditional face-to-face learning and ICT supported learning including both offline and online learning irrespective of the control over time, location, path or speed [34]. BL in the preparation of university students includes a combination of mobile learning, e-learning, distance learning, and mass open courses.

BL is a third wave in designing and implementing learning environments that is used in public education, job training, and higher education. With the emergence of information communication technology and increased penetration rate of the Internet, using these facilities in learning environment has gradually made e-learning environment meet the shortcomings of the traditional face-to-face learning systems [35]. BL system was appeared to contribute to the effective achievement of learning outcomes, increasing the absorption of various audiences and decreasing some educational costs [36]. The goal of this movement is improving learning qualities, extending the boundaries of education and decreasing educational costs.

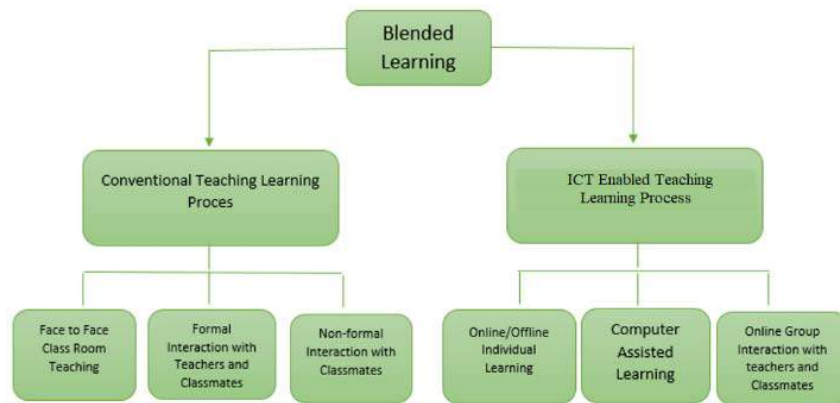The concept of BL is shown with the help of Figure 3 [33].

Figure 3. Concept of Blended Learning

The advantages of this model are: time saving, cost-effective, more effective and efficient Learning, the participants in accessing learning material, enables learners to learn the subject matter independently. Utilize materials available online, learners can conduct discussions with teachers or other learners outside of face-to-face Teaching, don't spend too much energy to teaching, Adding material enrichment through internet facilities, expand the range of learning/training, optimal results as well as enhance the attractiveness of learning, and etc [37]. The disadvantage of BL is the lack of required infrastructure and dearth of teachers having expertise in technological advancements.

5.3 Open Educational Resources

Open Education Resources (OERs) are one of the latest technological educational tools in present day society. Any form of learning and teaching materials that are freely accessible and are obtainable within the property right is termed Open Educational Resources (OERs) and may be used with an open license (Creative Commons). OERs embody course materials, modules, textbooks, lecture notes, assignments, tests, projects, computer code tools, audios, videos, and animations [38].

OERs are teaching, learning and research materials in any medium – digital or otherwise – that reside in the public domain or have been released under an open license that permits no-cost access, use, adaptation and redistribution by others with no or limited restrictions. The new definition explicitly states that OER can include both digital and non-digital resources. Also, it lists several types of use that OER permit, inspired by 5R activities of OER [39].

5R activities/permissions were proposed by David Wiley, which include:

- **Retain** – the right to make, own, and control copies of the content (e.g., download, duplicate, store, and manage)
- **Reuse** – the right to use the content in a wide range of ways (e.g., in a class, in a study group, on a website, in a video)
- **Revise** – the right to adapt, adjust, modify, or alter the content itself (e.g., translate the content into another language)
- **Remix** – the right to combine the original or revised content with other material to create something new (e.g., incorporate the content into a mashup)
- **Redistribute** – the right to share copies of the original content, your revisions, or your remixes with others (e.g., give a copy of the content to a friend) [40].

Advantages of using OER include:

- Expanded access to learning – can be accessed anywhere at any time
- Ability to modify course materials – can be narrowed down to topics that are relevant to course
- Enhancement of course material – texts, images and videos can be used to support different approaches to learning
- Rapid dissemination of information – textbooks can be put forward quicker online than publishing a textbook
- Cost saving for students – all readings are available online, which saves students hundreds of dollars [41].

Disadvantages of using OER include:

- Quality/reliability concerns – some online material can be edited by anyone at anytime, which results in irrelevant or inaccurate information
- Limitation of copyright property protection – OER licenses change "All rights reserved." into "Some rights reserved [42] so that content creators must be careful about what materials they make available
- Technology issues – some students may have difficulty accessing online resources because of slow internet connection, or may not have access to the software required to use the materials [41].

5.4 Massive Open Online Courses (MOCCs)

Massive Open Online Courses (MOOCs) are web based online courses for an unlimited number of participants held by professors or other experts. The term MOOC was originally used by George Siemens and Stephen Downes in 2008, and since then has gained popularity in the USA especially when Sebastian Thrun, a Stanford professor offered an artificial intelligence course for free [43]. MOOCs are a new addition to the open educational provision. They are offered mainly by prestigious universities on various commercial. MOOCs are among the latest e-learning initiative to attain widespread popularity among many universities.

So far, MOOCs can be characterized as follows:

- they are online courses
- with no formal entry requirement
- no participation limit
- are free of charge
- and do not earn credits [44].

Basically, any individual with an Internet connection can join a MOOC, to access the available resources, interact with other students, reflect and share what they have learned with others [45] [46]. MOOC are the structured courses where e-content is provided to the learner in the form of a virtual class through a web-based portal, preferably by LMS (Learning Management System). They can be accessed by any suitable device i.e., desktop, laptop, tablet or smart-phones. The e-content is arranged in a logical sequence, either in topic-wise format or weekly format for learners to meet specific learning outcomes. In addition to e-content, there are various activities provided to the virtual group of learners like online quizzes, discussion forums, live chat and live videos [47].

Nowadays, users can access the courses via mobile devices together with tablets, smartphones, than ever before. By considering the issue and for ease of the users, suppliers are providing mobile applications for their MOOCs. Moreover, these applications will support multiple platforms like android and iOS, permitting the learners to use mobile devices to induce enroll, access to course content, and participate in altogether course activities [48].

As of December 2020, more or less 180 million students are registered for the MOOC courses, offered by quite 950 universities and around 16300 courses [20], offered by numerous suppliers like Coursera, edX, Future Learn, Swayam [49].

In Table 1 are show the top MOOC providers look in terms of users and offerings: [49].

Table 1				
	Learners	Courses	Microcredentials	Degrees
Coursera	76 million	4,600³	610	25
edX	35	3,100	385	13
FutureLearn	14	1,160	86	28
Swayam	16 million	1,130	0	0

The advantage of MOOCs is that one can learn according to own pace of learning at any time convenient to you. Other advantage of MOOCs is that it will make learning learner centric and interactive unlike our traditional method of teaching, which is basically teacher centric [33].

The disadvantage of MOOCs is that human learns best socially, hence it is not suitable for individuals who struggle with motivation. Secondly, low completion rate is the major disadvantage. Around 5% percent of the total enrolled learners are able to complete MOOCs [34].

Conclusions

E-learning information systems are known to be the most used recent IT facilities in higher academic institutions. Technological advancements and e- learning is an approach that requires the reframing and restructuring of the traditional mode of teaching and learning. The research has highlighted that e-learning is not so similar to the traditional ways of learning in those numerous institutions and industry factors might have an impact on the overall success of an e-learning strategy. For preparing higher educational institutions to adopt e-learning it requires a well-designed plan that includes all the individuals of the educational hierarchy starting from top to the bottom. Learning or e-learning is also inseparable from various advantages and disadvantages. But behind it all, learning through e-learning is very supportive in the current learning process. This paper has been presented a background for e-learning in higher education establishments, requirements, and techniques of e-learning in teaching and learning in n higher education establishments such as Open Educational Resources (OERs), Blended Learning, Flipped Classroom (FC), and Massive Open Online Courses (MOOCs).

REFERENCES

[1] Adina-Petruta Pavela, Andreas Fruthb, & Monica-Nicoleta Neacsuc (2015). ICT and E-Learning – Catalysts for Innovation and Quality in Higher Education. Procedia Economics and Finance, 23(2015), 704 – 711. doi: 10.1016/S2212-5671(15)00409-8

[2] S. Kannadhasan1, M. Shanmuganantham2, Dr. R. Nagarajan3 and S. Deepa, The Role of Future E-Learning System and Higher Education, International Journal of Advanced Research in Science, Communication and Technology (IJARSCT), Volume 12, Issue 2, December 2020.

[3] Himanshu Agarwal1, G. N. Pandey2, Impact of E-Learning in Education, International Journal of Science and Research (IJSR), ISSN (Online): 2319-7064.

[4] Goyal S, (2012). E-Learning: Future of Education, Journal of Education and Learning. Vol.6 (2) pp. 239-242.

[5] Ulka Toro (Gulavani) and Millind Joshi, ICT in Higher Education: Review of Literature from the Period 2004-2011, International Journal of Innovation, Management and Technology, Vol. 3, No. 1, February 2012

[6] K. Balasubramanian, Willie Clarke-kah, "ICTs for higher education. Background paper from the common wealth of learning UNESCO," World Conference on Higher Education Paris, 2009.

[7] A. Garcia-Valcarcel Munoz-Repiso and F. J. Tejedor, "Use of information and communication technology in higher education and lecturers competencies,"

[8] B. Loing, "ICT and higher education - general delegate. of ICDE at UNESCO," 9th UNESCO / NGO, Collective Consultation on Higher Education, 2005, 6-8 April

[9] O. Ron, "The role of ICT in higher education for the 21st century: ICT as a change agent for education, Edith Cowan University, Perth, Western Australia

[10] M. Fengchun, "Constructive approach to ICT in education," APPLIEDUNESCO, Bangkok, 2010

[11] Y.S.Kiranmayi,"Management of higher education in India," Crown Publication, New Delhi, 2009

[12] Alshurideh, M., & Alkurdi, B. (2012). The Effect of Customer Satisfaction upon Customer Retention in the Jordanian Mobile Market: An Empirical Investigation. European Journal of Economics, Finance and Administrative Sciences, 47, 69-78

[13] Tarhini, A., Hone, K., & Liu, X. (2014a). The effects of individual differences on e-learning users' behaviour in developing countries: A tructural equation model. Computers in Human Behavior, 41, 153-163

[14] Darawsheh, S., ALshaar, A., & AL-Lozi, M. (2016). The Degree of Heads of Departments at the University of Dammam to Practice Transformational Leadership Style from the Point of View of the Faculty Members. Journal of Social Sciences (COES&RJ-JSS), 5 (1), 56-79.).

[15] Hubackova, S., & Golkova, D. (2014). Podcasting in Foreign Language Teaching. Procedia Social and Behavioural Sciences, 143, 143-146

[16] Alenezi, A., & Shahi, K. (2015). Interactive E-Learning through Second Life with Blackboard Technology. Procedia Social and Behavioural Sciences, 176, 891-897.

[17] Clark, R., & Mayer, R. (2011). E-Learning and the Science of Instruction: Proven Guidelines for Consumers and Designers of Multimedia Learning. Pfeiffer; 3rd Edition (August 16, 2011).

[18] Maqableh, M., Masa'deh, R., & Mohammed, A. B. (2015). The Acceptance and Use of Computer Based Assessment in Higher Education. Journal of Software Engineering and Applications, 8 (10), 557.

[19] Andersson, A., Grönlund, A. (2009). A conceptual framework for E-learning in developing countries: A critical review of research challenges. The Electronic Journal on Information Systems in Developing Countries, 38(2), pp. 1-16.

[20] Wright, N. (2010). E-Learning and implications for New Zealand schools: A literature review, Report to the Ministry of Education, New Zealand, pp. 23-27

[21] Andreea-Maria Tîrziua, Cătălin Vrabieb, Education 2.0: E-Learning Methods, 5th World Conference on Learning, Teaching and Educational Leadership, WCLTA 2014

[22] Himanshu Agarwal, G. N. Pandey, Impact of E-Learning in Education, International Journal of Science and Research (IJSR) ISSN (Online): 2319-7064

[23] Attila Nagy, The Impact of E-Learning, ICT Business Consultancy, Budapest, Hungary

[24] Keller, C., Hrastinski, S., & Carlsson, S. A. Students' Acceptanc of E-Learning Environments: A Comparative Study in Sweden and Lithuania. International Business, 395-406.

[25] Tarhini, A., Teo, T., & Tarhini, T. (2016). A Cross-Cultural Validity of the E-Learning Acceptance Measure (ElAM) in Lebanon and England: A Confirmatory Factor Analysis. Education and Information Technologies, 21 (5), 1269-1282

[26] Algahtani, A.F. (2011). Evaluating the Effectiveness of the E-learning Experience in Some Universities in Saudi Arabia from Male Students' Perceptions, Durham theses, Durham University.

[27] Nageswara Rao Posinasetti (2014). What are the advantages and challenges of online learning and teaching? Retrieved May 12, 2018, from https://www.researchgate.net/post/What_are_the_advantages_and_challenges_of_online _learning_and_teaching

[28] https://helea rning.wordpress.com/requirements-of-e-learning/

[29] Europass Teacher Academy| Flipped classroom; 2020url= https://www.teacheracademy.eu/course/flipped-classroom/

[30] Bajunury, A., An Investigation into The Effects of Flip Teaching on Student Learning. Master's Thesis, Ontario Institute for Studies in Education of the University of Toronto.

[31] S. Bal and M. Gupta, "Technology and E-Learning in Higher Education Technology and E-Learning in Higher Education," no. May, 2020.

[32] Ina Blau, Tamar Shamir-Inbal, Re-designed flipped learning model in an academic course: The role of co-creation and co-regulation, DOI: 10.1016/j.compedu.2017.07.014

[33] Satinder Bal, Monika Gupta, Technology and E-Learning in Higher Education, https://www.researchgate.net/publication/341734948

[34] A. Picciano, C. Dziuban, and C. Graham, "Blended learning: Research perspectives," vol. 2, 2014.

[35] S.Bocconi& G. Trentin, G. Modelling blended solutions for higher education: teaching, learning and assessment in the network and mobile technology era. Educational Research and Evaluation. (2014), 20(7-8), 516-535, DOI: 10.1080/13803611. 2014.99636.

[36] C.J.Bonk,& C.R. Graham (Eds.). Handbook of blended learning: Global Perspectives, local designs. SanFrancisco, CA: Pfeiffer Publishing. (2012). P, 211- 214.

[37] Kintu M J, Zhu C and Kagambe E 2017 Blended learning effectiveness: the relationship between student characteristics, design features and outcomes International Journal of Educational Technology in Higher Education

[38] Khalid Al-Hussaini, Huda al-qozani, A review of E-Learning in Higher Education, https://www.researchgate.net/publication/349847609

[39] Wiley, David; Hilton Iii, John Levi (2018). "Defining OER-Enabled Pedagogy". The International Review of Research in Open and Distributed Learning. 19 (4). doi:10.19173/irrodl.v19i4.3601

[40] http://opencontent.org/definition/

[41] Open Chemistry Education Resources: Advantages and Disadvantages". Board of Regions of the University of Wisconsin System. Retrieved 24 April 2019

[42] "Open Chemistry Education Resources: Advantages and Disadvantages". Board of Regions of the University of Wisconsin System. Retrieved 24 April 2019.

[43] Hu, H. (2013). MOOC migration. Diverse: Issues in Higher Education, 30(4), 10-11.

[44] Michael Gaebel, Book: MOOCs Massive Open Online Courses, pg 3, January 2013

[45] Kop, R. (2011). The challenges to connectivist learning on open online networks: Learning experiences during a massive open online course. International Review of Research in Open and Distance Learning

[46] Koutropoulos, A., Gallagher, M. S., Abajian, S. C., de Waard, I., Hogue, R. J., Keskin, N. O.,& Rodgriguez, C. O. (2012). Emotive Vocabulary in MOOCs: Context & Participant Retention. European Journal of Open, Distance and E-Learning

[47] Chatterjee, P., & Nath, A., Massive open online courses (MOOCs) in education—A case study in Indian context and vision to ubiquitous learning. In MOOC, Innovation and Technology in Education (MITE), 2014 IEEE International Conference on pp. 36-41, 2014.

[48] J. Chauhan, "An Overview of MOOC in India," no. July 2017, 2018, doi: 10.14445/22312803/IJCTT-V49P117.)

[49] https://www.classcentral.com/report/mooc-stats-2020

The Experience in TUMnanoSAT Launch Preparation

Viorel Bostan[1*], Valentin Ilco[2*], Vladimir Melnic[3*], Alexei Martiniuc[4*], Vladimir Vărzaru[5*], Nicolae Secrieru[6*]

Abstract: The National Center for Space Technologies of Technical University of Moldova (TUM) team was selected by the United Nations Office for Outer Space Affairs (UNOOSA) and Japan Aerospace Agency (JAXA) for the 4th round of the KiboCUBE Program for the launch of the TUMnanoSAT nanosatellite from the International Space Station (ISS). In this paper, a brief overview of the educational and scientific missions of TUMnanoSAT, the impact on system design and the educational opportunities are presented by these challenges. The primary mission of TUMnanoSAT is to provide hands-on experience to students in designing, building, and testing a space system with a specific task/mission. There are described basic testing procedures of this nanosatellite of systems, including structure, electrical power supply communications and attitude control.

Keywords: TUMnanoSAT nanosatellite, International Space Station, KiboCube module, JAXA, UNOOSA

1. Introduction

The National Center for Space Technologies (NCST) of Technical University of Moldova (TUM) has been oriented towards a series of nanosatellites, according to the international standard CubeSat. In 2019, the NCST team participated in the fourth round of the KiboCUBE Program with the "TUMnanoSAT" nanosatellite project proposal and won this competition for free launch by JAXA. This project includes the student-initiative design and fabrication of critical components, including the payload and CubeSat modules.

TUM spurred the installation of facilities such as a clean room to support building, testing, and integration of space hardware. Through this process, students acquired experience with industrial level integration and testing procedures. Undergraduate teams working on TUMnanoSAT lead the design and fabrication of the payload, structure, and system integration, providing experience with systems engineering, technical writing, and various cross-disciplinary applications. Over fifty undergraduate students, several graduate students and faculty members from several departments were involved in this project in both the development and testing of the TUMnanoSAT nanosatellite subsystems to enhance understanding of the fundamentals of engineering.

KiboCube program for the NCST of TUM has a major impact on the improvement of the quality of engineering studies based on modern space technologies, attracting young students to develop and strengthen scientific research in space exploration. The purpose of this paper is

---

[1] Technical University of Moldova, Space Technologies Center, Chisinau, Rep. of Moldova
* Corresponding author: nicolae.secrieru@cnts.utm.md

to present the overview of the TUMnanoSAT nanosatellite and to describe our testing and verification experience in preparation for its launch.

2. TUMnanoSAT setup and overall systems

NCST of TUM, focusing on the international standard CubeSat, decided to develop a series of satellites with specific and efficient missions. For the first mission of TUMnanoSAT our primary objective is to verify under real conditions the functionality of the various satellite modules and subsystems for future missions. The internal 3D schema and its real stack implementation of satellite modules are presented in figure 1. The basic missions of these satellites are:
- testing of nano-structure-based sensors in space conditions;
- to establish effective communication subsystem "satellite-ground station" with the possibility to   modify the communication rate range and ensure high reliability;
- to check the communication protocol "satellite-ground station" with different levels of access;
- testing of power supply system and the search for the optimal modes of accumulated energy distribution;
- testing of sensors subsystem for satellite attitude determining (magnetometers, micro-gyroscopes, sun sensors) in order to optimize process control satellite attitude;
- testing of the COTS electronic components operation in conditions of radiation, including
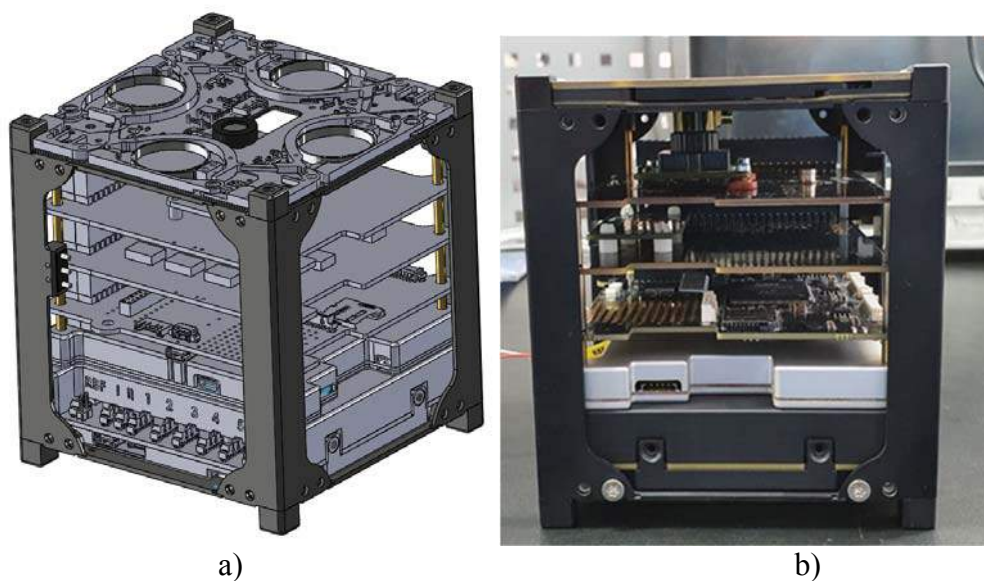

a)   b)

Figure 1. Overview of TUMnanoSAT:
a) Internal 3D schema;   b) real stack of nanosatellite modules.

the onboard computer, digital memories.

2.1. TUMnanoSAT structure

The main purpose of the structural subsystem is to provide a rigid, reliable structure that would withstand all harsh launch conditions. Also the main idea in structural subsystem designing is maximizing usable interior space while minimizing the complexity of subsystem. The basic constraints imposed to TUMnanoSAT structure are given by the CubeSat Design Specifications and JEM Payload Accommodation Small Satellite

Deployment Interface Control Document. Following these standards, TUMnanoSAT dimensions are 100 mm x 100 mm x 113.5 mm. The material used in TUMnanoSAT sctructure is aluminum alloy 6061. Also due to the fact that TUMnanoSAT is designed to be launched from Internation Space Station 3 deployment switches were added to rails. The switches should phisically cut all power lines in the satellite, so when the satellite is installed in deployer no early deployment of antennas or subsystem should be activated. The finite element model of the structure was created by using ANSYS Mechanical. The mass properties were used to construct a model with approximately equal mass as the components. The natural frequency and static load simulations by ANSYS Workbench Modal analysis results that it has revealed that minimum fundamental frequency is 366.57[Hz] which is higher than 60[Hz] and the maximum stress on the satellite was 94.5 MPa, 100.8 MPa and 19.5 MPa in the necessary limits of loads. Stress levels on various parts of the satellite are displayed in Figure 2 show the FEM with input load, acceleration and constraint condition for each analysis cases. The margin of safety for the various components was computed using a factor of safety of 1.5 for yield strength (Fty) and 2.0 for ultimate strength (Ftu).

Real following vibration tests were performed along X, Y and Z axes, with low level sinusoidal sweep and random vibration. The verification points are: no breakage in main structure; main structure needs to satisfy specified natural frequency; natural frequency before
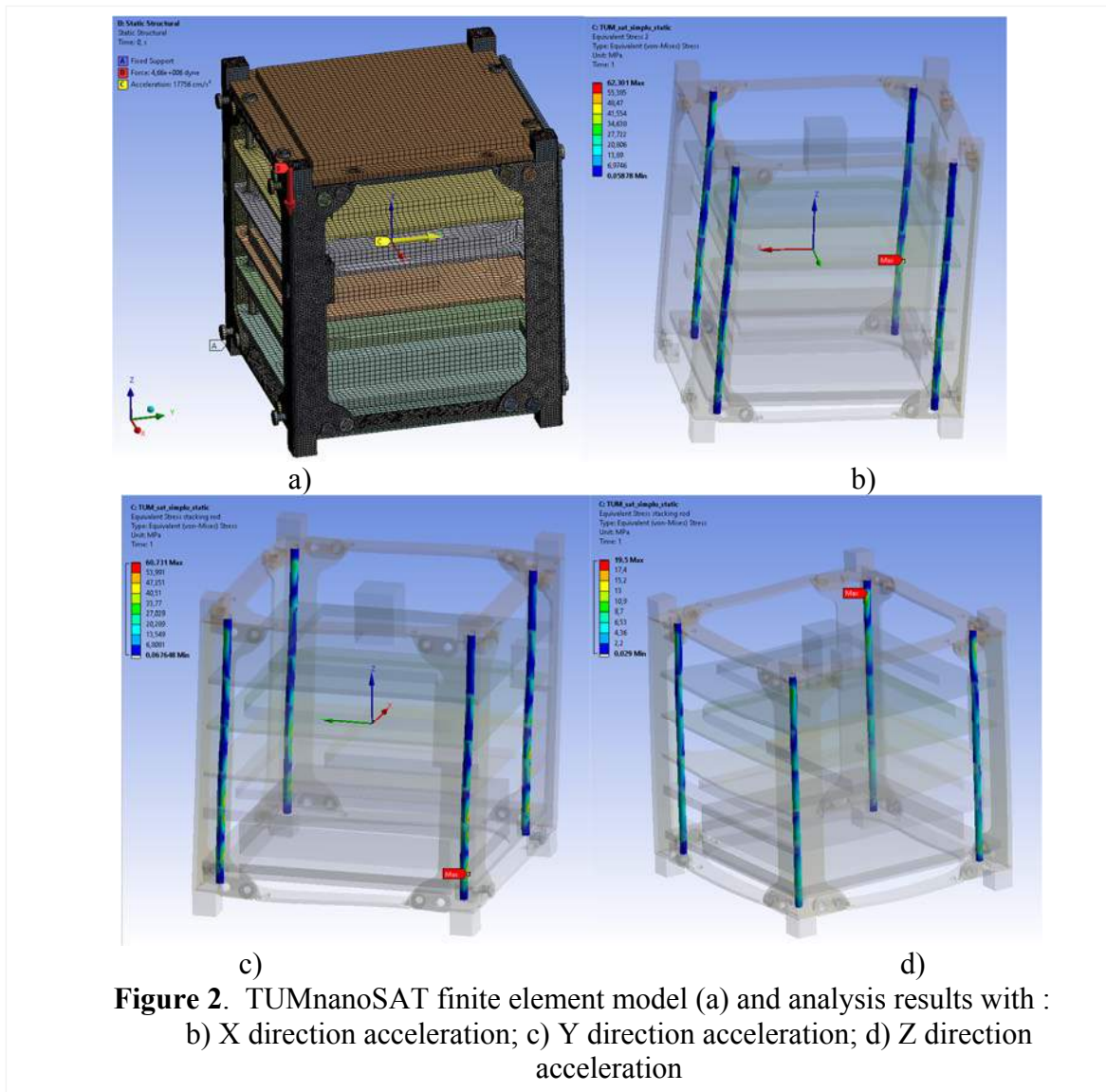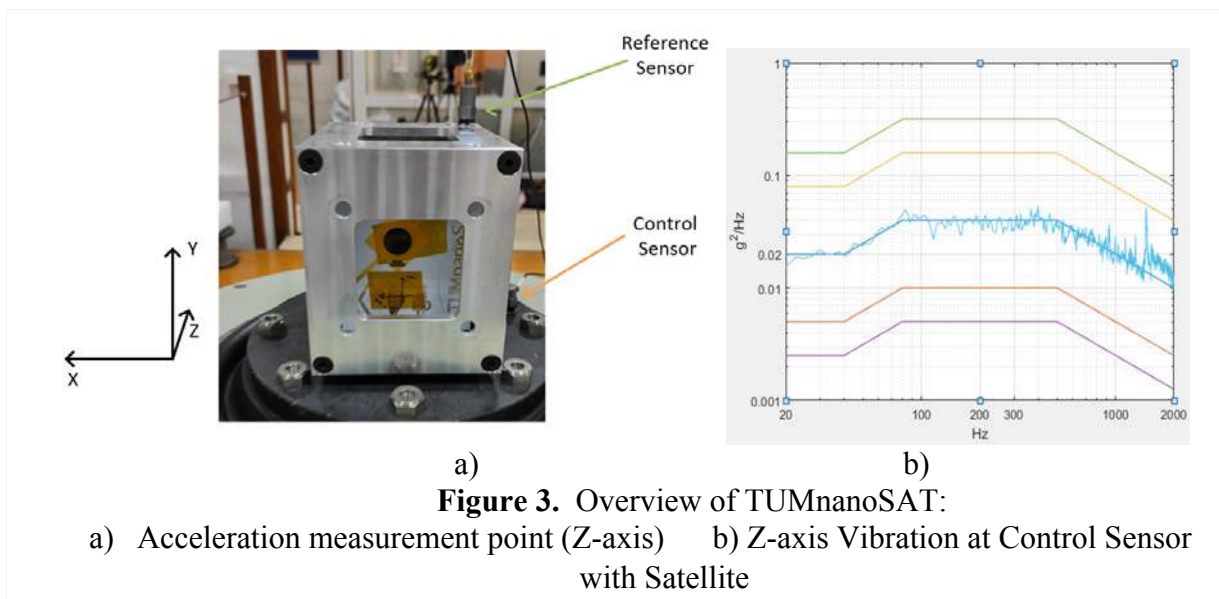

Figure 2. TUMnanoSAT finite element model (a) and analysis results with :
b) X direction acceleration; c) Y direction acceleration; d) Z direction
acceleration

and after tests need to remain unchanged; no improper antenna deployment, and no malfunction to cubesat; no breakage in grass material such as solar battery cover; no loosening in all fasteners. Low level sinusoidal sweep is adequate for model verification of simple structures with relatively rigid components, whose flexibility is confined to mounting bracketry or frequency isolation hardware. It is performed on each axis with the frequency 20~2000 [Hz] and amplitude 0,5 [G].

The random vibration test level It is performed with the frequency 20~2000 [Hz] and amplitude 02-04 **[G^2/Hz]**. This level is the envelope of the environments for HTV, Space X

a)   b)
Figure 3. Overview of TUMnanoSAT:
a) Acceleration measurement point (Z-axis)   b) Z-axis Vibration at Control Sensor
with Satellite

Dragon and NG Cygnus (reference: JX-ESPC-101132). This test level was defined by Structure Fracture Control Evaluation Form. Some results are presented in the figure 3.

2.2 The power subsystem of TUMnanoSAT

The power subsystem of TUMnanoSAT has one integrated Li-Po battery pack that contains two Varta Li-Po cells with a   total capacity of 10 Wh. Also in EPS (Electrical Power Subsystem) are five solar panels. Each Solar Panel Channel has a DC-DC step-up converter with Maximum Power Point Tracking (MPPT). The output energy for each solar panel is monitored. The Solar Panel Channels can handle input voltages up to 5.5V and the current maximum threshold for overcurrent protection is set to 1.8A. The operating temperature range is from -40 °C to +150 °C and the over temperature threshold is set to +155 °C (the module will turn off if this threshold is reached and restart automatically when the temperature decreases to +130 °C). The efficiency of the step-up convertors is up to 95%. The step-up convertors work at 100 kHz fixed frequency. The duty cycle is controlled by the MPPT algorithm. The boosted output voltage can be accessed through the PC/104 connector for additional functionality such as charging of the external battery pack, super capacitors, etc. The general diagram of power subsystem is presented in the figure 4.

All nanosatellite subsystems require a nominal voltage stabilized by 3.3V or 5V for normal operation. The voltage on the battery can vary in the 3.5V - 4.2V range, so for 3.3V voltage the DC-DC converter with the Buck (Step-Down) topology will be used, and for 5V - DC-DC converter with the Boost (Step-Up topology). To assure a correct and efficient power distribution it was created a simulation model for power subsystem in Simulink. For the
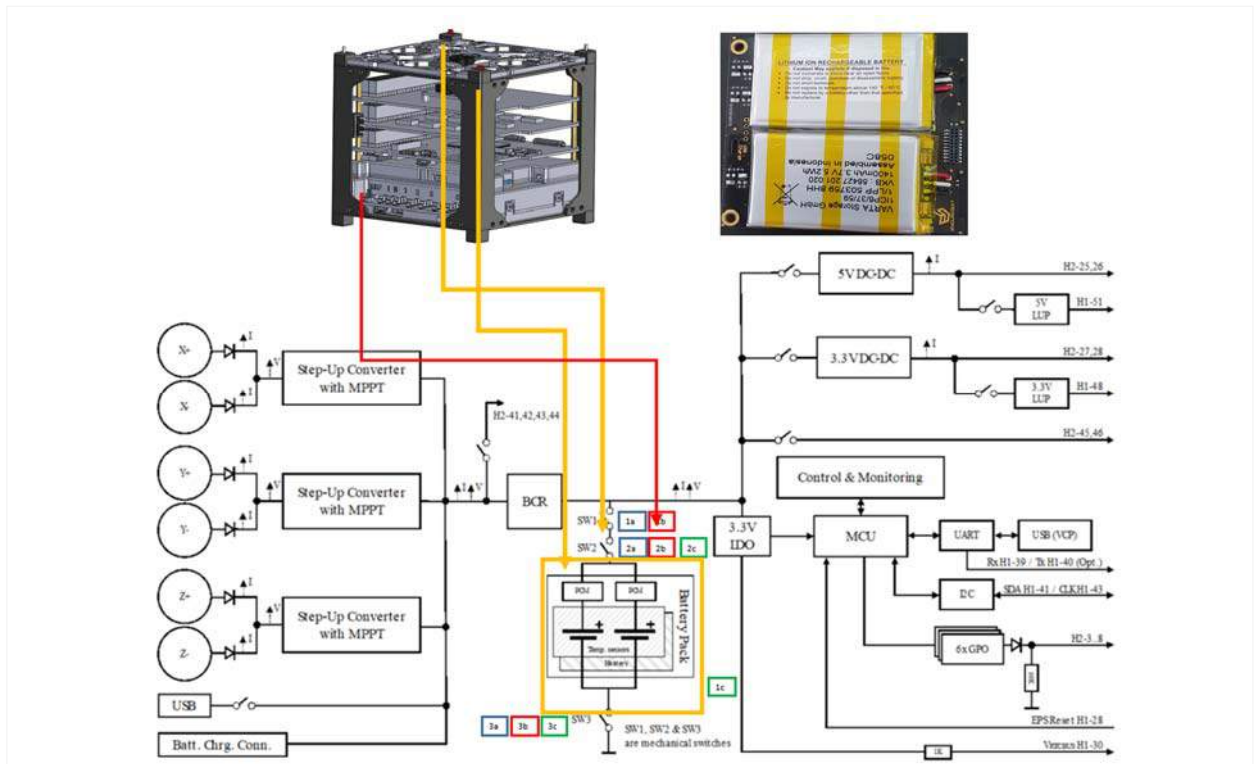
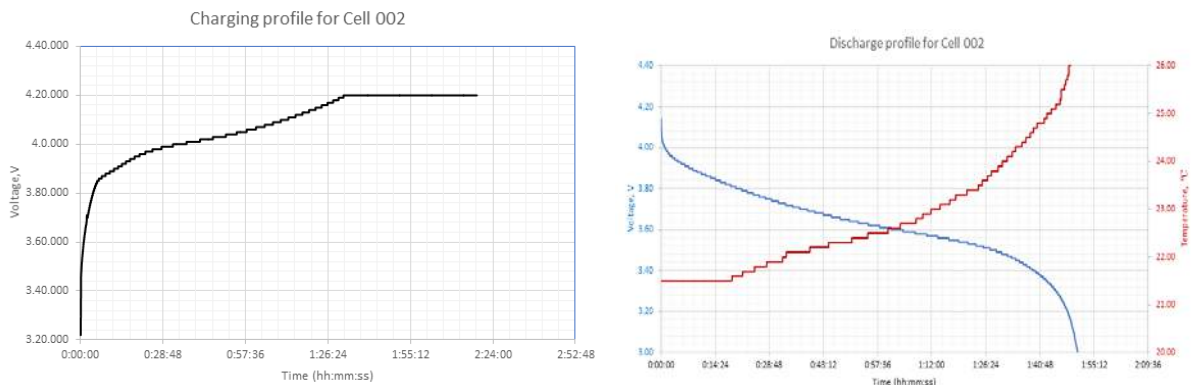**Figure 4**. Diagramm of the power subsystem of TUMnanoSAT.

Figure 5. Batteries characteristics
(Left : Charge,   Right: Discharge)

simulation, the converter models from the standard Simulink library were used. The parameters of the converters have been set according to the technical specifications of all components from EPS. The simulation permits showed that Overall battery state of charge increases after a full cycle (sun and shadow), which shows that in the given configuration, all nanosatellite subsystems will be sufficiently fed without disturbance for any length of time, until the photovoltaic panels, the battery or the appearance of some faults in the control system, but not for the consumption case 1.0W. For EPS reliability were used s hardware and firmware battery protection. Each battery has its own overcurrent, overcharge and overdischarge protections ensured by integrated protection circuit module (PCM). Special firmware algorithm is implemented for protection of the batteries from short circuit, deep discharge and overheating.

The EPS subsystem was subjected to real tests, priority was given to the characteristics of the batteries, being COTS components. Therefore, charge and discharge characteristics tests are performed for each battery cells before and after the environmental tests. From these tests, it is confirmed that charge and discharge characteristics do not change due to the environmental tests and are within the nominal range (figure 5). It is important prior to handover after the environment tests for TUMnanoSAT , Charge/Discharge Characteristic of battery inside nanosatellite is measured to see that there is no damage. To be mentioned that the Charge/Discharge Characteristics test was measured the range between maximum voltage and minimum voltage.

2.3 Communication Subsystem

The communication subsystem is responsible for receiving commands, sending telemetry and payload data. The efficiency of the satellite-ground station communication depends on the distribution of the level functions on the satellite components. The distribution of level functions is proposed as follows in figure 6:

- The physical level is achieved by the RF module: the transmission / reception concomitantly the modulation / demodulation of radio signals, in particular AFSK of the data provided or accumulated by the local microcontroller of the communication mode.

- The level of encapsulation / decapsulation of data according to the AX.25 protocol is performed on the on-board computer (OBC) of the nanosatellite;

- The application level is performed on the on-board computer (OBC) of the nanosatellite, which includes the acquisition of data from the basic sensors, including payload data and captured images.

Therefore, the communication software is done by the following processes, which was developed within FreeRTOS:

- Application Communication Task - the application communication process with the ground station

- DataLink Task - the transport process / communication link;

- Channel / Physical layer Com Task - the process of transmitting / receiving the physical level at communication.

In order for any radio amateur to be able to connect to the "university" satellite in the ground station - university satellite communication system, the AX.25 protocol is recommended as a standard - data transfer protocol at channel level (second lower level in OSI model). It is intended for communication between radio amateurs, which is why it is widely used in amateur packet-based radio communication networks.

The TUM Space Technology Center has a good terrestrial infrastructure for satellite communications, monitoring and control. A further development of a satellite data capture system with flexible configuration is based on SDR technology. The telemetry communications station is endowed with specialized equipment to ensure upward and downward linkages of the satellite in orbit flight with the ground infrastructure. It is connected to a set of telemetry antennas and to the parabolic antenna with mixed purpose. The telemetry antennas and the parabolic antenna are able to orient on two axes towards the nanosatellite in orbit flight through the actuator drivers of Rotor BIG-RAS HR model.

The stations can operate in the two main radio amateur bands for communication with small satellites. These bands are the VHF (2m) and UHF (70 cm) band. The antennas, mounted on the mast, are connected with RF ecoflex cable to the LNAs (Low Noise Amplifiers). X-Quad 70cm and X-Quad 2m to LNA SP70 and LNA SP200 respectively. The next node connected from the LNAs consists of coaxial relays which split the signal for feeding it into the ICOM IC-9100 and USRP B200/E310 to be further processed. Besides the main RF connections there is also a data line connection from the PC Ground station to the signal processing units (ICOM and USRP) and a control line connection to the rotator controller and relays.
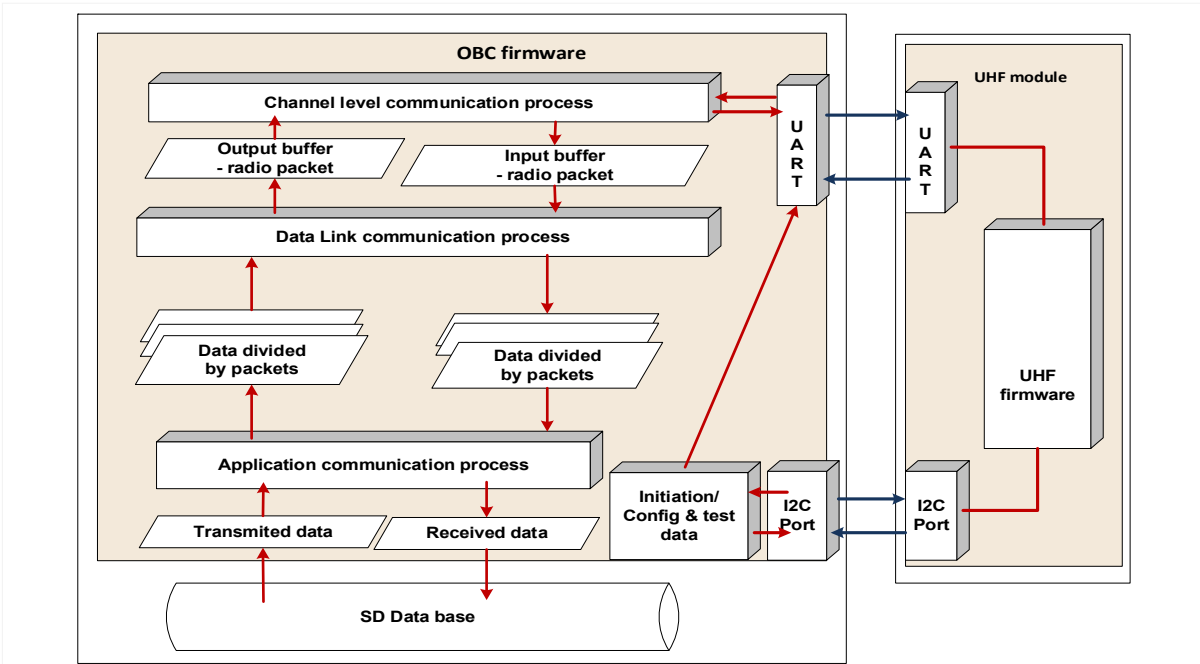

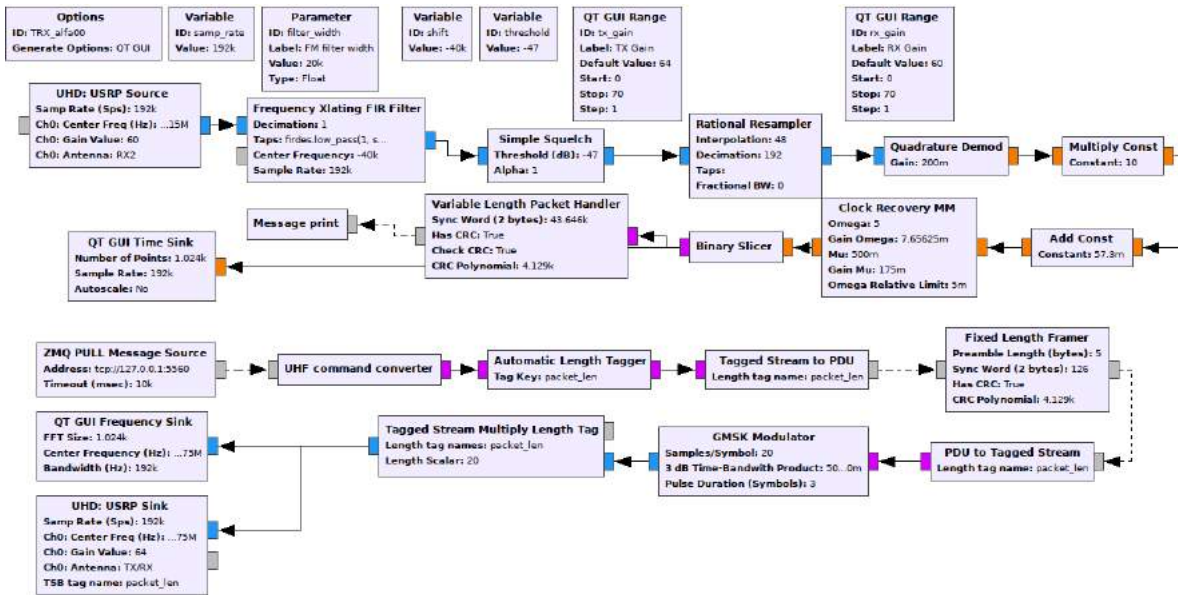**Figure 6.** Hierarchy and interaction of nanosatellite communication processes.

Figure 7. Example of the implementation in GNU Radio
of the communication algorithm with the nanosatellite "TUMnanoSAT".

The "TUMnanoSAT - Ground Stations" communication test scenario consists in checking the connection with the nanosatellite, configuring/setting/resetting the parameters of its modules and requesting payload data or images by the ground station operator, as well as sending the requested data from the satellite to the station. Due to the elaboration of transceiver type algorithms for the peripheral device USRP B200 and USRP E310 of the ground stations of NCST, we had the possibility to check efficiently communication through a semi-duplex channel with the nanosatellite "TUMnanoSAT".

In the result of communication tests it was confirmed, that the procedures and algorithms for communication, which performs the diversified dialogue with different transmission rates, with different ways of packing&encoding messages ensures an efficient and reliable communication of nanosatellites with ground stations.

2.4 Attitude and Orbit Control Subsystem

The attitude control subsystem is a very important one for any mission. In the case of TUMnanoSAT, a low-performance ADCS system is required to orient the nanosatellite to the Nadir direction, because the camera is low resolution and has a large aperture angle (56 degree), on the other hand the antenna also has a transmit/receive diagram with an angle of 120 degrees. Based on these, the following requirements were formulated to the ADCS components. The TUMnanoSAT is equipped with five Solar Panels. There are a network of sensors and a magnetorquer on the Solar Panel PCB and they can be interfaced to an Attitude Determination and Control System (ADCS). The network can be all or a combination of the following: temperature sensor, Sun sensor, magnetorquer, and gyroscope. The temperature sensor and Sun sensor (photodiode) are positioned on the top surface of the solar panel whereas the magnetorquer and gyroscope are positioned within the solar panel and not visible. The magnetorquer is a series of large electrical coils positioned over several layers of a multi-layer PCB. Furthermore, the PCB is equipped with a connector for an external magnetorquer. To calibrate sensors and to test magnetorquers and

attitude control algorithms was build a facility to simulate geomagnetic conditions for the satellite.

The verification of the attitude control algorithms was performed in the terrestrial magnetic field simulation stand. This stand is an elaboration of NCTS and ensures in a computerized way the creation of the magnetic field as intensity and direction in any point of the orbit of the nanosatellite. The results obtained confirm the correctness and quality of the satellite orientation, which are partially shown in Figure 8.
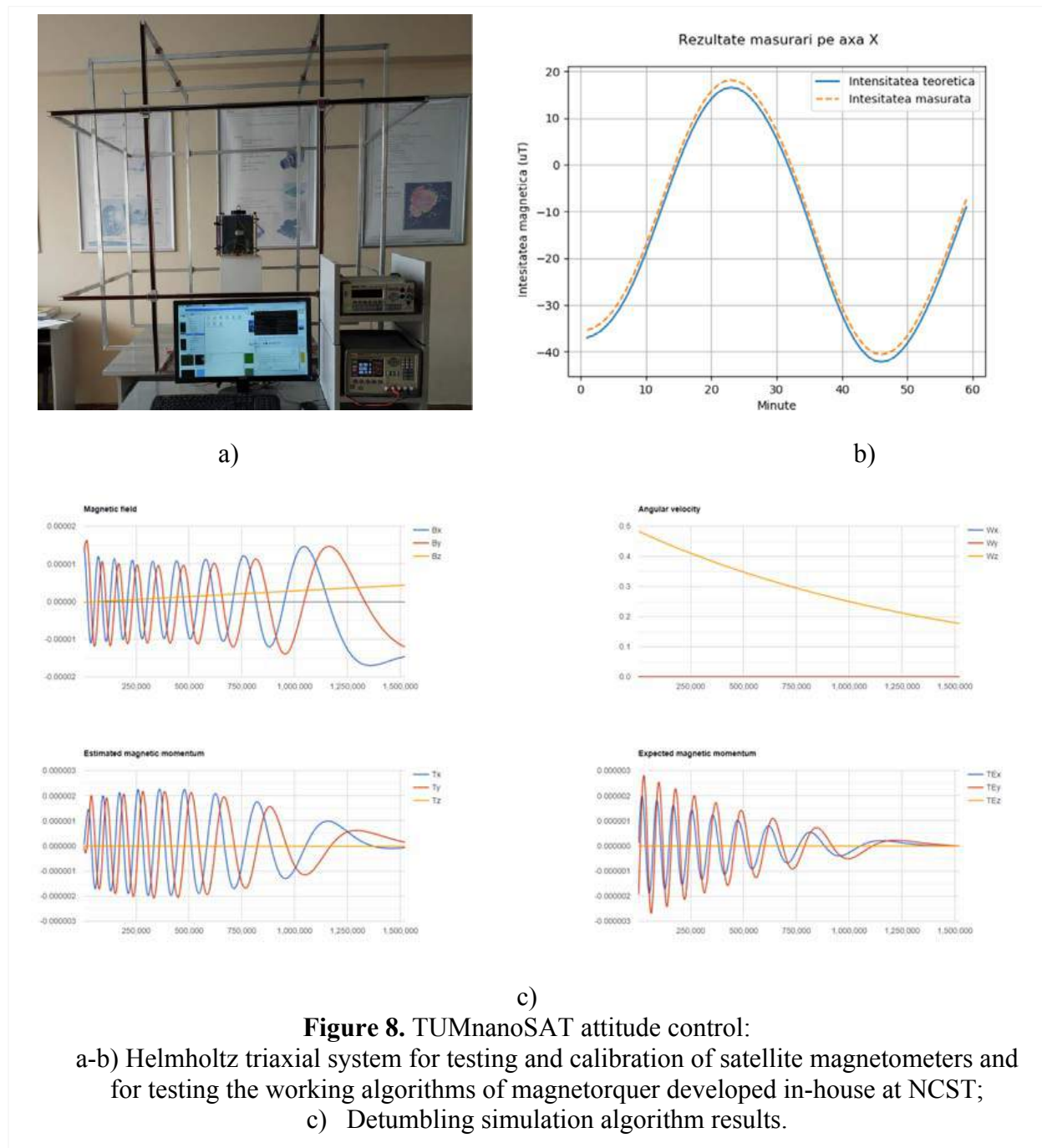

a)

b)

c)

Figure 8. TUMnanoSAT attitude control:
a-b) Helmholtz triaxial system for testing and calibration of satellite magnetometers and for testing the working algorithms of magnetorquer developed in-house at NCST;
c)   Detumbling simulation algorithm results.

3. Discussion and Conclusions

The TUMnanoSAT for KiboCube design is compliant with the Safety Requirements reported in the "JEM Payload Accommodation Handbook Small Satellite Deployment Interface Control Document (JX-ESPC-101133)", especially the specific ones related to the operations inside the ISS, including the possibility to be handled by astronaut on board.

High level functional tests on TUMnanoSAT subsystems and assemblies are required for validation. Functionality of the components shall be verified in different moments during the acceptance campaign. It should be noted that testing TUMnanoSAT nanosatellite was conducted by NCST staff with infrastructure of the ROSA on base of cooperation agreement between the TUM and the Space Science Institute.

This project of the first TUMnanoSAT nanosatellite within the KiboCube program includes several missions. Starting from the general concept, a 3D model of the TUMnanoSAT satellite was developed during the Critical Design Review stage and finally the nanosatellite was made the flight mode, figure 9. These missions are mainly with educational objectives, in the realization of which the students are involved, other objectives are with elements of research and technological verifications. The experimental tests in terrestrial conditions give us confidence in their efficient operation in space conditions.

Based on the KiboCube TUMnanoSAT project, the TUM Space Center aimed to directly involve students in each phase of the development of CubeSat space missions: design, development and testing of nanosatellite subsystems and processing and use of spatial data to promote students' interest in engineering and space technologies.

Acknowledgements

a)   b)
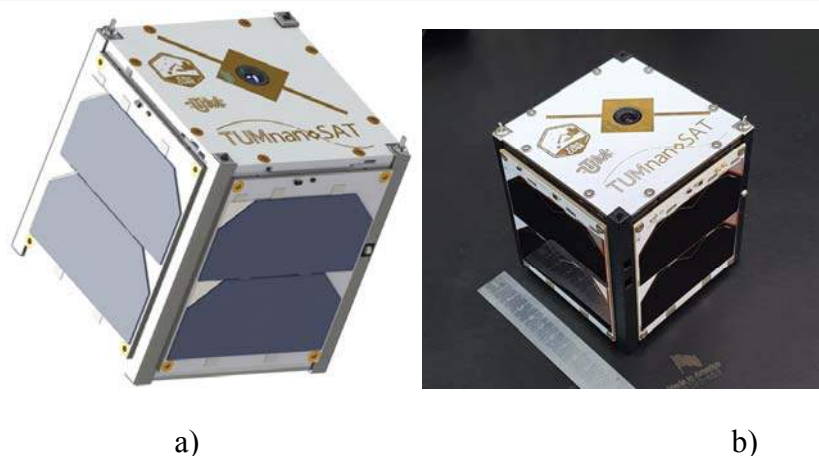
Figure 9. TUMnanoSAT final assembly:
a) 3D model of the TUMnanoSAT satellite after Critical Design Review stage;
b) Real TUMnanoSAT after final assembly.

References

J. Farkas, (2005). CPX: Design of a Standard Cubesat Software Bus, California State University, California, USA, 2005.

L. Dusseau et al., (2005). CUBE SAT SACRED: a student project to investigate radiation effects, In: RADECS 2005 Proceedings, Cap d'Agde, France, 2005.

B. Larsen, The Montana nanosatellite for science, engineering, and technology for the AFRL/NASA university nanosat program.

J. Bouwmeester et al., (2008). Advancing nanosatellite platforms: the Delfi program, - In: Proceedings of the 59th International Astronautical Congress, Glasgow, Scotland 2008.

J. Bouwmeester, J. Guo, (2010). Survey of worldwide pico- and nanosatellite missions, distributions and subsystem technology. - Acta Astronautica 67 (2010) 854–862 pp.

CEOS EO handbook – catalogue of satellite missions. –In: http://database.eohandbook.com/database /missiontable.aspx

World's largest database of nanosatellites, more than 1700 nanosats and CubeSats. – In: http://www.nanosats.eu/

CubeSat Design Specification (CDS) Rev. 13, (2013). The CubeSat Program, Cal Poly SLO, 2013. – In: http://cubesat.org

TUMnanoSAT proposal for CubeSAT Mission Application for the Fourth Round in the framework of United Nations/Japan Cooperation Programme on CubeSat Deployment from the International Space Staation (ISS) Japanese Experiment Module "KiboCube". – Technical University of Moldova. Chişinau, 2019. 63 p.

Infrastructure of the Spatial Sciences Institute (ROSA - Romania) In: http://www2.spacescience.ro/?page_id=22&lang=en

The United Nations/Japan Cooperation Programme on CubeSat Deployment from the International Space Station (ISS) Japanese Experiment Module (Kibo) "KiboCUBE" – In: http://www.unoosa.org/oosa/en/ourwork/psa/hsti/kibocube_2019.htm

Signal performance with eon-xr technology and frequency simulation mode with radio telescope on the MATLAB platform

Vehebi Sofiu[1]*, Faton Kabashi[2]*, Naim Baftiu[3]*

Abstract: The idea of using a large spherical plate using eon-xr technology is a depressing feature of the simulation representations in the 3D system of representing elements with a broad-spectrum characteristic that allows a telescope to operate with a large surface area of radius 250 m, which is arranged in a Y-shaped formation and acts as a single telescope with a range of 24 miles (38 kilometers) in the entire hanging space with an opening angle of 112º. The shape of the telescope function according to the technology represents the largest radio telescope in the universe which traverses radio waves whose frequencies are simulated with wavelengths through the MATLAB platform. Generating frequencies of magnetic wave vary in different wavelengths of about 0.05 inches or 65 miles (120km). In this research, light has been used as a great variety of cosmic phenomena including planets, fossil fuel clouds and dust, which have formed black holes in space. The large radio telescope is positioned at a 40º zenith angle and corrects spherical deviations in the ground to represent complex transformational systems from the adjustability of the vectorial system in the form of polarizations to discrete convergence transformation zones. To capture a signal on the operating system of the radio transmitter using a hardware platform interface for processing the simulation of data recorded in the FM transmission spectrum in a file which is read as a spectrum analyzer in the System toolbox that highlights the local stations of the transmission. Technology research has reduced the cost of electronics as a source of information which empowers scientific instruments globally with collaboration offers for all users and developers of CASPER applications such as compatibility of programming and collaboration environments.

Keywords: Radio telescope, wavelength, transform signals, specter performance, MATLAB

1.0 Large radio telescope

The radio telescope is an astronomical instrument consisting of a radio receiver and an antenna system used to detect radio frequency radiation between a wavelength of 0.05 inches or 65 miles which observes celestial bodies radiating electromagnetic waves in the spectral area of electromagnetic waves. The radio telescope shown in figure 1 has a 76 m diameter guided paraboloid antenna. The reflective surface of the Arecibo telescope fills a naturally occurring plate-shaped device with a diameter of 305 m. The Arecibo installation is equipped with a radar transmitter for studying radar signals reflected by such celestial objects as their planets and satellites. Technological development trends over the years have made it possible to make continuous improvements to increase the reliability of new electronic amplifiers with low noise and ultra-advanced resolution that today the telescope is used all over the world [1].

[1] [1,2]UBT- Higher Education Institution, Pristinam Kosova; [3]University of Prizren, Prizren, Kosova
∗ Corresponding author: vehebi.sofiu@ubt-uni.net

A radio telescope according to eon-xr technology is simply a telescope that was created to receive radio waves from space. In its simplest form and has three ingredients:

- Great beginning of the verse
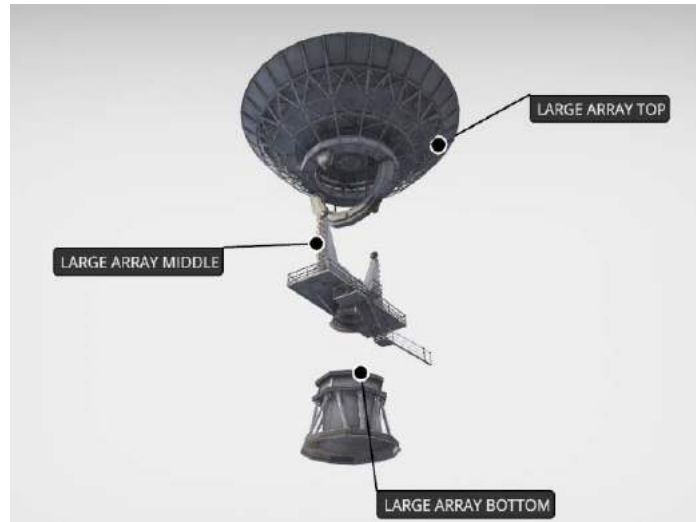
- Large middle of the group

- Big end of group [2]

Figure 1: Large Array Radio Telescope eon-xr

An antenna is a metal device that serves to radiate or receive radio waves. In a word, it represents a transitional structure between free space and reference device. [3]

The transmitting device or transmission line may take the form of a coaxial line or hollow tube and is used to carry electromagnetic energy from the transmitting source to the antenna or from the antenna to the receiver. In this case we have the transmitting antenna and the receiving antenna. [4]

The transmission line is presented in line with Z_c (characteristic impedance) and the antenna is presented as Z_a

$$Z_a=(R_l+R_r) +jX_a \tag{1}$$

which is connected to the transmission line.

- R_l submitted conductivity and dielectric losses associated with the antenna structure.

- R_r represents the radiation resistance that serves to represent the radiation of the antenna.

- X_a represents the imaginary part of the impedance associated with the antenna radiation.

Ideally, the energy generated by the source should be totally transferred to Rr, which serves to indicate the radiation of the antenna. [5]

Steady waves can be reduced and stored energy can be minimized by adjusting the Z_a to Z_c of the line. In addition to receiving or transmitting power, an antenna in an advanced wireless

system is usually needed to amplify the radiation energy in some directions and extinguish it in other directions. There are one or more antennas to collect incoming radio waves. Most antennas are parabolic plates that reflect radio waves to a receiver, in the same way as a curved mirror that can focus visible light at a point. The receiver and amplifier are used to amplify the very weak radio signal to a measurable level. These days amplifiers are extremely sensitive and normally cool to very low temperatures to minimize interference due to the noise generated by the movement of atoms in the metal (called thermal noise). Most radio telescopes nowadays record directly on a disk memory form of computer memory as astronomers use sophisticated software to process and analyze data. [7]

1.1 The performance of the large radio telescope

The Tadio Large Aperture Telescope is a Arecibo spherical telescope that illustrates the optical geometry of the FAST and its extraordinary features: support structure, secondary reflector, main active reflector of 500 m which directly corrects spherical deviation and partial spatial of cable-driven amplifier, servomechanism with adjustable secondary system to hold the most precise parts of the receivers and a parallel robot. Inside the cab, multi-beam and multi-band receivers will be installed, covering a frequency range of 70MHz - 5 GHz. Based on the Communications Toolbox mode, simulated forms of signals with different frequencies can be used to capture RF signals from the air with data generation interferences using the Radio Defined Radio (SDR) hardware. Effective visualization is the best way to communicate information even when the data modeling according to the programming platform is presented in complex forms. [8]

The platform used by MATLAB simply extracts information about any signals used that it can capture in the workspace or directly into a file for processing after capture in the Simulator.

The capture function is used to record the FM Transmission spectrum in a file which is later read again in a DSP System Toolbox spectrum analyzer that highlights the communication peaks corresponding to the local transmission stations. The wave capture function is used to receive an LTE frame from a local antenna in the workspace with the MATLAB application. The LTE Toolbox is used to decipher the known physical cell identifier to verify the reception shown in Figure 2. Large radio and telescope systems involve all technological stakeholders in order to follow innovative trends for the near future by alluding to optimal specifications and structural criteria which are unified within and outside community structures. [9]
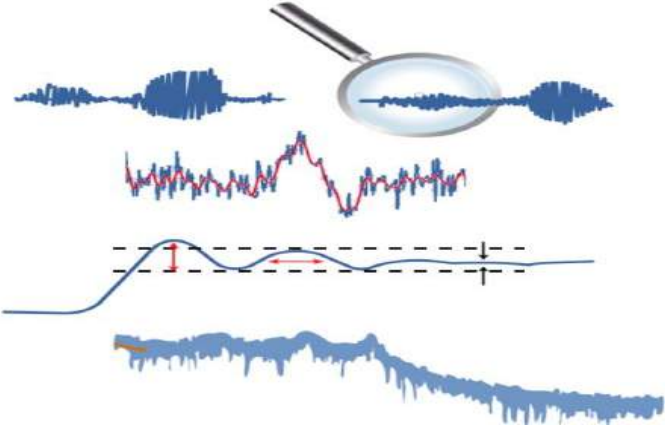
The simulation information is given with the same frequencies $f_1 = f_2$ and different $f_1 \neq f_2$ through two communication fields from 0 Hz to 30 Hz and magnitudes from 0-1 figure 3. The

communication signals with the analytical signal application have generated data different of constant shape and sinusoidal shape. The obtained data were filtered with the Filter Desingh application describing the time frequency during exploration as the impulsive response of the signal processing tools as the required response. [10]
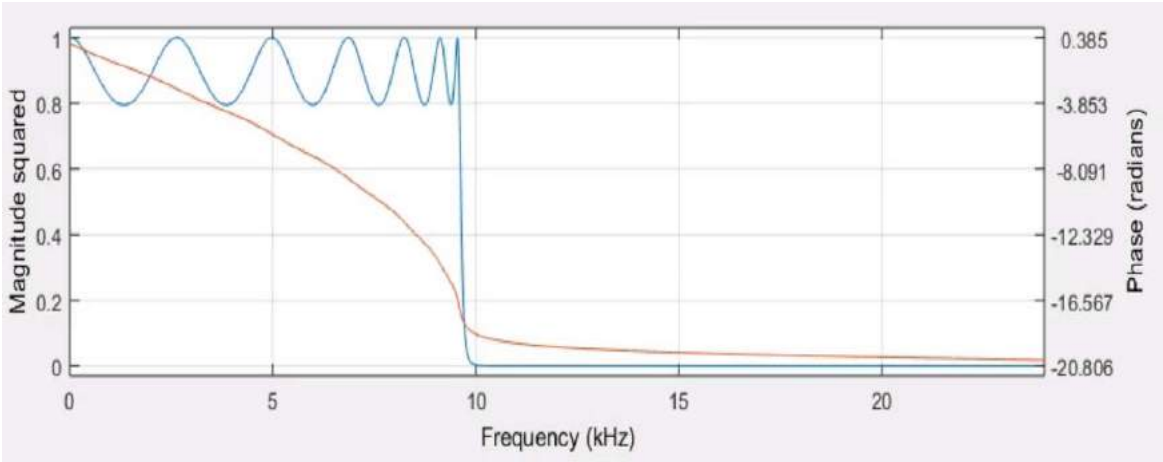

Figure 3: Communication signal between frequencies with filter analyzer

1.2   Signal power spectrum

The use of key concepts to update signal integrity through rules of acceptance and analytical approximation with numerical and measured data ensures the integrity of mathematical path design and improvement as an engineering practice for performance improvement [11]. The power spectrum is estimated through the Fourier transform using the direct analytical form according to equation (1). Frequency signal data is converted into data received as a function of time. Based on the data simulation and simulation download we provide pulse waves by the way of transmitting wave motions divided according to the samples in equal frequency positions or variable depending on the given modeling which adjusts the positions through the spatial interpolation used in the spatial values. located at x-y coordinates as the control routine on the MATLAB platform. The uniform signal sampling platform defines the connections of the autocorrelation function to the modeled signal data in a uniform network. Detection of lost samples at points of change resembles signals of the power spectrum which is made through Furie transformations.

There are two techniques of Fourier analysis:

- Fourier analysis solves the periodic signal - the energy signal in an infinite sum of sinusoidal waves.

- Fourier analysis performs a similar role in the analysis of non-periodic signal which are most used in power signal processing.

Infinite signals have components of sinusoidal waves whose frequency is the main component imposed on the amplitude of the signal. [12]

Spectral power is represented by the relation:

$$\text{Fs(f)} = \frac{1}{T} \int_0^T v_{xx}(t)\, e^{-j2\pi m f_1 t} dt \qquad\qquad m = 0,1,2,3\ldots \qquad (2)$$

$$\text{Fs[m]} = \sum_{n=1}^{N} v_{xx}[n] e^{-\frac{j2\pi mn}{N}} \qquad\qquad m = 0,1,2,3\ldots\ldots N \qquad (3)$$

v_{xx} (t) and v_{xx} [n] are autocorrelation bonds, whose functions have symmetry and the sine terms in the Fourier series are zero and the function takes a simplified form including the real cosine cut. [13]

$$Fs(f) = \frac{1}{T} vxx(t) \cos(2\pi m f t) dt \qquad\qquad m=0,1,2,3\ldots\ldots \qquad (4)$$

$$Fs[m] = \sum_{n=0}^{N-1} v_{xx}[n] \cos(\frac{2\pi nm}{N}) \qquad\qquad m=01,2, 3\ldots N \qquad (5)$$

Equations (4) and (5) represent cosmic transformations.

The energy transformation approach is a direct relation of the analog signal x (t) which is related to the signal size of the integrated square over time according to:

$$E = \int_{-\infty}^{\infty} |x(t)|^2 dt \qquad (6)$$

A major attribute in generating power data in the integrated squares part that refers to spectral power densities is the Parseval theorem [14]:

$$\int_{-\infty}^{\infty} |x(t)|^2 = \int_{-\infty}^{\infty} |X(f)|^2 df \qquad (7)$$

The Praseval connection allows us to calculate the energy of a signal from the Furier series:

$$\int_{0}^{T} (|f(t)|)^2 = T \sum_{n=-\infty}^{\infty} ((|c_n|)^2) \qquad (8)$$

Therefore $|x(t)|^2$ is equal to the energy density function over the frequency or simply the energy spectrum (FS).

In the "direct access", the energy spectrum is also counted as square form energy:

$$FS(f) = |X(f)|^2 \qquad (9)$$

From the generated sampled data, we have constructed power spectra with data uniformed by the signal models as part of the noises generated by the different frequencies from 0 to 0.3 amplitudes shown as in figure 4. In these different estimates are derived the results of spectrograms at the specified frequency determining the treatable time velocity and the structured modeling time of 4ms. [15]
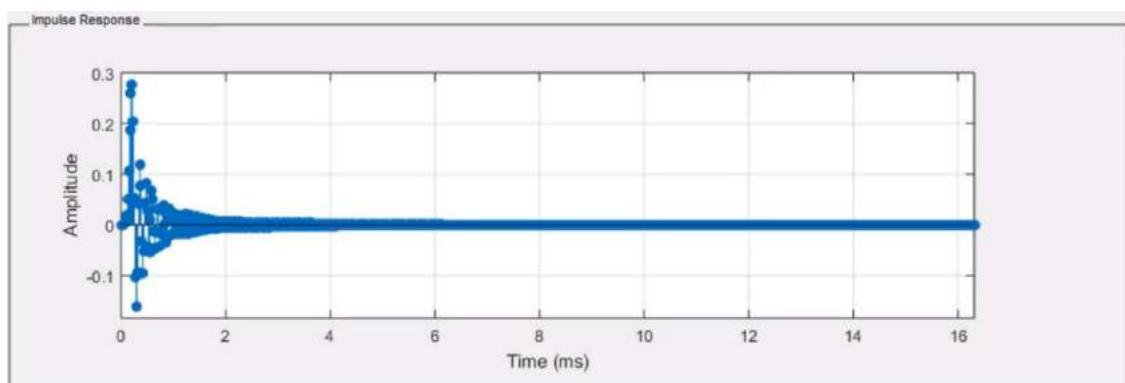

Figure 4: Presentation of time amplitudes obtained from noise

In practice it is much more important to make some characteristic measurements of waveforms before classifying the signal. The measurements capture quantitative descriptions

of the existing state and the differences of the signals produced by the activity of the simulated samples by generating data modeled by identifying the characteristic features (sound, frequency, time and speed) as a technique of signal processing with automated measurements. data obtained from the MATLAB platform shown in Figure 5. [16]
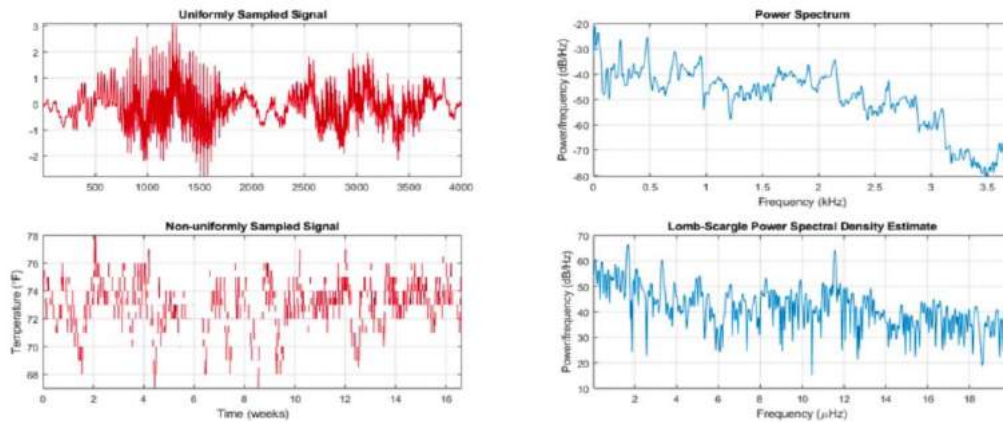

Figure 5: Difference of sampled power-frequency signals

Signals which have poor radio coverage are channeled from the food tree to a receiver located in the focus cabin located on top of the telescope which has several brass tubular horns. Radio receivers amplify the input signal of the system which optimizes different frequency applications and optimizes different frequency applications. Wave interference consists of two or more separate antennas widely connected to transmission lines. Controlling and digitizing analog transmitter follicles is acceptable if the frequency of reception and the frequency of transient transmission of energy are close to the band of interest. [15]

1.3 Frequency and time simulation mode

The time-dependent frequency simulation mode accelerates the simulation of systems with different frequencies which characterize the maximum step size for the variables of variable operators. Phase analysis of such systems uses blocks of Periodic Operators of Physical Signals. Frequency simulation analyzes the transient effects and modality of the data generated to perform the phase analysis of a model. [16]

The obtained data are based on anaclitic calculations whose variables are divided into two categories:

- Time variables with nominal period $2\pi / \omega_0$

- Frequency variables at nominal frequency, $x = d_x + a_x \cos(\omega_0 t) + b_x \sin(\omega_0 t)$

The time simulation mode is limited by a small fraction of the nominal frequency. The effects of accelerating the solution of complex problems in the case of the presentation of sinusoidal variables allowed by the variable selector with large steps. The frequency and time simulation modal should have a slow dynamic in relation to the simulated values obtained compared to the constant value variables. [17]

Signal blockages outside the physical network are not considered valid sinusoidal sources and we cannot execute frequency simulation data that does not meet the criteria of model analysis. [18]

Conclusion

Classroom 3.0 learning applications are based on eon-xr technology that offers practical benefits over implementation of complex 3D problem solving even remotely.

The use of analytical practices has updated the signal transmission through the analytical approximation of Fourier transforms for the generating power of numerical data and metered data.

Generation of sampled data according to power spectra from signal modeling as part of the noise generated their frequencies range from 0 to 0.3 amplitudes.

MATLAB platform applications are used in the same operating field with different frequencies between communications from 0HZ to 30 HZ.

The transformation approach gives the large power data generated in the integrated squares part which refers to the spectral power density from the Parseval theorem.

Signals with poor wave coverage are channeled from the data source to the top of the large telescope which amplifies and optimizes different frequencies by using phase analysis of systems in blocks.

The provision of generating modulations depends on the way of transmitting the wave movements of communications in separate frequencies according to the simulation samples in equal frequency positions.

The connections of the uniform autocorrelation functions have the analytical symmetry of the transformations in the Fourier series are simplified to the real part. Analytical data of energy furrier transformations are an adaptation of the interactive data language provided by simulated modeled measurements.

Frequency adjustment accelerates the modulation of systems with different frequencies which characterize the variability of periodic signal operators which directly illustrates the spherical deviation with adjustable secondary system to keep the most precise parts of the receivers in the system.

Frequency dependence on time accelerates the simulation of different speeds that characterize the magnitude of coverage of physical operators.

Reference

[1] Kemneth. I. Kellermann; Ellen N. Bouton; Sierra S. Brandt; The National Radio Astronomy Observatory and Its Impact on US Radio Astronomy, USA, 2021

[2] www.eon-xr (Large Array Radio Telescope, USA, 2021

[3] Constantine A.Balanis; Antenna theory analysis and design", 2014.

[4] Mario Garcia-Sanz; Robust Control Engineering; 2017

[5] William A. Imbriale; Large Antennas of the Deep Space Network; 2008

[6] Bernard F. Burke; An Introduction to Radio Astronomy 3rd Edition; 2010

[7] Spectrum Management for Science in the 21st Century, USA, 2010

[8] Claus O. Wilke; Fundamentals of Data Visualization; 2019

[9] James W. Mar, Harold Liebowitz; Structures Technology for Large Radio and Radar Telescope Systems, 2003

[10] *Daniel Aronsson;* Modeling and Simulation of Signal Processing Applications with MATLAB and Simulink; 2021

[11] Eric Bogatin; Signal and Power Integrity, 2020

[12] Khamies M. A. El-Shennawy; Fourier Series and Power Spectra; 2014

[13] John Semmlow, Signals and Systems for Bioengineers, 2012

[14] https://support.lumerical.com/hc/en-us/articles/360034394274-Using-Parseval-s-theorem-to-check-for-energy-conservation-between-the-time-and-frequency-domain

[15] Modeling and Simulation of Systems Using MATLAB and Simulink; Modeling and Simulation of Systems Using MATLAB and Simulink,2011

[16] Dac-Nhuong Le, Abhishek Kumar Pandey, Sairam Tadepalli, Pramod Singh Rathore, Jyotir Moy Chatterjee; Network Modeling, Simulation and Analysis in MATLAB, 2019

[17] Mahamed Nahavi; Signals and Systems; Californija, 2012

[18] Katalin Popovici, Pieter J. Mosterman; Real-Time Simulation Technologies: Principles, Methodologies, and Applications, 2013

[19] Elena Cordero; Luigi Rodino, Time-Frequency Analysis of Operators; 2020

[20] Franz Hlawatsch; Time-Frequency Analysis and Synthesis of Linear

Sun Dyeing of Wool Yarns with *Pyracantha coccinea* Roem. Fruits

Selime ÇOLAK[1], Meruyert KAYGUSUZ[2*], Fatoş Naslihan ARĞUN[3]

Abstract: People have used the natural dyes for millennia and have perfected the art of natural dyeing. Today's consumers have preferred using natural dyed fabrics or clothes, so the appeal of natural dye is returning. Most natural dyeing methods have required a heat source to extract dye. Solar dyeing relies on natural heat from the sun. Aside from being environmentally friendly and super low cost, this method requires very few tools and little work, and results in non-repeatable, beautiful colors. *Pyracantha coccinea* Roem. or scarlet firethorn is one of the shrubs belonging to the Rosaceae family, which remains green in summer and winter. It has plentiful orange-red globose fruits in the form of grape clusters. The most important feature of the plant is that it is resistant to cold and drought. For this reason, it is used to create hedges since even in winter, the fruits on it do not fall off, creating a decorative image. In this study, ecological sun dyeing process of wool carpet yarns with *P. coccinea* fruits extract at different pHs was investigated. When the colors obtained were evaluated, it was seen that the use of different chemicals can create different tones of brown color in wool yarns. Thus, it was revealed that *P. coccinea* fruits can be used as a natural dye source and the sun dyeing method is appropriate for textile dyeing.

Keywords: Eco-friendly method, Sun dyeing, Natural dyes, *Pyracantha coccinea,* Wool yarns

1. Introduction

Natural dyes have a historical, cultural and economic importance and value in the coloring of textile products. The art of using plant dyes has been improved today with the development of science and technology, and has gone far beyond the traditional practices (Erdem Işmal, 2019). Recently, awareness of humans and their grown demands on eco-protection, eco-safety and health have created new approaches for the use of natural colorants that have no adverse effects on the environment and aquatic ecosystem (Yusuf et al., 2017). The issue of advanced approaches for natural bio-resources and bio-based colorants and their sustainable use for functional clothing is currently being reconsidered in textile research and development. Therefore, the appeal of natural dyes is returning.

The interest in natural dyes, especially in the textile industry, is increasing day by day. The reason for this situation is that synthetic dyes can have allergic, toxic and carcinogenic effects on the human body and environmental concerns that have arisen recently. Not only to prevent

health problems, but also to prevent the degeneration of cultures and their loss by losing their values, people show interest in products that carry the traces of their cultures and take their source from nature. Based on this idea, aesthetic perception also changes (Taylan and Atlıhan, 2018). Many craftsmen and textile designers or artists have also started to use natural materials and natural dyes.

Most natural dyeing methods have one thing in common; a heat source is required to extract dye. Sun dyeing or solar dyeing is different by the type of heat source used. Solar dyeing relies on natural heat from the sun, whereas other dye methods commonly use artificial heat sources like an electric stove top. Aside from being environmentally friendly and super low cost, this method of natural dyeing is suitable for everyone and can be completed in just a few steps (Irwin, 2020). Solar dyeing is a natural method that requires very little work and results in non-repeatable, beautiful colors. It also requires very few tools, unlike stove-top dyeing and other dyeing techniques. It is an easy, natural and enjoyable way to give the yarn color and character (Ffrench, 2017).

Pyracantha coccinea Roem. or scarlet firethorn is one of the thorny perennial shrubs belonging to the Rosaceae family, which is up to three meters tall and remains green in summer and winter. It produces small, bright red berries. The fruit can be cooked to make jellies, jams, sauces and marmalade (www.wikipedia). Its red fruits, which are in the size of peas, are also known by names such as "dog apple", "rabbit apple" and "bird apple" (Sarıkürkçü and Tepe, 2015). It is naturally found in Tekirdağ, Istanbul, Bursa, Bolu, Zonguldak, Sinop, Tokat, Trabzon, Artvin, Konya, Ankara, İçel and Hatay regions in our country (Kambur, 2009). The most important feature of the plant is that it is resistant to cold and drought. For this reason, it is used to create hedges since even in winter, the fruits on it do not fall off, creating a decorative image.

In this study, ecological sun dyeing process of wool carpet yarns with *P. coccinea* fruits extract at different pHs was investigated.

2. Material and Method
2.1. Materials
The plant samples used in the research were collected from Gerzele region of Denizli Province in September 2020 and their fruits were separated (Fig. 1).

Figure 1. The collected *Pyracantha coccinea* (a) and its separated fruits (b)

Double twisted wool (100%) carpet yarn was used. Tannic acid (Tekkim, Turkey) was used in the mordanting process. pH adjustment was performed by vinegar and sodium bicarbonate.

Four glass jars with lids were used for sun dyeing process. The glass transmits the sun rays and contributes to the heating of the dye solution inside the jars.

2.2. Method
Extraction of plant dye
100 g of fresh *Pyracantha coccinea* fruits were immersed in 2 L of water and boiled for 2 hours. The extract was cooled for 30 minutes. The remnants of plant matter were removed from the extract and the obtained dye solution was used in subsequent applications. pH value of the dye solution was determined to be 5.5.

Preparation of yarn
Wool yarn was washed in a solution of soda and detergent in order to remove the impurities on them. They were made ready for dyeing by rinsing several times with warm water.

Sun dyeing application
In the solar dyeing applications plant materials can be used directly putted in jars with yarn or fabrics, but in our case the extraction of dye solution was carried out to produce an even dye. The equal amount (300 mL) of the prepared dye solution from *P. coccinea* was transferred to each glass jar. The first jar with only extract solution was marked as control. In the second jar pH of the dye solution was adjusted to 3.5 with vinegar. The pH value of the solution in the third jar was arranged to 9.0 by sodium carbonate. To the dye solution in the fourth jar tannic acid was added as biomordant and pH was measured to be 5.0 (Fig. 2). 1 g of wool yarn was placed in each dye solution. All the jars were closed with lids and were left in sunny place to sun dye for one week. Long agitation may cause fibers to felt (Ffrench, 2017). After solar dyeing process, the wool yarns were squeezed, rinsed with water and dried at room temperature. Color evaluations were made for the dried samples.

Figure 2. The arranged dye solutions for sun dyeing: a) control with pH 5.5, b) pH 3.5 by vinegar, c) pH 9.0 by carbonate and d) pH 5.0 by tannic acid

3. Results and Discussion

The most suitable fibers for natural dyeing are cationic fibers such as wool and polyamide because they absorb the color beautifully. The raw material of woven handicraft products is wool. It can be shown that natural dyed products do not adversely affect humans and the environment, unlike synthetic products, and these materials, which are already a part of nature, are evaluated and presented to human use by producing healthy products (Çolak et al., 2020). The obtained colors of wool carpet yarns after sun dyeing with *P. coccinea* in four different pHs are shown in Figure 3.
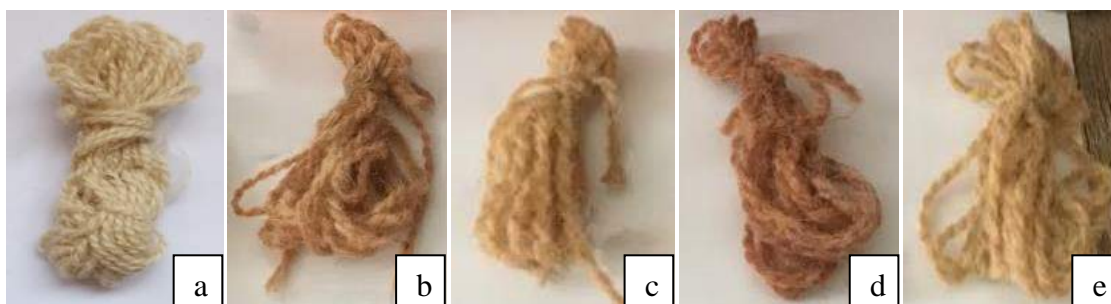
Figure 3. Colors of wool yarns a) undyed, b) control pH 5.5, c) pH 3.5, d) pH 9.0 and e) with tannic acid pH 5.0

As seen from Fig. 3, different color and tones have emerged as a result of the sun dyeing with *P. coccinea* fruits extract. While the color of the raw wool yarn was light beige, the color of the yarn dyed with the *P. coccinea* extract in the dyeing trial without using any mordant or chemical substance was in brown tone (Fig. 3). Whereas the adjustment of pH of the dye solution to 3.5 by vinegar was resulted in fulvous color of the yarn, the arrangement of pH to 9.0 by sodium bicarbonate caused obtaining of darker tone of yarn (Fig. 3). Even though the use of biomordant causes to change the dye solution to dark, the obtained color shade of the yarn was ivory or paler fulvous than the tone provided by the dye solution with pH 3.5. The color of the yarn, which was mordanted with tannic acid and dyed with the extract, created a light color (Fig. 3). In our study, this color difference is thought to be caused by both arrangement of pH and the use of biomordant. Furthermore, the higher pH as 5.5 and 9.0 resulted in obtaining of darker tones. Tannic acid is a mordant that makes chemical bonds between the dye molecules and the functional groups of the fibers, and generally change the color produced by the dye (El Khatib et al., 2016). It was stated that for best results the solar dyeing process can be performed longer, but in summer most dyes will give long lasting beautiful color after two to three weeks if placed in a sunny spot (Aka, 2019). In this study it was determined that one week of solar dyeing was enough to obtain effective coloration of wool yarn especially at mild acidic and basic pHs.

The process of dyeing involves adsorption of the dye on the fiber surface and then spreading it to the inside. The process of adsorption and dispersion depends on the nature of the fibers to be dyed. Fiber and animal fibers (such as wool and silk) containing amine and carboxylic groups are aliphatic (Al-Khateeb, 2019). The chemical composition of wool makes it chemically compatible with most types of pigments. It was reported that *P. coccinea* fruits are good source of glutathione, vitamin C, β-carotene and lycopene (Çöteli and Karataş, 2017). Beta carotene is a natural pigment that gives an yellow-red or orange color and is used in food coloring. The carotenoid dye structure has long-chain conjugated double bonds, which acts as chromophore (Gupta, 2019) and gives a yellow to red color (Venil et al., 2020). In addition, the natural wool has the ability to easily absorb dyes.

4. Conclusions

In this study, the wool carpet yarns were put in the dye solution obtained from the fruits of *P. coccinea* and solar dyeing process was carried out after pH adjustment. When the colors obtained were evaluated, it was seen that different pHs can create different tones in wool yarns. It is understood from the results obtained that darker colors are obtained at slightly acidic pH as 5.5 or at basic pH 9.0, while light colors are obtained at more acidic pHs as 3.5 with vinegar and 5.0 by tannic acid. Thus, in the light of the data obtained, it was revealed

that *P. coccinea* fruits can be used as a natural dye source and solar dyeing method is appropriate and creative for dyeing of wool fibers.

Solar dyeing is by far the easiest and most straight forward of all the natural dyeing methods. It is enjoyable to watch the color change every day as the yarns are exposed to the sun. It was seen that this method works well with natural fiber. It is also a great way to connect with the surroundings since natural solar dyeing uses natural materials such as leaves, flowers, veggies or fruits as in our case. It should be taken into consideration that the geographical location and time of year will influence the temperature that solar dye reaches and this can affect the resulting colour.

References

Aka, V.M.A. (2019). The Beginners Guide to Solar Dyeing. https://lacreativemama.com/beginners-guide-solar-dyeing/ Accessed on 20.08.2021.

AL-Khateeb, D. S. M. (2019). Extraction Dyes From Two Natural Plants Olive Leaves and Beta vulgaris and The Uses in dyeing Textile. J. Phys.: Conf. Ser. 1294.

Çolak, S., Kaygusuz, M., Arğun, F.N. (2020). Dyeing of Wool Yarns with *Parthenocissus quinquefolia* L. Leaves Extract. In "Theory and Research in Engineering", Ed. A. Hayaloğlu, Gece kitaplığı, Ankara.

Çöteli, E.and Karataş, F. (2017). Ateş Dikeninin (*Pyracantha coccinea* Roemer var. lalandi) Kırmızı Meyvelerindeki A, E, C Vitamini, β-Karoten, Likopen, Glutatyon ve Malondialdehit Miktarlarının Araştırılması. Fırat Üniv. Fen Bilimleri Dergisi, 29(1), 41-46.

El Khatib, E. M., Ali N. F., El-Mohamedy, R. S. R. (2016). Enhancing dyeing of wool fibers with colorant pigment extracted from green algae. Journal of Chemical and Pharmaceutical Research, 8(2), 614-619.

Erdem İşmal, Ö. (2019). Doğal boya uygulamalarının değişen yüzü ve yenilikçi yaklaşımlar, YEDİ: Sanat, Tasarım ve Bilim Dergisi, Yaz 2019 (22), s. 41- 58.

Ffrench, C. (2017). Kissed by the Sun: The Art of Solar Dyeing. https://spinoffmagazine.com/kissed-sun-art-solar-dyeing/ Accessed on 20.08.2021.

Gupta, V. K. (2019). Fundamentals of Natural Dyes and Its Application on Textile Substrates, In "Chemistry and Technology of Natural and Synthetic Dyes and Pigments", Eds. A. K. Samanta, N. S. Awwad and H. M. Algarni, IntechOpen.

Irwin, C. (2020). Beginner's guide to solar dyeing. https://caitlynirwin.com/blog/beginners-guide-to-solar-dyeing Accessed on 20.08.2021.

Kambur, S. (2009). *Rhus coriaria* L., *Pyracantha coccinea* M. Roemer, *Cotoneaster nummularia* Fisch.&Mey. Türlerinin Tohum ve Çimlenme Özelliklerinin Belirlenmesi. Yüksek Lisans Tezi. Artvin Çoruh Üniversitesi Fen Bilimleri Enstitüsü Orman Mühendisliği Anabilim Dalı, 34 p.

Sarıkürkçü, C. and Tepe, B. (2015). Biological activity and phytochemistry of firethorn (*Pyracantha coccinea* MJ Roemer). Journal of Functional Foods, 19, 669-675.

Taylan M, Atlıhan Ş. (2018). Tekstil Tasarımında Doğal Elyaf ve Doğal Boya Kullanımı. Idil, 7(43), 319-326.

Venil, C. K., Velmurugan, P., Dufossé, L., Devi, P. R., Ravi, A. V. (2020). Fungal Pigments:

Potential Coloring Compounds for Wide Ranging Applications in Textile Dyeing. J. Fungi 6(68), 1-24.

Yusuf, M., Shabbir, M., Mohammad, F. (2017). Natural Colorants: Historical, Processing and Sustainable Prospects. Nat. Prod. Bioprospect. 7, 123-145.

Internet sources:

https://en.wikipedia.org/wiki/Pyracantha_coccinea Accessed on 20.08.2021.

Synthesis and Characterization of Cellulose Acetate from Waste Spartium Juncem Flowers

Özlem Karaboyacı[1*], Semra Kılıç[2]

Abstract:

In this study, it was aimed to re-incorporate spartium junceum flowers, which became garbage after essential oil extraction, into the raw material cycle through cellulose extraction and to ensure recycling. Cellulose extracted from waste flowers is a commercial product and used in the synthesis of cellulose acetate, which is the raw material of our further studies. Cellulose and holocellulose were extracted from waste flowers for the synthesis of cellulose acetate. Later, both were used to synthesize cellulose acetate. At the end of the study, cellulose acetate was obtained with a yield of 8.37% by cellulose extraction from waste flowers, while cellulose acetate was obtained with a yield of 8.14% in the holocellulose method.

Keywords: Cellulose, Cellulose Acetate, Waste Spartium Junceum Flowers, Extraction

1. Introduction

Cellulose is one of the natural polymers produced by living plant organisms (Şahin, 2019). Plant, herb and in trees. Cellulose, which forms the cell wall of plants, is produced with an annual synthesis amount of 10^{-10}-10^{-11} tons. It is the most abundant carbohydrate in nature. (Arslan et al., 2014)
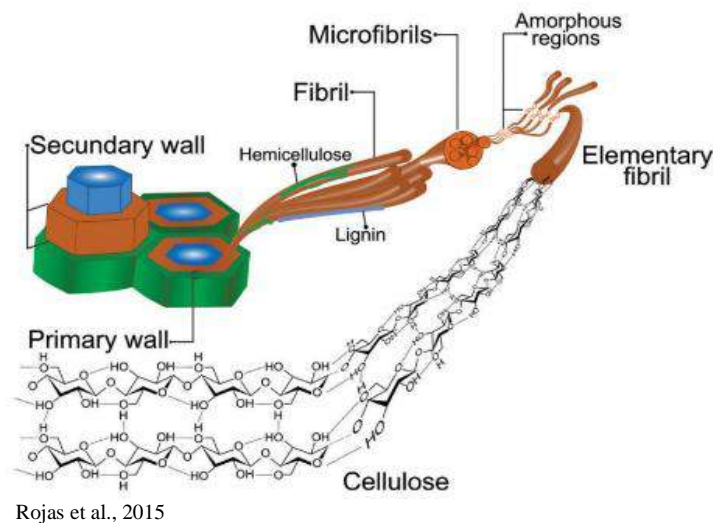

Rojas et al., 2015

Figure 1. Progressive Structure of Cellulose from Plants

[1] Süleyman Demirel University, Engineering Faculty, Bioengineering Department, Isparta, Turkey
[2] Süleyman Demirel University, Science and Literature Faculty, Biology Department, Isparta, Turkey
* Corresponding author: ozlemkaraboyaci@gmail.com

Cellulose Esters

Cellulose esters are formed by the reaction of cellulose molecules with hydroxide. Cellulose The formation of esters is theoretically possible for all inorganic and organic acids. These esters Among the commercial and technological aspects, the most important ones are cellulose nitrate, cellulose xanthate and cellulose acetate. (Kırıcı et al., 2001)

Cellulose Acetate and Type

Cellulose acetate is a natural polymer, that is widely used in various industries, cigarette, material for plastic, film, and paint. Mechanical durability, high abrasion resistance, transparency, dyeability, machinability diversity, It is the most important organic acid sourced cellulose derivative with its moldability and high dielectric properties. (Kırıcı et al., 2001) Cellulose consists of two types, fiber and plastic. Largest Market cellulose fiber dominates its share.
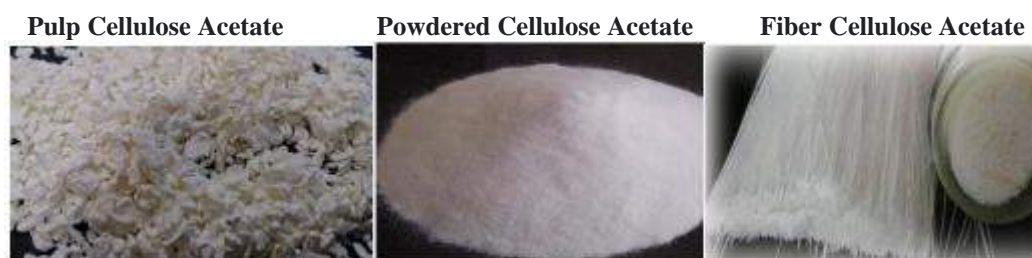
Pulp Cellulose Acetate **Powdered Cellulose Acetate** **Fiber Cellulose Acetate**

Figure 2. Cellulose Acetate and Types

It was made from cellulose by acetylation process. Cellulose could be isolated from plants or biomass. Empty palm oil bunches (EPOB) and dried jackfruit leaves (DJL) are two sources of biomass that is available in Indonesia.

Indonesia is one of the countries with the largest palm oil plantations in the world. Therefore, many palm oil factories are established in Indonesia and produce a lot of empty bunches of palm oil. Empty palm oil bunches are the biggest waste in processing palm into palm oil. The average production of empty palm oil bunches is 20-23% of total oil palm production in Indonesia. The content of cellulose in empty palm oil bunches is 38.76% . In addition to palm oil bunches there is another potential material, that is jackfruit leaves. Indonesia is a tropical country so it's suitable to grow plants, including jackfruit plant. This plant is found in almost all parts of Indonesia and is favored by most people.

Therefore, jackfruit leaves will be used for cellulose acetate raw materials. The cellulose content of dried jackfruit leaves is 21.45% (Tristantini et al., 2018). Cellulose acetate, one of the important derivatives of cellulose which are industrially more important and it is estimated that annually 1.5 billion pounds are manufactured globally (Das et al., 2014). Brazilian paper and cellulose industry aggregates about 220 companies which produce around 10.1 million metric tons of cellulose and 8.6 million metric tons of paper each year. This production corresponds to 1.4% of Brazilian gross domestic product (GDP) and makes Brazil the seventh major producer of cellulose – leader in the production of short fiber cellulose and 11th in the production of paper. Brazilian paper and cellulose products are manufactured exclusively from wood of forests planted in degraded areas, avoiding the cut of native trees(Rodrigues et al., 2008).

2. Material ve Method

2.1. Cellulose Extraction

The cellulose extraction of waste spartium junceum flowers was made by the Kurschner and Hoffer method (1931). Approximately 2 g of sample was treated with 100 mL of 1:4 (V/V mixture of nitric acid and ethanol and allowed to boil under reflux for 1 hour. After boiling for 1 hour, the sample was filtered and this process was repeated 3 times. After cooling, the remaining cellulose was filtered off and washed with distilled water until the filtrate was neutralized.

2.2. Holocellulose Extraction

Holocellulose is the carbohydrate complex that remains after the lignin substance of the plant has been removed. In the study, the chlorite method developed by Wise and Karl (1962) was used to determine the amount of holocellulose.

80 mL of distilled water was added to 2.5 g of waste flower pulp. By adding 0.3 mL of acetic acid and 0.75 g of sodium chloride, the reaction was carried out at 80°C for 1 hour under reflux. Afterwards, 0.3 mL of acetic acid and 0.75 g of sodium chloride were added again and waited for 1 hour. This process was repeated 3 times in total. After 3 hours, the mixture was filtered. The drying process was carried out by washing with distilled water and acetone. For the production of cellulosic fiber, it is necessary to convert the cellulose and holocellulose we have obtained into cellulose acetate.

The cellulose acetate production reaction was described by Djuned et al. 2014, Filho et al. The studies of 2008 and Cerqueira et al. 2007 were examined, modified in accordance with our study, and reactions were carried out as described below.

2.3. Obtaining Cellulose Acetate from Cellulose

1 g of cellulose was added to 25 mL of acetic acid and stirred for 1 hour for activation. 0.1 mL of sulfuric acid and 30 mL of acidic anhydride were added to the mixture as catalysts and stirring continued for 4 hours at room temperature (22 °C). After 4 hours, the mixture was filtered to remove unreacted particles. By adding 500 mL of distilled water to the obtained filtrate, it was waited for the hydrolysis to start and the precipitation of cellulose acetate to take place. The precipitate was filtered and washed with distilled water until the pH was 7. It was dried in an oven at 105 °C.

2.4. Obtaining Cellulose Acetate from Holocellulose

1 g of holocellulose was added to 25 mL of acetic acid and stirred for 1 hour for activation. 0.1 mL of sulfuric acid and 30 mL of acidic anhydride were added to the mixture as catalysts and stirring continued for 4 hours at room temperature (22 °C). After 4 hours, the mixture was filtered to remove unreacted impurities. By adding 500 mL of distilled water to the obtained filtrate, the precipitation of cellulose acetate was expected. The precipitate was filtered and washed with distilled water until neutralized. It was dried in an oven at 105 °C.

Figure 3. Cellulose acetate derived from holocellulose

Figure 4. Cellulose acetate derived from cellulose

3. Results

Holocellulose and cellulose obtained from the wastes of the broom (spartium junceum) flower were converted into cellulose acetate. It was observed that there was a color difference between the cellulose acetates. As can be seen in the figures, it has been observed that the cellulose acetate obtained from cellulose (Figure 4) is more yellowish than the cellulose acetate obtained from holocellulose (Figure 3). As a result of experimental studies; While cellulose acetate was obtained with 8.37% yield from cellulose, cellulose acetate was obtained with 8.14% yield from holocellulose.

FTIR spectra of cellulose acetates obtained from cellulose and holocellulose are shown in Figures 5 and 6. The fact that both spectra are very similar to each other shows that the same purity product was obtained in both methods. In the FTIR spectra, 1748, 1384 and 1240 cm^{-1} bands corresponding to the characteristic bands C=O, C-H and -CO- of acetyl cellulose are clearly observed in both spectra.
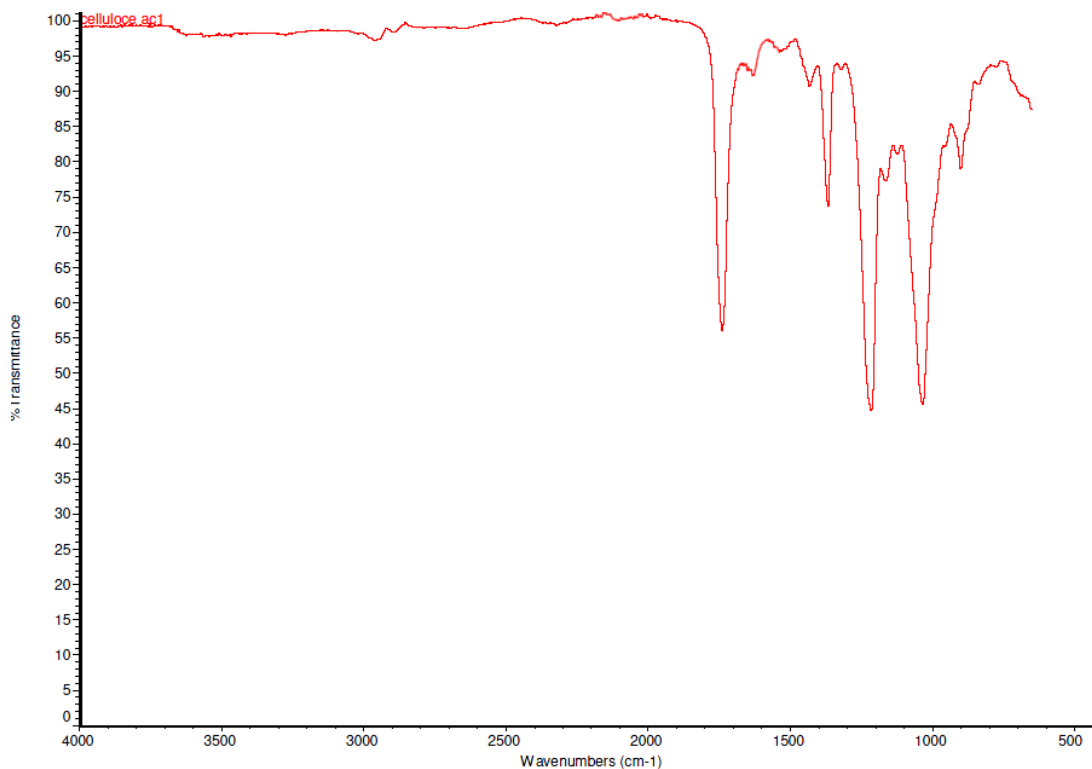

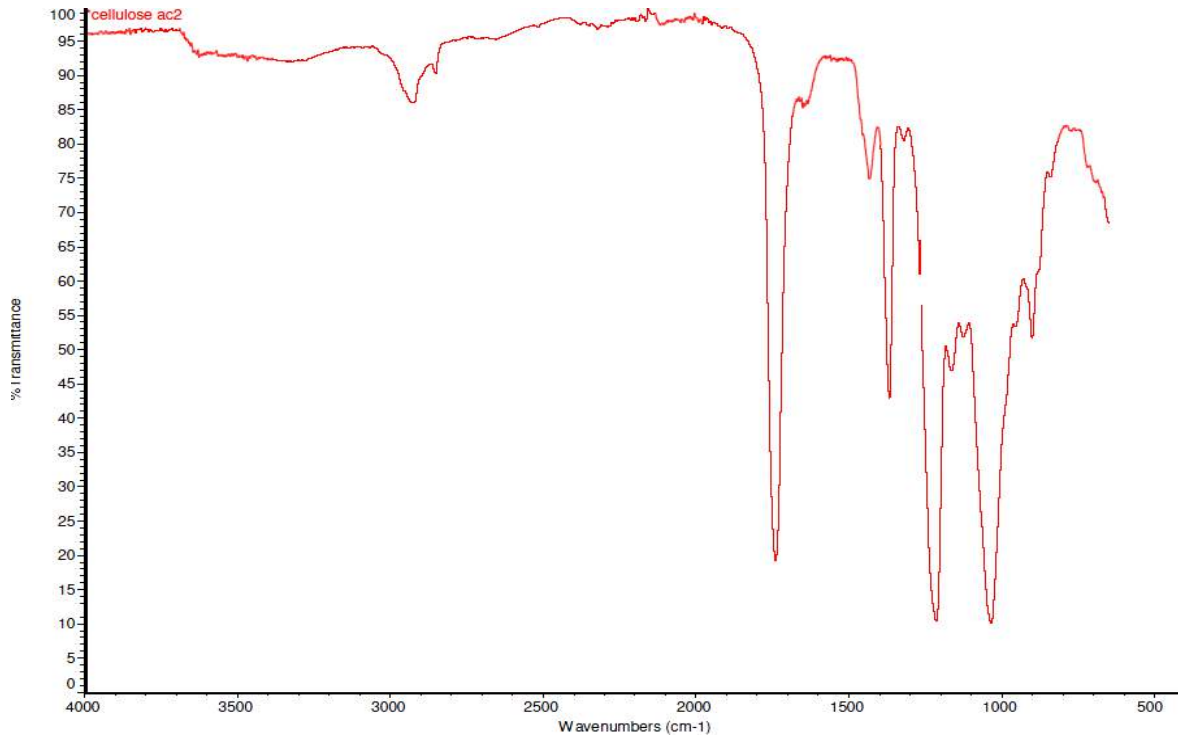**Figure 5.** FTIR spectrum of Cellulose Acetate derived from cellulose

Figure 6. FTIR spectrum of Cellulose Acetate derived from holocellulose

4. Discussion and Conclusions

The positive effect of the recycling of flower waste (pulp) released as a result of the distillation of broom (*Spartium junceum*) plant and the data we obtained were examined. With the implementation of recycling, the amount of waste going to garbage will be reduced, and less space and energy will be used for the transportation and storage of these wastes. FTIR spectra show that cellulose acetate was successfully synthesized from the waste flowers. Obtained cellulose acetate can be used in fiber, nano fiber spinning in the next stages.

References

Arslan, S., & Erbaş, M. (2014). Selüloz ve Türevi Diyet Liflerin Özelliklei ve Fırın Ürünlerinde Kullanım İmknaları. Gıda(39), s. 243-250.

Cerqueira, D. A., Rodrigues Filho, G., Silva Meireles, C. (2007). Optimization of sugarcane bagasse cellulose acetylation. Carbohydrate Polymers, 69(3), 579-58

Das, A. M., Ali, A. A., & Hazarika, M. P. (2014). Synthesis and characterization of cellulose acetate from rice husk: Eco-friendly condition. Carbohydrate polymers, 112, 342-349.

Djuned, F. M., Asad, M., Ibrahim, M. N. M., Daud, W. R. W. (2014). Synthesis and characterization of cellulose acetate from TCF oil palm empty fruit bunch pulp. BioResources, 9(3), 4710-4721.

Kırıcı, H., Ateş, S., Akgül, M. (2001). Selüloz Türevleri ve Kullanım Yerleri. Fen ve Mühendislik Dergisi, 4(2), s. 119-130.

Pinestrength, (2017). COST Action FP1406: Pine pitch canker strategies for management of Gibberella circinata in greenhouses and forests (Pinestrength). http://www.pinestrength.eu

Rodrigues Filho, G., Monteiro, D. S., da Silva Meireles, C., de Assunçao, R. M. N., Cerqueira, D. A., Barud, H. S., Messadeq, Y. (2008). Synthesis and characterization of cellulose acetate produced from recycled newspaper. Carbohydrate Polymers, 73(1), 74-82.

Rojas, J., Bedoya, M., Ciro, Y. (2015). Cellulose-Fundamental Aspects and Current Trends. Current Trends in the Production of Cellulose Nanoparticles and Nanocomposites for Biomedical Applications

Şahin, H. T. (2019, Ağustos 7). Selüloz ve Kağıt Üretimi Üzerine Bir Değerlendirme. Ağustos 12, 2020

Tristantini, D., Sandra, C. (2018). Synthesis of cellulose acetate from palm oil bunches and dried jackfruit leaves. In E3S Web of Conferences (Vol. 67, p. 04035). EDP Sciences.

TÜİK, (2015). Turkish Statistical Institute. http://www.tuik.gov.tr/Start.do (Date of Access: 12.04.2017)

Determination of Volatile Component and Saponin Content of Jujube Tree Leaves Pre-Fruit and Post-Harvest

Musa Denizhan Ulusan[*1]**, Mustafa Karaboyacı**[2]

Abstract: In this study, leaf volatile components and saponin contents of cultured jujube trees grown in Isparta region in spring and autumn were analyzed. There is a very developed sector in the Isparta region where essential oils of plants such as lavender and rose essential oils are obtained. For this reason, the volatile components of the leaves of the jujube tree, which has been used for centuries for medicinal and various purposes, were studied with the SPME method and 18 volatile components were determined before the fruiting period and 14 components after the harvest season. Leaves contains 2,49 mg/mL saponin before fruiting 4,29 mg/mL after harvest season.

Keywords: Ziziphus zizyphus, jujube, leaf, volatile, saponin

1. Introduction

Jujube Tree is a thorny tree with a height of 4-5 meters that blooms with fragrant yellow flowers between April and May. The fruits of the tree are red-brown bark, hard-seeded, the wild ones are in the size of a elaeagnus, and the grafted cultivated plants are in the size of an average walnut. Although the original homeland of jujube (Ziziphus zizyphus) is Syria, it is a plant that has been grown in China for 4000 years and is known to have 400 varieties. India, Russia, Southern Europe, North Africa, the Middle East and Anatolia are its natural spread areas. The jujube plant, which was taken to the United States in 1837, found a place to grow in the southwestern region of the country (Yılmaz, 2019).

Jujube is a temperate climate plant and subsides up to 1700 meters above sea level, withstanding down to -20ºC degree. It is resistant to excessive precipitation on drained and fertile soils. It is not affected by drought. It can grow well in sandy-loam neutral or slightly alkaline soils in regions with an altitude of 0-1500 m, annual average temperature 7-13°C in winter and 37-48°C in summer, and an annual average rainfall of 120-2200 mm (Kavas and Dalkılıç, 2015).

When the literature about the plant is examined, it is seen that there are many studies on the usage areas of its fruits, wood and leaves. Outlaw et al, (2002), in their study explained the versatile uses of the plant as follows: Few plants are as versatile as the jujube. First, the wood itself is valuable. Strong, durable, and smooth, it is used for the manufacture of musical instruments, artwork, carts and miscellaneous items. It has also been crafted into gears and caskets, which bring honor to the deceased. Second, it is a source of fodder for cattle, camels, and goats. Third, it has been used medicinally for 3000 year. All parts of the plant kernel,

[1] Süleyman Demirel Üniversity, Isparta, Turkey
[2] Süleyman Demirel Üniversity, Engineering Faculty, Chemical Engineering Department, Isparta, Turkey
* Corresponding author: denizhanulusan@sdu.edu.tr

flower, fruit, leaves, bark, wood, and root have been used medicinally. Fourth, the fruit has been used for every imaginable edible purpose fresh, dried, candied, in teas in myriad recipes, and for the production of wine and vinegar. Last, the jujube is a major honey source in China.

As can be understood from this beautifully summarized sentence, every part of the plant is used, from the fruit to the stem, bark and leaves. Since our article is about the leaves of the plant, let's focus on the studies on the leaves.

Elaloui et al (2016) conducted a study on the phytocomponents of jujube plants harvested in Tunisia. At the end of the study, they found that, Z. jujuba leaf extracts were distinct due to their richness in linolenic, palmitic, oleic, and linoleic acids, and in β-Sitosterol, stigmasterol and flavonoid compounds especially rutin and apigenin that justified their use in cosmetics and in pharmacology.

Guo et al (2011) performed a study about determining triterpenic acids, saponins and flavonoids in the leaves of two Ziziphus species. They found fourteen constituents including three flavonoids, two saponins and nine triterpenic acids in Z. jujuba and Z. jujuba var leaves. They found that jujube leaves are rich in quercetin-3-O-rutinoside and triterpenic acids, they could be the promising natural sources for future industrial research of quercetin-3-O-rutinoside and triterpenic acids with potential benefits for human health.

Damiano et al (2017) studied antioxidant and antibiofilm activities of secondary metabolites from Ziziphus jujuba leaves used for infusion preparation. They reported that jujube leaf infusion is a healthy antioxidant bedtime beverage, associate it to an unreported anti-caries activity. Z. jujuba Mill. leaf extracts could be also employed for the development of alternative or adjunctive natural anti-caries prevention remedies, as well as included in products for oral hygiene such as toothpastes and mouthwashes.

In this study, we tried to elucidate the changes in the volatile components and saponin content of the leaves of the jujube plant grown in the Isparta region before fruiting in the spring and after the fruits are harvested in the autumn.

2. Material and Methods

Ziziphus zizyphus fresh leaves were collected from the cultivated fields of Isparta Gönen region on 10 June and 10 November. The leaves were saved in the shade at room temperature and ground for aallysis with the aid of a rondo. Powdered leaves (10.0 g) was extracted at room temperature with 100 mL distilled water for 12 hours and filtered.

2.1. Determination of total saponins

The total saponins contents of Ziziphus zizyphus leaves extracts were determined by the vanillin-sulfuric acid method (Hiai et al., 1976). 0,25 mL of extracts were reacted with 0,25 mL vanillin/etanole (8%) and 2 mL sulfuric acid (72%). Than the mixture was incubated at 60 °C for 10 min. After the incubation mixture was cooled for another 15 minute at room temperature, followed by absorbance measurement at 538 nm. Quillaja saponin was used as a standard and the content of total saponins was expressed as Quillaja equivalents.

2.2. Determination of volatile components

GC-MS SPME technique was used in the analysis of the volatile components of the leaf extracts. The SPME technique is a simple and sensitive sample preparation method that extracts the components in the sample to be analyzed by absorbing the fiber coated with a thin polymeric stationary phase on silica.

3. Results

Figure 1 shows the extracts of jujube leaves. It can be seen from the picture leaves collected before the fruit season gives more clear extracts. After the harvest season, the pigments contained in the leaves increase and a darker solution is obtained. In addition, the stable foam layer clearly observed on the solutions is an indication that both contain saponins.
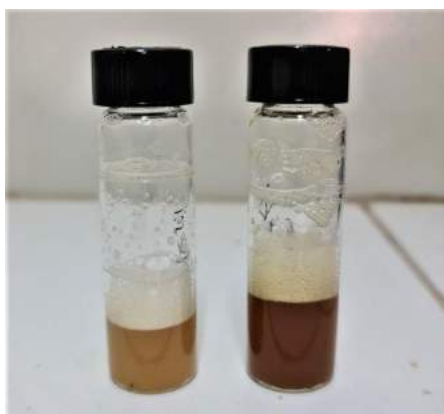

Figure 1. Extracts of jujube leaves, on left june extract on right november extract

Peak	Name	Area
1	Ethyl alcohol	4,76
2	Propanenitrile, 2-hydroxy-2-methyl- (CAS) Acetone cyanohydrin	3,16
3	2,3-Butanedione (CAS) Diacetyl	2,68
4	Hexane (CAS) n-Hexane	21,38
5	1-Propene, 3-bromo- (CAS) Allyl bromide	2,33
6	2-Hexenal, (E)- (CAS) (E)-2-Hexenal	2,06
7	6-Methyl-5-hepten-2-one	3,33
8	dl-Limonene	2,05
9	6-Octen-1-ol, 3,7-dimethyl-, formate (CAS) Citronellyl formate	4,89
10	Benzofuran, 2,3-dihydro-	18,76
11	Guaiacol 4-vinyl-	5,04
12	Eugenol	19,68
13	5,9-Undecadien-2-one, 6,10-dimethyl- (CAS) Dihydropseudoionone	9,88

Table1. Volatile components of jujube leaves after harvest season on november

Table 1 shows the volatile component of jujube leaves after harvest. As seen from the table hexane, benzofuran, eugenol and dihydropseudoionone are the major components of the leaves. 14 volatile components were detected in leaves by SPME method. But these four components make up 69,7 percent of the total components.

Table 2 shows the result of SPME analysis at the end of water extraction of leaves collected from jujube tree in June before fruiting. As a result of the analysis, 18 different components were identified. The main of these compounds are ethyl alcohol, 2-pentanone, 2-hexenal, 3-octanone, 3-octanone, eugenol and 3-methylpentane. These 7 compounds constitute 75,51 percent of the total components and the ratio of all of them is over five percent. But the presence of 23,63% of ethyl alcohol alone is too high to ignore. It also contains a high rate of 14,35% eugenol.

The total amount of saponin determined according to the method of Hiai et al., 1976 was determined as an average of 2,49 mg/mL in the leaves before fruiting period. In the leaves collected in November after the fruit harvest, this rate was found to be 4,29 mg/mL on average. As can be seen, the plant continues to produce saponin as long as the leaves remain on the tree, so this rate is higher in autumn leaves.

Peak	Name	Area
1	Ethanol (CAS) Ethyl alcohol	23,63
2	Propanenitrile, 2-hydroxy-2-methyl- (CAS) Acetone cyanohydrin	2,26
3	2,3-Butanedione (CAS) Diacetyl	2,90
4	Pentane, 3-methyl- (CAS) 3-Methylpentane	5,12
5	2-Pentanone (CAS) Methyl propyl ketone	9,30
6	2-Hexenal, (E)- (CAS) (E)-2-Hexenal	9,40
7	2-Hexen-1-ol, (Z)- (CAS) Cıs-Hex-2-En-1-Ol	3,47
8	2-Heptanone (CAS) Heptan-2-one	1,85
9	7-Octen-2-one	2,29
10	3-Octanone (CAS) Eak	7,65
11	2-Octanone (CAS) Octan-2-one	6,06
12	Octanal (CAS) n-Octanal	2,73
13	l-Limonene	1,85
14	Linalool	2,63
15	Phenol, 4-ethenyl-2-methoxy-	1,33
16	Eugenol	14,35
17	5,9-Undecadien-2-one, 6,10-dimethyl- (CAS) Dihydropseudoionone	1,10
18	1,2-Benzenedicarboxylic acid, bis(2-methylpropyl) ester	2,08

Table 2. Volatile components of leaves extracted before fruit season on june

4. Discussion and Conclusions

In this study, the volatile components and saponin contents of the leaves of jujube trees grown in the Isparta region were analyzed. As it is known, secondary metabolites produced by plants vary according to the climate and soil structure of the region where they are located. For this reason, this preliminary study on the analysis of the injured components contained in this plant, which has been used for medicinal purposes for centuries and which has been extensively cultivated in this region in recent years, and in which sectors it can be used, offers new ideas to researchers and us.

References

Guo, S., Duan, J. A., Tang, Y., Qian, Y., Zhao, J., Qian, D., ... & Shang, E. (2011). Simultaneous qualitative and quantitative analysis of triterpenic acids, saponins and

flavonoids in the leaves of two Ziziphus species by HPLC–PDA–MS/ELSD. Journal of pharmaceutical and biomedical analysis, 56(2), 264-270.

S. Hiai, H. Oura, T. Nakajima. (1976). Color reaction of some sapogenins and saponins with vanillin and sulfuric acid. Planta Med., 29 pp. 116-122

Yılmaz, G. (2019). Hünnap (zizyphus zizyphus) ağacı yaprak ve meyve ekstratlarının antioksidan ve antimikrobiyal özelliklerinin araştırlması (Master's thesis, Namık Kemal Üniversitesi).

Kavas, İ., Dalkiliç, Z. (2015). Bazi Hünnap Genotiplerinin Morfolojik, Fenolojik ve Pomolojik Özelliklerinin Belirlenmesi ve Melezleme Olanaklarinin Araştirilmasi. Adnan Menderes Üniversitesi Ziraat Fakültesi Dergisi, 12(1), 57-72.

Outlaw Jr, W. H., Zhang, S., Riddle, K. A., Womble, A. K., Anderson, L. C., Outlaw, W. M., Thistle, A. B. (2002). The jujube (Ziziphus jujuba Mill.), a multipurpose plant. Economic Botany, 56(2), 198-200.

Elaloui, M., Laamouri, A., Ennajah, A., Cerny, M., Mathieu, C., Vilarem, G., Hasnaoui, B. (2016). Phytoconstituents of leaf extracts of Ziziphus jujuba Mill. plants harvested in Tunisia. Industrial crops and products, 83, 133-139.

Dye Sensitized Solar Cell Production by Doctor Blade Method Using Bezathren Yellow 5GF Vat Dye

Kamila Sobkowiak[1*], Mustafa Karaboyacı[2]

Abstract: In this study, the structure and working principle of dye-sensitized solar cells were investigated, as well as the production process of them from cheap organic vat dyes. The conductive glass part of the cell was produced with SnO_2 nano coating by spray pyrolysis method. In order to increase the efficiency of conductive glasses, the doping with fluorine was applied. FTO glass surfaces was coated with TiO_2 by the very famous easy to operate method doctor blade method.

The current-voltage (J-V) values of the prepared solar cells under light and dark conditions were measured with an A.M 1.0 solar simulator and the efficiency calculation was made for each cell with the obtained values. The highest efficiency $\eta = 0.00429$ % was obtained for solar cell sensitized with Bezathren Yellow 5GF dye prepared by paste method.

Keywords: DSSC, Vat dyes, solar cell, FTO,

1. Introduction

The development of renewable energy sources becomes an alternative focus point to reduce the use of fossil resources. The most abundant and remarkable energy source is photovoltaic or solar energy that converts solar energy directly into electrical energy (Feldt, 2013; Fukurozakia et al., 2013). Solar energy is the main renewable energy source available today because it provides energy for growth and development to all living beings in the world through the process of photosynthesis. An important advantage of solar energy is that it can be used locally and commercially. Solar energy benefits not only the individual owners but also the environment. Solar energy can be turned into useful heat or electricity. Electricity is a form of energy that can be made accessible easily. For this reason, scientists and engineers are currently trying to use solar radiation to generate electricity directly with economic devices (Kumar et al., 2015).

Vat dyes are a type of dyestuff that maintains its importance in cotton dyeing due to its high fabrication fastness. They show high fastness to wet processes. Good wet fastness is due to the formation of water-insoluble compounds. Light fastness is also generally very good. Vat

[1] Lodz University of Technology, Chemistry Faculty, Polymer and Dye Technology Department, Lodz, Poland
[2] Süleyman Demirel University, Engineering Faculty, Chemical Engineering Department, Isparta, Turkey
* Corresponding author: camilla.river.50@gmail.com

dyes are not only resistant to light, acids and alkalis, but also to strong oxidizing bleaches. Vat dyes are water insoluble dyes so before applying it to dyebath in needs to be e reduced to water soluble leuco form and after dye is absorbed to the fiber than it needs to be re-oxidised to the original form.

These reduction oxidation properties of vat dyes gave us the idea that they can also be used in solar cells. Bezathren Yellow 5GF Vat Dye produced by CHT Bezema ad it is redox potential – 840 mV accurding to its MSDS. Also Egerton and Assaad, (1970) studied about photochemical behaviour of vat dyes and they reported that photo reduction of some vat dye are possible.

For preparing the solar cell, simplest method for depositing titania paste on FTO glass substrate was used. The technique is known as doctorblade method and the thickness of the titania layer is determined by the thickness of a adhesive tape placed on both sides FTO glass.

2. Material and Methods

Some combinations were applied, and various results were obtained as described below.

2.1. HNO$_3$ method

3 g of TiO$_2$ was mixed with HNO$_3$ and 2 drops of wetting agent giving a medium density paste. Two sides of the surface were covered with a tape. Thin smooth layer of the paste was distributed on the conductive glass surface. The tape was removed. Afterwards, the glass was heated in the oven for 30 min in 500°C

2.2. H$_2$O method

3 g of TiO$_2$ was mixed with distilled water and 2 drops of wetting agent giving a medium density paste. A thin smooth layer of the paste was distributed on the conductive glass surface. Afterwards, the glass was heated in the oven for 30 min in 500°C.

2.3. H$_2$O + Ethanol method

3 g of TiO$_2$ was mixed with mixture of 1:1 distilled water and ethanol and 2 drops of wetting agent giving a medium density paste. A thin smooth layer of the paste was distributed on the conductive glass surface. Afterwards, the glass was heated in the oven for 30 min in 600 °C.

2.4. TiO$_2$ + Dye premixed method

TiO$_2$ was mixed with dye, distilled water and 2 drops of wetting agent giving a medium density paste. A thin smooth layer of the paste was distributed on the conductive glass surface. Afterwards, the glass was heated in the oven for 30 min in 400°C.

3. Results

In the material method section, the preparation of 4 different paste methods was explained. In the "2.4. TiO2 + Dye premixed method" method, which is the method number 4, a completely homogeneous and surface-covering titanium coating was obtained and the experiments were continued on this. In other trials, the TiO_2 coating was partially or completely removed from the surface after the dye solution was impregnated. For this reason, those trials have not been studied further. s

Figure 1 shows the J-V curves of DSSC prepared with Bezathren Yellow 5GF. Table 1. shows the J_{SC}, V_{OC}, P_{in}, FF and efficiency values of the solar cell. Solar cell was prepared by paste method using only TiO_2 solution and was sintered at 400°C. The dye and mixture of H_2O + ethanol as a solvent was placed on the coated surface afterwards.
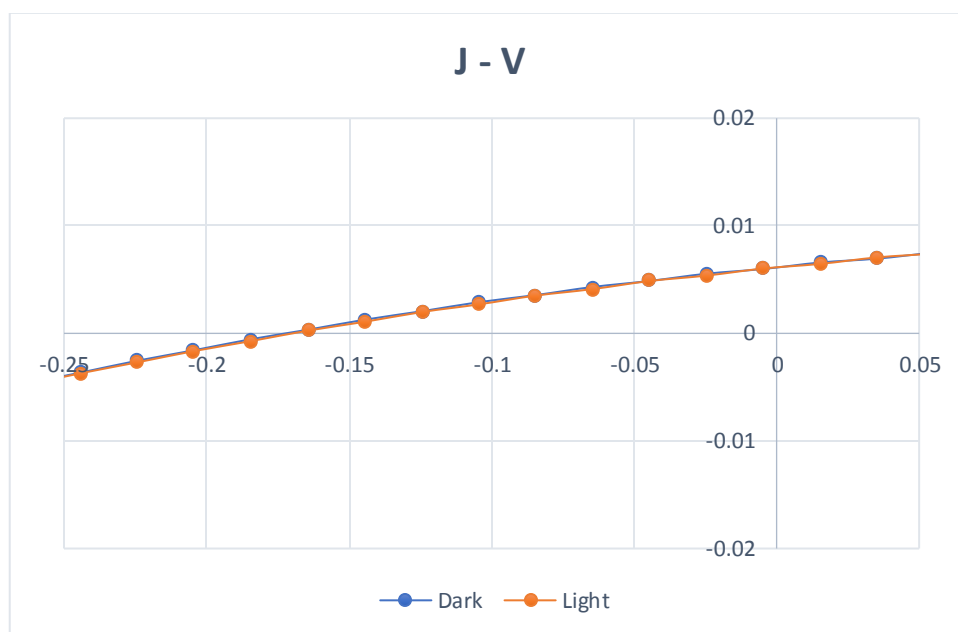

Figure 1. J - V graph of solar cell measured with AM 1.0 Solar Simulator

Table 1. Results for Bezathren Yellow 5GF

Sample	J_{SC} (mA)	V_{OC} (V)	P_{in} (Watt)	Fill factor (%)	Efficiency (%)
Paste method	0.01	0.213	1.5	30.21	0.00429

4. Discussion and Conclusions

Results shows us vat dyes are photo sensitive and can be used for solar cells. However, the yield result obtained from this experiment is as low as 0.00429%. We intend that the study will be useful in terms of being a preliminary study on the preparation of dye-sensitive solar

cells with vat dyes, and giving us and those interested in the subject in the future. The other attractive point of the subject is the cheapness and abundant availability of vat dyes.

References

Feldt, S. (2013). Alternative redox couples for dye-sensitized solar cells (Doctoral dissertation, Acta Universitatis Upsaliensis).

Fukurozaki, S. H., Zilles, R., Sauer, I. L. (2013). Energy payback time and CO2 emissions of 1.2 kWp photovoltaic roof-top system in Brazil. Int J Smart Grid Clean Energy, 2, 164-9.

Egerton, G. S., & Assaad, N. E. N. (1970). Photochemical Behaviour of Vat Dyes I—Reaction with the Polymer Substrate. Journal of the Society of Dyers and Colourists, 86(5), 203-208.

Kumar, A., Richhariya, G., & Sharma, A. (2015). Solar photovoltaic technology and its sustainability. In Energy sustainability through green energy (pp. 3-25). Springer, New Delhi.